Jubilee Conference Proceedings

NCK-days 2012

crossing borders in coastal research

Enschede, 13-16 March 2012

University of Twente

Editors:

W.M. Kranenburg

E.M. Horstman

K.M. Wijnberg

NCK contact information:

NCK c/o Deltares
P.O. Box 177
2600 MH Delft
The Netherlands
www.nck-web.org

Cover: Aerial photograph of the Zandmotor (13-10-2011), courtesy Rijkswaterstaat.

ISBN: 978-90-365-3342-3
DOI: 10.3990/2.165

Organization NCK-days 2012:

This 20th edition of the NCK-days is organized by the University of Twente, Department of Water Engineering & Management.

The local organizing committee consists of:

K.M. Wijnberg

E.M. Horstman

W.M. Kranenburg

UNIVERSITY OF TWENTE.
Water Engineering & Management

These NCK-days are supported by:

NWO
Netherlands Organisation for Scientific Research

J.M.Burgerscentrum
Research School for Fluid Mechanics
TUD, TUE, UT, RUG, RUN, UL, WUR, UU

Koninklijke Boskalis Westminster nv
International Dredging & Marine Contractors

HKV CONSULTANTS

Waddenacademie

IGS
INSTITUTE FOR INNOVATION AND GOVERNANCE STUDIES

Van Oord
Marine ingenuity

Rijkswaterstaat
Ministry of Infrastructure and the Environment

Deltares
Enabling Delta Life

Editorial

Dear NCK colleagues and guests,

On behalf of the Water Engineering and Management department of the University of Twente we bid you all a very warm welcome to the NCK-days 2012 in Enschede! This year's meeting is a special edition of this annual event, celebrating the 20th anniversary of the Netherlands Centre for Coastal Research. As part of the celebrations, this year's edition is accompanied by these NCK Jubilee Conference Proceedings, which we prepared for you with pleasure and present to you with proud.

In this book you will find short peer reviewed papers of authors from all over the NCK community, giving an impression of the state of the art of Coastal Research in the Netherlands. Special contributions from éminence grise and the present NCK chairman illuminate the history of NCK and discuss the future challenges to the NCK-community. An international perspective is put forward in the papers of the keynote speakers. The various contributions are alternated by the most beautiful pictures of this year's NCK photo competition.

Also this year's excursion is a special one as part of the celebrations. It will bring you to the Ems-Dollard estuary, and highlights the motto for the 4th lustrum 'Crossing borders in coastal research' in more than one way: not only by crossing over from the marine to the fluvial domain, but also by crossing the border to Germany.

We truly hope that you will enjoy these NCK-days and that oral presentations, posters, the excursion, and all occasion for informal contacts during this meeting may reinforce the collaboration within the NCK-community and the productivity of Dutch coastal research.

Wouter Kranenburg
Erik Horstman
Kathelijne Wijnberg

Enschede, February 2012

UNIVERSITY OF TWENTE.
Water Engineering & Management

nck
netherlands centre for coastal research

NCK photo competition

Alma de Groot: Low tide at Conwy

Jury: This photo shows rays of sunlight spreading their warm glow over mudflats bordering a small coastal town. The photographer captured a multitude of contrasts: low mud and high hills, man and nature, water and land. The curvature of the tidal creeks in the foreground is not only exemplified by the backlighting, but also reflected in the skyline of the rolling hills in the background.

Content

Program NCK-days 2012

TUESDAY March 13th		
20:00 - 22:00	**Registration & Ice-breaker** Drienerburght, University of Twente, building 44	

page

WEDNESDAY March 14th (all presentations are in room Waaier 4)		
8:30	**Registration & Coffee** Waaier (Foyer), University of Twente, building 12	
9:00	**Opening** Suzanne Hulscher, Chair Water Engineering & Management group, University of Twente	
9:15	**Introduction** Ad van der Spek, Chair Program Committee NCK	
9:30 - 10:40	**Session 1: Estuaries & tidal basins (I)**	
9:30	**KEYNOTE: Hendrik Antoon Lorentz and the problem of the Zuiderzee tides** Anne Kox (University of Amsterdam)	49
10:10	**Zuiderzee is now called IJsselmeer: Process-based Modeling** Ali Dastgheib	91
10:25	**Tidal asymmetries in estuaries due to channel-flat interactions, a simple model** Niels Alebregtse	79
10:40 - 11:00	**Coffee break** Waaier (Foyer)	
11:00 - 12:00	**Poster session (Waaier, Foyer)**	
11:00 - 11:20	**'Zeepkist' presentations of posters** See the list of titles and authors at the end of this program	4
11:20 - 12:00	**Poster market**	
12:00 - 13:00	**Lunch** Waaier (Foyer)	
13:00 - 14:25	**Session 2: Estuaries & tidal basins (II)**	
13:00	**KEYNOTE: A large scale morphodynamic process-based model of the Gironde estuary** Catherine Villaret (Saint Venant Laboratory for Hydraulics)	69

13:40	**Simulating the large-scale spatial sand-mud distribution in a schematized process-based tidal inlet system model** Freek Scheel	190
13:55	**Influence of basin geometry on equilibrium and stability of double inlet systems** Ronald Brouwer	85
14:10	**Variability of currents and vertical stratification in the Marsdiep** Jurre de Vries	119
14:25 - 14:45	**Coffee break** Waaier (Foyer)	
14:45 - 16:10	**Session 3: Sediment transport**	
14:45	**KEYNOTE: Laboratory experiments for wave-driven sand transport prediction** Tom O'Donoghue (University of Aberdeen)	61
15:25	**Vortex tubes in the wave bottom boundary layer** Martijn Henriquez	143
15:40	**Erodibility of soft fresh water sediments: the role of bioturbation by meiofauna** Miguel de Lucas Pardo	111
15:55	**Monitoring silt content in sediments off the Dutch Coast** Ronald Koomans	157
16:30	**Bus pick-up**	
17:00 - 19:00	**Social event in Roombeek, Enschede** Guided tours through Twentse Welle museum and the Roombeek area!	
19:00 - 22:30	**Conference dinner** Twentse Welle, Het Rozendaal 11 (where the Roomweg crosses the bus lane), Enschede	

page

THURSDAY March 15th (all presentations are in room Waaier 4)		
9:00 - 10:25	**Session 4: Coastal wetlands & deltas**	
9:00	**KEYNOTE: Bio-physical linkages in coastal wetlands – implications for coastal protection** Iris Möller (University of Cambridge)	51
9:40	**Flow routing in mangrove forests: field data obtained in Trang, Thailand** Erik Horstman	147
9:55	**Highlights of Dutch and US coastal graduation projects in the Mississippi Delta after Hurricane Katrina** Mathijs van Ledden	235
10:10	**Modeling plan-form deltaic response to changes in fluvial sediment supply** Jaap Nienhuis	173

10:25 - 11:20	**Poster session (Waaier, Foyer)**	
10:25 - 11:20	**Poster market & Coffee**	
11:20 - 13:00	**Session 5: Nearshore oceanography & shelf**	
11:20	**KEYNOTE: Nearshore Physical Oceanography: Recent Trends and Future Prospects** David Huntley (Plymouth University)	41
12:00	**Rip Current Observations at Egmond aan Zee** Gundula Winter	245
12:15	**Hydrodynamics of the Rhine ROFI near IJmuiden** Janine Nauw	167
12:30	**Observations of suspended matter along the Dutch coast** Carola van der Hout	207
12:45	**Quantified and applied sea-bed dynamics of the Netherlands Continental Shelf and the Wadden Sea** Thaiënne van Dijk	223
13:00 - 14:00	**Lunch** Waaier (Foyer)	
14:00 - 15:10	**Session 6: Surfzone-beach-dune system (I)**	
14:00	**KEYNOTE: Surfzone-beach-dune interactions** Patrick Hesp (Louisiana State University)	35
14:40	**Dune development and aeolian transport along the Holland coast** Sierd de Vries	125
14:55	**Connecting aeolian sediment transport with foredune development** Joep Keijsers	153
15:10 - 15:30	**Coffee break** Waaier (Foyer)	
15:30 - 16:30	**Session 7: Surfzone-beach-dune system (II)**	
15:30	**Nearshore evolution at Noordwijk (NL) in response to nourishments, as inferred from Argus video imagery** Gerben Ruessink	179
15:45	**Assessing dune erosion: 1D or 2DH? The Noorderstrand case study** Pieter van Geer	229
16:00	**Probabilistic assessment of safety against dune retreat along the Northern-Holland coast** Wim van Balen	197

16:15	**Effects of 20 years of nourishments: Quantitative description of the North Holland coast through a coastal indicator approach** Giorgio Santinelli	185
16:30 - 17:00	**Closure and prizes**	

FRIDAY March 16th		
full day	**Excursion Ems-Dollard estuary**	

page

POSTERS			
1	Marcel Bakker	**Towards a three-dimensional geological model of the North Sea subsurface**	81
2	Gerben de Boer	**OpenEarth: using Google Earth as outreach for NCK's data**	97
3	Alma de Groot	**Measuring and modeling coastal dune development in the Netherlands**	105
4	Matthieu de Schipper	**Morphological developments after a beach and shoreface nourishment at Vlugtenburg beach**	115
5	Dusseljee / Jansen	**An efficient method to assess erosion risks in tidal basins**	131
6	Menno Eelkema	**Ebb-tidal delta morphology in response to a storm surge barrier**	137
7	Lodder / Van Geer	**MorphAn: A new software tool to assess sandy coasts**	161
8	Wing Yan Man	**Short term morphological wave impact on the Zandmotor; a conceptual model**	165
9	Abdel Nnafie	**Nonlinear response of shoreface-connected sandridges to offshore sand extraction for a realistic inner shelf slope**	177
10	Meinard Tiessen	**Numerical modeling of physical processes in the North Sea and Wadden Sea with GETM/GOTM**	191
11	Karen van Bentum	**The Lagos coast – Investigation of the long-term morphological impact of the Eko Atlantic City project**	201
12	Mick van der Wegen	**Levee development along tidal channels**	213
13	Julia Vroom	**Tidal divides**	241

About the Netherlands Centre for Coastal Research (NCK)

OBJECTIVES

The Netherlands Centre for Coastal Research (NCK) has been founded in 1992 with the aim:

- to increase the quality of the coastal research in the Netherlands by enhancing cooperation between the various research streams and to guarantee the continuity of coastal research in the Netherlands by exchange of expertise, methods and theories between the participating institutes;
- to maintain fundamental coastal research in The Netherlands at a sufficient high level and to enhance the exchange of knowledge to the applied research community;
- to reinforce coastal research and education capacities at Dutch universities and
- to strengthen the position of Dutch coastal research in a United Europe and beyond.

ORGANIZATION

The NCK was initiated by the coastal research groups of Delft University of Technology, Utrecht University, WL | Delft Hydraulics and Rijkswaterstaat RIKZ. Early 1996, the University of Twente and the Geological Survey of The Netherlands joined NCK, followed by the Netherlands Institute for Sea Research (NIOZ, 1999), the Netherlands Institute for Ecology – Centre for Estuarine and Marine Ecology (NIOO-CEME, 2001), UNESCO-IHE Institute for Water Education (2004) and Wageningen IMARES (2008).

The NCK Program Committee establishes the framework for the research and other activities to be carried out by NCK. Based hereon, researchers prepare proposals, which NCK submits for funding to national and international agencies. Several times a year, the Centre organizes workshops and/or seminars aimed at promoting cooperation and mutual exchange of information. Furthermore, exchanges of young researchers are encouraged and possibilities for sabbaticals are pursued. Through the participating institutes, researchers have access to several facilities. The universities offer computing facilities. Field data can be accessed from data banks at Rijkswaterstaat and Deltares. The researchers of NCK may use numerical model systems developed at Deltares and Rijkswaterstaat. Deltares and Delft University of Technology offer various hydraulic laboratory facilities. Advanced equipment for field measurements is available at Utrecht University and at Rijkswaterstaat. Rijkswaterstaat and the Netherlands Institute for Sea Research can provide research vessel support. Through access to these facilities the necessary opportunities to advance the frontiers of knowledge of coastal processes are provided.

Since 1998, the NCK has a part time Program Secretary, with - in cooperation with the Programming Committee – the task to draft and to keep up to date the NCK research program, to stimulate joint NCK research projects, and to increase the visibility of NCK, both inside the NCK partner organizations and external (national and international). At the moment, ir. Claire van Oeveren is the NCK Program Secretary. Secretarial support is provided by Mrs. Jolien Mans.

The NCK Programming Committee and the Program Secretary are supervised by the NCK Supervisory Board. The various bodies are composed as follows (1/1/2012):

NCK Supervisory Board

Prof.dr.ir. H.J. de Vriend (chairman)	Deltares, Delft
Ir. M.C. van Oeveren (secretary)	NCK (Deltares), Delft
Dr. R. Allewijn	RWS-WD, Lelystad
Prof.dr.ir. M.J.F. Stive	TUD, Delft
Prof.dr. ir. H. Ridderinkhof	Royal NIOZ, Den Burg
Prof.dr. P.M.J. Herman	Royal NIOZ , Yerseke
Prof.dr. P. Hoekstra	UU, Utrecht
Prof.dr. S.J.M.H. Hulscher	UT, Enschede
Ir. J. de Schutter	UNESCO-IHE, Delft
Dr. H.J. Lindeboom	IMARES Wageningen UR

NCK Program Committee

Dr. A.J.F. van der Spek (chairman)	Deltares, Delft
Ir. M.C. van Oeveren (secretary)	NCK (Deltares), Delft
Ir. A.P. de Looff	RWS-WD, Lelystad
Dr.ir. B.C. van Prooijen	TUD, Delft
Prof.dr.ir. G.S. Stelling	TUD, Delft
Prof.dr. P.M.J. Herman	Royal NIOZ , Yerseke
Dr. M. van der Vegt	UU, Utrecht
Dr. K.M. Wijnberg	UT, Enschede
Dr. Th. Gerkema	Royal NIOZ, Den Burg
Prof.dr.ir. J.A. Roelvink	UNESCO-IHE, Delft
Prof.dr.ir. J.C. Winterwerp	Deltares, Delft
Dr.ir. M.J. Baptist	IMARES Wageningen UR

NCK photo competition

Thorsten Balke: Haamstede, Zeeland

Jury: This photo shows long shadows stretching out in the foreground making the piles look even longer and stronger. The photographer's viewpoint shows breaking waves behind the fortress of piles so their line-up accentuate their function. The sediment in front has delicate natural ridges broken-up by footprints emphasising the human impact on beach morphology.

NCK-partners

- **Delft University of Technology**
- **University of Twente**
- **University of Utrecht**
- **UNESCO-IHE**
- **Rijkswaterstaat**
- **Deltares**
- **IMARES**
- **Royal Netherlands Institute for Sea Research**

Coastal Research and Engineering at
Delft University of Technology

Bram C. van Prooijen[1],Marcel J.F. Stive[2], Wim S.J. Uijttewaal[3], Henk M. Schuttelaars[4], Cees van Rhee[5]

[1]Section of Hydraulic Engineering, Faculty of Civil Engineering, Delft University of Technology, the Netherlands, B.C.vanProoijen@TUDelft.nl

[2]Section of Hydraulic Engineering, Faculty of Civil Engineering, Delft University of Technology, the Netherlands, M.J.F.Stive@TUDelft.nl

[3]Section of Environmental Fluid Mechanics, Faculty of Civil Engineering, Delft University of Technology, the Netherlands, W.S.J.Uijttewaal@TUDelft.nl

[4]Department of Applied Mathematical Analysis, Faculty of Electrical Engineering, Mathematics and Computer Science, Delft University of Technology, the Netherlands, H.M.Schuttelaars@TUDelft.nl

[5]Section of Offshore and Dredging Engineering, Faculty of Mechanical Engineering, Marine Technology & Materials Science, Delft University of Technology, the Netherlands, C.vanRhee@TUDelft.nl

INTRODUCTION

Delft University of Technology (DUT) is part of a longstanding history of hydraulic engineering and research in the Netherlands. The university aims at educating engineers on a scientific basis, conducting research to extend scientific knowledge, and contributing to society in formulating its problems and finding appropriate solutions. We do this in close cooperation with national and international partners. The Netherlands Center for Coastal Research (NCK), of which DUT was one of the initiators, forms an important national platform.

In the field of coastal engineering, three faculties are involved in NCK: the Faculty of Civil Engineering and Geosciences (CEG); the Faculty of Electrical Engineering, Mathematics and Computer Science (EEMCS); and the Faculty of Mechanical, Maritime and Materials Engineering (3ME). A brief overview of the DUT activities is given below, with an emphasis on the research activities. We refer to our website www.TUDelft.nl for general information or http://repository.TUDelft.nl for publications.

EDUCATION

In the field of coastal engineering, DUT aims at educating BSc-, MSc- and PhD-graduates who can combine scientific knowledge and engineering skills. In the BSc-phase, fundamental knowledge like hydrodynamics is taught to ensure a scientific background in combination with project oriented education to improve engineering and design skills. In the MSc-phase a more in depth background is developed in understanding processes in coastal systems from detailed turbulence to large-scale basin development. A strong link with practice is made in the MSc-thesis project, which is often carried out in collaboration with partners outside the university. In the PhD programme, students develop into independent researchers, who find their way in the scientific community, non-profit organisations such as ministries and knowledge institutes, and in profit organisations like consultancy firms and dredging companies.

Apart from the traditional master tracks, CEG participates in the Erasmus Mundus Master in Coastal and Marine Engineering and Management (CoMEM). This is a two-year, English taught international MSc-programme, in which five European universities participate.

Since 2009, DUT offers the possibility to obtain a double degree at the National University of Singapore (NUS) and at DUT in the field of Hydraulic Engineering and Water Resources Management.

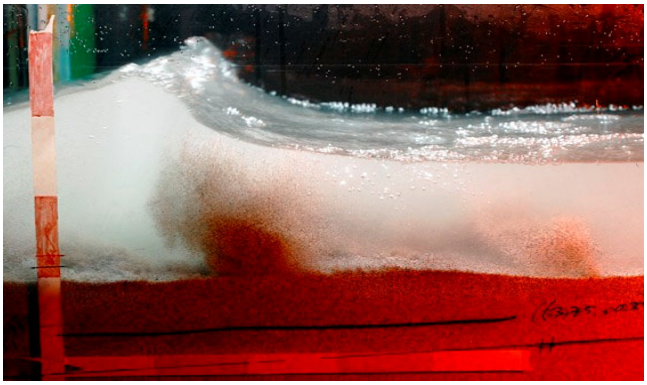

Figure 2: Laboratory experiments give new insights in the behaviour of processes, in this case on sediment erosion due to waves (source: M. Henriquez, M.Henriquez@TUDelft.nl, Foto © Sam Rentmeester/FMAX).

RESEARCH

The goal of coastal research at Delft University of Technology is to understand the dynamics in coastal areas, with an emphasis on physical processes. Research activities are based on: numerical modeling, field measurements, laboratory experiments, and system analyses. In most studies several of these methods are combined. Research is often carried out in close cooperation with national and international partners from small-scale projects and large-scale multi-disciplinary programs.

Figure 3: Field measurements are carried out by means of a devices mounted on a jetski. A jetski is specifically useful in the shallow near shore region. (source: M. de Schipper, M.A.deSchipper@TUDelft.nl)

Numerical models have been developed by DUT as principle developer, like SWAN (www.SWAN.TUDelft.nl) or SWASH (http://swash.sourceforge.net/). Both models simulate waves in the coastal zone. Furthermore, DUT has been and still is involved in the development of many other models such as XBeach (a model to simulate beach morphodynamics) or ASMITA (an aggregated model for tidal inlets). These models are applied by universities, institutes, consultancy firms and contractors all over the world. All these models have in common that the processes are incorporated in a physically sound way. Research is also carried out by applying numerical models on different aggregation levels. On the one hand idealized models are applied, in which the system is reduced to its very essence, e.g. the idealized models for equilibria of tidal inlets. On the other hand complex models are applied, containing numerous processes. We believe that especially an integral approach of the use of various types of models on different aggregation levels will lead, in combination with field experiments, to a better understanding of coastal systems.

A large body of research is based on experiments carried out in the university laboratories (at CEG and 3ME). Specific devices in this laboratory are wave flumes; the shallow water flume; a carousel; a settling column and a sediment transport flume. With detailed measurements, like Particle Image Velocimetry and Laser Doppler Velocimetry, we aim at understanding the fundamental processes behind wave dynamics, turbulence, and sediment dynamics. These measurements often lead to better parameterization of complex processes. Specific attention is recently paid to incorporating the effects of biology (vegetation, benthic fauna) into numerical models, in close cooperation with ecologists.

Since several years, DUT pays more attention to field measurements. With a special equipped DUT-jetski, bathymetries can be mapped in shallow waters and velocities can be measured. Recently, an ERC Advanced Grant by the EU was awarded. Over the coming five years this grant will be used for the 'Nearshore Monitoring and Modelling: Inter-scale Coastal Behaviour' project. This large-scale observation and measurement programme that focuses on the coastline in the area around The Hague aims to provide good long-term predictions concerning coastal change processes, which have so far been lacking.

By means of combining different methods, like data analysis and numerical modeling, coastal systems are explained. Such analyses have been carried out for several areas like the Texel Inlet. At present the Voordelta, the Yangtze Estuary and several other systems around the world are analyzed to understand the past and to predict the future.

SOCIETAL RELEVANCE

All our education and research efforts are aimed at serving society. Because of the nature of our research, this contribution becomes practically available after a medium-term period, but sometimes more direct. Also the attempts to integrate environmental issues in research have lead to enhanced solutions. Staff members participate in national advisory boards such as the 2nd Delta Committee and international advisory boards, such as the Sea dike Guidelines Vietnam and G2G Mekong Advisory Board. To strengthen the relation with other institutes and companies, several staff members from those companies are part-time employed at the DUT.

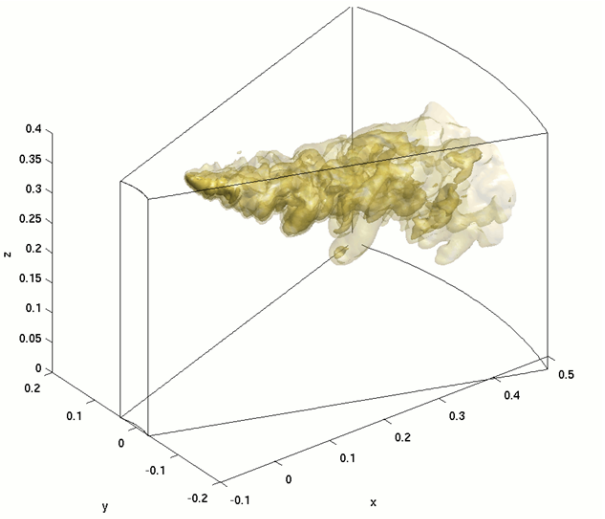

Figure 1: Large Eddy Simulation of a dredging plume. High resolution simulations are used to obtain better insights in the processes to simulate these complex flows on a more aggregated level. (source: Lynyrd de Wit, l.dewit@TUDelft.nl).

University of Twente

Department of Water Engineering & Management

INTRODUCTION

Since 1992, the University of Twente is providing a research and educational program in Civil Engineering, which aims at embedding (geo)physical and technical knowledge related to infrastructural systems into its societal and environmental context.

The department of Water Engineering and Management (WEM) is organised along two research themes: (1) Marine & Fluvial Systems and (2) Water Management. The former deals with fundamental research aimed at achieving a better grasp of the physical processes in surface water systems to support better management decisions. The latter focuses on comprehending the complex interactions between natural, socio-economic and policy processes relevant to the governance of water resources. A significant part of the research concerns shared issues, like diagnosing and dealing with uncertainties and handling different temporal and spatial scales in modelling and management.

The theme of Marine & Fluvial Systems deals with natural processes and human intervention. Both fundamental scientific questions are addressed as well as the exploration of options for management of these systems. Regarding marine systems, we investigate the natural morphodynamic processes and how they interfere with large-scale human activities at sea and in the coastal zone.

MISSION AND AMBITION

The mission of the Water Engineering & Management department is to carry out research and provide education in the areas of water systems and management. Our aim is to increase our understanding of the natural processes in water systems and the socio-economic processes that affect these systems, and to develop tools to support the management of rivers, river basins, seas and coastal zones. The key vision of the group is that water-related problems – all vitally relevant to society, by their nature – such as flooding, tsunamis, water scarcity, pollution and ecological deterioration, can only be solved through a multi-disciplinary approach, involving both knowledge of engineering science and expertise from the natural, social and policy sciences.

RESEARCH HIGHLIGHTS

Regarding marine systems, WEM identifies five research lines, which will be outlined below.

Marine morphodynamics, seabed patterns

The complexity of the morphodynamics of shallow shelf seas is expressed e.g. by the occurrence of tidal sandbanks and sandwaves (Figure 1). These large-scale patterns are dynamic and play a crucial role in the conflicts between economical activities (sand extraction, navigation, pipelines, wind farms) and other interests (coastal safety, ecology). Sustainable sea use requires an adequate understanding of large-scale pattern dynamics.

WEM develops idealized process-based hydrodynamic (Figure 2) and morphodynamic models (Figure 3) and geostatistical data analysis techniques. Primary aim is to understand the physical processes, related to both autonomous dynamics and the response to human intervention. These studies are/have been carried out within European projects (e.g., PACE, HUMOR), NWO-innovation schemes (VICI, VENI) and other STW-projects.

Nearshore sediment transport processes

Understanding the complex hydrodynamic and sediment transport processes of the nearshore zone is both scientifically challenging and practically relevant. Particularly the cross-shore sediment fluxes are greatly influenced by the detailed characteristics of the wave motion, the seabed and sediment. At the same time, cross-shore sediment transport is a crucial factor in the sediment balance of the coastal system and thus crucial for developing efficient shore nourishment strategies.

WEM investigates sediment transport under waves (influence of wave asymmetry and skewness) in different regimes, e.g. ripples (Figure 4) and sheet flow (Figure 5). This is done using both experimental and process-based modeling techniques. This research has taken place in EU-funded projects (SANDPIT) and in the Dutch-UK project SANTOSS (funded by STW-EPSRC). To develop an improved sand transport model for the nearshore zone, a new STW-EPSRC project “Sand transport under irregular and breaking wave conditions” will focus on the roles of irregular waves and breaking waves.

Biogeomorphology

The study of the dynamic interaction between morphodynamics and biology/ecology is a recent development. WEM investigates this in various environments: estuaries, seas and the coastal zone (Figure 6). These studies link to recent research programmes such as Building with Nature.

Dune and beach dynamics

Sandy shorelines along inhabited coasts are usually subject to coastal management intervention. WEM investigates the long-term morphodynamics of dunes and beaches in response to these interventions (Figure 7). Furthermore, to obtain long time series of coastal evolution, WEM contributes to the development of video-based monitoring techniques (Figure 8).

Policy processes in coastal management

Coastal management problems are embedded in a natural and social system characterized by complexities, leading to uncertain decision making processes. WEM investigates the interplay of specialist knowledge and actors’ perceptions in these processes, aimed at improving societal embedding of coastal management.

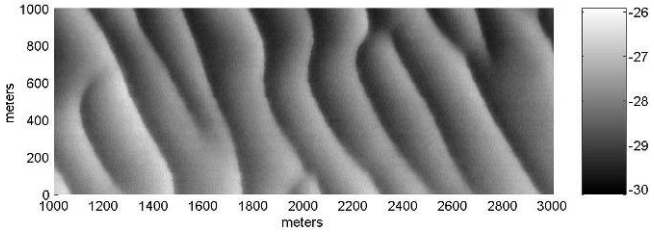

Figure 1. Bathymetric chart of tidal sandwaves in the North Sea, showing bed level in m below MSL (image courtesy A.A. Németh).

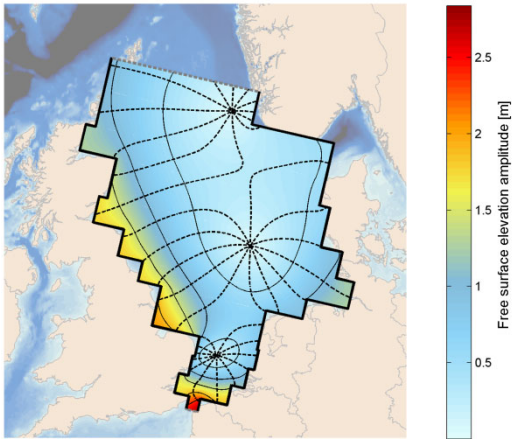

Figure 2. M2-amphidromic system in the North Sea as reproduced with an idealized tidal model (image courtesy J.J. Velema).

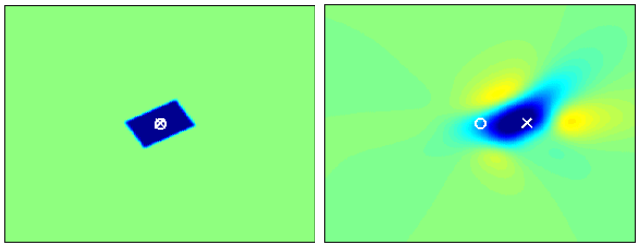

Figure 3. Long-term evolution of a large-scale sand pit (blue) in a tide-dominated offshore environment. Model results showing gradual deformation and migration (image courtesy P.C. Roos).

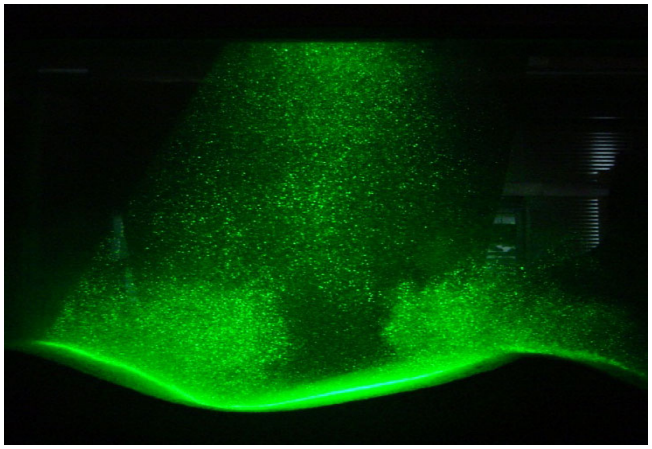

Figure 4. Laser illumination of suspended sediment particles above vortex ripples in an oscillatory flow tunnel (photograph courtesy J.J. van der Werf).

Figure 5. Flume experiments of sheet flow under breaking waves (photograph courtesy J.L.M. Schretlen).

Figure 6. Mangrove forest affecting intertidal hydro- and morphodynamics (photograph courtesy E.M. Horstman).

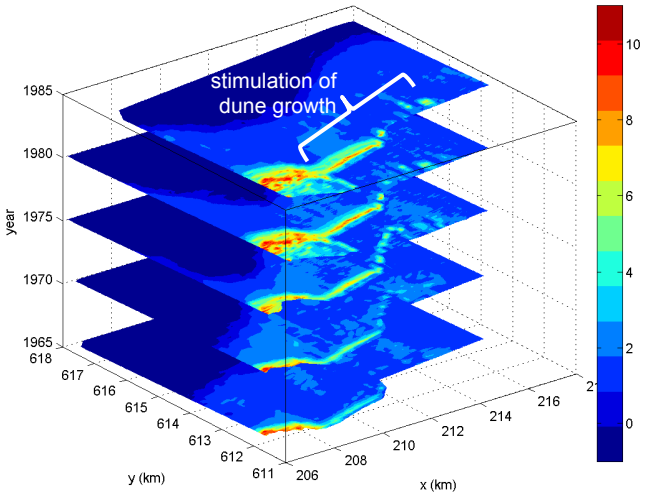

Figure 7. Beach and dune evolution at Schiermonnikoog (1965-1985; image courtesy L.M. Bochev-van den Burgh).

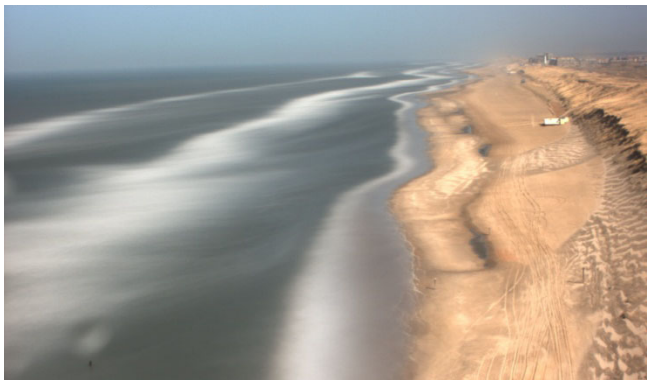

Figure 8. Argus video time exposure image of Egmond beach (source: http://cil-www.oce.orst.edu/).

University of Utrecht

Institute for Marine and Atmospheric Research Utrecht (IMAU)

ABOUT IMAU

Utrecht University, founded in 1636 is one of the older Universities in Europe. With more than 28.000 students, 8000 staff and 650 full-time professors it also is the largest University in the Netherlands. The University has always focused strongly on research and in 2010, for example, 468 candidates received a PhD degree from Utrecht University.

The coastal research group at the IMAU is divided over two departments: the department of physics and astronomy at the faculty of Science and the department of physical geography at the faculty of Geosciences. Our main aim is to increase the fundamental understanding of the hydrodynamic and morphologic behavior of sedimentary coastal environments, including shallow shelf seas and the shoreface. The research approach is based on a combination of research methodologies that are highly complementary and comprise the collection and analysis of new field data, the development and analysis of both process-oriented numerical models as well as idealized mathematical models and the implementation and application of Data-Model Integration (DMI) techniques. The research is carried out in strong cooperation with national and international research partners. Beneath we show several examples of research that has been carried out in recent years and an outlook to the coming years.

EXAMPLES OF RESEARCH PROJECTS

Dynamics of subtidal sand bars

In co-operation with Deltares and Unesco-IHE, we developed a fully coupled, wave-averaged cross-shore process model that can accurately predict both offshore and onshore migration of subtidal sandbars during periods of high waves and intermediate lower waves. Consistent with field observations, the simulated offshore bar migration takes place during storms when large waves break on the bar and is due to the feedback between waves, undertow, suspended sediment transport, and the sandbar. Simulated onshore bar migration is predicted for energetic, weakly to non-breaking conditions and is due to the feedback between near-bed wave skewness, bedload transport, and the sandbar. The model also shows considerable skill in predicting the multi-year sandbar migration, with the strength of the breaking-induced alongshore current playing an interestingly large role in the growth and subsequent decay of a sandbar as it progresses offshore. The evolution of the intertidal beach is still poorly predicted, which has stimulated considerable field efforts to understand sand transport under breaking waves in water depths less than 2 m (see Figure 1). In addition to their cross-shore motion, subtidal sandbars can also change in plan-view shape. Remotely sensed video (Argus) images of the nearshore have, for example, highlighted that crescentic subtidal sandbars continuously change their wavelength due to splitting or merging of individual crescents in response to the inevitable time-varying offshore wave-forcing. Furthermore, alongshore inner-sandbar variability can be remarkably similar to outer-bar variability, indicating some sort of coupled behavior. Non-linear models are now used to test hypotheses underlying merging-splitting and morphological coupling.

Figure 1. Measurement array to study turbulence and sediment suspension in breaking wave conditions.

Shoreface-connected sand ridges

An active line of research is on the dynamics of shoreface-connected sand ridges (hereafter sfcr) on the inner shelf. These bedforms are found in depths of 10-20 m and they occur in patches. Each patch consists of 5-10 ridges, which are about 5 km spaced apart, several meters high and which migrate several meters per year along the coast. These ridges form due to positive feedbacks between a storm-driven flow, waves and the sandy

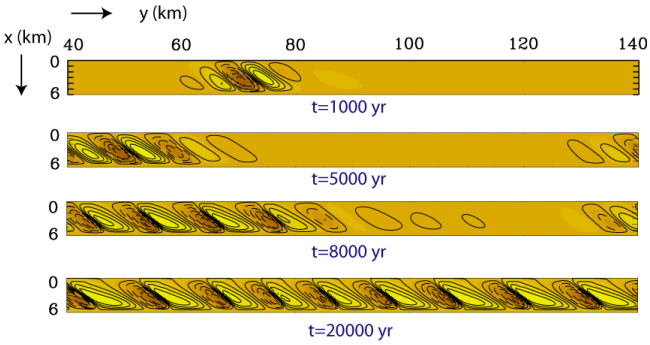

Figure 2. Bottom pattern (light: crests, dark: troughs) at different times. In each panel the coast is at the top. The ridges migrate alongshore in the direction of the storm-driven flow (negative y direction). Patch behaviour is observed up to 8000 years after initial formation.

bottom of the shelf. An important finding of recent years was that the patch behavior of sfcr was modeled and explained for the first time (see Fig. 2). This was done by extending a model, which simulates the finite-amplitude evolution of sand ridges, such that it accounted for wave shoaling and wave refraction processes. The model results suggest that patch behavior is a transient phenomenon, and thus observed sfcr are still in their developing stage.

Another highlight of this project concerned the modeling and interpretation of the distribution of mean grain size and sorting over sfcr. It was found that, in the case of a sediment mixture, the finest grains are found slightly upcurrent of the crests. The mechanisms responsible for this pattern are the positive feedbacks between the evolving ridges and the waves (which stir sediment from the bottom), enhanced erosion of sediment if the bed surface gets rougher, and hiding processes. The latter account for the fact that fine grains are less exposed to fluid stress than coarse grains, which reduces their entrainment into the water.

Dynamics of estuarine channels and channel networks

Our knowledge on the dynamics of estuarine channel networks is still very limited. In recent years a large project has been dedicated to the dynamics of the shelf and estuarine channel network of the Berau, Kalimantan, Indonesia. Based on field data and the results obtained by numerical models we were able to explore the processes that drive transport of water in a channel network. Tides transport water in an upstream direction by covariation of water levels and velocity (Stokes transport), while water is carried downstream by mean Eulerian currents. While in a single channel estuary the Stokes transport is exactly balanced by an Eulerian transport, in channel networks this is in general not the case. Water that is transported landward in one channel can be transported seaward in another one. Geometric differences between the channels and the relative importance of tides over river discharge determine the distribution of water over the network.

The morphodynamic evolution of the estuarine channel network is strongly influenced by the exchange of sediment at the junctions. We obtained field data that clearly reveal how the interaction of tides, freshwater and local bathymetry and geometry result in very intricate flow patterns and how this affects the exchange of suspended sediment between the channels that join at the junction. In the near future we will further explore how these sediment transport processes influence the dynamics of an ETM and the morphodynamic evolution the entire network. The results will be applied to the Yangtze and Pearl river estuary in China and the Rotterdam Rijnmond area in the Netherlands.

Mosselwad

Mussel beds are important biogenic structures in the intertidal and subtidal environment of the (Dutch) Wadden Sea. They are partly able to stabilize the substrate of the Wadden Sea, to improve the water quality, to establish important habitats for many (benthic) species and to provide food for water birds and other organisms. Mussel beds also represent characteristic and scenic landscape units in an area of outstanding natural beauty: since June 2009, the Wadden Sea has been recognized as an important new UNESCO World Heritage Site. In the Wadden Sea though, the area covered by stable mussel beds demonstrates a large variability from year to year and from location to location, in particular in the Western Wadden Sea. One can only speculate about the reasons and, so far different explanations have been offered. In general the stability of mussel beds is determined by a range of physical and ecological processes and conditions. The interdisciplinary research programme MOSSELWAD will be testing a number of hypothesis for the (lack of) stability of mussel beds and will consider aspects such as coverage, density and predation. The coastal research group of Utrecht University will focus on the physical/hydrodynamic processes and conditions that can play a decisive role in the development of stable mussel beds. In particular the study is initiated to: (1)Determine the effect of waves, in combination with wind and tides in eroding mussel beds; (2) Establish the hydrodynamic boundary conditions for the settlement and stable development of mussel beds; (3) Evaluate the effect of mussel bed patterns in relation to stability; (4)Understand the musselbed-sediment interactions, both in terms of erosion (resuspension of suspended matter) and biodeposition.

Based on a first field experiment near Texel we concluded that waves can cause erosion of mussel beds. The largest waves came from easterly directions due to limitations in wind fetch for the other directions. At the mussel bed waves did not break but lost their energy mainly due to the strong bottom friction above the very rough mussels. The strong correlation between the contour of the mussel-bed and the areas that experienced largest shear stresses suggest a strong relation between wave forcing and mussel bed survival. This hypothesis will be further tested in coming years.

TO CONCLUDE

We have described several examples of research that has been carried out at the Utrecht University. There are lines of research that were not highlighted in this text. Further information on these projects, the measurement techniques being used and the models being developed and applied can be found at www.coastalresearch.nl and at www.imau.nl.

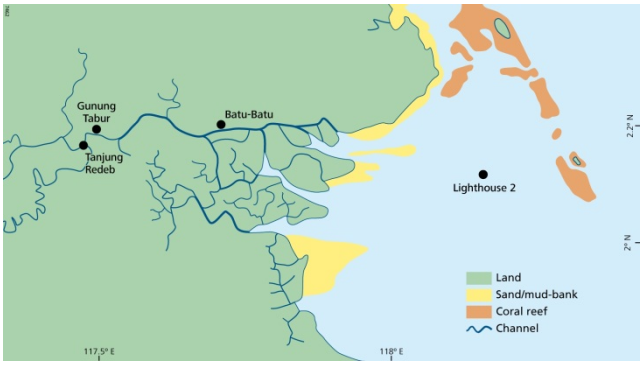

Figure 3. Map of the Berau shelf and estuarine channel network in Indonesia. At Tanjung Redeb two rivers join to form the Berau river that splits close to Batu-Batu in an estuarine channel network. The shelf hosts large areas of coral reefs.

UNESCO-IHE Institute for Water Education

Chair Group of Coastal Systems and Engineering & Port Development

UNESCO-IHE

UNESCO-IHE is the largest international postgraduate water education facility in the world. It is established as a UNESCO 'Category I' institute operating under direct responsibility of UNESCO.

The Institute confers fully accredited Masters of Science degrees and promotes PhDs. Since 1957 the Institute has provided postgraduate education to more than 14,500 water professionals from over 160 countries, the vast majority from the developing world.

Over 130 PhD fellows are currently enrolled in water-related research and numerous research and capacity development projects are carried out throughout the world.

Mission and vision

UNESCO-IHE envisions a world in which people manage their water and environmental resources in a sustainable manner, and in which all sectors of society particularly the poor, can enjoy the benefits of basic services. Our mission is to contribute to the education and training of professionals and to build the capacity of sector organizations, knowledge centers and other institutions active in the fields of water, the environment and infrastructure, in developing countries and countries in transition.

UNESCO-IHE centers its education, research and capacity development programmes around Water Security, Environmental Integrity, Urbanisation, Water Management and Governance, Information and Communication Systems, as well as in the emerging areas of Conflict Management and Climate Adaptation. Through each of these themes, the Institute addresses the major issues and challenges faced by many developing countries and countries in transition.

Core Activities

- *Education, Training and Research* for water sector professionals, engineers, scientists, consultants and decision makers working in the water, environment and infrastructure sectors.
- *Water Sector Capacity Development* for water sector ministries and departments, municipalities, water boards and water utilities, universities, training and research institutes, industries, non-governmental and private sector organizations, particularly in developing countries and countries in transition.
- *Partnership Building and Networking* for knowledge centers, public and private sector organizations worldwide.
- *Global Policy Forum on Water and Environment* involving UNESCO Member States, National Committees of the International Hydrological Programme, World Water Council and many other stakeholders.
- *Standard Setting for Education and Training* for water-related academies, universities, and other education and training agencies in the water sector.

Education and Training

UNESCO-IHE offers a wide range of accredited educational programmes, tailor-made training & online training courses for

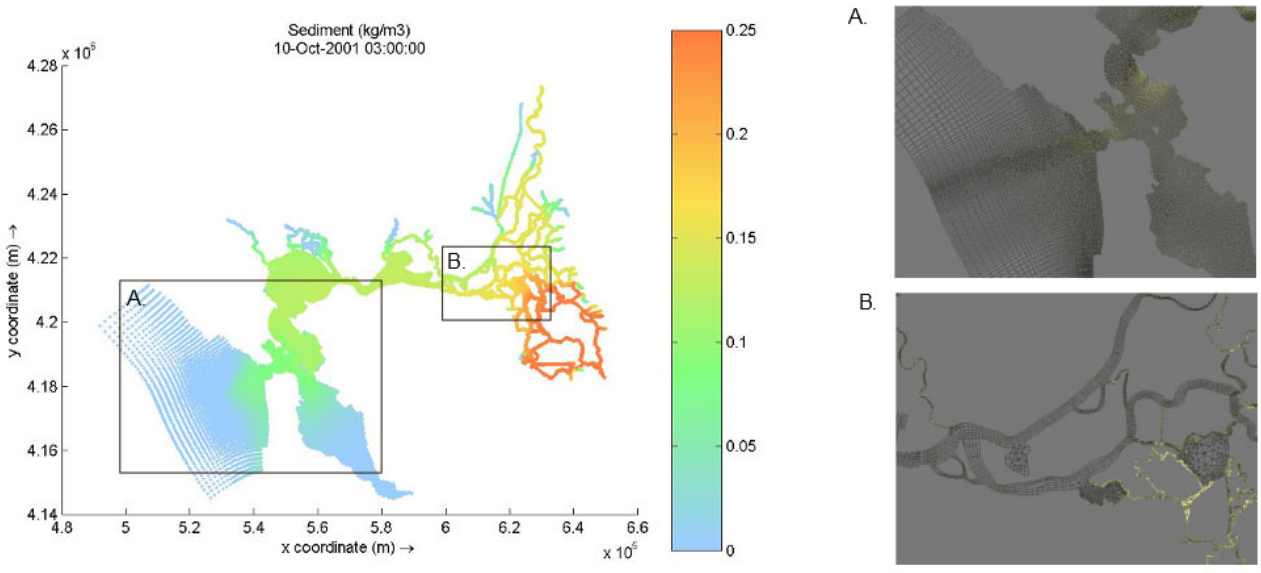

Figure 1. Sediment concentration (kg/m^3) in the San Francisco Bay Area for the wet period (winter). In detail the grid generated in DFlow for the coastal area and delta

engineers, scientists and managers working in the water, environment and infrastructure sectors. UNESCO-IHE is implementing its educational activities increasingly with partner institutes, making water education more accessible and affordable for an increasing numbers of students.

Research

Research is a vital component of UNESCO-IHE's mission. The Institute's research activities focus on and contribute to the knowledge base concerning the water environment, and therefore complement its education and capacity development activities. One of the Institute's main assets is its ties to the developing world. These links provide an excellent opportunity to perform an almost constant reality check, since water issues that developing countries face require new and innovative solutions.

Capacity Building

UNESCO-IHE provides capacity development services to knowledge institutes and water sector organizations around the world. Through these operations, the Institute increases its global impact and helps to build sustainable organizations that are equipped to properly manage water resources and deliver water services to all communities. Services include institutional development projects, tailor-made training and policy advice.

Alumni

UNESCO-IHE encourages its 14,500 alumni community members from over 160 countries to actively engage in knowledge and information exchange. Alumni reach senior positions in their home countries and become nationally and internationally recognized experts in their fields of expertise. Many have made significant contributions to the development of the water and environmental sectors. UNESCO-IHE alumni have access to and remain part of a global network, consisting of alumni, guest lecturers, experts and renowned centers of knowledge, together providing a vast source of expertise available to the sector.

CHAIR GROUP OF COASTAL SYSTEMS AND ENGINEERING & PORT DEVELOPMENT

The Chair Group of Coastal Systems and Engineering & Port Development is part of the Department of Water Science and Engineering of UNESCO-IHE. The group currently counts 2 professors, 1 assistant professor, 1 senior lecturer, 3 lecturers and 12 PhD students. It is responsible for the MSc programme of Water Science and Engineering - specialization Coastal Engineering and Port Development.

Research

The research conducted within the group mainly focuses on four aspects:

- Integrated modeling of coastal processes and evolution;
- Performance and reliability of flood defense systems;
- Port development;
- Port-related hydrodynamic and morphological modeling.

Integrated modeling of coastal processes and evolution

The objective of this research line is to develop knowledge and modeling tools to predict hydrodynamic and morphological phenomena in the coastal zone, as a result of natural processes and human interference, directly and through climate change impacts. The focus is on improving long-term predictions of coastal morphology via process based, scale aggregated and probabilistic modeling and on developing open-source software for predicting coastal behavior, at various spatio-temporal scales (Figure 1, Figure 2).

Performance and reliability of flood defense systems

Here the objective is to improve the understanding, models and techniques for the performance of coastal structures under variety of loading conditions and of flood defense systems including natural and man-made defenses. This includes the assessment of flooding risks under climate change conditions, and research to estimate socio-economically viable setback lines.

Port development

The research in the field of port development concentrates on ship traffic modeling, design of port master plans and expansion plans, including adaptive port planning.

Port-related hydrodynamic and morphological modeling

Topics include the influence of port extensions on coastal processes, solutions to harbor siltation problems and wave penetration studies.

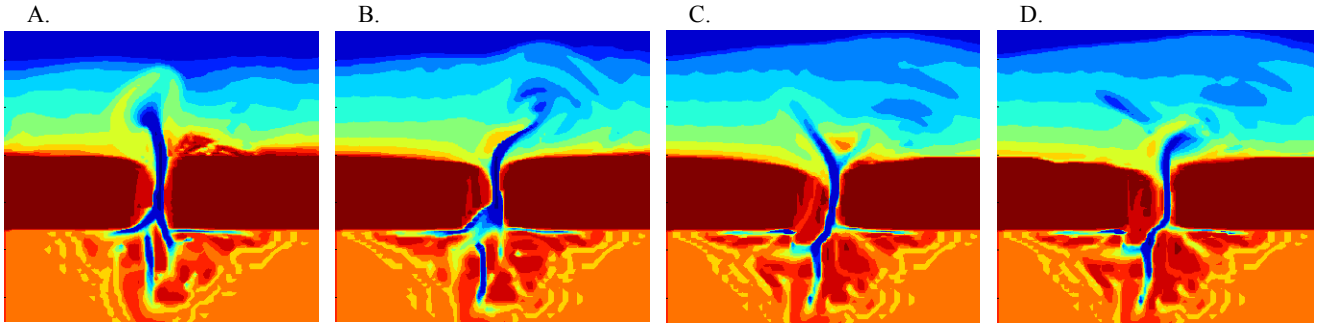

Figure 2. The cyclic behavior of the tidal inlet system in a wave dominated regime, simulated by a process based model. A. Evolution after 10 years; B. After 23 years; C. After 30 years; D. After 33 years.

Rijkswaterstaat

INTRODUCTION

Rijkswaterstaat is responsible for the construction, management and maintenance of the Dutch water system and for everything needed to control it properly: dunes, dams and storm surge barriers and some of the dikes, river dams and river banks. Rijkswaterstaat coordinates, manages and gives guidance. This is done with the assistance of the private-sector parties responsible for executing projects and in partnership with water authorities, municipalities, provinces and other stakeholders.

The Netherlands abounds in water, with major rivers, canals, the IJsselmeer region, the Southwest Delta, the North Sea and the Wadden Sea. Rijkswaterstaat works to keep people's feet dry and to ensure a sufficient supply of clean water.

DUTCH POLICY

The aim of government policy in 2010 was to get and keep the main water system up to standard at a cost acceptable to the public. In September 2010 the Delta Programme was presented to the House of Representatives. The programme contains the proposed decisions necessary to ensure water safety and freshwater supplies up to 2015, together with the measures needed for subsequent years. The new Water Act came into force in December 2009. It aims for an integrated, uniform, efficient and public-oriented approach to our work in this area. It will therefore impact on how Rijkswaterstaat issues permits and enforces their terms. The National Water Plan for 2009-2015 forms the main basis for Rijkswaterstaat's current activities.

ORGANISATION OF PRIMARY FLOOD DEFENSES

Rijkswaterstaat's main concern is to ensure strong primary flood defences: dunes, weirs, dams, dikes and large engineering structures such as the storm surge barrier in the Eastern Scheldt and the Barrier Dam (the Afsluitdijk). The water authorities and Rijkswaterstaat work towards a flood protection standard for the coastal areas of the Netherlands of 1:4000 and 1:10.000 for the Randstad. To reach some of these goals, Rijkswaterstaat works on:

- the *Storm Surge Warning Service*. This service provides the necessary information during high water such as water levels, information about the consequences of flooding, and measures to reduce the damage.

- *National Flood Risk Assessments* (VNK). This project maps the current flood risks using innovative methods. The risk of flooding is coupled with the flood consequences, which are expressed in economic impact and the amount of victims.

- (besides the water authorities) testing whether the primary flood defences are up to legal standards. This test is obliged every five years according to the Water Act. The test results are the basis for reinforcements that can be taken on and prioritized in the *High-Water Protection Programme* (HWBP).

- the programme *Strength of and Hydraulic Load on Water Defences* (SBW). In this program the strength of the water defense and the hydraulic loading are studied. The results of this program determine the previously described test criteria.

- the secretarial office of the Expert Group Water Safety (*Expertise Netwerk Waterveiligheid* - ENW). ENW Works on knowledge development related to flood defenses.

COASTAL MAINTENANCE

The Dutch coast is 340 km long and protects our country from the sea. Sand nourishments are essential to maintain the coastline. There are three types of nourishments; beach, shoreface and channel wall nourishments. Rijkswaterstaat is responsible for maintaining the coastline at the 1990 level, i.e. the basic coastline. Annually we supply the coast with a total of 12 million cubic meters of sand, either offshore or on the beaches at locations where erosion has taken place.

RESEARCH AND DEVELOPMENT

Rijkswaterstaat investigates new coastal nourishment methods, such as the *Sand Motor*, the *channel wall nourishments* and the *differentiated shoreface nourishment*, explained below. Besides these innovative developments there is the regular research programme *Knowledge for Primary Processes - Coastal Management and Maintenance* (KPP), commissioned by Rijkswatertstaat and executed by Deltares.

Figure 1. Shore Face Nourishment.

Figure 2. Sand Motor Ter Heijde.

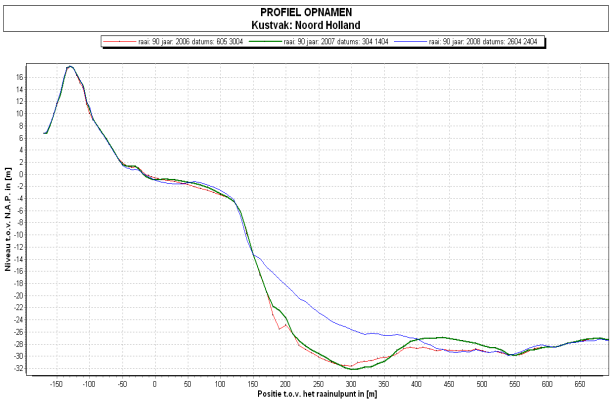

Figure 3. Channel wall nourishment in Den Helder.

The Sand Motor involves depositing 21.5 million cubic meters of sand off the coast of Ter Heijde. The idea is that wind, waves and sea currents will gradually spread the sand along the coast of South Holland, allowing natural growth of the coast. This way, the project will contribute to coastal safety and create more space for nature and recreation. The project will generate new knowledge on building with nature's help and whether this nourishment strategy is cost-effective.

There is one type of erosion that cannot be compensated for: erosion due to the movement of tidal channels. Therefore, to reduce channel migration, channel wall nourishments have been introduced. The first nourishment of this type was executed in 2005 in the province of Zeeland, followed by channel wall nourishments in Den Helder, Walcheren en Zeeuws Vlaanderen in the years after.

The differentiated shoreface nourishment of Heemskerk is another innovative nourishment, where the sand is deposited at different locations. Based on prior modeling research, the differentiated shoreface nourishment appears to create faster and larger sand accretion caused by enhanced local hydraulics and sand transport, especially around the heads of the nourishments. Heemskerk is considered a good and safe location to test this theory. Therefore the nourishment of Heemskerk consists of two separate nourishments (one at -5 m NAP and one at -6 m NAP) with a gap in between to increase the number of heads. The nourishment will be extensively monitored to test the model results.

As mentioned above Deltares has been commissioned by Rijkswaterstaat - Waterdienst to develop the knowledge needed to carry out an effective nourishment strategy (spatially and temporally). Deltares organized the KPP in a number of sub-projects. In order to link the project results to the actual nourishment practice of Rijkswaterstaat, the subprojects focus on the validation of a number of hypotheses on which the present nourishment strategy is based. *State of the Coast*, the *Functionality of the Coastal Foundation and the Redistribution of Nourished Sediment* and the *Exchange of the Tidal Basins and the Mophodynamics of the Wadden Islands*, are some examples of the sub-projects within this multi-year program. For example in the *State of the Coast* the impact of nourishments are identified for a number of indicators along the Dutch coast. Learned lessons from the past are further used to improve future nourishment strategies. Moreover, there is the sub-project *Ecologic Design of Nourishments* (*Ecologisch Gericht Suppleren*) that focus on the effects of nourishments on, primarily, the ecological and the related physical system.

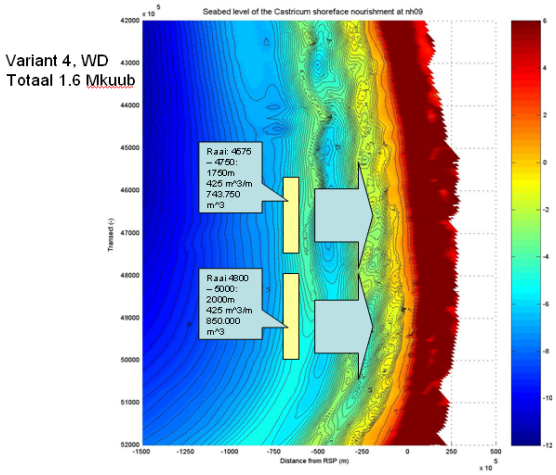

Figure 4. Differentiated shoreface nourishment Heemskerk.

Deltares

ABOUT DELTARES

Deltares (www.deltares.nl) is a leading independent research and internationally operating specialist consultancy institute (not-for-profit) for water and subsurface issues with its base in the Netherlands, employing some 800 water and subsurface experts. Throughout the world, our advanced expertise enables safe, clean and sustainable living in deltas, coastal areas and river basins. With this goal in mind, we develop knowledge, innovative products and services, pool our knowledge with others, and make the results available. We advise governments and the private sector, and use our expertise to make sound and independent assessments of the physical condition of deltas, coastal areas and river basins.

In 2007, Delft Hydraulics fully merged into Deltares, together with GeoDelft, the Soil and Groundwater department of TNO and research departments of the Dutch Department of Public Works, Transport and Water Management. Through the combination of the former institutes, we have excellent resources of appropriate expertise based on more than 300 years of experience.

In supporting public authorities, private parties and society, Deltares acts as:

- research and development centre,
- knowledge broker,
- knowledge and information centre,
- specialist advisor and
- assessor and analyst.

Our range of roles can be seen in our work throughout the world. Our consultancy work picks up where others leave off, often in the exploratory stages of a project, with independent advice using the latest advances. We extend our knowledge base in government research programmes and contract research for contractors and the engineering sector, teaming up with universities and other research institutions along the way. In the process, we encourage innovations, and speed up the pathway making new advances available for application in practice.

To live and work comfortably and safely in the narrow confines of coastal areas and river basins, local residents need smart approaches to the subsurface and the water systems. Deltares supplies answers to social issues by combining technical expertise with an understanding of political, administrative and economic processes. This interdisciplinary approach, our independent position, and our role as an authority with a reputation for integrity mean we can get pro-actively involved in public debate, implementing our strategic principle: ‘Enabling Delta Life’.

Water and the subsurface involve not only technological issues, but also natural processes, spatial planning and administrative and legal processes. We apply our understanding of those processes in an integrated way, improving the quality of life in deltas, coastal areas and river basins. The integrated approach allows us to come up with innovative solutions.

MARINE AND COASTAL SYSTEMS

By understanding how coasts and seas work as a system, we can make the most of natural processes in planning and management. This means building with nature, sustainable hydraulic engineering projects in coastal areas and smart coastal maintenance making the most of natural forces. Deltares expertise about the effect of weather conditions on natural processes, coastal defences and hydraulic engineering ranges from everyday conditions to extreme events like storm tides, tsunamis and hurricanes.

Deltares supports policy and management for coastal zones (for example with Integrated Coastal Zone Management). The areas we work in cover climate change or the impact of measures for protecting water and ground quality. We have integrated our knowledge of ecosystems in models that are used to implement European initiatives such as the Water and Marine Strategy Framework Directives.

We also help government authorities tackle pollution and disaster management more effectively. We develop prediction systems for early warnings and to advise on public works. The potential of the physical system has to be managed so that large numbers of people can live and work close to the sea without too much impact on natural processes. Deltares provides consultancy services for hydraulic engineering projects that make this possible. We work on coastal protection, recreation, energy supplies and transportation infrastructure.

IMARES Wageningen UR

INTRODUCTION

IMARES is the Institute for Marine Resources and Ecosystem Studies. A leading, independent research institute that concentrates on research into strategic and applied marine ecology.

We carry out scientific support to policies (50%), strategic RTD programmes (30%) and contract research for private, public and NGO partners (20%). Our key focal research areas cover ecology, environmental conservation and protection, fisheries, aquaculture, ecosystem based economy, coastal zone management and marine governance.

IMARES primarily focuses on the North Sea, the Wadden Sea and the Dutch Delta region. It is also involved in research in coastal zones, polar regions and marine tropical areas throughout the world and in specific fresh water research.

IMARES has some 235 people active in field surveys, experimental studies, from laboratory to mesocosm scale, modelling and assessment, scientific advice and consultancy. Our work is supported by state-of-the-art in-house facilities that include specialist marine analysis and quality labs, outdoor mesocoms, specific field-sampling devices, databases and models. The IMARES quality system is ISO 9001 certified.

We collaborate with fellow research specialists, about 20% of our research is contracted to partner institutes in the Netherlands and abroad. Our research is regularly published in international peer reviewed publications. As part of Wageningen UR, IMARES has close ties with Wageningen University and the Van Hall Larenstein University of Applied Sciences. Both universities cater for Bachelor, professional Master and academic Master education programmes. The institute runs a PhD programme together with Wageningen University.

FACTS AND FIGURES

- Annual turnover of € 30 Million
- 235 employees
- 60 % has an academic degree
- 8 professors and 2 lectors
- 30 PhD students
- >120 (Scientific) publications annually
- Active in ICES, Ascobans and EFARO

PUBLICATIONS

In 2011 IMARES contributed to

- 26 publications in journals without impact factor.
- 56 publications in journals with an average impact factor of 2.32.

ORGANISATION

As per 1 January 2012 our organisation structure is as follows:

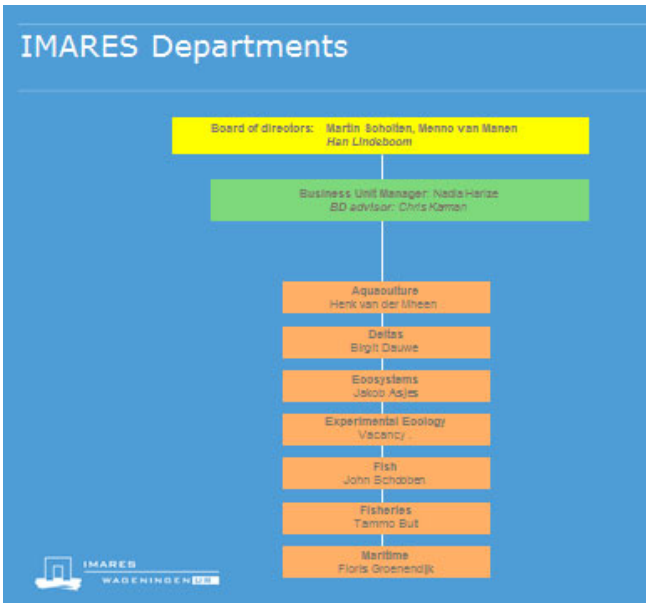

Figure 1. Organization structure of IMARES

IMARES AND COASTAL RESEARCH

Declining biodiversity, vanishing intertidal zones, problems with freshwater supply... The growth of the world population and rising sea levels are causing increased pressure on coastal ecosystems. Low-lying delta areas are most vulnerable to the effects of increasing urbanization and agriculture. IMARES, part of Wageningen UR (University & Research centre) has a leading role in the Building with Nature programme, which provides an innovative, sustainable and cost-effective method for intervention. The name of this initiative says it all: Natural processes are deployed as building blocks to solve ecological problems. A defining characteristic of the programme is that it is supported by a consortium of business, government and research institutions.

Projects

Our researchers often work on existing projects. One example is the Zandmotor (sand engine) off the Dutch coast, built by dredging companies Boskalis and Van Oord. This hook-shaped peninsula is comprised of 21.5 million cubic metres of sand, and

is designed for wind, waves and currents to spread the sand along the coast, causing it to expand in a natural way. This means better protection for the land, while natural habitats get more breathing space and biodiversity increases. Another example of a coastal protection project can be found in the Dutch province of Zeeland, where the construction of flood barriers in the Oosterschelde estuary is causing the tidal areas there to rapidly disappear. Researchers from IMARES are now investigating the possibilities to preserve and restore these areas by using a layer of dead oyster shells to create new, natural oyster beds. These subsequently stabilise the edges of the plateaus and counter erosion. The first test results are promising. Further north, work is underway at full speed on the construction of Maasvlakte 2, a major expansion of the Rotterdam port. The project involves the extraction of lots of sand off the shore, which is having negative consequences for the relevant ecosystems. Biodiversity and productivity can recover much better if, instead of leaving the sea floor flat after sand extraction, irregular terrain is artificially created. Another ongoing land reclamation project in Singapore is of a different nature: There, our researchers are looking at the governance aspects of marine projects. IMARES is also carrying out experiments in Singapore into the effects of water turbidity on coral reefs.

Excellent research facilities

Our researchers are real field workers who go out both to sea and on land to take measurements and calculations. IMARES also has at its disposal excellent research facilities, including chemical and biological laboratories. Our 'mesocosms,' tools which represent an intermediate stage between an aquarium and actual bodies of water, allow us to carry out reliable research in controlled conditions. Research subjects include the effect of toxic substances released into the environment and opportunities for the cultivation of seaweed for the needs of the offshore industry.

Broad-based innovations

The 'golden triangle' – i.e. a balanced combination of business, government and research institutions – has proven to be a highly effective form of cooperation and is being imitated worldwide. The defining characteristic of this concept is its process-oriented approach – the choice of stakeholders to involve in a project and the method of communication are clearly defined in the initial phase. This prevents situations in which solutions are implemented that later prove to be unfeasible, or in which processes are made ineffectual through repeated compromises. Building with Nature is a typically Dutch form of cooperation which leads to genuinely broad-based and ground-breaking innovations.

IMARES HIGHLIGHTS

IMARES highlights can be found in the dossiers on our website: http://www.imares.wur.nl/UK/research/dossiers/

- Sustainable development in the Arctic region
- Storing CO_2 in sub-seabed geological formations of the North Sea
- Plastic waste in the sea
- Eel and Eel Fishing in The Netherlands
- Seals in the Wadden Sea
- By-catch and beaching among porpoises
- Innovative fishing gear
- Antarctic research
- Fisheries research at sea
- Darwin's Beagle journey
- Research in the tropics – Caribbean Netherlands
- Marine Protected Areas in the coastal zone, North Sea and high seas
- Mauritania resource management
- Biodiversity research

Figure 2. IMARES studies human activities in sensitive areas.

Royal Netherlands Institute for Sea Research NIOZ

NCK-
past, present & future

Special contributions by:

- **J. Dronkers**
- **A.J.F. van der Spek**

NCK photo competition

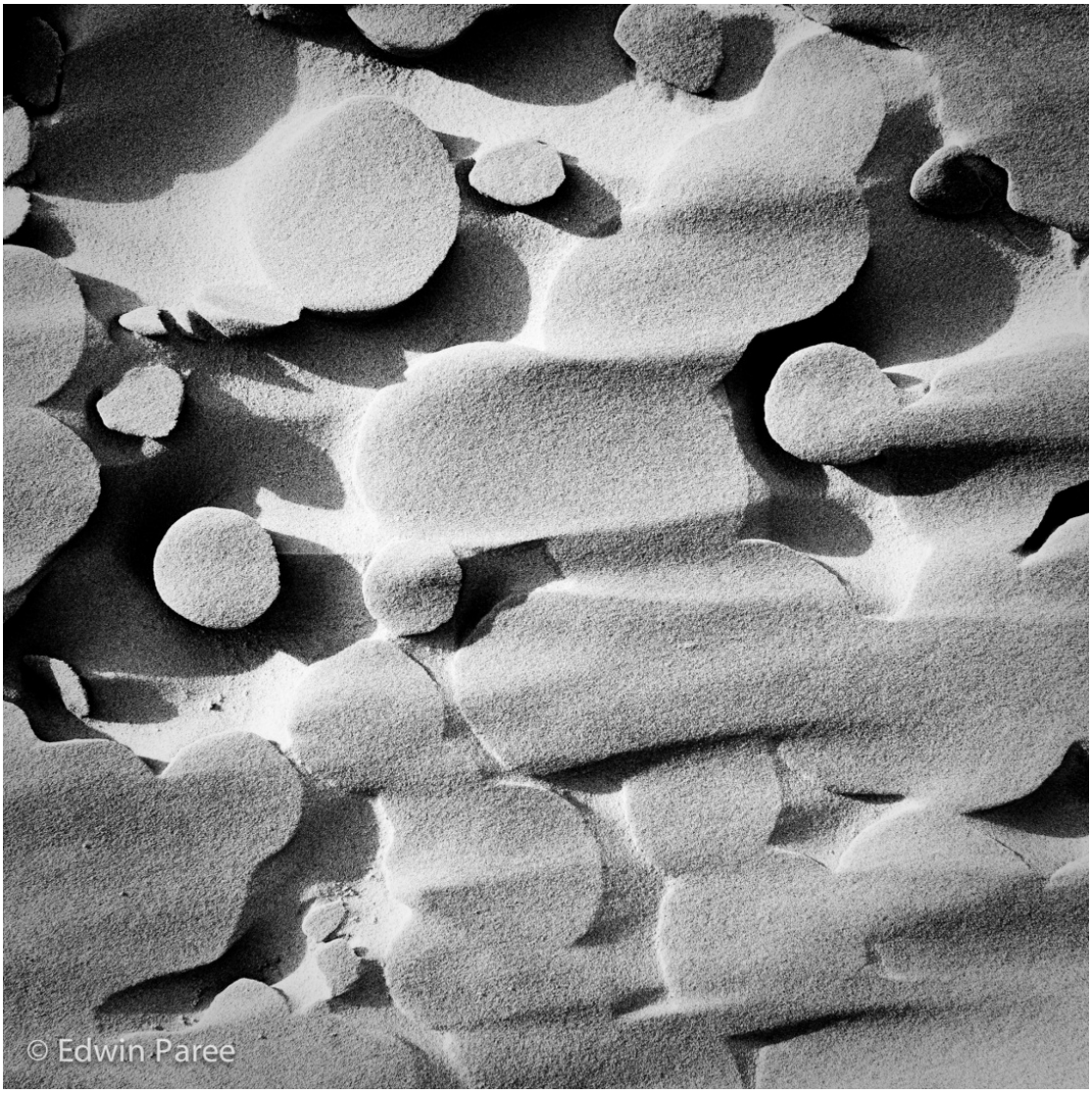

Edwin Paree: Terschelling

Jury: This puzzling picture makes you wonder how nature is able to make abstract art from sand. Sun heating and wind erosion led to a magnificent blend of almost perfect circular pillars contrasted with sharp edges. The photographer used floodlight to bring lively shadows in the details of the sandy surface, which is not flat but undulated.

DOI: 10.3990/2.166

Looking back on 20 years of NCK

J. Dronkers
Deltares, P.O. Box 177, 2600 MH, Delft, The Netherlands, Job.Dronkers@deltares.nl

I will be retiring this year. That is an additional reason for me to look back on 20 years of NCK. I see the NCK as one of the most significant initiatives in my discipline in which I was involved during my career. It brings me a sense of contentment that I could contribute to this initiative.

The NCK overlaps with a bloom in Dutch coastal research. That is due to the work of many. But in my experience, certain persons played a key role in that they provided innovative impulses to our coastal research. That I am highlighting them in my retrospective should not be interpreted as a denial of the significance of many others. Among these many others who I should perhaps have mentioned are colleagues in other countries who have enriched the discipline with insights that we have gratefully used in the Netherlands.

The NCK did not just happen overnight. We had the privilege of being able to build on a particularly bountiful inheritance. With that, I would like to start my retrospective.

– PRELUDE – A FEW IMPORTANT MILESTONES

When the storm surge barrier in the Eastern Scheldt became operational in 1986, people felt that the Netherlands had completed its battle against the sea. The vision of Johan van Veen, the spiritual father of the Delta Plan, had been realized. Although that dam in the Eastern Scheldt could have been a closed one, as far as he was concerned.

Johan van Veen was a visionary and, moreover, a tenacious go-getter, in spite of how modest he might appear to outsiders. One of his starting points was: In order to beat the enemy, you first have to get to know him well. In the 1930s, for example, he had investigated tidal currents in the North Sea so as to understand how they were influenced by seabed morphology. His PhD thesis of 1936 gives evidence of deep insight in physical oceanography. We could call Johan van Veen the first Dutch morphologist, but the term did not exist yet at the time. At Rijkswaterstaat (the executive arm of the Dutch Ministry of Infrastructure and the Environment), he had established the Algemene Studiedienst, where young engineers and a young mathematician – my father – were challenged to learn how to simulate hydrodynamic processes for major interventions in the coastline, after the example of the great physicist Hendrik Lorentz. Because already back then, long before the disastrous storm surge of 1953, Johan van Veen knew that the Netherlands needed a Delta Plan to remain safe from flooding.

But the battle against the sea had not been won yet after the construction of the Eastern Scheldt storm surge barrier. Calculations with the electrical simulator “Deltar” – also one of Van Veen’s brainchildren – showed that the lower river region was not yet sufficiently protected. The Deltar, an ingenious machine which heavily taxed The Hague’s electricity grid, soon was replaced by the first numerical mathematical models, however. They confirmed the precarious situation of the lower river region and offered the possibility of calculating various hydraulic engineering solutions. Eventually, this led to the design of the storm surge barrier in the New Waterway, which was finished in 1997.

Meanwhile, the way the Netherlands thought of its relationship with water had changed radically. The idea that we could win the fight against the water once and for all was replaced by the awareness that we had to deal differently with water. "Omgaan met Water" (Dealing with Water) was the title of a memorandum written by a team of young scientists, led by Henk Saeijs, in 1985. Henk Saeijs, a former plantation manager in Sumatra in the 1950s, studied biology in Wageningen upon his return to the Netherlands. He was driven, a goldmine of ideas, and a charismatic inspirer. As head of the environmental department of Rijkswaterstaat in Middelburg, he was closely involved in the Eastern Scheldt studies. It gave him the insight that technological solutions alone cannot provide definite answers for water problems facing the Netherlands. The ideas of Saeijs can be seen as the first pointers toward the concept of “Building with Nature”, which the NCK later shaped. But Omgaan met Water went further, as it did not only incorporate natural processes, but also offered a home to societal processes in solving water problems. Omgaan met Water was the overture to Integral Water Management and also a source of inspiration for Integrated Coastal Management.

At that same environmental department, which was initially located in ’s Heer-Arendskerke, the first steps on the road to morphodynamics were taken at the start of the 1970s. Joost Terwindt had been appointed to study the effects of the constructions in the Eastern Scheldt on the development of the salt marshes and shoals. An important question that had to be answered first was: In which conditions do salt marshes and shoals develop? The research was carried out by a team of young physical geographers, led by Luc Kohsiek. Luc Kohsiek, currently dike warden in the Province of Noord-Holland and previously substitute Director-General at Rijkswaterstaat, is a tawny and confident guy, with a special talent for pinpointing the essence of complex matters and translating them into appealing images. The result of the investigation was a bit of a jolt for the builders of storm surge barrier. The new concept of "zandhonger" – sand demand – entered the stage: The salt marshes and shoals were doomed to disappear over time as a result of the construction of the barrier and the compartmentalization dams. This tough lesson also contributed toward readying people’s mind for the notion of “Building with Nature”.

Some others had started even earlier to venture into the area of morphodynamics. While working on his PhD in the 1950s, Henk Postma, geochemist at the NIOZ (Royal Netherlands Institute for Sea Research) on Texel, became puzzled by the phenomenon of

shoal accretion in the Wadden Sea. He came up with the ingenious mechanism of settling lag, the lagging of resuspension after sedimentation, which explains how net transport is possible in an oscillating flow. It was not until decades later that it became clear how important the non-linearity of transport processes is for the morphodynamics of tidal basins. Later, Henk Postma would inspire many young scientists to unravel more details of the processes of self-organization in tidal systems, when he was director of NIOZ. The work done in this area by Sjef Zimmerman and his own students after him, including Huib de Swart, is globally seen as ground-breaking. Not surprisingly, the field of morphodynamics became one of the main pillars of the NCK's research.

After the flood disaster of 1953, the focus had shifted away from the dune coast. After all, the dune coast had shouldered the storm. Still, the dune coast was not doing very well in many locations. One engineer at Rijkswaterstaat had already put his teeth into the issue, T. Edelman. In those days, engineers hardly ever wrote scientific publications and Edelman adhered to that tradition. His work therefore is not very well known, but no less important. Edelman noticed how strongly coastal profiles fluctuate from year to year, as well as seasonally. Periods of strong erosion, during storms, alternate with periods of coastal accretion, in calm conditions, while long-term trends hide behind these fluctuations. He did not only see these processes through the glasses of the engineer, but also through the glasses of the geologist who looks for connections at greater spatial and temporal scales. He realized that long systematic series of measurements were paramount, in this respect. It is notably due to him that that Rijkswaterstaat started its annual coastal measurements in 1964. All Dutch coastal morphologists as well as the NCK owe Edelman for having been the instigator of the JARKUS program and for his far-reaching views.

Edelman's work did not escape the attention of everyone. In 1984, the "Directie Noordzee" was established, which among other things was responsible for the management of what we call the coastal foundation ("kustfundament") nowadays. Chief engineer Cees van den Burgt had hired a physical geographer to that end. Hans Wiersma notably had a broad view and was a networker pur sang. Someone with whom you enjoy having a drink and who will not let you pin him to a formal job description. He realized that an interplay of disciplines was required to tackle the erosion problems of the coast, by making connections between coastal processes at various time scales – from surf beat to coastal genesis. He managed to get a special group of people to sit down at the table, including the geologists and geographers Saskia Jelgersma, Dirk Beets and Joost Terwindt, and the hydraulic engineers Cees d'Angremond, Herman Wind, Huib de Vriend, Marcel Stive and Jan van de Graaff. He also came up with the name of the project aimed at advancing our understanding of coast-forming processes: Kustgenese (Coastal Genesis).

Next, Rijkswaterstaat had to be convinced. Walter Van der Kleij ruled over the A division (in which A is the acronym for Aqua), which is currently part of the I&M Directorate-General Water en Ruimte; although he was of small stature, people looked up to him. When the ideas about Kustgenese had ripened sufficiently, Van den Burgt hopped on his bicycle to update Van der Kleij. He was successful: Finances were secured and Van der Kleij became a sort of godfather to Kustgenese. In those days, people started speculating about increased sea level rise as a result of global warming. Kustgenese was given the assignment to look into that as well. Ton Kuik became project manager of Kustgenese, which meanwhile had grown into a mega project in which dozens of researchers were involved. There was a need for clear targets and tight coordination, a role for which information analyst Ton Kuik was particularly well suited.

The insights from Kustgenese were ground-breaking and gave rise to a fundamental revision of Dutch coastal policy. The first person to see that was Tjalle de Haan, at the time Van der Kleij's policy officer. The traditional ideas about coastal defense were abandoned: Hard constructions like seawalls were abolished in favor of sand nourishment and natural dynamics. This newfangledness, later summarized in the motto "soft where possible, hard where required", initially met with incomprehension and resistance from managers and politicians. People spoke about "carrying sand to the sea", with horror. Tjalle de Haan has Frisian blood and is stubborn; he won't let go, once he is certain of something. In 1990, the memorandum "Kustverdediging na 1990" was sent to the House of Representatives, in order to determine the new Dutch coastal policy. From now on, funds for sand nourishment along the coast would be set aside in the government's budget, with sand mined offshore in the North Sea, such that there would be no deterioration of the Dutch coast, at any location.

ESTABLISHMENT OF THE NCK

When the last one of the 23 supporting studies of Kustgenese was submitted and Dutch Parliament had agreed on the coastal memorandum, a post-partum depression was hanging over the research community of Kustgenese. Hans Wiersma sensed that perfectly well, and launched the idea of a permanent association: An organization that was to retain the multidisciplinary cooperative spirit of Kustgenese by ensuring that the coastal researchers would be able to exchange ideas about their research projects. That is how the NCK came about.

The NCK started in 1992 with 4 partners, namely the parties that had contributed big time to Kustgenese: Delft University of Technology (departments of Fluid Mechanics and Hydraulic Engineering), WL | Delft Hydraulics, Utrecht University (IMAU) and Rijkswaterstaat (RIKZ). The directors of those partners had a seat on the Supervisory Board; their roles were predominantly ceremonial. The actual cooperation was to be shaped within the program commission, supported by the NCK secretariat. The first chair of the program commission was Joost Terwindt; Ad van Os was its secretary, and would remain so for 13 years. Joost Terwindt was succeeded in 1997 by yours truly, who in 2003 passed the baton to Piet Hoekstra. As of last year, 2011, Ad van de Spek is chair. The secretariat was taken over by Stefan Aarninkhof in 2004, by Mark van Koningsveld in 2006 and by Bert van der Valk in 2007. Claire van Oeveren became program secretary last year.

New partners have joined the NCK over the years: NITG-TNO (Geological Survey), the University of Twente (Civil Engineering and Management), NIOZ, NIOO-CEMO, UNESCO-IHE and Imares. These partners enriched the NCK with a host of new disciplines. However, physical coastal research has always remained at the core of the NCK.

WHAT IS THE NCK?

The objectives drawn up at the launch of the NCK revealed a great deal of ambition:

- Quality improvement of coastal research through increased cooperation among research disciplines;
- Continuity of coastal research in the Netherlands through exchange of knowledge and methods among the partners;
- Maintaining fundamental coastal research at a sufficiently high level;
- Increasing knowledge exchange with the applied research community;
- Strengthening of coastal research and education at the Dutch universities;
- Enhancing the position of Dutch coastal research internationally.

As a result, the university partners obtained more research staff: 2.5 fte were financed by Rijkswaterstaat and 1.5 fte worth of senior researchers were made available by WL | Delft Hydraulics. The appointed researchers were given the task to design a research program for the NCK, submit it to the program commission for approval and subsequently take care of its execution by coordinating the research programs of the participating institutes.

In the eyes of the founders, the NCK was a continuation of the Kustgenese project. They probably did not realize fully yet that a new situation had developed after Kustgenese. Kustgenese was driven by an urgent societal question: How do we fight the continuous retreat of the Dutch coast? After Kustgenese, this question had received sand nourishment strategies as a reply. In addition, Kustgenese had generous earmarked funding and a relatively pristine research field in front of it, where pearls were easy to find.

The NCK lacked these ingredients. As a result, the program commission did not have a clear focus. The university groups, of course, each selected the discipline in which they could shine scientifically. The non-university partners carried out demand-driven research, which did not easily fit within the long-term research topics of the NCK program. The program commission did not actually have that much coordination to do. In spite of that, the somewhat misleading designation program commission has always remained.

The immediate impact of research in policy and management of the coast had been an important catalyst for entangling various disciplines in coastal research. That is why within the NCK, Rijkswaterstaat was assigned the important role as driver of knowledge integration. In addition, Rijkswaterstaat also had the roles of user of research results and research sponsor. Within the NCK, there has always been a great deal of discussion about these roles of Rijkswaterstaat, certainly in the days when Rijkswaterstaat had its own coastal research department at the former RIKZ. Did the NCK assist Rijkswaterstaat or did Rijkswaterstaat assist the NCK? Should the NCK focus on societal benefits or predominantly on the advancement of knowledge? Opinions within the NCK differed. In 2007, the partners Rijkswaterstaat (RIKZ), TNO (RGD) and WL | Delft Hydraulics merged into the new institute Deltares, and the discussion about the immediate benefits of the NCK for coastal management and coastal policy ebbed away.

Cooperation does not go without saying. That is what I experienced when I was at the center of the NCK, as member and later as chair of the program commission. Researchers are head-strong people, who don't want to be told what to do. The differences of opinion in the program commission sometimes led to heated discussions. That we found a solution in spite of that was notably due to two persons who radiated so much wisdom that the rational mind eventually conquered emotion: Joost Terwindt and Marcel Stive. You can easily call them the "patres familias" of the NCK.

The NCK never was a programming or coordinating organization in coastal research. The NCK is in fact a network organization. As a network, the NCK functioned well for 20 years, and it ensured that researchers of the participating parties interacted with one another to exchange knowledge and cooperate. The greatest added value of the NCK is in the area of knowledge transfer between different research disciplines and knowledge transfer from experienced researchers to researchers who are just starting out.

Each year, the NCK days bring together a large number of people from the research community, while in addition, workshops on specific topics are organized frequently. The NCK summer school has already been a great success for ten years, enjoying increased interest every year, also from other countries. Its initiator was Huib de Swart who saw his summer school, originally focused on morphodynamics, grow into a multidisciplinary coastal research summer school. This success, in his eyes slightly too exuberant, meanwhile has caused him to organize a summer school on morphodynamics in parallel.

The NCK has ensured that every coastal researcher in the Netherlands can lean on the entire research community, and is able to use all models and instruments that have already been developed. These are conditions for gaining optimal yield from coastal research. To which special achievements did it lead? I will address that hereafter.

REMARKABLE ACHIEVEMENTS, CATALYZED BY THE NCK

Coastal morphodynamics

The term coastal morphodynamics is still new. I do not know who introduced the term, but it is quite clear who put the concept on the map. That is Huib de Vriend, who was the initiator and driving force for three large European projects (G6M, G8M and PACE) in the area of coastal morphodynamics, in the first years of the NCK. The phenomenon of morphodynamics had been known for some time, but the crucial importance of feedback mechanisms for the resilience of the coastal system was less well known, such as the tendency for autonomous recovery after extreme erosion or after human interventions. Better insight in these feedback mechanisms reveals possibilities for strengthening these self-regulating dynamics of the coast through smart interventions. The impulses by Huib de Vriend grew into a flourishing research branch within the NCK community; it attempts to fathom various aspects of morphodynamics and capture them in models.

The research of the inherent instability of coastal systems, which drives the formation of many coastal forms, was stimulated strongly by Huib de Swart. Huib de Swart developed

mathematical methods for the analysis of instability development and he initiated a large number of PhD projects in this area. Is it due to the NCK that both Huibs, in spite of their rather self-willed characters, were able to inspire and complement each other? One of the PhD students of Huib de Swart, Suzanne Hulscher, subsequently established her own, internationally acclaimed research group for the study of the morphodynamics of the sea floor as full professor at the University of Twente.

The morphodynamics virus also infected the other NCK partners. A great deal of research into bank behavior off the Dutch coast under the influence of bound long waves was carried out at Delft University of Technology and at WL | Delft Hydraulics, inspired by Jurjen Battjes and Marcel Stive. Important contributions included those of Ad Reniers, Dano Roelvink and Gerben Ruessink. And many others, standing on the shoulders of these innovators, have contributed to the world-wide reputation of the Netherlands in the area of coastal morphodynamics research. I will later get back to the societal benefits of this kind of research.

Mud

The Netherlands has a sandy coast, yet mud plays an important role in it. The silting up of shipping channels and ports entails considerable maintenance costs. But there are many other aspects. The laboratory experiments of Jan van de Graaff and Paul Sistermans have shown, for example, that the physical properties of sandy soils can change significantly even if they contain only a small percentage of mud. This is also evident from the Eems-Dollard project on the erodibility of mudflat shoals, which was initiated by Joost Terwindt. But the presence of a small fraction of mud also has a large influence on the soil fauna and soil vegetation, which in turn determine physical soil properties such as erodibility, net sedimentation and roughness. Mudflats and tidal marshes therefore create their own conditions for their development and thus play an important role in the morphodynamics of tidal systems. The consequences of this new insight were investigated by Peter Herman and his research group at NIOO-CEMO. This knowledge appeared to be highly relevant for environmental impact studies and for projects of recovery and creation of nature areas.

From the early years of the NCK, studies were carried out to describe the physical properties of mud in models. The main pioneer in this area was Wim van Leussen, who recorded the flocculation behavior and the related sedimentation velocity of mud, with the mud camera he designed. Later, Johan de Kok and Han Winterwerp and others applied these insights and relationships in mathematical models, with which various mud-related practical problems were analyzed, such as the occurrence of mud layers and turbidity maxima in estuaries and the mud recirculation from the Loswal to the Rotterdam Waterway. These models are also of great importance for understanding the primary production in the Dutch coastal waters. This ecosystem research largely takes place outside the NCK framework, however.

Field research

Nature does not always like its measurements taken. In 20 years of NCK, quite a few expensive measuring instruments were lost in the surf. Some more were dragged off by fishing gear. But that didn't discourage the NCK partners. After all, field data are essential for testing hypotheses regarding coastal behavior and for developing new theories. Initially, all field work was the exclusive domain of Rijkswaterstaat and of the physical geographers at Utrecht University. Jointly, they developed the tripod measurement frames, the WESP and the CRIS, which played an important role in corroborating Kustgenese's ideas on the effectiveness of the nourishment strategy for coastal preservation. This research was carried out in the European NOURTEC project initiated by Jan Mulder, in Rijkswaterstaat's KUST2000 program and in the EU project COAST3D coordinated by Leo van Rijn. In these projects, Aart Kroon, Gerben Ruessink and Piet Hoekstra organized the field work.

The Argus camera, a smart way of measuring in the surf zone, was imported from the US. As addition to the JARKUS measurements, this yielded insight into the short-term coastal behavior and, moreover, enabled monitoring of foreshore nourishments. Also owing to the advanced analysis software developed by Stefan Aarninkhof and other NCK members, the Argus camera is now a commonly used measuring instrument on beaches all over the world.

Another "exotic tool" is the jet ski which since a few years is used very successfully for coastal bathymetry surveys. Students from Delft ended the hegemony for field measurements in the Netherlands from Utrecht; their jet ski company is now also asked to carry out surveys in other countries. Other innovating measurement techniques are the MEDUSA measurement probe developed by Rob de Meijer at the University of Groningen, for quick scans of the sea floor surface composition, and the measurement kit which Herman Ridderinkhof of NIOZ has mounted on the ferry to Texel in order to gain better insight into the sediment exchange between the Wadden Sea and the coastal zone.

Considerable progress was made in techniques for the analysis and interpretation of coastal field data. Gerben de Boer of Deltares, for example, developed the OpenEarth system, which enables combining and visualizing coastal data, such that it yields much more information at a glance.

Observations sometimes have an immediate impact on coastal management. The first observations with the wave measurement set-up at Petten, for example, revealed that the period of storm waves off the Dutch coast had always been largely underestimated until then. That made clear that the safety level against flooding did not meet the requirements along the entire coast, as a result of which additional coastal reinforcement measures had to be taken.

Models

Every hypothesis can be considered a model. But in order to test theories for natural coastal configurations, to analyze observations or to carry out effect predictions, complex models are often required, in which processes are represented in great detail. In the 20 years of the NCK, an extensive model kit was developed, largely based on Guus Stelling's numerical solution methods. This model kit has been used as research means in many NCK projects and has contributed greatly to the advancement of knowledge.

An important component is the numerical wave model SWAN by Nico Booij and Leo Holthuisen, which has become the global standard for wave simulations in coastal waters. For the simulation of coastal morphology processes, Delft3DMOR is generally considered a top model around the world; major trumps of Delft3DMOR are the morphological time scaling procedure of Dano Roelvink and the sediment transport formulations of Leo

van Rijn. These numerical models have paved the way for realistic simulations of non-linear processes in complex morphological systems, for instance, sediment exchange between tidal basins and the adjoining coastal zones and the development of the channel-and-shoal systems in estuaries. The reliability of the model formulations was tested in a large number of real-life studies, including the EU projects SEDMOC and SANDPIT, coordinated by Leo Van Rijn. Especially for wave-dominated sandy coasts, Ap van Dongeren and Dano Roelvink developed the XBEACH model. Leo Postma and Han Winterwerp developed DELWAQ routines for the simulation of mud transport; among other things, they enabled an understanding of the very high turbidity of many European estuaries and investigated the effectiveness of repair measures. The model kit developed by NCK partners (predominantly WL | Delft Hydraulics and Delft University of Technology) over the years is frequently used by Dutch consultancies for complex coastal engineering projects around the world and contributes to the strong image of the Netherlands as the country of hydraulic engineering expertise.

Examples of the immediate importance of models for coastal management in practice are the drawing up of the sand budget for the Dutch coast and the quantification of nourishment requirements. Also, models have contributed to a new insight with far-reaching policy consequences. This was the case for the transport atlas of the North Sea by Will de Ruijter and Leo Postma, which showed that polluting substances that enter the Netherlands with the Rhine water at Lobith partly end up in the German Wadden Sea. This insight contributed to the large-scale remediation program of pollution sources along the entire Rhine river.

Building with Nature

The concept of "Building with Nature" was put on the map by Ronald Waterman. Building with Nature stands for a hydraulic engineering philosophy which breaks with the traditional practice of controlling the forces of the sea by means of hard constructions. Ir. T. Edelman and probably also several geologists already realized in the 1950s that the forces of the sea not just aim at breaking down sand coasts, but more often produce coastal accretion. But it took several decades before this awareness was translated into the practice of hydraulic engineering. The Eastern Scheldt studies and Kustgenese provided the push for it. The practice of Building with Nature is founded on insight in the natural coastal processes and their self-organizing capacity. Without the knowledge of coastal morphodynamics accumulated in 20 years of NCK, the concept Building with Nature would have remained an empty shell.

Building with Nature is the hydraulic engineering practice which uses natural processes and materials naturally present in the coastal system, as much as possible. The best known application of Building with Nature is the foreshore nourishment strategy for coastal maintenance, which was studied extensively and optimized by the NCK partners. It became clear that natural processes (waves) do not only carry nourished sand from the breaker zone to the beach, but also contribute (wind) to strengthening of the dune zone and to increasing the dunes' drinking water storage capacity.

The Building with Nature concept for sandy shores was elaborated by Jan Mulder in the sand strategy. This sand strategy takes natural coastal morphology processes at different scales of time and space (for example, processes ranging from the time scale of a storm surge to the time scale of a meter of sea level rise) into consideration, in order to achieve sustainable coastal management. The Sand Engine at Kijkduin is a practical embodiment of this sand strategy.

Building with Nature is not only applicable to the maintenance of sandy coasts. Stimulating the development of vegetation offers possibilities for improving the safety of hard dams and dikes, while ecological values are restored or added. Edelman already wrote about this in the 1960s, and Tjalle de Haan had already started a subdivision on ecotechnology in Middelburg in the 1980s, in support of the Eastern Scheldt works. Mindert de Vries and colleagues of the biological and morphological disciplines at the NCK are presently developing and testing a wide range of new techniques. They call it eco-engineering: Ecosystem development aimed at optimizing societal services. Examples are the development of mussel beds (in the Wadden Sea) and oyster reefs (in the Eastern Scheldt) which absorb wave action, stimulate sedimentation, improve water quality as a result of their filtering action, and create a living environment for many other natural organisms that play a role in the marine food web. In short, assigning roles of hydraulic engineer and water manager to organisms!

The Netherlands, the world's top coastal engineering country

Over the centuries, The Netherlands has built up a great reputation as a country with hydraulic engineering know-how. This reputation creates a lot of goodwill for the Netherlands and carries over to the economic position of the Netherlands in the world. It is therefore important for the Netherlands to maintain and enhance this reputation. The water sector, and notably coastal hydraulic engineering, is recognized as one of the top sectors of Dutch expertise for knowledge export. The NCK plays an important role in this: Through the hydraulic engineering innovations for which the NCK is a major breeding ground, and through the transfer of knowledge and experience within the NCK to new generations of water experts. Also owing to the NCK, knowledge of Building with Nature is currently an important new motor for the export of Dutch hydraulic engineering know-how to the rest of the world.

CONCLUSION

Quite some time ago, Johan van Veen, master of the sea, gave the example of how studying the fundamental properties of nature provides the insight in how to make the Netherlands safe and liveable. The NCK followed in these footsteps and has paved new roads in the past 20 years. But the sea keeps challenging us, both in the Netherlands and elsewhere on the planet. Work to do for a new generation of NCK people!

NCK photo competition

Dano Roelvink: Abidjan, Côte d'Ivoire

DOI: 10.3990/2.167

NCK; the road ahead

A.J.F. van der Spek
Subsurface and Groundwater Systems Unit, Deltares, 3508 AL, Utrecht, The Netherlands, Ad.vanderSpek@deltares.nl;
chairman NCK Program Committee

INTRODUCTION

Twenty years of NCK is a milestone that asks for both celebration and reflection. Reflection on what we have accomplished in those years and some thoughts on where we want, or need, to go in the coming years. Job Dronkers' contribution gives a first-hand report on the history of coastal research in The Netherlands, the founding of NCK and the 'winding road' that led us to where we stand today. My contribution will address the road ahead. It reflects my personal ideas and is by no means an official NCK policy plan.

NCK, THE FIRST 20 YEARS

The Netherlands Centre for Coastal Research NCK is not what the name suggests: a building where a predominantly scientific staff researches the ins and outs of the Dutch coast. In fact, it is more or less the opposite: it is a platform for the exchange of knowledge and expertise, the sharing of data and tools, and collaboration of scientists from different disciplines and with different backgrounds that work in different institutes. The Centre works as a network, a network that provides access to knowledge, experience, facilities, etc. As Job describes, NCK never was a programming or co-ordinating organization in coastal research. Instead, it was, and still is, a network organization that encourages and facilitates transfer of knowledge, from one research discipline to the other and from senior, experienced researchers to junior ones. Thus, the expertise of the entire coastal research community is available to that same community. Important ways to accomplish this are part-time secondment of senior staff of applied research institutes to universities, the yearly symposium "NCK-days" and the bi-yearly NCK Summer School. The "NCK-days" provide an opportunity for PhD and masters students to present their plans, ideas and results, both orally and as posters, and to learn from the feedback they will get, usually in the form of animated discussions. This is the sound basis of the NCK network. The large number of 'alumni' of the network that continues to attend these symposia strengthens this. The NCK Summer School is a must for all PhD students working within the NCK partner institutes. Both the lecture programme and the case studies presented in the Summer School reflect the wide range of subjects that is covered by the NCK partners. Finally, NCK partners have joined forces to write research proposals for national and European funding organizations in the past. And they will continue to do so.

NCK IN 2012

So where do we stand today? Concentrating on the national level, we see an increasing call for coastal development. The national programme to reinforce the so-called 'weak links' in the coastal defence sparked off a series of plans for upgrading of the local infrastructure, especially in coastal towns, in combination with the improvement of the sea defences. However, several plans are not directly related to coastal defence issues but are concentrating on local spatial planning, in some cases including seaward extensions of the coastline. Simultaneously, coastal maintenance with sand nourishment has proven to be successful in stopping structural erosion of the coast. Repeated nourishment of the coast of North- and South-Holland has stabilized or locally even prograded the coastline. This success triggered studies into optimization of the nourishment strategy (Can we reach the same effect with less effort? Can we reach more effect, or less negative impact, with the same effort?) and inspired plans for large-scale interventions with sand. The trend over the last decade is one of increasing volumes of individual nourishments, from beach nourishments of several hundred thousand cubic meters of sand, to shoreface nourishments of up to 2 million cubic meters, to channel-wall nourishments of more than 5 million cubic meters. It culminated in the mega-nourishment *Zandmotor* that has been created along the coast of southern South-Holland in 2011. The presumed beneficial effects of the *Zandmotor* have already inspired plans for new mega-nourishments elsewhere. This recent trend in (spatial) planning for coastal development is illustrated by the Delta Programme Kust. Coastal safety has become one of the issues for the future of our coast instead of being the leading issue. Moreover, spatial planners are, in general, unaware of the functioning of the natural coastal system. Applying the latest insights and knowledge of the functioning of the natural coastal system in the process of planning and designing for the future might pay off in designs more in line with nature, resulting, e.g., in smaller costs for maintenance of the design in the long run. Unfortunately, coastal experts are presently hardly involved in this planning process.

More generally, experts need clients and stakeholders to ask the right questions in order to be able to give relevant answers. But how can non-experts identify the right questions? This is a challenge for the years to come: How can the coastal research community introduce its expertise and experience in the societal discussions on coastal matters? This is not only a matter of presentation, of 'show and tell', but also of learning to appreciate

the issues that play a role in the decision making. Generally speaking, scientific and/or technical arguments are competing with political, economic, administrative and other arguments, leading to decisions that are not always recognized by experts. Learning to appreciate the complexity of decision making, e.g., by participating in such a process, will improve the communication between experts and non-experts. Serious gaming might prove to be a valuable tool in this.

WHERE ARE WE HEADING?

NCK and the outside world

Does the changing outside world ask for a new or different NCK? The world in which we have to operate is becoming increasingly complex. New skills and capabilities are necessary to continue our work: learning to understand coastal systems and sharing that knowledge with society. That brings up the 'classic' discussion within NCK: Do we need to expand our network with new disciplines and partners or should we stick to the present mix of partners and seek co-operation with other parties and/or networks? A serious risk of expansion is a decline in interest and enthusiasm of the students and staff of the present partners that might not appreciate or recognize the relevance of new subjects for their daily work. This would seriously hamper the functioning of the network. So, what is the connection between the present partners? Presently we incorporate disciplines with their basis in physical and biological processes that result in erosion, transport and deposition of sediments, leading to changes in (geo-) morphology and, on a larger scale, changes of landscapes both above and below sea level. The overarching subject of NCK is the functioning and evolution of sedimentary coastal systems, both in a natural state and man-influenced. My suggestion is that parties that fit this picture should be welcome to participate in our network.

Another question is: Does the outside world know, or even better, recognize NCK as the expert network on sedimentary coastal systems? Discussions with parties outside the field of operation of NCK lead to the conclusion that this is not always the case. Apparently, one of the recommendations for the future of NCK that was noted in 2007[1] still holds: "... create an external NCK profile through external networking". This is a subject that needs urgent action!

New developments

Apart from ongoing research on more traditional subjects such as sediment transport, surf-zone bar behaviour, etc., we have seen an increasing attention over the past years for subjects such as:

- The interaction of beaches and dunes, including aeolian transport processes;
- The interaction of hydrodynamic and aeolian processes on the beach and the numerical modeling of that interaction;
- The application of numerical process models for time scales of decades and centuries, resulting in building of stratigraphy of complete coastal systems; and
- An expansion of the interest in the morphodynamics of muddy coasts and a starting interest in gravel dynamics.

The introduction of new, cheap and increasingly smaller sensors and highly mobile and easy-to-launch platforms have made quickly deployable monitoring methods reality. A good example is NEMO, the jet-ski based echo-sounding system that has proven its value in the monitoring of the progress of the reinforcement of the Delfland coast. These new monitoring systems have boosted data gathering in the field and will likely lead to increased understanding of short-term variability of coastal morphology. Moreover, the launching of smart data bases with flexible data formats and open-access facilities such as Google Earth and Open Earth, permits fast combination of data and realistic presentation of data. This will likely become a standard for the coming years.

New developments in the world of process modeling such as the on-line coupling of model systems, more realistic schematization of boundary conditions and the growing number of state-of-the-art, open-source numerical models all open up new possibilities for research and bring models within reach of new research groups.

All above-mentioned developments show that coastal research in The Netherlands is alive and kicking. In the years to come, it will continue on 3 tracks, that are complimentary:

1. Expansion of system knowledge, based on observations and data collection in the field, and enabling the building of hypotheses on functioning of coastal systems;
2. Modeling, both numerically and conceptually of natural systems; and
3. Experimenting, both in the field and lab and numerically, to test hypotheses.

The implementation and subsequent evolution of large-scale sandy interventions, such as the *Zandmotor* and the artificial dunes at Vlugtenburg along the Delfland coast, not only is an excellent chance to deepen our understanding of that coastal system, it also creates new opportunities for co-operation in research. The latter is illustrated by the leading role that NCK partners have in proposing and execution of research in this area. Hopefully we can transplant that model of operation to other areas.

We have got work to do!

[1] Hoekstra, P, JPM Mulder, MJF Stive, SJHM Hulscher & M van Koningsveld, 2007. NCK – Past, present and future. In: Book of Abstracts, 15th Anniversary NCK – International Symposium IJmuiden, June 13-15, 2007, p. 45-51.

Keynote papers

- **P.A. Hesp**
- **D.A. Huntley**
- **A.J. Kox**
- **I. Möller**
- **T. O'Donoghue and D.A. van der A**
- **C. Villaret, N. Huybrechts and A.G. Davies**

NCK photo competition

Edwin Paree: Western Scheldt

DOI: 10.3990/2.168

Surfzone-beach-dune interactions

P.A. Hesp
Department of Geography and Anthropology, 227 Howe Russell Geosci. Bldg., Louisiana State University, Baton Rouge Louisiana, USA 70803. pahesp@lsu.edu

ABSTRACT

This paper reviews the wave-beach-dune model of beach and dune interactions formulated by Hesp [1982] for micro-tidal beaches in eastern and southern Australia, and examines additions to, and more recent research principally on that model, but also briefly examines other models based on sediment supply variations. The model contends that dissipative beaches are characterized by high wave driven sediment supply, wide, low gradient beaches, maximum fetch, maximum aeolian sediment transport, largest foredunes and largest dunefields or dune systems, while reflective beaches are the opposite (minimal wave and wind driven sediment transport, narrow steep beaches, small foredunes and limited dunefield /dune system development. Intermediate beaches display a trend from high to low transport conditions, foredune size and dunefield development with a trend from dissipative to reflective. Future research ideas are also presented.

INTRODUCTION

The original generation of the wave-beach-dune model of beach and dune interactions was formulated by Hesp [1982] for micro-tidal beaches in eastern and southern Australia, although it might be argued that it would work in many cases for meso-tidal beaches (<~4m range). Most of these beaches were apparently not limited in sediment supply during the Holocene transgression and particularly in the last 7000 years. Sea level crossed the present around 6,500 to 7000 years ago, rose a little higher (perhaps 1m in eastern Australia) and eventually fell to the present following a typical southern hemisphere pattern.

The model development followed the publication of a robust micro-tidal beach model with reasonably high predictability [Wright and Short, 1984]. The beach model enabled one to classify micro-tidal beaches into six states with characteristic morphologies, mobility, and modes of erosion and accretion. Subsequent research has extended the original model to meso- and macro-tidal beaches [e.g. Short and Masselink, 1993; Masselink and Turner, 1999]. An understanding of beach and backshore morphology for different surfzone-beach types allowed Hesp [1982] to develop actual and theoretical links between backshore morphology, potential aeolian transport, foredune state and morphology, and dunefield type and development [Short and Hesp, 1982].

SURFZONE-BEACH STATE

The micro-tidal beach models classified beaches into six states, with the dissipative state at the high wave energy (>2.5m) extreme and reflective state at the low wave energy (<1m) extreme. Four intermediate beach states occur between these states [Wright et al, 1979; Short and Wright, 1983; Wright and Short, 1984]. Dissipative beaches are characteristically high wave energy beaches and have the highest potential onshore sediment supply [Hesp, 1988]. Note however, that beaches may also be dissipative because of the presence of very fine sand (hence low gradient), or abundant sand, so some dissipative beaches may, in fact, be low wave energy beaches. They are typically wide, display flat to concave morphologies (no berms), low gradients and minimal backshore mobility. The latter refers to the coefficient of variation of mean shoreline position (see Short [1999], his table 7.1), and in reality refers to the amount of volumetric and profile change the beach and backshore experiences over time and through erosion to accretion phases. Reflective beaches are characteristically low wave energy beaches with low potential onshore wave driven sediment transport. Note that they may also be moderate to high wave energy where sediments are coarse sand to boulders. They are relatively steep, narrow, linear to terraced (i.e. display a berm form) morphologies, with low backshore mobility. Intermediate beaches range from wide, relatively flat beaches with low gradient berms and low mobility at the higher energy end of the spectrum, through moderate width with beaches with pronounced berms and high mobility to narrow beaches and moderate to low mobility berms at the reflective end of the range. Rips dominate surf zone processes in the intermediate range (Figure 1).

SURFZONE TO BEACH SEDIMENT TRANSPORT

Hesp [1982; 1999] and Short and Hesp [1982] argued that dissipative surfzones had the highest potential wave driven onshore transport while reflective beaches had the lowest, based on observations of Holocene sediment volumes contained in barrier systems developed landwards of those beaches. Some have argued that this premise (highest onshore transport on dissipative beaches, lowest on reflective) is fallacious, partly it seems because (i) there are minimal measurements of surfzone sediment transport, (ii) some of the measurements that exist tend to show that dissipative beaches are characterized by offshore transport (but not all – see e.g. Aagaard et al. [2004]; Miot da Silva [2011, in review]), (iii) models such as SBEACH and CROSMOR generally predict offshore transport [e.g. Larson and Kraus, 1989; van Rijn et al., 1999; Aagaard et al., 2002], and (iv) the observational time scales are substantially different (hours to days for surfzone observations versus 6-7000 years for Holocene barrier volumetric calculations).

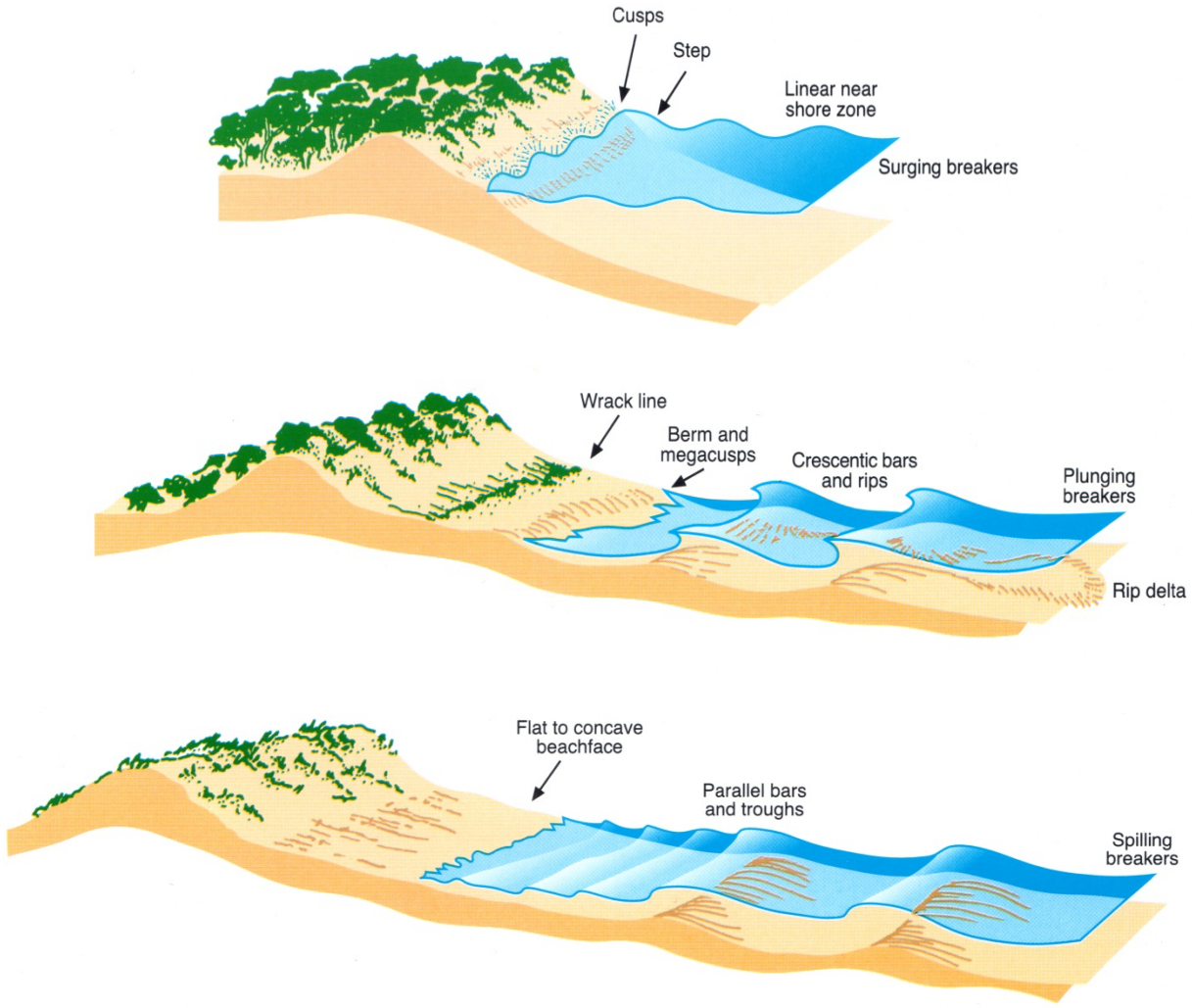

Figure 1. Schematic diagrams of the three micro-tidal surfzone-beach types, dissipative, intermediate and reflective. Also shown are the typical (for temperate environments) foredune stages and vegetation cover (modified from [Hesp, 2000]).

As Aagaard et al. [2004] note, "most field and laboratory observations suggest that the transport of sand and the movement of nearshore bars are directed offshore when the waves are breaking" (p. 206). Despite this, large-scale coastal evolution

models predict onshore sediment transport and barrier formation during rising sea levels (given a suitable substrate gradient) [e.g. Roy et al., 1994; Cowell et al recent papers], and geological research of various barrier types indicates the same [e.g. Woodroffe, 2002; Davis and Fitzgerald, 2004; Dillenburg and Hesp, 2009]. It is also a fact that very many of the largest barrier and coastal dunefields in the world are found on high energy dissipative and high energy intermediate beaches (see Hesp [in press]).

Houser [2009] states that "existing beach-dune models do not consider how and when sediment gets transferred to the backshore…" (p. 742). The wave-beach-dune model does not examine nor predict the "how" of grain by grain transport, nor concern itself with bar migration and sediment delivery to the beach, but there are an increasing number of studies that have and do [e.g. Wijnberg and Kroon, 2002; Shand et al., 2003; Aagaard et al., 2004, 2011; Miot da Silva and Hesp, 2010; plus the Argus observation systems worldwide], and certainly more are required. However, for the scale of model building examined by Hesp [1982] and others [e.g. Psuty, 1988, 2004; Sherman and Bauer, 1993] this is unnecessary since, in fact, the wave-beach-dune model explicitly considers the net sediment delivery to the beach by providing long term data on beach-surfzone profiles and their dynamics (width, mobility, modal state, modes of erosion and accretion etc.; - see Figure 7.7 in Short [1999]; and profile measurements by e.g. Sonu [1973]; Holman and Bowen [1982]; Stive and deVriend [1995]; Stive et al. [1999] and many others). These data have been, or can be utilized to examine "when" sediment is delivered to the beach by scrutinizing the profile data and associated wave energies for various beaches [e.g. Short, 1979], but again, this is unnecessary for model building at meso- and macro-scales. The beach profile data provide evidence of sediment delivery to, and from the beach, the "how" is therefore irrelevant to meso-scale model building, and defining modal surfzone-beach behavior is the only necessary criteria required for the next step linking the beach supply to the dunes.

BEACH-BACKSHORE WIDTH AND MORPHOLOGY, FETCH, AND POTENTIAL AEOLIAN TRANSPORT

Beach width is important in determining fetch which is critical for determining the volume of sand delivered across the backshore and to dunes [Davidson-Arnott, 1988, 2010; Davidson-Arnott and Law, 1996; Bauer and Davidson-Arnott, 2002; Houser, 2009]. Dissipative beaches display the widest morphologies and hence have the highest potential fetches compared to reflective beaches with a gradient from wide to narrow through the intermediate range. There are constraints however, not noted in the original model, including (i) at low tide, dissipative beaches may have a considerable wet to moist zone due to groundwater drainage, and (ii) as one moves from the micro-tidal to meso- and macro-tidal ranges, groundwater drainage is significant and the width of the dry upper beach can be limited.

Beach morphology is important because the greater the morphological variability, the more likely that wind velocity decelerations and variations take place across the backshore. Hesp [1982; 1999] showed that the wind flow across a wide, low gradient but curvilinear, dissipative beach displayed minimal flow variation and gradually accelerated across the backshore, thus maximizing potential aeolian transport. The wind flow over the berm crest of an intermediate beach was accelerated but decelerated leeward of the berm crest. High narrow berms typical of some reflective beaches display significant flow disturbance and deceleration leeward of the berm crest [Short and Hesp, 1982] (see Figure 2).

Modeling by Sherman and Bauer [1993] indicates that the conceptual and empirical observations of Hesp [1982] and Short and Hesp [1982] are confirmed. Sherman and Lyons [1994] modeled wind flow and potential sediment transport across three beach morphologies: a flat beach, low berm and high berm profiles, and found that sand transport off the dissipative beach was 20% higher than off the reflective beach if just slope and grain size were taken into account. When moisture content was added, transport rates were nearly two orders of magnitude higher off the dissipative beach compared to the reflective beach. Note, however, that each beach had the same width (100m wide), whereas actual reflective beaches and many intermediate beaches are considerably narrower than dissipative beaches.

Beach mobility is important because the greater the beach mobility, the greater the morphological variability. The latter affects the fetch such that the beach width is at times quite narrow, at times quite wide, particularly for intermediate beaches. It is also important because alternating episodes of cut and fill result in varying beach morphologies which then affect airflow and sediment transport as indicated above.

Thus, the link between surfzone-beach state, aeolian sediment transport and landward dunes is that modal dissipative beaches have maximum potential aeolian sediment transport (low mobility, wide fetch, flat, low gradient morphology), reflective beaches have minimal potential aeolian sediment transport (low mobility, short fetch, steep, narrow beach and/or high narrow berms), and intermediate beaches range from relatively high potential at the dissipative end to low potential at the reflective end. Houser and Hamilton [2009] provide supporting evidence for these relationships in a study of surfzone-beach interactions in NW Florida.

Note that a minimal sediment supply ("minimal" is currently undetermined) is required.

AEOLIAN SEDIMENT TRANSPORT AND FOREDUNE MORPHOLOGY

An examination of foredune heights and volumes on dissipative to reflective beaches allows one to examine the validity of the links above. Since established foredunes occupy a foremost backshore position, they are a medium term indicator of beach and backshore processes. Hesp [1988] measured incipient and established foredune volumetric changes over several years at Myall Lakes National Park in NSW, Australia to find that a modal reflective beach with the same wind exposure as a modal dissipative beach received 60% less sand than the dissipative beach over the same survey period. Intermediate beach volumes ranged from relatively high to relatively low between the dissipative and reflective beaches.

Surveys of established foredunes, which have been present for potentially several hundred years, provide further evidence that there is a strong link between surfzone-beach type and foredune height and volume. Hesp [1982; 1988] demonstrated that in the Myall Lakes National Park in NSW, Australia, the smallest established foredunes, with lowest sediment volumes were found on reflective beaches, while the highest and largest foredunes occurred on dissipative beaches. Similar results are reported by Davidson-Arnott and Law [1990]. Intermediate beaches followed

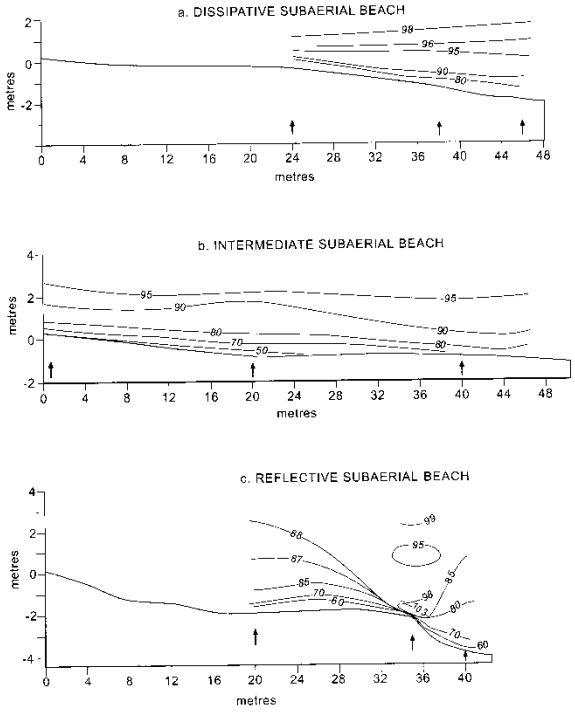

Figure 2. Mean wind speed iso-lines measured with cup anemometry over a dissipative, intermediate and reflective beach (modified from [Hesp, 1999]). An increase in topographic variability leads to an increase in wind field variability such that, on average, wind speeds are least disturbed, and show the greatest landward accelerations on dissipative beaches.

a trend from low to high volumes on lowest to highest energy intermediate beaches respectively (see reviews in Sherman and Bauer [1993] – their Table 1, and Bauer and Sherman [1999]).

Miot da Silva and Hesp [2010] and Miot da Silva [2011; in review] examined wave driven sediment supply, winds, aeolian transport, foredune development and dunefield evolution for an embayment in southern Brazil and found that shoreline orientation to the predominant wind and wave regime was important in driving sediment delivery to foredunes, but also that the alongshore gradient in surfzone-beach type (low energy dissipative in the south, increasingly higher energy intermediate towards the north, moderate to high energy dissipative in the north) resulted in greater sediment supply towards the north and the largest foredunes occurred in the northern portion of the embayment.

Houser and Mathew [2011] found that an increase in available fetch was correlated with an increase in dune height. They further state however, that the washover channels occur on the widest and lowest gradient dissipative beaches, while the largest dunes on Padre Island are "fronted by a foreshore that is relatively steep and short" (p. 70). Note, however, their dissipative and intermediate beaches appear to be only slightly different in terms of gradient. They argue that the highest dunes occur where the backshore is higher and where there is more sediment available. They thus believe that sediment availability is more important there than transport potential. It is unlikely that 2 periods of Lidar observations as obtained by Houser and Mathew [2011] are sufficient to establish relationships about modal beach states. It is true that at times more intermediate beach-backshore profiles have higher berms and therefore less moist or wet surface areas than dissipative beaches, but the Short and Hesp [1982] model shows that it is the higher mobility of these beaches that reduces the long term sediment input to dunes, something that Houser and Mathew [2011] do not consider. In addition, dune height is a less useful parameter to use for estimating relationships between beach state, aeolian sediment delivery and dune development; estimates of dune volume provide a much more accurate means of determining such relationships.

FOREDUNE ECOLOGY

The vegetation cover, species richness and zonation of foredunes is determined by several factors, but sediment supply and sand deposition rate, and salt spray aerosol levels are two important factors [Hesp, 1991; Maun, 2009]. Simultaneous studies carried out on adjoining reflective, intermediate and dissipative beaches show that salt spray aerosol levels are related to surfzone-beach type. Dissipative beaches have the widest surfzones, the greatest number of breaking waves, and highest wave heights and the highest salt aerosol levels. Reflective beaches often have only one breaking wave, narrow to very narrow surfzones, and low wave heights and the lowest salt aerosol levels. All other factors being equal, foredune species richness and zonation tends to be greatest and narrowest respectively on reflective beaches (low sediment supply and salt aerosols), and lowest and widest on dissipative beaches (highest sediment supply, high salt aerosol levels [Hesp, 1988].

FOREDUNE STABILITY AND TYPE, EROSION PROCESSES AND DUNEFIELD DEVELOPMENT

Foredunes bear a morphological imprint dictated, in part, by modal surfzone-beach erosion and accretion modes, and the wind often accentuates this morphological imprint. Dissipative beaches are typically eroded by swash bores and undertow commonly associated with elevated water levels and storm surge. Beach erosion and dune scarping is laterally continuous alongshore, and at times catastrophic. Short and Hesp [1982] and Hesp [1988] theorized that such laterally continuous alongshore, large scale foredune scarping would on occasions lead to large scale foredune de-stabilization. Transgressive dunefields would most likely result from the breakdown of the large established foredune. In fact, whether foredunes exist or not, transgressive dunefields are most commonly found on high energy dissipative and high energy intermediate surfzone-beach systems (e.g. Australia, South Africa, Brazil coasts; west coast USA; east and west coast Mexico; NZ North Island west coast; Peru and Chile coasts; France, Spain and Portugal coasts). Recent research by Hesp et al. [2009], Martinho et al. [2009], Miot da Silva and Hesp [2010], and Miot da Silva [2011; in review] support this contention for southern Brazilian transgressive dunefield barrier systems.

Intermediate beaches are characterized by localized, arcuate rip embayment erosion during storms. Such arcuate erosion extends well into the foredune during extreme events resulting in large scale, but localized foredune scarping. Topographic funneling of the wind may result in the evolution of blowouts and eventually parabolic dunes at these locations. While Short and Hesp [1982] argued that higher energy intermediate beaches should be correlated with parabolic dune complexes, to date there has been little research conducted on this or evidence provided.

On SE Australian beach systems where overwash events are minor to absent, where sediment supply is generally not limited, and where an aggressive pioneer grass (Spinifex sp.) exists, relict foredune plains are common, particularly on the moderate energy intermediate beaches. Here established foredune stability is maintained to various degrees, and progradation over the last 6 – 7000 years has led to the development of foredune plains.

Reflective beaches are characterized by accentuated swash during storms and laterally continuous alongshore beach erosion. Recovery is fairly rapid. Foredunes remain relatively stable over time, and because they are typically small, with limited sediment supply, little dune transgression results. Thus reflective beaches are characterized by a single foredune, or a few relict foredunes.

THE ROLE OF SEDIMENT SUPPLY

Sediment supply is clearly a critical factor in all this. If there is no sediment supply, or very little, a dissipative surfzone-beach system will operate to use all the sediment available to build the surfzone and beach and there may be no dune at all. At the other extreme, a high to very high sediment supply on a low energy reflective beach will result in the development of a wide foredune plain. Several examples may be found on the Western Australian coast, for instance.

Psuty [1988, 2004] has produced several versions of a beach-dune model which uses sediment supply alone as the single factor driving changes or spatio-temporal evolutionary sequences to

foredunes (and sometimes other dune types). In these models high sediment supply from the beach and a negative dune budget results in the development of low foredunes or "beach ridges" (as indicated by Psuty [1988]), but this only applies strictly to foredunes, not any other dune types or systems. In addition, as Davidson-Arnott [2010] notes "in nature it is difficult to conceive of a situation with a large positive littoral sediment budget and negative dune budget so the curve on the right side of the diagram should more realistically flatten off around the neutral line" (p.263). Additionally, the creation of the curve is these models is unexplained, blowouts and parabolic dunes are only formed in negative beach budget situations (not true for many parabolic dune and transgressive dunefield systems), and the lower range of "present day dune development" compared to the "maximum"(?) development scenario (see Psuty [1988], figure 3) remains unexplained.

OTHER FACTORS

There is no doubt that sediment supply, wind energy, sea level state (transgressive, stable, regressive), return interval and magnitude of extreme storm events, and Pleistocene inheritance factors will all, at times, and in some places, be a controlling variable in beach-dune interactions. If sediment supply is limited, sea level is rising, and coastal erosion is the general rule, the models reviewed above may not work in part or perhaps at all.

FUTURE STUDIES

In order to move forward with the development of a more robust, higher predictability model (or models) we need to (at least):

(i) skill and field test present models and develop new models of surfzone and beach sediment transport;

(ii) conduct more combined wind flow and sand transport experiments across beaches of the modal types (dissipative through to reflective);

(iii) conduct computer model experiments of flow over different beach types;

(iv) obtain more data on surfzone-beach states, wave driven sediment transport over long time intervals for different surfzone-beach types, and compile data on their attendant dune systems in order to further test linkages between surfzone-beach and dune interactions;

(v) extend the models to meso-, macro-tidal and ultradissipative beach types;

(vi) develop a universal classification and definitions of low, medium and high sediment supply;

(vii) find coastal sites where it is possible to test (hopefully) one of the major factors driving coastal evolution at a time (e.g. marine and aeolian sediment supply, wave energy, wind energy, etc).

This list is not exhaustive.

ACKNOWLEDGEMENT

A special thanks to Douglas Sherman and Graziela Miot da Silva for their advice and assistance, Kathelijne Wijnberg for the invitation and support to attend the NCK-days 2012, and LSU and the NSF for grant and logistical support.

REFERENCES

Aagaard, T., Black, K.P. and Greenwood, B., 2002. Cross-shore suspended sediment transport in the surf zone: a field based parameterization. Marine Geology 185: 283-302.

Aagaard, T., Davidson-Arnott, R., Greenwood, B., and Nielsen, J., 2004. Sediment supply from shoreface to dunes: linking sediment transport measurements and long term morphological evolution. Geomorphology 60: 205-224.

Aagaard, T., Hughes, M.G. and Greenwood, B., 2011. Sediment transfer from bar to beach? Measurements using a pulse-coherent acoustic Doppler profiler. J. Coastal research SI 64: 2002-2006.

Bauer, B.O. and Davidson-Arnott, R.G.D., 2002. A general framework for modelling sediment supply to coastal dunes including wind angle, beach geometry, and fetch effects. Geomorphology 49: 89-108.

Bauer, B.O. and Sherman, D.J., 1999. Coastal Dune dynamics: Problems and prospects. In: A.S. Goudie, I. Livingstone and S. Stokes (eds), Aeolian Environments, Sediments and Landforms, 71-104. Chichester: J. Wiley and Sons

Davidson-Arnott, R.G.D., 1988. Temporal and spatial controls on beach/dune interaction, Long Point, Lake Erie; in: N.P. Psuty (ed), Dune/Beach Interaction. J. Coastal Research Special Issue No. 3: 131-136.

Davidson-Arnott, R.G.D., 2010. Introduction to Coastal Processes and Geomorphology. Cambridge Univ. Press, 442pp.

Davidson-Arnott, R.G.D. and Law, M.N., 1990. Seasonal patterns and controls on sediment supply to coastal foredunes, Long Point, Lake Erie; in: K.F. Nordstrom,

K.F. Psuty and R.W.G. Carter (Eds), Coastal Dunes: Form and Process, 177-200. Chchester: John Wiley and Sons.

Davidson-Arnott, R.G.D. and Law, M.N. 1996. Measurement and prediction of long-term sediment supply to coastal foredunes. J. Coastal Research 12 (3): 654-663.

Davis, R.A. Jr. and Fitzgerald, D.M., 2004. Beaches and Coasts. Blackwell Publishing, 419pp.

Dillenburg, S. and Hesp, P.A. (Editors), 2009. Geology and Geomorphology of Holocene Coastal Barriers of Brazil. Springer-Verlag Lecture Notes in Earth Sciences 107. Springer.

Dillenburg, S.R. and Hesp, P.A., 2009. Coastal Barriers – An Introduction. Chpt 1 in: S. R. Dillenburg and P. A. Hesp (Eds), Geology and Geomorphology of Holocene Coastal Barriers of Brazil. Lecture Notes in Earth Sciences, Vol 107: 1-15. Springer.

Hesp, P.A., 1982. Morphology and Dynamics of Foredunes in S.E. Australia. Unpubl. Ph.D Thesis, Dept. Geography, University of Sydney.

Hesp, P.A., 1988. Surfzone, beach and foredune interactions on the Australian south east coast. J. Coastal Research Spec. Issue 3: 15-25.

Hesp, P.A., 1991. Ecological processes and plant adaptations on coastal dunes. J. Arid Environments 21: 165-191

Hesp, P.A., 1999. The Beach Backshore and Beyond. In: A.D. Short (Ed), Handbook of Beach and Shoreface Morphodynamics: 145-170. John Wiley and Sons, Chichester.

Hesp, P.A., 2000; Coastal Dunes. Forest Research (Rotorua) and NZ Coastal Dune Vegetation Network (CDVN): 28pp.

Hesp, P.A., P. C. F. Giannini, C. Thaís Martinho, G. Miot da Silva and N. E. Asp Neto, 2009. The Holocene Barrier Systems of the

Santa Catarina Coast, Southern Brazil. Chapter 4 in: S. R. Dillenburg and P. A. Hesp (Eds), Geology and Geomorphology of Holocene Coastal Barriers of Brazil. Lecture Notes in Earth Sciences, Vol 107: 93-133. Springer.

Hesp, P.A., in press (due 2012). Dune coasts. In: Treatise on Estuarine and Coastal Science. Volume 3, Estuarine and Coastal Geology and Geomorphology. Elsevier. ISBN: 978-0-12-374711-2.

Holman, R.A. and Bowen, A.J., 1982. Bars, bumps and holes: Models for the generation of complex beach topography. J. Geophysical research 87: 457-468.

Houser, C., 2009. Synchronization of transport and supply in beach-dune interaction. Progress in Physical Geography 33(6): 733-746.

Houser, C. and Hamilton, S., 2009. Sensitivity of post-hurricane beach and dune recovery to event frequency. Earth Surface Processes and Landforms 34: 613-628.

Houser, C. and Mathew, S., 2011. Alongshore variation in foredune height in response to transport potential and sediment supply: South Padre Island, Texas. Geomorphology 125: 62-72.

Larson, M., and Kraus, N.C., 1989. SBEACH: Numerical model for simulating storm-induced beach change. CERC TR 89-9, 256pp.

Martinho, C.T., Dillenburg, S. R., Hesp, P.A., 2009. Wave energy and longshore transport gradients controlling barrier evolution in Rio Grande do Sul, Brazil. J. Coastal Research 25 (2): 285-293.

Masselink, G. And Short, A.D., 1993. The effect of tide range on beach morphodynamics and morphology.: A conceptual beach model. J. Coastal Research 9: 785-800.

Masselink, G. and Turner, I., 1993. The effect of tides on beach morphodynamics. In: A.D. Short (Ed.) Handbook of Beach and Shoreface Morphodynamics: 204-229. J. Wiley and Sons Ltd.

Maun, M.A., 2009. The Biology of Coastal Sand Dunes. Oxford Univ. Press, 265pp.

Miot da Silva, G., 2011. Wave dynamics and beach - dune interactions: Moçambique Beach, Santa Catarina Island, Brazil. In: Wang, P.; Rosati, J.D.; Roberts, T.M., (Eds.) 2011. Proceedings Coastal Sediments, Miami, Florida, 1: 725-738.

Miot da Silva, G. and Hesp, P.A., 2010. Coastline orientation, aeolian sediment transport and foredune and dunefield dynamics of Moçambique Beach, southern Brazil. Geomorphology 120: 258-278.

Miot da Silva, G., Siadatmousavi, S.M. and Jose, F. (in review). Wave-driven longshore sediment transport and beach-dune dynamics in a headland bay beach. Submitted to Marine Geology.

Nickling, W.G. and Davidson-Arnott, R.G.D. (1990) Aeolian sediment transport on beaches and coastal sand dunes. Proc. Canadian Symposium on Coastal Dunes: 1-35.

Psuty, N.P., 1988. Sediment budget and beach/dune interaction, in: N.P. Psuty (Ed), Dune/Beach Interaction. J. Coastal Research Special Issue No. 3: 1-4.

Psuty, N.P., 2004. The coastal foredune: A morphological basis for regional coastal dune development. In: M. Martinez and N. Psuty (editors), Coastal Dunes, Ecology and Conservation. Ecological Studies v. 171. Springer-Verlag, Berlin: 11-27.

Shand, R.D., Bailey, D.G., Hesp, P.A., and Shepherd, M.J., 2003. Conceptual beach-state model for the inner bar of a storm-dominated micro/meso tidal range coast at Wanganui, New Zealand. Proc. Coastal Sediments '03, 5th Internat. Symp. on Coastal Engineering and Science of Coastal Sediment Processes, May 18-23, Clearwater Beach, Florida, USA. (CD-Rom).

Sherman, D.J. and Bauer, B.O. (1993) Dynamics of beach-dune interaction. Progress in Physical Geography 17: 413-447.

Sherman, D. J. and Lyons, W. (1994) Beach-state controls on aeolian sand delivery to coastal dunes. Physical Geography 15: 381-395.

Short, A.D., 1979. Three-dimensional beach stage model. J. Geology 87: 553-571.

Short, A.D., 1999. Wave-dominated beaches. In: Short, A.D. (Ed.), Handbook of Beach and Shoreface Morphodynamics: 173-203. J. Wiley and Sons Ltd.

Short, A.D. and Hesp, P.A. (1982) Wave, Beach and Dune interactions in South Eastern Australia. Marine Geology 48: 259-284.

Short, A.D. and Wright, L.D., 1983. Physical variability of sandy beaches. In McLachlan, A. and Erasmus, T. (Eds.) Sandy Beaches as Ecosystems. Junk, The Hague: 133-144.

Sonu, C.J., 1973. Three dimensional beach changes. Journal of Geology 81: 42-64.

Stive, M.J.F., deVriend, H.J., 1995. Modelling shoreface profile evolution. Marine Geology 126, 235– 248.

Stive, M.J.F., Cloin, B., Jimenez, J., Bosboom, J., 1999. Long-term cross-shoreface sediment fluxes. Proceedings Coastal Sediments '99. ASCE, New York, pp. 505– 518.

Van Rijn, L.C., Ruessink, B.G., and Grasmeijer, B.T., 1999. Generation and migration of nearshore bars under non-to macrotidal conditions. Proc. Coastal Sediments '99, ASCE: 463-478.

Wijnberg, K.M. and Kroon, A., 2002. Barred beaches. Geomorphology 48: 103-120.

Woodroffe, C.D., 2002. Coasts. Form, process and Evolution. Cambridge Univ. Press, 623pp.

Wright, L.D., Chappell, J., Thom, B.G., Bradshaw, M.P., and Cowell, P.J., 1979. Morphodynamics of reflective and dissipative beach and inshore systems, southeastern Australia. Marine Geokogy 32: 105-140.

Wright, L.D. and Short, A.D. (1984) Morphodynamic variability of beaches and surfzones: A synthesis. Marine Geology 56: 92-118.

DOI: 10.3990/2.169

Nearshore Physical Oceanography: Recent Trends and Future Prospects

D.A. Huntley
Marine Institute, Plymouth University, Drake Circus, Plymouth, Devon, PL4 8AA, UK, D.Huntley@plymouth.ac.uk

ABSTRACT

This paper reviews the evolution of nearshore physical oceanography over the past forty years. Over this period there have been enormous changes in the equipment, computing power and concepts used by nearshore physical oceanographers. The greatest change in observational equipment has been the development of remote sensing methods which are now providing spatial mapping of nearshore features and their temporal changes over time periods ranging from seconds to decades. The vast increase in computing power is also transforming the field from reliance on simplified analytical theories to comparisons with fully physical numerical simulations in realistic domains. Conceptually, the field has evolved from a Newtonian deterministic approach to a realization of the importance of the stochastic nature of the environment and of interactions between different aspects of the nearshore system.

INTRODUCTION

In this paper, I review, from a personal perspective, the evolution of nearshore physical oceanography over the past forty years, with a particular focus on identifying the major trends and continuing weaknesses, and trying to identify future prospects.

Enormous strides have been made over the past forty years in describing the nearshore physical environment, in understanding it and in making relevant predictions (or at least knowing the limitations of predictions) about future states. In order to survey these changes, it is useful to consider developments in three related areas: developments in equipment for observing the nearshore environment, developments in computing capacity available to the nearshore researcher and developments in concepts applied to the nearshore environment. These three areas are closely intertwined and complement each other in the evolution of our science, as we shall see.

Figure 1. Waiting for high tide. An EM flowmeter (the discus under my hand) and a pressure sensor (the 'pot' on the aluminum frame) deployed in 1972.

FORTY YEARS AGO

The year 1972 was an auspicious year for nearshore physical oceanography! In that year, Jurjen Battjes published a seminal paper [Battjes, 1972] on the influence of the spectral nature of waves on the set-up of the water level at the shoreline, revealing in a startling way that the 'traditional' simplification of monochromatic, unidirectional waves approaching beaches could get things badly wrong. For example, for longshore currents, he showed that the directional spread of incoming waves could reduce the forcing by a factor of two.

It was also the year when electromagnetic current meters (EMs) were placed in the nearshore zone to measure, for the first time directly, the currents under waves as they shoal and break at the shoreline [Huntley and Bowen, 1975; figure 1]. Pressure sensors had been used for some time (including Barber and Ursell's observations of wave energy generated by storms half way across the world in the southern hemisphere [Barber and Ursell, 1948] and Tucker's observations [Tucker, 1950] of 'surf beat' from measurements of wave pressures off Peranporth in Cornwall, UK) but the addition of an ability to measure wave currents provided opportunities to interpret the wave motion in terms of wave directions and even to distinguish between wave types such as incident waves and edge waves and to begin to map out the flow patterns in and beyond the surf zone.

The resulting records of currents were immediately very interesting. The time series shown in figure 2, taken on that first deployment of the EM current meter, show clearly the change in the nature of the currents across the nearshore zone towards the shoreline, from the expected (though peaked) waves offshore to dominant longer period oscillations close to the shoreline. Comparisons of measurements on a steep beach and a beach of shallow slope also revealed important differences. As is usually the case when a new method of observation becomes available, the new means of in situ observation of nearshore hydrodynamics prompted a new burst of activity and new understanding of nearshore wave dynamics.

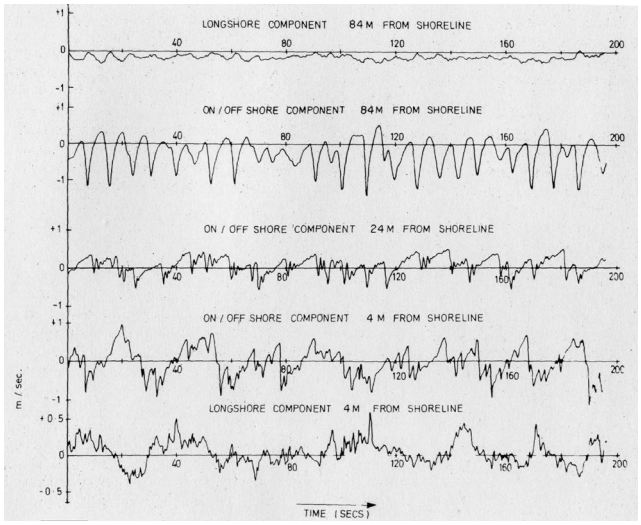

Figure 2. Current records from the first deployment of EM flow meters in the nearshore zone. The top two are the alongshore and cross-shore currents 84m from the shoreline, the third the cross-shore current 24m from the shoreline and the lowest two the cross-shore and alongshore currents 4m from the shoreline.

At the same time, the computing resources available to the researcher were growing rapidly but still very limited. The Institute where I worked in 1972 had only recently installed an IBM 1130 computer in a custom-built, air-conditioned room with a false floor to accommodate cabling. It boasted 64 kBytes of core memory and a punched card reader for data and program input. Apart from running embryonic 2D tidal models, its main role in nearshore physical oceanography was as a data analyzer. A data set from the EM current meters could be input from magnetic tape but the programs to analyze it came in the form of a box of punched cards. These were presented to the computer before going home in the evening and, with luck, resulted in a printout of results the following day. Of course, any errors in programming meant punching new cards and waiting a further day for new results (a great way to encourage careful programming the first time round!). By this slow process, spectra of the EM-derived currents could be produced and wave contributions at different frequencies separated.

But the limited computing resources had another, more interesting influence. It meant that the interpretation of the measurements remained largely constrained to highly simplified, generally analytical solutions to the basic hydrodynamic equations. Thus the background theory of edge waves leading the interpretation of the long-period motion observed in the currents close to the shoreline was based on assumptions of very small amplitude waves (similar to Airy theory of waves), simple cross-shore beach slopes (generally linear) and alongshore uniformity. Algorithms to compute the form of edge wave motion over arbitrary beach slopes (still alongshore uniform), and the realization that edge wave motion can be strongly sensitive to changes in cross-shore beach profile, didn't arrive for another six or so years. In the meantime, the knowledge that the simplified slopes were only an approximation provided a useful 'fudge factor' if the observations didn't quite fit the theory!

Forty years ago, the absence of sensors to measure short-term sediment response to waves, and the very limited role of computers in imposing realistic domains for wave motion, also meant that there was no challenge to the universal assumption that sediment moved in response to waves and currents and that any resulting patterns in beach morphology would reflect patterns in wave and current flow. Thus, the pursuit of edge waves in the natural environment was largely driven by an assumption that the form of cusps and nearshore bars reflected directly the flow patterns found in small amplitude edge waves over simple, unbarred topography.

This theoretical approach of relying on simplifications of the real physical environment and on simplifications of the basic hydrodynamic equations placed the field of nearshore physical oceanography forty years ago firmly in the 19th century tradition of reliance on analytical solutions to carefully chosen simplified situations. What was meant by increasing our understanding of the nearshore environment was centrally focused on linking observations to analytical solutions to simplified equation sets containing the key physical processes or processes responsible for given features. The underlying assumption was that if we got those processes right, the observed features would be 'explained' and potentially could be accurately predicted in a deterministic manner. As we will see, it is in this area of what we can expect as an 'explanation' for a phenomenon and the limits of predictability that the most radical, important and interesting changes have occurred over the last forty years.

THE CURRENT STATE OF THE ART

Let us now fast-forward to the present and see how the current state of the art compares to the situation forty years ago. Again here I will focus on the importance of equipment, computing and concepts as drivers of the radical changes that have occurred.

Developments in sensors

Of course, the first deployment of EM current meters was quickly followed by large-scale field campaigns where arrays of EM and other in situ sensors were deployed to measure the spatial structure of flows. The array of 42 sensors deployed over an area 520m long parallel to the shore and 500m offshore on Torrey Pines Beach, California in 1978 remains an outstanding example and allowed for the first time a clear demonstration of the expected spatial structure of long period edge waves [Huntley et. al. 1981], as well as providing data leading to a much better understanding of a whole range of nearshore processes, including the breaking of wave spectra [Thornton and Guza, 1983].

There have also been major advances in the development of sensors designed to measure sediment suspension by waves and currents. Point measurements by Optical Backscatter Sensors (OBSs) and acoustic sensors can now be complemented by acoustic sensors able to profile the suspended sediment concentrations over a range of depths. These sensors provide valuable insight into the complexities of sediment response to hydrodynamic drivers and have to some extent acted as constraints on the bewildering array of sediment transport algorithms on offer. It is probably fair to add, however, that this is still work in progress and a number of important factors remain unresolved. Chief amongst these factors are the difficulty of allowing for the strong dependence of sensor response on the size (and form, in the

case of fine, flocculated sediments) of sediment particles, the need for very fine vertical resolution of the concentration profile close to the seabed, where concentrations are highest and the hydrodynamic regime most complex (see Austin and Masselink, [2008], for an example of the current state of the art) , and the failure to date to find a workable means of measuring bedload transport at the seabed itself. Until these factors are better addressed our ability to improve our understanding of sediment transport under the full range of natural nearshore conditions remains limited.

More successful has been the development of sensors to monitor the evolution of bedforms in the nearshore zone. Acoustic sensors can now provide quantitative measurements of variations in bed elevation, including ripples and small sand waves [e.g. Austin et al. 2007] and are changing our perception of the nature of the seabed in the nearshore zone, not least in showing that bedforms persist even in the energetic surf zone.

The greatest recent advance in sensors for nearshore physical science has undoubtedly been in the development of methods of remote sensing of substantial areas of the nearshore zone. Most influential has been the Argus video-imagery system [Holman and Stanley, 2007], well known to anyone working in the field. The Argus system was originally set up to obtain maps of the locations and 2D-horizontal shapes of submerged nearshore bars through the breaking pattern over the shallower water over bars. The resulting time series showing the evolution of bars in response to forcing by offshore wave over periods of a year or more have been hugely influential in changing our perspective on bars, their dynamics and the processes responsible for forming them. In particular, the iconic 'movie' of a year in the life of bars on Palm Beach, Australia, produced by Rob Holman and his group at Oregon State University, could reasonably be called 'paradigm-changing' in its influence on the research community. No longer could simple ideas of a bar being the product of a single edge wave field be sustained; the temporal and spatial variability of the observed bars was clearly much more complex and there were strong hints that the evolution of bars depends as much on pre-existing conditions as on the immediate forcing by waves.

Further development of the Argus technology has now led to its use not only for spatial mapping of topography, which can now include quantitative estimates of water depths as well as horizontal shapes (figure 3), but also for estimation of wave directional spectra, wave refraction and nearshore currents [Holman and Stanley, 2007].

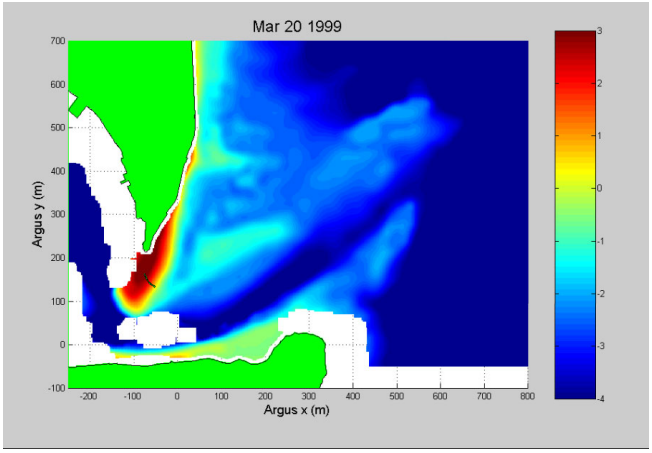

Figure 3. Bars at Teignmouth, Devon, UK. The bed elevations are given by the color bar to the right. These contours are derived from Argus images over several tidal cycles. With acknowledgement to Dr Kenneth Kingston, Plymouth University.

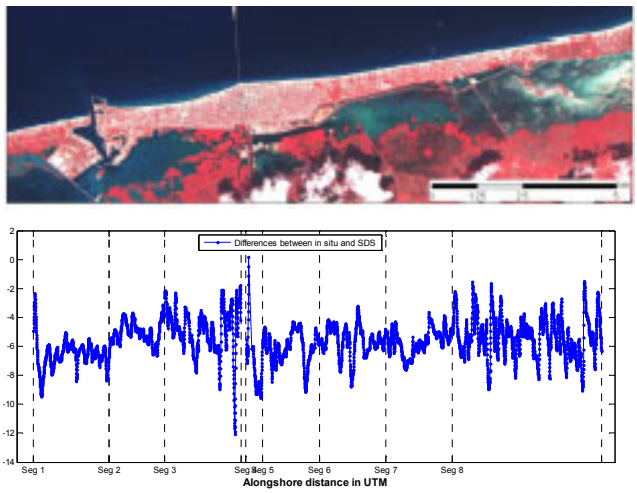

Figure 4. Upper panel: Satellite image of the northern coast of Yucatan, Mexico. Lower panel: The difference in position (meters) between the satellite-derived shoreline and the shoreline measured in situ using GPS. With acknowledgement to Gabriela Garcia Rubio, Plymouth University.

Satellites are also coming into use for evaluating nearshore processes, in particular showing their value in mapping, over large spatial scales, trends in shoreline erosion or accretion. Figure 4 shows an example of the accuracy of a satellite-derived shoreline along the north shore of the Yucatan Peninsula, Mexico, based on images from the SPOT satellite. The comparison with in situ measurements of the shoreline changes is very encouraging and confirms that the technique has great promise, particularly for regions with little or no other data on shoreline change.

By mapping, often in great detail, the spatial structure and temporal variation of nearshore morphology over a wide range of timescales, these new remote sensing techniques force the science of nearshore physical oceanography to confront the complexities of the real situation and expose the inadequacies of the simplified ideas which dominated the field forty years ago. Interpretation in terms of analytical solutions to greatly simplified scenarios no longer provides a satisfying explanation of the observed features. Fortunately, however, the concurrent development of computing power means that the need to rely on simplified cases is diminishing, as we show in the next section.

Developments in computing

It hardly needs to be said that computers have now come to dominate almost all aspects of life, not least in science. In our field, whereas forty years ago a computer was a tool for forecasting relatively simple hydrodynamic features such as tides and surges and for analyzing (slowly!) digital data from sensors, today computers impinge on almost all aspects of nearshore physical oceanography. In particular I want to emphasize three areas where computers have made, and continue to make, major changes to the pursuit of our science. Firstly computing power is

now such that it can handle many of the complexities of the full equations of wave motion within realistic computational domains, thus removing the need for simplifying assumptions and simplified physical domains. Secondly it can be used to investigate the influence of complex, stochastic, boundary forcing and thus assess the predictability of the nearshore system. Thirdly it can include interaction between different features of the nearshore zone (waves and longshore currents; waves and nearshore circulation; waves and 2D topography and so on). Some examples of each of these areas will be given in this section.

Forty years ago, the numerical description of waves in the nearshore zone was generally limited to Airy theory, based on assuming sinusoidal waves with a single period and wavelength, and of a height much smaller than either the wavelength or the water depth. Today, computing power is beginning to allow computation of random wave shoaling and breaking using the full 3D Navier-Stokes equations, the only simplification being in the parameterization of turbulence by Reynolds averaging. These Reynolds-averaged Navier-Stokes (RANS) models can include all of the influences of realistic wave heights, non-linear wave distortion and wave breaking with none of the empirical input required by less complete models.

To date, application of RANS models to shoaling and breaking waves has been limited to shore-normal wave propagation with alongshore uniformity. The first such simulation was by Lin and Liu [1998] who successfully simulated 20s of data from a single breaking wave in the laboratory and this was followed by a simulation by Chopakatia et al. [2008] of wave propagation and breaking over the barred beach at Duck, North Carolina during the 1990 Delilah experiment. They simulated a 35.5 minute period, driving the outer boundary 800m offshore with measured wave time series. The results are generally good, with wave heights predicted with rms errors of around 0.04m and mean flows well predicted given the model assumption of alongshore uniformity. Wave breaking is directly included in RANS models and was identified in the model of Chopokatia et al. [2008] as the region where the maximum kinetic energy of turbulence exceeded a chosen threshold, with good agreement with observed breaking patterns in the field.

The computational requirements of RANS models will continue to limit their direct application to nearshore problem for some time to come, but their use to test different empirical parameterization used in simpler, less computer-intensive models has been demonstrated by Fuhrman et al. [2009] and Ruessink et al. [2009], who both tested the relative sensitivity of sediment transport under waves to the influences of wave height, velocity skewness, asymmetry and other variables, coming, intriguingly, to different conclusions about which influences are dominant!

Of more immediate value to the prediction of nearshore wave conditions are models which include non-linear effects but in simplified forms. Boussinesq theory relaxes the Airy theory assumption of infinitesimally small wave heights compared to water depth and wavelength and has been the subject of intensive research over the past forty years or more (for a review, see Huntley, in press]. Boussinesq models can now accurately model the propagation of waves from deep water right into the surf zone and in 2D domains, provided the slope of the seabed is small. These models do not inherently include wave breaking, which must be introduced empirically and there is still no consensus about how best this can be done [Cienfuegos et al., 2010] Nevertheless, modern Boussinesq models can accurately simulate the heights of shoaling and breaking waves over 2D topography and include the skewness and asymmetry effects known to be vital to sediment transport. The focus now needs to shift to testing and tuning these models for nearshore sediment transport and morphological modeling.

As waves move into very shallow water, the assumptions of Boussinesq theory break down and the Nonlinear Shallow Water Equations (NSWE) become more relevant. As with Boussineq theory, these equations have been the subject of important recent developments [Brocchini and Dodd, 2008].

Remarkably, however, despite these developments, Airy theory continues to dominate practical methods for predicting nearshore wave conditions, despite the fact that nearshore waves generally grossly violate the assumptions of Airy theory, most obviously by having wave heights comparable to water depths and to wave wavelengths! This is in part explained by the fact that measurements have shown that Airy theory still provides a reasonable quantitative description of many features of nearshore waves (e.g. the relationship between wave height and wave currents; Guza and Thornton [1980]). Where Airy theory fails, empirical parameterizations can generally be patched in to cover the deficiencies. For example, to describe wave breaking through the surf zone, the earliest parameterization was to assume that breaking wave height is a fixed fraction of the local water depth, but this has generally now been replaced by more complex empirical descriptions of wave breaking in terms of roller dissipation and energy conservation. These parameterizations can be tuned to match a particular feature of the nearshore wave field, for example wave height through the surf zone, but such tuning can produce non-physical results for other features, for example the fraction of breaking waves in the surf zone (figure 5).

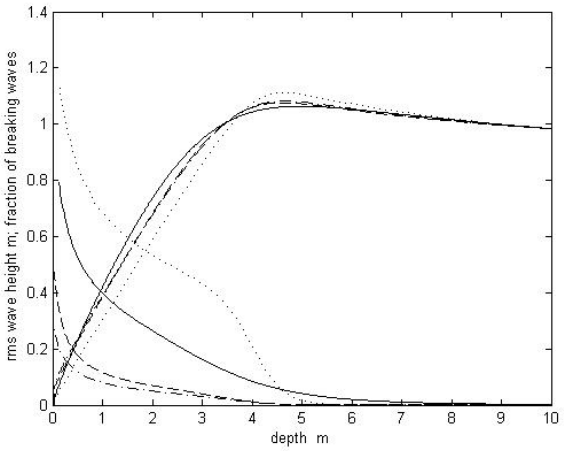

Figure 5. Predictions of shoaling and breaking of waves of 1m deep water height and period 10s propagating over a beach slope of 0.01, for four breaking wave models. The curves reducing towards zero as the depth decreases show the modeled rms wave heights and curves increasing as depth decreases show the fraction of breaking waves. Solid line: Thornton and Guza [1983]; Dashed line: Battjes and Janssen [1978]; Dashed-dotted line: Baldock et al. [1996]; Dotted line: Lippmann et al. [1996]. Note that, despite the good match of wave heights, the predictions of the fraction of breaking differ widely and can exceed one.

Nevertheless, the relatively small computational demands of wave models based on Airy theory mean that they continue to be the most used models in practice, despite their clear scientific limitations. The move to more sound physical models remains limited by computer power.

Whilst the move towards more complete physical models of nearshore waves is clearly valuable, another factor of equal, and arguably even more, importance is the fact that the forcing of a real nearshore system by incident waves is stochastic in nature. Random changes in the incoming wave field, whilst keeping integrated measures such as overall energy fluxes and directional spreads constant, can result in significant changes in the resulting response of the nearshore system. The possibility that system response might be sensitive to details of the incident forcing such as the sequence of varying wave heights (wave groupiness) and the chronology of storm-calm cycles, and that as a result predictability of future states in inevitably limited, has taken a surprisingly long time to enter the field of nearshore physical oceanography, particularly given that the seminal papers of Lorentz on non-predictability in meteorology were published as early as 1963 [Lorentz, 1963]. However the vastly increased computing power now makes it possible to make multiple model runs, each differing in the stochastic sequence of wave conditions, in order to assess sensitivities to this stochastic effect. Thus for example, de Vriend used an established morphodynamic model (Delft Hydraulics Unibest TC) to assess the sensitivity of bar evolution on the Dutch coast, over periods of 180 days and 10 years, to the chronology of storms incident on the coast (de Vriend: Presentation at NICOP Workshop, held at DHI, Copenhagen, June 1998). He concluded that the location and migration of the bars was relatively insensitive to stochastic variations but that the resulting bed elevations were chronology-dependent and therefore much less predictable. Similar conclusions were reached by Coco et al. [2001] in their model for beach cusps.

The third aspect of numerical modeling that is now possible with current computing power is the ability to consider directly the interaction between different features such as waves and currents and waves and evolving topography and there is no doubt that this has had a profound influence on our understanding of nearshore processes. Here I will focus on the interaction between waves and the resulting morphodynamic response, as an example of the implications of this aspect.

As previously mentioned, forty years ago, the universal assumption was that the hydrodynamics of the nearshore zone determined the morphological response which creates beach profiles, bars, channels and shoreline cusps. The starkest demonstration of the inadequacy of this approach came in 1993 with the publication by Werner and Fink [1993] of their self-organization model for beach cusps. A disarmingly simple model for the hydrodynamics of swash motion and an even simpler model for sand response were coupled so that changes in the morphology fed back directly to the hydrodynamic response. The result was the emergence, due to self-organization within the coupled system, of beach cusps with a marked degree of alongshore regularity and a wavelength in good agreement with those observed in the field. The cusps emerged without any pre-existing regular pattern in the flow field and thus the self-organisation model provided a completely different 'explanation' for cusps than the edge wave forcing model which had previously held sway. Subsequent detailed comparisons between observations and the self-organization model [Coco et al. 2000, 2001, 2003] have confirmed that the self-organization model is able to simulate a wide range of observed cusp characteristics, including growth to a quasi-equilibrium size and the observed variability in the alongshore spacing. It is now generally agreed that edge waves are not required for cusps to emerge and that they play only a minor role if they are present [Coco et al. 2001; Dodd et al., 2008].

Coupling between hydrodynamic and morphodynamic equations also plays a key role in the model used by Reniers et al. [2004] to simulate rip currents on an embayed beach. Their model produces a range of quasi-regular rip channels which are self-organizing when the incident waves have no directional spread but become primarily forced by quasi-steady flows generated by incident wave groups as the directional spread increases. Again, no correlation with simple edge wave wavelengths was found.

The success of the self-organization model of Werner and Fink [1993] is particularly extraordinary because of the simplicity of the hydrodynamic and sediment dynamic algorithms used. It appears that, at least for self-organized systems, inclusion of the feedback between water and sediment movement is overwhelmingly more important than getting details of the physics of either the water or sediment movement correct. This observation has led to a wide range of so-called 'abstracted models' which attempt to simulate a variety of nearshore (and other) morphological features (see Huntley et al. [2006], for a review). A major advantage of such models is that their demands on computational resources are relatively small so can be run many times with stochastically different forcing to provide an assessment of the intrinsic variability in their coupled systems.

Developments in concepts

The previous two sections have shown that the dramatic increase in resources available to the nearshore physical oceanographer have led to similarly dramatic changes in the way in which nearshore processes are perceived. Forty years ago the nearshore system was perceived through linear, Newtonian deterministic eyes, with hydrodynamic behavior decoupled from topographic response and a highly simplified view of incident wave forcing (typically unidirectional, monochromatic waves) and highly simplified descriptions of nearshore domains. The result was that an 'explanation' for any particular behavior was typically couched in terms of agreement with analytical solutions of simplified theoretical models which best fitted the limited observations available. We now have a much greater ability to observe large areas of nearshore systems and to track their evolution over a range of time scales. We can also now model numerically much more realistic computational domains with much more realistic physical processes. The result is a shift from explaining observations in terms of simplified, analytical results towards explanations based on agreement with numerical model outputs. Where models include details of the expected physical processes acting on the system, such an explanation might be in terms of the relative importance of the different physical processes which are included. For the highly simplified 'abstracted' models, however, emerging self-organized features are 'explained' by the strong coupling and feedback included in the model rather than any particular physical process, an interesting and fundamental change in perception of the meaning of 'explanation'!

There is also a much greater (though perhaps still not universal) appreciation of the intrinsic limits to the predictability of the nearshore environment. As we have seen, some features (for example some mean length scales of morphological features) have been found to be relatively insensitive to the stochastic nature of wave forcing but others (for example the bed elevations associated with morphological features) are much more unpredictable. The need to address such limits to predictability is also an important recent conceptual change.

FUTURE PROSPECTS

This brief and personal view of the evolution of nearshore physical oceanography over the past forty years does suggest some trends which might be expected to continue and develop into the future.

In terms of equipment development, notwithstanding the insensitivity of many morphological features to details of sediment transport, there remains an outstanding need for better in situ sensors to measure sediment in motion in the nearshore zone. Sediment transport algorithms can currently only be tested against limited and incomplete data sets and are therefore uncertain and limited to narrow ranges of environmental conditions. It is unfortunately difficult to see where major advances are likely in this area of research but combinations of optical and acoustic techniques probably still form the best available approach. Remote sensing techniques for the nearshore environment are also still being developed and will continue to be central to the development of research in the future.

It is obvious that numerical modeling will continue to increase in importance for providing explanations and predictions of nearshore behavior. However there are several directions that use of increased computing power could go. Improving the physical description of relevant physical processes will take up more computing time. For example have seen that there is a hierarchy of available numerical models for nearshore waves and it is clearly desirable to move increasingly towards those which include better, less empirical, descriptions of fundamental processes. Alternatively any increase in computing power could be used to improve the coupling between nearshore features. As we have seen, it is now clear that coupling between hydrodynamics and morphological response is vital if at least some nearshore phenomena are to be properly understood and simulated. Coupled models however demand more computer time than decoupled models, either through the need for concurrent running of interacting equation sets or through the use of more complex equations. A third possibility would be to use additional computing power to assess sensitivity to the stochastic forcing that is the natural feature of a nearshore system. We have seen that some nearshore features are particularly sensitive to forcing characteristics such as the detailed form of incident wave groupiness or the chronology of storms.

Of course there is not a single best answer to the question of where increased computing power should be directed. The optimum approach will vary depending on the particular nearshore feature of interest and research will continue in all three directions. However, it is important to recognize that there is a choice to be made.

For example, the surprising success of abstracted models in reproducing many of the features of at least some quasi-regular morphological features in the nearshore zone (cusps, large-scale longshore bars, ripples, sorted bedforms) suggests that improvements in the physical processes should be included in the models only as they reveal deficiencies in simulating particular features. For beach cusps, for example, changes to the sediment transport algorithm are found to influence the rate at which cusps grow but have only a small influence on the length scales and equilibrium relief of the cusps. In this case use of computing power to investigate sensitivity to changing wave forcing and to pre-existing morphological conditions might be more appropriate.

Finally it is worth pointing out that models to simulate nearshore behavior have now developed to the point where they can begin to be used as research tools in their own right. We have already seen the example of the use of RANS models by Fuhrman et al. [2009] and Ruessink et al. [2009] to investigate the relative importance of different processes in determining the response of sediment to waves, with a view to providing better empirical descriptions for simpler models. Huntley et al. [2008] show how an abstracted model of ripples can be used to investigate how a ripple field responds (or not) to a change in the current field above them. It is likely that such numerical 'thought experiments' will be increasingly common in the future.

REFERENCES

Austin, M. J and G. Masselink (2008). The effect of bedform dynamics on computing suspended sediment fluxes using optical backscatter sensors and current meters. Coastal Eng. 55(3), 251-260.

Austin, M. J., G. Masselink, T. J. O'Hare and P. E. Russell (2007). Relaxation time effects of wave ripples on tidal beaches. Geophys. Res. Let. 34, L16606, doi:10.1029/2007GL030696

Baldock, T. E., P. Holmes, S, Bunker and P. van Weert (1998). Cross-shore hydrodynamics within an unsaturated surf zone. Coastal Engineering 34(3-4): 173-196

Barber, N. F. and F. Ursell (1948). The generation and propagation of ocean waves and swell: 1. Wave periods and velocities. Phil. Trans. Roy. Soc. London, Series A; Mathematical and Physical Sciences, 240 (824), 527-560.

Battjes, J. A. (1972). Set-up due to irregular waves. Proceedings of the 13th International Conference of Coastal Engineering. New York, ASCE

Battjes, J. A. and J. P. F. M. Janssen (1978). Energy loss and set-up due to breaking of random waves. 16th International Conference on Coastal Engineering, Hamburg, ASCE, New York.

Brocchini, M. and N. Dodd (2008). Nonlinear shallow water equation modeling for coastal engineering. Journal of Waterway, Port, Coastal and Ocean Engineering 134(2): 104-120

Chopakatia, S. C., T. C. Lippmann and J. E. Richardson (2008). Field verification of a computational fluid dynamics model for wave transformation and breaking in the surf zone. Journal of Waterway, Port, Coastal and Ocean Engineering 134(2): 71-80.

Cienfuegos, R., E. Barthelemy and P. Bonneton (2010). Wave-breaking model for Boussinesq-type equations including roller effects in the mass conservation equations. Journal of Waterway, Port, Coastal and Ocean Engineering 136(1): 10-26.

Coco, G., T. K. Burnet, B. T. Werner and S. Elgar (2003). Test of self-organisation in beach cusp formation. J. Geophys. Res., 108(C3), 3101, doi: 10.1029/2002JC001496.

Coco, G., D. A. Huntley and T. J. O'Hare (2000). Investigation of a self-organised model for beach cusp formation and development. J. Geophys. Res. 105, 21,991-22,002.

Coco, G., D. A. Huntley and T. J. O'Hare (2001). Regularity and randomness in the formation of beach cusps. Marine Geology 178: 1-9.

Dodd, N., A. Stoker, D. Calvete and A. Sriariyawat (2008). On beach cusp formation. Journal of Fluid Mechanics 597: 145-169.

Fuhrman, D. R., J. Fredsoe and B. M. Sumer (2009). Bed slope effects on turbulent boundary layers: 2. Comparison with skewness, asymmetry and other effects. Journal of Geophysical Research-Oceans 114(C03025).

Guza, R. T. and E. B. Thornton (1980). Local and shoaled comparisons of sea surface elevations, pressures and velocities. Journal of Geophysical Research 85(C3): 1524-1530.

Holman, R. A and J. Stanley (2007). The history and technical capabilities of Argus. Coastal Engineering, 54 (6-7), 477-491.

Huntley, D. A. (in press). Nearshore Processes: Waves. in.: Shroder, I. (Ed-in chief), Sherman, D. (Ed.) Treatise on Geomorphology. Academic Press, San Diego. Vol. 10.

Huntley, D. A. and A. J. Bowen (1975). Comparison of the hydrodynamics of steep and shallow beaches. Chapter 4 in: Nearshore Sediment Dynamics and Sedimentation. Hails, J and Carr A. (Eds). John Wiley and Sons, London.

Huntley, D. A., G. Coco and T. J. O'Hare, (2006). Abstracted modelling as a tool for understanding and predicting coastal morphodynamics. J. Coastal Res. SI49, 21-27. Proceedings of ICS2004, Itajai, Brazil.

Huntley, D. A., Coco, G., K. R. Bryan and A. B. Murray. (2008). Influence of "defects" on sorted bedform dynamics. Geophys. Res. Let. 35, L02601. doi: 10.1029/2007GL030512

Huntley, D. A., R. T. Guza, and E. B. Thornton. (1981). Field observations of surf beat, 1. Progressive edge waves. Journal of Geophysical Research 86(C7): 6451-6466.

Lin, P. and P. L. F. Liu (1998). A numerical study of breaking waves in the surf zone. Journal of Fluid Mechanics 359: 239-264.

Lippmann, T. C., A. H. Brookins and E. B. Thornton (1996). Wave energy transformation on natural profiles. Coastal Engineering 27: 1-20

Lorentz, E. N. (1963). Deterministic non-periodic flow. J. Atmos. Sci. 20, 131-141.

Reniers, A., E. B. Thornton and J. A. Roelvink (2004). Morphodynamic modeling of an embayed beach under wave-group forcing. Journal of Geophysical Research 109(C01030).

Ruessink, B. G., T. J. J. van den Berg and L. C. van Rijn (2009). Modeling sediment transport beneath skewed asymmetric waves above a plane bed. Journal of Geophysical Research-Oceans 114(C11021)

Thornton, E. B. and R. T. Guza (1983). Transformation of wave height distribution. Journal of Geophysical Research 88(C10): 5925-5938

Tucker, M. J. (1950). Surf beats: Sea waves of 1 to 5 min. period. Proceedings of the Royal Society Series A 202: 565-573

Werner, B. T. and T. M. Fink (1993). Beach cusps as self-organised patterns. Science 260: 968-971.

Hendrik Antoon Lorentz and the problem of the Zuiderzee tides

A.J. Kox

Paper confidential

NCK photo competition

Luca van Duren: Diatomees on the Wad

DOI: 10.3990/2.170

Bio-physical linkages in coastal wetlands – implications for coastal protection

I. Möller
Cambridge Coastal Research Unit, Department of Geography, and Fitzwilliam College, University of Cambridge, CB2 3EN, Cambridge, UK, iris.moeller@geog.cam.ac.uk

ABSTRACT

Coastal wetlands have, for many decades, fascinated ecologists and geomorphologists alike. The existence of terrestrial vegetation communities in highly saline and hydraulically extremely dynamic environments has provided an ideal opportunity to study both ecological adaptation mechanisms to physical stressors as well as the importance of vegetation to landform evolution. In recent years, however, the importance of understanding the linkages between the biological and physical factors that control coastal wetland functioning and evolution has been brought into focus within the conservation, engineering, and policy sector. This is largely the result of a rising awareness of the value of coastal wetlands resulting from the services they provide to society. Those services include their role as natural sea defenses, a role that is becoming increasingly significant in the context of ever increasing coastal population densities alongside environmental pressures (e.g. sea level rise and increasing storm frequencies) arising from climate change. This paper reviews how, over the past quarter of a century, advances in field, laboratory, and numerical modeling approaches have made particular inroads into the quantification of the sea defense role of coastal wetlands. It is becoming increasingly clear that the sea defense function itself is complex and highly context dependent. Although there is now an urgent need for improved ecologically-informed engineering solutions, these are unlikely to be successful without future research finding appropriate ways of scaling up hydraulically important parameters to the landscape scale and defining the physical and biological process thresholds that control the continued provisioning of the sea defense function of coastal wetlands in the face of potential extreme events and sea level rise.

INTRODUCTION

Coastal wetlands exist on most of the world's coastlines and their value has been brought to the attention of national and international conservation bodies through the recognition of the ecosystem services they provide [MEA, 2005; UKNEA, 2011]. While coastal wetlands have long been the focus of academic study, this recognition of their societal values, the increasing human pressures faced by, and climate change impacts on, these environments have been the catalyst for a stronger focus of coastal research on the linkages between biological and physical processes within coastal wetlands in recent years [Allen, 2000; Gedan et al., 2010; Spencer and Möller, 2012].

Coastal mangrove and saltmarshes provide a range of ecosystem services, with the UKNEA [2011] identifying particularly their provisioning (e.g. agricultural), climate regulatory (e.g. carbon sequestration [Chmura et al., 2003]), and hazard regulatory (e.g. flood defense and wave dissipation [Gedan et al., 2011] functions. Underpinning these particular functions are a range of 'supporting services', such as primary production, soil formation, water quality regulation, etc. [Beaumont et al., 2008]. The assessment (and quantification) of all of these functions requires a detailed understanding of bio-physical linkages within the wetland systems, but particular linkages become important with respect to particular services. The potential for individual services to exist in 'trade-off' relationships with other services must thus be kept in mind when focusing on any individual service.

This paper focuses on the importance of recent research into the bio-physical linkages within coastal wetlands, both saltmarshes and mangroves, for the assessment of the particular service of flood and storm protection. In doing so, several important bio-physical linkages that determine the continued existence of coastal wetlands in particular environmental contexts are only briefly highlighted, but the reader is referred to the wealth of existing literature that addresses these wider controls on saltmarsh/mangrove functioning [Allen, 2000; Allen and Pye, 1992; Woodroffe, 2002].

THE NATURE OF BIO-PHYSICAL LINKAGES IN COASTAL WETLANDS

Coastal wetlands exist in the upper intertidal zone, characterized by halophytic vegetation communities and regular tidal inundation. While saltmarshes and mangroves differ markedly in vegetation structure, landform development, and geographical distribution (mangroves being restricted to the tropics [Woodroffe, 2002]), both types of wetland typify what can be seen as the most fundamental bio-physical linkage: vegetation mediates the coastal morphodynamic principle linkage between hydrodynamics and sediment transport through its modification of water flow paths and currents and sediment provision, capture, and retention (Fig. 1). Within this general relationship, it is important to remember the fundamental difference in the time-scale over which biological controls operate (generally beyond the seasonal time-scale) compared to the time-scale of hydrodynamic processes (seconds (e.g. waves) to seasonal (spring-neap tidal cycles)). Thus, over short, instantaneous time-scales (waves and tidal current flows), the presence of biota plays a rather passive part (i.e. providing an obstruction to currents or waves), while over longer, lagged, geomorphological time-scales (> annual), it becomes an active component of the dynamic morphological evolution of the system

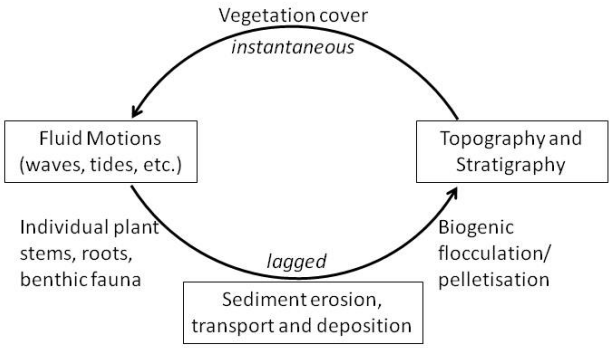

Figure 1. The influence of biota on the morphodynamic linkage between coastal morphology, fluid motions that interact with it, and sediment erosion, transport, and deposition [adapted from from Cowell and Thom, 1994].

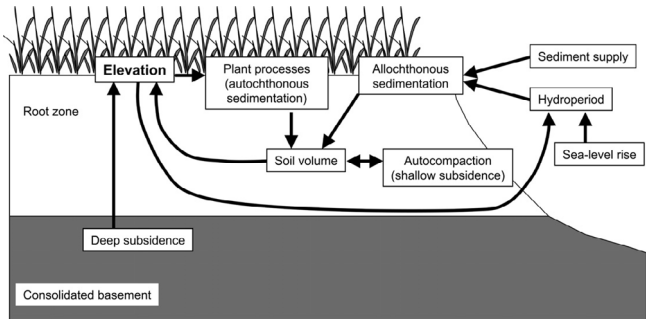

Figure 2. The range of biological and physical influences on the vertical adjustment of coastal marshes through surface sedimentation [French 2006 (adapted from USGS 1994)].

as a whole (i.e. contributing to landform evolution directly and indirectly (Fig. 1)).

A large body of literature exists that addresses these general bio-physical feedbacks in more detail, with arguably the greatest volume of work addressing the feedbacks involved in controlling the wetland response to sea level rise. Here, the alteration of relative sea level through vertical growth of the marsh surface is facilitated by the dense vegetation cover decreasing flow velocities and turbulence upon inundation [see e.g. Christiansen et al., 2000; Leonard and Luther, 1995], as well as contributing organic material for marsh surface and sub-surface sedimentation [French, 2006] (Fig. 2).

Amongst other important insights, this body of work has highlighted that the multitude of bio-physical feedbacks that exist in wetland ecosystems operate on a vast range of time-scales and that time- and space- scales in wetland evolution are tightly linked as illustrated in Spencer and Möller's [2012] review of mangrove system functioning (Fig. 3). Furthermore, it has become increasingly obvious that the relationship between individual biological and physical parameters changes beyond certain, as yet largely undefined, process thresholds [Bouma et al., 2009; Koch et al., 2009; Morris et al., 2002].

THE SEA-DEFENSE ROLE OF COASTAL WETLANDS

The view that coastal wetlands act as important sea defenses has been voiced in the United States as early as the late 19th Century [Gedan et al., 2011], but more formal scientific study into the sea defense role did not begin until the mid-1970s [Wayne, 1976], since when there have been numerous field, laboratory, and numerical modeling studies on the topic [Anderson et al., 2011; Gedan et al., 2011]. Before discussing these approaches in more detail, it is useful to highlight that, bound up in discussions on the sea defense role of coastal wetlands is the common failure to recognize that the 'sea defense' function itself is highly complex. There are two aspects to this complexity:

First, there are a series of hydrodynamic processes against which 'defense' may need to be provided. These include, for example, elevated water levels during meteorological surges or river-flow induced estuarine floods (such as in the Mississippi Delta [Wamsley et al., 2009]), storm generated waves, boat generated waves (a common cause of erosion in Venice lagoon [Dabala et al., 2005]), or tsunami waves (e.g. the Asian Tsunami of 2005 [Tanaka et al., 2007]). Although the first two of these hydrodynamic coastal threats, elevated water levels and wind generated waves, often coincide, each of these processes is rather different in nature and interacts with the wetland's vegetation and morphological features differently. It is thus unfortunate that many discussions of the 'sea defense' function of coastal wetlands do not recognize that protection against one threat does not necessarily afford the same protection against another and that different wetland properties potentially become significant in relation to different threats.

Secondly, the provision of efficient 'sea defense' requires either the dissipation of hydrodynamic energy incident upon the shore and/or an increased resistance of the shore to damage from hydrodynamic energy impacts. Investigations into the sea defense function of coastal wetlands must thus address both those factors that determine the resistance of the wetland to erosion and those factors that determine the degree to which the wetland affects the hydrodynamic process that poses the threat. Looking at the sea defense function of coastal wetlands from both these perspectives highlights the location-specific nature of this function: even in situations with identical hydrodynamic threats, the resistance of one wetland to erosion may be much lower than that of another, thus resulting in one wetland providing a 'better' (longer lasting) sea defense service.

The complexity of the sea defense function of coastal wetlands has only been openly addressed in recent reviews on the subject [Shepard et al., 2011; Gedan et al., 2011], but its recognition means that the translation of the results from scientific studies that focus on only <u>one</u> element of the process (e.g. the effect of the vegetation-induced surface roughness on waves) cannot easily be translated into engineering guidelines that must consider the <u>full</u> sea defense functionality of a wetland.

In recognition of some of the points raised above, Shepard et al. [2011] divide the sea defense function of coastal wetlands into wave attenuation, shoreline stabilization, and floodwater attenuation. For the purposes of this review, the resistance of wetlands to incident hydrodynamic energy (shoreline stabilization) will not be discussed in detail, but the reader is referred to Shepard et al. [2011] and to the reviews on the geomorphology of coastal

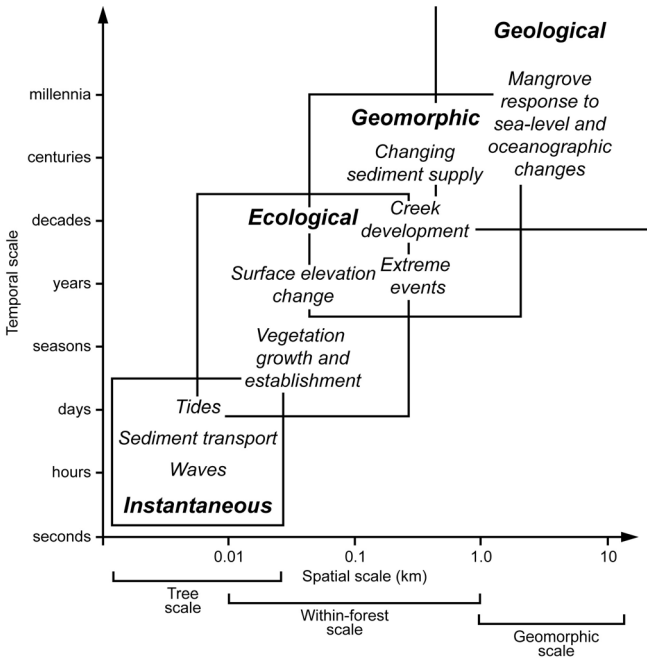

Figure 3. Time-space relationships of biological and physical processes within mangrove forest systems. Bio-physical linkages and feedbacks can be identified at a range of scales [from Spencer and Möller, 2012].

wetlands provided by Allen [2000], Woodroffe [2002], and Spencer and Möller [2012] and on the impact of extreme events on wetlands [Cahoon et al., 2006; Tanaka et al., 2007; Vermaat and Thampanya, 2006]. In view of the very different nature of tsunami waves compared to wind-generated waves, the sea-defense role of wetlands as discussed here is thus most sensibly split into: (i) flood control (water level regulation), (ii) wind wave dissipation, and (iii) mitigation of tsunami damage. The linkages between biological and physical factors vary widely with respect to each one of these three functions, necessitating their separate discussion.

Flood control

The flood control function of coastal wetlands concerns the impact that the existence and location of a coastal wetland can have on regional or local water levels during flood events. This function could also be described as 'water flow regulation' and its specific operation depends on the cause of the flood event.

Flow retardation over vegetated intertidal surfaces at the small, vegetation canopy scale, is well documented through field and laboratory studies. Leonard and Luther [1995], for example, showed that turbulent kinetic energy in *Juncus roemerianus* wetlands in Florida and *Spartina alterniflora* marshes in Louisiana was reduced by up to 65% of the original energy after a distance of only 3m. While water depths in those micro-tidal field sites were low (under 45 and 20 cm in the Florida and Louisiana sites, respectively), such evidence suggests that significant flow retardation occurs over vegetated intertidal surfaces, thus slowing/delaying the progression of tidal flows / meteorological surges.

Numerical modeling studies (see below) have largely confirmed such flow reduction effects over wetland surfaces, though they have also highlighted that this flow reduction effect can be complex, and may produce zones of higher flow within the canopy, as in Shi et al.'s [1996] study on flows within saltmarsh (*Spartina*) vegetation. Fonseca and Cahalan [1992] recorded significant flow reduction (40% over a 1m long test section) in seagrass beds, but observed a rapid reduction in flow reduction when water depth exceeded plant size. Plant height and alignment played an important role in controlling shear stress and current reduction in these experiments, but all laboratory studies indicate a strong interaction of the plants with the flow through hydrodynamic drag and the generation of turbulent eddies around the obstructions. In addition to plant height and alignment, stem density has proved to be of importance in determining shear velocities within the vegetated zone [Fonseca et al., 1982].

Within mangroves, evidence for such flow retardation at the landscape scale has been observed by Krauss et al. [2009] where, during two hurricanes, water levels were reduced by as much as 9.4cm/km across a mangrove area in Florida. Evidence for high friction effects on water levels is also provided by Wolanski et al. [1992], who report water surface slopes of up to 1m per 1000m distance on the ebb tide within mangroves, when seaward flows are reduced over the high friction vegetated surfaces. Once flows are restricted to the channel system within wetlands, ebb peak velocities may exceed flood peak velocities, thereby acting to maintain the channel system. This phenomenon has also been observed in saltmarshes [Bayliss-Smith et al., 1979].

In a general sense, estuarine studies have shown that the presence of high-friction intertidal surfaces leads to a modification of the progression of the tidal wave into and out of the estuary, such that, where friction is high, the landward increase in tidal high water is counteracted by tidal energy dissipation over those surfaces [Dyer, 1997]. By implication, the loss of such high friction surfaces can thus lead to an increase in tidal high water within the estuary, resulting in a heightened flood risk. Feedback relationships between tidal asymmetry and the transportation and deposition of sediment, however, clearly also operate in the reverse, where high friction surfaces lead to the capture of fine sediments around the flood and ebb slack water phases [Dronkers, 1986].

With respect to protection (water level regulation) during storm surges, the flow retardation over vegetated intertidal surfaces and channelization in the creeks within such surfaces has been incorporated into numerical storm surge models [Wamsley et al., 2010; Loder et al., 2009]. While such models suggest that wetlands have the potential to reduce elevated water levels during surges (*ca.* 1m reduction over 50-60km in the case of Louisiana wetlands), this effect has also been shown to be highly sensitive to bathymetry and wetland geomorphology, as well as individual storm characteristics [Wamsley et al., 2010]. Moreover, such models have also highlighted that, in certain circumstances, increases in surge elevations can result from increases in wetland elevations [Loder et al. 2009]. With respect to wetland morphology, Loder et al. [2009] identified the degree of marsh segmentation / fragmentation as being of particular importance to the landward conveyance of the surge. Table 1, adapted from Anderson et al. [2011] lists some of the findings of key field studies to date.

Table 1. Key field studies on wave dissipation over saltmarsh and mangrove vegetation [adapted from Anderson et al. 2011].

Author and year of study	Distance (m)	Dominant species	Wave height (or *energy*) reduction over distance
Wayne 1976	20	Spartina alterniflora	77% over first 10m, 66% over second 10m
Knutson et al., 1982	10	*Spartina alterniflora*	65% (*88%*)
Brinkman et al., 1997	150	Rhizophora spp.	(*50%*)
Möller et al., 1999	180	Mixed saltmarsh community (Limonium vulgare, Aster Tripolium, Atriplex portulacoides, Salicronia spp., Spartina spp., Suaeda maritima, Plantago maritima, Puccinellia maritima	61%
Möller and Spencer, 2002	163	Aster, Suaeda, Puccinellia, Salicornia, Limonium spp.	(*88%*)
	10	Aster, Suaeda, Puccinellia, Salicornia, Limonium spp.	(*43.8%*)
Möller, 2006	10	Spartina anglica, Salicornia spp.	15-20%
	10	Spartina anglica, Salicornia spp.	11-17%
	10	Salicornia spp.	10-12%
Mazda et al., 2006	100	*Sonneratia* spp.	(*50%*)
Quartel et al., 2007	100	Kandelia candel, Sonneratia sp., Avicennia marina	74%
Vo-Luong and Massel,2006	40		50% (*50%-70% over 20m*)
Lövstedt and Larson, 2010	5-14	Phragmites australis	4-5% per meter
Möller et al., 2011	4	Phragmites australis	(*17-72%*)

Wind wave dissipation

As mentioned above, on the time-scale of an individual inundation event, the bio-physical linkage between the vegetation of the coastal wetland and waves that travel across it, is one in which the vegetation elements act, to varying degrees, as passive obstructions to water currents. Progress in understanding the effect that such an obstruction has on the propagation of waves has been achieved through field, physical and numerical modeling.

Early field and modeling studies

The first published field study of wave height reduction over saltmarshes concerned wind waves of relatively small magnitude (< 5 cm) over short (10m) distances within a micro-tidal *Spartina alterniflora* marsh on the East coast of the United States [Wayne, 1976]. Average energy loss of 77 % and 66 % was recorded in that experiment over the two 10m long successive sections of the 20m long transect. No additional studies were published until Knutson's [1982] field experiment in which the dissipation of boat generated waves was observed over relatively short *S. alterniflora* marsh transects in Florida. The study by Knutson [1982] reported wave height reductions of, on average, 65% (88% wave energy loss) over 10m marsh surface for waves up to 17cm in height. In the UK, basic physical model experiments with assumed additional friction effects over plywood models of seawalls fronted by 'marsh' (berms) suggested that an 80m wide macro-tidal saltmarsh platform (with a 2m high steep seaward 'cliff' and inundation depths of 2m above the platform) would reduce incident deep water wave heights of 1.75m to less than 0.8m at the landward end of the platform [Brampton, 1992]. These early results, based on very specific assumptions about marsh configuration and hydrodynamic conditions, were promptly used by the UK Environment Agency to estimate cost savings on sea walls with fronting saltmarsh, but Table 1 illustrates that estimates based on one individual study must be treated with extreme caution, due to a high spatial and temporal variability within the wave dissipation process.

None of the above early studies considered the effect of varying water depths, varying incident wave conditions, or vegetation type, or indeed, with the exception of the physical scale model of Brampton [1992], included any comparison with unvegetated surfaces in a similar setting. Brampton's model, however, remained untested against field data in macro-tidal marsh settings until the studies of Moeller et al. [1996] and Möller et al. [2002] produced field measurements over macro-tidal marshes on the North Norfolk and Essex coast of the UK. This field data showed good agreement with the model of Brampton: a marsh edge cliff producing a rapid, localized, shoaling of waves, followed by rapid attenuation over the vegetated marsh surface (Fig. 4).

Geomorphological and hydrodynamic contexts

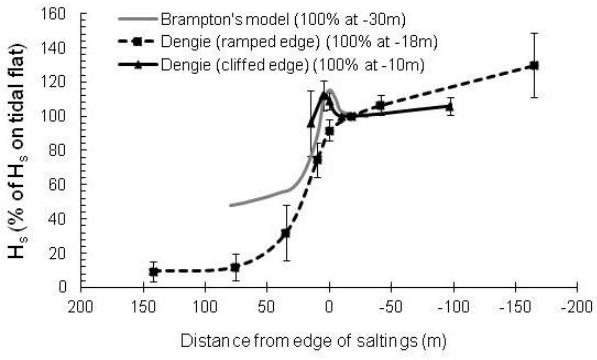

Figure 4. Comparison of wave height reduction along shore-normal transect from right to left: unvegetated tidal flat (negative distances) across the wetland margin (zero distance) and onto the vegetated marsh (positive distances); for model of Brampton [1992] and field data of Möller and Spencer [2002] (see text).

Both Brampton's model and the Essex coast (Dengie, UK) [Möller et al., 2002] field data set show that, when encountering a cliffed marsh edge, wave height temporarily increases over the submerged cliff, before undergoing a rapid decline, while ramped marsh edges exhibit a smoother, but rapid, reduction in wave energy landward of the marsh edge (Fig. 4), highlighting that wave dissipation over wetland surfaces is a process that is significantly affected by what might be called 'meso-scale morphological variations'. Such variations include the occurrence of morphological features such as cliffs, mud-mounds, tidal creeks, and salt-pans, all of which cause wave refraction, shoaling, diffraction, and breaking, and thus wave energy reduction or transmission over distances of 1-100m [Möller et al., 2002]. Consideration of the effect of such features, however, continues to pose a challenge and is thus rare or absent in studies on wave attenuation over wetland surfaces.

Brampton's model and the field data from Dengie also suggested a rapid, non-linear reduction in wave energy landward of the marsh edge. As might be expected, given the rapid attenuation of the oscillatory wave motion with depth beneath the water surface, however, the data from Dengie shows that the nature of that decline appears to depend on water depth and incident wave energy conditions [Möller et al., 2002] (Fig. 5). A range of studies have followed a similar approach of recording wave dissipation along shore-normal transects in other field settings, e.g. in mangroves [Furikawa et al., 1997; Quartel et al., 2007] and micro-tidal reed bed settings [Lövsted and Larson, 2010; Möller et al., 2011; Möller et al., 2009] under a range of water depth and wave conditions. The review by Gedan et al. [2011], however, highlights that the relationship between wave dissipation, water depth, and incident wave energy remains anything but clear, with contradictory field evidence from different settings and types of vegetation. Aside from the more obvious distinction between fully submerged vegetation canopies (e.g. macro-tidal saltmarshes) and partially emergent vegetation (e.g. micro-tidal settings or mangroves), the varying structural characteristics of different species of vegetation (vertical structure, flexibility/stiffness, buoyancy, and canopy density) most likely explain this large variability in field measurement [Möller et al., 2011; Mazda et al., 2006].

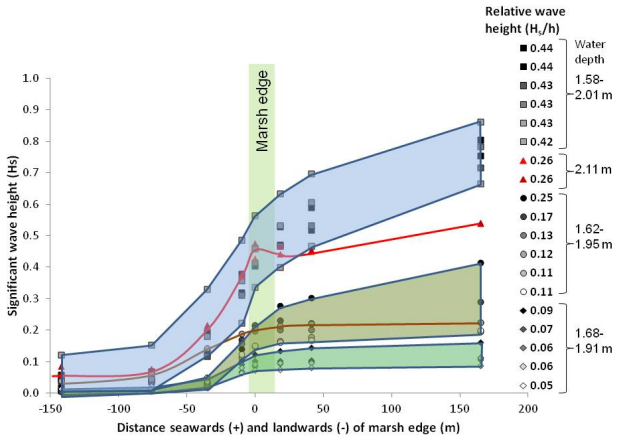

Figure 5. Wave height / water depth control on patterns of shore-normal wave dissipation across unvegetated tidal flat (right side) to vegetated marsh (left side of marsh edge); data from the ramped marsh at Tillingham, Dengie, UK.

The importance of vegetation characteristics

Field studies that explore the direct linkage between vegetation properties and wave dissipation are still few and far between, but separate studies clearly suggest variations in wave attenuation between species, with, in the case of mangroves, Brinkman et al. [1997], e.g., reporting a 50% reduction in wave energy over 150m of *Rhizophora* covered surfaces, while Mazda et al. [2006] suggest the same reduction over 100m of *Sonneratia* mangrove in similar conditions. In the case of mangroves, Mazda et al. [1997 and 2005] have also been able to capture the structural complexity of mangrove trees to a degree and relate the 'effective length scale' (L_E) (the ratio of the proportion of vegetation within a volume of water to the surface area of that vegetation projected into the flow direction) to tidal flow, but not wave, reduction in *Rhizophora* and *Bruguiera* mangroves.

In saltmarshes, Möller et al. [1999] reported seasonal variations in wave dissipation over the Dengie marshes, UK, for measurements made under similar hydrodynamic conditions. Such variations may be explained by seasonal changes in vegetation density, although no direct measurements of the latter were included in the study. Möller [2006] found indications of relationships between wave dissipation over short (20m) transects of *Salicornia*, *Spartina*, and a mixed canopy, and estimates of the projected area of vegetation obstructing wave-induced flow as derived from photographs of a strip of vegetation of known width taken horizontally against a background plate. In a more detailed field experiment, Neumeier and Amos [2006] found that 10-20% attenuation of wave orbital-velocities occurred in the denser part of a *Spartina* canopy below a height of about 30-40cm from the bed, where the lateral obstruction by the vegetation, as determined from horizontal photography and biomass estimates, became significant. The importance of vegetation stiffness to wave dissipation was aptly demonstrated by the flume experiments of Bouma et al. [2005] in which relatively stiff *Spartina* vegetation caused waves to be dissipated approximately three times as efficiently as the more flexible *Zostera* counterparts. Quantitative relationships between structural properties of wetland vegetation and wave dissipation under particular hydrodynamic conditions, however, are still lacking, though Feagin et al.'s [2010] report on structural measurements of a series of different coastal wetland plant species, provides a step in the right direction.

Vegetation does not necessarily reduce wave or tidal currents at the scale of individual vegetation elements. Furukawa et al. [1997], for example showed that individual mangrove stem and root elements are able to generate significant flow jets and eddies around them, with root-mean-square velocities within those jets equal to three times the mean flow velocity. Furthermore, anecdotal evidence reported from field observations suggests that, where present at low densities on eroding saltmarsh margins, individual saltmarsh plants can interact with incident waves in ways that enhance erosion at the small (plant) scale (Fig. 6(a)). Depending on the spacing between plants, such small scale erosion can then act to initiate large-scale erosion features, such as surface gullies that lead to creek bank mass failure (Fig. 6(b)). Feagin et al. [2009] identify similar effects with respect to roots on exposed marsh cliff sections.

Figure 6. (a) Individual Salicornia plants acting together with wave action as erosive agents, encouraging (b) larger scale erosion features and mass failure of creek bank sediments at Tillingham, Essex, UK (Photograph: I. Möller).

Controlled laboratory experiments

The recognition that the interaction between the orbital motion of surface waves and the vegetation present at the bed is complex and that this interaction depends on (a) hydrodynamic conditions and (b) vegetation properties has led to several authors investigating the phenomenon under controlled laboratory conditions, of which that of Bouma et al. [2005] has already been mentioned above. One of the key challenges in this context is the need to scale down the vegetation elements and/or hydrodynamic conditions within standard laboratory wave flumes. Thus, such studies have arguably contributed more towards understanding the nature of flow patterns around plant elements than the dependency of the process on vegetation canopy characteristics at the landscape scale, or on water depth and wave height variation.

Due to the physical size of mangrove plants, laboratory flume experiments with natural vegetation are restricted to saltmarsh, reed, or seagrass vegetation. Key studies include those of Fonseca and Cahalan [1992] on four species of seagrass common in the Gulf of Mexico, Coops et al. [1996a and 1996b] on emergent reed (Phragmites), and Tschirky et al.'s [2000] studies using *Scirpus americanus* vegetation typical of Great Lake wetlands. The seagrass study results indicate that the energy of waves (wave height < 0.05m) can be reduced by as much as 76 % over a 1m test section [Fonseca and Cahalan, 1992]. Plant density and water depth were identified as factors that control wave attenuation. Shoot density, however, appeared to be less influential than other factors such as plant morphology, flexibility and movement in affecting flow and wave reduction. Streamlining is important in reducing the area of the plant exposed to the flow and therefore the stress experienced by the plant.

Vegetation in Coops et al.'s [1996a] experiment was only partly submerged, but exposed to higher waves (0.23m). The results indicate much smaller reductions in wave height (< 29 %) than in the seagrass experiment although reductions were significantly higher on the vegetated areas than the unvegetated areas when the vegetation was fully developed. Coops et al. [1996a] also showed that the presence of vegetation can significantly reduce the amount of wave-induced erosion, although the amount of reduction in erosion depends on the type of species, substrate, and surface morphology.

In addition to the positive influence of high stem densities and the negative influence of high water depths on wave attenuation, Tschirky et al.'s [2000] study suggested, contrary to the field studies referred to above, that attenuation increased slightly under larger incident wave heights.

Other studies, such as those of Augustin et al. [2009] have used artificial vegetation, in this case cylindrical wooden dowels and polythene foam tubing. Although valuable for the validation of numerical models that assume a rather simplistic vegetation structure (see below), the limitations of such work become clear when considering the importance of plant flexibility and structure identified by field and flume studies with natural vegetation.

Numerical modeling

In the absence of field and laboratory observations during extreme water depth / wave energy events, when the capacity of wetlands to act as a sea defense becomes of greatest interest to coastal managers and engineers, numerical modeling offers one avenue to at least assess whether the fundamental physics of the process of wave attenuation by vegetation has been adequately understood theoretically and can be mathematically captured.

The numerical modeling of wave attenuation over wetland surfaces has to account for wave breaking in the reduced water depth and for drag and inertial forces around the vegetation elements. Wave energy dissipation due to wave breaking is largely a function of wave parameters (wave height, length, and period) and water depth (i.e., the morphology of the intertidal zone) and can be numerically approximated if these parameters are known. The drag and inertial forces induced by the 'rough' vegetation cover, however, are more difficult to parameterize. The correct representation of the biomechanics of the vegetation elements is clearly critical in this regard. While the representation of vegetation as simple vertical cylinders has been commonly adopted [e.g. Dalrymple et al., 1984; Dean and Bender, 2006] this is not always appropriate, in particular, where plant structure is complex (such as in the common North-west European saltmarsh species *Atriplex portulacoides*) or species are flexible (such as in the case of seagrass or kelp).

One of the earlier studies to recognize the importance of representing the swaying motion of submerged or partially submerged vegetation in wave transformation models is that by Knutson et al. [1982]. He incorporated an empirical drag coefficient, C_P, into his model, such that the rate of wave height

reduction from incident waves (H_0) to waves a certain distance (x) across the wetland can be expressed as a function of the bulk drag coefficient of the entire canopy (C_D), average plant stem diameter (d), average stem spacing (Δs), water depth (h), and incident wave height (H_0):

$$\frac{H}{H_0} = \frac{1}{1 + Ax} \quad (1)$$

Where:

$$A = \frac{C_P C_D d}{6\pi \Delta s^2 h} H_0 \quad (2)$$

Based on field measurements gathered by observing the reduction of boat generated waves over *Spartina alterniflora* marshes in Chesapeake bay, a value of 5 was determined for C_P as leading to the best prediction of observed attenuation. Most numerical approaches towards representing the interaction between plants and waves involve the incorporation of a plant-dependent drag coefficient of a similar nature (and its inverse relationship to the Reynolds number [see e.g. Asano et al., 1992]) and this approach has since been expanded by, for example, Mendez and Losada [2004] with validation and calibration against results from laboratory experiments with artificial kelp.

More recently, however, alternative algebraic model formulations suggest that, for highly flexible vegetation at least, the resistance resulting from the presence of a group of plant elements can be as much as four times that derived from a simple summation of the drag imposed by individual stems [Anderson et al., 2011].

Tsunami protection

Although mangroves have been thought to act as coastal protection in a more general sense, the Asian tsunami of 2004 caused much debate about their actual effectiveness as tsunami protection and the means by which this is achieved. Anecdotal evidence abounds as to the protection that was afforded by fringing mangrove areas to landward lying communities [Danielsen et al., 2005; Baird and Kerr, 2008], but the sudden and unpredictable nature of tsunami events as well as the large canopy size of mangrove forests makes this effect less easy to study by field and physical model approaches.

The long length and period and high velocity (430km, 37s, and 200 ms^{-1} in the case of the 2004 tsunami [Spencer, 2007]) mean that the impact of a tsunami wave on coastal vegetation differs significantly from that of storm generated waves or raised water levels under a meteorological surge. Such waves generate extreme wave run-up in very short periods of time upon arrival at the coast (up to 50m run-up above mean sea level (MSL) near the earthquake epicenter in Sumatra in 2004 [Spencer, 2007]).

Under such extreme hydrodynamic impact, mangrove vegetation itself can suffer significant damage (as it did in 2004 [see Dam Roy and Krishnan, 2005]) and, while, in the process of suffering this damage, water levels and flows may well be reduced, the destruction of the vegetation leaves the coast more vulnerable to high wave action than before the event. In addition, the debris created by mangrove destruction, interacts with the flow of water during the event, potentially blocking or diverting water flows. Teo et al. [2009], in their attempt to model the effect of mangrove vegetation on a tsunami, describe a two-fold approach of (i) increased drag (friction) as introduced by mangrove presence, and (ii) the effect of the mangrove in blocking the flow of water due to the specific 'porosity' of the mangrove forest. The likelihood of mangrove damage during the passage of a tsunami, however, creates a difficulty in modeling the sea defense function, as both friction and blockage effects are likely to change during an individual event.

Bearing these difficulties in mind, however, existing studies suggest that key controls on the efficiency with which mangroves attenuate tsunamis are bathymetry and coastal configuration and mangrove species (and species composition) [see Spencer and Möller, 2012]. Thus, Hiraishi and Harada [2003], for example, modeled a decrease in the maximum flow pressure (in N m^{-2}) with increasing mangrove tree density, using data from the 1998 tsunami in Papua New Guinnea.

FUTURE CHALLENGES

Much progress has been made in recent years on better understanding bio-physical linkages within coastal wetland systems. The disciplinary boundary between ecological studies into coastal wetland functioning and geological and geomorphological studies into landform evolution has become less divisive in the context of the growing recognition of ecosystem service provisioning by wetlands. An increasing number of studies now appreciate the tight linkage between the presence of vegetation and benthic fauna and the water and sediment fluxes through and across the wetland system. Arguably, two key challenges remain, however, regarding our understanding of how bio-physical linkages affect the sea defense function of coastal wetlands.

Firstly, there is the issue of scale-dependency of the varying marsh characteristics that determine coastal protection functions. At small spatial scales of 1-10m, the effect of wetland surfaces on wave dissipation, for example, can be understood as a function of parameters that can be recorded at discrete and distinct locations along the cross-shore profile (notably vegetation type, structure, and density, as well as water depth and incident wave energy). At larger spatial scales of 10-100m wave refraction and diffraction through surface topographical features (creeks and salt pans for example) are likely to become equally important or at least cannot be ignored. At those larger scales, however, it is still unclear how vegetation type, structure, and density might be most suitably parameterized and measured in practice (so as to link them to the wave dissipation effect), at least where vegetation cover is patchy and non-uniform. How best to aggregate those vegetation characteristics relevant to the wave dissipation function of coastal wetlands in patchy communities (such as those typical of mature, mixed European salt marsh communities) at the larger, marsh-wide, scale remains a fundamental challenge for future research.

Secondly, growing evidence from extreme events such as hurricanes in the Gulf of Mexico (in the case of surge and wave dissipation) and the Asian tsunami, illustrates the importance of the quantification of process thresholds or 'tipping points'. Such thresholds can be conceptualized as describing the switching from a system in which the biological elements act to mediate hydrodynamic energy (such as the reduction in surge elevations,

flow velocities, or wind generated waves) to one in which the presence of biological elements enhances the erosive impact of water flows (such as in sparsely vegetated marshes with high incident wave energy (Fig. 5) or where mangrove debris adds to the destructive impact of tsunami waves propagating inshore). Any serious incorporation of bio-physical linkages into coastal management plans requires some assessment of the likelihood with which such process thresholds may be exceeded within a given time frame and further research is thus required to identify where those process thresholds lie.

Thus, while much progress has been made in understanding bio-physical linkages in saltmarsh systems, for this knowledge to be used successfully in predictive models that evaluate the sea defense function of coastal wetlands for the purpose of its incorporation into coastal management approaches, progress in these two areas is now needed.

ACKNOWLEDGEMENT

This review and the thoughts expressed therein result from many years of research and this includes a range of research projects funded, amongst others, by the UK Environment Agency, The Royal Society, the Natural Environment Research Council (NERC), and the UK Department for the Environment and Rural Affairs (DEFRA). I am indebted to Dr T Spencer for collaboration on most of those projects and for fruitful discussions over the years. I am also grateful to Dr A McIvor for very useful short-notice comments on the text.

REFERENCES

Allen, J.R.L. (2000), Morphodynamics of Holocene saltmarshes, a review sketch from the Atlantic and Southern North Sea coasts of Europe, Quaternary Science Reviews 2000, 19,1155-1231.

Allen, J.R.L. and K. Pye (eds) (1992), Saltmarshes, Morphodynamics, conservation and engineering significance. Cambridge University Press, Cambridge.

Anderson, M.E., J. McKee Smith, and S.K. McKay (2011), Wave dissipation by vegetation. US Army Corps of Engineers. Note ERDC/CHL CHETN-I-82, 22pp.

Asano, T., H. Deguchi, and N. Kobayashi (1992), Interactions between water waves and vegetation. Proceedings of the 23rd International Conference on Coastal Engineering, ASCE, 2710-2723.

Augustin, L.N., J.L. Irish, and P. Lynett (2009), Laboratory and numerical studies of wave damping by emergent and near-emergent wetland vegetation, Coastal Engineering, 56(3), 332-340.

Baird, A.H., and A.M. Kerr (2008), Landscape analysis and tsunami damage in Aceh, comment on Iverson & Prasad (2007), Landscape Ecology, 23, 3–5.

Bayliss-Smith, T.P., R. Healey, R. Lailey, T. Spencer, and D.R. Stoddart (1979), Tidal flows in salt marsh creeks, Estuarine and Coastal Marine Science, 9, 235-255.

Beaumont, N.J., M.C. Austen, S.C. Mangi, and M. Townsend (2008), Economic valuation for the conservation of marine biodiversity, Mar. Poll. Bull., 56, 386–396.

Bouma, T.J., M.B. De Vries, G. Peralta, I.C. Tanczos, J. van de Koppel, and P.M.J. Herman (2005), Trade-offs related to ecosystem engineering, a case study on stiffness of emerging macrophytes, Ecology, 86, 2187–2199.

Bouma T.J., M. Friedrichs, B.K. van Wesenbeek, S. Temmerman, G. Graf, and P.M.J. Herman (2009), Density dependent linkage of scale-dependent feedbacks, a flume study on the intertidal macrophyte Spartina anglica, Oikos, 118, 260–268.

Brampton, A.H. (1992), Engineering significance of British saltmarshes. In: Allen, J.R.L., and K. Pye (eds) Saltmarshes. Morphodynamics, conservation and engineering significance. Cambridge University Press, Cambridge.

Brinkman, R.M., S.R. Massel, P.V. Ridd, and K. Furakawa (1997), Surface wave attenuation in mangrove forests. Proceedings, 13th Australasian Coastal and Ocean Engineering Conference, 2, 941–979.

Cahoon, D.R., P.F. Hensel, T. Spencer, D.J. Reed, K.L. McKee, and N. Saintilan (2006), Coastal wetland vulnerability to relative sea level rise, Wetland elevation trends and process controls. In Verhoeven, T.A., B. Beltan, R. Bobbink, and D.F. Whigham (eds), Wetlands and Natural Resource Management. Ecological Studies, 190, 271-292. Springer, Berlin.

Cahoon, D.R. (2006), A review of major storm impacts on coastal wetland elevations, Estuaries and Coasts, 29(6A), 889-898.

Chmura, G.L., S. Anisfeld, D. Cahoon, and J. Lynch (2003) Global carbon sequestration in tidal, saline wetland soils, Global Biogeochemical Cycles, 17, 1-12.

Christiansen, T., P.L. Wiberg, and T.G. Milligan (2000) Flow and sediment transport on a tidal salt marsh surface, Estuarine, Coastal, and Shelf Science, 50, 315-331.

Coops, H., N. Geilen, H.J. Verheij, R. Boeters, and G. van der Velde (1996a) Interactions between wave, bank erosion and emergent vegetation, an experimental study in a wave tank, Aquatic Botany, 53, 187-198.

Coops, H., and G. van der Velde (1996b) Effects of waves on helophyte stands, mechanical characteristics of stems of Phragmites australis and Scirpus lacustris, Aquatic Botany, 53, 175-185.

Cowell, P.J., and B.G. Thom (1994) Morphodynamics of coastal evolution. In: Carter, R.W.G., and C.D. Woodroffe (eds) Coastal evolution, late Quaternary shoreline morphodynamics, Cambridge University Press, Cambridge, 33-86.

Dabalà, C., N. Calace, P. Campostrini, M. Cervelli, F. Collavini, L. Da Ros, A. Libertini, A. Marcomini, C. Nasci, D. Pampanin, B.M. Petronio, M. Pietroletti, G. Pojana, R. Trisolini, L. Zaggia, and R. Zonta (2005), Water quality in the channels of venice, Results of a recent survey. In: Fletcher, C.A., and T. Spencer (2005), Flooding and Environmental Challenges for Venice and its Lagoon, Cambridge, Cambridge University Press, 617-630.

Dalrymple, R., J. Kirby, and P. Hwang (1984) Wave diffraction due to areas of energy dissipation, Journal of Waterway, Port, Coastal and Ocean Engineering, 10(1), 67-79.

Dam Roy, S., and P. Krishnan (2005), Mangrove stands of Andamans vis-a`-vis tsunami, Current Science, 89, 1800–1804.

Danielsen, F., M.K. Sørensen, M.F. Olwig, V. Selvam, F. Parish, N.D. Burgess, T. Hiraishi, V.M. Karunagaran, M.S. Rasmussen, L.B. Hansen, A. Quarto, and N. Suryadiputra (2005), The Asian tsunami, a protective role for coastal vegetation, Science, 310, 643.

Dean, R.G., and C.J. Bender (2006), Static wave setup with emphasis on damping effects by vegetation and bottom friction, Coastal Engineering, 53, 149-156.

Dronkers, J. (1986), Tidal Asymmetry and Estuarine Morphology, Neth. J. Sea Res., 20(2/3), 117–131.

Dyer, K.R. (1997), Estuaries, A Physical Introduction. John Wiley and Sons, London.

Feagin, R.A., J.L. Irish, I. Möller, W.M. Williams, R.J. Colon-Rivera, and M.E. Mousavi (2010), Short communication, Engineering properties of wetland plants with application to wave attenuation, Coastal Enginering, 58(3), 252-255.

Feagin, R.A., S.M. Lozada-Bernard, T.M. Ravens, I. Möller, K.M. Yeager, and H.H. Baird (2009), Does vegetation prevent wave erosion of salt marsh edges?, Proceedings of the National Academy of Sciences of the United States of America, 106(25), 10109-10113.

Fonseca, M.S., and J.A. Cahalan (1992), A preliminary evaluation of wave attenuation by four species of seagrass, Estuarine, Coastal and Shelf Science, 35, 565-576.

Fonseca, M.S., J.S. Fisher , J.C. Zieman , and G.W. Thayer (1982), Influence of the seagrass, Zostera maina L., on current flow, Estuarine, Coastal and Shelf Science, 15, 351-364.

French, J.R. (2006). Tidal marsh sedimentation and resilience to environmental change, exploratory modelling of tidal, sea-level and sediment supply forcing in predominantly allochthonous systems, Marine Geology, 235, 119-136.

Furukawa, K., E. Wolanski, and H. Mueller (1997), Currents and sediment transport in mangrove forests, Estuarine, Coastal and Shelf Science, 44, 301-310.

Gedan, K.B., M.L. Kirwan, E. Wolanski, E.B. Barbier, and B. Silliman (2010), The present and future role of coastal wetland vegetation in protecting shorelines, answering recent challenges to the paradigm, Climate Change, 106, 7-29. doi, 10.1007/s10584-010-0003-7.

Hiraishi, T., and K. Harada (2003), Greenbelt tsunami prevention in South Pacific region, Available from, /eqtap.edm.bosai.go.jp/useful_outputs/report/hiraishi/data/papers/greenbelt.pdfrS.

Knutson, P.L., R.A. Brochu, W.N. Seelig, and M. Inskeep (1982), Wave damping in Spartina alterniflora marshes, Wetlands, 2, 87-104.

Koch, E.W., E.B. Barbier, B.R. Silliman, D.J. Reed, G.M.E. Perillo, S.D. Hacker, E.F. Granek, J.H. Primavera, N. Muthiga, S. Polasky, B.S. Halpern, C.J. Kennedy, C.V. Kappel, and E. Wolanski (2009), Non-linearity in ecosystem services, temporal and spatial variability in coastal Protection, Front Ecol Environ 2009, 7(1), 29–37, doi,10.1890/080126

Krauss, K.W., T.W. Doyle, T.J. Doyle, C.M. Swarzenski, A.S. From, R.H. Day, and W.H. Conner (2009), Water level observations in mangrove swamps during two hurricanes in Florida, Wetlands, 29(1),142-149.

Leonard, L.A., and M.E. Luther (1995), Flow hydrodynamics in tidal marsh canopies, Limnology and Oceanography, 40 (8), 1474-1484.

Loder, N.M., J.L. Irish, M.A. Cialone, and T.V. Wamsley TV (2009), Sensitivity of hurricane surge to morphological parameters of coastal wetlands, Estuarine, Coastal, and Shelf Science, **84(4), 625-636.**

Lövstedt, C.B., and M. Larson (2010), Wave damping in Reed, Field measurements and mathematical modelling, Journal of Hydraulic Engineering, 136(4), 222-233.

Mazda, Y., D. Kobashi, and S. Okada (2005), Tidal scale hydrodynamics within mangrove swamps, Wetlands Ecology and Management, 13, 647–655.

Mazda, Y., M. Magi, Y. Ikeda, T. Kurokawa, and T. Asano (2006), Wave reduction in a mangrove forest dominated by Sonneria sp, Wetlands Ecology and Management, 14, 365–378.

Mazda, Y., E. Wolanski, B. King, A. Sase, D. Ohtsuka, and M. Magi (1997), Drag force due to vegetation in mangrove swamps. Mangroves and Salt Marshes, 1, 193–199.

MEA (Millennium Ecosystem Assessment) (2005), Ecosystems and Human Wellbeing, Synthesis, Island Press, Washington, DC.

Méndez, F.J., and I.J. Losada (2004), An empirical model to estimate the propagation of random breaking and nonbreaking waves over vegetation fields, Coastal Engineering, 51(2), 103-118.

Moeller, I., T. Spencer, and J.R. French (1996), Wind wave attenuation over saltmarsh surfaces, Preliminary results from Norfolk, England, Journal of Coastal Research, 12(4), 1009-1016.

Möller, I. (2006), Quantifying saltmarsh vegetation and its effect on wave height dissipation, results from a UK East coast saltmarsh, Journal of Estuarine, Coastal, and Shelf Sciences, 69(3-4), 337-351.

Möller, I., T. Spencer, J.R. French, D.J. Leggett, and M. Dixon (1999), Wave transformation over salt marshes, A field and numerical modelling study from North Norfolk, England, Estuarine, Coastal and Shelf Science, 49, 411-426.

Möller, I., T. Spencer, and J. Rawson (2002), Spatial and temporal variability of wave attenuation over a UK East-coast saltmarsh, Proceedings of the 38th International Conference on Coastal Engineering, Cardiff, July 2002.

Möller, I., J. Lendzion, T. Spencer, A. Hayes, and S. Zerbe (2009), The sea-defense function of micro-tidal temperate coastal wetlands, In: Brebbia, C.A., G. Benassai, and G.R. Rodriguez (eds), Coastal Processes, WIT Transactions on Ecology and the Environment, 126, 51-62.

Möller, I., J. Mantilla-Contreras, T. Spencer, and A. Hayes (2011), Micro-tidal coastal reed beds, Hydro-morphological insights and observations on wave transformation from the southern Baltic Sea, Estuarine, Coastal and Shelf Science, 92(3), 424-436.

Morris, J.T., P.V. Sundareshwar, C.T. Nietch, B. Kjerfve, and D.R. Cahoon (2002), Responses of Coastal Wetlands to Rising Sea Level, Ecology, 83, 2869–2877.

Neumeier, U,. and C.L. Amos (2006), The influence of vegetation on turbulence and flow velocities in European salt-marshes. Sedimentology**, 53(2), 259-277**.

Quartel, S., A. Kroon, P.G.E.F. Augustinus, P. Van Santen, and N.H. Tri (2007), Wave attenuation in coastal mangroves in the Red River Delta, Vietnam, Journal of Asian Earth Sciences, 29, 576-584.

Shepard, C.C., C.M. Crain, and M.W. Beck (2011), The protective role of coastal marshes, A systematic review and meta-analysis, PLoS ONE, 6(11), e27374. doi,10.1371/journal.pone.0027374

Shi, Z., J.S. Pethick, and K. Pye (1995), Flow structure in and above the various heights of a saltmarsh canopy, a laboratory flume study, Journal of Coastal Research, 11(4), 1204-1209.

Spencer, T., and I. Möller (2012), Mangrove Systems, In: Sherman, D.J. (ed.), Coastal Geomorphology (Treatise in Geomorphology Vol. 10), Elsevier, Amsterdam.

Spencer, T. (2007), Coral reefs and the tsunami of 26 December 2004, generating processes and ocean-wide patterns of impact, Atoll Research Bulletin, 544, 1–36.

Tanaka, N., Y. Sasaki, M.I.M. Mowjood, K.B.S.N. Jinadasa, and S. Homchuen (2007), Coastal vegetation structures and their functions in tsunami protection, experience of the recent Indian Ocean tsunami, Landscape Ecological Engineering, 3, 33–45.

Teo, F.Y., R.A. Falconer, and B. Lin (2009), Modelling effects of mangroves on tsunamis, Water Manag., 162, 3–12.

Tschirky, P., K. Hall, and D. Turcke (2000), Wave attenuation by emergent wetland vegetation, Proceedings of the 27th International Conference on Coastal Engineering, ASCE, 865-877.

UK NEA (UK National Ecosystem Assessment) (2011), The UK National Ecosystem Assessment Technical Report, UNEP-WCMC, Cambridge.

Vermaat, J.E., and U. Thampanya (2006), Mangroves mitigate tsunami damage, a further response, Estuarine, Coastal and Shelf Science, 69, 1–3.

Vo-Luong, H.P., and S.R. Massel (2006), Experiments on wave motion and suspended sediment concentration at Nang Hai, Can Gio mangrove forest, Southern Vietnam, Oceanologia, 48, 23–40.

Wamsley, T.V., M.A. Cialone, J.M. Smith, J.H. Atkinson, and J.D. Rosati (2010), The potential of wetlands in reducing storm surge, Ocean Engineering, 37, 59–68.

Wamsley, T.V., M.A. Cialone, J.M. Smith, B.A. Ebersole, and A.S. Grzegorzewski (2009), Influence of landscape restoration and degradation on storm surge and waves in southern Louisiana, Natural Hazards; 51: 207–224.

Wayne, C.J. (1976), The effects of sea and marsh grass on wave energy, Coastal Research Notes; 4 (7): 6-8.

Wolanski, E., Y. Mazda, and P. Ridd (1992), Mangrove hydrodynamics, In: Robertson, A.I., and D.M. Alongi DM (eds), Tropical Mangrove Ecosystems, American Geophysical Union, Washington, DC, 4–62.

Woodroffe, C.D. (2002), Coasts: Form, process and evolution, Cambridge University Press, Cambridge.

DOI: 10.3990/2.171

Laboratory Experiments for Wave-Driven Sand Transport Prediction

T. O'Donoghue[1] and D.A. van der A[2]

School of Engineering, University of Aberdeen, AB24 3UE, Scotland, [1]T.ODonoghue@abdn.ac.uk; [2]D.A.vanderA@abdn.ac.uk

ABSTRACT

Since the first NCK-Days 20 years ago, a significant body of large-scale laboratory experiments on wave-driven sand transport has been conducted in oscillatory flow tunnels and large wave flumes. The experiments have yielded measures of net sand transport rates for a wide range of flow and sand conditions and have provided insights that have informed the development of practical predictors for sand transport in oscillatory flows and under waves. An overview of these experiments and a commentary on some of the important insights and quantitative results is presented. Particular attention is given to unsteady aspects of the sand flux for ripple regime and fine sand sheet-flow conditions, the role of flow acceleration on bed shear stress and net transport, and the differences in net transport and transport processes occurring in tunnel oscillatory flows and occurring under progressive surface waves.

INTRODUCTION

Twenty years ago, the year of the first NCK-Days, *Dibajnia and Watanabe* [1992] published a formula for predicting sheet-flow sand transport under waves and currents. The formula uses a half-cycle approach whereby sand transported in each half-cycle of the near-bed oscillatory flow (Figure 1) is calculated based on a representative velocity for that half-cycle. The Dibajnia and Watanabe predictor is classed as "semi-unsteady" because it accounts for an unsteady (phase lag) effect whereby a proportion of sand entrained during one half-cycle remains in suspension and is transported during the following half-cycle. The half-cycle approach has since been adopted by others as the basis for more developed predictors [*Dibajnia and Watanabe*, 1996, 1998; *Camenen and Larson*, 2006; *Silva et al*., 2006; *Van der Werf et al*., 2007; *Van der A et al.*, subm.]. Other practical formulae, not based on the half-cycle approach, have also been developed in the intervening years including *Ribberink* [1998], *Drake and Calantoni* [2001], *Dohmen-Janssen et al*. [2002], *Soulsby and Damgaard* [2005], *Nielsen* [2006], *Van Rijn* [2007], *Wang* [2007], *Gonzalez-Rodriguez and Madsen* [2007] and *Suntoyo et al*. [2008]. All of these predictors have the following in common: they comprise simple formulae making them readily useable within morphological models and they aim to capture essential processes within these formulae through parameterizations based on laboratory experiments.

The focus of this paper is on the laboratory experiments that have informed the development of the practical formulae for wave-driven sand transport. It presents an overview of the laboratory experiments of the last 20 years or so and indicates how insights and quantitative results from the experiments have been used to develop the predictors. The focus is on experiments conducted at large scale, by which we mean flows with period $T >$ 4 s and real sands (mostly in the range 0.12 mm $\leq d_{50} \leq$ 0.54 mm). Studies at this scale have been conducted in large wave flumes such as the GWK in Hannover and the Deltaflume in The Netherlands, and in large oscillatory flow tunnels such as the LOWT in The Netherlands, the AOFT in Aberdeen and the TOFT in Tokyo.

MEASURED NET SAND TRANSPORT RATES

Perhaps the most important contribution from experiments towards the development of practical predictors is the body of net sand transport rates measured for well-defined hydrodynamic and sand conditions, which can be used to calibrate and test the predictors. The transport rates are obtained by applying the conservation of mass principle to the measured pre- and post-test bed profiles and the volumes of sand collected from the ends of the test section at the end of an experiment. The same cannot be done in the field; indeed measurement of *total* net sand transport under waves is still not practically feasible in field conditions.

The database first described by *Van der Werf et al*. [2009] now contains 226 measured net transport rates for a wide range of full-scale conditions. Figure 2 presents the measured net transport rates

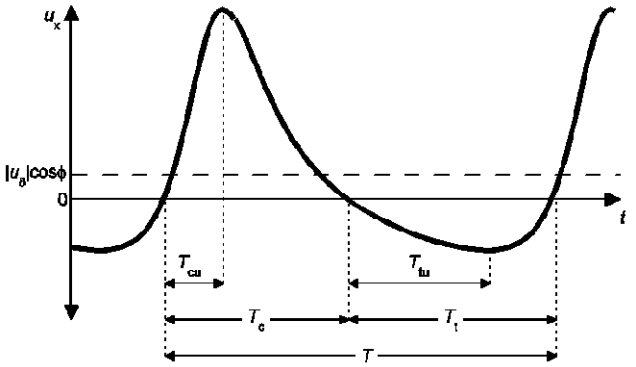

Figure 1. Definition sketch for near-bed velocity input to predictor; subscript "c" and "t" refer to wave crest and trough respectively. u_δ is steady current at angle ϕ to wave direction.

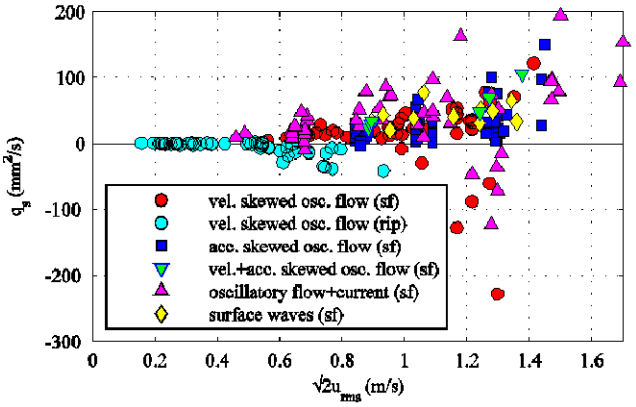

Figure 2. Measured net transport rates from large-scale laboratory experiments (sf =sheet flow; rip = rippled beds).

plotted against $\sqrt{2}u_{rms}$, where u_{rms} is rms free-stream horizontal orbital velocity. The results cover the ripple and sheet-flow regimes, progressive non-breaking surface waves, regular and irregular oscillatory flows with velocity and/or acceleration skewness and oscillatory flows with superimposed current. The range of net transport rates for given $\sqrt{2}u_{rms}$ in Figure 2 reflects the fact that transport rate depends on sand size, flow period and shape and whether the near-bed flow is generated by surface waves or is generated in an oscillatory flow tunnel. For oscillatory flows without superimposed current, it is the asymmetry in the flow kinematics between the positive and negative flow half-cycles that drives the transport: for velocity-skewed flow (circles in Figure 2), the asymmetry is asymmetry in velocity, with higher peak positive than peak negative velocity (a la Stokes-type wave); for acceleration-skewed flow (square symbols in Figure 2) the asymmetry is asymmetry in acceleration with higher peak positive than peak negative accelerations (sawtooth-type flow).

RIPPLE REGIME

A large number of full-scale laboratory experiments have been conducted over the past 20 years involving wave-generated sand ripples, both in wave flumes [*Thorne et al.*, 2003; *Williams et al.*, 2004; *Cataña-Lopera and Garcia*, 2006; *O'Hara Murray et al.*, 2011] and in oscillatory flow tunnels [*Ribberink and Al-Salem*, 1994; *Ahmed and Sato*, 2001; *O'Donoghue and Clubb*, 2001; *Sleath and Wallbridge*, 2002; *Van der Werf et al.*, 2006].

Primarily because of its impact on bed roughness, ripple geometry has been a main focus for many studies [*Dumas et al.*, 2005; *O'Donoghue et al.*, 2006; *Pedocchi and Garcia*, 2009]. Based on combined data from large-scale experiments covering a wide range of sand sizes, 2D and 3D ripples and regular and irregular flows, *O'Donoghue et al.* [2006] proposed the following Nielsen-type formulae for ripple height, η, and ripple length, λ:

$$\frac{\eta}{a} = m_\eta \left\{0.275 - 0.022\psi^{0.42}\right\} \quad (1)$$

$$\frac{\lambda}{a} = m_\lambda \left\{1.97 - 0.44\psi^{0.21}\right\} \quad (2)$$

where ψ is mobility number and the multiplier m for η or λ depends on sand size. Figure 3 shows the general good agreement between ripple dimensions calculated using Equations (1) and (2) and the corresponding measured ripple dimensions for the data used by *O'Donoghue et al.* [2006].

For practical sand transport predictors, ripple dimensions are important in quantifying the bed roughness for shear stress estimation and, for half-cycle-type formulations, determining the phase lag parameter which controls the degree of sharing of entrained sand between the present and subsequent flow half-cycle, as described below. Rippled bed roughness is commonly scaled to the ripple height, $k_s \propto \eta$, or to the product of ripple height and steepness, $k_s \propto \eta^2/\lambda$.

A number of large-scale experiments have studied the detailed sand transport processes occurring over ripples [*Ribberink and Al-Salem*, 1994; *Thorne et al.*, 2003; *Van der Werf et al.*, 2006; *O'Hara Murray et al.*, 2011]. Sediment transport over rippled beds has two components: a suspended component and a bedload component associated with ripple migration. During positive (onshore) flow, the onshore velocities transport sand along the stoss slope and over the ripple crest. Some of this sand is entrained in the developing lee vortex, which also entrains sand from the lee slope. The vortex increases in size as the flow slows, entraining more sand from the lee slope as it does so. The sand-laden vortex is then ejected into the main flow above the ripple at about the time of flow reversal, contributing to the negative-directed (*offshore*) suspended sediment transport. A proportion of the sand that has been carried up the stoss slope and over the ripple crest during the onshore flow does not get carried into suspension by the lee vortex. Instead it slumps down the onshore side contributing to *onshore* ripple migration. The same processes occur during the offshore flow half cycle. There is non-zero net transport if there is asymmetry between the two half-cycles, caused by asymmetry in the freestream flow. For example, for velocity-skewed oscillatory flow, the ripples are asymmetric, with steeper lee (onshore) slopes than stoss (offshore) slopes; the lee

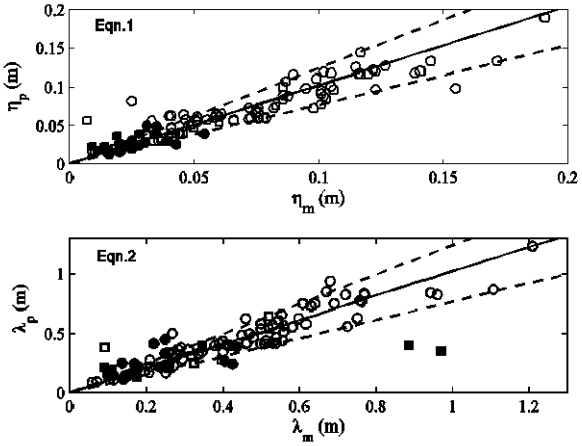

Figure 3. Ripple dimensions calculated using Equations (1) and (2) plotted against corresponding measured ripple dimensions; open/solid symbols correspond to 2D/3D ripples and circles/squares correspond to regular/irregular flows [after O'Donoghue et al., 2006].

vortex is much stronger than the stoss vortex and more sand is ejected at the onshore-offshore flow reversal than at the offshore-onshore reversal, resulting in much lower onshore-directed suspended sand transport. At the same time, such flows cause onshore ripple migration. For velocity-skewed flow therefore, net suspended transport is offshore while net bedload transport is onshore and the net total transport (magnitude and direction) depends on the relative magnitudes of these two contributions.

The entrainment of sand during one half-cycle, its ejection into the flow at flow reversal and subsequent transport in the opposite direction during the following half-cycle, is a "phase lag" effect in the sense that the entrained sand concentration lags the flow velocity. Half-cycle transport predictors can account for this effect through a "phase lag parameter" which controls the proportion of sand entrained during one half-cycle that is transported in the following half-cycle. For example, in the "santoss" predictor [*Van der A et al*., subm.], the phase lag parameter is

$$P_i = \alpha \frac{\eta}{2\left(T_i - T_{iu}\right)w_s} \tag{3}$$

where w_s is sand settling velocity, the T's are as indicated in Figure 1 with subscript i being c or u for wave crest or trough respectively and α is a calibration parameter. The phase lag parameter represents the ratio of a representative "stirring height" and the sand settling distance within the decelerating phase of the flow half-cycle; for rippled bed, the stirring height is taken as proportional to ripple height. The higher the value of P, caused by higher ripples or a shorter flow deceleration phase, the greater the proportion of entrained sand that is carried over to the following half-cycle. Other predictors define phase lag parameters in a different way but with the same purpose of controlling the proportion of sand that is carried over to the following half-cycle [e.g. *Van der Werf et al.*, 2006; *Camenen and Larson*, 2007].

OSCILLATORY SHEET-FLOW

Sheet flow occurs when wave-generated near-bed flow velocities are high, ripples are washed out and sand is transported in a water-sand mixture layer that is of order cm in thickness. Sheet-flow transport is considered a form of bed load, although textbook definitions of bed load or suspended load do not strictly apply. Based on laboratory experiments conducted in the LOWT [*Ribberink and Al-Salem*, 1994, 1995], *Ribberink* [1998] observed a near quasi-steady response in sheet flow sand concentration relative to the oscillating freestream flow velocity for sands with d_{50} > 0.2mm and flows with period T > 4s. Observations of the fundamental processes, combined with measures of net sand transport for a range of conditions, led to Ribberink's quasi-steady bedload transport formula in which the instantaneous transport rate, $\phi(t)$, is directly related to the instantaneous (Shields) shear stress, $\theta(t)$, in a formula of the following kind:

$$\phi(t) = m\left|\theta(t)^n\right| \frac{\theta(t)}{\left|\theta(t)\right|} \tag{4}$$

where m and n are calibration coefficients. For velocity-skewed flows given by $u(t) = u_1 \sin(\omega t) - u_2 \cos(2\omega t)$, with velocity skewness $R = (u_1+u_2)/2u_1$ and rms velocity u_{rms}, net transport based on Ribberink's quasi steady formula can be shown to be

$$\phi_N = \frac{\alpha m}{\left[1+\left(2R-1\right)^2\right]^n} \theta^n_{\sqrt{2}u_{rms}} \tag{5}$$

where α depends on R and n only. Figure 4 shows a comparison of Equation (5) (R = 0.63, n = 1.65 and m =11) against measured (non-dimensional) net sand transport rates for velocity-skewed oscillatory flows with $R \approx 0.63$. For the coarser sands (d_{50} > 0.2mm), sheet-flow net transport rates are positive and increase with increasing Shields, and the Ribberink predictor is seen to agree well with the measured transport rates, supporting the validity of the quasi-steady approach for these coarser sands. However, the net transport results for the finer sands ($d_{50} \leq$ 0.2mm) show a contrary behaviour: net transport rates are initially positive but become negative at higher Shields and show very high negative net transport at high Shields. For the finer sands therefore, the wave-generated sand transport process is not quasi-steady: it is an unsteady process and the degree of unsteadiness depends on the flow condition and the sand size.

The unsteady behaviour seen in the net transport results for fine sand in Figure 4 is also seen in detailed process measurements for sheet flow conditions measured in the AOFT and LOWT oscillatory flow tunnels. Example measurements of the intra-wave erosion depth and sheet-flow layer thickness obtained via detailed concentration measurements within the sheet-flow layer are presented in Figure 5, which shows example results for three cases: (a) 0.27mm sand in a velocity-skewed flow; (b) 0.13mm sand in velocity-skewed flow; (c) 0.15mm sand in acceleration-skewed flow. In the case of Figure 5(a), we see a near quasi-steady behaviour in the time-dependent erosion depth and sheet-flow layer thickness for the medium sand. In contrast, we see strong unsteadiness in Figure 5(b) for the case of fine sand in the same velocity-skewed flow as in Figure 5(a). In this case, a proportion of sand entrained during each flow half-cycle does not settle back to the bed before flow reversal, and the proportion is greater for the positive flow half-cycle than for the negative flow half-cycle because positive velocity is higher and deceleration time is shorter; the result is deeper erosion and thicker sheet-flow layer thickness soon after the positive-negative flow reversal compared with after the negative-positive reversal.

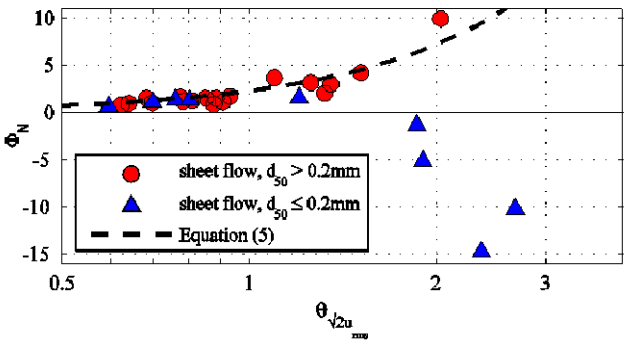

Figure 4. Measured net transport rates for sheet-flow, velocity-skewed oscillatory flow with R ≈ 0.63 and calculated net transport using Equation 4 with m=11, n=1.65 and R=0.63.

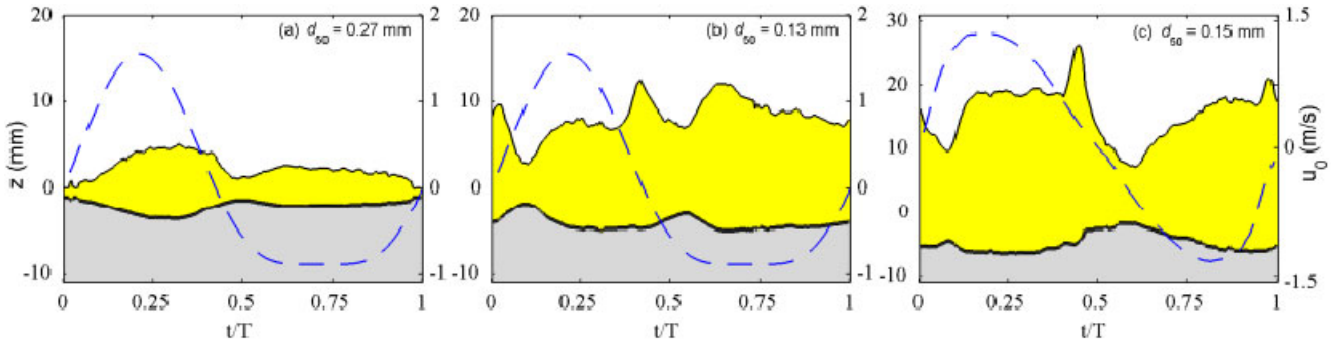

Figure 5. Measurements of erosion depth (black line) and sheet-flow layer thickness (shaded yellow) for (a) medium and (b) fine sand in a velocity-skewed flow and (c) for fine sand in acceleration-skewed flow; the free-stream velocity is indicated by the dashed line.

As for ripples, there is therefore a phase lag effect in sheet-flow transport processes, and the effect is stronger for finer sands and shorter period flows. For the santoss half-cycle-based predictor [*Van der A et al*., subm.], a phase lag parameter for sheet flow is defined similarly to Equation (3), but with sheet flow layer thickness, δ_s, replacing ripple height as the representative stirring height. Recourse is again made to measurements from large-scale experiments to estimate δ_s. For example, *Ribberink et al*. [2008] propose $\delta_s/d_{50} = \beta\theta_{max}$, with calibration factor β = 10.6. For velocity-skewed oscillatory flow, the phase lag parameter for the positive half-cycle is greater than that for the negative half-cycle because (a) δ_s is greater due to higher Shields and (b) flow deceleration time is shorter ($(T_c - T_{cu}) < (T_t - T_{tu})$); the result is a greater proportion of positive half-cycle-entrained sand being carried into the following negative half-cycle than negative half-cycle sand being carried into the following positive half-cycle, as seen in Figure 5. Other half-cycle predictors use a phase lag parameter similar in concept to that of the santoss predictor for sheet flow conditions [*Camenen and Larson*, 2006; *Silva et al*., 2006]. For net transport in sinusoidal flow with superimposed current, *Dohmen-Janssen et al.* [2002] applied a "reduction factor", r, to Ribberink's quasi-steady predictor (Equation (4)) with r depending on a version of the phase lag parameter and the ratio between the current velocity and the amplitude of the sinusoidal velocity. There are other predictors for sheet-flow transport [*Soulsby and Damgaard*, 2005; *Nielsen*, 2006; *Wang*, 2007; *Gonzalez-Rodriguez and Madsen*, 2007, *Suntoyo et al.* 2008] which do not account for phase lag effects and so are limited to relatively coarse sand conditions.

ACCELERATION EFFECTS

For oscillatory flow, bed shear stress is usually related to the square of the flow velocity via a friction factor dependent on relative roughness a/k_s, where $a = \sqrt{2}u_{rms}T/2\pi$ and T is flow period. On this basis, net transport in acceleration-skewed (sawtooth-type) flow should be zero because of the symmetry in velocity (and, therefore, bed shear stress) between the positive and negative flow half-cycles. However, experiments by *King* [1991] and, later, full-cycle acceleration-skewed oscillatory flow experiments by *Watanabe and Sato* [2004] and at larger scale by *Van der A et al*. [2010] showed that acceleration asymmetry can generate significant net sand transport in the direction of highest acceleration, and increasing net transport with increasing acceleration skewness. The net transport arises from an asymmetry in bed shear stress caused by the asymmetry in acceleration: higher flow acceleration generates higher bed shear stress because the boundary layer has less time to develop before peak velocity is reached.

The effects of acceleration skewness on oscillatory boundary layer dynamics and bed shear stress were studied in detail by *Van der A et al.* [2011]. An example result is presented in Figure 6, which shows the asymmetry in bed shear stress between the positive and negative flow half-cycles for oscillatory flow with high acceleration skewness alongside the symmetrical bed shear stress behaviour of the corresponding sinusoidal flow. *Van der A et al.* report values as high as 1.8 for the ratio of peak positive to peak negative bed shear stress. A number of practical predictors account for this acceleration effect on bed shear stress, including *Watanabe and Sato* [2004], *Silva et al*. [2006], *Nielsen* [2006] and *Gonzalez-Rodriguez and Madsen* [2007], *Camenen and Larson* [2007], and *Suntoyo et al.* [2008].

The santoss predictor [*Van der A et al*., subm.] is driven by bed shears stress, with bed shear stress evaluated separately for each half-cycle. In this predictor the acceleration skewness effect on the bed shear stress is accounted for by adjusting the relative roughness to $\left(2T_{iu}/T_i\right)^{\alpha} a/k_s$, where, as before, the T's are as indicated in Figure 1 with subscript i being c or u for wave crest or trough respectively, and α is a calibration parameter. So, for example, a forward-leaning crest half-cycle has $(2T_{cu}/T_c)^{\alpha} < 1$, leading to higher friction factor and bed shear stress compared to the equivalent sinusoidal flow for which $(2T_{cu}/T_c)^{\alpha} = 1$. This

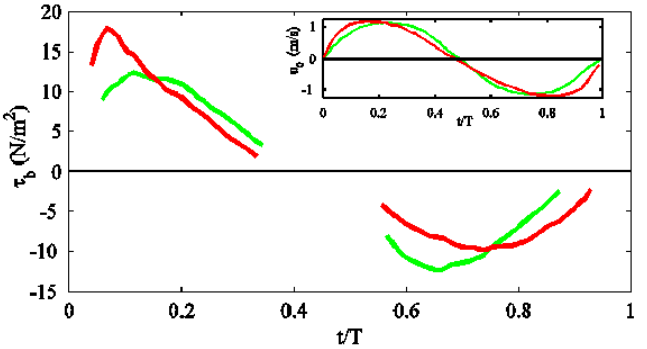

Figure 6. Measured bed shear stress time-series for sinusoidal (green) and acceleration-skewed (red) oscillatory flows over fixed rough bed. (T = 6s, $u_{0max} \approx$ 1.1 m/s, k_s = 14mm).

approach of effectively adjusting the relative roughness through the effective a is similar to that used by *Gonzalez-Rodriguez and Madsen* [2007] in their approach to account for acceleration in the bed shear stress.

As for velocity-skewed flow, phase lag effects become significant for acceleration-skewed flow when the sand is fine and the flow period is relatively short. However, in contrast to velocity-skewed flow, for which phase lag effect augments the negative transport, phase lag tends to augment the *positive* transport in the case of acceleration-skewed flow (for a forward-leaning wave). This is because the deceleration time for the negative half-cycle (T - T_{tu}) is less than that for the positive half-cycle (T_c - T_{cu}), so that sand entrained in the negative half-cycle has less time to settle before the flow reverses. The effect is seen in Figure 5(c), which shows time-varying erosion depth and sheet-flow layer thickness for a fine sand in a pure acceleration-skewed flow: erosion depth and sheet-flow layer thickness are greater at the negative-positive flow reversal than at the positive-negative flow reversal; a greater proportion of sand entrained during the negative half-cycle is carried into the following positive half-cycle than is carried from the positive half-cycle into the following negative half-cycle. For half-cycle-based practical predictors, the effect is captured via the phase lag parameter as previously defined.

PROGRESSIVE WAVE EFFECTS

Of the 226 large-scale laboratory conditions for which net transport has been measured, 11 correspond to progressive, non-breaking waves in a large wave flume; all other cases are for oscillatory flows in large oscillatory flow tunnels. Figure 7 shows progressive wave net transport rates plotted against $\sqrt{2}u_{rms}$ for sands with $0.21 \le d_{50} \le 0.27$mm, with the data coming from two independent experimental series [*Dohmen-Janssen and Hanes*, 2002; *Schretlen et al*., 2011]. Also shown are measured net transport rates from large-scale oscillatory flow tunnel experiments with near-bed velocity-skewed flows and sand size similar to those of the progressive wave cases. The results indicate that net transport rates for medium sand under progressive waves are higher than transport rates in "similar" oscillatory flows. Moreover, *Schretlen et al*. [2010] report that net transport for fine sand ($d_{50} \approx 0.15$mm) is *positive* under progressive waves, in contrast to the *negative* net transport measured for fine sand in strong velocity-skewed oscillatory flows (as seen, for example, in Figure 4). The indication is that boundary layer streaming and/or horizontal advection of sand contributes significantly to the net transport. Unfortunately, unlike for tunnel flows, detailed boundary layer measurements with which to better understand the streaming and the boundary layer shear stresses are lacking for large-scale waves over fixed rough beds. However, *Kranenburg et al*. [2011] used a numerical model that can simulate both wave flume and oscillating tunnel flows to show that the wave-induced streaming does indeed contribute to the higher net transport rates seen under progressive waves. With the exceptions of *Nielsen* [2006], *Van Rijn* [2007] and *Van der A et al*. [subm.], existing practical predictors make no distinction between oscillatory near-bed flow as occurs in tunnels and oscillatory near-bed flow generated by progressive surface waves. Both *Nielsen* [2006] and

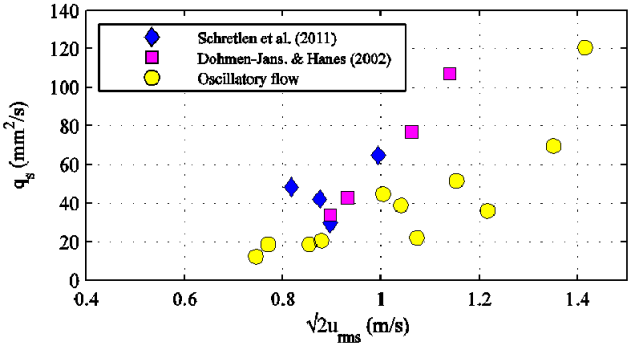

Figure 7. Measured sand transport rates from progressive surface waves [Dohmen-Janssen and Hanes, 2002; Schretlen et al. 2011] and oscillatory flow tunnel experiments with "similar" flow and sand conditions ($0.21 \le d_{50} \le 0.27$mm; $0.57 < R < 0.72$; $5s < T < 10s$).

Van der A et al. [subm.] account for the effect of wave-related positive streaming by adding a positive wave Reynolds stress, τ_{wRe}, in the following manner:

$$\theta_i = \frac{\frac{1}{2} f_w |u_i| u_i + \tau_{wRe}}{(s-1) g d_{50}} \tag{6}$$

where τ_{wRe} is evaluated using

$$\tau_{wRe} = \frac{2}{3\pi} \rho f_w \frac{u^3}{c} \tag{7}$$

in which f_w is friction factor, s is sediment specific gravity, g is acceleration due to gravity, ρ is water density and c is wave speed.

Kranenburg et al. [2011] have also shown that other wave-related processes are at work, which impact particularly on the net transport of fine sand: (i) vertical advection of sand by vertical orbital velocities, which causes sand to settle faster at the end of the onshore flow and settle slower at the end of the offshore flow; and (ii) higher concentration peaks and enhanced flux at times of maximum positive velocity caused by horizontal gradients in the horizontal sediment flux. In the santoss predictor [*Van der A et al*., subm.], account is taken of (i) by simple adjustment of the sand settling velocity under the wave crest, w_{sc}, and wave trough, w_{st}, as follows:

$$w_{sc} = w_s + v_r \quad ; \quad w_{st} = \max\left[\left(w_s - v_r\right), 0\right] \tag{8}$$

where w_s is settling velocity in still water and v is the amplitude of orbital vertical velocity at reference height r above the bed, with r equal to ripple height for rippled bed and equal to sheet-flow layer thickness for sheet flow. In the same predictor, account is taken of (ii) through a correction to the phase lag parameter P_i (Equation (3)) that increases P_i under the wave crest and reduces P_i under the trough; see *Van der A et al*. [subm.] for details.

CONCLUSION

Since the first NCK-Days 20 years ago, a significant body of large-scale laboratory experiments on wave-driven sand transport has been conducted in oscillatory flow tunnels and very large wave flumes. The experiments have yielded measures of net sand transport rates for a wide range of flow and sand conditions and have provided insights that have informed the development of

practical predictors. Consequently, the most developed predictors now account for the ripple and sheet flow regimes, unsteady phase lag effects, wave shape effects including flow acceleration, and the differences between oscillatory flow as occurs in tunnels and oscillatory flow generated by progressive surface waves. The paper has presented a brief overview of the experiments along with indications of how insights and quantitative results have been used to develop the predictors.

Although the body of experimental work is substantial, it is the case that some hydrodynamic conditions have received more attention than others. For example, despite recent significant work, experiments involving progressive surface waves are still relatively few and more experimental research is needed with fixed and mobile beds under large-scale surface waves to better measure the fundamental processes. However, the most significant shortfall in the coverage of experiments to date is arguably the fact that they are limited to non-breaking wave conditions, which of course means that the attendant predictors are limited to non-breaking waves. For this reason a primary objective of further research in this area must be to conduct large-scale experiments with breaking waves, measuring net transport rates and fundamental processes as before, and to look to extend practical predictors to accommodate breaking wave conditions.

ACKNOWLEDGEMENT

Much of the Aberdeen research reported in this paper was conducted in collaboration with Jan Ribberink and colleagues at the University of Twente over the past number of years. The "santoss" work mentioned in the paper refers to our recent collaboration on the SANTOSS project ('SANd Transport in OScillatory flows in the Sheet-flow regime') funded by the UK's EPSRC (GR/T28089/01) and STW in The Netherlands (TCB.6586).

REFERENCES

Van der A, D. A., T. O'Donoghue, and J. S. Ribberink (2010), Measurements of sheet flow sediment transport in acceleration-skewed oscillatory flow and comparison with practical formulations. Coastal Engineering, 57(3), doi: 10.1016/j.coastaleng.2009.11.006.

Van der A, D. A., T. O'Donoghue, A. G. Davies, and J. S. Ribberink (2011), Experimental study of the turbulent boundary layer in acceleration-skewed oscillatory flow. Journal of Fluid Mechanics, 684, 251-283, doi:10.1017/jfm.2011.300.

Van der A, D. A., J. S. Ribberink, J. J. van der Werf, T. O'Donoghue, R. H. Buijsrogge, and W. M. Kranenburg (submitted), New practical sand transport formula for non-breaking waves and currents. Coastal Engineering.

Ahmed, A. S. M., and S. Sato (2001), Investigation of bottom boundary layer dynamics of movable bed by using enhanced PIV technique, Coastal Engineering, 43(4), 239–258. doi:10.1142/S0578563401000360.

Camenen, B. and M. Larson (2006), Phase-lag effects in sheet flow transport, Coastal Engineering, 53(5-6), 531-542, doi: 10.1016/j.coastaleng.2005.12.003.

Camenen, B., M. Larson (2007), A total load formula for the nearshore. Proceeding Coastal Sediments '07. ASCE, New Orleans, Louisiana, USA.

Cataña-Lopera, Y. A., and M. H. Garcia (2006), Geometry and migration characteristics of bedforms under waves and currents Part 2: Ripples superimposed on sandwaves, Coastal Engineering, 53(9), 767-780, doi: /10.1016/j.coastaleng.2006.03.007.

Dohmen-Janssen, C. M., D. M. Hanes (2002), Sheet flow dynamics under monochromatic nonbreaking waves. Journal of Geophysical Research, 107(C10), 3149, doi:10.1029/2001 JC001045.

Dohmen-Janssen, C. M., D. Kroekenstoel, W.N. Hassan, and J. S. Ribberink (2002), Phase lags in oscillatory sheet flow: experiments and bed load modelling, Coastal Engineering, 46(1), 61-87, doi:10.1016/S0378-3839(02)00056-X.

Drake, T. G., and J. Calantoni (2001), Discrete particle model for sheet flow sediment transport in the nearshore. Journal of Geophysical Research, 106(C9), 19,859-19,868, doi: 10.1029/2000JC000611.

Dibajnia, M., and A. Watanabe (1992), Sheet flow under non linear waves and currents. Proceedings 23rd International Conference on Coastal Engineering, ASCE, 2015-2028.

Dibajnia, M., and A. Watanabe (1996), A transport rate formula for mixed sands. Proceedings 25th International Conference on Coastal Engineering, ASCE, 3791-3804.

Dibajnia, M. and A. Watanabe (1998), Transport rate under irregular sheet flow conditions. Coastal Engineering, 35(3), 167-183, doi:10.1016/S0378-3839(98)00034-9.

Dumas, S., R. W. C. Arnott, and J. B. Southard (2005), Experiments on oscillatory-flow and combined-flow bed forms: Implications for interpreting parts of the shallow-marine sedimentary record. Journal of Sedimentary Research, 75(3), 501-513, doi:10.2110/jsr.2005.039.

Gonzalez-Rodriguez, D., and O. S. Madsen (2007), Seabed shear stress and bedload transport due to asymmetric and skewed waves. Coastal Engineering, 54(12), 914-929, doi:10.1016/j.coastaleng.2007.06.004.

King, D. B. (1991), Studies in oscillatory flow bedload sediment transport. PhD thesis, University of California, Sand Diego.

Kranenburg, W. M., J. S. Ribberink, R. E. Uittenbogaard (2011), Sand transport by surface waves: can streaming explain onshore transport? Proceedings of the International Conference on Coastal Engineering, 32(2010), Paper#: sediment.11.

Nielsen, P. (2006), Sheet flow sediment transport under waves with acceleration skewness and boundary layer streaming. Coastal Engineering, 53(9), 749-758, doi: 10.1016/j.coastaleng.2006.03.006.

O'Donoghue, T., and G. S. Clubb (2001), Sand ripples generated by regular oscillatory flow, Coastal Engineering. 44(2), 101-115, doi: 10.1016/S0378-3839(01)00025-4.

O'Donoghue, T., J. S. Doucette, J. J. van der Werf, and J. S. Ribberink (2006), The dimensions of sand ripples in full-scale oscillatory flows, Coastal Engineering, 53(12), 997-1012, doi: 10.1016/j.coastaleng.2006.06.008.

O'Hara Murray, R. R., P. D. Thorne, D. M. Hodgson (2011), Intrawave observations of sediment entrainment processes

above sand ripples under irregular waves, Journal Geophysical Research, 116(C01001), doi:10.1029/2010JC006216.

Pedocchi, F., and M. H. Garcia (2009), Ripple morphology under oscillatory flow: 2. Experiments, Journal Geophysical Research, 114(C12015), doi:10.1029/2009JC005356.

Ribberink, J. S., and A. A. Al-Salem (1994), Sediment transport in oscillatory boundary layers in cases of rippled beds and sheet flow. Journal of Geophysical Research, 99(C6), 12,707-12,727. doi:10.1029/94JC00380.

Ribberink, J. S., and A. A. Al-Salem (1995), Sheet flow and suspension of sand in oscillatory boundary layers. Coastal Engineering, 25(3-4), 205-225, doi: 10.1016/0378-3839(95) 00003-T.

Ribberink, J. S. (1998), Bed-load transport for steady flows and unsteady oscillatory flows, Coastal Engineering, 34(1-2), 59-82, doi:10.1016/S0378-3839(98)00013-1.

Ribberink, J.S., J.J. van der Werf, T. O'Donoghue, and W.N.M. Hassan (2008), Sand motion induced by oscillatory flow: sheet flow and vortex ripples. Journal of Turbulence, 9(20), 1-33, doi: 10.1080/14685240802220009.

Van Rijn, L. C. (2007), Unified view of sediment transport by currents and waves. I: Initiation of motion, bed roughness, and bed-load transport. Journal of Hydraulic Research, 133(6), 649-667, doi: 10.1061/(ASCE)0733-9429(2007)133:6(649).

Schretlen, J. L. M., J. S. Ribberink, T. O'Donoghue (2011), Boundary layer flow and sand transport under full scale surface waves. Proceedings of the International Conference on Coastal Engineering, 32(2010), Paper#: sediment.4.

Sleath, J. F. A., and S. Wallbridge (2002), Pickup from rippled beds in oscillatory flow. Journal of Waterway, Port, Coastal and Ocean Engineering. 128(6), 228-237, doi: 10.1061/(ASCE) 0733-950X(2002)128:6(228).

Soulsby, R. L., and J. S. Damgaard (2005), Bedload sediment transport in coastal waters. Coastal Engineering, 52(8), 673-689, doi:10.1016/j.coastaleng.2005.04.003.

Suntoyo, H. Tanaka, and A. Sana (2008), Characteristics of turbulent boundary layers over a rough bed under saw-tooth waves and its application to sediment transport. Coastal Engineering, 55(12), doi: 10.1016/j.coastaleng.2008.04.007.

Silva, P. A., A. Temperville, and F. Seabra Santos (2006), Sand transport under combined current and wave conditions: A semi-unsteady, practical model. Coastal Engineering, 53(11), 897-913, doi:10.1016/j.coastaleng.2006.06.010.

Thorne, P., A. G. Davies, and J. J. Williams (2003), Measurements of near-bed intra-wave sediment entrainment above vortex ripples. Geophysical Research Letters, 30(20), doi:10.1029/2003GL018427.

Wang, Y.-H. (2007), Formula for predicting bedload transport rate in oscillatory sheet flows, Coastal Engineering, 54(8), 594-601, doi:10.1016/j.coastaleng.2006.12.003.

Watanabe, A., S. Sato, (2004), A sheet-flow transport rate formula for asymmetric forward-leaning waves and currents. Proceedings 29th International Conference on Coastal Engineering. World Scientific, 1703–1714.

Van der Werf, J. J., J. S. Ribberink, T. O'Donoghue and J.S. Doucette, (2006), Modelling and measurement of sand transport processes over full-scale ripples in oscillatory flow. Coastal Engineering, 53(x), 657-673, doi :10.1016/j.coastaleng. 2006.02.002.

Van der Werf, J. J., J. J. L. M. Schretlen, J. S. Ribberink, and T. O'Donoghue (2009), Database of full-scale laboratory experiments on wave-driven sand transport processes. Coastal Engineering, 56(7), 726-732, doi: 10.1016/j.coastaleng.2009. 01.008.

Van der Werf, J. J., J. S. Ribberink, and T. O'Donoghue (2007), Development of a new practical model for sand transport induced by non-breaking waves and currents. Proceedings Coastal Dynamics '07, ASCE, 1-14.

Williams, J.J., P. S. Bell, P. D. Thorne, N. Metje, and L. E. Coates (2004), Measurement and prediction of wave-generated suborbital ripples, Journal Geophysical Research, 109(C02004), doi: 10.1029 /2003JC001882.

NCK photo competition

Ali Dastgheib: Lighthouse

DOI: 10.3990/2.172

A large scale morphodynamic process-based model of the Gironde estuary

C. Villaret[1], N. Huybrechts[1,2] and A.G. Davies[3]

[1] Saint Venant Laboratory for Hydraulics (Université Paris Est, joint research unit EDF R&D – CETMEF – Ecole des Ponts ParisTech), 6 quai Watier, 78400 Chatou, France, catherine.villaret@edf.fr

[2] Roberval Laboratory, LHN (joint research unit UTC-CETMEF), UMR CNRS 6253, Centre de recherches de Royallieu, B.P. 20529, 60206 Compiègne Cedex, France

[3] School of Ocean Sciences, Bangor UniversityMenai Bridge, Anglesey LL59 5AB, UK

ABSTRACT

We present here our effort to develop a morphodynamic model of the Gironde estuary, using a process-based approach. In this complex and strongly dynamical environment, internal coupling between the flow (Telemac-2d) and sediment transport models (Sisyphe) allows the representation of detailed sediment processes and interactions with the bed, using a bed roughness feedback method. In this complex and highly heterogeneous environment, the sediment bed composition had to be schematized assuming 3 classes of bed material. Model results could be further improved by accounting for the cohesive sediment (consolidation processes). Thanks to parallelization of the codes, the simulation takes only 18 hrs on 8 processors (linux station) to calculate the 5-year bed evolution, at the basin scale (150 km).

INTRODUCTION

Estuaries are located worldwide at the boundary between the marine and terrestrial spheres. They represent the most dynamic sedimentary environment, as well as a highly valuable area for the diversity of their ecosystems. They evolve in response to tidal (marine), wind and wave forcing (atmospheric) and fluvial influence. This highly energetic environment is also characterized by its high non-homogeneity in sediment types and bed features, with mixtures of marine sand input at the mouth of the estuary and muddy fine sediment entering from the rivers. The richness of the flora and fauna adapts locally to the diversity of the morphodynamic features: tidal marshes are a nesting area for migrating birds, flood channels bring in marine fish, while ebb channels influence nutrients and fresh water species in the system.

Most estuaries and bays located on the French Atlantic shore have endured strong alluvial bed evolutions in the last decades. These bed evolutions affect the morphodynamic equilibrium, with important consequences for various economic activities and environmental issues. The diversity of the ecosystems can be endangered under the pressure of economic development (industries, tourism, and navigation). The effect of human interference needs to be monitored in order to preserve the environmental equilibrium and ensure sustainable development. Numerous applications include the impact of dredging activities, construction of dikes, etc… on the morphodynamic equilibrium and their consequences on the biodiversity.

Morphodynamic processes in estuaries are driven by **complex interactions** between various hydrodynamic, biological and morphological **processes**. The morphodynamic response acts at a wide range of time scales, which may vary from hours to days (short term), from months to decades (medium term), hundreds of years (long term) or millennia (geological scales). In term of spatial scales, bedforms range from micro-scale bed features (ripples, megaripples of the order of 10 cm to meters, dunes, sand banks; ebb and flood channels can be classified as meso-scale (100 m to km), whereas the entire estuary evolves at the macro-scale (10-100 km). Different approaches can be applied to model the morphodynamic response of the estuarine system, depending on the scale of application. Geo-morphodynamic models, also called behavior-oriented models, are designed for long term simulation. They can be applied for example to study the effect of global changes (e.g. sea level rise) on the large scale morphodynamic features. They are based on empirical rules and expert analysis of long term bathymetric data. This approach is however limited by the lack of physical insight [e.g. Karunarathna et al., 2008]. Process based models are designed to represent the detailed physical interaction between the flow and the sediment transport processes. The filtering scale is the time step of the model (of the order of a few seconds) which allows representation with great accuracy of the detailed mean flow variation for a particular combination of tidal signal, atmospheric and flooding event [e.g. Huybrechts, et al., 2011]. Spatial variations in the bathymetry are filtered at the model grid size which varies from 10-100 m, such that the small scale bed features need to be parameterized by bed roughness coefficients.

Despite their complexity, process based models still rely on some empirical parameterization of the complex flow/sediment transport interactions. They are mainly designed to study the short term morphodynamic response of the system to human interference [Chini and Villaret, 2007].The objective of this paper is to discuss the state of the art and the limits of process models to study the medium to long term bed evolutions in complex estuarine systems. Morphodynamic factors have been extensively applied in order to reduce the computational cost [van der Wegen and Roelvink, 2008]. Model predictions could be extended over geological time scales, leading to realistic as well as stable model results [van der Wegen, 2010]. However, this simplifying method introduces an additional source of uncertainty and becomes

questionable in the presence of mixed sediment, where consolidation and biological processes interact at their own time scales. Thanks to the optimization of numerical schemes, parallelism, as well as tremendous progress in the performance of computers, bed evolution can be calculated on basin scale (10-100 km) and for the medium term (years to decades), without the use of hydrodynamic filtering methods.

Our framework is the open source finite element Telemac system (http//www.opentelemac.com) which has been developed over 20 years at EDF R&D. Our case study is the Gironde macro-tidal estuary located South West of France, which is the largest estuary in Western Europe. The tide propagates approximately 170 km inland from the Bay of Biscay. Its importance to the economy is related to the presence of several ports, including the harbor of Bordeaux as well as various industries, fisheries and tourism activities. Despite the large density of population and its important economic development, the Gironde estuary remains one of the most natural estuaries [Natura, 2000].

We start in Part II with a brief review of existing morphodynamic process-based models and present in more detail the open source Telemac system. In Part III, we discuss some of the local/short term and global issues which can be addressed by a two-dimensional process morphodynamic model. In Part IV, we present the large scale (2D depth-averaged) morphodynamic model of the Gironde estuary.

MORPHODYNAMIC MODELS

After a short review of existing process-based morphodynamic models, we present here the finite element Telemac system (focusing on 2D modules) which is used in the large scale morphodynamic application.

Review of morphodynamic models

Numerous morphodynamic models have been developed and applied in the past 30 years in order to predict the sediment transport rates and resulting bed evolution in complex environments. Comprehensive morphodynamic modeling systems like ECOMSed [Hydroqual, 2002], Mike21 [Warren and Bach, 1992], Delft3D [Lesser et al., 2004] and ROMS [Warner et al., 2008] generally include different flow options (from 1D to 3D), a wave propagation model and a sand transport model including bed-load and suspended load (for a review, see for example Papanicolaou et al. [2008]).

Most existing morphodynamic modeling systems rely on finite difference methods and are therefore constrained by the use of boundary fitted (orthogonal curvilinear horizontal coordinate systems, sigma stretched vertical coordinates) which are only suitable for simplified geometry.

The Telemac system

Like other comprehensive models, the Telemac system comprises various modules to calculate the flow (Telemac-2d or -3d), the waves (Tomawac) and the sediment transport (Sisyphe), which can be chained or internally coupled [cf. Villaret et al., 2011]. In comparison with other comprehensive modeling systems, the main originality lies in the efficiency and flexibility of the finite elements. All modules of the Telemac system are based on unstructured grids and finite-element or finite volume algorithms. The sources and user manuals can be downloaded from the Telemac website: http://www.telemacsystem.com. One important feature is parallelism with domain decomposition.

Different numerical methods are available, as described by Hervouet [2007]. The method of characteristics, kinetic schemes and others can be applied to calculate the convective terms in the momentum equation. The wave equation as well as providing a method of smoothing free surface instabilities is particularly well suited for large scale applications. The use of implicit schemes enables relaxation of the CFL limitation on time steps (typically, values of Courant numbers up to 10 or 50 are acceptable).

For the treatment of tidal flats, a new algorithm based on segments ensures positive water depths and mass conservation without extra limitation of the time step [Hervouet et al., 2010].

The Telemac-2D flow module solves the shallow water equations (momentum and continuity), with several options for the horizontal diffusion terms (depth-averaged k-ε, Elder model (1959) or constant eddy viscosity models) and source terms (atmospheric pressure gradients, Coriolis force …).

$$\frac{\partial h}{\partial t}+\frac{\partial hU}{\partial x}+\frac{\partial hV}{\partial y}=0 \tag{1}$$

$$\left.\begin{aligned}\frac{\partial U}{\partial t}+U\frac{\partial U}{\partial x}+V\frac{\partial U}{\partial y}&=-g\frac{\partial Z_s}{\partial x}+\frac{\tau_x}{h}+\frac{1}{h}div(h\nu\, grad(U))\\ \frac{\partial V}{\partial t}+U\frac{\partial V}{\partial x}+V\frac{\partial V}{\partial y}&=-g\frac{\partial Z_s}{\partial y}+\frac{\tau_y}{h}+\frac{1}{h}div(h\nu\, grad(V))\end{aligned}\right\} \tag{2}$$

Where h is the water depth, and U, V the horizontal mean velocity components. The first term on the right hand side of the equations of motion is the pressure gradient (Z_s is the free surface elevation), the second is the bottom friction, and the third, the horizontal diffusion. The mean bottom shear stress τ_0 (τ_x, τ_y) enters the momentum equation (Eq. 2).

The bed (total) shear stress represents both the combined effect of skin friction and additional drag (pressure) forces acting on the bed in the presence of bedforms. In 2D models, it is related to the mean (depth-averaged) flow velocity $|U|=\sqrt{U^2+V^2}$ by a quadratic friction coefficient denoted C_D:

$$\tau_0=\frac{1}{2}\rho C_D U^2 \tag{3}$$

Different options are available for the choice of friction coefficient. Assuming a logarithmic velocity profile up to the free surface, the friction coefficient can be related to the representative equivalent bed roughness, denoted k_s:

$$C_D=2\kappa^2\left[Ln(\frac{30h}{ek_s})\right]^{-2} \tag{4}$$

where κ (=0.4) is the von Karman constant and e=exp(1).

The equivalent bed roughness coefficient k_s is represented in terms of the characteristic bedform dimensions averaged over the grid scale. This single scale represents therefore a wide spectrum of bedforms including the effect of grain skin friction, micro-scale ripples (typically of the order of 10cm) and mega ripples and dunes that scale with the water depth. The macro-scale features (typically of the order of 100 m) are typically smaller than the grid size in large scale models, and their effect needs to be parameterized also.

The bed roughness is generally determined based on a trial and error procedure in order to reproduce the available hydrodynamic data.

The morphodynamic model Sisyphe calculates the sediment transport rates, decomposed into bed-load and suspended load, and the resulting bed evolution. The model is applicable to non-cohesive sediment, composed of either uniform grains or multi-grains, characterized by their mean size and density, as well as cohesive sediments and mixtures. Detailed information on the sediment transport processes can be found in the Sisyphe user manual [Villaret, 2010] and in Villaret et al. [2011].

A choice between 10 classical transport formulae is available to predict the bed load Q_b as a function of the hydrodynamic bed shear stress, corrected for skin friction. For the suspended load, we solve an additional transport equation for the depth-averaged suspended sediment concentration transport equation, where the source term represents the net erosion (E) minus deposition (D) flux.

For non-cohesive sediments, the erosion flux (E) is expressed in terms of an 'equilibrium' reference concentration [e.g. Van Rijn, 1984] which is defined at a reference elevation whereas, for cohesive sediments, the Krone-Partheniades relation relates the erosion rate to the excess bed shear stress minus the resistance of the bed to erosion, which varies as a function of mud composition and consolidation state. The deposition flux (D) is calculated as the product of settling velocity W_s and the near bed concentration.

The variation of bed elevation can be derived from a simple mass balance, as expressed by the Exner equation:

$$(1-p)\frac{\partial Z_f}{\partial t} + Div\left(\vec{Q_b}\right) + \left(E - D\right) = 0 \qquad (5)$$

where p is the bed porosity (p~0.4 for non-cohesive sediment), Z_f the bottom elevation, Q_b the solid volume transport rate (bed-load) per unit width, and the last term represents the net erosion (E) minus deposition (D) flux.

Sediment transport rates are calculated as a function of the local skin friction, which is calculated from the hydrodynamic friction τ_0 by use of a skin friction correction parameter (μ<1). The skin friction correction parameter μ is the ratio of skin and total friction ($\mu = \frac{C_d'}{C_d}$) where C_d' is the quadratic friction coefficient corresponding to the skin roughness, which, for flatbed conditions, is proportional to the mean grain size ($k_s' = 3d_{50}$).

Internal coupling and method of feedback

The sediment transport model (Sisyphe) relies on a complete description of the flow field, through internal coupling with the flow module; at each time step, the hydrodynamic model (Telemac-2D or -3D) calculates the flow field and sends to Sisyphe the spatial distribution of the main hydrodynamic variables: water depth h, horizontal depth-averaged flow velocity components U and V, and the quadratic friction coefficient C_d. The bed roughness parameter has been identified as the key parameter regarding sediment transport rate predictions.

In order to avoid possible inconsistency between the morphodynamic model and hydrodynamic model, a method of feedback for the bed roughness, decomposed into skin friction and drag friction, has been developed [cf. Villaret et al., 2011]. According to van Rijn [2007], the total bed roughness can be decomposed into a grain roughness k_s', a small-scale ripple roughness k_r, a mega-ripple component k_{mr}, and a dune roughness k_d:

$$k_s = k_s' + \sqrt{k_r^2 + k_{mr}^2 + k_d^2} \qquad (6)$$

Both small scale ripples k_r and grain roughness k_s' have an influence on the sediment transport laws, while the mega-ripples and dune roughness only contribute to the hydrodynamic model (total friction). In the bed roughness feed-back method, the total bed roughness calculated by Sisyphe is sent to Telemac-2d and converted into quadratic friction coefficient. The total bed roughness is sent to the 2D- hydrodynamic model and converted into a friction parameter for sediment transport rate predictions, before calculating the bedload transport Q_b and erosion rates (E).

Assuming local equilibrium conditions between the flow and bed morphology, the value of the roughness for each bedform component depends on a mobility parameter ($U^2/\Delta g d_{50}$, where U is the flow velocity and Δ the excess of relative density) and the median diameter of the bed material d_{50}, with different expression for silt, sand or gravel. In summary the roughness can be expressed as a function of the following parameters (Eq. 2).

$$k_s = fct\left(\frac{U^2}{\Delta g d_{50}}, d_{50}, d_{silt}, d_{sand}, d_{gravel}\right) \qquad (7)$$

where d_{silt}=0.02 mm, d_{sand} =0.062 mm and d_{gravel}=2 mm. Further, the formulation of van Rijn [2007] for k_s is sensitive not only to the sediment grain size but also, where dunes and mega-ripples are concerned, to the water depth.

This method has been selected as the most accurate for the lower alluvial regime (ripples and dunes) as typically met in estuarine conditions [Huybrechts et al., 2010b]. For waves and combined waves and currents, ripple dimensions can be calculated as a function of the wave parameters. Here such estimations have been implemented only in the case of the Dee estuary [see Villaret et al., 2011] again based on the methodology of van Rijn [2007] which, for combined waves and currents, utilizes a wave-current mobility number $(U^2+U_w^2)/\Delta g d_{50}$ wherein U_w is the near-bed wave velocity amplitude.

The procedure above for the prediction of the bed roughness accounts only for the turbulent form drag exerted by the physical bed roughness, i.e. the roughness associated with the physical dimensions, shapes and asymmetries of sub-grid-scale bed features, of which dunes are normally of greatest importance. In addition, however, *wave-current interaction* in the seabed boundary layer should, in principle, be included as a further factor enhancing the total drag felt by the (tidal) flow. Wave stirring in the near-bed layer can greatly enhance the turbulence intensity and this should be reflected, in turn, in the bed roughness k_s. Van Rijn [2007] proposed a formulation that typically enhances the 'physical roughness' k_s by a factor of between 2 and 5 times due to wave-current interaction. One conceptual uncertainty here, however, is whether the k_s enhancement should be applied to some or all of the four component parts of k_s involved in Eq.(6) ; there is presently insufficient experimental evidence here, particularly regarding k_d and k_{mr}.

Another limitation arises in the use of Eq.(6) when time-varying flows such as tidal flows are involved. While spatial variations in k_s are potentially important in determining the strength of the mean flow locally in a computational domain, large temporal

variations are typically predicted to occur also through the use of Eq.(6) *instantaneously* as the computation proceeds. These temporal variations in k_s through a tidal cycle may, in practice, be unrealistically large, particularly for dunes, due to the present lack of any bed form history effects in our simulations. From observations made in time-varying river flows Paarlberg et al. [2010] have pointed out that observed dune heights do vary significantly in time, exhibiting a hysteresis lag with regard to the flow strength, and Coleman et al. [2010] have proposed a predictive scheme for k_s in such circumstances. However, intra-tidal variation in k_s may actually be relatively small due to the time scales required for dunes to evolve. At the present stage of this research we do not yet have sufficient field evidence to propose a suitable formulation for the history effect in k_s and this represents a clear priority for future study.

THE GIRONDE ESTUARY

The Gironde macro-tidal estuary extends from the confluence of the Garonne and Dordogne Rivers to the mouth on the Atlantic coastline. Its width ranges from 3.2 to 11.3 km wide downstream for a length of 170 km. The central part is characterized by a complex geometry, with the presence of different channels separated by elongated sand banks and characterized by a high turbidity level due to cohesive sediments coming from both rivers.

The estuary can be classified as macro-tidal, hyper-synchronous and with an asymmetric tide (4 h for the flood 8 h 25 for the ebb). The tidal amplitude near the mouth of the estuary ranges from 2.2 m to 5.4 m during the spring-neap cycle, higher than 4m further upstream. The river discharge ranges from 50 up to 2000 $m^3.s^{-1}$. During flood events, the river flow rate becomes occasionally greater than 5000 $m^3.s^{-1}$.

Sediment bed composition

The bed composition is highly variable in space: gravel and sand can be found at the mouth of the estuary as well as upstream of the tributaries. Contrarily, the channel bed is dominated by the mud except for some sand banks from the mouth to the tributaries [Allen, 1972]. Information concerning the bed material is generally provided qualitatively: areas of sand, mud or gravel are reported on maps. A measurement campaign was performed in 2009 which provides detailed quantitative information on the spatial variation of the sediment granulometry and composition in the central part: 39 samples were collected for a study area about 10 km length in the vicinity of the velocity measurements. The median diameter sizes from 0.01 mm to 0.35 mm and the space-averaged value of the median diameter for the 39 samples is 0.03 mm. At the estuary mouth, the median diameter of the bed material ranges within 0.25 and 0.38 mm [Port Autonome de Bordeaux, 2002]. The bed material of the Gironde is thus composed of a mixture of mud and of highly graded sand. Some bed forms are locally observed near sand bank or at the mouth even if the mud seems to dominate the bed material in the central part. For instance, Allen [1972] reports the presence of dunes about 1 m height and 10 m long a little bit upstream the location of the velocity measurements (Fig. 1). More recently, such large scale bed forms are reported in the same area in the main channel on the right side. Typical dimensions of those small scale dunes are about 5.5 m in length with a height of approximately 70 cm.

Bathymetric evolutions

In the central part of the estuary, morphodynamic features evolved drastically from 1994 to 2005 as monitored through regular bathymetric surveys (Fig. 2). Those bed evolutions are either due to anthropogenic or natural origins and may also notably be attributed to large amounts of dredging volumes.

The bed evolutions are measured through bathymetry surveys made every 5 years, since it takes about 4 years to cover the whole estuary from Bordeaux to Verdon station. A better accuracy is expected in the central part of the estuary and model validation will be focused on this part. A rather coarse grid is applied in both maritime and fluvial parts, where the bathymetry has not be updated. In the central part of the estuary, morphodynamic features evolved drastically from 1994 to 2005 and more detailed bathymetric data sets are available for years 2000 and 2005. The 1995 bathymetry is used as an initial condition of the morphodynamic model whereas the 2000 data is used to compare the measured bed evolutions with model predictions. The 2005 bathymetry is used in the hydrodynamic model validation. The 1995-2000 differential bathymetry is used for morphodynamics model validation.

Hydrodynamic data

The tide propagation can be analyzed through water levels, which are measured every 5 min at nine hydrometric stations along the estuary from the Verdon station at the mouth to the harbour of Bordeaux, located 10 km upstream of the confluence between the Dordogne and Garonne rivers (Fig. 3). Measurements of flow rates are available every hour at the upstream boundary.
Velocity measurements are sparser in comparison to the water level data. For instance, ADCP velocity profiles were measured by EDF R&D in August 2006 at 3 points located along the same cross section, approximately 5 km downstream Pauillac station (Fig. 3) and at 5 points along the estuary from September to October 2009 (7 points were measured, as shown on Fig. 1, but only 5 of them were successful). Both events are used to calibrate and validate the hydrodynamic model [Huybrechts et al., 2012].

Turbidity measurements

The suspended load and related water quality parameters have been measured at four stations along the estuary [www.magest.u-bordeaux1.fr] since 2005. This monitoring gives information on the turbidity variation along the estuary as a response of seasonal variation in the river flow rates. Three stations are located in the tributaries whereas one station is located in the estuary itself at Pauillac station (Fig. 3). The turbidity data can be converted into massive sediment concentration using a conversion factor of 0.0023 [Commarieu, 2007]. However during the two velocity field surveys (August 2006; September-October 2009) used to calibrate the hydrodynamics, the turbidity data are not available at Pauillac station. Therefore, two events of sediment transport data collected in August 2007 are selected: from 1st to 5^{th} (spring tide) and from 7^{th} to 11^{th} (neap tide). It is assumed that the hydrodynamic conditions in August 2007 are similar as the hydrodynamic conditions in August 2006 during the velocity survey and thus that the hydrodynamic calibration of the model still remains valid.

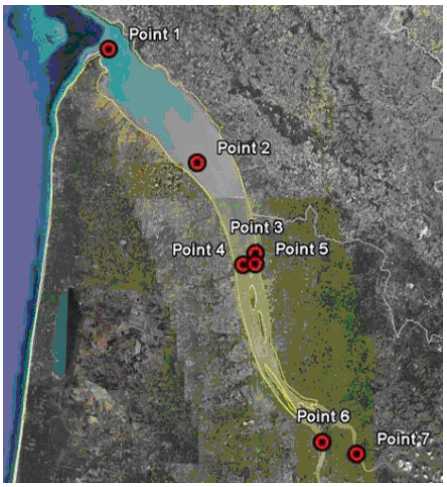

Figure 1. ADCP velocity measurements along the Gironde estuary (Sept 2009 campaign).

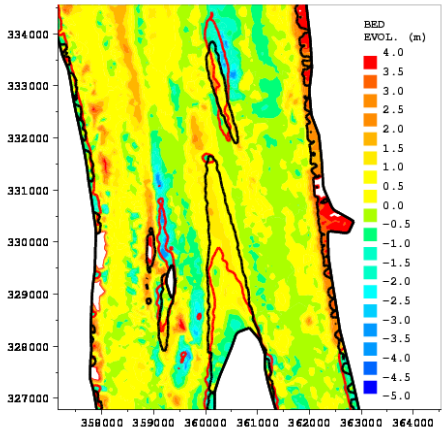

Figure 2. Bed evolution from 1995 to 2000 with iso-line zero (in red is 1995 data, in black, 2000).

MORPHODYNAMIC MODEL

We present here our ongoing effort to develop a process-based model to describe the sediment transport rate and medium term evolution in the Gironde estuary. The 2D approach (Telemac-2d/Sisyphe) has been selected here as a good compromise between model accuracy and CPU time.

Grid mesh and extension

The numerical domain covers the whole estuary: from the Bay of Biscay (mouth near Verdon, Fig. 3) to La Reole and Pessac, considered as the limit of the tide influence in the tributaries. The numerical domain is extended into the coastal zone (30~40 km from Verdon station) in order to impose the tide height in deep water. The unstructured triangular mesh comprises 22 650 nodes. The cell lengths extend from 50 m in the refined central part and up to 2,5 km offshore. At the mouth (Fig. 4(a)), a mesh size of 100 m is imposed in the smallest flow section. The mesh is also refined around the navigation channel where bathymetric gradients are expected. In the central part (Fig. 4(b)), the coarser mesh size is about 200m. The mesh becomes finer near the power plant between Trompeloup and Patiras islands.

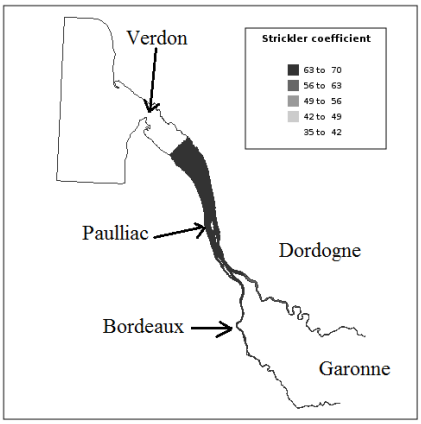

Figure 3. Spatial distribution of the calibrated friction coefficient for the hydrodynamics.

Boundary conditions

The tidal components are issued from a global oceanic model [Lyard et al., 2006] and are recomposed following Schureman [1968] methodology. The tide height is composed of 46 harmonic waves [Huybrechts et al., 2011].

Flow rates are imposed at the upstream boundary and the tide height at the maritime downstream boundary for the hydrodynamics.

Equilibrium conditions are applied for the sediment transport rate (suspended sediment concentration and bed-load transport rates) in order to insure zero-evolution on the boundaries.

Bed roughness prediction

The feasibility of the van Rijn's bed roughness predictor method has been assessed, and the method of feedback leads to stable results. However in order to achieve best agreement with the measurements of flow velocity, the predicted (total) bed roughness converted into Strickler, had to be time-averaged and slightly adjusted by a trial and error procedure in order to obtain a set of best fit coefficients. The best fit (adjusted) set of friction coefficients are compared to their predicted mean values in Table 1. In order to predict the bed roughness k_s, information on the bed material composition (such as d_{50}) needs to be provided. At the mouth and in the coastal area, a median diameter equal to 0.31 mm is selected. In the central part, a value 0.03 mm is imposed

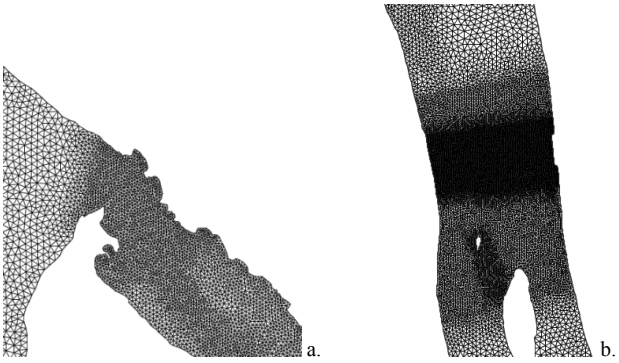

Figure 4. Grid mesh of the large scale model (22 650 nodes); (a) Zoom of the maritime part. (b) Zoom on the central part.

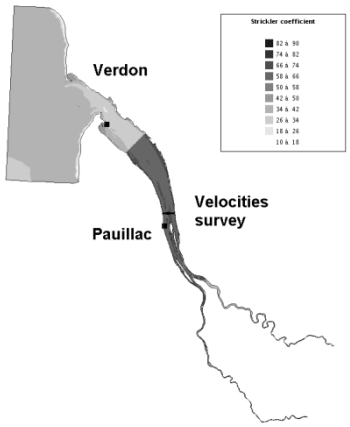

Figure 5. Spatial distribution of the calculated (Strickler) friction coefficient for the hydrodynamics based on van Rijn [2007].

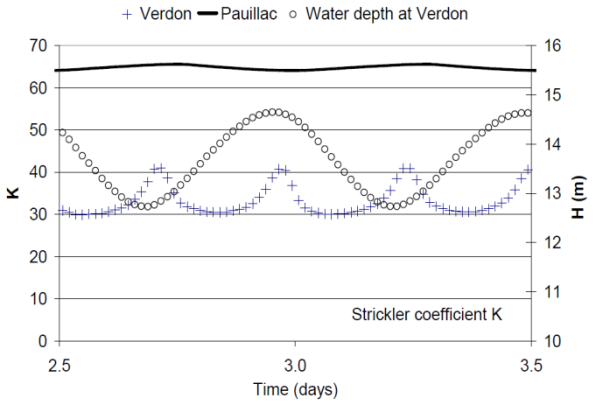

Figure 6. Time variation of the calculated Strickler coefficient at Pauillac and Verdon stations during a tidal cycle.

[Huybrechts et al., 2010b]. At each node of the grid, a time and space variable roughness can be predicted according to the method of van Rijn. Both spatial distribution and time variation are shown on Figure 5 and 6.

At Verdon (mouth of the estuary) and Pauillac (centre part) stations, time evolutions of the predicted friction coefficient are plotted (Fig. 6). During a tidal cycle, the Strickler coefficient at Verdon varies from 28.8 to 41 $m^{1/3}/s$ with a time-averaged value of 32.6 $m^{1/3}/s$, whereas it varies from 63.6 to 66 $m^{1/3}/s$ with a time-averaged value of 64.8 $m^{1/3}/s$ at Pauillac. The maximum Strickler coefficient corresponds to low or high tide (Fig. 6). At the mouth, the Strickler coefficient has a larger gap between the minimum and maximum value since bed forms such as dunes can develop. In the central part, the median diameter corresponds to fine cohesive material and the model predicts a quasi-constant value of the roughness which is in good agreement with the calibrated value. More significant differences are observed at the mouth where the van Rijn equation seems to predict too much friction, which is possibly due to the neglected effect of waves and wave-current interactions as discussed in Davies and Thorne [2008].

Hydrodynamic model validation

The hydrodynamic model results obtained with the predicted time-varying bed roughness and the calibrated constant roughness are compared with the measurements and the results previously obtained with the calibration (see Fig. 7). The top figures show the tidal signal at two points (Verdon and Pauillac stations) and the bottom figures, the velocities.

As expected, the tidal signal obtained with the van Rijn equation has a slightly smaller amplitude than the measurement at the Verdon station, which is consistent with a possible overestimate of the friction in the maritime part. This may be due to the neglected effect of waves. At Pauillac, the accuracy of both model results is equivalent in comparison to the data. However, the amplitudes of the velocity signal are significantly under-predicted using the van Rijn equation. For the morphodynamic computations, the calibrated Strickler coefficients are kept, while we further assume fully non-cohesive sediments. Therefore, the effect of fine cohesive sediment which presumably inhibit the development of bedforms in the central part are implicitly included into the value of the Stickler coefficient.

Table 1. Comparison between predicted mean (time-averaged) and calibrated constant values of the Strickler coefficients at two stations.

Strickler coefficients $[m^{1/3}/s]$	Verdon	Pauillac
Predicted (mean)	32.6	64.8
Calibrated (constant)	37.5	67.5

Morphodynamic model results

In the present contribution, the bed material is treated as a mixture of silt, fine sand and medium sand. For this test case, the cohesive effects are not included into the sediment transport. Some new developments on the cohesive effects are still in process [Van et al., 2011] to integrate for instance mud consolidation.

The variability of the sediment distribution along the Gironde estuary is schematized by assuming an initial uniform sediment distribution for each geo-morphological unit. In the upper river part, the bed sediment is composed of silt (d_{50}= 60 µm), whereas the maritime part is made of medium sand (d_{50}= 310 µm). In the central part, the bed is made of a mixture of 50% of fine sand (d_{50}= 210µm) and 50% of silt (d_{50}= 60µm).

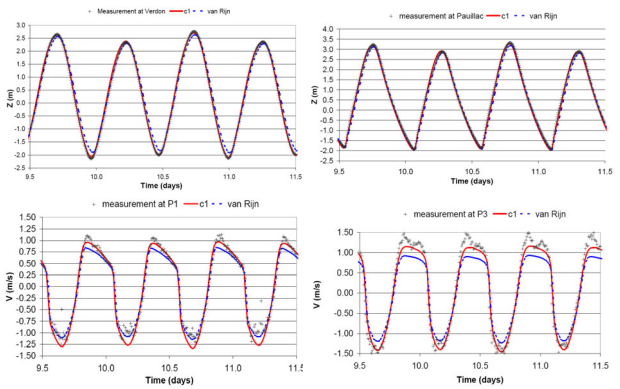

Figure 7. Comparison between the model results (c1 in red are the calibrated results c2, in blue the results obtained with the van Rijn predictor). The black points are the data.

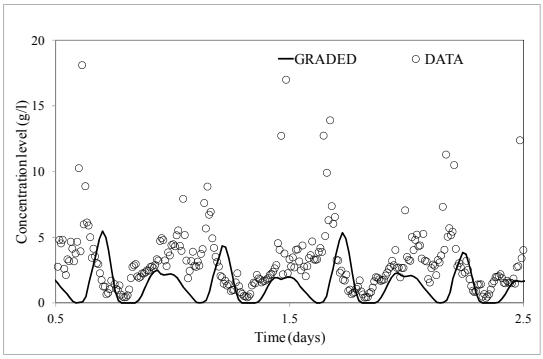

Figure 8. Time-varying concentration in g/l calculated at Pauillac (t=0 corresponds to the August 1st 2007 (OhTU).

The grain size distribution calculated by the model after one year is shown on Fig. 9(b). In the maritime part, the fine sediment is flushed out and deposited offshore, which is in qualitative agreement with observations (Fig. 9(a)). In the central part, very fine (cohesive) sediment is dominant downstream of the Patiras island and deposits area, whereas coarser sediment is predominant in the deeper channels, as observed by Boucher [2009].

Sediment transport predictions are highly sensitive to the sediment granulometry and bed composition as well as to the choice of transport formula. In the present application, transport rates are dominated by the presence of very fine particles in suspension. The suspended load is highly sensitive to the choice of settling velocity, which can be deduced from the grain diameter using a semi-empirical formula [cf. van Rijn, 1984]. The reference length delineating the bed-load and suspended load is taken at 0.5 k_s as suggested by van Rijn, where k_s is the equivalent bed roughness. Influences of the ripples on the skin friction and thus on the transport rates are incorporated for all the performed computations. Model results are in qualitative agreement with turbidity measurements from the Magest survey. Time-varying concentrations calculated at the Pauillac station are shown in Figure 8.

Best agreement in the central part, at Pauillac station, is obtained by adjusting the settling velocity to 1.8 mm/s for the finer grain size and by lowering the empirical coefficient in the van Rijn formula (0.05 instead of 0.15). In comparison to the data (see Fig. 7), the model tends globally to underestimate the peaks in concentrations. The overall time-variation is qualitatively well reproduced.

In the large scale morphodynamic model, the sequence of dry or flood seasons can be imposed at the upstream boundaries based on measured flow rates from January 1st 1995 to December 31st 2000. During this sequence of dry and flood seasons, the flow rate in the Garonne River decreases down to 60 m^3/s during the dry season and reaches its maximum, up to 4000 m^3/s, during winter floods. In Fig. 10(b), we show the 5-year bed evolution. The bed evolution is overall, in both qualitative and quantitative agreement with the 5-year differential bathymetry, shown in Fig. 10(a).

The growth rate of the Patiras island and associated deposition rates of the fine particles downstream of the island are over-estimated by roughly a factor 2. This discrepancy may be due to some uncertainty in the representation of physical processes as well as some uncertainty in the bathymetric data. Indeed, the 1995 historical bathymetry data set is based on digitalized bathymetrical maps, from mono-beam bathymetry (the original data was not available). So the final uncertainty in the differential bathymetry is difficult to assess. The measured bed evolution in the vicinity of the banks is probably unrealistic.

The model gives overall reasonable estimates of the bed evolution despite the fact that the calculated shape of the deposit in the lee of the central island is not well reproduced. This is not surprising since this bank is dominated by mud processes which are not presently accounted for.

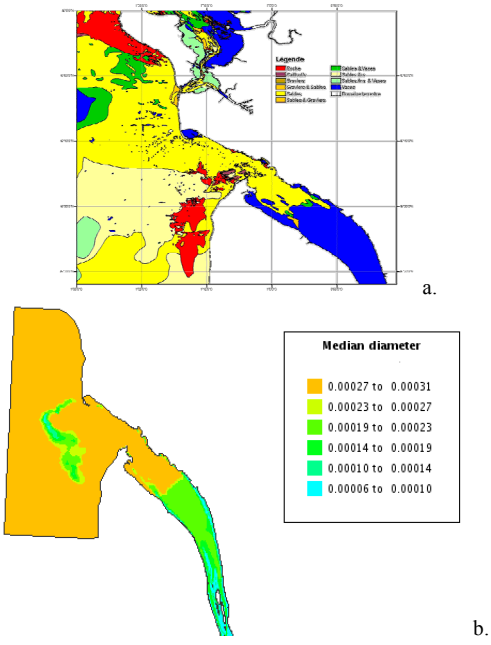

Figure 9. Grain size distribution: (a) Measurements (provided by Shom). (b) Predicted mean diameter.

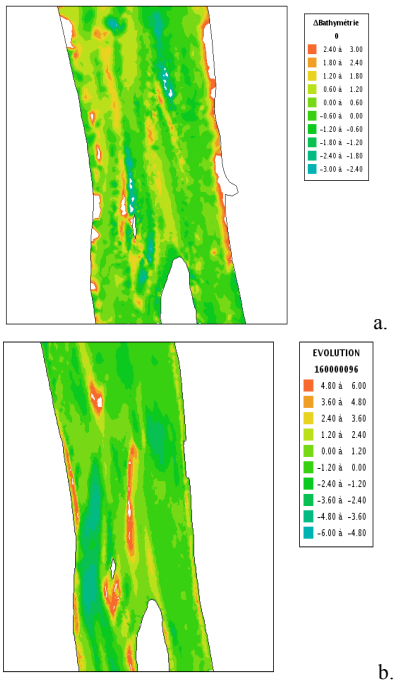

Figure 10. 5-year Bed evolution in the central part (1995-2000): (a) The differential bathymetry. (b) The calculated bed evolution.

CONCLUSIONS

A 2D morphodynamic process-based model has been applied to predict the bed evolution in a complex estuarine system: the Gironde estuary. Thanks to recent progress in the numerical methods and extensive use of parallelization, medium term predictions (order of decades) can be achieved at the basin scale (150 km) without the use of hydrodynamic filtering methods nor morphodynamic factors. With a time step of 100 s, 5 years of bed evolution requires approximately 18 hrs of computational time using 8 processors (Intel Xeon-3.33 GHz).

The model (Telemac-2d/Sisyphe) presented here takes into account complex interacting processes between the flow and sediment transport. In particular, a method of feedback for the bed roughness which avoids inconsistencies between the flow and sediment transport model, has been proved to give physically realistic as well as stable numerical results. For validation, model results could be further improved by slightly adjusting the predicted time-averaged mean friction coefficients in order to get a set of best fit coefficients (constant). The bed friction predictor can therefore be viewed as a way to guide a time-consuming trial and error procedure, on physically sound basis.

Sediment transport processes include the coupling between bedload and suspended load, as well as sand grading effects. Here only 3 sand classes were considered which is a very crude schematization of the high heterogeneity in the sediment bed composition. We only account for the non-cohesive processes. The effect of cohesion and mixed sediment processes needs to be accounted for using the consolidation model [cf. Van et al., 2011]. The effect of waves is discussed in Villaret et al. [2011].

ACKNOWLEDGEMENTS

The authors thank the “Grand Port Maritime de Bordeaux (GPMB)”, the “Service Hydrographique et Océanographique de la Marine (SHOM)”, Etablissement Public Territorial du Bassin de la Dordogne" and "Département de l'équipement- DDE 33 for providing their data.

REFERENCES

Allen G.P., 1972, Etude des processus sédimentaires dans l’estuaires de la Gironde, Phd Thesis Université de Bordeaux. 314p.

Boucher, O., 2009, Note sur les analyses de granulométrie Laser sur les échantillons de sédiments prélevés en Gironde, rapport Cetmef.

Chini N., Villaret C., 2007: Numerical modelling of the bed evolution downstream of a dike in the Gironde estuary, *Proceedings of the River, Coastal and Estuarine Morphodynamics Conference. 7p.*

Coleman, S. E., Zhang, M. H., & Clunie, T. M. (2005). Sediment--Wave development in subcritical water flow. Journal of Hydraulic Engineering, 131(2), 106-111.

Commarieu M.V., 2007: Oxygénation des eaux dans un estuaire hyperturbide, observations in-situ, expérimentation et modélisation, Thèse de l’Université de Bordeaux, 175 p.

Davies, A.G. , Thorne P.D., 2008: Advances in te study of moving sediments and evolving seabed, Surv. Geopys, DOI.1007/s10712-008-9039-x

Hervouet J.M., 2007: Hydrodynamics of free surface flow modelling with the finite element method, Wiley. ISBN 978-0-470-03558-0, 341p.

Hervouet J.M., Razafindrakoto E., Villaret C., 2011: Dealing with dry zones in the free surface flow, a new class of advection schemes, IAHR Congres. Brisbane, Australia.

Huybrechts N., Villaret C., Lyard F., 2011: Optimized predictive 2D hydrodynamic model of the Gironde estuary (France). (….Journal of Waterway, Coast, Port and Ocean engineering).

Karunarathna H., Reeve D., Spivak M., 2008: Long term morphodynamic evolution of estuaries: an inverse problem, Estaurine Coastal and Continental Shelf Science 77, 385-395.

Lesser G.R., Roelvink J.A., van Kester J.A.T.M., Stelling G.S, 2004: Development and validation of a three dimensional morphological model, Coastal Engineering, 51, pp. 883-915.

Lyard, F., Lefevre, F., Letellier, T., Francis, O., 2006: Modelling the global ocean tides: modern insights from FES2004”, Ocean Dynamic, Vol 56 (5-6), pp 394-415.

Paarlberg, A.J., Dohmen-Janssen, C., Hulscher, J.M.H., Termes, P., & Schielen, R. (2010). Modelling the effect of time-dependent river dune evolution on bed roughness and stage. Earth Surface Processes and Landforms, 35, 1854–1866 (2010) DOI: 10.1002/esp.2074.

Papanicolaou A.N., Elhakeel M., Krallis G., Prakash S., Edinger J., 2008 : Sediment transport modelling review - Current and Future Development, Journal of Hydraulic Engineering, 134(1).

Schureman, P. (1958) “Manual of harmonic analysis and prediction of tides”, US Department of Commerce, Coast and Geodetic Survey, Washington, US.p317.

Van L.A., Pham Van Bang D., 2011: On the self weight of consolidation mixtures, River Coastal Estuarine Morphodynamics Conference, Beijing sept. 2011.

Van der Wegen, M., Roelvink, J.A., 2008: Long term morphodynamic evolution of a tidal embayment using a 2D process-based model, Journal of Geophysical Research, Vol. 113, C03016, doi: 10.10292006JC003983.

Van der Wegen, M. 2010, Modeling morphodynmaic evolution in alluvial estuaries, PHD Thesis , Delft University of Technology, ISBN 978-0-415-59274-1 (Taylor &Francis Group).

Van Rijn, L.C. 1984 : Sediment transport, part III: bed forms and alluvial roughness, *J. Hydraul. Eng.-Asce*, 110(12), 1733-1754.

Van Rijn, L.C., 2007: Unified view of sediment transport by currents and waves. 1. Initiation of motion, bed roughness, and bed-load transport”, *J. Hydraulic Eng.* 133(6), pp 649-667.

Villaret, C., et al., 2011: Morphodynamic modeling using the Telemac finite-element system. Computers & Geosciences, doi:10.1016/j.cageo.2011.10.004

Villaret C., Huybrechts N., Davies A.G., Way O., 2011: Effect of bed roughness prediction on morphodynamic modelling: Application to the Dee estuary (UK) and to the Gironde estuary (France), Proceedings of the 34th IAHR World Congress, Brisbane (Australia).

Warner J.C., Sherwood C.R., Signell R.P., Harris C.K., Arango H.G., 2008: Development of a three-dimensional, regional, coupled wave current and sediment transport model, Computer and Geosciences, 34, pp. 1284-1306.

Warren, I.R., Bach, H.K., 1992. MIKE 21: a modelling system for estuaries, coastal waters and seas. Environmental Software 7 (4), 229e240.

Short papers

Of the NCK-days 2012

NCK photo competition

Alma de Groot: Wad Schiermonnikoog

Tidal asymmetries in estuaries due to channel-flat interactions, a simple model

N.C. Alebregtse, H.E. de Swart and J.T.F. Zimmerman

Paper confidential

DOI: 10.3990/2.174

Towards a three-dimensional geological model of the North Sea subsurface

Marcel Bakker[1], Sjef Meekes[2], Sytze van Heteren[1], Denise Maljers[1], Bob Paap[3], Simon Fitch[4], Vincent Gaffney[4] and Ben Gearey[4]

[1]TNO Geological Survey of the Netherlands, PO Box 80015, NL-3508 TA Utrecht, The Netherlands, marcel.bakker@tno.nl
[2]TNO Sustainable Geo-Energy, PO Box 80015, NL-3508 TA Utrecht, The Netherlands
[3]Deltares Subsurface and Groundwater Systems, PO Box 85467, NL-3508 AL Utrecht, The Netherlands
[4]IBM Visual and Spatial Technologies Centre, The University of Birmingham, Edgbaston B15 2TT, United Kingdom

ABSTRACT

The Geological Survey of the Netherlands is extending the 3D model of the Quaternary record as created for the onshore part of the country to the North Sea realm. Onshore, cores are the most important source of information. Offshore, seismic data are at least equally valuable. A recent pilot study has shown that 2D and 3D seismic data, originally collected for hydrocarbon exploration, are very useful in delineating much shallower stratigraphic units. This is best achieved by interpreting 3D seismic surveys together with high-resolution 2D seismic lines and well data. In the pilot, focus has been on the Oyster Grounds and Silver Well areas in the central part of the Dutch continental shelf. The units modeled thus far include Middle- to Late-Pleistocene strata that have accumulated in the North Sea Basin. The 3D seismic surveys reveal some remarkable, well-preserved sedimentary features that may be difficult to recognize in 2D profiles but are clearly visible in horizontal time slices. Examples include intricate early Holocene tidal-channel systems and striking sets of tunnel valleys formed during multiple glacial episodes. The level of detail provided by the time slices enables paleolandscape scholars to reconstruct environmental settings of Mesolithic (mostly Holocene) times.

.

INTRODUCTION

Geological models are quantitative, user-oriented predictions of subsurface architecture and properties in 3D space [*Van der Meulen et al.,* in prep.]. They can be easily queried by end users of geological information to answer questions or make decisions in their respective areas of expertise. Two types of model have been developed for the onshore part of the Netherlands in recent years: (1) layer-based ones, with tops and bases of lithostratigraphic units only, and (2) voxel models composed of a regular grid of 3D pixels (voxels) with associated parameter values. These parameters include lithological characteristics, geotechnical, geochemical and hydrological attributes, and stratigraphy.

Geological modeling has replaced traditional mapping, which focused on producing qualitative visualizations of the subsurface. By using profile-type legends ('Unit X on top of Unit Y on top of Unit Z'), maps depicting the shallow subsurface provide some information on the variability of sedimentary successions, but digital geological models are much better able to show this variability. Although the maps have considerable detail, application possibilities are limited because they are not tailor-made for specific purposes. They have been used mainly for illustrative purposes, and have contributed significantly to our understanding of process-response relationships and to the development of geological concepts, including aspects of preservation.

After a successful transition onshore, resulting in the models DGM, NL3D and GeoTOP developed by the Geological Survey of the Netherlands, offshore geological mapping is now being

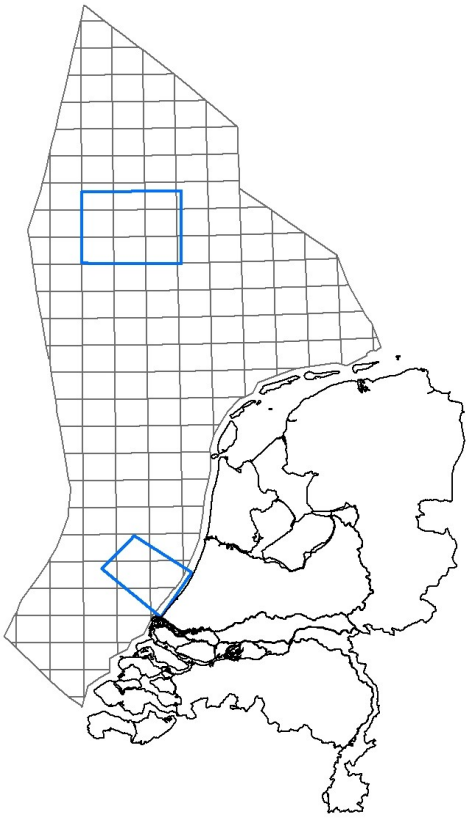

Figure 1. Pilot areas North and South on the Dutch shelf.

Table 1: Number and penetration depth of boreholes in pilot areas. Number of petroleum-exploration boreholes in parentheses.

Location	Boreholes 0-5 m	Boreholes 5-12 m	Boreholes 12-50 m	Boreholes >50 m
Pilot area North	35	39	5	1 (11)
Pilot area South	788	282	111	3 (34)

replaced by digital geologic modeling as well. Protocols developed and lessons learned during the development of these onshore models are used as much as possible, but marine mapping and modeling offers its own specific challenges requiring adjustments in approach and methodology. These challenges are related to differences between onshore and offshore data types and data densities. The land data come primarily from boreholes, whereas the offshore has been mapped with a balanced combination of boreholes and geophysical surveys, even for the upper 50 m. Also, the density of boreholes (point data) decreases significantly with increasing distance from the shore (Table 1), forcing us to rely increasingly on 2D (cross-sections) and 3D (full coverage in x, y, z) seismic data. A second challenge associated with marine mapping is the dynamic nature of this environment. Much more than onshore, sediment is being transported to such an extent that maps of the shallow subsurface may be out of date after as little as a decade.

Here, we report on the development of a protocol for modeling the shallow (upper 100s of m) subsurface of the Dutch part of the North Sea. Efforts to optimize data density are highlighted, as they determine the scale at which lithostratigraphic and lithological units can be recognized and mapped in light of the limited number of boreholes. Using this new protocol, lithological horizons are being digitized to form a layer-based model for two pilot areas (Figure 1), and initial steps are undertaken to build a voxel model that will allow seamless integration with onshore voxel models.

DATA TYPES

Borehole logs and laboratory analyses

Borehole logs are extracted from the DINO database developed and hosted by the Geological Survey of the Netherlands. Most information comes from shallow boreholes, typically up to 12 m deep but locally up to several 100s of m. The logs of some hydrocarbon-exploration wells provide information for the upper 100s of m as well. Most boreholes up to 5 m deep provided little-disturbed core samples. The vast majority of deeper boreholes were made with counterflush or related techniques resulting in disturbed samples. Per depth interval, borehole logs provide qualitative, visually assessed information on lithology and stratigraphy. For many boreholes, one or more samples were analyzed in the laboratory, most frequently for quantitative measures of grain-size parameters, micropaleontology or age.

Seismic profiles and time slices

In marine seismic-reflection surveys, acoustic waves generated by a seismic source towed by or mounted to a vessel are used to obtain information on the subsurface. When a seismic wave encounters a boundary between two materials with different acoustic properties, some of the energy in the wave will be reflected at the boundary, while some of the energy will continue through the boundary. The amplitude of the reflected wave depends on the impedance contrast between the two materials, which is greatest at the water-seabed interface.

A distinction can be made between high-resolution single- or multi-channel systems using frequencies of 100-1000 Hz and low-resolution multi-channel systems using <100 Hz. High-frequency single-channel systems record through short hydrophones. Their vertical resolution is on the order of a few meters, but they suffer from quality loss below first seabed multiple. High-frequency multi-channel systems record through hydrophone arrays in cables (streamers). Vertical resolution is on the order of meters below 100 ms (100 ms two-way travel time (TWTT) ≈ 75-80 m, including the water column), but lower in shallower units. Low-frequency multi-channel systems record through km-long hydrophone arrays. Vertical resolution is 5-15 m, depending on the frequency, on survey and source characteristics in relation to target geometry and on post-survey processing [*Praeg,* 2003]. In general, information of the upper 100-200 ms is lost. When acquisition parameters and processing are optimized for the shallow subsurface, however, information may be obtained from the seabed downward (starting at about 50 ms) when water depth is at least 40 m. In 3D surveys, multiple streamers are deployed in parallel to record data suitable for 3D interpretation of the structures beneath the seabed. Most 3D surveys employ low-frequency systems, which work best in deeper waters and cover very large areas efficiently at a coarse resolution [*Fitch et al.,* 2005].

Data collected via a single cable or streamer are displayed as vertical cross-sections through the subsurface. In our traditional surveys conducted for mapping purposes, distances between adjacent profiles are typically on the order of 10 km or more. Such a wide spacing is commonly sufficient to understand the overall architecture and formation of sedimentary systems, and may be good enough for pre-planning purposes, but render maps unsuitable for most applied use. Not all reflections can be correlated among lines, and most architectural elements have lateral dimensions smaller than can be resolved in a 10 x 10 km grid.

Data collected with multiple parallel streamers may be displayed as vertical cross sections, time slices or horizon slices. Time slices are sections of 3D seismic data having a certain arrival time. Because of spatial variability of sound velocity in the subsurface, they are near-horizontal rather than perfectly horizontal depth slices. Because of their map view, time slices are very suitable to identification of landscape elements as reflected in seismic amplitude. Horizon slices show the spatial pattern of particular reflections, created by tracing these reflections on all survey lines and interpolating the resulting data. Thus, features

can be extracted not only in planform but also in 3D, providing depth (and relative age) relationships.

WORKFLOW

Stratigraphic framework

The stratigraphic framework for the pilot studies is provided by published 1:250,000 map sheets made jointly by the British, Belgian and Dutch geological surveys during the 1980s and 1990s, and by the lithostratigraphic overview of *Rijsdijk et al.* [2005]. The borehole and seismic data are used to identify and map the tops of stratigraphic units. In identifying these units, well-defined reflections of 2D and 3D seismic datasets are linked and labeled systematically from the mid-Miocene unconformity upward, focusing on vertical (TWTT) mismatches at line intersections. These mismatches relate in part to positioning inaccuracies of older surveys.

Petrel project

At the core of the interpretation activities, a mother file was created in Petrel, a software application for the visualization and analysis of aggregated reservoir data from multiple sources. This mother file hosts all interpreted horizons. For interpretation, elements of the mother file are copied onto local hard drives. Changes and additions made on such local copies are exported regularly to the mother file.

Although the 3D seismic data allow superior visualization of even small sedimentary units, they are not ideally suited for the development of an overall stratigraphic framework of shallow (<300 m) units in Petrel. Therefore, we started reinterpreting high-quality 2D seismic lines collected during the 1980s and 1990s for the 1:250,000 maps. These lines were labeled, linking the major reflections to boundaries between stratigraphic units, and providing metadata including certainty of interpretation and name of interpreting geologist. The labeling scheme (for both bounding reflections and seismic facies) is summarized and updated in a table that includes information on reflection strength, internal reflection configuration, external form of bounded unit, degree of transparency and position relative to the reference datum (mean sea level).

The resulting framework is validated and supplemented with 3D seismics. By scrolling up and down in 3D seismic cubes at intersection planes with 2D seismic profiles, seismic facies and reflections identified on the 2D data can partly be assigned to depositional settings and environments. More subtle features on the 2D lines that were missed initially are labeled as part of this validation step. Finally, the 3D data are interpreted in their own right.

The seismic interpretations are validated with borehole data and with the results of laboratory analyses.

Export to modeling software (ISATIS)

The horizon slices as reconstructed in Petrel are exported as x-y-t grids with a time rather than a depth value for each x-y coordinate. The t values are translated into z values using seismic-wave velocities of x ms^{-1}. The resulting output is imported into Isatis, geostatistical software used to generate a digital geological model.

WORKFLOW OUTPUT

Pilot area North

The northern pilot area offers high-quality 3D seismics supplemented with 2D seismics and few boreholes. Using the workflow developed as part of the pilot study, we reconstructed the top of the Lower-Pleistocene Markams Hole Formation for an area of 55 x 65 km (Figure 2). When viewed at this large scale, this horizon slice provides a general impression of highs and lows, with an overall deepening from the southwest to the northeast. The eastern half of the image shows more complicated patterns associated with faults.

When zooming in and intersecting seismic profiles or horizon slices with time slices, sub-kilometer-scale patterns visible on the time slices provide direct indications of depositional environments. Some features can be easily recognized and interpreted, such as tunnel valleys, iceberg-scour marks and various channel fills. Tunnel valleys are large, valleys formed by meltwater under Pleistocene ice sheets near their margins. They may be up to 100 km long, kilometers wide and 100s of meters deep. The scour marks of icebergs, formed in open-marine waters beyond ice-sheet margins, appear as thin lines, commonly with a fairly uniform direction. Channel fills show intricate meandering and dendritic patterns (Figure 3). They may be tidal or fluvial in origin, and Pleistocene or Holocene in age.

The clear visibility of some of the smaller features on time slices is most likely related to the presence of shallow gas [cf. *Schroot and Schüttenhelm*, 2003], either formed in situ (*e.g.*, organics in tidal-channel fills) or supplied from an external source.

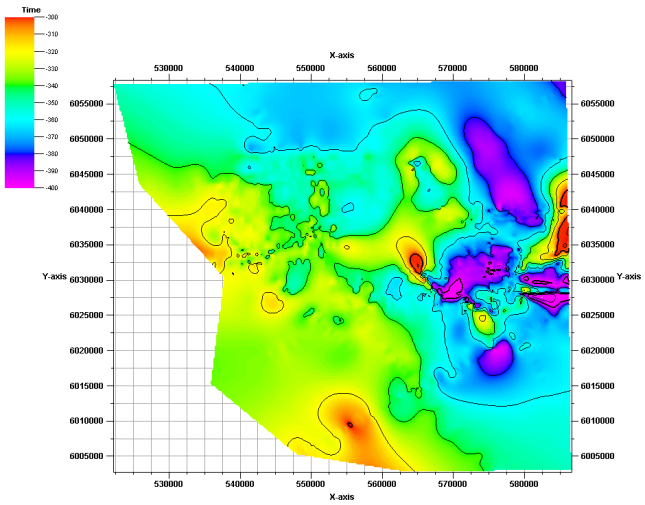

Figure 2. Horizon slice of Markams Hole Formation in pilot area South. Darker graytones denote lows.

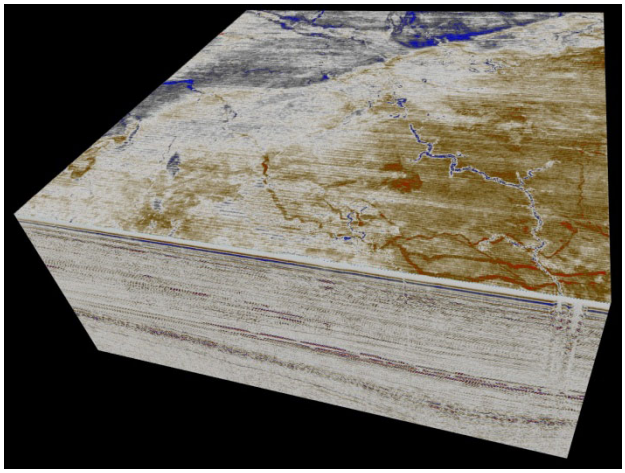

Figure 3. 3D seismic cube of a 20 x 20 km area with early Holocene tidal-channel systems in the time slice.

Pilot area South

The southern pilot area offers low-quality 3D seismics supplemented with 2D seismics and abundant boreholes. The low quality of the 3D seismics for the upper subsurface units in these shallower waters is related to system settings targeted at optimizing data quality for the deeper, petroleum-bearing units, and to a paucity of sediments containing shallow gas. Using the workflow developed as part of the pilot study, we were able to identify the remains of a once near-continuous horizon of Basal Peat covering the Pleistocene landscape that drowned during the early Holocene.

Validation with borehole data shows that the Basal Peat imaged on the time slices of the 3D seismics is very thin and buried under no more than a few m of clastic sediment. The fact that very shallow, decimeter-thick organic units can be identified and mapped using acoustic methods with a vertical resolution of 5-15 m shows the possibilities of our new approach. A disadvantage is the persistence of the gas-related reflections. Although the Basal Peat is very thin, its apparent thickness as derived from subsequent time slices is on the order of 10s of meters. When borehole data are scarce, it may be difficult to constrain the real thickness of imaged units.

DISCUSSION

From the pilot study, it has become apparent that the joint use of 2D and 3D seismics offers the best chance to extract detailed information, both laterally and vertically, from acoustic datasets. Time slices from 3D seismics are useful for identifying familiar sedimentary features such as channel fills and deltas. They can also be used for an initial validation of non-parallel anomalies on seismic profiles, such as clinoforms and irregular reflections. The temptation to focus on 3D seismic cubes and ignore 2D data should be resisted. Sedimentary features that cannot immediately be identified on the basis of their planform are commonly visible on seismic profiles as well, providing additional information on size and shape needed for interpretation. Because of their superiority in vertical resolution, high-frequency 2D seismics are also a good starting point for selecting and digitizing reflections for which horizon slices are constructed.

Digital geological models that include 3D seismic data are superior in detail to those relying exclusively on 2D seismic data and boreholes. For most end users of geological information, such detail is essential. Marine archeologists, for example, rely heavily on time-slice interpretation for paleolandscape reconstructions [*Fitch et al.*, 2005]. They need to be able to recognize former coastlines, fertile lowlands, and drainage patterns and directions.

The availability of 3D seismics for large parts of the North Sea, related to the abundance and distribution of petroleum reservoirs, provides a unique opportunity to model the shallow subsurface at a spatial resolution comparable to that of the onshore voxel models NL3D (250 x 250 x 1 m) and GeoTOP (100 x 100 x 0.5 m) and layer-based model DGM (100 x 100 m). This similarity in resolution will make it easier to work toward an integrated land-sea model of the shallow subsurface. Such a model will help understand subsurface-related processes that are unrelated to the present North Sea shore. Hydrological models, for example, may be optimized when the distribution of units with various hydraulic properties is known both on- and offshore. The creation of a digital geological model for the entire North Sea, and its integration with existing or future onshore models for North Sea countries will be a key step in the development of a web-accessible geo-model for all of Europe.

CONCLUSIONS

The joint use of 2D and 3D seismic data is very useful in delineating shallow stratigraphic units, revealing features that may be difficult to recognize in 2D profiles. A new workflow is used to delineate unit boundaries and to map features as small as 10s of meters laterally and as thin as a decimeter. The presence of shallow gas enhances many of these features but also leads to vastly overestimated apparent thicknesses. The resulting improvement in mapping resolution is a key step toward an integrated land-sea model of the shallow subsurface.

REFERENCES

Fitch, S., K. Thomson, and V. Gaffney (2005), Late Pleistocene and Holocene depositional systems and the paleogeography of the Dogger Bank, North Sea, Quaternary Research, 64, 185-196.

Praeg, D. (2003), Seismic imaging of mid-Pleistocene tunnel-valleys in the North Sea Basin – high resolution from low frequencies, Journal of Applied Geophysics, 53, 273-298.

Rijsdijk, K. F., S. Passchier, H. T. J. Weerts, C. Laban C., R. J. W. van Leeuwen, and J. H. J. Ebbing (2005), Revised Upper Cenozoic stratigraphy of the Dutch sector of the North Sea Basin: towards an integrated lithostratigraphic, seismostratigraphic and allostratigraphic approach, Netherlands Journal of Geosciences, 84(2), 129-146.

Schroot, B. M. and R. T. E. Schüttenhelm (2003), Expressions of shallow gas in the Netherlands North Sea, Netherlands Journal of Geosciences, 82(1), 91-105.

Van der Meulen, M. J., F. S. Busschers, S. H. L. L. Gruijters, J. L. Gunnink, P. Kiden, D. Maljers, J. Stafleu, W. O. van Berkel, M. J. van Bracht, T. M. van Daalen, F. G. van Geer, S. F. van Gessel, S. van Heteren, R. J. van Leeuwen, R. W. Vernes, and W. E. Westerhoff (in prep.), Geological surveying in the Netherlands: trends and perspectives, Netherlands Journal of Geosciences.

DOI: 10.3990/2.175

Influence of basin geometry on equilibrium and stability of double inlet systems

R.L. Brouwer[1] , H.M. Schuttelaars[2] and P.C. Roos[3]

[1]Section of Hydraulic Engineering, Delft University of Technology, P.O. Box 5048, 2600 GA Delft, The Netherlands, r.l.brouwer@tudelft.nl

[2]Institute of Applied Mathematics, Delft University of Technology, Mekelweg 4, 2600 GA Delft, The Netherlands, h.m.schuttelaars@tudelft.nl

[3]Department of Water Engineering and Management, University of Twente, P.O. Box 217, 7500 AE, Enschede, The Netherlands, p.c.roos@utwente.nl

ABSTRACT

This study investigates the influence of basin geometry on the cross-sectional stability of double inlet systems. The inlet is in equilibrium when the amplitude of the inlet velocities equals the equilibrium velocity (~1 m s^{-1}). This equilibrium is stable when after a perturbation the cross-sections of both inlets return to their original equilibrium value. The necessary amplitudes of the inlet velocities are obtained using an idealized 2DH hydrodynamic that calculates tidal elevation and flow in a geometry consisting of several adjacent rectangular compartments.

Model results suggest that regardless of the inclusion or exclusion of bottom friction in the basin, stable equilibrium states exist. Qualitatively, the influence of basin geometry does not change the presence of stable equilibrium. Quantitatively, however, taking a basin surface area of 1200 km^2, equilibrium values can differ up to a factor 2 depending on the geometry of the basin.

INTRODUCTION

Barrier island coasts are highly dynamical systems that serve as a first defense for the hinter lying mainland. Examples are the Wadden Sea coast of the Netherlands, Germany and Denmark, the U.S. East Coast and the Ria Formosa in Southern Portugal. Understanding the mechanisms causing these (multiple) tidal inlet systems to be cross-sectionally stable is of importance to anticipate the effects of natural or man-made changes in these systems. Examples are sea level rise, barrier island breaching and basin reduction. Following *Escoffier* [*1940*] an inlet is considered to be in equilibrium when the amplitude of the inlet velocity equals the equilibrium velocity. The equilibrium is stable when after a perturbation the cross-section of that inlet returns to the original equilibrium state.

In calculating the amplitude of the inlet velocity it is customary to use a semi-empirical cross-sectionally averaged equation for the flow in the inlet and to assume a uniformly fluctuating water level, the so-called pumping mode, for the basin. In particular the use of the pumping mode in these lumped models needs justification as by definition water levels inside the basin vary in amplitude as well as phase. It is postulated that the validity of the use of the pumping mode depends among others on the basin dimensions including depth and geometry, i.e. length to width ratio when the surface area is assumed constant. This in turn can cause inlet velocities to vary and therefore change the stability of the inlet system.

The goal of this study is twofold: 1) to investigate the influence of basin geometry on the equilibrium and stability of *double* inlet systems and 2) to compare the results with a cross-sectionally averaged pumping mode model (e.g. *van de Kreeke et al., 2008*). To this end, an idealized 2DH hydrodynamic model is developed based on *Roos & Schuttelaars* [*2011*] and *Roos et al.* [*2011*] that calculates tidal elevation and flow in a schematized geometry of a tidal inlet system. This approach will be explained in the next section together with the definition of cross-sectional stability. Subsequently, the model results are presented using so-called flow diagrams. We finalize our study with a discussion, conclusions and an outlook for future research.

METHODOLOGY

Cross-sectional stability

In this study the focus is on cross-sectional stability. Following *Escoffier* [*1940*] an inlet is assumed to be in equilibrium if the amplitude of the cross-sectionally averaged inlet velocity is equal to the so-called equilibrium velocity $\hat{u}_{eq}$, generally taken as 1 m s^{-1} [*Bruun et al., 1978*]. The equilibrium is stable when after a perturbation of the equilibrium, the cross-sectional areas return to these equilibrium values. For inlets that are in equilibrium and assuming average weather conditions (as opposed to storm conditions) there is a balance between the volume of sediment entering and leaving the inlet. Following *van de Kreeke* [*2004*], the volume of sediment entering the inlet is taken as a constant fraction of the littoral drift, while the volume leaving the inlet is taken proportional to a power of the ebb tidal velocity amplitude. The difference between the amount of sediment that enters and leaves the inlet during a tidal cycle is uniformly distributed over the inlet length if this difference is positive; if negative the inlet is eroded uniformly. Hence, sediment exchange between inlet and basin is assumed to be negligible. Under these assumptions, the rate of change of the cross-sectional area can be written as [*van de Kreeke et al., 2008; de Swart & Zimmerman, 2009*]

$$\frac{dA_j}{dt} = \frac{M}{l_j}\left(\left(\frac{\hat{u}_j}{\hat{u}_{eq}}\right)^n - 1\right). \quad (1)$$

Here, A_j is the cross-sectional area of inlet j (m^2); t is time (s); l_j is the length of inlet j (m); M is a constant fraction of the littoral drift (m^3 s^{-1}); $\hat{u}_j$ is the cross-sectionally averaged velocity amplitude of compartment j (m s^{-1}); and n is a power whose value depends on the adopted sand-transport law. Here n is assumed to be 3. If $\hat{u}_j = \hat{u}_{eq}$, it follows that $dA/dt = 0$. This implies that the inlet system is in equilibrium.

Hydrodynamic model formulation

As shown in Eq. (1), the response of the inlet cross-sectional area and the equilibrium state is governed by the amplitude of the cross-sectionally averaged inlet velocities $\hat{u}_j$ that, in general, follows from a numerical or analytical model. In this study, the velocities are calculated using an idealized 2DH hydrodynamic model based on the modeling approach described in *Roos & Schuttelaars [2011]; Roos et al.* [*2011*]. Compared to the more classical lumped models of tidal inlets [*e.g. van de Kreeke et al., 2008*], our new hydrodynamic model has the following properties. (1) Since the adjacent sea/ocean is contained in the model geometry, the tidal wave past the inlet system is part of the solution. In turn, this implies that the amplitude and phase differences between the two inlets are automatically calculated and need not be imposed externally. (2) Amplitude and phase differences within the tidal basin are accounted for, which is important for rather elongated and shallow tidal basins. (3) Bottom friction in the basin is also accounted for, which is particularly realistic for shallow tidal basins. (4) The hydrodynamic method is quick, thus allowing for extensive sensitivity analyses with respect to the geometrical and physical characteristics of the system. (5) Our schematization ignores the complex channel-shoal patterns by assuming a uniform depth. (6) The model can be readily extended to systems with more than two inlets.

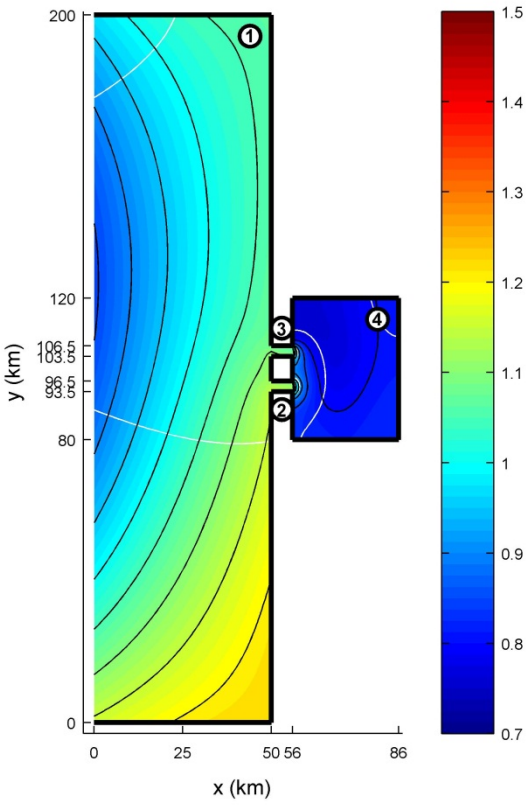

Figure 1. Co-tidal chart for a double inlet system with a basin geometry of 30×40 km. Elevation amplitudes are in meters, co-phase lines are depicted in white with intervals of 30° and co-range contours are depicted in black with intervals of 0.05 m. Compartment dimensions are listed in Table 1.

Table 1. Compartment dimensions of an inlet system representing the Marsdiep-Vlie system in the western Dutch Wadden Sea.

Fig.	j	b_j (km)	l_j (km)	h_j (m)
1,3	1	200	50	25
1,3	2,3	3	6	15
1,3	4	40	30	$5^{(1)}$; $1\times10^{6\ (3)}$
2a,b,c	1	200	50	25
2a,b,c	2,3	variable	6	variable
2a,b,c	4	$80^{(a)}$; $40^{(b)}$; $20^{(c)}$	$15^{(a)}$; $30^{(b)}$; $60^{(c)}$	5
4	1	200	50	25
4	2,3	variable	6	variable
4	4	40	30	1×10^6

Superscripts above a parameter value refer to the corresponding figure

Our model calculates tidal elevation and flow in a geometry consisting of several adjacent rectangular compartments. Figure 1 shows an example of such a geometry for a double inlet system resembling the Marsdiep-Vlie system in the Dutch Wadden Sea. It consists of four compartments of length l_j, width b_j and (uniform) depth h_j (j = 1,…,4). Compartment 1, which has an open boundary to the left, represents the ocean/sea. Compartment 2 and 3 are the two inlet channels of rectangular cross-section. Compartment 4 is the tidal basin. In each compartment, conservation of momentum and mass is expressed by the depth-averaged shallow water equations including Coriolis effects, and linear bottom friction on the f-plane:

$$\frac{\partial u_j}{\partial t} - fv_j + \frac{r_j u_j}{h_j} = -g\frac{\partial \eta_j}{\partial x}, \quad (2)$$

$$\frac{\partial v_j}{\partial t} + fu_j + \frac{r_j v_j}{h_j} = -g\frac{\partial \eta_j}{\partial y}, \quad (3)$$

$$\frac{\partial \eta_j}{\partial t} + h_j\left[\frac{\partial u_j}{\partial x} + \frac{\partial v_j}{\partial y}\right] = 0. \quad (4)$$

Table 2. General parameter values resembling the Marsdiep-Vlie system in the western Dutch Wadden Sea.

M (m^3 $year^{-1}$)	$\hat{u}_{eq}$ (m s^{-1})	Ω (rad s^{-1})	ϑ (^oN)	c_D (-)	γ (-)	Z_{M2} (m)	ω (s^{-1})	g (m s^{-2})
5×10^5	1	7.292×10^{-5}	53	2.5×10^{-3}	0.005	1	1.4×10^{-4}	9.81

For compartment j, u_j and v_j are the depth-averaged flow velocity components in along-basin (x)- and cross-basin (y)-direction, respectively, and η_j is the free surface elevation. Furthermore, $f = 2\Omega\sin\vartheta$ is a Coriolis parameter (with $\Omega = 7.292\times10^{-5}$ rad s^{-1} the angular frequency of the Earth's rotation and $\vartheta \sim 53$ºN the central latitude of the system) and $g = 9.81$ m s^{-2} the gravitational acceleration. The linear bottom friction coefficient is defined as $r_j = 8c_DU_j/3\pi$ obtained from Lorentz' linearization of a quadratic friction law [*Zimmerman, 1982*] with a default value of the drag coefficient $c_D = 2.5\times10^{-3}$. The current amplitude of a classical Kelvin wave without bottom friction is assumed as the typical flow velocity scale $U_j = Z_{M2}\sqrt{(g/h_j)}$. Here $Z_{M2} = 1$ m is typical for the dominant M2-tide.

The model geometry displays different types of boundaries. At the closed boundaries, a no-normal flow condition is imposed. Next, continuity of elevation and normal flux is required across the topographic steps between the adjacent compartments.

Analogous to the classical *Taylor* [*1922*] problem, the system is forced by a single incoming Kelvin wave with angular frequency ω and typical elevation amplitude Z_{M2}, entering through the open boundary of compartment 1. Due to the Coriolis effect the Kelvin wave travels upward along the coast past the two inlets, thus forcing the flow in the inlet system. This effect is negligible inside the inlets, as its dimensions are generally small compared to the Rossby deformation radius. The traveling Kelvin wave along with other waves is allowed to radiate outward at the open boundary of compartment 1.

Flow diagram

To determine the equilibrium cross-sectional areas and their stability, the results are expressed in terms of a so-called flow diagram [*van de Kreeke et al., 2008*]. Using the hydrodynamic model described above the cross-sectionally averaged velocity amplitudes $\hat{u}_1$ and $\hat{u}_2$ are calculated for multiple combinations of (A_1,A_2). The cross-sections are varied by enlarging the width b_j of the inlet compartments and calculating the corresponding depth h_j. This is done using the assumption of a geometrically similar rectangular cross-section [*O'Brien & Dean, 1972*]. Hence, the ratio $\gamma = h_j/b_j$ is constant for all cross-sections; where γ is chosen to be 0.005. From $\hat{u}_1(A_1,A_2)$ and $\hat{u}_2(A_1,A_2)$, equilibrium velocity curves are constructed for both inlets. The equilibrium velocity curves represent the locus of (A_1,A_2)-values for which $\hat{u}_1 = \hat{u}_{eq}$ and $\hat{u}_2 = \hat{u}_{eq}$, respectively. The intersections of the two curves represent sets of equilibrium cross-sectional areas. To determine the stability of the equilibrium, vectors are added to the flow diagram. These vectors are the unit vectors in the direction of $d\vec{A}/dt$ calculated from Eq. (1). The unit vectors indicate the direction in which the values of cross-sectional areas change when they are not in equilibrium.

RESULTS

In this study, three basin geometries ($l_4\times b_4$) are chosen with a constant basin surface of 1200 km^2: 15×80 km, 30×40 km and 60×20 km (see Table 1). Other general parameter values used in the calculations are denoted in Table 2 and are roughly based on

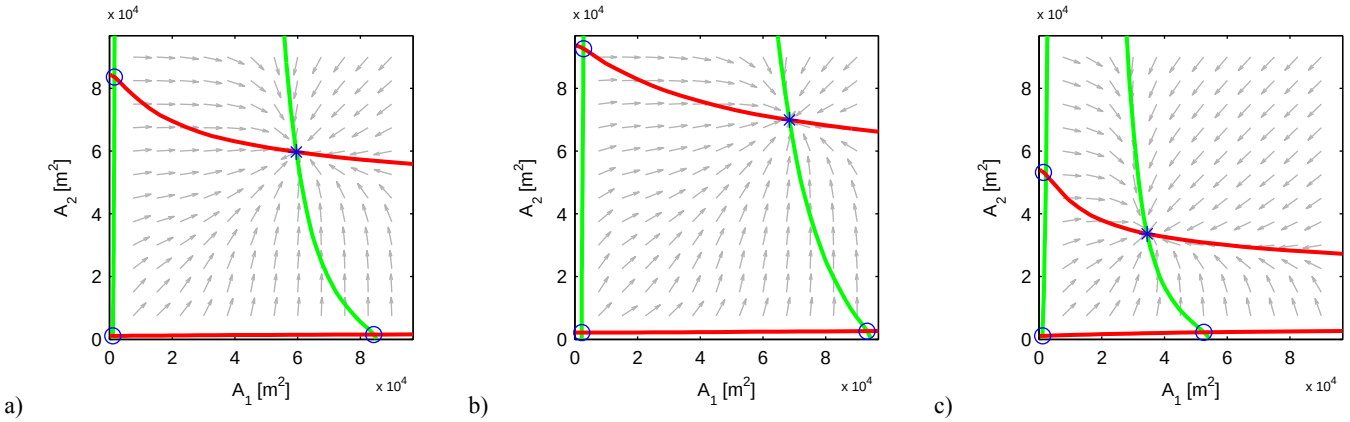

Figure 2. Flow diagrams for different basin geometries: a) 15×80 km, b) 30×40 km and c) 60×20 km. The green and red solid line corresponds to the equilibrium velocity curves of inlet 1 and 2, respectively. The gray vectors indicate the direction in which the values of the cross-sectional areas change when they are not in equilibrium. Blue circles indicate an unstable equilibrium and the blue cross a stable one.

the Marsdiep-Vlie system in the western Dutch Wadden Sea. For each configuration the centerline of the tidal basin is on the same position as the centerline of the ocean and the centerlines of the inlet channels are 10 km apart and symmetrically positioned with respect to the centerlines of the ocean and basin.

Bottom friction in the basin

A typical result of the model with dimensions resembling the Marsdiep-Vlie system is shown in Fig. 1, which shows a co-tidal chart for a basin geometry of 30×40 km. Other dimensions of the system are listed in Table 1. It follows that due to bottom friction amplitudes and phases show a spatial variability of approximately 10 cm and 30°, respectively. Moreover, amplitudes decay from approximately 1.1 m in the inlets to approximately 0.75 m inside the basin.

Flow diagrams are used to determine how this spatial variability of amplitudes and phases influences the stability of the system for different basin geometries. This is shown in Figs. 2a, b and c for a basin geometry of 15×80 km, 30×40 km and 60×20 km, respectively. It follows that for all three cases next to three unstable equilibriums, a single stable equilibrium exists. Moreover, the influence of basin geometry has a large quantitative influence on the equilibrium values of the cross-sectional areas. The largest equilibrium values are found for the 30×40 km geometry (Fig. 2a), i.e. $(A_1,A_2) \approx (7\times10^4, 7\times10^4)$. The other basin shapes lead to smaller equilibrium values (Figs. 2a and 2c); $(A_1,A_2) \approx (6\times10^4, 6\times10^4)$ for the 15×80 km geometry and $(A_1,A_2) \approx (3.5\times10^4, 3.5\times10^4)$ for the 60×20 km geometry. This leads to a difference in equilibrium values up to a factor 2 depending on the geometry of the basin.

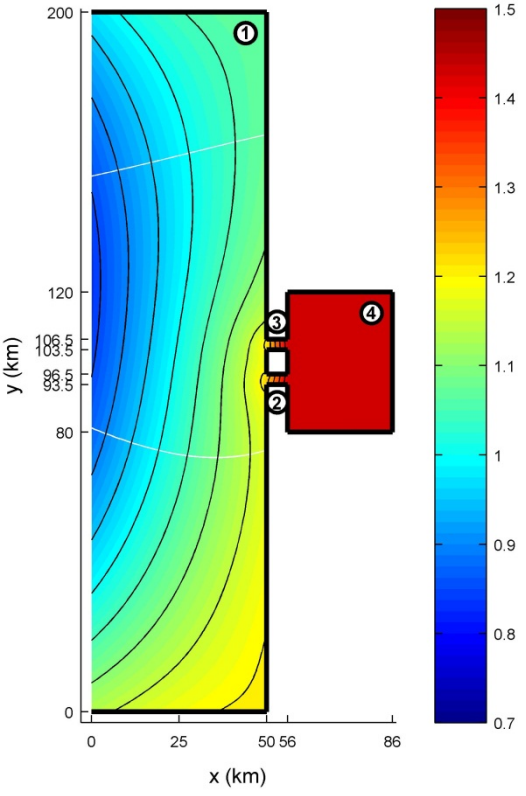

Figure 3. Co-tidal chart for a double inlet system with a basin geometry of 30×40 km. Elevation amplitudes are in meters, co-phase lines are depicted in white with intervals of 30° and co-range contours are depicted in black with intervals of 0.05 m. Compartment dimensions are listed in Table 1.

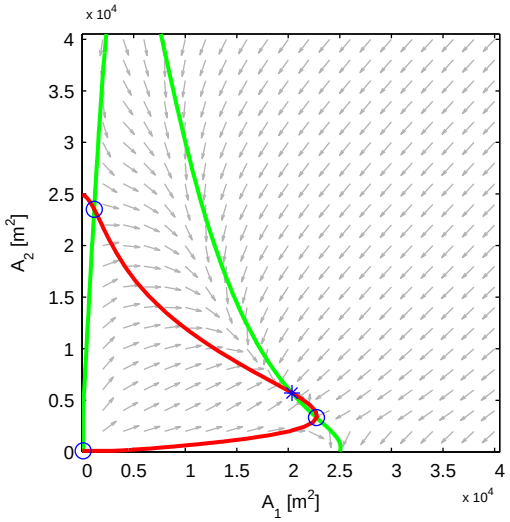

Figure 4. Flow diagram for a basin geometry of 30×40 km, no bottom friction in the basin ($c_D = 0$) and basin depth $h_4 = 1\times10^6$ m. The green and red solid line corresponds to the equilibrium velocity curves of inlet 1 and 2, respectively. The gray vectors indicate the direction in which the values of the cross-sectional areas change when they are not in equilibrium. Blue circles indicate an unstable equilibrium and the blue cross a stable one.

No bottom friction in the basin

It is interesting to determine to what extent the results of our idealized 2DH hydrodynamic model can be compared with results from the classical lumped model approach. Apart from other assumptions, an important one in that approach is a uniformly fluctuating water level inside the basin. Results by *van de Kreeke et al.* [*2008*] show that for a double inlet system with a single basin and relatively long inlet channels two equilibriums exist, none of which is stable.

To approximate the pumping mode with our model we consider a basin geometry of 30×40 km with $c_D = 0$ and $h_4 = 1\times10^6$ m. This results in the co-tidal chart depicted in Fig. 3. A clear difference with the case including bottom friction (Fig. 1) is that in the absence of bottom friction amplitudes are amplified from approximately 1.25 m in the inlet channel to approximately 1.4 m inside the basin. Furthermore, amplitudes and phases in the basin do not display (visual) spatial variability. The corresponding flow diagram for the 30×40 km basin is depicted in Fig. 4. It follows that, similar to the case with bottom friction, four equilibriums exist, one of which is stable with equilibrium values of $(A_1,A_2) \approx (2\times10^4, 0.6\times10^4)$.

DISCUSSION

Care should be taken to compare the results of our model with the lumped model of *van de Kreeke et al.* [*2008*] as even with $c_D = 0$ and $h_4 = 1\times10^6$ m the water motion does not satisfy the pumping mode approximation. Other differences are the presence of physical mechanisms automatically accounted for in our 2DH model approach. Examples are resonance, radiation damping and entrance/exit losses. Comparing Fig. 4 with Fig. 2b shows that the equilibrium velocity curve of inlet 2 (red) has retreated to almost within the equilibrium velocity curve of inlet 1 (green). It is to be expected that when our model more closely approximates the assumptions in the model by *van de Kreeke et al.* [*2008*] the stable equilibrium at $(A_1,A_2) \approx (2\times10^4, 0.6\times10^4)$ will disappear, thus leading to two unstable equilibriums.

CONCLUSIONS AND OUTLOOK

In this study, we have investigated the influence of basin geometry on the stability of double inlet systems. To this end, an idealized 2DH hydrodynamic model was developed that calculates the spatial characteristics of tidal flow in a schematized geometry of a tidal inlet. Tidal inlet stability has been investigated by combining the inlet velocity amplitudes from this model with *Escoffier's* [*1940*] classical stability method.

The flow diagrams based on our model suggest that regardless the inclusion or exclusion of bottom friction in the basin stable equilibrium states exist. Moreover, qualitatively the basin shape does not change the presence of stable equilibriums. Quantitatively, a more elongated basin shape, in (*x*)- or (*y*)-direction, generally corresponds to significantly smaller equilibrium values. Specifically, taking a basin surface area of 1200 km^2, equilibrium values can differ up to a factor of approximately 2 depending on basin shape.

Inspired by the above conclusions, future research should focus on the following aspects.

- Examine the cause(s) of the large influence of basin geometry on the equilibrium values when assuming a constant basin surface area.
- Extend the sensitivity analysis to investigate the roles of physical mechanisms such as bottom friction, radiation damping, resonance and entrance/exit losses on the stability of double inlet systems.
- Investigate the influence of the position of the inlet channels with respect to where they connect the ocean to the tidal basin (in our case this position was assumed constant and the mutual distance between the inlet channel was relatively short).
- Investigate the consequences of alternatives for the similarity approach regarding the cross-sections of the tidal inlets (by which we assumed a constant factor γ when constructing the flow diagrams in Figs. 2 and 4).

REFERENCES

Bruun, P. Mehta, A.P., Johnsson, I.G. (1978), Stability of tidal inlets: theory and engineering, Elsevier Scientific Publishing Co., The Netherlands.

Escoffier, F.F. (1940), The stability of tidal inlets, Shore and Beach, 8 (4), 111-114.

van de Kreeke, J. (2004), Equilibrium and cross-sectional stability of tidal inlets: application to the Frisian Inlet before and after basin reduction, Coastal Engineering, 51 (5-6), 337-350, doi: 10.1016/j.coastaleng.2004.05.002.

van de Kreeke, J., Brouwer, R.L., Zitman, T.J., Schuttelaars, H.M. (2008), The effect of a topographic high on the morphological stability of a two-inlet bay system, Coastal Engineering, 55 (4), 319-332, doi:10.1016/j.coastaleng.2007.11.010.

O'Brien, M.P. and Dean, R.G. (1972), Hydraulics and sedimentary stability of coastal inlets, 13th International Conference on Coastal Engineering, Vancouver, Canada, 761-780.

Roos, P.C. and Schuttelaars, H.M. (2011), Influence of topography on tide propagation and amplification in semi-enclosed basins, Ocean Dynamics, 61 (1), 21-38, doi:10.1016/S0278-4343(97)00007-1.

Roos, P.C., Velema, J.J., Hulscher, S.J.M.H., Stolk, A. (2011), An idealized model of tidal dynamics in the North Sea: resonance properties and response to large-scale changes, Ocean Dynamics, 61 (12), 2019-2035, doi:10.1007/s10236-011-0456-x

de Swart, H.E., Zimmerman, J.T.F. (2009), Morphodynamics of Tidal Inlet Systems, Annual Review of Fluid Mechanics, 41, 203-229, doi:10.1146/annurev.fluid.010908.165159.

Taylor, G.I. (1922), Tidal oscillations in gulfs and rectangular basins, Proceedings of the London Mathematical Society, s2-20 (1), 148-181.

Zimmerman, J.T.F. (1982), On the Lorentz linearization of a quadratically damped forced oscillator, Physics Letters, 89A, 123-124.

DOI: 10.3990/2.176

Zuiderzee is now called IJsselmeer*: Process-based Modeling

A. Dastgheib[1] and J.A. Roelvink[2]
[1]UNESCO-IHE, PO Box 3015, 2601 DA Delft, The Netherlands, a.dastgheib@unesco-ihe.org;
[2]UNESCO-IHE, PO Box 3015, 2601 DA Delft, The Netherlands, d.roelvink@unesco-ihe.org,
Deltares, PO Box 177, 2600 MH Delft, the Netherlands,
Delft University of Technology, Delft, the Netherlands

* from Zuiderzeeballade

ABSTRACT

Constructing a closure dam such as Afsluitdijk causes an instantaneous change in tidal wave propagation and flow field in the basin which triggers extensive morphological changes in the adjacent tidal basin. These morphological changes may continue for centuries before the whole system reaches a new "equilibrium" state, which is different from the "equilibrium" in case the closure would not have been done. In this paper we have used Delft3D to investigate the characteristics and time scale of the morphodynamic effects of construction of the Afsluitdijk. In this research we focused on tidal forces only. A schematized bathymetry with a uniform depth is used in the model with the land boundary of Waddenzee before the closure. A morphological simulation is carried out for 4000 years. Using this procedure ensures us that the morphological "equilibrium" state which is reached in this simulation is only due to the tidal forcing. In subsequent runs we have applied a closure after 1000, 2000 and 3000 years and continued the simulation while the closure dam was included in the model. The main outcome of this research is that as soon as the closure is applied the sediment transport regime of the basins changes from exporting to importing, which corresponds with the existing hypothesis based on measurements at Marsdiep.

INTRODUCTION

Closure dams in lowland countries such as The Netherlands are traditionally used to protect tidal inlets, rivers and estuaries from occasional storm surge events, and/or to provide possibilities to reclaim new land from the tidal basin area. Constructing a closure dam often causes an instantaneous change in tidal wave propagation and flow field in the basin which triggers extensive morphological changes in the adjacent tidal basin. These morphological changes may continue for centuries before the whole system reaches a new "equilibrium" state, which can be different from the "equilibrium" in case the closure would have not been done. (Figure 1).

After the construction of the Afsluitdijk in 1932, the tidal basin area in the Western Dutch Waddenzee decreased from around

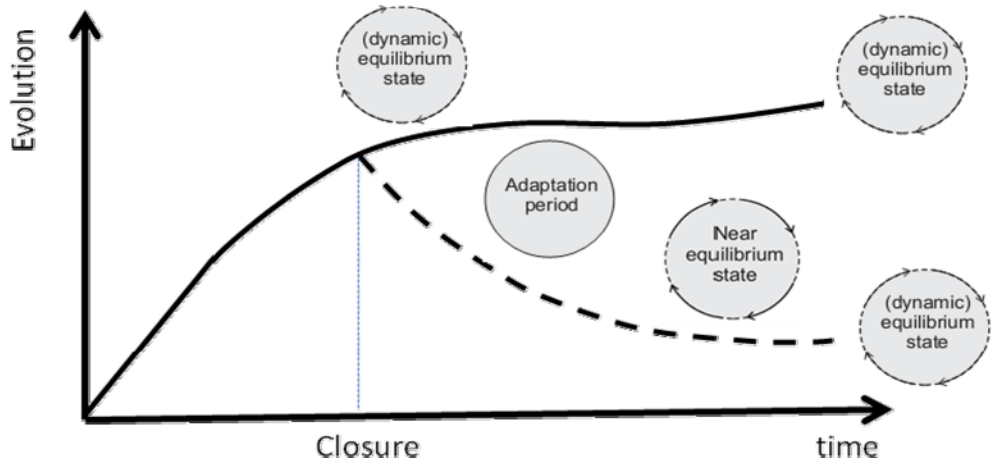

Figure 1. Description of the effect of closure dams (Stages of the evolution from Elias, 2003)

4000 Km2 to 700 Km2 and as it was predicted beforehand the tidal prism increase for about 26%. This dramatic change is the main reason for the ongoing morphological changes in the new Dutch Waddenzee. Elias (2003) based on data and short-term simulations, extensively described the morphological changes due this closure, and suggested a conceptual model that explains the impact of the closure on the tidal basins.

In recent years advances in the knowledge of numerical modeling of the physical processes together with technological developments made it possible to use process-based models for mid- and long-term morphological simulations, and study the morphological behavior of the complex coastal systems such as tidal basins.(Hibma et al 2003, Van Leeuwen at al. 2003, Dastgheib et. al. 2008, Van der Wegen and Roelvink 2008, Van der Wegen et. al. 2008, Dissanayake et. al. 2009a,b). Using a process-based model and considering a realistic analogue approach (Roelvink and Reniers, 2012) we can select an important process in the morphological changes of tidal basins and give more insight into the effect of large human interventions such as closure dams on that specific process and consequently on the morphological behavior of the tidal basin.

AIM OF STUDY

In this study we have used a numerical process based model to investigate the characteristics and time scale of the morphodynamic effects of the construction of the Afsluitdijk and to determine the characteristics of the Dutch Waddenzee tidal basin without closure dam only due to tidal forcing.

DESCRIPTION OF THE MODEL

The model which is used in this study is the 2DH version of the Delft3D model, described in Lesser et al (2004) in detail. Basically the governing equation of the same model is integrated over depth. This model is a finite difference-scheme model which solves the momentum and continuity equations on a curvilinear grid with a robust drying and flooding scheme. For this exploratory study, the simplest possible physics (depth-averaged shallow water equations, simple transport formula) are applied. In this study the empirical relation of Engelund-Hansen is used for sediment transport.

Following Roelvink (2006) we have used the so called online approach. In this approach the flow, sediment transport and bed-level updating run with the same (small) time steps (Lesser et al, 2004, Roelvink, 2006). Since the morphologic changes are calculated simultaneously with the other modules the coupling errors are minimized. But, as described in Lesser et al (2004), because this approach does not consider the difference between the flow and morphological time step, a ‘morphological factor’ to increase the depth changes rate by a constant factor (n) should be applied (Roelvink, 2006). So after a simulation of one tidal cycle in fact the morphological changes in n tidal cycle are modeled.

MODEL SETUP

Model Domain

A model for the Waddenzee before closure is set up. The land-boundary of the model is determined using historical maps together with the borders of Dutch new municipalities. In this study our interest is to set up a model with a reasonable computational time that can simulate long-term (~ 4000 years) morphological changes. The grid we generated is a compromise between enough resolution in the inlets (at least 10 at the gorge) and having as few cells as possible. In this study the average spacing between grid lines inside the basins is about 350 m. The grid cells are smaller inside the basins and they are much bigger at the offshore boundary. The grid mesh covers only the area under the high water and the other parts of the barrier islands are excluded from the model. Figure 2 shows the domain and the computational grid of the model.

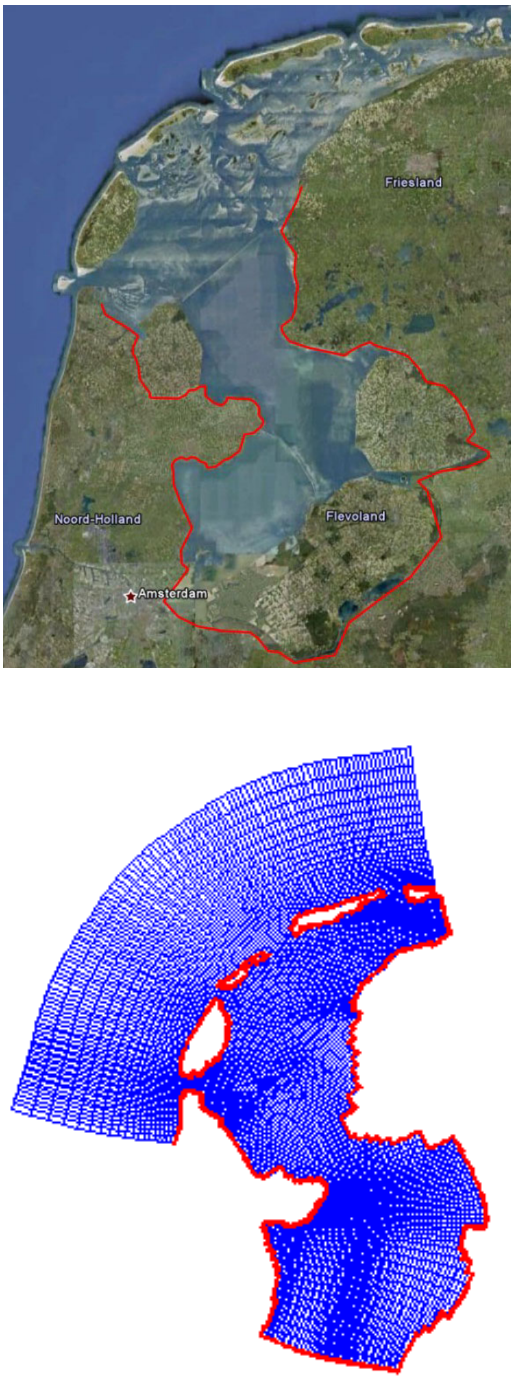

Figure 2. land boundary and the computational grid of the model

Forcing

The only hydrodynamic force which is chosen for the simulations in this study is the tidal forcing and other forces such as wave and wind are not included in the simulations.

In order to determine the boundary conditions of this local model, a calibrated model for the vertical tide in the North Sea, called 'ZUNO', is used.

Referring to Van de Kreeke and Robaczewska (1993), we neglect the spring neap cycle and consider the dominant forcing by M2 and over-tides. Therefore the ZUNO model is run with the forcing boundary conditions of M2, M4 and M6 until a periodic solution was reached. During this run the tidal level variations at the boundaries of local model are recorded.

From the results of ZUNO model the recorded tidal variations at local model boundaries are analyzed and M2, M4 and M6 are extracted for these boundaries. These components are used to form boundary conditions for the local model.

The boundaries for the local model consist of 3 boundaries: one boundary at the sea side and two other lateral boundaries. The sea side boundary is chosen to be a water level boundary, while the lateral boundaries are Neumann boundaries, where the alongshore water level gradient is prescribed (Roelvink and Walstra, 2004).

Initial Bathymetry

The initial bathymetry which is used in the simulations of this study is a flat bathymetry inside the basins without any kind of ebb-tidal delta outside the inlets. Therefore the model simulates the mechanism of building and changing the ebb-tidal delta outside the basin and channel and shoal patterns inside based on the applied forces and the available sediment. In this case the uniform depth of this flat bathymetry is equal to average depth of the basins.

Scenario of simulations

In this study a morphological simulation is carried out for 4000 years including the whole domain (Waddenzee together with the Zuiderzee) to achieve a reasonable computational time a MorFac of 300 is applied. Using this procedure ensures us that the morphological "equilibrium" state which was reached in this simulation is only due to the tidal forcing. To investigate the effect of the morphological conidian at the time of closure, in subsequent runs we have applied the closure after 0, 1000, 2000, 3000 and 4000 years and continued the simulation including the closure dam (the same model domain excluding the Zuiderzee).

RESULTS AND DISCUSSIONS

Morphological evolutions

Figure 3. shows an example of the morphological evolution with and without the closure, in this figure the resulting bathymetry of the whole domain in year 2000 is shown. It is clear that in the first 2000 years the channels in Vlie and especially Marsdiep are penetrating into the Zuiderzee and this procedure continues for the next 2000 years if there is no Afsluitdijk, the main channels of Marsdiep is connected to the Zuiderzee and has a south easterly direction. However in the case in which the closure is applied at the year of 2000 the main channel in Marsdiep rotates towards the east and the connection between Vlie and Marsdiep is cut. The areas closer to the closure dam is silted up and some flat areas are developed in that area.

Instantaneous changes due to closure

At each closure time we carried out two hydrodynamic/sediment Transport model and compared the discharge of water and sediment passing though the Texel inlet and the water level at Den Helder station before and after the closure, Figure 4 shows the outcome of this comparison for closure at 1000 years and 3000 years. Over all we can observe some tidal asymmetry in the flood and considerable reduction in ebb-Sediment transport due to the closure. Therefore we can conclude that before the closure Texel is ebb-dominant both for tidal-flow and tidal transport, thus, exporting sediment. After the closure Texel is still ebb-dominant for tidal-flow but flood-dominant for tidal transport and importing sediment, this result is in agreement with Elias et. al (2004) descriptions of the effect of the construction of the closure dam on Texel inlet. Also we can see that the tidal range increases by about 20% which is comparable with what happened in reality.

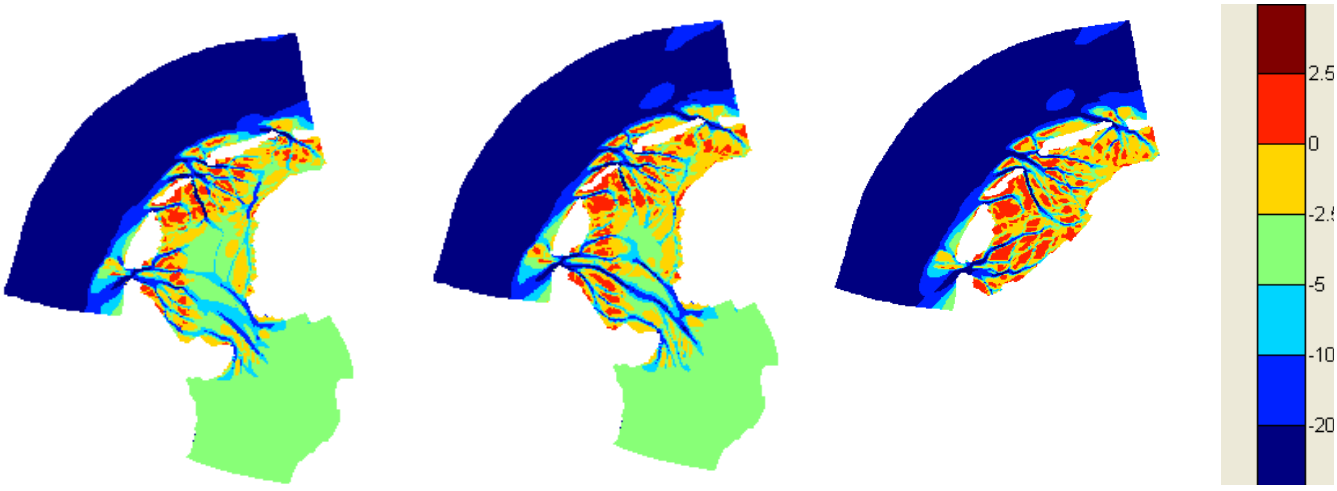

Figure 3. From left to right :Resulting bathymetry in year 2000,in year 4000 without the closure, and in year 4000 with the closure dam included in year 2000

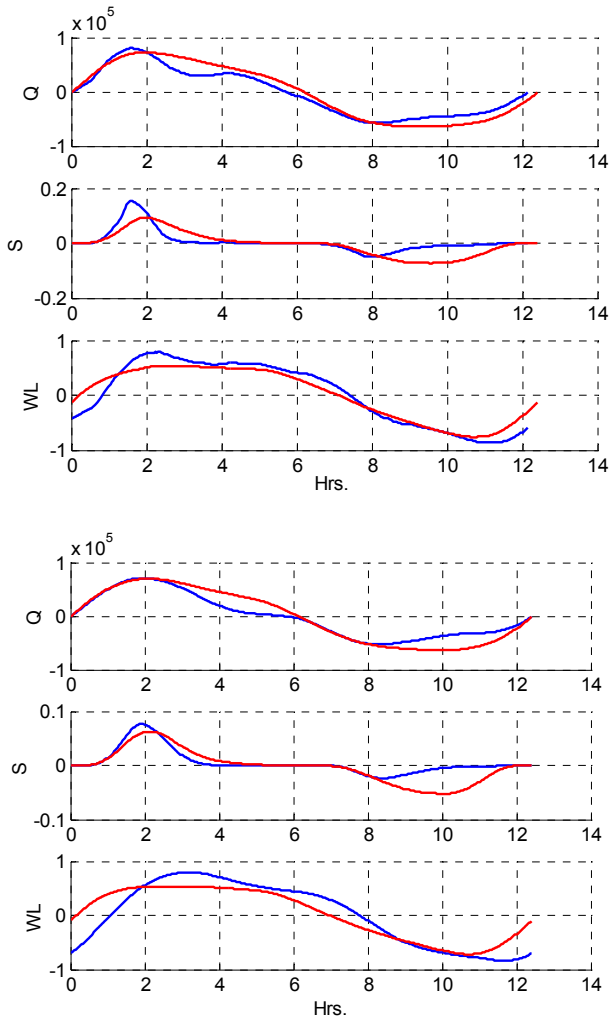

Figure 4. Discharge, Sediment Transport and water level in Texel inlet before (red) and after (blue) the closure at year 1000 (top) and 3000 (bottom)

This change from being ebb-dominant to being flood dominant for tidal transport, changes the regime of the tidal basins in Waddenzee from an exporting system to an importing system. Figure 5 shows the sediment exchange between North Sea and Waddenzee through Texel and Vlie inlets in 4000 years morphological simulation without the closure together with the change of the import export regime due to the closure at different times.

CONCLUSIONS

The main conclusions can be summarized as follows:

- Even considering tidal forcing only it is possible to show the change in import/export regime of Texel (Waddenzee)
- After the closure Texel is ebb-dominant for tidal flow but becomes flood-dominant for tidal transport.

REFERENCES

Dastgheib, A., Roelvink, J.A., Wang, Z.B., 2008. Long-term process-based morphological modelling of the Marsdiep Tidal Basin, Marine Geology, 256, 90-100.

Dissanayake, D.M.P.K., Roelvink, J.A., Ranasinghe, J.A., 2009a. Process-based approach on tidal inlet evolution – Part II, Proc. International Conference in Ocean Engineering, Chennai, India. CD Rom.

Dissanayake, D.M.P.K., Roelvink, J.A., Van der Wegen, M., 2009b. Modelled channel pattern in a schematised tidal inlet. Coastal Engineering 59, 1069 – 1083

Elias, E. P. L., Stive, M. J. F., Bonekamp, J. G. and Cleveringa, J. 2003 Tidal inlet dynamics in response to human intervention Coastal Engineering Journal, 45(4), 629-658.

Elias, E.P.L.; Stive, M.J.F., and Roelvink, J.A., 2004. Impact of back-barrier changes on ebb-tidal delta evolution. Journal of Coastal Research SI(42).

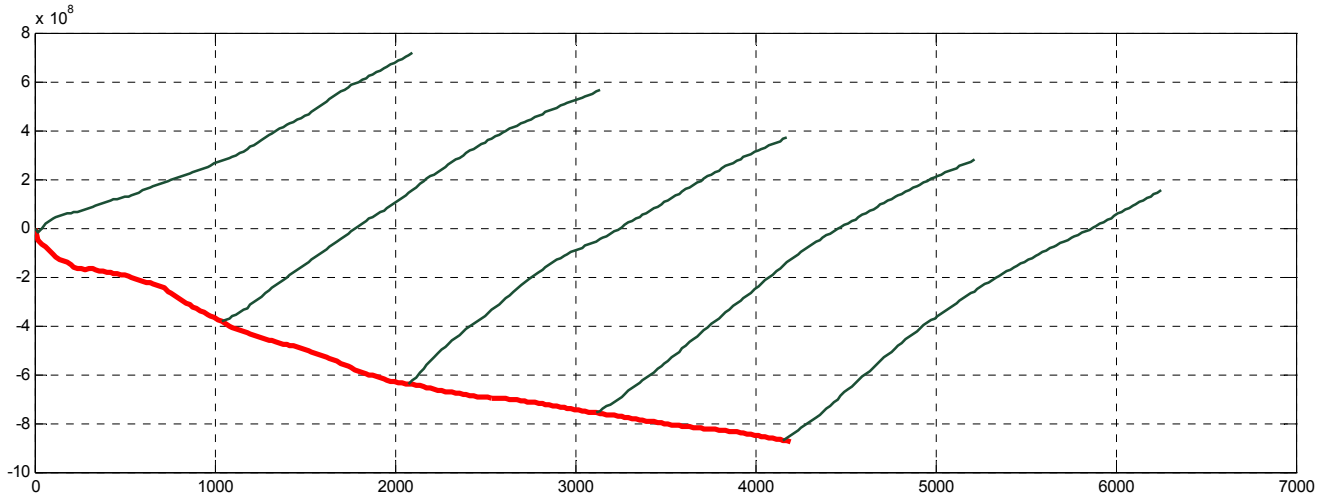

Figure 5. Sediment Exchange between North Sea and Waddenzee in 4000 years morphological simulation and the change of the import export regime due to the closure at different times, (+:import, - : export)

Hibma, A., De Vriend, H. J. and Stive, M. J. F. 2003. Numerical modeling of shoal pattern formation in well-mixed elongated estuaries Estuarine, Coastal and Shelf Science, 57, 981-991.

Lesser, G. R., Roelvink, J. A., Van Kester, J. A. T. M. and Stelling, G. S. 2004. Development and validation of a three-dimensional model. Coastal Engineering, 51, 883-915.

Roelvink and Reniers, 2012. A guide to modeling coastal morphology. World Scientific Publishing co.

Roelvink, J.A. 2006. Coastal morphodynamic evolution techniques, Coastal Engineering 53, pp. 277-287.

Roelvink, J.A., Walstra, D.J., 2004. Keeping it simple by using complex models, Advances in Hydroscience and Engineering, Volume V1, 1-11

Van der Kreeke, J., Robaczewska, K., 1993. Tide-induced residual transport of coarse sediment; application to the Ems estuary. Netherlands Journal of Sea Research 31, 209-220.

Van der Wegen, M., and J. A. Roelvink 2008, Long-term morphodynamic evolution of a tidal embayment using a two-dimensional, process-based model, Journal of Geophysical Research Volume 113, Issue 3, 8 March 2008, Article number C03016

Van der Wegen, M., Z.B. Wang, H.H.G. Savenije and J.A. Roelvink 2008, Long-term morphodynamic evolution and energy dissipation in a coastal plain, tidal embayment, Journal of Geophysical Research Volume 113, Issue 3, 24, Article number F03001

Van Leeuwen, S.M., Van Der Vegt, M., De Swart, H.E., 2003. Morphodynamic of ebb-tidal deltas: a model approach. Estuarine, Coastal and Shelf Science 57, 899–907.

DOI: 10.3990/2.177

OpenEarth: using Google Earth as outreach for NCK's data

Gerben J. de Boer[1,2,4,*], Fedor Baart[1,2], Ankie Bruens[1,6], Thijs Damsma[3,4], Pieter van Geer[1], Bart Grasmeijer[5], Kees den Heijer[1,2], Mark van Koningsveld[2,3,4], Giorgio Santinelli[1], et al.

[1] Deltares, P.O. Box 177, 2600 MH, Delft, the Netherlands.

[*] Gerben.deBoer@deltares.nl

[2] TU Delft, Hydraulics Engineering + Section of Environmental Fluid Mechanics.

[3] Van Oord dreding and marine contractors.

[4] Ecoshape, Building with Nature.

[5] Alkyon, Arcadis.

[6] Rijkswaterstaat Kustlijnzorg program.

ABSTRACT

In 2003 various projects at Deltares and the TU-Delft merged their toolboxes for marine and coastal science and engineering into one toolbox, culminating in 2008 in an open source release, known as OpenEarthTools (OET). OpenEarth adopts the wikipedia approach to growth: web 2.0 crowd sourcing. All users are given full write access to help improve the collection. Quality is assured by version control, tracking all changes. OpenEarth started as a social experiment to investigate whether crowd sourcing was possible in our community of marine and coastal researchers. The answer is yes: over 1000 users registered, now enjoying over 5000 contributions from over 100 contributors. The most important asset is a general toolbox to plot any data type in Google Earth. With this toolbox it has become very easy for marine and coastal experts to disseminate their data via Google Earth. It enables the NCK community to make its data available to end-users and the general public with only little effort. They can now consume our data as simple as watching YouTube: DataTube. In this paper it is shown that OpenEarth has added important value by analyzing a wide range of marine and coastal data types from NCK simultaneously in Google Earth. To match the traditional gap between specialist knowledge and end users, Google Earth is shown to be a very powerful tool. The possibilities for outreach by NCK are manifold.

INTRODUCTION

The Netherlands is one of the flattest, lowest and flood-prone countries around the world. Yet, the Netherlands has probably the best digital elevation model (DEM) of the world: 1m nation-wide coverage with the AHN DEM [AHN]. For the dynamic dune rows and foreshore a time dependent DEM is available between 1996 and present at 5 m resolution. This data is made openly available by Rijkswaterstaat, and allows for detailed study of marine and coastal dynamics, not only by analyzing trends in the wealth of data itself, but also as input or validation for a wide range of models. The cost of such mass gathering of data, Lidar in this case, will drop in the future, leading to an even bigger wealth of data. This trend is known as the Digital Data Deluge [e.g., e-IRG, 2010]. However, the scientific use of this abundance of data is still far from optimal. The main reason for this is that the dedicated, often self-made software used by of marine and coastal scientists and engineers cannot handle such large quantities of data and can hardly handle the wide variety. This applies even more to the use of this wealth of data by policy makers and the general public. These latter groups cannot use the dedicated software used by marine and coastal scientists. Instead, they have to rely on the condensed data products and visualizations produced by the experts. These products and visualizations are often produced by various experts, during various projects, over many years. This makes it difficult to keep track of all the information that is available. And is, amongst others, hampering quality improvement and knowledge sharing as outlined in Nature [Merali, 2010]. In an ideal world, scientists and end-users have easy access to all raw data (from various data sources) as well as all derived products (e.g. Coastal State Indicators). Why is it not possible for end users to 'fly' through all data and CSIs at once, comparing the development of different indicators, for different time-periods and for different areas? Could this not support the decision making by managers and the draw up of expert advise by scientists and engineers? Matching this gap between specialist knowledge and end users has been discussed in literature [e.g. Van Koningsveld, 2003]. By developing and/or applying existing state-of-the-art techniques to share and visualize data we attempt to contribute to bridge this gap. In this paper we describe a first exploration to what extent all marine and coastal data and data products from NCK can be combined into one simple viewer for non-specialists. To do this we made use of the [OpenEarth] approach to data, models and tools. OpenEarth is the data management solution in [Building with Nature] and [MICORE]. We here present the result to the NCK-community to open a discussion with coastal scientists and managers regarding the additional value, future possibilities and future demands. What we are in fact looking for is an analog of YouTube for viewing marine and coastal data: 'DataTube'. The aim of this paper is to test whether such a 'DataTube' is already possible for a wide range of data, with existing technologies.

Web Services for graphics: OGC WxS and KML

At national, EU and international level many initiatives and projects are trying to enable non-specialists to visualize all kinds of geospatial data [Percivall, 2010]. The INSPIRE directive aims to provide a top-down overall framework for dissemination of all geospatial data in the EU [INSPIRE]. In the Netherlands a national registry was launched to host the meta-data of all

governmental geospatial data, including marine and coastal data [NGR]. This website will link to 'DataTube' links were users can actually obtain the data. Generally, initiatives like these have chosen to rely on the international openGIS standards known as WxS. These standards have been issued by the [OGC] consortium to disseminate geospatial data over the web. WxS is the shorthand for a range of Web Services where the letter x denotes the specific standard. The most mature standard is WMS, short for Web Mapping Service [WMS]. WMS is meant for exchange of graphics of grid plots over the web. For the exchange of vector data, such as line elements and dots, there is a the WFS standard, short for Web Feature Service [WFS]. Separate WxS protocols exist for exchange of data over the web. Please refer to [Hankin et al, 2012; Baart et al., 2012] for a comparison of the three most mature ones: OGC's WCS, short for Web Coverage Service, OPeNDAP from the ocean community and GTS from the World Meteorological Organisation (WMO). However, our purpose here is only to enable plotting of marine and coastal data over the web, not exchange of the actual data. For our purpose WMS and WFS are sufficient. These two WxS protocols provide very powerful tools to visualize any data into viewers for the general public over the web. However, the specialists in the realm of marine and coastal science and engineering have hardly any experience with these protocols. Moreover, the actual implementation of these protocols in plotting (server) and viewing (client) software is lagging behind. Especially time-dependency, 3D views and non-orthogonal grids lag implementation. For instance, to our knowledge, time dependent WxS-complaint software for grids has only been implemented in pre-release software [Adaguc]. And curvi-linear and unstructured grids, very often used in marine and coastal models, are not supported by any existing WxS software yet. This means that these protocols are not appropriate *yet* for our aim, although their specifications were designed for this very purpose. Fortunately, another protocol is already capable of dealing with these aspects: [KML]. This is an open standard based on xml file format syntax and is recognized as standard by the same OGC body that wrote the WxS services. However, KML is not in the repertoire of the top-down organizations that implement INSPIRE directive. KML, however, is the backbone of the simplest and most powerful viewer for the general public we could find: the free [Google Earth] viewer. In contrast to WMS and WFS viewers, this KML viewer is already well-known by end-users and the general public (Fig. 1). (Google earth also supports stationary WMS.) KML is an open standard, so anyone can make a viewer that can interpret KML plots. Google Earth is the most advanced viewer available though. Currently, plotting data in Google Earth and encoding data as KML plots are therefore de facto the same. Note that because KML is an open standard, choosing KML does not necessarily mean limiting oneself to Google Earth. The Google Earth viewer has already implemented all aspects that are lagging for WxS viewers: 3D, time-dependency and unstructured grids are already included. The aim of this paper is to test whether a 'DataTube' for all marine and coastal data is already possible with existing technologies. In this paper we chose to test whether the existing KML plotting standard with the Google Earth viewer can enable a DataTube for marine and coastal data.

Fig. 1. A powerful example of DataTube-like outreach to general public: Google Earth show with a range of custom data for children in the brand-new California Academy of Sciences building, one of the largest museums of natural history in the world. Here a smooth map of Africa is overlaid on the Google Earth background.

Reading guide

In section 2 we introduce the community tools that we developed to plot data in KML (Google Earth). This software was written in Matlab, a commercial programming language that is used most widely by marine and coastal scientists and engineers in the NCK community. With the [OpenEarth] community [Van Koningsveld, 2010] we developed a generic, coherent toolbox for many atomic plot types in KML. In section 3 we test this toolbox with a wide range of large data sets currently used by the NCK community. We describe the specifics of the data and show whether we can plot it in KML in a manner that is readily useable by end-users. In section 4 we discuss the performance of plotting in KML, before we conclude in section 5 that plotting marine and coastal data in Google Earth can be considered a successful proof-of-concept solution to enable better collaboration between experts and end-users.

METHOD: OET GOOGLEPLOT

OpenEarth community and workflow

Matlab is one of the most commonly used programming languages for data analysis by marine and coastal scientist and engineers in NCK. In 2003, a number of scientists from Deltares and the TU-Delft merged their Matlab toolboxes for marine and coastal science and engineering into one toolbox, culminating in open source release as OpenEarthTools (OET) in 2008. OpenEarth adopts the wikipedia approach to growth: web 2.0 crowd sourcing. All users are given full write access to help improve the collection. Quality is assured by version control tracking all changes in [SubVersion], the same tool used by professional software engineers worldwide. OpenEarth started as social experiment to investigate whether crowd sourcing was possible in our community. The answer is yes: over 1000 users registered, now enjoying over 5000 contributions from over 100 contributors. One of the most powerful toolboxes of OpenEarth is the GooglePlot toolbox. GooglePlot was developed in 307 revisions by 20 developers. They devised a set of Matlab functions that can plot

any atomic data type with one coherent toolbox. The GooglePlot toolbox is designed to be the primary example of the OpenEarth quality control guidelines. For each GooglePlot plot function the settings were made customizable. Proper default values for all settings were chosen, which can be requested by calling the function without arguments. Common code fragments were detected in the toolbox and put into a separate subtoolbox. For each function in the GooglePlot toolbox a dedicated unit test was conceived. These test were coded into a unit test function that is run periodically to test ongoing performance of the entire toolbox. The rigorous test approach was included to deal with the typical shortcoming found in computer code made by scientists and engineers [Merali, 2010].

Plot types in KML

The first atomic data types to be implemented were the native plot types of Matlab. For intuitive use, the same nomenclature as Matlab was kept with KML as prefix: KMLline, KMLpcolor for 2D orthogonal and curvi-linear grids, KMLmesh/KMLsurf for 3D wire meshes and surfaces (flying carpets), KMLquiver for arrows, KMLmarker, KMLtext, KMLcontour derivatives for different contour lines, KMLtrimesh/KMLtrisurf for unstructured grids and KMLpatch for set of filled polygons. More atomic plot types were added in a later stage, going beyond the range offered by native Matlab plots: KMLcolumn/KMLcylinder, KMLcurtain for vertical time-space flying carpets, KMLcurvedarrrows for arrows that move in time and are curved following the streamlines. The latter function contains a dedicated particle-tracking implementation, with sophisticated seeding/decay algorithm. The most advanced function of GooglePlot is KMLfigure_tiler that can be used to chop up a grid datasets of any size into a collection of standard tiles [Thijs Damsma, pers.com.]. This method is known as a quad-tree [Wiliams, 1983] with universal texture, and is the very same technique that Google Earth uses view all the worlds satellite imagery. With this function, our toolbox has rivaled the capabilities of Google Earth imagery.

Coordinate conversion

Plotting in KML requires per definition latitude-longitude coordinates with the WGS84 datum, the same one used by GPS systems. KML and Google Earth have chosen to abandon support for the zillion coordinate systems in use. The choice of supporting only one single global coordinate system has greatly facilitated the ease of disseminating data via Google Earth. End-users, unknown to the difficulties and pitfalls of different coordinate systems, now have zero chance of running into coordinate conversion issues. Instead, coordinate issues have to by solved by scientists and engineers who make the KML files. Although coordinate conversion is not native knowledge of marine and coastal scientists and engineers, acquainting oneself with coordinate systems is a relatively simple task to them. Marine and coastal raw data is often only available in x-y coordinates. For just the NCK community these include for already: Rijksdriehoek for nearshore, UTM31-ED50 and UTM31-WGS84 for offshore, Lambert for Belgian waters, a German system in the Ems, latitude-longitude on WGS84, ED50 and ETRS89 globes, and many custom satellite projections, often polar stereographic. OpenEarth contains the ConvertCoordinates toolbox that can now convert almost any coordinate type to WGS84 lat-lon [Maarten van Ormondt, pers. com.]. Now coordinates can be mapped in batch mode directly from the data that scientist and engineers work with. ConvertCoordinates is subject to the same rigorous test procedure as GooglePlot, including the single free calibration coordinate provided by the [Kadaster]. With these two toolboxes a powerful and reliable toolbox was created for the marine and coastal specialists in NCK. It enables them to plot with little effort any kind of marine and coastal data in KML.

RESULTS: A RANGE OF DATA

Does it work for the range of data sets in NCK?

To test the OpenEarth GooglePlot toolbox, we choose a wide range of large datasets that that covers the usage and availability for marine and coastal scientists and engineers in the Dutch NCK community. We selected freely available datasets that underpin the research and advice of almost everyone in the NCK community. These are key assets of NCK in our opinion. And these are the sets are worth disseminating to decision makers and the general public. For each of these datasets an attempt is made to plot it as KML into Google Earth. The kmls are publicly available via http://kml.deltares.nl. In section 4 we will analyze to what extent we succeeded.

Maps: North Sea grain sizes (Geological Survey of NL)

The Geological Survey of the Netherlands (TNO/Deltares) compiled grain size maps of the bed of the Dutch part of the North Sea [Sytze van Heteren, pers. com]. These maps have a resolution of 200m and are available for D10, D50 and D90 grain sizes and %-occurrence maps for mud and cobbles. These maps were compiled from a dataset of over 13,000 sediment cores/grabs [DINO]. This test set represents all time-independent map products such as DEMs and GIS rasters. It is shown to work successfully in KML in Fig. 2.

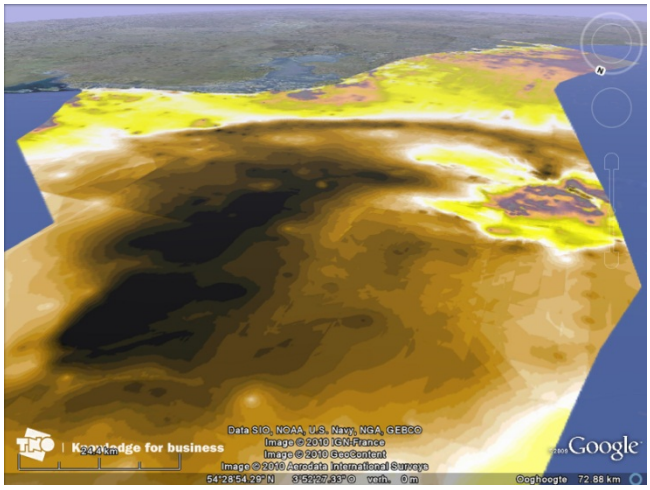

Fig. 2. D50 grain sizes, seen from central North Sea towards Europe. Data credit: Geological Survey of the Netherlands (TNO/Deltares). Image credit: Google Earth™ mapping services.

Transect time stacks: JarKus (Rijkswaterstaat)

Since 1965 Rijkswaterstaat annually collects cross shore dune profiles along the entire Dutch coast at 100m alongshore intervals [Minneboo, 1995]. The data covers the area inland behind the first dune row to an offshore water depth over 8 m, with 5 m

resolution. The data product is currently generated from ship-based soundings offshore, a dedicated device in the swash zone and Lidar in the dry foreshore and the dunes. The near shore sand bar zone is annually updated, whereas the datasets extends to a depth 8 m only at 5 or 10 year intervals only (*doorlodingen*). This test set represents all kinds of profile data and is shown to work successfully in KML in Fig. 3.

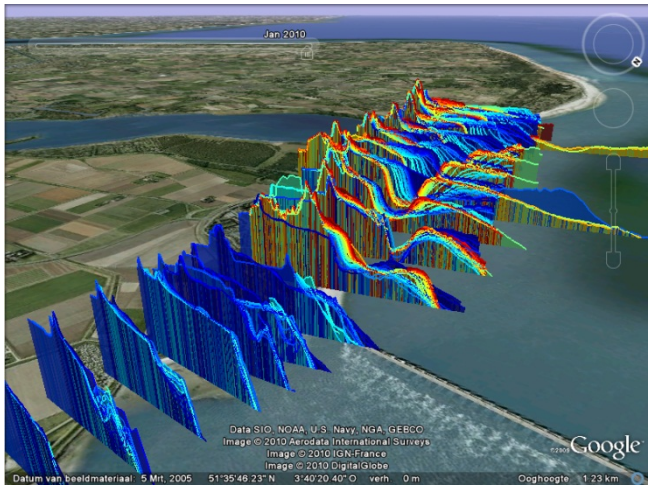

Fig. 3. Plot of JarKus profiles around the Eastern Scheldt barrier from 1965 to 2010 with a cross-shore resolution of 5 m. The color represents the time at which a profile was collected (blue =old, red=recent). Data credit: Rijkswaterstaat. Plot credit: Claire van Oeveren Theeuwes (Deltares). Image credit: Google Earth™ mapping services. Note the time slider.

Map time stacks: vaklodingen bathymetry (Rijkswaterstaat)

Since 1927 Rijkswaterstaat makes bathymetry soundings of the Dutch waters from deeper water up to the beach and into the tidal inlets of Zeeland and the Wadden Sea [Wiegmann et al., 2005]. Data is available as orthogonal grids with 20 m resolution at time intervals of about 7 years. This time dependency is needed due to the large morphological changes in the sedimentary beds of the Dutch waters. The early data consists of digitized navigation charts originally compiled from lead lines, the most recent are based on single and multi beam surveys. The product is chopped up into more almost 180 tiles known as “kaartblad”, which are offshore extrapolations of the standard 10km x 12km tiles from the 1:25.000 Dutch Topographic map definitions [Kadaster]. This bathymetry data is used to make legally binding sand balances; an important analyses in the context of the Dutch sustainable coastal policy (maintaining the sediment buffer in the so-called coastal foundation). The vaklodingen are shown to work successfully in KML in Fig. 4. To highlight small vertical variations a 500 element long colormap was developed with shading effects on top [Thijs Damsma, pers.com.]. A second time-dependent grid set is shown to work successfully in KML in Fig. 5: The *Kusthoogte* dataset with a resolution of 5 m. This dataset is also available as tiles, but smaller ones: 5 km by 6 km tiles from the 1:10.000 Dutch Topographic map definitions. Both datasets are very large. The raw ASCII vaklodingen data are about 23 GB, in netCDF it reduces to ca. 4GB. The raw Kusthoogte data is 2 GB, because they are already stored in binary ArcGIS files. Viewing these complete datasets for all times at once would require GBs of memory on the computer where Google Earth runs. However, 4Gb is beyond the physical limit of 32 bit PCs. Only the native Google Earth quad-tree with universal texture implemented in the GooglePlot KMLfigure_tiler function allows end-users to view these data in Google Earth. For 2D data plotted in this type, Google Earth only loads the subset that is actually visible. 3D plotting of all data within view is again beyond the capacities of normal PCs. We chose a successful approach with a light KML overview of the boundary boxes of all tiles (Fig. 6) with links to 3D KML visualizations of individual tiles at one time (Fig. 7).

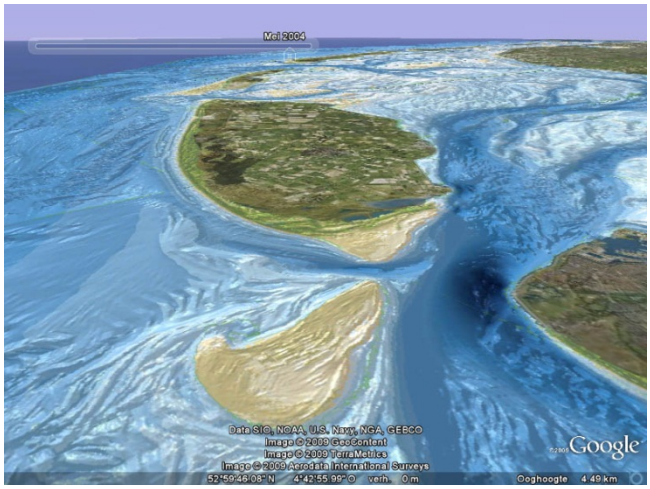

Fig. 4. Map of bathymetry in Western Wadden Sea in May 2004. Data credit: Rijkswaterstaat. Plot credit: Thijs Damsma (Van Oord). Image credit: Google Earth™ mapping services. Note the time slider.

Fig. 5. Map of Kusthoogte *bathymetry dataset in 2008. This dataset was collected with Lidar at a very low water and binned to cells of 5 m. Lidar can only get bathymetry soundings for locations that are dry, therefore there are data gaps in the channels. Data credit: Rijkswaterstaat. Image credit: Google Earth™ mapping services. Note the time slider.*

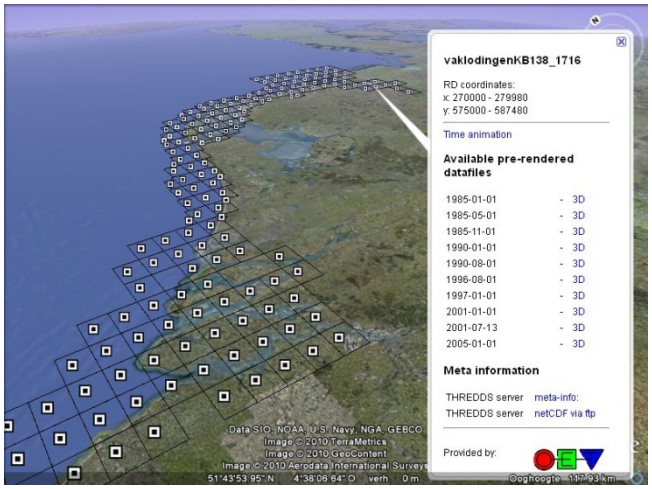

Fig. 6. Overview map of vaklodingen with spatio-temporal meta-data and links to 3D data of individual tiles. Data credit: Rijkswaterstaat. Image credit: Google Earth™ mapping services.

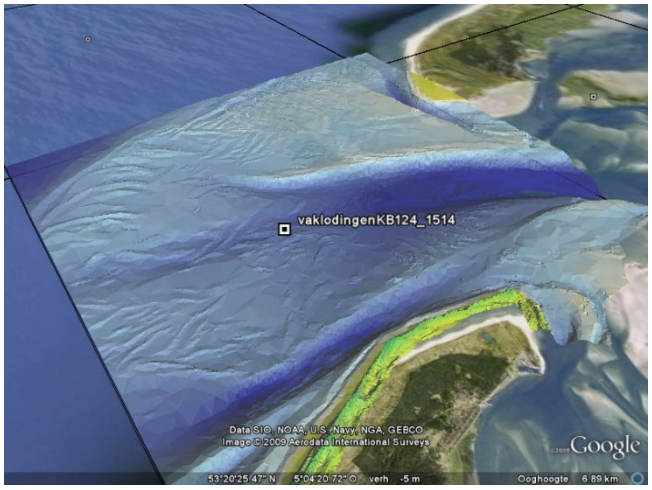

Fig. 7. 3D visualization that allows for a 'fly through' of one vaklodingen tile at one time instance. Data credit: Rijkswaterstaat. Image credit: Google Earth™ mapping services. Plot credit: Thijs Damsma (Van Oord).

Time series (Rijkswaterstaat)

Since the late 1900's Rijkswaterstaat records water levels offshore, along the coast and at inland waters. Initially only low and high water were recorded, but modern data are available at 10 min. intervals. For some stations over 100 years continuous recordings is available. Since the 60's, water quality parameters are collected at the water surface on a weekly basis, reduced to bi-monthly at some locations now due to gradually improved water quality in Europe. This set is called MWTL *(Monitoring Waterstaatkundige Toestand des Lands*). Recorded parameters include salinity, temperature, suspended sediment concentrations, pH, Chlorophyll, and many nutrients and pollutants. Since the 80's also wave periods, directions and heights are available from about 6 buoys. Gradually time series in the central North Sea become available for physical parameters via international collaboration and oil companies. The time series are stored in the offline DONAR database from Rijkswaterstaat, and available via a dedicated web service [Waterbase]. We show all locations of the MWTL water quality stations to work successfully in KML in Fig. 8. For each dot a meta-data pop-up appears as shown in Fig. 9.

Lines: Dutch beach lines (Rijkswaterstaat)

From the aforementioned JarKus dataset dedicated Coastal State Indicators (CSI) are extracted. A CSI typically yields one number per cross shore transect. Since 1990, the Dutch coastal policy aims at preventing further retreat of the coastline. Therefore, the yearly Momentary Coastline (MKL) and the Testing Coastline (TKL) are derived from the Jarkus dataset. In case of structural exceedance of the reference coastline (BasisKustlijn BKL), local nourishments are considered. In addition, the position of low water, high water and dune foot and many other indicators [Santinelli et al., this NCK volume] are derived from JarKus. The CSIs can simply be plotted as time dependent alongshore lines, i.e. shape files. In Fig. 10 they are shown to work successfully in KML.

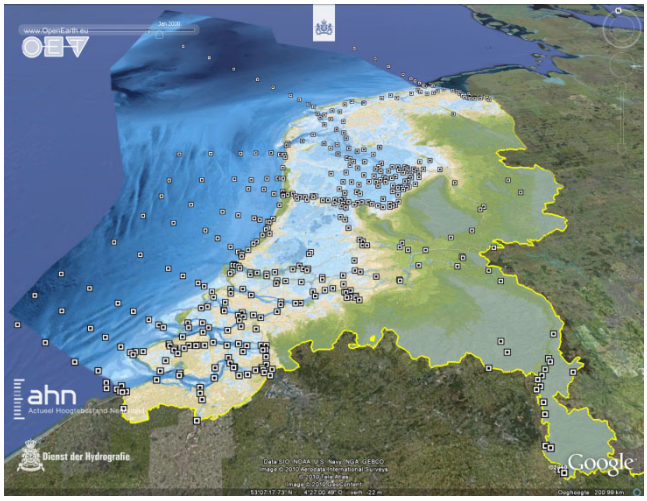

Fig. 8. Locations of MWTL water quality measuring locations on top of the 200m North Sea bathymetry from the Hydrographic Office (www.hydro.nl) and the 100m MaaiVeld *set from TNO. Data credit: Rijkswaterstaat. Image credit: Google Earth™ mapping services.*

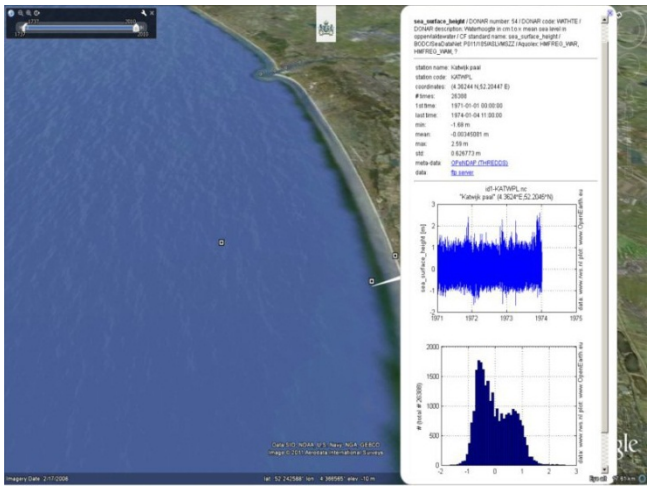

Fig. 9. For each location in Fig. 6 a pop-up is available with statistical data and a preview of the time series and a histogram. Data credit: Rijkswaterstaat. Image credit: Google Earth™ mapping services.

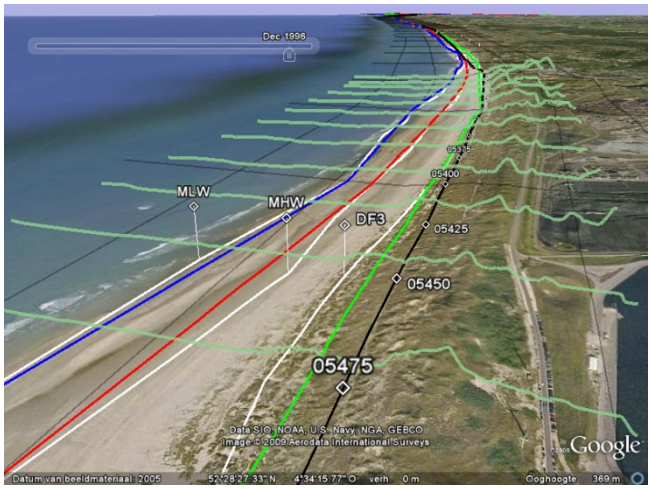

*Fig. 10. Example of JarKus profiles in one year (viz. Fig. 3) with beach line indicators overlaid. Data credit: Rijkswaterstaat. (DF3 = Dune Foot 3m). The alongshore numbers on the black line indicate the beach poles (*strandpaal*). Data credit: Rijkswaterstaat + Deltares. Image credit: Google Earth™ mapping services.*

Scatter points: Sieve curves Wadden Sea (Rijkswaterstaat)

Nearly 9000 sediment cores (surface grabs) were collected in the Wadden Sea by Rijkswaterstaat in the 80's and 90's. These data are part of the Sediment Atlas Wadden Sea executable that is available for download [sediment atlas] and allows for data export as txt file. This set is included to test performance of OpenEarth for any kind of data with a non-spatial or temporal dimension, such as grain sizes/classes, wave directions, wave frequencies. In Fig. 9 they are shown to work successfully in KML.

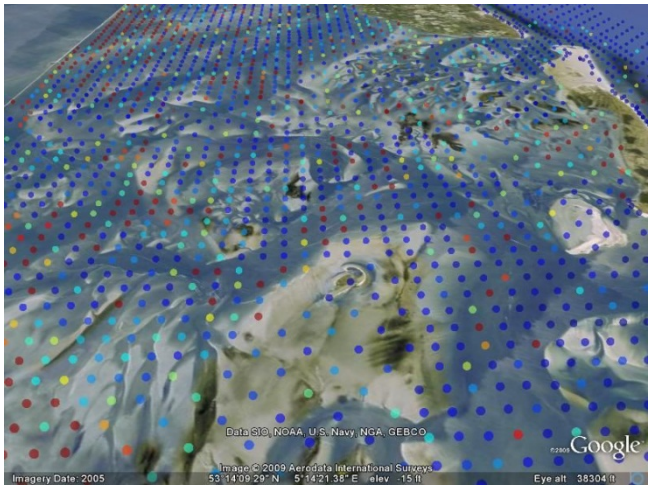

Fig. 11. The mud percentage in the bed in the Western Wadden Sea, calculated from data in the Sediment Atlas. Data credit: Rijkswaterstaat. Image credit: Google Earth™ mapping services.

North Sea sediment samples (Geological Survey of NL)

The North sea grain size maps of the North Sea were compiled using sediment cores and surface grabs of the North Sea bed. These datasets contain the primary sediment type per sample layer. In Fig. 12 they are shown to work successfully in KML. For these data a dedicated OET GooglePlot function was developed to be able to plot these cores as 3D cylinders.

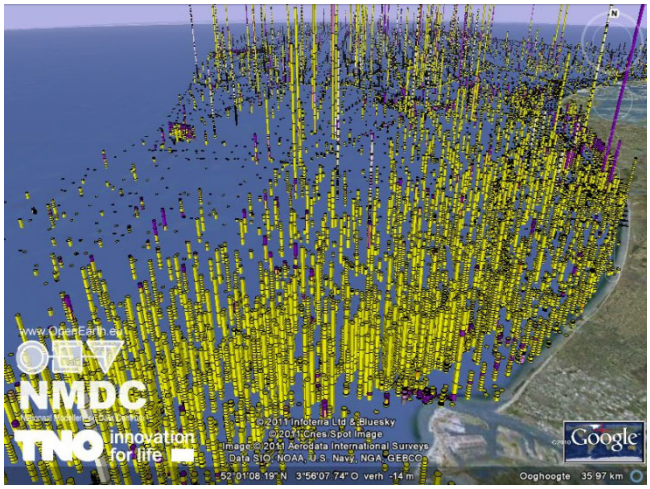

Fig. 12. All > 13,000 open sediment cores data available on the North Sea plotted simultaneously. Data credit: Geological Survey of the Netherlands [DINO] via [NODC] format. Plot credit: Gerben de Boer (Deltares in NMDC context). Image credit: Google Earth™ mapping services.

Nourishments (Rijkswaterstaat)

The Dutch coast has been eroding over more than a thousand years. Coastal retreat puts coastal functions (e.g. safety against flooding) under pressure. Since 1990, the Dutch policy aims at structural prevention of a further retreat of the coastline, but in the meantime taking the valuable dynamical behavior of the coast into account. Therefore, sand nourishments have been preferred over hard structures to counteract the systematic erosion. Since 1952 Rijkswaterstaat registered the nourishments along the Dutch coast. To analyze the morphological development of the Dutch coast, this nourishment record is essential (as large amounts of sediments have been nourished). Therefore the nourishment database is an essential dataset for NCK research. In Fig. 13 it is shown to work successfully in KML.

Fig. 13. Beach and foreshore suppletions since 1952. The area indicates the sand volume (assumed 1 m thick), the color indicates the nourishment type (red=beach, green=under water). Data credit: Rijkswaterstaat. Image credit: Google Earth™ mapping services.

CONCLUSION: DATATUBE WORKS

The aim of this paper was to test whether it is possible to plot a wide range of data from the NCK community for easy viewing by end-users and the general public. The successful examples in section 3 have shown that the existing technologies, KML in combination with the OpenEarth community toolboxes, are capable of plotting almost any data type for ready viewing by non-specialist users. The opportunities for outreach by NCK are abundant. We can consider a 'DateTube' feasible.

DISCUSSION: DATA DELUGE SEARCH

We started this paper by stating that there is a gap between specialist knowledge and end-users. The difficulty to keep track of all information from experts was the main cause for this. Plotting of all data in KML has solved this issue. However, the gap between specialists and end-users does not appear to have ceased. In contrary, feed-back from end-users learned us that a new challenge has arisen. The supply of readily available data in Google Earth is now so huge, that end-users have difficulty in finding the correct data. They are basically overwhelmed and have expressed a need for filters to group data into manageable clusters for specific purposes. Our experiment has shown that giving away data has created more work for experts: only they have the knowledge to do this filtering. Some experts are still reluctant to open up their data though. They fear that their expert work might not be needed any more. Our pilot DataTube has showed the opposite. Anyone opening up his data will immediately be contacted by the overwhelmed end-users. In the past, control over data access was profitable, in the future only control of data filters will become valuable. The next challenge for marine and coastal scientists and engineers is therefore to create search options for end-users to find the correct KMLs. Top-down INSPIRE-like philosophies propose to make central inventories, catalogs, that allow to search data. There is a special OGC protocol for this: CSW: Catalogue Service for Web. However, we think it will become a challenge to keep such central catalogues up to date with the speed at which end-users can now generate new KML files. We believe that a different search option is worth investigating too: regular search enginers. We have shown that viewing data is now as simple as viewing YouTube. YouTube offers a similar deluge of information as a collection of KML files, and it is not subject to complaints from overwhelmed users. The reason is that YouTube offers a simple and powerful search box to search the movies. We therefore envision a future where KML should be as easy as to search as movies. Our next challenge to therefore to tag each KML with specific micro-information and user votes, so that general search engines can find them as easy as YouTube movies. Only then DataTube is complete: open data and simple searches.

REFERENCES

Adaguc, http://adaguc.knmi.nl.

AHN, Actueel Hoogtebestand Nederland, http://www.ahn.nl.

Baart, F.; de Boer, G.J.; de Haas, W.; Donchyts, G.; Philippart, M.; van Koningsveld, M.; Plieger, M., 2012. A comparison between WCS and OPeNDAP for making model results and data products available through the internet. Trans. in GIS, accepted.

Building with Nature, http://www.ecoshape.nl.

DINO, http://www.dinoloket.nl.

e-IRG, 2009. Report on data management, e-IRG Data management Task Force, http://www.e-irg.eu.

Google Earth, http://earth.google.com.

Hankin S.C., Blower J.D., Carval Th., Casey K.S., Donlon C., Lauret O., Loubrieu Th., Srinivasan A., Trinanes J., Godoy O, Mendelssohn R., Signell R., De La Beaujardiere J., Cornillon P., Blanc F., Rew R., Harlan J. (2010). NETCDF-CF-OPENDAP: standards for ocean data interoperability and object lessons for community data standards processes. Oceanobs 2009, Venice Convention Centre, 21-25 Sep. 2009, Venice. http://archimer.ifremer.fr/doc/00027/13832.

INSPIRE directive, http://inspire.jrc.ec.europa.eu.

Kadaster, kernnetpunt, https://rdinfo.kadaster.nl/pics/publijst1.gif.

KML, http://www.opengeospatial.org/standards/kml.

Merali, Z, 2010. Error… Why scientific computing does not compute. Nature, 467 775-777.

MICORE, http://www.micore.eu.

Minneboo, F.A.J., 1995. Jaarlijkse kustmetingen Rijkswaterstaat RIKZ, rapport RIKZ-95.022.

NGR, Nationaal GeoRegister, http://www.nationaalgeoregister.nl.

NODC, http://www.nodc.nl..

OGC, http://www.opengeospatial.org.

OpenEarth, http://www.OpenEarth.nl.

Percivall, G., 2010. The application of open standards to enhance the interoperability of geoscience information. International Journal of Digital Earth, 3(1), 14-30.

Sediment Atlas Wadden Zee, http://www.waddenzee.nl.

SubVersion, http://subversion.tigris.org/.

Van Koningsveld, M., de Boer, G.J., Baart, F., Damsma, T., den Heijer, C., van Geer, P., de Sonneville, B., 2010. OpenEarth - inter-company management of: data, models, tools & knowledge.WODCON XIX, September 2010. China, Beijing.

Van Koningsveld, M., 2003. Matching specialist knowledge with end user needs. Bridging the gap between coastal science and coastal management. PhD thesis, Twente University, Enschede, The Netherlands. ISBN 90-365-1897-0.

Waterbase, Rijkswaterstaat, http://live.waterbase.nl.

WFS, http://www.opengeospatial.org/standards/wfs.

Wiegmann, N. R. Perluka, S. Oude Elberink, J. Vogelzang, 2005. Vaklodingen: de inwintechnieken en hun combinaties. AGI Rijkswaterstaat, Rapp.Nr. AGI-2005-GSMH-012.

Wiliams, 1983, Pyramidal parametrics, ACM Siggraph Computer Graphics, 1983, 17(3), 1-11.

WMS, http://www.opengeospatial.org/standards/wms.

ACKNOWLEGDEMENTS

Part of this study have been carried out (i) by Deltares in the framework of the KPP-B&O Kust and KPP-Kustbeleid projects, both commissioned by Rijkswaterstaat Waterdienst, (ii) by Van Oord and Deltares in the data management case (DM) of Building with Nature, (iii) by TU Delft in the data management workpackage of the EU FP7 MICORE project, (iv) by Deltares in the *Verbetertraject voor visualisatie en user interfaces* of NMDC. Numerous other projects contributed parts as well. We are very grateful to the open marine and coastal data from Rijkswaterstaat and the Geological Survey of the Netherlands (TNO/Deltares).

DOI: 10.3990/2.178

Measuring and modeling coastal dune development in the Netherlands

A.V. de Groot[1], S. de Vries[2,3], J.G.S. Keijsers[1], M.J.P.M. Riksen[1], Q. Ye[2,3,4], A. Poortinga[1], S. M Arens[5], L.M. Bochev-Van der Burgh[6], K.M. Wijnberg[6], J.L. Schretlen[6], J.S.M. van Thiel de Vries[2]

[1]Land Degradation and Development Group, Wageningen University, P.O. Box 47, 6700 AA Wageningen, The Netherlands, alma.degroot@wur.nl

[2]Section of Hydraulic Engineering, Delft University of Technology, Delft, 2628 CN, The Netherlands

[3]Deltares, P.O. Box 177, 2600 MH Delft, The Netherlands

[4]UNESCO-IHE, Westvest 7, Delft, The Netherlands

[5]Bureau for Beach and Dune Research, Iwan Kantemanplein 30, 1060 RM Amsterdam, The Netherlands

[6]Water Engineering and Management, University of Twente, P.O. Box 217, 7500 AE, Enschede, The Netherlands

ABSTRACT

In the past couple of years, new coastal-dune research has sprung up in the Netherlands. In this paper, we give an overview of ongoing projects at Wageningen UR, Deltares, TU Delft and UTwente: how these are connected and what type of questions are addressed. There is an increasing demand for the understanding and prediction of coastal dune dynamics, both on the short (year) and long (100 years) term. We approach this from a variety of angles: scientific and applied, short-term and long-term, data-driven and model-based, biotic and abiotic, process-based and rule-based, and focused on components and integrated. We give examples of results and end with a discussion of the benefits of this integrated approach.

INTRODUCTION

Coastal dunes are an important feature along the Dutch coast. They have a variety of functions, including coastal defense against flooding, recreation, drinking water supply and nature conservation. Coastal dunes develop through the interplay of sand transport by the wind and the sea, and vegetation growth (Figure 1) [*Martínez and Psuty*, 2008]. Large-scale sand supply is a strong driver for the type of dunes that will develop, but sea-level excursions, storm magnitude and frequency, wind and wave climate, beach width and shape, and dominant grain size all exert an influence on coastal dune formation on a variety of spatial and temporal scales [*Sherman and Bauer*, 1993; *Short and Hesp*, 1982]. Next to these complex interactions, man has strongly modified the coast by management practices such as dune reinforcements [*Nordstrom and Arens*, 1998].

Although coastal-dune research has already been done in the Netherlands for a long time, recently many new initiatives have started and new collaborations are explored. In this paper, we give an overview of ongoing projects that include the aeolian aspect of dune formation, how these are connected, and what type of questions are addressed. The recent interest in coastal dunes is inspired by both scientific questions and societal developments. From a scientific point of view, biogeomorphology and linkages between systems (e.g. underwater – above water) have become hot topics, and dunes are perfect examples of systems fitting within these concepts. Additionally, the dynamics of sediment transport continue to form a major scientific theme. From a management perspective, the impact of small and large coastal management practices such as dynamic coastal defense and the related (mega-) nourishments has gained much attention, raising questions on impacts and future developments. Further, global (climate) change is expected to significantly affect dynamic sedimentary coasts such as those with dunes.

Questions regarding coastal dunes thus range from the scale of seconds and meters, to the scale of the entire Dutch coast over a century. In the past, valuable research has been done on these issues, although that often addressed specific coastal locations, or only part of the system components, or concerned for arid rather than coastal systems. To increase our knowledge on coastal dunes, improve prediction capability under management scenarios (e.g. Sand Engine, long-term nourishment strategies) and climate change, and contribute to the daily engineering practice, a variety of projects has been developed. In the next sections we discuss these projects and preliminary results.

Figure 1. Dune formation on Ameland.

FRAMEWORK

The linking factor in the projects presented here is the aeolian processes building coastal dunes. Additionally, storm erosion and other hydrodynamic processes, management, and vegetation growth are included to various degrees. The positioning of the projects is given in Figure 2. The approaches can be divided into data-driven and model-driven, with Bayesian network analysis as hybrid in between. The combination of data and modeling is essential for understanding and predicting coastal dune formation. Data is used as basis for hypothesis and model development, including calibration and validation. Models, in their turn, give

direction to data collection and further hypothesis development. A variety of model approaches is used, ranging from strongly process-based to behavior-oriented. In Bayesian networks, both field data and model-generated data can be used.

Temporal scales from hours up to a century are considered, related to spatial scales from metres to hundreds of kilometres. All studies have practical relevance, related to nourishment design, safety, and nature conservation. Their result can be used in daily management and engineering practice, for example within the context of EcoShape and Knowledge for Climate (Figure 2). We will describe the projects of Figure 2 in the next section, starting with data-driven projects and ending with modeling approaches.

PROJECTS

Aeolian sediment transport on the beach

Starting at the beach and at the smallest timescale, aeolian sediment transport is an important process in the development of dune geomorphology. In a beach environment, aeolian sediment transport is governed by saltating streamers. Although these have small temporal and spatial scales, their net effect is what drives aeolian sediment supply to the dunes. The saltation process is typically described on a small temporal (sec) and spatial (cm) domain, whereas total aeolian sediment transport is often studied on a much larger scale. Both approaches find difficulties in describing the process, because of the inherent spatial-temporal complexities of aeolian sediment transport. Results from the different scales are not easily inter-comparable, as data obtained from a small spatial or temporal domain cannot be easily extrapolated to a larger scale.

To gain more insight into the process of aeolian sediment transport and geomorphologic development, researchers from Wageningen University performed a field study at Ameland [*Poortinga et al.*, in prep.]. They measured the meteorological conditions, sediment fluxes (Figure 3) and groundwater height spatially at the beach. A camera on the top of a dune acquired an image of the area every five minutes. The transport patterns under various wind regimes and other meteorological conditions were identified and compared with larger scale meteorological data and annually surveyed elevation transects (JARKUS) [*Keijsers et al.*, in prep.]. Results can be found in Keijsers et al. (this issue). Later, these results will be used to build a short-term sediment transport model.

Figure 3. Sediment catcher on the beach of Ameland.

Sediment transport from beach to hinterland

Moving from the beach into the established dunes, increased atmospheric nitrogen deposition is perceived as a severe threat to dune ecosystems by reducing landscape dynamics and biodiversity. Wageningen University investigates if dynamic dune management can reduce these negative impacts on soil and vegetation, by creating the opportunity for sand to be transported in suspension far into the dune field during storms.

To get an idea of the quantity and range of this occasional suspension transport behind foredune, a pilot project was started on four locations along the Dutch coast: Ameland, Kwade Hoek, Voornsduin and Solleveld. So-called MDCO sediment traps (Marble Dust COllector) were installed to measure vertical

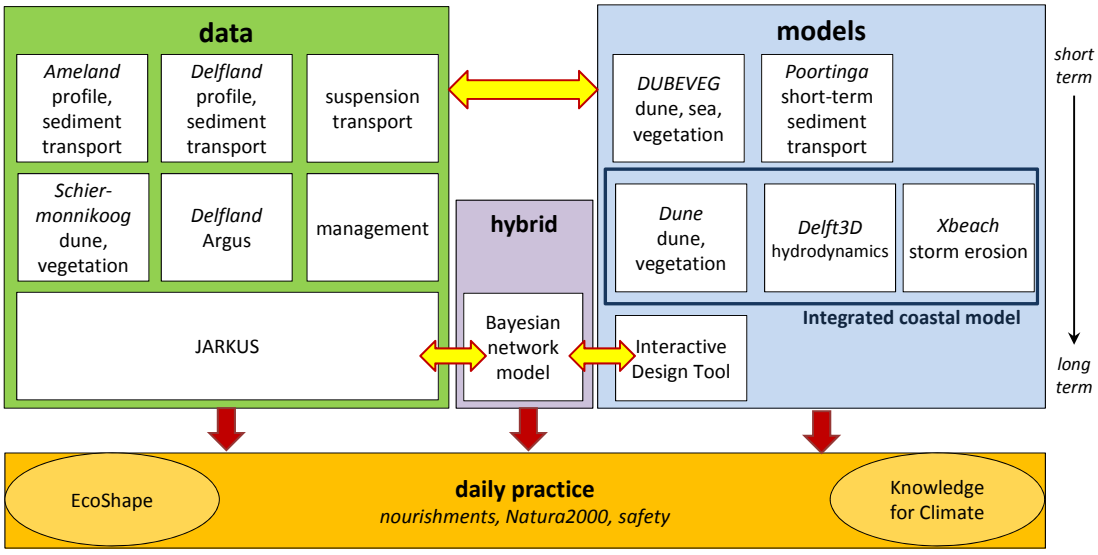

Figure 2. Framework of dune research, showing the data and models described in this paper.

sediment deposition in transects running landwards from the foredune (Figure 4).

The first results show that sedimentation amount and pattern mainly depend on foredune characteristics, for instance related to the presence of dynamic dune management. Further research will identify the impact of this sedimentation on soil properties and vegetation.

Figure 4. MDCO sediment trap for vertical sand deposition.

Foredune volume

On a larger timescale, foredune volume depends on the balance between dune erosion through wave attack and dune growth via aeolian transport. For the purpose of modeling foredune development over 10 to 100 y, Wageningen University tries to identify a limited set of factors that control the rate of sediment input to the dunes. Beach width is thought to be an important factor, as it controls sediment available for transport, wind fetch length and wave dissipation (limiting storm erosion). An analysis of 30 years of JARKUS beach and dune profile data of Ameland shows that this expected relationship between beach width and foredune growth is not evident at annual scale (Figure 5). Although strong erosion seems less frequent at beaches wider than 200 m, growth rates are not necessarily higher at wider beaches.

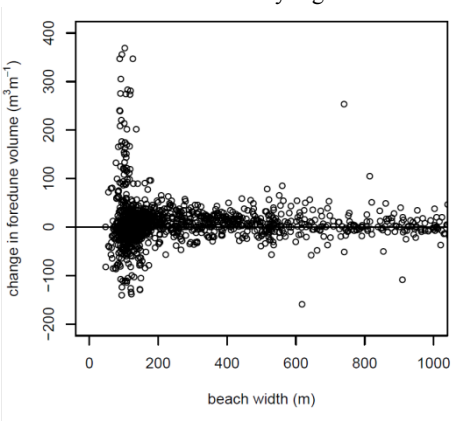

Figure 5. Annual changes in foredune volume and their corresponding beach widths at Ameland. Each point represents a single profile and year.

As beach width alone is not a good predictor of foredune growth at this location and time scale, further factors will be analyzed. The ultimate purpose is to design a long-term model to explore the possible effects of changing conditions on foredune development.

Long-term foredune evolution under management interventions

Recent work at the University of Twente also considers the understanding and prediction of aggregated scale evolution (10 year+) of foredunes, but focuses on the effects of management interventions on it. To analyze the relation between spatio-temporal variability in the cross-shore shape of the foredune and the applied management interventions, 49 year of JARKUS profiles along the Holland coast were analyzed [*Bochev-van der Burgh et al.*, 2011; in press]. At the decadal scale, measures that were applied in response to erosional events and aimed at restoring the pre-erosion state (flattening dune scarps, erecting sand fences, planting marram grass), left less imprint on foredune shape than proactively applied measures that aimed at creating a buffer for erosion. A case study on Schiermonnikoog (Figure 6) showed that proactive intervention strategies tend to leave a larger imprint on the decadal scale than reactively applied measures, because they interfere with the foredune system at a higher hierarchical level.

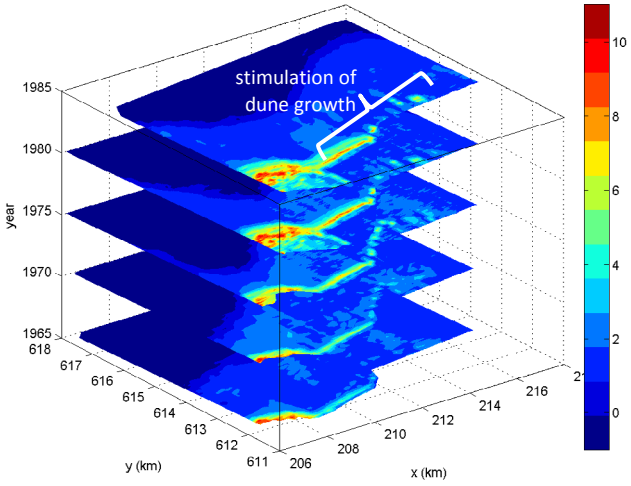

Figure 6. Topographic development at Schiermonnikoog from 1965 to 1985. The artificial stimulation of dune growth was only partially successful. Note: the cross-shore distance has been exaggerated 5 times; elevation in m + NAP.

For understanding morphological evolution beyond the process scale, such as the decadal scale evolution of managed foredunes, behavior-oriented modeling approaches seem promising. To develop aggregation rules, exploratory work has started to extract patterns in persistence of depositional areas around an artificially created dune, using Argus video imagery (Figure 7).

Figure 7. Argus image collected at Vlugtenburg beach (The Netherlands) showing depositional features at the landward side of a dune-like feature created by ground-moving equipment.

Foredune response to nourishments and changed management

When further zooming in on management practices affecting foredune development, a notable change in Dutch coastal management policy was in 1990. Coastal erosion is now primarily combatted using sand nourishments, and foredunes are much less intensively managed. This management change has had two main effects on the foredune system. Firstly, the sediment budget of the foredune system has changed. Roughly 25% of the nourished volume is transferred into the dunes by aeolian processes [*Arens et al.*, in prep.]. In many cases, the formerly negative sediment budget of the foredune changed into positive.

Secondly, the less intensive foredune management has resulted in an increase in the importance of natural processes, which is reflected in a more natural appearance of the foredunes. The northern part of the Holland coast shows increased dynamics, blowout development, increased inland sand transport (Figure 8). In contrast, the southern part mainly shows the development of new incipient foredunes in front of the former foredunes, leading to increased stabilization. The cause of this distinction between north and south lies probably in the interaction between shoreface, beach and foredunes. This issue needs to be resolved to 1) fully understand the response mechanisms to nourishments and 2) to be able to use nourishments more precisely as a management tool, meeting both coastal defense and nature requirements [*Arens et al.*, in press].

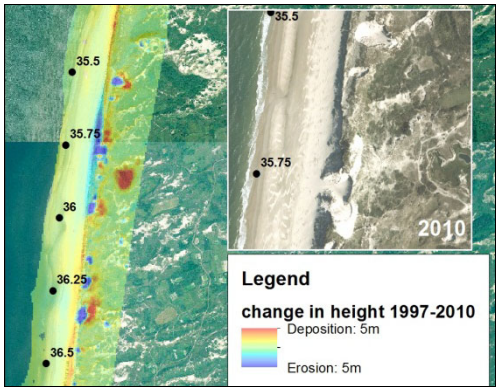

Figure 8. Blowouts in the foredunes of Noord-Holland, Bergen-Egmond evident from elevation changes (left) and aerial photographs (right).

Bayesian network modeling

The results from the above studies can be further exploited for evaluating existing models for dune development and forming a basis for new process formulations [*De Vries et al.*, this issue]. An example of such application is a data-driven model in the form of a Bayesian network model. At Delft and Wageningen, such a model for the Holland Coast is being set up, starting with dune volume changes and beach slope (Figure 9). A Bayesian model uses the underlying data and specified connections between these data to provide a prediction of the expected value, its standard deviation and distribution based on conditions selected by the user. For instance, when selecting a specific beach slope and location, the network model gives the expected dune-volume change. The Bayesian network model can easily be extended towards other domains, such as nourishment locations or Wadden Islands. Additional parameters (such as MKL volumes, foreshore slopes, marine conditions) can be added to fine-tune these data-based predictions.

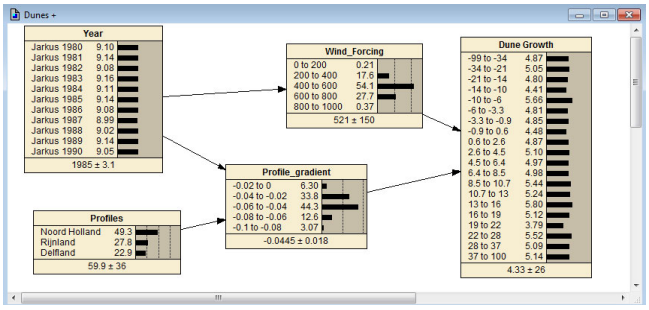

Figure 9. Example of the structure of a Bayesian network model. Selecting specific cases in the boxes on the left will give the corresponding distribution of the output variable on the right.

Dunes in an Interactive Design Tool for the Holland coast

A direct application of the findings of the above projects is a user-friendly, long-term model of the Holland Coast that is developed as part of the EcoShape program. This Interactive Design Tool allows stakeholders in the coastal zone to quickly see the effect of management interventions such as nourishments on the development of the coast on a timescale of 100 years. Google Earth is used as interface, and calculation time is kept as short as possible so that it can be used during stakeholder working sessions (Figure 10). As dunes are important features in how people perceive the coast, the model will be extended with a dune model that is currently under construction. The expertise of Wageningen UR, Deltares and TU Delft is combined to come to an efficient model design, where the challenge lies in predicting dune behavior with a minimum of input parameters and calculation time.

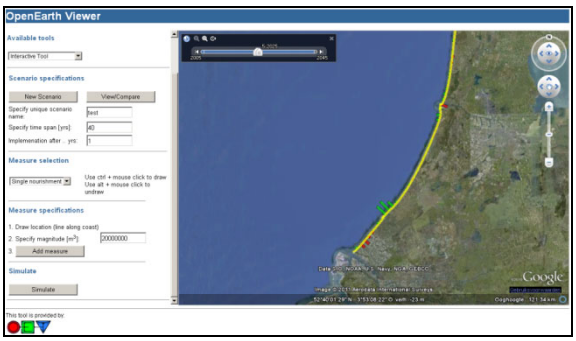

Figure 10. Screenshot of the Interactive Design Tool developed within Ecoshape.

Ecological optimization of dynamic coastal defense

Although dune formation, sea processes and vegetation development are closely interlinked, not much is known yet on the role of the vegetation. To study under which conditions ecologically valuable swales (NL: duinvalleien) develop, the DUBEVEG dune model was built at Wageningen University. This model integrates dune formation, vegetation growth, and sediment transport by the sea. The simulations show that vegetated swales develop if the beach is sufficiently wide to create accommodation

space for new dune formation (Figure 11). After a new seaward dune has established, dune-slack vegetation establishes in the low-lying swale between the new dune and the previous foredune. The model is further used to study the impact of nourishments on the development of ephemeral swale [*De Groot et al.*, in prep.] and will be validated using a GIS-based analysis of dunes and vegetation of the recently developed green beach on Schiermonnikoog.

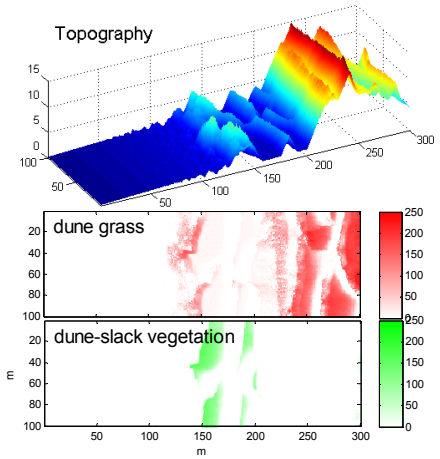

Figure 11. Simulated topography (upper panel) and vegetation biomass (lower panels) after 15 years, using the DUBEVEG model.

A modeling shortcut: from data to engineering practice

A second approach to integrate dune-forming factors in a modeling environment is undertaken at Deltares. To predict morphological changes at mega-nourishments such as the Sand Engine, an ecomorphological modeling approach is desired. The essence of ecomorphological modelling is to identify and represent the links between the hydrodynamic, morphodynamic, water quality and ecological processes involved on the appropriate spatial and temporal scales. This can be achieved by coupling various individual models. A method to do this is through ESMF (Earth System Modeling Framework), which is an open-source software framework for building and coupling various types of related models. The individual models are reformulated into smaller components, for instance I/O systems or computational kernels. The ESMF then provides toolkits to assemble the components into an integrated model system. Currently, in Delft an Integrated Coastal Model consisting of Delft3D-FLOW (hydrodynamics), Xbeach (storm events, low-frequency waves) and Dune (aeolian transport and dune formation) is under testing (Figure 2) [*Baart et al.*, submitted]. It will eventually be applied to predict dune dynamics related to mega sand nourishments such as the Sand Engine.

DISCUSSION AND CONCLUSIONS

The Dutch coast is an excellent place to study dune formation. It has extensive stretches of dunes, with ample variation in dune form and the degree of management. Further, dunes fulfill important functions for society. There is an unparalleled historic coastal dataset available, mostly for free, of which especially JARKUS is a well-used resource for studying long-term dune and coastal development. Its worth is again highlighted by its featuring in many of the studies of this paper.

The projects described in this paper started mostly independently. In parallel to the overarching NCK community, we found that there are large benefits in collaboration. Even if similar questions are addressed, universities and institutes all have their specific strengths and interests, so that research turns out to be complementary (cf. Figure 2). Advantages include: learning from each other's experience, standardizing methods, improve strategic planning, seeing the bigger perspective, having more opportunities for scientific discussion, and network building for young researchers. We further aim at keeping in contact with other Dutch groups investigating aspects of dune formation, such as OSL dating of storm erosion (Netherlands Centre for Luminescence dating, Delft), saltating streamers (UU), long-term coastal development and dune erosion (Deltares), and vegetation ecology (UvA).

The aim of the authors is Science for Impact: improving scientific understanding together with solving real-world problems from the management and engineering practice. The variety in approaches, timescales and spatial scales of the current studies (Figure 2) will provide a toolbox for doing so. The results of the presented projects are and will become available through scientific publications, reports, and the open knowledge databases of Deltares and EcoShape. In the scope of the Dutch Deltaprogramma and climate change, interest in coastal dunes continues, and new research proposals are actively being developed to continue and expand the current line of work.

ACKNOWLEDGEMENTS

The following funding has made our work possible: Knowledge for Climate (AdG and JK), EcoShape (AdG, SdV, KW, JS), WUR IPOP (AdG), OBN and Kustlijnzorg (BA), and LOICZ-ALW (LBvdB). Various colleagues at Deltares, TU Delft and Wageningen UR are thanked for their inspiring discussions. The authors greatly acknowledge the data made publicly available by KNMI and Rijkswaterstaat.

REFERENCES

Arens, S. M., L. Van der Valk, and S. P. Van Puijvelde (in prep.), Response of Dutch foredunes in changes in management.

Arens, S. M., Q. L. Slings, L. H. W. T. Geelen, and H. G. J. M. Van der Hagen (in press), Restoration of dune mobility in the Netherlands, in *Restoration of coastal dunes*, edited by M. L. Martinez, J. B. Gallego-Fernandez and P. Hesp, Springer.

Baart, F., J. Den Bieman, A. Luijendijk, J. A. Roelvink, M. J. F. Stive, J. S. M. Van Thiel de Vries, and Q. Ye (submitted), An integrated coastal model for aeolian and hydrodynamic sediment transport, in *EGU 2012*, edited.

Bochev-van der Burgh, L. M., K. M. Wijnberg, and S. J. M. H. Hulscher (2011), Decadal-scale morphologic variability of managed coastal dunes, *Coastal Engineering*, *58*(9), 927-936.

Bochev-van der Burgh, L. M., K. M. Wijnberg, and S. J. M. H. Hulscher (in press), Foredune management and foredune morphodynamics: A case study of the Netherlands' coast, *Journal of Coastal Conservation*.

De Groot, A. V., F. Berendse, M. J. P. M. Riksen, A. C. W. Baas, P. A. Slim, H. F. Dobben, and L. Stroosnijder (in prep.), Modelling the effects of environmental factors and nourishments on coastal dune formation and associated vegetation development.

Keijsers, J. G. S., A. Poortinga, M. J. P. M. Riksen, and A. V. De Groot (in prep.), Aeolian sediment transport at the beach of Ameland (part II): foredune development.

Martínez, M. L., and N. P. Psuty (2008), *Coastal Dunes: Ecology and Conservation*, Springer-Verlag, Berlin, Heidelberg.

Nordstrom, K. F., and S. M. Arens (1998), The role of human actions in evolution and management of foredunes in The Netherlands and New Jersey, USA, *Journal of Coastal Conservation*, *4*(2), 169-180.

Poortinga, A., J. G. S. Keijsers, S. M. Visser, M. J. P. M. Riksen, and A. C. W. Baas (in prep.), Aeolian sediment transport at the beach of Ameland (part I): measuring aeolian sediment fluxes.

Sherman, D. J., and B. O. Bauer (1993), Dynamics of beach-dune systems, *Progress in Physical Geography*, *17*(4), 413-447.

Short, A. D., and P. A. Hesp (1982), Wave, beach and dune interactions in southeastern Australia, *Marine Geology*, *48*(3-4), 259-284.

DOI: 10.3990/2.179

Erodibility of soft fresh water sediments: the role of bioturbation by meiofauna

M. A. de Lucas[1], M. Bakker[1], J. C. Winterwerp[1], T. van Kessel[2] and F.Cozzoli[3]
[1]Environmental Fluid Mechanics, Delft University of Technology, 2628CN, Delft, The Netherlands, m.a.delucaspardo@tudelft.nl
[2]Sediment Transport and Morphology, Deltares, 2629HD, Delft, The Netherlands
[3]Netherlands Institute of Sea Research (NIOZ) 4400 AC Yerseke, The Netherlands

ABSTRACT

Markermeer is a large and shallow fresh water lake in The Netherlands. It has a 680 km^2 surface and a 3.6 m mean water depth. Markermeer is characterized by its high turbidity, which affects the lake ecosystem seriously. As part of a study that aims to mitigate this high turbidity, we studied the water bed exchange processes of the lake's muddy bed. The upper cm's – dm's of the lake bed sediments mainly consist of soft anoxic mud. Recent measurements have proved the existence of a thin oxic layer on top of the soft anoxic mud. This oxic layer is believed to be responsible for Markermeer high turbidity levels. Our hypothesis is that the oxic layer develops from the anoxic mud, and due to bioturbation. In particular we will refer to bioturbation caused by meiobenthos. The objective of this study is to determine the influence of the development of the oxic layer on the water-bed exchange processes, as well as the role of bioturbation in this processes. This is done by quantifying the erosion rate as a function of bed shear stresses, and at different stages of the development of the oxic layer. Our experiments show that bioturbation increases the erosion rate of Markermeer sediments, and therefore affects the fine sediment dynamics of the lake.

INTRODUCTION

Markermeer is a large artificial fresh water lake located in the centre of The Netherlands. Together with the northern IJselmeer it is the largest natural fresh water reservoir of Europe. This area is known as the IJselmeer Region. During the last decades, the lake has experienced a decrease in its ecological values. [*Noordhuis & Houwing, 2003; van Eerden & van Rijn, 2003*]. This is may be caused by a food web that is not functioning optimally. Fine sediments, which are in significant concentrations in the water column, are considered to be an important pressure on the food web of the lake [*Van Kessel et al, 2008*]. Moreover, water quality problems are often related to sediment composition and transport in Markermeer [*Van Duin, 1992*]. Therefore, fine sediments in the system seem to be a key factor towards an explanation of the negative trend over the last decades. As a part of a study that aims to mitigate Markermeer high turbidity, we studied the water bed exchange processes of the lake's muddy bed.

The upper cm's – dm's of the lake bed sediments mainly consist of soft anoxic mud. Recent measurements have proved the existence of a thin oxic layer on top of the soft anoxic mud. Thin oxic layers on the mud surface exert a pronounced influence upon the exchange of substances across the mud water interface [*Mortimer, 1942*]. In fact, the sediment concentration in Markermeer's water column is dominated by erosion and sedimentation of this oxic layer [*Vijverberg, 2008*]. Our hypothesis is that the oxic layer develops from the anoxic mud. The main mechanism responsible for the development of the oxic layer would be bioturbation.

Bioturbation includes the processes of feeding, burrowing and locomotory activities of sediment dwelling benthos [*Fisher & Lick, 1980*]. The activity of this benthic biota severely affects sediment dynamics [*Le Hir et al., 2007*]. Previous researchers have measured the effect of bioturbation in the erodibility of sediments [*Willows et al., 1998; Widdows et al., 1998 and 2000; Amaro et al., 2007*]. The erodibility of sediments was characterized through the turbidity of the water in an annular flume. Our approach focuses on quantifying the erosion rate as a function of bed shear stresses. We quantified those erosion rates at several time stages within the development of the oxic layer. Our aim is a better understanding of the physics associated to bioturbation driven erosion.

MARKERMEER PHYSICAL DESCRIPTION

Lake Markermeer did not existed before the 20th century. The IJsselmeer Region used to be the Zuiderzee, a shallow inlet from the North Sea of about 5000 km^2. During the Zuiderzee era there was a landward fine sediment flux, caused by tide and estuarine circulation. Thick layers of clay and loam were deposited as a result of this flux. Then in the 20th century, the Zuiderzee works took place, and the morphology of the region changed significantly. Figure 1 illustrates the differences in bottom composition between the two periods, as well as the differences in morphology. Markermeer was created in the upper reaches of the old sea inlet, with finer bottom sediments and smaller depths than the northern IJsselmeer. The dike separating the lakes, known as the Houbtrijdijk, does not allow for the fine sediments to be transported outside of Markermeer anymore.

Markermeer is a shallow lake, with a mean water depth of 3.6 m. About 90% of the lake has a water depth between 2 and 5 m [*Vijverberg, 2008*]. The total surface of water, including Lake IJmeer, is 691 km^2 [*Coops et al, 2007*]. The volume of stored

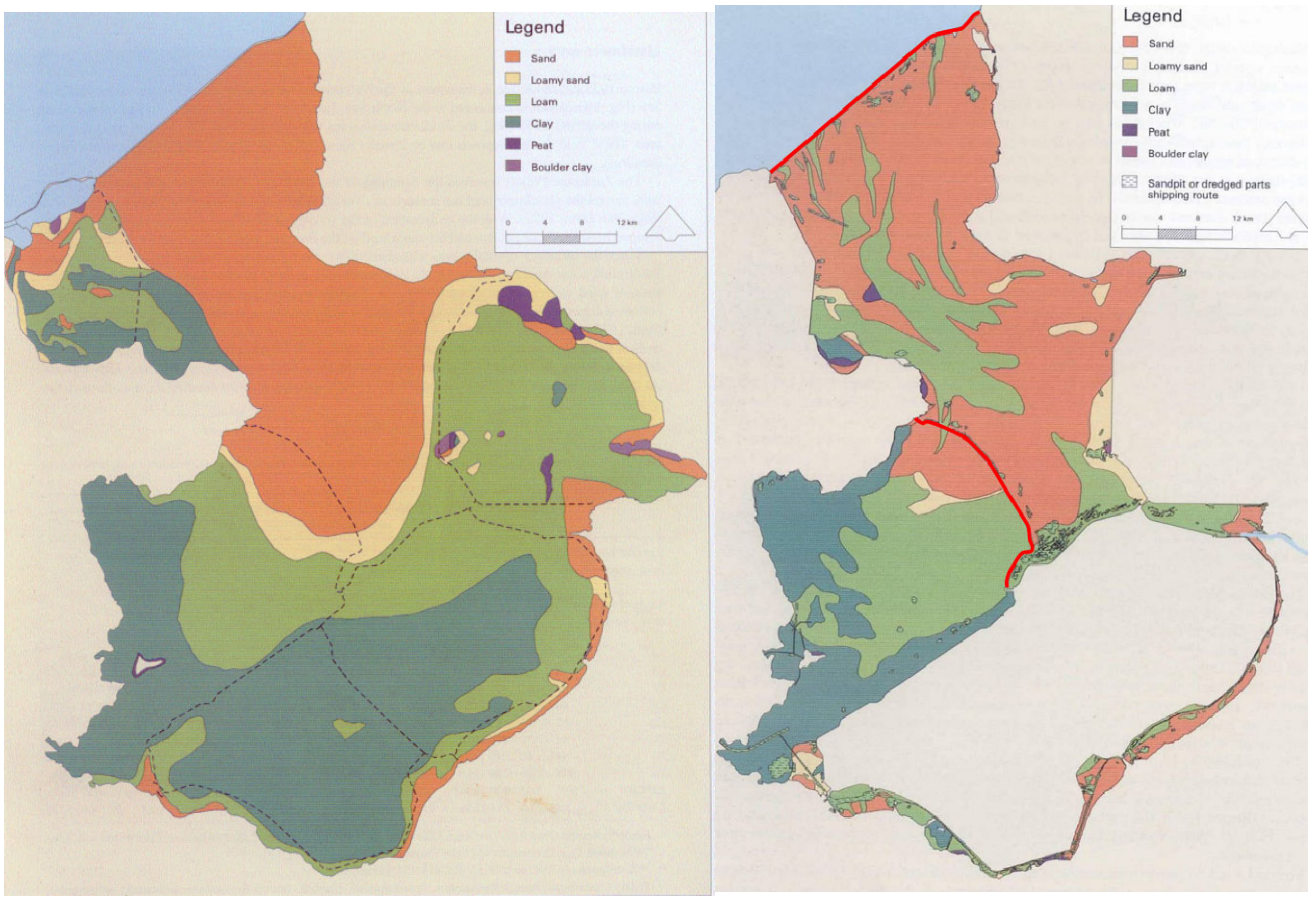

Figure 1. The left panel shows the sea inlet bottom composition during the Zuiderzee era. The right panel shows the current Markermeer bottom composition, after the execution of the Zuiderzee works [Lenselink & Menke, 1995]. Green represents loam and dark green represents clay.

water is about 2.5 10^9 m^3 [*Van Duin, 1992*]. The residence time ranges between 6 and 18 months [*Vijverberg, 2008*]. The water temperature during 2010 was 13.6±5.4 °C.

The large scale flow pattern in Markermeer is mainly dominated by wind induced flow [*Vijverberg, 2008*]. Wind induces horizontal circulations of water. This circulations may have opposite directions in surface and near the bottom, which results in a complex 3D flow pattern [*Vijberverg, 2008*]. Different large scale circulation patterns can occur depending on wind direction [*van Kessel et al, 2008*]. This water circulation is responsible for the fine sediment transport over the system. Wind also generates waves which, together with currents, induce bed shear stresses that may resuspend sediments from the bed of the lake. The relationship between wind speed and suspended solids in Markermeer is shown in Figure 2. Wind-induced-waves have a more important effect on the re-suspension of sediments from the bed than wind-induced-currents in Markermeer [*Royal Haskoning & WLDelft Hydraulics, 2006*].

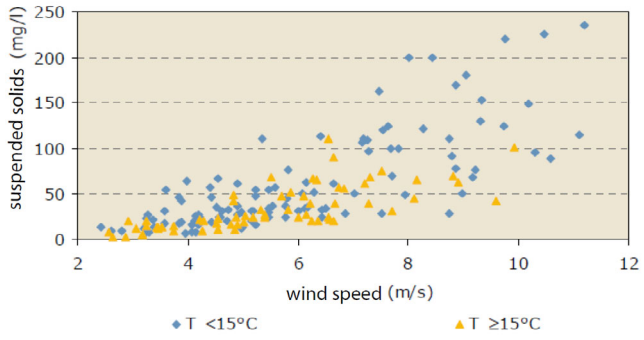

Figure 2. Relationship between wind speed and suspended solids in Markermeer [Noordhuis, 2010]

METHODS

Markermeer anoxic mud sediment samples were placed in cylindrical containers, with Markermeer water on top. These containers were kept in a small chamber, in which temperature and light conditions were controlled to mimic field conditions. We choose 6.5 °C and no light exposition. An initial erosion experiment was performed to every anoxic mud sample. Then several individuals of *Tubifex*, a characteristic benthic species of Markermeer, were added to the sample. The *Tubifex* individuals were obtained by sieveing oxic mud through 250µm and 500 µm sieves. The oxic mud started to develop on top of the anoxic mud,

upon which a series of erosion experiments was executed. The erosion rate under several bottom shear stresees was determined with these experiments. The samples were tested at several stages within the oxidized layer development process. A defaunated control sample was also studied for its erodibility. This sample was defaunated with Gamma Rays treatment in the Nuclear Reactor Institute Delft. The erosion experiments were performed in an UMCES-Gust Erosion Microcosm System. This microcosm was calibrated at Deltares. The resulting calibration curve can be seen in Figure 3. An OSLIM turbidity meter was installed at the suction outlet of the microcosm, with which the turbidity of the out-flowing water was measured. The turbidity meter was calibrated with samples of different concentrations of the sediments to be tested. Equation 1 shows how the eroded mass was calculated from the turbidity data:

$$E = c \cdot Q \cdot \Delta t \qquad (1)$$

Where E is the eroded mass (g), c is the sediment concentration (g/l) in the out-flowing water, Q is the discharge (l/s) of water through the suction outlet, and Δt (s) is the interval between two measurements of the turbidity meter. The erosion rate (g/m^2 s) was then calculated by means of dividing the eroded mass by the surface of the microcosm bed, and by the number of seconds within each bed shear step.

We performed erosion experiments at 2, 4, 6 and 8 days since the beginning of the bioturbation process. The same measurement frequency was applied for the defaunated sample.

RESULTS AND ANALYSIS

Figure 4 shows the results of our first set of experiments. The erosion rate of a two days-old oxic layer, is larger than the erosion rate of an anoxic layer. This holds for most of the bed shear stresses applied. The erosion rate of a four days-old oxic layer, is larger than the erosion rate of an two days-old oxic layer. This also holds for most of the tested bottom shear stresses. However, the erosion rate of a six days-old oxic layer is larger than the erosion rate of a four days-old oxic layer only for 0.8 Pa. This is probably caused by the high mortality of *Tubifex* in the six days oxic layer experiment. Finally the erosion rate of an eight days old oxic layer is larger than the erosion rate of a six days old oxic layer. This holds for most of the tested bottom shear stresses.

The oxic layer thickness was 1 mm after two days, 1.3 mm after four days, 2 mm after six days, and 2.5 mm after eight days. The erosion rate of the defaunated sample was always between 0 and 0.1 (g/m^{2}s) for every bottom shear stress, and it did not show any time evolution. An oxic layer did developed on the defaunated sample as well. However, its thickness was 1 mm only, and constant over time. We believe that the oxic layer in the defaunated sample was caused by the diffusion of oxygen only.

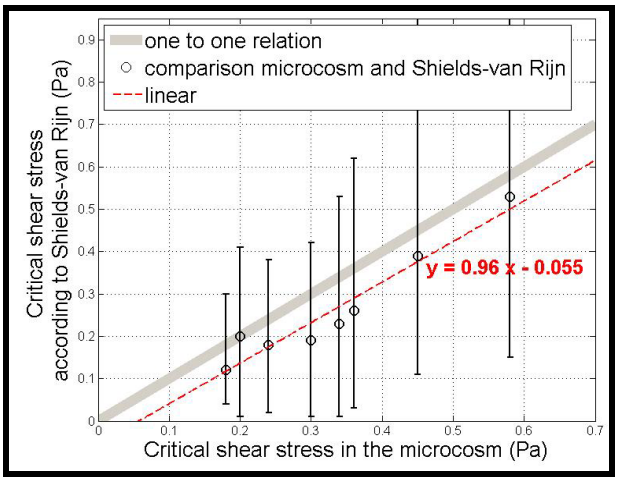

Figure 3. Calibration curve of the UMCES-Gust Erosion Microcosm System. The error bars were calculated by using d10 and d90 (instead of d50) for the calculation of the critical shear stress according to Shields-van Rijn.

DISCUSSION

Overall we can conclude that bioturbation increases the erosion rate of Markermeer sediments under bottom shear stresses of 0.4 to 0.8 Pa. The larger the bioturbation time, the larger the increase in erosion rate. The defaunted sample did not experienced any increase in erosion rate over time under any of the studied bottom shear stresses. Thus oxidation can not be responsible of the decrease in bed shear strength.

The results has important implications for the fine sediment dynamics of Markermeer. Without biota effects, significant erosion of the bed, and therefore a turbid water column, would only be possible under bed shear stresses larger than 0.8 Pa. Waves larger than 0.8 m would be needed for producing a 0.8 Pa bottom shear stress (given a wave period of 5 s, a sediment bed with a d50 of 80 μm, and a depth of 3 meters). Those wave heights occur only under storm conditions in Markermeer. However, the reality is that Markermeer is characterized by a high turbidity. Therefore, and given the very particular characteristics of Markermeer (e.g. shallowness, muddy bottom), the benthic fauna is causing a major contribution for the characteristic turbid state.

ACKNOWLEDGEMENT

The authors thanks to Peter Herman, Gerard Kruse, Bram van Prooijen, Marinus Hom and Ruurd Noordhuis for the support and guidance on this paper and related work.

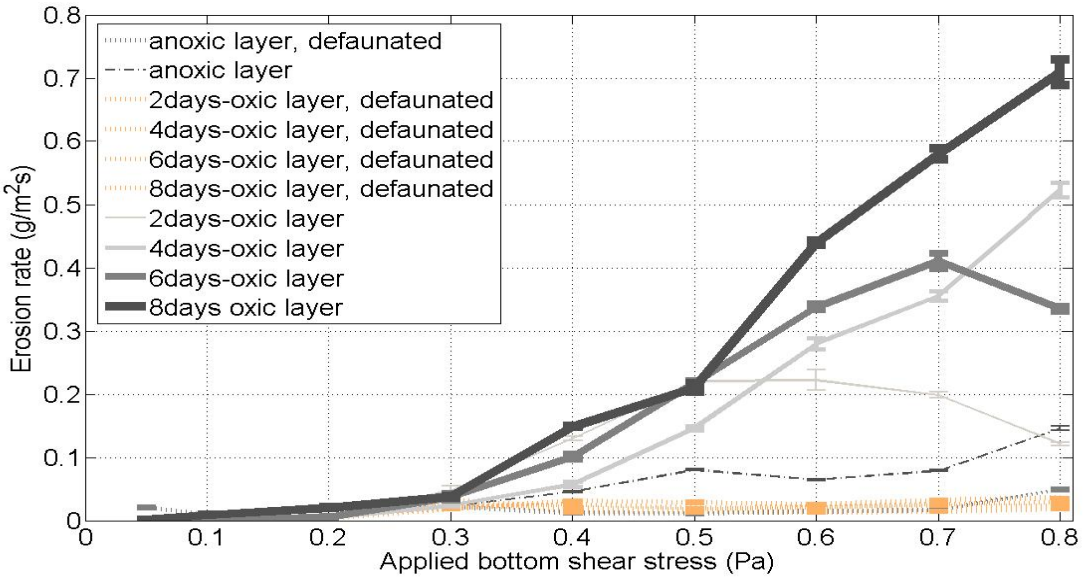

Figure 4.Effect of bioturbation on the erodibility of Markermeer sediments.

REFERENCES

Noordhuis R, Houwing EJ (2003) Afname van de Driehoeksmossel in het Markermeer. RIZA rapport 2003.016.

van Kessel T, de Boer G, Boderie P (2008) Calibration suspended sediment model Markermeer. Deltares report Q 4612.

van Eerden M, van Rijn S (2003) Redistribution of the Cormorant population in the Ijsselmeer area. CRGB 5: 33 - 37.

van Duin E H S (1992) Sediment transport, light and algal growth in the Markermeer—a two dimensional water quality for a shallow lake. Ph.D. thesis, Wageningen University.

Vijverberg, T. (2008). Mud dynamics in the Markermeer. MSc-thesis Delft University of Technology, Delft, The Netherlands.

Mortimer, C. H. (1942). The Exchange of Dissolved Substances Between Mud and Water in Lakes. The Journal of Ecology 30.1: 147-201.

Fisher, J. B. and Lick, W.J. (1980). Vertical mixing of lake sediments by tubified oligo-chaetes. J. Geophysical Research, 85: 3997--4006.

Hir, P. L., Y. Monbet, and F. Orvain (2007). Sediment erodability in sediment transport modelling: Can we account for biota effects? Continental shelf research.

Willows, R., J. widdows, and R. Wood (1998). Influence of an infaunal bivalve on the erosion of an intertidal cohesive sediment: A flume and modelling study. Limnology and Oceanography 43 (6), 1132-1343.

Widdows J., Brinsley M. D., Salkeld P. N., Lucas C. H. (2000). Influence of biota on spatial and temporal variation in sediment erodability and material flux ona tidal flat (Westernschelde, The Netherlands). Marine Ecology Progress Series 194: 23-37

J. Widdows, M.D. Brinsley, N. Bowley, C. Barrett (1998). A benthic annular flume for in situ measurement of suspension feeding/biodeposition rates and erosion potential of intertidal cohesive sediments. Estuarine, Coastal and Shelf Science, 46 (1) (1998), pp. 27–38

Amaro T P F, Duineveld C A, Bergman M J N, Witbaard R, Scheffer M. the consequences of changes in abundance of Callianassa subterranea and Amphiura filiformis on sediment erosion at the Frisian Front (south-eastern North Sea). Hydrobiologia (2007) 589:273-285.

Coops H, Kerkum FCM, van der Berg MS, van Splunder I (2007) Submerged macrophyte vegetation and the European Water Framework Directive: assessment of status and trends in shallow, alkaline lakes in the Netherlands. Hydrobiologia (2007) 584:395–402.

Royal Haskoning & WL Delft Hydraulics (2006), Verdiepingsslag en maatregelen slibproblematiek Markermeer – Analyse kennisleemten en inventarisatie maatregelen, authors Van Ledden et al , Royal Haskoning and WL Delft Hydraulics.

Lenselink G, Menke U. Atlas geology and soil of the Markermeer. Rijkswaterstaat, Directie IJsselmeergebied.

Noordhuis R (2010). Ecosysteem IJsselmeergebied: nog altijd onderweg. Trends en ontwikkelingen in water en natuur van het Natte Hart van Nederland. Rijkswaterstaat Waterdienst.

DOI: 10.3990/2.180

Morphological developments after a beach and shoreface nourishment at Vlugtenburg beach

M.A. de Schipper[1], S. de Vries[1], R. Ranasinghe[1,2], A.J.H.M. Reniers[3] and M.J.F. Stive[1]

[1]Section of Hydraulic Engineering, Delft University of Technology, P.O. Box 5048, 2600 GA, Delft, The Netherlands, M.A.deSchipper@TUDelft.nl

[2]Department of Water Engineering, UNESCO-IHE, P.O. Box 3015, 2601 DA, Delft, The Netherlands

[3]Rosenstiel School of Marine and Atmospheric Science, University of Miami, FL 33149-1098, Miami, USA

ABSTRACT

Typically a beach is out of equilibrium after a nourishment is installed. To observe how a nourished beach behaves on the timescale of storms a monitoring campaign was set up at Vlugtenburg beach after a nourishment in the spring of 2009. Here we show a sediment budget analysis of the first 2.5 years for a coastal domain spanning 1750 m alongshore from -9 to +5 m NAP. To investigate the redistribution of nourished sand different sections of the profile are examined. Observations show that the initial response (first 6 to 12 months after construction) is large where the sediment eroded from the beach is transported offshore to form a subtidal bar. In the following period (until present) the losses in the domain are on the order of 40 m^3 per m alongshore per year. These losses are concentrated in the profile around the waterline.

INTRODUCTION

For the last decades Dutch coastal policy requires to maintain the coastline at its 1990 location. A large part of the Dutch coast suffers from structural erosion and to prevent coastal retreat these parts are nourished every few years. The total volume of these nourishments is 12-15 million m^3 per year and this large volume is likely to increase in the upcoming decades. Over time, the nourishment strategy has evolved from a direct protection approach to a feeder approach. Hence, instead of placing the sand on the beach or dune where it directly benefits safety, sand is rather placed on the shoreface or alongshore concentrated. The underlying hypothesis is that natural processes redistribute the sand over the profile and alongshore.

To make optimal use of natural forces it is essential to understand how (nourished) sand is redistributed over time. Within this context a coastal stretch is monitored from the completion of a large beach and foreshore nourishment onwards.

The objective of the current paper is to show the morphological response observed at the nourished Vlugtenburg beach. Special attention is given to the redistribution of sand along the profile, transforming the artificial man made profile to a more natural profile.

FIELD SITE AND NOURISHMENT

The nourishment under investigation is the '*Duincompensatie*' project at Vlugtenburg beach, close to the town of Hoek van Holland on the southwest part of the Dutch coast. This part of the Dutch coast, called Delfland, is a 17 km long open sandy coast long intersected by the harbourmoles of the port of Rotterdam and Scheveningen.

Notorious for its structural erosion, a large nourishment scheme was initiated in 2008, strengthening the Delfland coast with 12.5 million m^3 of sand on shoreface, beach and dune.

The largest coastline reinforcement on the Delfland coast has been executed in the spring of 2009 at Vlugtenburg beach, located approximately 3 km north of the harbourmoles of the port of Rotterdam. Prior to the construction, Vlugtenburg beach had a slightly concave coastline (Figure 1a). The coastline planform shape of the coastline was straightened by moving the shoreline up to 300 m. The nourished volume is about 2500 m^3 per m alongshore in the middle of the field site (Figure 1b).

The extensive beach and shore face nourishment created a new profile (Figure 1) consisting of an artificial dune 200 m from the old dune foot. The lens-shaped area in between the old and new dune row forms a new dune valley and is intended to become a nature reserve.

OBSERVATIONS

The newly constructed area is surveyed monthly since the completion of the construction in April 2009. The alongshore extent of the observed coastal cell is 1745 m centered around the beach entrance. The surveyed area is subdivided in 22 profiles roughly 80 m apart (Figure 1c). These profiles extend 900 m offshore to approximately -9 m NAP. Dutch datum level (NAP) used here is around mean sea level. On the landward side the profiles are bound either by the dune foot on the new dune (app. 5 m NAP) or the crest of the old dunes (app. +10 m NAP).

Approximately half of the profiles extend beyond the new dune row through the dunevalley into the old dunes. These profiles are used to evaluate the aeolian transport in the dune valley, which are not discussed here. Sea and landward limits of the profiles are selected rather far apart to obtain a closed sediment balance in cross-shore direction (at least on the timescales discussed here).

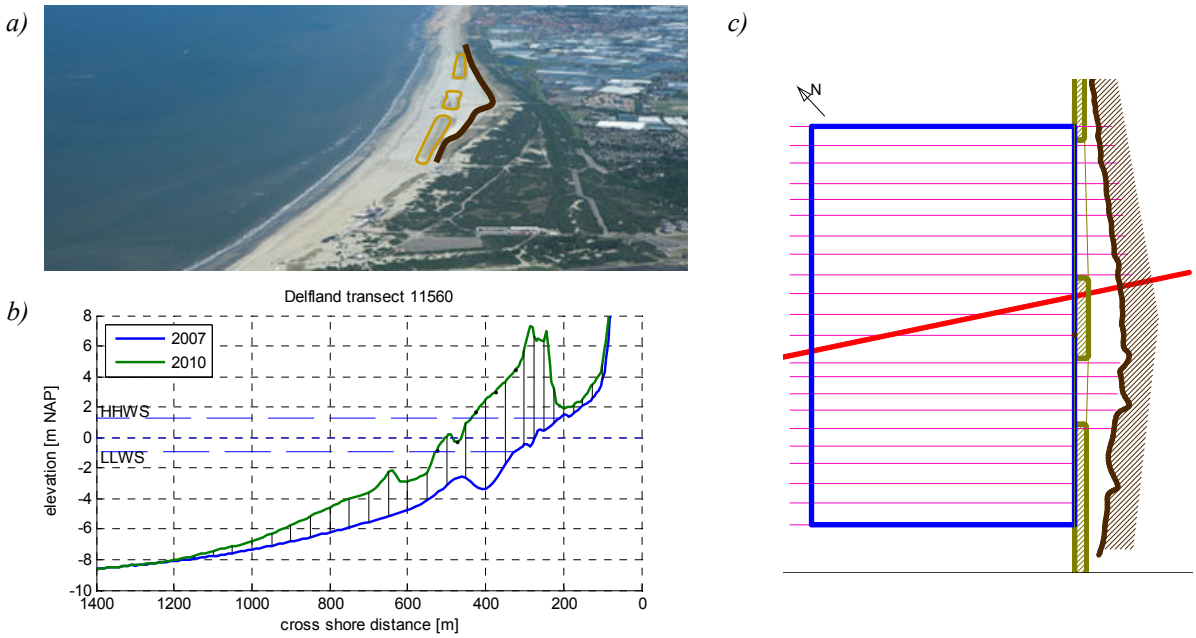

Figure 1. a) Overview of the Vlugtenburg field site. Old dune (app. +10 m NAP) shown as the dark brown line. New constructed foredune (app. +6 m NAP) given by the brown line. b) Jarkus profiles before and after construction of the nourishment. c) Overview of the survey area. 22 TUD profiles given by the magenta lines, Jarkus 115.60 profile in red. Sediment budgets are calculated within the blue rectangle.

Surveys are executed using two techniques, walking and jetski surveys. The sub aerial part of the profile is surveyed using RTK-GPS backpack surveys. These backpack surveys have accuracy in the order of 3 cm and extend to the low water line. The sub aqueous part of the profile is surveyed using the TUD survey jetski. The jetski is equipped with a single beam echosounder and Real Time Kinematic-GPS to acquire depth sounding with accuracy in the order of 5 cm (*van Son et al.* [2010]). Vertical displacements of the jetski due to tide and waves are compensated using the elevation of the jetski recorded by the GPS.

A substantial part of the error in the jetski surveys is the estimation of the speed of sound, used by the echo sounder. As the sound speed is dependent on the seawater temperature, it is calculated each survey with the Mackenzie formula (*MacKenzie* [1981]) using the daily averaged water temperature measured offshore at Europlatform. From March 2011 onwards, sound speed is measured during the survey on location using a sound velocity profiler, thereby also including salinity effects on the sound speed.

Surveys are typically executed during spring tide resulting in maximum overlap of both techniques. Jetski surveys are executed around high tide and backpack surveys around low tide. Transects of both jetski and backpack surveys are in line and the same profiles are surveyed since the beginning of the field campaign reducing the need of interpolation of the survey data over large distances between survey lines.

Both walking and jetski surveys result in *x,y,z* data points scattered around the predefined survey lines. The scattered data are interpolated to the shore-normal profiles with a cross-shore step size of 5 m.

RESULTS

Sediment budget

Sediment budget is calculated for the area seaward of the dunefoot of the new foredune (Figure 1c, blue box).

Topography maps are constructed out of the 22 shore normal profiles and integrated to obtain monthly sediment volumes in the area.

Annual Jarkus profiles every 250 m alongshore are interpolated calculated to the same grid. Jarkus profiles of 2007 and 2010 were used, to compute the nourished volume. Jarkus profiles of 2008 and 2009 were not used here as they extend only to -7m NAP (2008) or are measured during construction (2009).

The nourished volume with respect to the Jarkus 2007 elevation is presented in Figure 2 for all TUD surveys. As can be seen from the figure the total amount of nourished sediment in the control area was in the order of 2.7 million m^3.

The additional volume decreases with approximately 200.000 m^3 over the domain (i.e. 115 m^3 / m alongshore) within the two and a half years investigated here (Figure 2).

The first 6 to 12 months show a rapid decrease in sediment volume after which a more gradual loss of sediment can be observed. In the last 12 to 18 months the volume fluctuates, but a small downward trend of app. 70.000 m^3/yr (i.e. ~40 m^3 / m /yr) can be distinguished.

Timeseries of sediment volume in the area show slight variability on a monthly time scale. This variability originates partly from small inaccuracies *O* (0.5 %) in the sound speed which

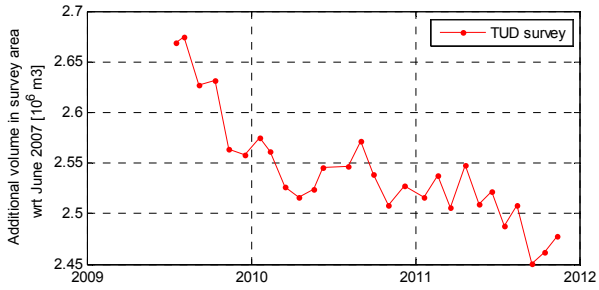

Figure 2. Sediment volume within the full alongshore stretch. Volume obtained from interpolation of Jarkus 2010 profiles given by the triangle.

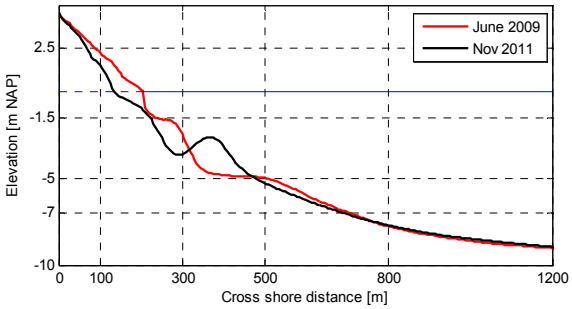

Figure 3. Alongshore averaged profile just after construction (in red) and in November 2011 (in black). Mean water level given by the solid blue line.

affects the depth measurement. Sound speed estimates/measurements in this area are prone to small errors, since the field site is close to the river mouth of the Rotterdam harbor. Sound speed profiles occasionally show strong temperature fluctuations as well as shear in salinity of 15 to 27 ppt over depth depending on the tidal phase. Consequently sound speed is varying over depth, spatially and temporally, even within a single survey. These variations yield to *O* (5 cm) over/underestimation at the deeper parts of the profile which influences sediment budget. This variability also partly be due to the (varying) sediment fluxes across the borders of the domain.

Redistribution of nourished sand over the profile

Profiles show that a large redistribution of sand occurs (Figure 3). Initially a steep sloping profile was created by the nourishment, especially below the low water line from -2 to -4 m NAP. Over time extensive erosion has taken place on the upper profile, and over a 2.5 year period the mean water level has shifted 75 m landward. The beach is consequently much smaller at present than in the first months after construction. Sediment from high up the profile has partly settled in the nearshore forming a large subtidal bar (Figure 3). This subtidal bar originated from the beach and migrated in the first 12 months towards 200 m from the low tide water line. Ever since the bar crest has moved back and forth but remains mostly stable.

The slope of the most active part of the profile (+1.5 to -4 m) is reduced as a result of these changes. To investigate the redistribution of sediment over the profile the domain is subdivided in various coastal sections, ranging from close to the dunes to far offshore. In addition, a division is also made based on elevation. The first approach indicates primarily if sand is moving landward or seaward, the latter shows if sand is moving up or down the profile.

Sediment balances for cross-shore boxes and elevations are shown in Figure 4a and 4b respectively. Cross-shore boxes are divided at cross-shore locations 100, 300, 500 and 800 m, elevation sections are divided by the +2.5, -1.5 ,-5 and -7 m NAP contour lines.

In the deep and offshore zones of the profiles a significant sedimentation of *O* (50 m^3/m alongshore) is observed. This is further confirmed by the profiles showing a bed level increase of about 10 cm at -9 m NAP. This is surprising as the seaward limit of the profiles was selected quite far offshore to obtain a closed sediment balance.

As discussed previously, a small scatter is found in the sediment volumes due to the sound speed. As the absolute error increases with depth, the largest scatter is found in the most seaward / deepest sections.

Subdivision in cross-shore boxes (Figure 4a), shows very clear the shift of sand offshore from the beachface (magenta line) to a subtidal bar (black line). The large losses observed near the waterline, are compensated by the formation of the bar. In the last year no clear migration of the bar was observed, and the volume changes in this section of the profile have become very small. The majority of the losses observed in profiles in this last year can be attributed to the zone around the water level (magenta line in both panels).

The observed changes are correlated with nearby wave data to investigate the impact of storm events. It is observed that in autumn when wave forcing is strong, the profile adaptation is accelerated, whereas in spring changes are less pronounced. Higher up the profile the volume changes are much more gradual, showing less seasonality.

DISCUSSION

Results falsify the initial hypothesis of a cross-shore closed sediment balance using an offshore limit of -9 m NAP. Considering the observed bed level changes at seaward side of the domain (over 1 km from the shoreline at a waterdepth of 9 m) it is likely that the closure depth is deeper and sediment is leaving the domain offshore. On the landward side of the profiles no significant bed level changes were observed. However, it is well possible that sand is transported by wind beyond the landward border of the domain towards the dune valley and the old dune row. First estimates of the volume transported towards the dunes is the dune growth in the area over the last decades of *O* (30 m^3 / m / yr) (*De Vries et al.* [2011] Figures 3,4). Visual observations of the area as well as the profile data that extend to the old dune confirm a deposition of windblown sand of this order of magnitude in front of the old dune row.

It is therefore open to discussion how much of the ~40 m^3 / m / yr losses as obtained from the sediment budget analysis for the last period can be contributed losses in either the alongshore or the

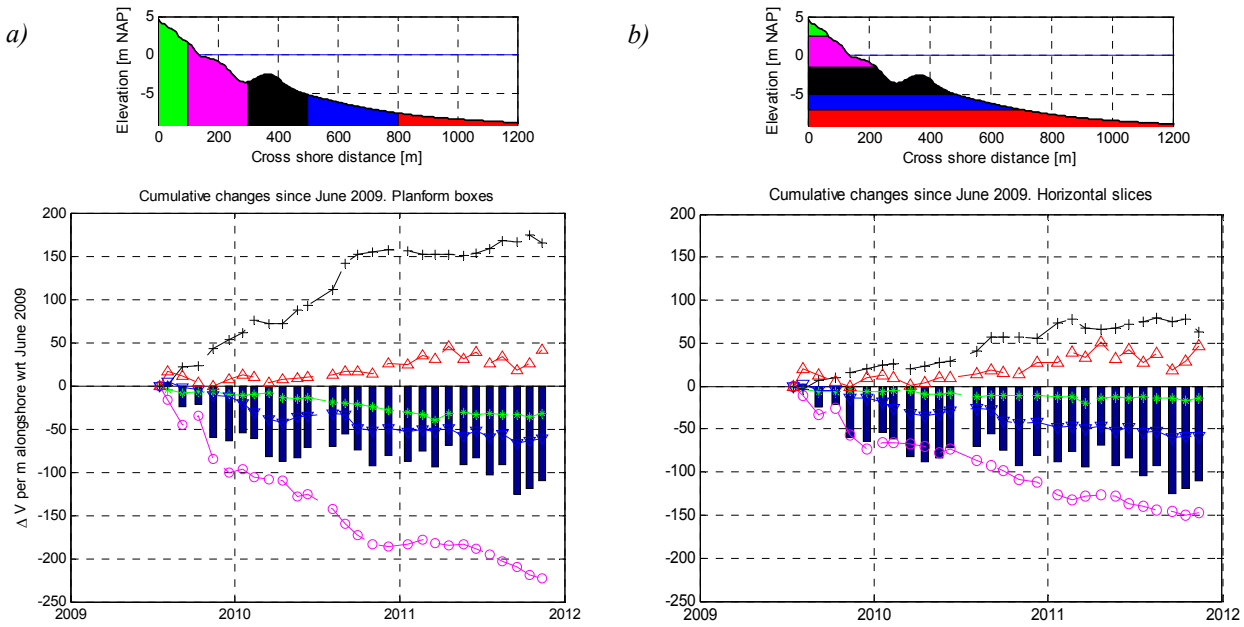

Figure 4. Alongshore averaged volume changes since the start of the monitoring in June 2009, subdividing in cross-shore boxes (left panel) and elevations (right panel). Different cross sectional areas are given in colors, clarified by the cross section above. Bar graphs show the profile averaged behavior (identical in both panels).

cross shore (seaward or landward). Ongoing investigation of the individual profiles and the dune area will provide more insight in this.

Surveys in deep water are found to be noisy at this field site due to the vicinity of a river mouth, hampering a conclusion on the morphological changes due to storms at the very deep parts of the profiles. In the shallow zone and/or with sufficient morphological variations these errors are insignificant. As a result deeper parts of the profiles however are less suited to investigate on a monthly scale.

CONCLUSIONS

Two and a half years of morphodynamic data were collected and analysed after a nourishment was installed at Vlugtenburg beach. Monthly surveys (28 in total) show in detail the transition from man-made profile shape towards a more natural profile.

Observations show that over the entire period about 200.000 m3 of sediment (115 m^3 per m alongshore) is lost from the survey area, which is less than 10 % of the nourished volume. The morphodynamic evolution can be characterized by two periods; first a period of 6 to 12 months of rapid changes followed by a second period of more stable topography. Sand is redistributed quickly within the profile. In the first period of very rapid response sand high up the profile is displaced to from a subtidal bar, thus reducing the steep construction profile slope to a more milder slope. In the following 14 to 22 months (until present) morphological changes are milder, showing a gradual loss of about 30-40 m^3 per m alongshore per yr.

ACKNOWLEDGEMENTS

M. de Schipper and S. de Vries were funded by the innovation program Building with Nature under project code NTW 3.2 and 2.1 respectively. R. Ranasinghe and M. Stive are supported by the ERC-Advanced Grant 291206 – NEMO. The 'Kustlijnzorg' program is greatly acknowledged for their support in the development of the TUD survey jetski. The Ministry of Transport and Infrastructure and Open Earth Tools are acknowledged for the use and distribution of the Jarkus data.

The Building with Nature program is funded from several sources, including the Subsidieregeling Innovatieketen Water (SIW, Staatscourant nrs 953 and 17009) sponsored by the Dutch Ministry of Transport, Public Works and Water Management and partner contributions of the participants to the Foundation EcoShape. The program receives co-funding from the European Fund for Regional Development EFRO and the Municipality of Dordrecht.

REFERENCES

MacKenzie, K. V., 1981. Nine-term equation for sound speed in the ocean. Journal of the Acoustical Society of America, 70(3), 807-812

van Son, S., Lindenbergh, R., de Schipper, M.A. , de Vries, S., Duijnmayer, K., 2009. Using a personal watercraft for monitoring bathymetric changes at storm scale. International Hydrographic Conference. Cape Town, South Africa.

de Vries S., Southgate H., Kanning W and R. Ranasinghe, 2011. Dune development and aeolian transport along the Holland coast.*This issue.*

DOI: 10.3990/2.181

Variability of currents and vertical stratification in the Marsdiep

J.J. de Vries[1], H.M. van Aken[1] and J.J. Nauw[1]
[1]Physical Oceanography, NIOZ Royal Netherlands Institute for Sea Research, Landsdiep 4, t' Horntje, the Netherlands, jurre.de.vries@nioz.nl

ABSTRACT

Velocity and salinity data is presented from 22 13-hour anchor stations (AS) collected between 2004 and 2011 at different locations in the Marsdiep. For 13 of the 22 AS, the largest velocities occur close to the surface during the entire tidal cycle. For the other 9 AS, a mid-depth velocity maximum is observed during the late flood phase in combination with a vertically stratified water column and strong cross-stream velocities. A mid-depth maximum has only been observed towards springtide conditions. Cross-stream circulation cells with velocities up to 0.4 m/s are present during different phases of a tidal cycle together with a vertically stratified water column. Vertical stratification is highly variable within a tidal cycle and seems to be driven by cross-stream circulation patterns. The onset of vertical stratification is during the late ebb (flood) phase and it can persist until the consecutive peak flood (ebb) phase. Stratification is observed just as frequently during springtide as during neaptide conditions. It suggests that changes in fresh water influx are more important for vertical stratification than changes in tidal stirring driven by the spring/neaptide cycle. These observations show that vertical stratification is more frequent and important in the Marsdiep than previously thought.

INTRODUCTION

The Marsdiep is a highly dynamic tidal inlet where the current structure is influenced by a variety of processes. In the past, the water column was always assumed to be mainly well-mixed due to the strong tidal currents up to 2 m/s [*Postma,* 1954; *Zimmerman,* 1976]. Data on the occurrence of density stratification were, however, lacking. Research of the last decade has shown that stratified conditions can occur [*Buijsman and Ridderinkhof ,* 2008] and according to *Groeskamp et al.,* [2011] they can only occur during slack tides under certain conditions. Strong cross-stream circulation cells may develop during different phases of the tide driven by friction, channel curvature, Coriolis and/or lateral density gradients [*Buijsman and Ridderinkhof,* 2008].

The main source of fresh water is from the IJsselmeer sluices at Den Oever (DO) and Kornwerderzand (KWZ). All fresh water of DO and one-third of the fresh water of KWZ is assumed to be transported to the North Sea through the Marsdiep inlet via the Malzwin channel, the southern branch of the Marsdiep channel [*Zimmerman, 1976*]. The northern branch of the Marsdiep, the Texelstroom channel, is connected to the Vlie channel and the KWZ sluices. The presence of fresh water and differential current shear leads to density fronts, which occur frequently in the Marsdiep and are highly dynamic in time and space.

In this paper, a description of the variability of currents and vertical stratification is presented from data collected between 2004 and 2011 during 22 13-hour anchor stations (AS) in 4 different locations in the Marsdiep (Figure 1).

MEASUREMENTS

During 13-hours AS, velocity data was collected with a downward-looking shipboard ADCP while remaining at anchor. AS were collected at different locations and during different seasons. During AS28-57, a Nortek was used at a frequency of 1.0 MHz and with a bin size of 1 m.

During AS28-57, a 1200 kHz RDI workhorse and a bin size of 0.25 m was used. A 2 ping ensemble was recorded every 2 seconds. The ADCP was located 1 m below the water level and a blanking distance of 0.5 m was used. The ADCP was calibrated prior to each AS. Velocity data is corrected for movement and heading of the ship. Velocity output is given in earth coordinates (velocity in east-west, north-south and the vertical direction).

Measurements of salinity and temperature over the entire water column were recorded every 20 minutes during the AS with Seabird Conductivity, Temperature, Depth sensors. The sensors were attached to a metal frame. Velocity and CTD measurement were post-processed and quality controlled.

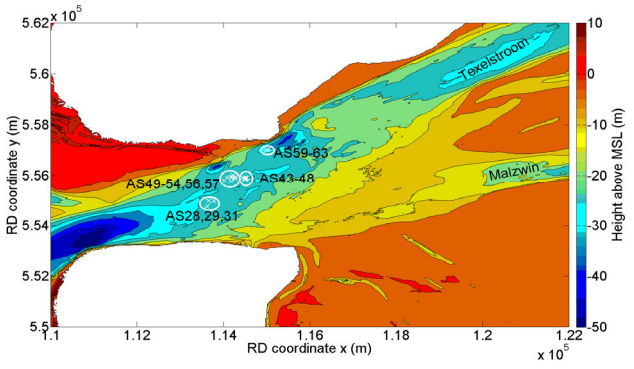

Figure 1. Bathymetric map of the Marsdiep inlet and the bifurcation of the Marsdiep channel into the Texelstroom to the north and the Malzwin channel to the south. The anchor stations are indicated with AS. Four areas are distinguished from southwest to northeast:1) AS28,29,3;2) AS 49-54,56,57;3) AS43-48;4) AS59-63 (source: Rijkswaterstaat).

ANALYSIS

For each AS, a sine was fitted through the depth-averaged east-west and north-south velocity with a period of the dominant semidiurnal tidal constituent M2 (12 hours and 25 minutes) using a least-squares method

$$u = a_{M2}cos(\omega t - \varphi_{M2}), \quad (1)$$

where u is the measured depth-averaged flow velocity (m/s), a_{M2} is the amplitude of the M2 constituent (m/s), ω is the tidal frequency (Hz), t is the time (s) and φ_{M2} is the phase.

The diurnal inequality and the spring/neaptide modulations are hidden in this signal. The amplitude and phase lag between the east-west and north-south velocities are used to compute the tidal ellipse parameters described in *Pawlowicz et al.* [2002]. The tidal ellipse parameters are the semi-major axis (SEMA), which is the maximum speed axis of the M2 constituent, the eccentricity (ECC) which is the ratio between the minimum and maximum speed axis. Negative (positive) values indicate (anti-) clockwise rotation. The inclination (INC) is the inclination between the SEMA and the east velocity axis in anti-clockwise direction. The phase (PHA) is the moment (in degrees) during the M2 at which the maximum current speed is reached. The alongstream (primary) and cross-stream (secondary) currents are determined by rotating the horizontal velocity vector over INC for each individual AS.

RESULTS

Tidal Ellipse parameters

Grouping of the AS in 4 areas shows that the SEMA varies between 1.08 and 1.28 m/s. The standard deviation of the SEMA of each group is mostly dependent on the range of measurements days along the lunar (read spring/neaptide) cycle. The eccentricity is small at all areas indicating that the tide is almost rectilinear. The inclination varies between 27 and 35 degrees and is dependent on the location of the area and the bathymetry. The orientation of the Marsdiep channel at AS28,29,31 is more east-west than for the other areas resulting in a smaller INC. The bathymetry in the Marsdiep and Texelstroom channel is highly variable which might cause a certain degree of tidal rectification explaining the largest standard deviation in the AS59-63 area. This area is characterized by large depth changes on a small spatial scale. During each AS, the measurement location is not exactly the same but describes a loop-8 kind of pattern around the anchor with an alongstream and cross-stream range of 100 and 50 m respectively. PHA is between 34 and 315 degrees for the AS. No mean and standard deviation can be calculated from the PHA at each area, since PHA is in degrees/radians. For example, the mean of 0 and 360 degrees, would result in a PHA of 180 degrees, which is a phase error of 180 degrees. The PHA values indicate that the tidal wave is between a progressive and standing wave character. Weather conditions and fresh water influx are neglected from this analysis and require further analysis.

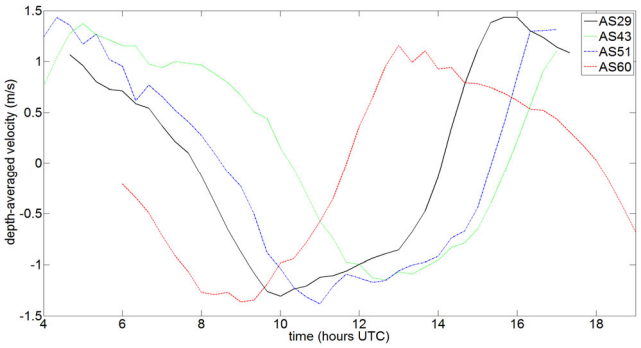

Figure 2. Depth-averaged velocity during AS29,43,51,60.

Alongstream and cross-stream velocity

A general trend of all the AS is that the late ebb phase and slack before flood (SBF) period is shorter than the late flood phase and slack before ebb (SBE) period (Figure 2). This tidal asymmetry is a consequence of the phase difference between the M2 and M4 tidal constituent as already discussed by *Friedrichs and Aubrey* [1988] and described by *Dronkers* [1986].

Besides the tidal asymmetry, a characteristic of the alongstream velocity profile is that it seems to have two states. During 13 of the 22 AS, a velocity profile was observed with the largest velocities close to the surface over the entire tidal cycle as exemplified in Figure 3a. Such profiles remind us of the canonical polynomial 'van Veen' profiles. However, during 9 AS, the maximum velocities were observed at mid-depth during the late flood phase (Figure 4a). The difference between the surface

Table 1: Averaged (grey) and standard deviation (white) of tidal ellipse parameters of M2 constituent for each area. Lunar cycle indicate on which days AS were done in the neap/spring cycle with 1 being neap- and 7 being springtide conditions.

Area	depth [m]	lunar cycle	SEMA [m/s]	ECC [-]	INC [deg]
AS28,29,31	23.30	5	1.28	0.02	27.67
	0.42		0.04	0.01	1.52
AS49-54,56,57	23.48	3,4,6,7	1.23	0.02	31.84
	1.25		0.08	0.01	1.19
AS43-48	23.58	1,2,5,6	1.08	0.02	35.07
	0.70		0.17	0.01	0.96
AS59-63	29.52	3,4	1.16	0.02	35.17
	1.42		0.06	0.01	2.52

velocity and the mid-depth maximum can be up to 1 m/s. A mid-depth maximum always coincided with strong cross-stream circulation cells (in northwest direction at the bottom and in southeast direction at the surface) and a strong vertical stratification. AS with a mid-depth maximum flow velocity during the late flood phase has been observed in all areas except the AS28,29,31 area. During the late flood phase of AS28,31, the water column was well-mixed and cross-stream velocities were small. During AS29, the water column was vertically stratified but a strong cross-stream circulation cell (in southeast direction at the bottom and in northwest direction at the surface) only formed around SBE. It is not known if the right conditions do occur at AS29,29,31 for the occurrence of a mid-depth maximum during the late flood phase.

So far, a mid-depth velocity maximum has only been observed towards and during springtide conditions. However, the fresh water influx has been neglected so far. Several longer datasets of flow velocity, surface salinity data and sluice discharge are available which will be used to include the influence of variations in fresh water discharge on the vertical velocity profile. During vertically stratified conditions, strong cross-stream velocities are usually observed during the peak and late phase of flood and ebb (Figure 4b) with velocities up to 0.3-0.4 m/s.

During well-mixed conditions, cross-stream currents are small or absent (Figure 3b). The cross-stream circulation cell is generally characterized by southwestward (northeastward) directed surface (bottom) currents. However, cross-stream circulation cells in the opposite direction can also occur (Figure 3b, between 9 and 13 hours UTC).

Vertical stratification

Vertical stratification is highly variable in time. Vertical

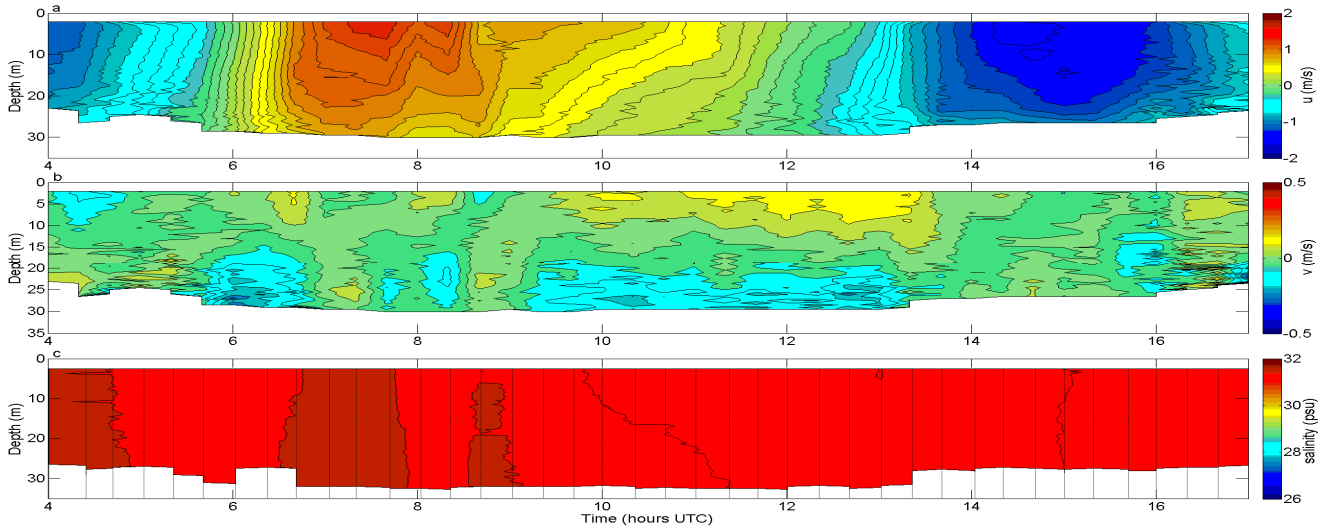

Figure 3. Alongstream (a) and cross-stream (b) velocity and salinity (c) over depth during AS61. Positive (negative) alongstream values are flood (ebb) velocities. Negative (positive) cross-stream values are directed to the southeast (northwest).

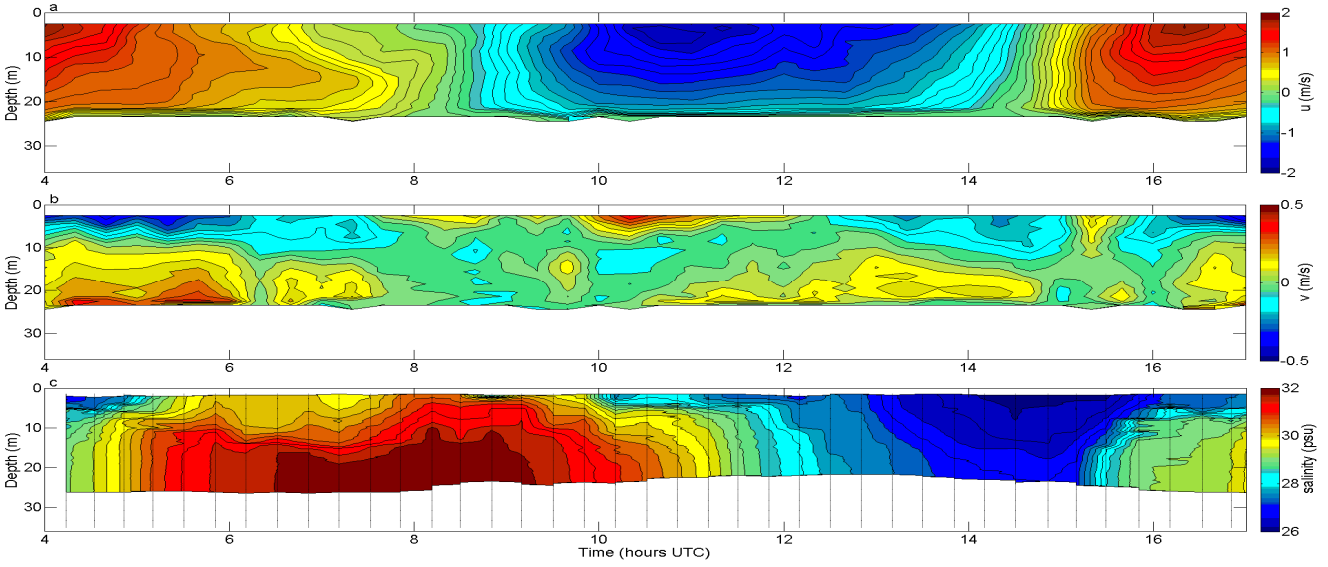

Figure 4. Alongstream (a) and cross-stream (b) velocity and salinity (c) over depth during AS46.

stratification may already develop during the late flood (ebb) phase and it can persist until the consecutive peak ebb (flood) velocities are reached. Mean bottom to surface salinity differences during an AS are approximately 1 psu, but may increase to 2-4 psu during the late ebb and flood phase and the slack tides. The periodic vertical stratification during SBE and SBF differs in magnitude and duration for each AS. Vertical stratification is always accompanied by strong cross-stream currents. Cross-stream currents, driven by lateral density-gradients, channel curvature and Coriolis, change the lateral salinity structure and enable the formation of a vertically stratified water column. It is still an open question what the contribution is of the alongstream and lateral salinity gradient on the generation of vertical stratification. Taking all 4 areas into consideration, it is striking that vertical stratification is observed during neaptide as well as during springtide conditions.

DISCUSSION AND CONCLUSION

Some interesting features have been observed in the alongstream and cross-stream flow velocity profiles, especially the mid-depth velocity maximum during the late flood phase. A mid-depth maximum in the alongstream velocity profile during late flood has also been found by *Jay and Smith* [1990] in the Colombia River Estuary during highly stratified conditions. *Geyer* [1988 in *Jay and Smith,* 1990] relates this subsurface maximum to the 'baroclinic forcing in the pycnocline, in combination with weak mixing'. However, the Colombia River Estuary is a highly stratified estuary with a salt wedge, whereas the Marsdiep is classified as a well-mixed estuary which is occasionally weakly stratified [*Buijsman and Ridderinkhof*, 2008]. The strong lateral baroclinic forcing and the stratified conditions are also present during the late ebb phase, but no mid-depth maximum is observed during any of the 22 AS during the late ebb phase. The tidal asymmetry and the related time period of the late flood and ebb phase might play another important role in the formation of a mid-depth velocity maximum. To better understand this phenomenon in a periodically stratified basin as the Marsdiep, the mixing characteristics during flood and ebb require more research. A better understanding of the mid-depth maximum is important for the estimation of sediment and nutrient transport in the Marsdiep. The strong circulation cells that occur during the flood and ebb phase are also important for sediment and nutrient transport and are an important agent for lateral transport of salt and heat. The cross-stream circulation cells are driven by lateral density gradients, channel curvature and to a lesser extent Coriolis forcing [*Buijsman and Ridderinkhof*, 2008]. Via the lateral salt flux, the water column can become vertically stratified if mixing is not too strong. Tidal straining, as described by *Simpson et al.* [1990] can be another mechanism that drives the generation of vertical stratification. However, the spring/neaptide modulation in vertical stratification as a result of the variation in tidal stirring has not been observed. The relative contribution of the longitudinal and lateral salinity gradients and their relation to stratification requires further research.

The periodic stratification during the slack tides is observed to occur just as frequently during neaptide as during springtide conditions. The asymmetry in the magnitude and duration of the vertical stratification may be of influence to estuarine circulation as described by *Geyer et al.* [2000], *Lerczak and Geyer* [2004], *Scully et al.* [2009] and others. In the Marsdiep, the fresh water influx through the sluices (of which the discharge is only during the ebb phase) is highly variable within a year (Figure 5) from a daily to seasonal timescale. It can result in large variations in stratification, density-driven flows and the alongstream vertical flow profile. The asymmetry in stratification between flood and ebb and their link to the fresh water influx is not investigated yet. Stratification influences the vertical distribution of turbulence, which is important for sediment and nutrient transport [*Joordens et al.*, 2001].

Another complicating factor is that the Malzwin is usually fresher than the Texelstroom during ebb. Besides the AS, long-term velocity data (3 times 1 month) is available in combination with surface and bottom temperature and salinity data to further

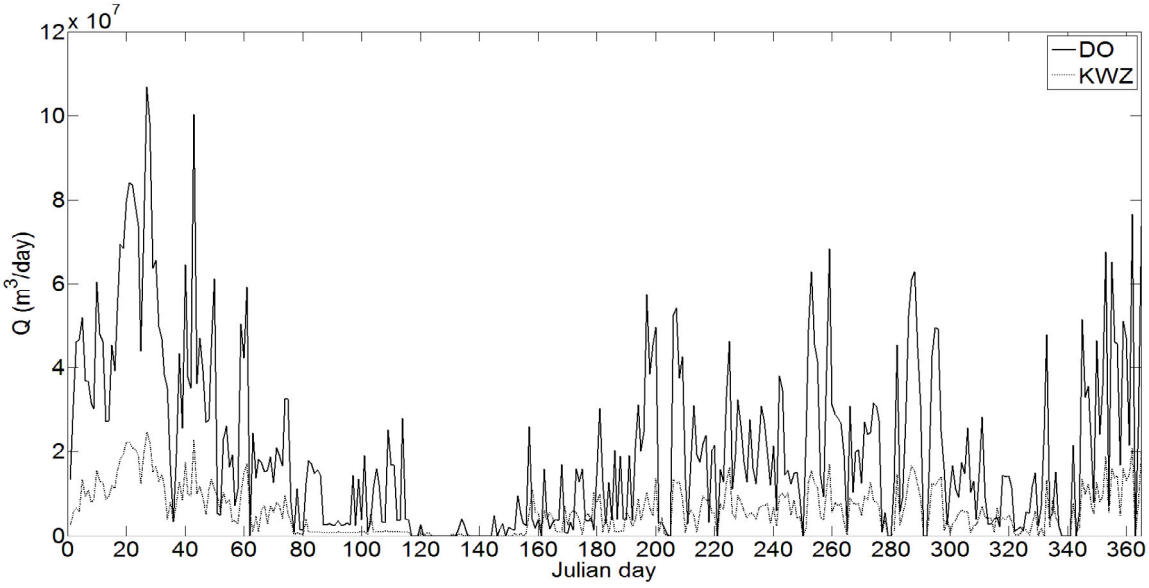

Figure 5. Discharge during 2011 at Den Oever and one third of the discharge at Kornwerderzand which flush into the North Sea through the Marsdiep inlet (source: Rijkswaterstaat).

investigate the asymmetry in vertical stratification. Also, the General Ocean Turbulence Model (GOTM, see Umlauf and Burchard, [2005] for a review) will be used to further investigate the interaction between the alongstream and cross-stream velocity profile, stratification and fresh water influx.

The influence of wind has been left out so far, but will be studied in the future. Wind contributes to the net subtidal transport [*Buijsman and Ridderinkhof*, 2007] and may also increase or decrease vertical stratification [*Souza and Simpson*, 1997].

In this paper, observations of 22 anchor stations in the Marsdiep have shown that the alongstream vertical current structure varies strongly over time with an unexpected mid-depth velocity maximum during the late flood phase when the flow is stratified and strong cross-stream circulation cells are present. Cross-stream currents are highly variable from an intra- to intertidal timescale.

The same is valid for stratification. Stratification occurs during the late ebb and late flood phase and during the slack tides during neaptide and springtide conditions and may persist until maximum current velocities are reached. It is hypothesized that the strong cross-stream circulation cells generate periodical vertical stratification. The interaction of the along-stream, cross-stream velocity profile, stratification, turbulence and the contribution of wind in the Marsdiep will be investigated further over the next years.

AKNOWLEDGEMENTS

All the students, researchers, technicians and the crew of the research ship Navicula are thanked for their contribution to the data collection in the Marsdiep over the last decade.

REFERENCES

Buijsman, M.C., H. Ridderinkhof (2007), Water transport at subtidal frequencies in the Marsdiep inlet, Journal of Sea Research, 58, 255-268

Buijsman, M.C., H. Ridderinkhof (2008), Variability of secondary currents in a weakly stratified inlet with low curvature, Continental Shelf Research, 28, 1711-1723

Dronkers, J. (1986), Tidal asymmetry and estuarine morphology, Netherlands Journal of Sea Research, 20, 117-131

Friedrichs, C.T., D.G. Aubrey (1988), Non-linear tidal distortion in shallow well-mixed estuaries: a synthesis, Estuarine, Coastal and Shelf Science, 27, 521-545

Geyer, W.R., J.H., Trowbridge, M.M., Bowen (2000), The dynamics of a partially mixed estuary, Journal of Physical Oceanography, 30, 2035-2048

Groeskamp, S., J.J. Nauw, L.R.M. Maas (2011), Observations of estuarine circulation and solitary internal waves in a highly energetic tidal channel, Ocean Dynamics, 61, 1767-1782

Jay, D.A., J.D., Smith (1990), Circulation, density distribution and neap-spring transitions in the Colombia River Estuary, Progress in Oceanography, 25, 81-112

Joordens, J.C.A., A.J. Souza, A. Visser (2001), The influence of tidal straining and wind on suspended matter and phytoplankton distribution in the Rhine outflow region, Continental Shelf Research, 21, 301-325

Lerczak, J.A., W.R. Geyer (2004), Modeling the lateral circulation in straight, stratified estuaries, Journal of Physical Oceanography, 34, 1410-1428

Pawlowicz, R., B. Beardsley, S. Lentz (2002), Classical tidal harmonic analysis including error estimates in MATLAB using T_TIDE, Computers and Geosciences, 28, 929-937

Postma, H. (1954), Hydrography of the Dutch Wadden Sea, Archive Neerlandais Zoologiques, 10, 405-511

Scully, M.E., W.R. Geyer, J.A., Lerczak (2009), The influence of lateral advection on the residual estuarine circulation: a numerical modeling study of the Hudson River Estuary, Journal of Physical Oceanography, 39, 107-124

Simpson, J.H., J. Brown, J. Matthews, G. Allen (1990), Tidal straining, density currents, and stirring in the control of estuarine stratification, Estuaries, 13, 125-132

Souza, A.J., J.H., Simpson (1997), Controls on stratification in the Rhine ROFI system, Journal of Marine Systems, 12, 311-323

Umlauf, L., H. Burchard (2005), Second order turbulence closure models for geophysical boundary laters. A review of recent work, Continental Shelf Research, 25, 795-827

Zimmerman, J.T.F. (1976), Mixing and flushing of tidal embayments in the western Dutch Wadden Sea, PhD thesis, 1-239

DOI: 10.3990/2.182

Dune development and aeolian transport along the Holland coast

Sierd de Vries[1,2], Howard Southgate[1], Wim Kanning[1] and Roshanka Ranasinghe[1,3].
[1]Section of Hydraulic Engineering, Delft University of Technology, Delft, 2628 CN, The Netherlands
[2]Building with Nature, EcoShape, Burgraadt Building, Dordrecht, 3311 JG, The Netherlands
[3]Department of Water Engineering, UNESCO-IHE, PO Box 3015, 2601 DA Delft, The Netherlands
Sierd.deVries@tudelft.nl; W.Kanning@tudelft.nl; H.N.Southgate@tudelft.nl; R.Ranasinghe@unesco-ihe.org

ABSTRACT

This paper presents an analysis of annual to decadal dune behavior along the Holland Coast. In the database of the JAarlijkse KUStmeting (JARKUS) a very large collection of yearly measured profiles is available for analysis. These measured profiles are used to extract a selection of parameters relevant to the development of dunes which are inter-comparable in time and between profiles. Special attention is given to dune volume changes and parameters which could influence aeolian transport such as the beach slope and annual wind conditions.

It is found that the beach slope is significantly correlated with dune volume changes on an annual timescale. No temporal lag between the two parameters is found. Additionally, annual wind conditions are found not to correlate with dune volume changes; windy years do not show different dune volume changes than relatively quiet years.

The results of this analysis provides new insight on processes governing aeolian transport and how to model aeolian transport and dune development. Extending the analysis to more areas along the Dutch coast could give more information on specific processes regarding dune behavior.

INTRODUCTION

The dune area along the Dutch coast is subject to natural variability as well as variability induced by anthropogenic activity (Bochev-van der Burgh et al. 2011). Natural variability is a result of aeolian and marine processes. Whereas nourishments change the dune morphology directly or indirectly via the influence on transport processes.

Annual dune volume changes are considered as a measureable parameter representing dune development. Figure 1 gives an overview of processes influencing the dune volume change. In this paper we focus on aeolian transport and therefore dune volume changes in relation to wind forcing and beach slope (profile shape in Figure 1) in particular.

DATA AND METHOD

Two datasets are used for this study. (1) The Holland coast section of the Dutch JAarlijkse KUStmenting (JARKUS) see Figure 2. (2) Wind measurements gathered at a weather station at IJmuiden by the Royal Dutch Meteorological Institute (KNMI). Both datasets are elaborated upon below.

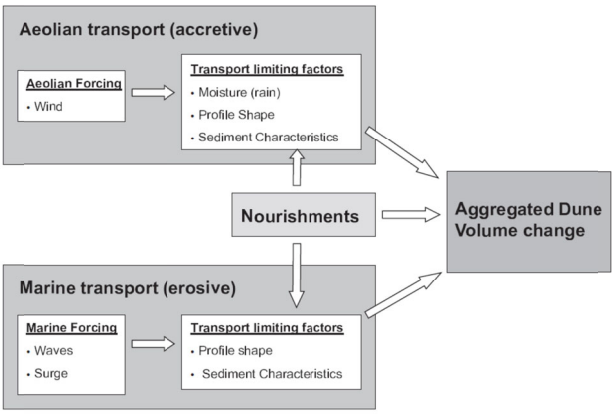

Figure 6. Conceptual representation of dune volume change aggregated over time. Accretive periods are alternated with erosive periods. Nourishments directly affects the dune volume changes as well as transport limiting factors

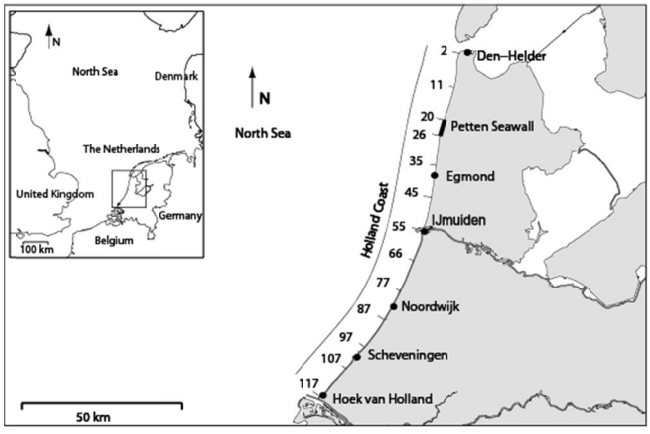

Figure 7. Overview of the Holland coast. Numbers indicate alongshore kilometers with respect to the most northern point of the Holland coast. The Petten sea wall and the harbors of IJmuiden and Scheveningen are indicated

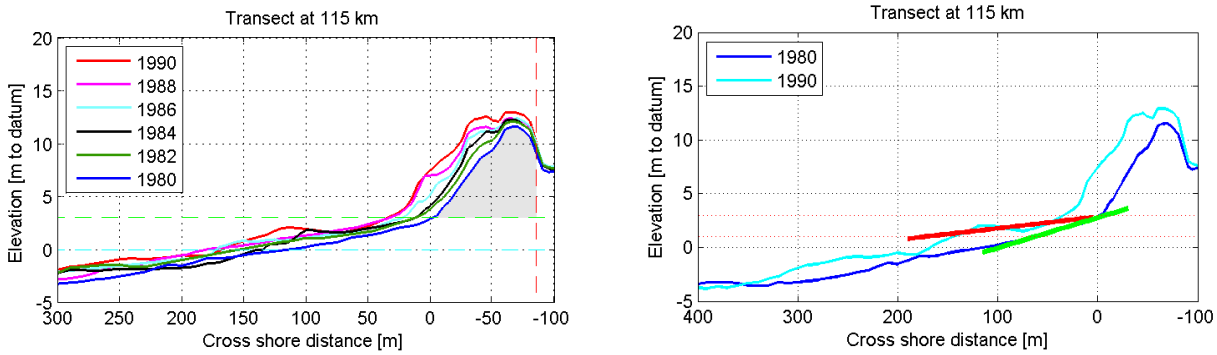

Figure 3.- Left panel shows the definition of the dune volume where the colored lines show profile measurements at an arbitrary transect location. The vertical red dashed line indicates the stable point boundary the green dashed line the dunefoot level and the gray area the dune volume derived for 1980 - Right panel shows the derived beach slope for an arbitrary transect location and two arbitrary years.

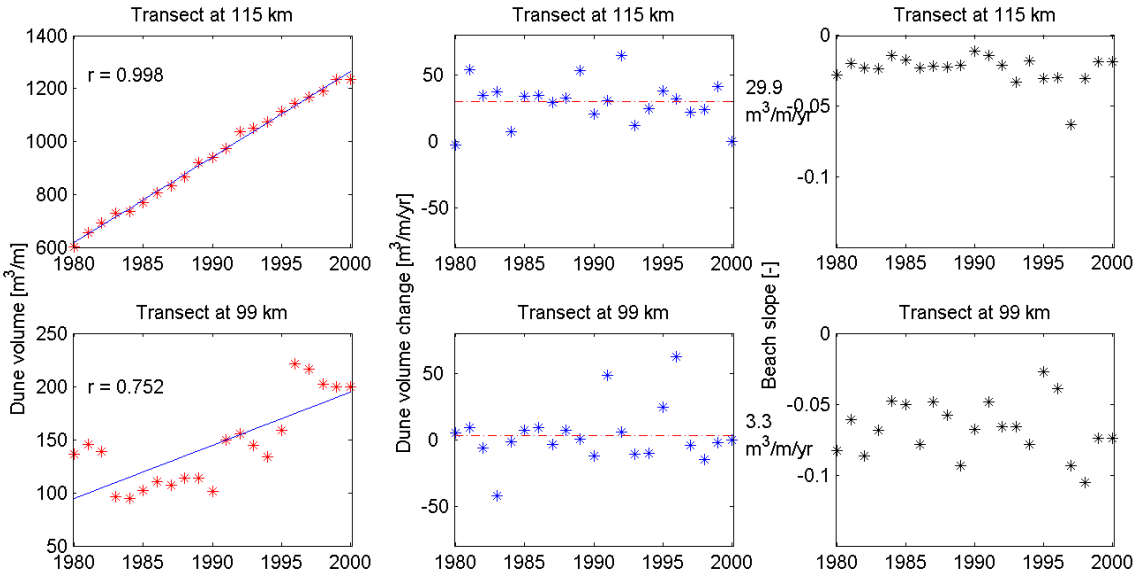

Figure 4. Left panel shows dune volume development over time at two different transect locations. Middle panels shows the associated dune volume changes over time together with the mean dune volume changes indicated. Right panel shows the development of beach slope over time.

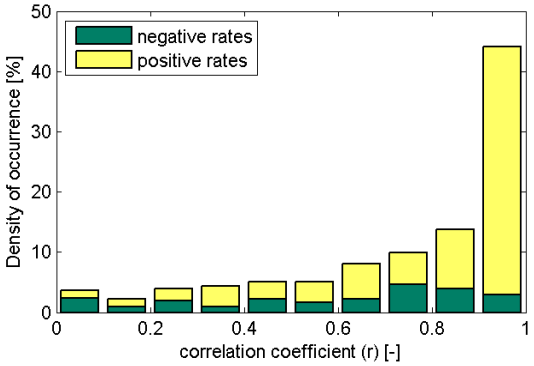

Figure 5. Density of occurrence of correlation coefficients fitting a linear trend on dune volume development at every transect location.

JARKUS - data

The Holland coast section of the JARKUS data consists of 593 annual profiles covering 117km with 250m spacing. The time window considered is 1980-2000. The annual profiles are used to derive Dune Volumes (DV) and beach slopes.

Dune Volume (DV)

In order to derive Dune Volumes using the measured profiles from the JARKUS dataset generic boundaries are needed. In this paper we choose the dunefoot level at +3 m NAP as a lower limit boundary of the dune volume. For the second boundary a landward static point is derived using a timeseries. The static point is located where the vertical variance of the bed level elevation is lower than a certain limit. Figure 3 (left panel) shows the dune volume over consecutive years together with the defined boundaries. Boundaries and dune volumes are derived for every transect location. Therefore references vary and absolute values of dune volumes are dependent on these references. As a result the absolute values of dune volumes are not of particular interest because they are not intercomparable between transect locations. However the year to year changes in dune volume are intercomparable. Figure 4 shows the development of the dune volume and dune volume changes for two arbitrary profiles.

It is shown that at particular transect locations the dune volume development is very well represented by a linear trend in time. Although the development of dune volume is not well represented by a linear trend at all transect locations (also shown in Figure 4), a large percentage of transect locations is. Figure 5 shows that around 44% of all measured transect locations show correlations coefficients of 0.9 and higher.

Beach Slope

In this paper the beach is defined as the part of the transect bordered by the dune (at +3 m NAP) and the Mean Water Level (MWL). The beach slope is defined as the gradient of the best linear fit using a least square method. Figure 3 (right panel) shows the beach slope for an arbitrary transect at two moments in time. Beach slopes are generally between 0 and -0.1 and show some variability in time, see Figure 4.

Wind conditions – Resultant Drift Potential

Following the method of Fryberger 1979, the Drift Potential (DP [m3/m/s]) is the transport potential of measured wind conditions. Equation 1 is used to calculate wind speed (u) to potential transport (q_r) where u_{t0} is the transport velocity for the initiation of aeolian transport.

$$q_r \propto (u^2 - u_{t0}^2)u \qquad (1)$$

Equation 1 is a simplified version of the sediment transport formulation by Hardisy and Whinehouse (1988). While only the effect of the variability of wind on the variability on transport is of interest all other (wind independent) constants are assumed to be averaged out due to (later) normalization.

Representative values of wind speed and direction for 1 day measured at IJmuiden weather station are used to calculate DP's. Yearly Resultant Drift Potentials (RDP's) en the associated Resultant Drift Directions (RDD's) are calculated using vector summation of all daily DP's. Figure 6 shows the wind rose for IJmuiden wind station together with the derived annual RDP

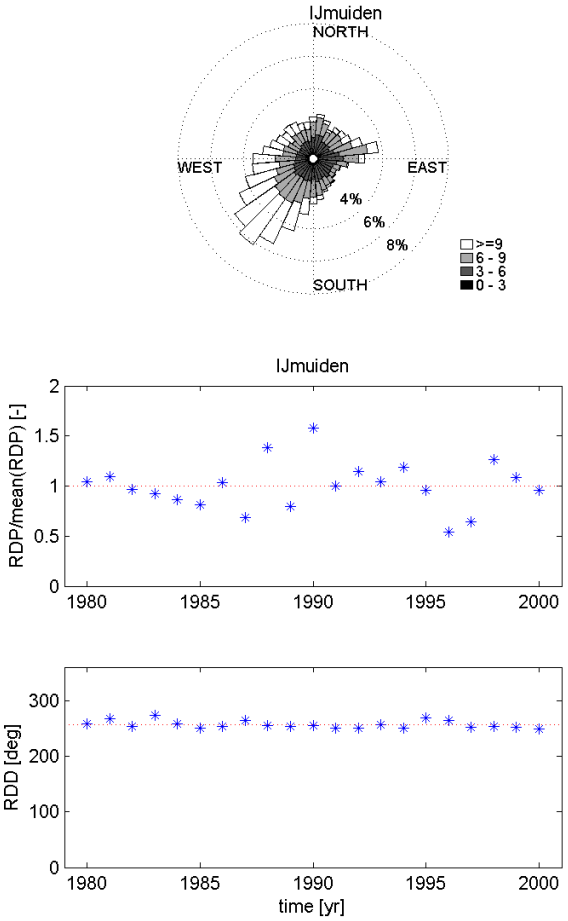

Figure 6. Wind conditions measured at IJmuiden weather station from the period 1980-2000.

(normalized with the mean) and RDD. It is shown that the annual RDP's vary around the mean with a factor 2. Moreover the RDD seems to be very constant in time averaging around 256 degrees.

CROSS-CORRELATIONS

Using the data series derived above, cross correlations are used to show to what extend parameters are related.

Dune Volume changes and RDP.

Given that dune growth is partly governed by aeolian processes (Figure 1), it could be expected that dune volume changes correlate well with wind conditions. At this stage it is assumed that the wind conditions at IJmuiden are representative for the total Holland coast. The time series of dune volume changes at every profile location is correlated with the time series of normalized RDP's derived from the data measured at the IJmuiden station.

Testing cross correlations at every transect location on the 95% significance interval it is found that the number of transects where dune volume changes correlates positive and significant with wind speed is less than 3%. Therefore we find no correlation between wind speed and dune volume changes.

Note that while calculating RDP's, u_{t0} is assumed to be 5m/s based on results by Arens (1996). Other values ranging from 0-10 m/s are also tested with no significant change in results.

Dune Volume changes and Beach Slope.

Hardisty and Whitehouse (1988) quantify (empirically) the influence of bed slope on aeolian sediment transport rates. Their results imply that where the bed slope increases from 0 to 2 degrees, aeolian transport rates decrease in the order of 30-40%. Based on these findings, correlation between dune volume changes and beach slope are expected to some degree.

Figure 7 shows cross correlations at every transect location. A time lag is shown while a delay might be expected in the reaction of the dune volume changes on changes of beach slope. The percentage of transect locations where dune volume changes correlate significant with beach slope peak at a lag of zero on 11%. This indicates that there is some correlation between both parameters and no time lag is present. The transect locations where significant correlations are found are evenly distributed over the entire Holland coast.

DISCUSSION

The lack of correlation between wind conditions and dune volume changes could be explained by effects due to transport limiting conditions (Davidson Arnott and Law, 1990). Variability of these transport limiting processes could overshadow variability induced by wind forcing (e.g. when strong winds are accompanied with rain, transport might be limited to the point where no transport occurs). Based on these results, process based predictive models where wind forcing is used as primary forcing and therefore a large wind driven variability of sediment transport rates and as a result dune volume changes, should be reconsidered or adapted before using them for coastal situations.

The found correlations between beach slope and dune volume changes could possibly represent the effect of transport limiting conditions. The transport limiting processes could be represented by the upslope effect described by Hardisty and Whitehouse (1988). Also sediment supply from the marine zone could be very relevant where sediment supply can both, limit (or stimulate) transport and cause milder beach slopes. Future research might shed some more light on this.

CONCLUSION AND OUTLOOK

Conclusion

After the analysis it is concluded that:

1. A large part of dune volumes along the Holland coast develop linearly in time.
2. Variability in time of dune volume changes do not correlate with wind conditions
3. Variability in time of dune volume changes do correlate with local beach slope.

Outlook

This research fits into the framework presented by de Groot et. al. (2012, This Issue).

The described procedure of correlating parameters extracted from the JARKUS dataset could lead to new insight on governing processes relevant to dune development and coastal development

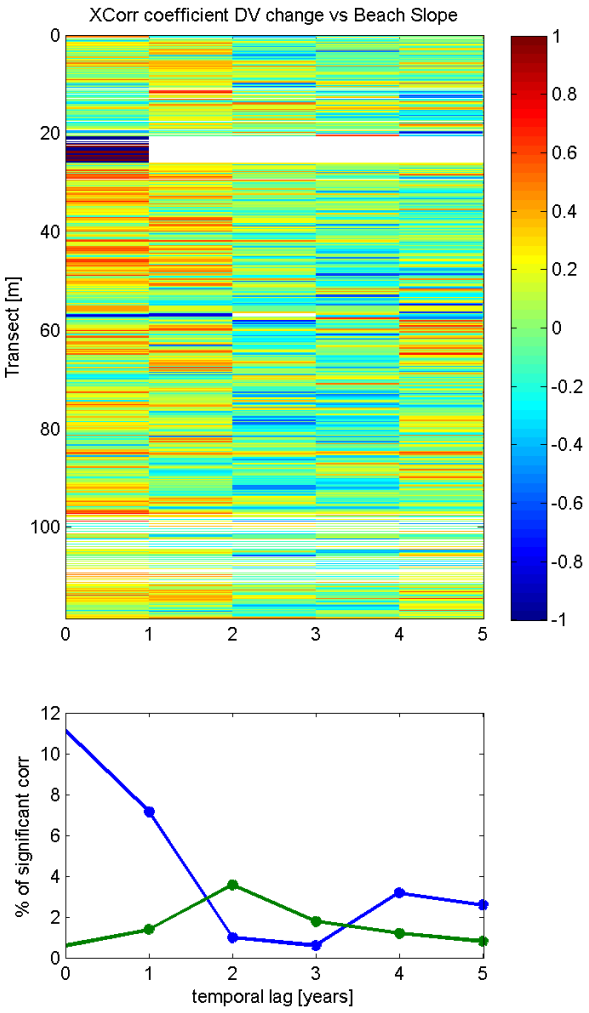

Figure 7. Top panel shows the cross correlation between dune volume change and beach slope at every transect location. Bottom panel shows the percentage of transect locations where a significant correlation (positive – blue line, negative – green line) is found.

in general. Based on the correlations, processes could be identified and quantified. According to the presented framework by de Groot et. al. (2012), the JARKUS data and the correlation procedures could further be exploited for the purpose of evaluating existing models for dune development as well as form a basis for new process formulations.

Setting aside a process based approach, the correlation and the data itself can be used as a basis for a data model. In a first effort, a Bayesian network model is set up based on the described data on dune volume changes and beach slope. Figure 8 shows such a network model. Using this model, a step of Bayesian interference provides a conditional prediction of the expected value (and its standard deviation) of dune volume change given beach slope at a given transect location. The Bayesian network model can easily be

extended towards other domains such as specific nourishment situations, Wadden islands or data from other countries. Moreover additional parameters (such as MKL volumes, foreshore slopes, marine conditions) could also be added to fine-tune these data based predictions

REFERENCES

de Groot, A., de Vries, S., Keijsers, J., Riksen, M., Ye, Q., Poortinga, A., Arens, S. M., der Burgh, L. B.-V., Wijnberg, K., Schretlen, J. and van Thiel de Vries, J. (2012), Measuring and modeling coastal dune development in the Netherlands, NCK-Days 2012, (This Issue).

Arens, S. M. (1996), Rates of aeolian transport on a beach in a temperate humid climate, Geomorphology, 17 (1-3), 3 – 18

Bochev-van der Burgh, L.M., Wijnberg, K.M. , Hulscher, S.J.M.H. (2011), Decadal-scale morphologic variability of managed coastal dunes, Coastal Engineering, 58 (9), 927 –936.

Davidson-Arnott, R. G. D., Law, M. N. (1990), Seasonal patterns and controls on sediment supply to coastal foredunes, long point, lake erie. In: Nordstrom, K. F., Psuty, N. P., Carter, R. W. G. (Eds.), Coastal Dunes: Form and Process. John Wiley & Sons Ltd., pp. 177–200.

Fryberger, S. (1979), Dune forms and wind regime. A Study of Global Sand Seas, USGS Professional Paper 1052, 137–16

Hardisty, J., Whitehouse, R. J. S., Apr. (1988), Evidence for a new sand transport process from experiments on saharan dunes. Nature 332 (6164), 532–534.

ACKNOWLEDGEMENTS

Sierd de Vries was funded by the innovation program Building with Nature. The Building with Nature program is funded from several sources, including the Subsidieregeling Innovatieketen Water (SIW, Staatscourant nrs 953 and 17009) sponsored by the Dutch Ministry of Transport, Public Works and Water Management and partner contributions of the participants to the Foundation EcoShape. The program receives co-funding from the European Fund for Regional Development EFRO and the Municipality of Dordrecht.

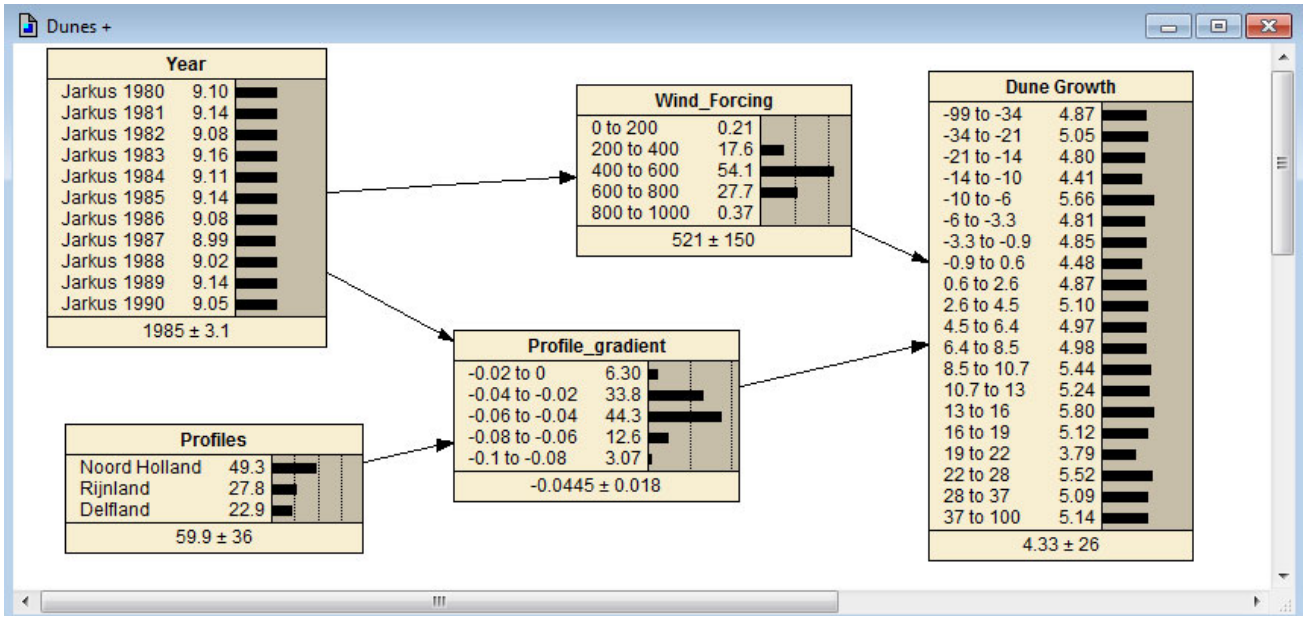

Figure 8. Initial Bayesian network model.

DOI: 10.3990/2.183

An efficient method to assess erosion risks in tidal basins

D.W. Dusseljee, A.L. de Jongste and M.H.P. Jansen [1]
[1]Witteveen+Bos B.V., P.O. box 2397, 3000 CJ Rotterdam, The Netherlands, d.dusseljee@witteveenbos.nl

ABSTRACT

Predicting erosion of channel banks and tidal flats due to wind waves in tidal basins involves multiple parameters. These parameters represent the hydrodynamic load onto a bank as well as the stability of a bank against erosion. An efficient method to predict bank erosion in tidal basins is by calculating the sediment stability parameter based on the initiation of motion of sediment particles, because this parameter includes both the oscillatory bed stress and the sediment characteristics. The loading by wind waves on banks and tidal flats can be quantified by the bed shear stress. Wave breaking can be quantified by means of the intensity parameter of energy dissipation by wave breaking. Calculation of the sediment stability parameter gives insight in the locations where erosion or sedimentation may occur in the future.

As a case study, the future reintroduction of the tide in Lake Grevelingen, in the Netherlands, is studied. The reintroduction of the tide may be combined with a tidal power plant in the Brouwersdam, between the North Sea and Lake Grevelingen. Reintroduction of the tide will change the wave load on intertidal areas in Lake Grevelingen. The effects of a tidal power plant in the Brouwersdam on erosion and the effectiveness of bank protection in Lake Grevelingen are analysed. The results of this morphological analysis are used as input for an environmental impact assessment. This case study shows that studying the initiation of motion is an efficient method to assess the local risks of (bank) erosion.

INTRODUCTION

Erosion of channel banks and tidal flats

Intertidal areas are often highly valuable and unique ecosystems. Erosion of the channel banks and tidal flats can be a serious threat to these areas. It is therefore important to understand and predict bank erosion of intertidal areas in tidal basins.

Methods available to examine bank erosion and the risks of bank erosion comprise measurement campaigns, physical scale modelling and/or numerical morphological modelling.

Bank erosion may be diagnosed by measurement campaigns. Many measurement techniques are available [*Thorne,* 1981]. In particular, remote sensing techniques have proven themselves very useful for measuring bank erosion [*Thoma et al.,* 2005]. Measuring changes – however valuable these measurements are – can only be done afterwards, and can most often not be used to predict the impact of a change on the system.

Another method to study erosion is through physical scale modelling. Physical scale modelling of bank erosion is appropriate to gain knowledge about natural processes under hypothetical situations. For meandering rivers, this has been carried by Utrecht University [*Kleinhans et al,* 2010]. However, physical scale modelling may easily suffer from scale effects, particularly in morphological scale modelling.

Morphological modelling of bank erosion is possible with numerical models, like Delft3D [*Deltares,* 2011]. At the moment, the standard numerical scheme of Delft3D for erosion does not allow erosion of the dry parts of banks. However, an optional scheme is implemented which can redistribute the erosion flux of wet cells over the adjacent dry cells.

Case study Lake Grevelingen

Bank erosion risks are also an issue in the policy analysis for Lake Grevelingen (MIRT Verkenning Grevelingen). Lake Grevelingen is the largest salt-water lake in Western Europe. This lake is a former estuary in the south-western part of the Netherlands which has been closed after the flood of 1953 by the construction of the Brouwersdam in 1971. Because of this closure, the tidal flow in the Grevelingen disappeared and the development of intertidal flats was hampered [*Deltares,* 2010; *Rijkswaterstaat Zeeland,* 2010]. However, the eroding forces of local wind waves persist. In absence of tidal water level variations, these forces now act on bank slopes at a constant level. As a consequence, the edges of tidal flats and banks have been eroded considerably (Figure 2). Therefore, many edges of tidal flats are now protected by bank protection and foreshore dams (Figure 1).

In a recent policy analysis on the future development of Lake Grevelingen, the possibilities to (partially) reintroduce the tide in Lake Grevelingen are studied. The reintroduction of the tide may be combined with a tidal power plant in the Brouwersdam, between the North Sea and Lake Grevelingen. The construction of a conduit in the Grevelingendam, the reconstruction of the Flakkeese flushing sluice and the construction of a navigation lock

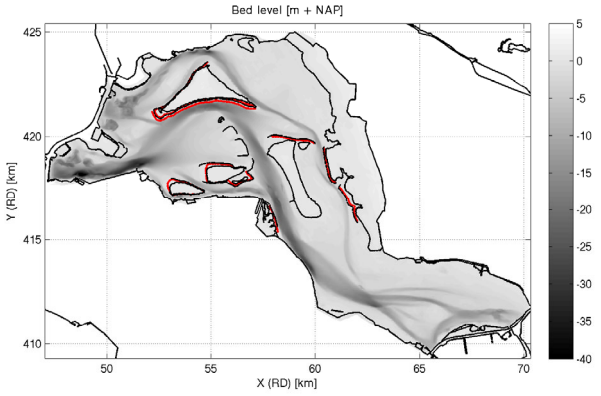

Figure 1. Bed level of Lake Grevelingen with the main protected banks (in red).

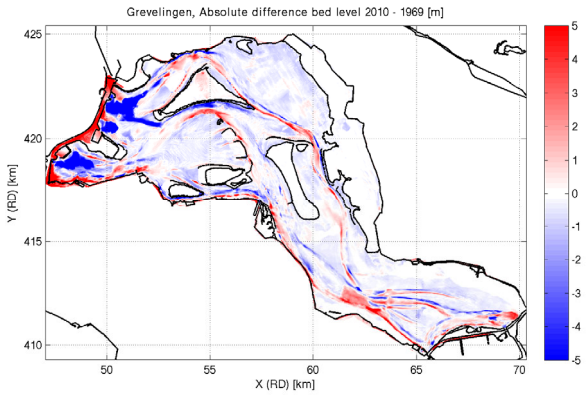

Figure 2. Bed level difference between 2010 and 1969 [m].

have also been considered [*Witteveen+Bos,* 2011].

It is important to determine the effects of reintroduction of the tide on the morphology of Lake Grevelingen and on the outer delta of Grevelingen estuary. Witteveen+Bos and Deltares have studied the morphological effects on sandbanks and channels in the outer delta and also on dispersion of mud and erosion of intertidal areas in Lake Grevelingen.

The effects of reintroducing the tide on erosion and the effectiveness of bank protection are analysed based on wave modelling and several morphological parameters in Lake Grevelingen. This purpose of this study is to describe this method to assess erosion risks in tidal basins. The results of this analysis are used as input for an environmental impact assessment [*Witteveen+Bos*, 2011].

METHODOLOGY

Morphology

Three morphological parameters are considered to determine the effect of waves on sedimentation and erosion patterns. These parameters indicate where erosion or sedimentation will change in the future:

1. the significant bed shear stress due to waves;
2. an intensity parameter of energy dissipation due to wave breaking;
3. an initial sediment stability parameter for waves.

Sediment can be stirred up and transported when near-bed velocities, caused by the oscillatory motion of waves, exceed the critical velocity for initiation of motion. The bed shear stress and the sediment stability parameter are directly derived from these near-bed velocities.

1. Significant bed shear stress

Here, the significant bed shear stress due to waves is the amplitude of the bed shear stress due to the orbital velocity amplitude directly above the boundary layer near the bed. These shear stress coefficients represent the influences of waves on the bed, with a shear stress increase occurring when water depths decreases or when the wave height increases. In deep water, the shear stress is very small since the orbital motion does not reach the bed. The significant shear stress (in [N/m²]) is defined as:

$$\tau_w = \frac{1}{2}\rho f_w u_b^2 \qquad (1)$$

In this formula, ρ is the density of water and f_w is the friction coefficient corresponding to an orbital velocity u_b. The maxima of the orbital velocity are equal to $u_b = \sqrt{2}\cdot U_{rms}$. U_{rms} is the root-mean-square value of the orbital velocity near the bed just outside the boundary layer [*Schiereck and Fontijn*, 1996]. The friction coefficient f_w may be determined by:

$$f_w = 0.00251\exp\left[5.21\cdot\left(\frac{A}{k_s}\right)^{-0.19}\right] \quad \text{for } \frac{A}{k_s} > 1.57$$

$$f_w = 0.3 \qquad \text{for } \frac{A}{k_s} \le 1.57 \qquad (2)$$

In these formulas, k_s is the Nikuradse roughness height. And A is the horizontal amplitude of the bed oscillation and according to:

$$A = \frac{u_b \cdot T_{m;bed}}{2\pi} \qquad (3)$$

In this formula, $T_{m;bed}$ is the mean wave period at the bed [*Soulsby et al.*, 1993].

2. Wave breaking parameter

The intensity parameter of energy dissipation due to wave breaking (in [m²/s]) shows where wave breaking and related wave energy dissipation will occur. This wave energy loss can produce a lot of turbulence which can stir up sediment. And the wave breaking induces a mean current through the associated radiation-stress gradients. This is why sediment transport is relatively high in the breaking zone.

The dissipation of energy due to wave breaking is defined as energy dissipation per unit of time due to wave breaking caused by decreasing water depth [*Delft University of Technology*, 2011].

3. Initial sediment stability parameter

The initial stability parameter shows where the bed material will be disturbed and sediment can move. Initiation of motion of sediment is defined as a dimensionless parameter S:

$$S = \frac{d_{50}}{d_{c;n50}} - 1 \qquad (4)$$

In this formula, d_{50} is the local median grain size of the bed (assumed to be 180 µm in Lake Grevelingen, based on [*Nieuwenhuize et al.*, 1995]) and $d_{c;n50}$ is the critical grain size diameter based on [*Schiereck and Fontijn*, 1996]:

$$d_{c;n50} = 2.15\frac{\hat{u}_b^{2.5}}{\sqrt{T_{m;bed}}(\Delta g)^{1.5}} \qquad (5)$$

In this formula, $\hat{u}_b$ is the maximum orbital velocity near the bed and $T_{m;bed}$ is the mean wave period near the bed. Negative values of S mean that sediment may be stirred up under the influence bed orbital velocities. Positive values of S indicate that the orbital velocities are relatively small and no initiation of motion will take place. This method is comparable with the theory of Shields for uniform flow [*Shields*, 1936] .

Numerical wave modelling with SWAN

Wave model set-up

The numerical spectral wave model SWAN [*Delft University of Technology*, 2011] is used to determine wave conditions in the tidal basin. SWAN is specially developed for application in environments with shallow water and reproduces wave processes like wind growth of the waves, depth-induced wave breaking and 'whitecapping', 'shoaling', refraction, wave transmission and wave reflection. SWAN is used to provide the relevant wave parameters needed to get insight in the (bank) erosion processes.

For the case Lake Grevelingen, a rectangular grid has been made with a resolution of 20 m (1225 by 805 grid points). The grid size is small enough to calculate the relevant processes near steep banks [*Van Vledder et al.*, 2008] and to include bank protections and foreshore defences.

Bathymetric records of Rijkswaterstaat are used for the wave model of Lake Grevelingen. Parts below NAP +0.1 m are measured recently (in 2008 and 2009). Bathymetric records of 1969 are used as a basis for bed levels above NAP +0.1 m, since at that time no high vegetation existed on the dry intertidal flats. More recent measurements do not give accurate information on the elevation of the intertidal flats because the data is not corrected for the presence of high vegetation.

Bank protections and foreshore defences are modelled separately (as obstacles) in SWAN and are not included in the bathymetry. The reason for this is, that these dams are small in relation to the grid size and reflection and transmission are modelled separately in SWAN. The foreshore dams are modelled with a height of NAP +0.0 m, a crest width of 4.0 m and a slope of 18.0 degrees. This results in a reflection coefficient of 0.3. Transmission has been modelled with the formulation of d'Angremond and Van der Meer [*d'Angremond et al.*, 1996].

The SWAN simulations are performed with the same physical and numerical settings as used for the Strength and Loading of Flood Defences Programme (SBW), as well as for the normative set of tools for the national assessment of flood defences (WTI) in The Netherlands.

Boundary conditions

To determine the change in wave conditions in Lake

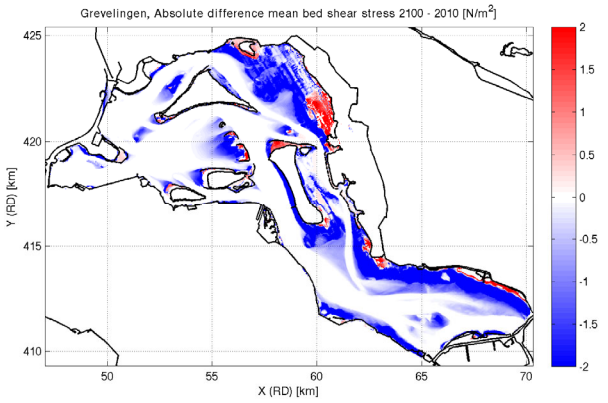

Figure 3. Difference in significant bed shear stress (2100 - 2010), daily conditions.

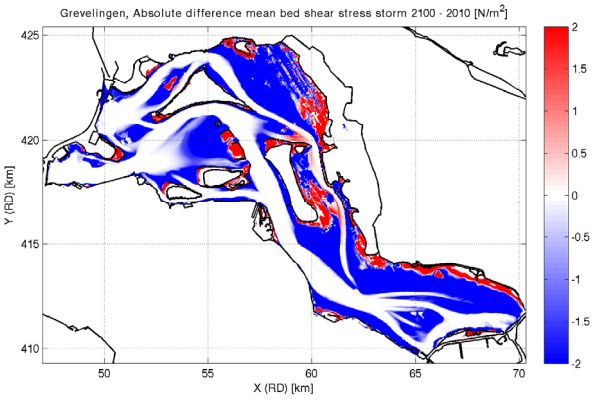

Figure 4. Difference in significant bed shear stress (2100 - 2010), storm conditions.

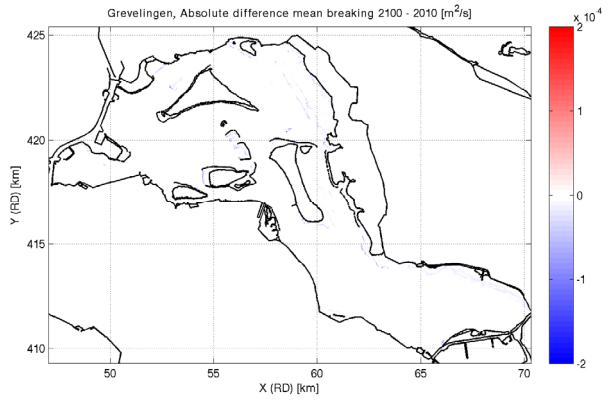

Figure 5. Difference in mean wave breaking (2100 - 2010), daily conditions.

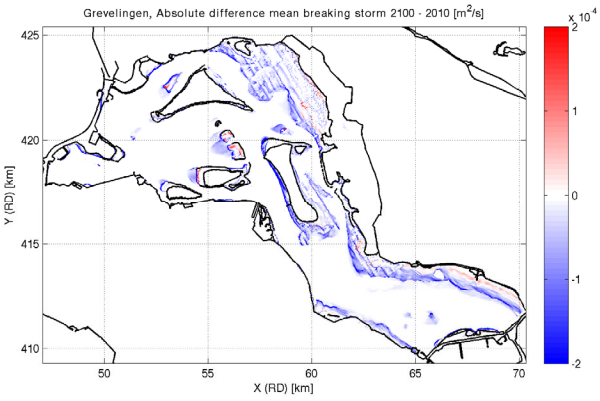

Figure 6. Difference in mean wave breaking (2100 - 2010), storm conditions.

Grevelingen, a set of stationary SWAN computations has been carried out. The individual simulations are made for a set of conditions each with a uniform water level, a uniform wind speed and a uniform wind direction.

The stagnant water level in the present situation is NAP -0.2 m. Mean conditions are used such that the future situation can be compared with the present situation. The future mean conditions are composed of a combination of three water levels, i.e. the sum of: ¼ of the low water level, ¼ of the high water level and ½ of the mean water level. The mean water level in Lake Grevelingen in 2100 is assumed to be NAP +0.75 m, the high water level NAP +1.0 m and the low water level NAP +0.5 m.

The wind speeds are based on wind statistics of KNMI measurement station Lichteiland Goeree for a period of 30 years (1981-2010). The wave conditions are determined for two different wind speeds: one which is not exceeded 50 % of the time (average daily conditions) and another for wind speeds that will not be exceeded 99 % of the time (yearly maximum storm conditions). These input conditions are summarized in Table 1.

Table 1: Applied wind directions and wind speeds.

wind direction (°N)	avg. wind speed (m/s)	99 % wind speed (m/s)	frequency of occurrence (%)
30	7.7	15.8	8.2 %
60	7.2	15.9	7.0 %
90	6.6	14.4	6.1 %
120	6.6	14.0	5.3 %
150	6.6	14.1	5.3 %
180	8.0	17.3	8.3 %
210	9.8	18.7	12.9 %
240	10.0	19.4	15.9 %
270	8.9	19.6	9.8 %
300	8.4	19.5	7.4 %
330	7.9	18.4	6.5 %
360	6.7	16.5	7.3 %

RESULTS

For Lake Grevelingen the situation in 2100 (with tide and with a mean water level of NAP +0.75 m) is computed and compared with the present situation (stagnant water level) by interpolating the stationary SWAN results over all wind directions.

1. Significant bed shear stress

The differences in significant bed shear stress in Lake Grevelingen between the situation in 2100 and the present situation are shown in Figure 3 and Figure 4. It appears that the orbital velocity and therefore the bed shear stresses will decrease (due to the higher water level).

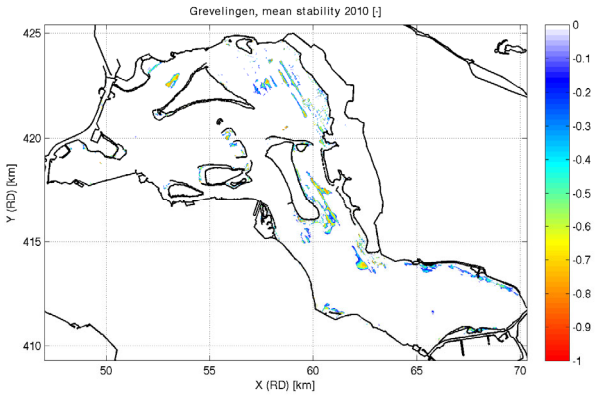

Figure 7. Mean stability of sediment in 2010, daily conditions.

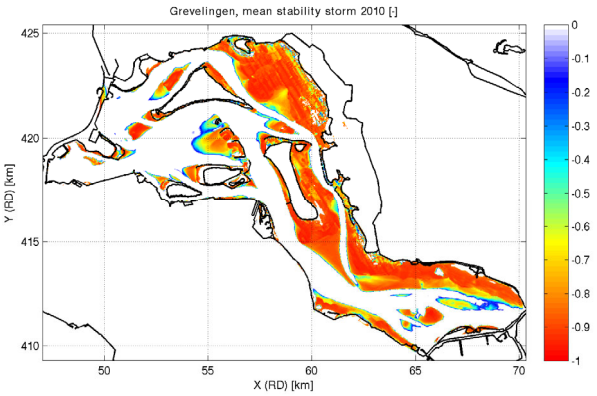

Figure 8. Mean stability of sediment in 2010, storm conditions.

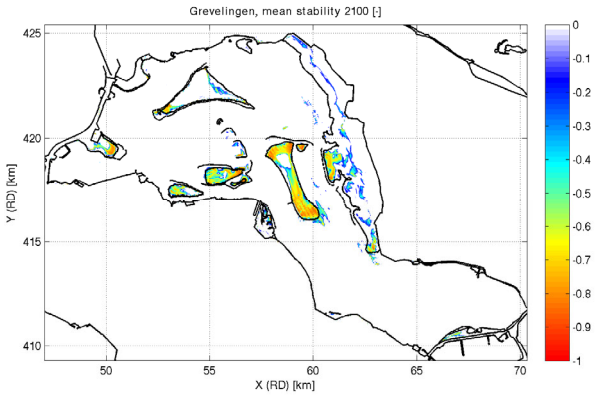

Figure 9. Mean stability of sediment in 2100, daily conditions.

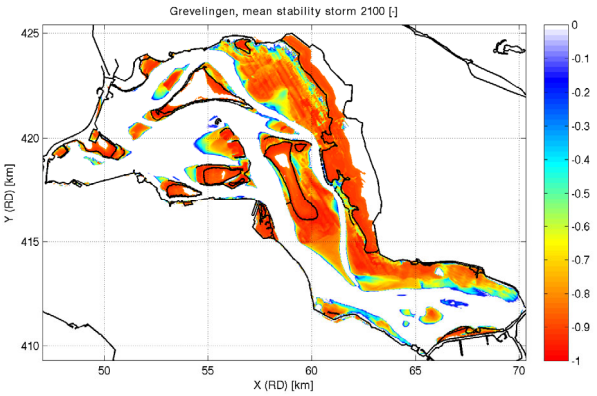

Figure 10. Mean stability of sediment in 2100, storm conditions.

Table 2: Change of parameters in 2100 behind foreshore dams relative to the reference year 2010.

	avg. wind	storm
rel. difference significant wave height	+107 %	+97 %
rel. difference bed shear stress	-33 %	-32 %

In shallow areas of the Grevelingen, the increase of the water level has a much larger influence on the bed shear stress than the increase in wave height. Only in very shallow areas (less than some decimetres), the bed shear stress will increase. This occurs under daily conditions during storm conditions.

Behind the foreshore dams, the wave heights increase and the bed shear stresses decrease in future situations (Table 2).

2. Wave breaking parameter

Wave breaking will decrease near the channel bank zones (Figure 5 and Figure 6). Therefore, less energy becomes available for sediment transport. A small increase of wave breaking will occur in higher parts in Lake Grevelingen in 2100. Wave breaking will move to higher located parts of Lake Grevelingen.

3. Initial sediment stability parameter

Figures 7, 8, 9 and 10 show the initial stability of sediment in the present situation and in 2100. A negative value means that sediment can start to move. Locations with positive values (stable) are indicated with a white colour.

Based on initial stability of sediment, it can be concluded that all low-lying areas will become more stable in the future, but that some higher parts may start eroding. The future higher water levels will cause drowning of parts of the tidal flats. And erosion may take place at these locations in future.

DISCUSSION

The combination of wave modelling and post-processing is a good method to quickly assess the risks of erosion of channel banks and tidal flats, in tidal basins. It is a simple analysis relative to full morphodynamic modelling, because of the dedicated combination of a small number of stationary simulations. This type of analysis shall off-course not be a replacement for monitoring programs. However, it can be used to get insight in the – spatial and temporal – patterns in the occurring physical processes.

Bed shear stress is a useful indicator of the influence of waves on the bed. However, an increase in bed shear stress does not necessarily mean that sediment transport will occur. Since the bed shear may be too low to initiate sediment motion.

The wave breaking parameter shows where wave breaking will occur and where waves will dissipate energy. This energy can cause sediment transport. However, wave breaking will not directly give insight in the risks of (bank / tidal flat) erosion either.

An efficient way to assess bank erosion in tidal basins is by means of the initial sediment stability parameter, because it includes both hydraulic loads on a bank and the strength of the bank. This has been presented for the case of reintroducing a tide in Lake Grevelingen.

The initial sediment stability parameter will not give the magnitude of sediment transport or the amount of erosion. However, this parameter can indicate at which locations erosion may occur in future.

Predicting bank erosion through evaluation of the initial sediment stability parameter is a conservative approach, because it is assumed that erosion may occur where grain stability is low.

ACKNOWLEDGEMENT

The presented work is part of a study commissioned by both Natuur- en Recreatieschap De Grevelingen and Rijkswaterstaat Zeeland, The Netherlands. The valuable contributions of Romke Bijker (ACRB) and Z.B. Wang (Deltares) are greatly appreciated.

REFERENCES

D'Angremond, K., J.W. van der Meer and R.J. de Jong (1996), Wave transmission at low-crested structures, ASCE Proc. ICCE, 1996.

Delft University of Technology (2011), SWAN scientific and technical documentation SWAN cycle III version 4.85, Delft.

Deltares (2010), Morfologische effecten getijdencentrale in de Brouwersdam. accompanied by 'MIRT Verkenning Grevelingen', draft version.

Deltares (2011), Delft3D-Flow user manual Hydro-Morphodynamics, Delft.

Kleinhans, M.G., W.M. van Dijk, W.I. van de Lageweg, R. Hoendervoogt, H. Markies and F. Schuurman (2010), From nature to lab: scaling self-formed meandering and braided rivers. River Flow 2010.

Nieuwenhuize, J., P.M.J. Herman en R.H.D. Lambeck (1995), De bodemsamenstelling van 36 meetpunten in het Grevelingenmeer in 1995 en een analyse van lange-termijnontwikkelingen (1967-1995).

Rijkswaterstaat Zeeland (2010), Invloed getij op oevers Grevelingen Meer.

Schiereck, G.J. and H.L. Fontijn (1996), Pipeline protection in the surf zone, 25th ICCE, Orlando, ASCE, New York.

Shields, A. (1936), Anwendung der Ähnlichkeitsmechanik und der Turbulenz Forschung auf die Geschiebebewegung Mitt. der Preuss. Versuchsamt. für Wasserbau un Schiffbau, Heft 26, Berlin, Deutschland.

Soulsby, R.L., L. Hamm, G. Klopman, D. Myrhaug, R.R. Simons, and G.P. Thomas (1993), Wave-current interaction within and outside the bottom boundary layer, Coastal Engineering, 21 (1993), 41 - 69, Amsterdam.

Thoma, D.P., S.C. Gupta, M.E. Bauer and C.E. Kirchoff (2005), Airborne laser scanning for riverbank erosion assessment. Remote Sensing of Environment 95 (2005) 493 - 501, doi:10.1016/j.rse.2005.01.012.

Thorne, C.R. (1981), Fields measurements of rates of bank erosion and bank material strength. Proc. of the Florence Symposium, June 1981, IAHS publ. no. 133.

Van Vledder, G. Ph., J. Groeneweg, A. van der Westhuysen (2008), Numerical and physical aspects of wave modelling in a tidal inlet, Coastal Engineering 2008, 424 - 436.

Witteveen+Bos (2011), MIRT-verkenning Grevelingen - milieueffectrapport, in cooperation with 'Natuur en Recreatieschap De Grevelingen'.

DOI: 10.3990/2.184

Ebb-tidal delta morphology in response to a storm surge barrier

M. Eelkema[1], Z.B. Wang[2], and A. Hibma[3]
[1] Hydraulic Engineering, Delft University of Technology, P.O. Box 5048, 2600 GA, Delft, The Netherlands, m.eelkema@tudelft.nl
[2]Deltares, P.O. Box 177, 2600 MH, Delft, The Netherlands
[3]Ecoshape Building With Nature, Burgemeester de Raadtsingel 69, 3311 JG, Dordrecht, The Netherlands

ABSTRACT

The Eastern Scheldt ebb-tidal delta morphology has been adapting for the past 25 years in response to the construction of the Eastern Scheldt storm-surge barrier in 1986. As a result of the barrier, there has been a decrease in tidal amplitudes, volumes, and average flow velocities, and there is hardly any sediment exchange through the barrier. Bathymetrical measurements of the ebb-tidal delta show multiple effects: (1) an overall decrease in sediment volume, (2) a decrease in morphological activity, (3) sedimentation in most channels, (4) northward reorientation of channels and shoals, and (5) an increase in wave-driven features. Some channels are showing stronger erosion since 1986. This, and the reorientation of other channels could be related to changes in the interaction between cross-shore and alongshore tide. Most of the erosion is located in shallower, wave-dominated regions, indicating that waves have become relatively stronger. The steady erosive trend, combined with the decline of morphological activity, points toward a system dominated by relatively small and mostly negative bed-level changes. This system is still far from any kind of equilibrium, and is steadfastly adapting itself to the new hydraulic forcing regime, even though sediment transport capacities have decreased.

INTRODUCTION

The Eastern Scheldt tidal inlet (Figure 1), located in the south-western part of the Netherlands, has experienced large changes in hydrodynamics and morphology in response to the construction of several dams in its basin (constructed between 1965 and 1970) and a storm surge barrier in the inlet (constructed between 1983 and 1986). This storm surge barrier is open under normal weather conditions, allowing the tide to pass through the inlet, but closes during storm surges. However, even though it was designed as an open barrier, it still has a strong effect on the tidal hydrodynamics, and through that, the morphology of the ebb-tidal delta.

As a result of the storm surge barrier, the average tidal flows inside and outside the basin have decreased (Vroon, 1994). The sediment budget of the Eastern Scheldt basin indicates that ever since the barrier has been in place, the basin has received virtually no sediment from outside. Apparently, the storm surge barrier is acting as a blockage for sediment transport.

This combination of effects has created a unique situation on the seaward side of the barrier: The ebb-tidal delta has experienced decreased tidal flow coming out of the inlet, but exchanges virtually no sediment with its basin. The morphological activity declined, and the sediment volume has decreased. However, it is yet unclear on what time scale the ebb-tidal delta is adapting, nor where the eroded sediment is transported to (Aarninkhof and Van Kessel, 1999; Cleveringa, 2008). The response of the ebb-tidal delta is an important factor in coastal maintenance policy, as we know from looking at other tidal inlets under the influence of human intervention (e.g. Van de Kreeke, 2006; Elias, 2006). Also, knowledge on the behavior of channels on the ebb-tidal delta can be valuable, because some of those channels are positioned very close to the coastline. A shift in the position of those channels might lead to increased coastal erosion.

The goal of this study is to gain understanding of the

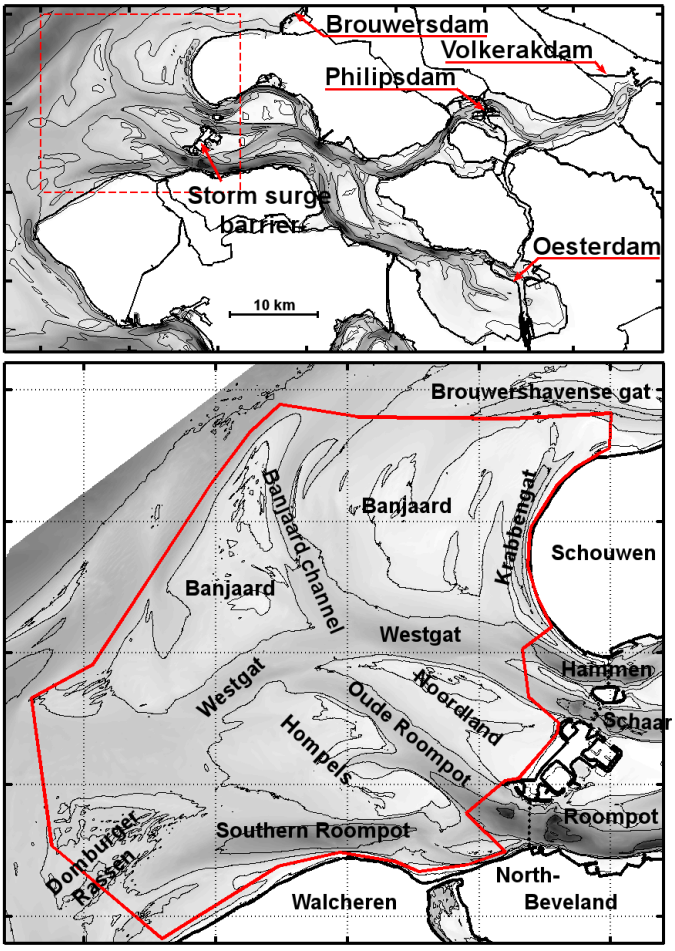

Figure 1. Overview of the Eastern Scheldt inlet. The red polygon in the lower figure indicates the area for which the activity and sediment volume in figures 4 and 5 are calculated.

behavior

of an ebb-tidal delta in response to the construction of a storm surge barrier by studying the Eastern Scheldt Inlet. In this paper we describe the observed morphological development of the Eastern Scheldt's ebb-tidal delta for the period between 1986 and 2008, i.e. the period after completion of the barrier.

STUDY AREA

Eastern Scheldt Inlet

The Eastern Scheldt (Figure 1) is an elongated tidal basin of approximately 50 km in length and a surface area of 350 km^2. Before 1965 A.D., this basin was also connected to two more tidal basins to the north through several narrow, yet deep channels. These connections were closed off with dams in the nineteen sixties as part of the so-called 'Deltaplan', designed mainly to improve safety against flooding. The inlet is located between two (former) islands called Schouwen and North Beveland, and consists of three main channels, separated by shoals. Seaward of the inlet the mean tidal range is 2.9 meters. The total tidal prism passing through this inlet before barrier construction was on average 1250 Mm^3 per tide (de Bok, 2001).

The long-term mean significant wave height measured 20 km offshore from Eastern Scheldt Inlet is 1.1 m, and waves higher than 4 m occur less than 0.2% of the time. The directional distribution shows two distinct wave directions, one from west southwest, and one from north northwest. Both directions are more or less equal in strength.

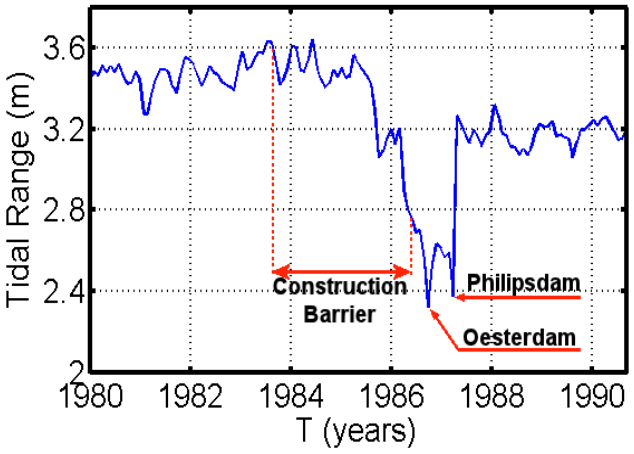

Figure 2. Tidal range measured in the centre part of the basin between 1980 and 1990 (adapted from Mulder and Louters (1994)).

Human Interventions

Between 1983 and 1986 a storm surge barrier was built in the

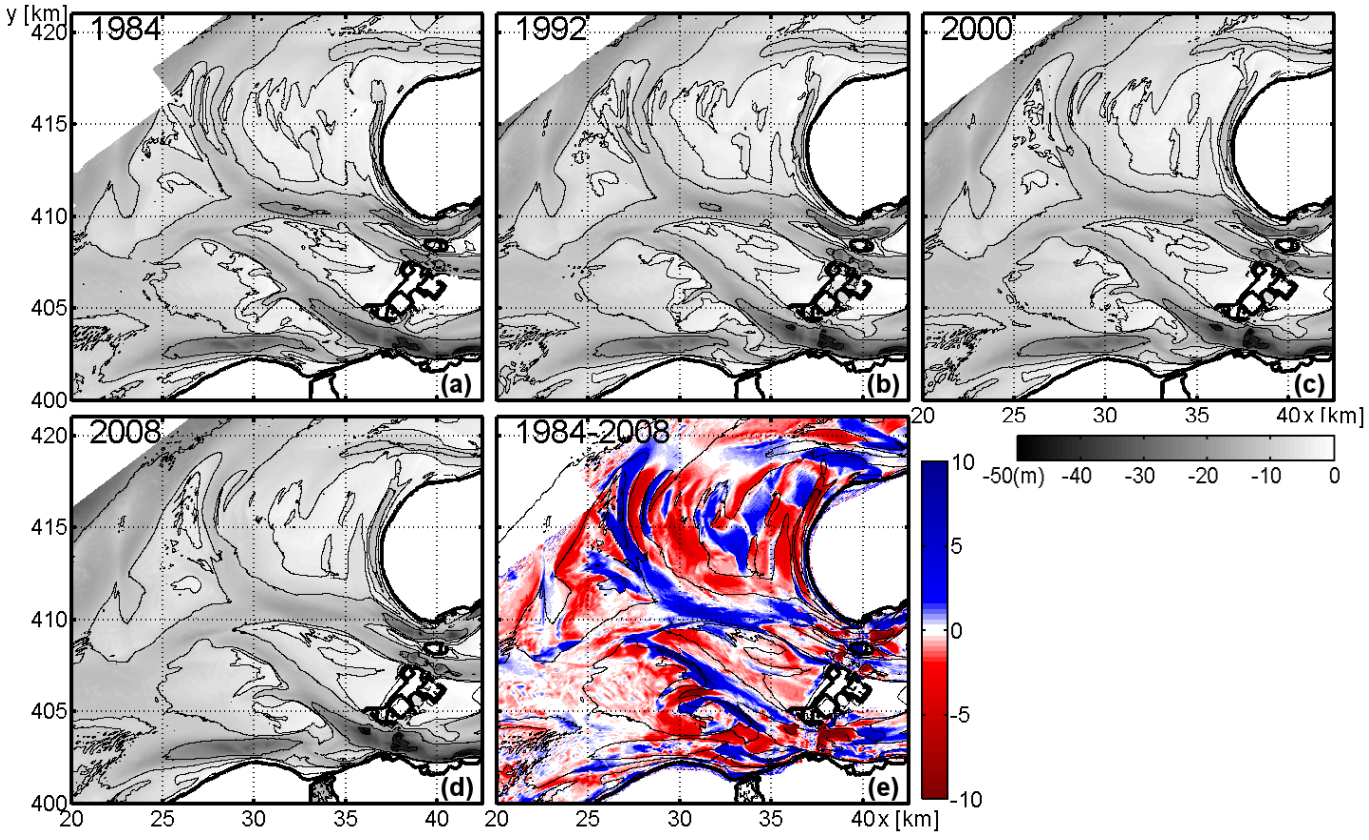

Figure 3. Bathymetry of the ebb-tidal delta between 1984 and 2008. (a through d) Bathymetry measured between 1984 and 2008. (e) Difference in bed level between 1984 and 2008 (red=erosion). Depths and differences are in m.

inlet channels in order to close off the inlet during storms while retaining the tide inside the basin during normal conditions. This barrier decreased the inlet's cross-section from 80.000 m^2 to 17900 m^2 (Vroon, 1994). Simultaneously with the barrier's construction, also two more dams (the Philipsdam and Oesterdam) were built near the landward end of the Eastern Scheldt basin (Figure 1). These dams were constructed in order to restrict the decrease of the tidal range by limiting the basin length and thereby increasing the reflection and amplification of the tidal wave. As a result of these dams, the total reduction in tidal range was limited to roughly 10% (Figure 2). The tidal prism was reduced to approximately 900 Mm^3 (de Bok, 2001).

MORPHOLOGICAL DEVELOPMENTS

Overall morphology

From the bathymetrical development of the ebb-tidal delta, measured every 4 years since 1960 (De Kruif, 2001), a view emerges of an ebb-tidal delta that is adapting itself to the presence of the storm surge barrier (Figure 3). Due to the drop in current velocities the magnitudes of the sediment transports must have decreased also. This decrease in transport is likely to be stronger than the decrease in flow, because of the non-linear relation between flow and transport. Most of the channels are no longer scouring, and some are becoming shallower. On the shoals, there is an increase in landward migrating saw-tooth bars, and most shoals are eroding and pushed northward (Figure 3e). Also, the seaward front of the ebb-tidal delta is eroding.

The construction of the storm surge barrier has caused a small clockwise reorientation of the main channels on the ebb-tidal delta, effectively caused by sedimentation on the southern sides and erosion on the northern sides of these channels. The growth of the Westgat and Roompot channels in seaward direction has stopped, and both channels are sedimentating in the areas seaward of the scour holes near the barrier. This trend is not seen everywhere on the ebb-tidal delta. Krabbengat and Banjaard Channels are still lengthening in northern direction. Krabbengat channel has also become deeper.

The reorientation of the channels and shoals could be related to the interaction between the alongshore tidal current and the tidal current coming out of the inlet (Aarninkhof and Van Kessel, 1999). According to Sha and Van den Berg (1993), the orientation and protrusion of ebb-tidal deltas are related to the relative phases and strengths of alongshore currents and currents coming out of the inlet. Because the current flowing in and out of the Eastern Scheldt has decreased in strength, the alongshore current going from southwest to northeast should have become relatively stronger on the ebb-tidal delta. This could explain the clockwise reorientation of most channels and shoals.

Morphological activity

The overall decrease in morphodynamics is clearly visible when it is quantified by computing a Morphological Activity Index (MAI), as used by Zimmermann (2009). This index is defined as the mean of the absolute bed-level changes calculated from the bathymetrical data of the ebb-tidal delta from 1960 to 2008 (Figure 4). The MAI is calculated according to:

$$MAI(t)=\frac{\sum_{i=1}^{n}\left|z_{year2}(x_i,y_i)-z_{year1}(x_i,y_i)\right|}{N(year_2-year_1)} \quad (1)$$

in which $t=(year_1+year_2)/2$, and $z_{year1}(x_i,y_i)$ and $z_{year2}(x_i,y_i)$ are the bottom depths with coordinates x_i and y_i measured in $year_1$ and $year_2$, respectively. N is the total number of locations where bottom depths are compared. The area for which the activity is calculated is shown as the red polygon in Figure 1.

In Figure 4 the MAI is shown along with the periods when the Volkerak Dam and the storm surge barrier were constructed. Apparently, between 1960 and 1984 the morphological activity was already quite high as compared to the post-1986 period, indicating that the ebb-tidal delta was still undergoing large changes in response to previous developments inside the basin. This activity increased in response to the implementation of the Volkerakdam and Brouwersdam in 1970, and remained more or less stable during the seventies and early eighties. This activity is mostly due to the increased flow coming from the basin. There was also a supply of sediment coming from the basin, but this supply decreased significantly during the seventies, while the morphological activity persisted (Van den Berg, 1986; Eelkema *et al*., 2011).

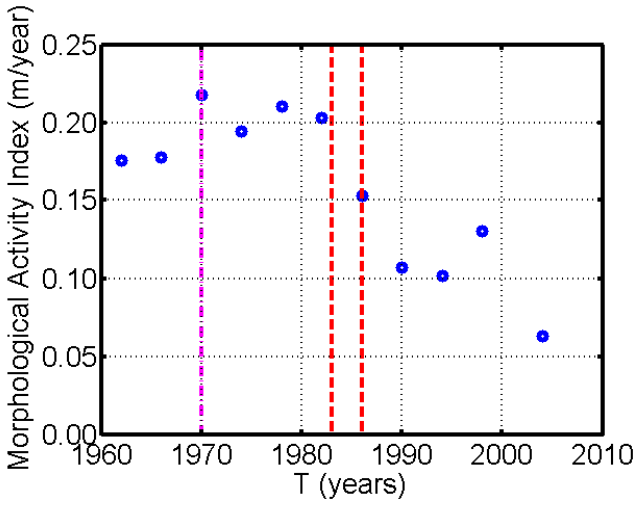

Figure 4. Morphological activity index. The vertical lines indicate the construction of the Volkerak Dam (1970) and the storm surge barrier (1983-1986). The calculation area is shown in Figure 1.

Figure 4 also shows the effect of the storm surge barrier. After the completion in 1986, the activity decreased sharply and continued to decrease even further after 2000. This indicates that the new situation on the ebb-tidal delta is such that there are hardly any large-scale or high amplitude bed-level changes occurring, and the area is characterized by a slow but continuous development towards a new state. The decline in activity is probably caused by the general decrease in flow velocity over the area. Because of the non-linear relation between flow velocity and transport, the morphodynamics are diminished much more relative to the hydrodynamics.

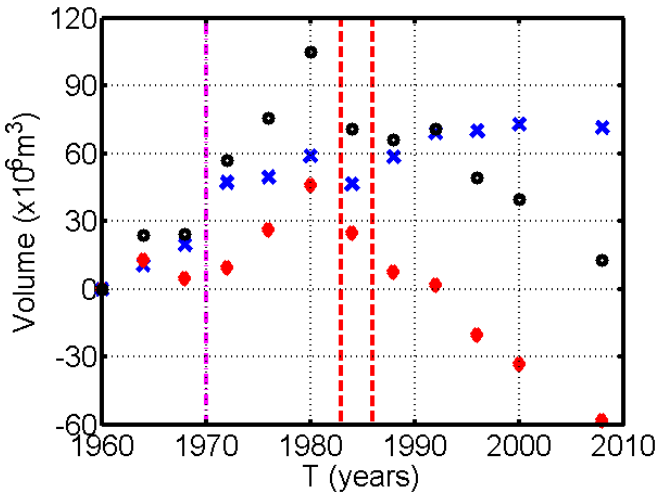

Figure 5. Cumulative sediment volumes relative to 1960. Blue crosses: cumulative sediment volume below -10 m depth. Red diamonds: cumulative sediment volume above -10 m depth. Black circles: total cumulative sediment volume. The vertical lines indicate the construction of the Volkerak Dam (1970) and the storm-surge barrier (1983-1986). The calculation area is shown in Figure 1.

Hypsometric & volumetric evolution

The effect of the barrier is also observable in the evolution of the hypsometry (red and blue symbols in Figure 5). Since 1986, the sediment volume of the ebb-tidal delta above -10 m below mean sea level has continuously decreased, signifying erosion of the shallow parts. The sediment volume below -10 m has increased since 1986, indicating sedimentation in the deeper parts. The erosion on the shallow parts of the ebb-tidal delta does not seem to have slowed since 1986, while on the other hand the volumes of the deeper parts do seem to have reached some sort of stable value. This figure also shows that the sediment volumes lost in the shallow parts are much larger than the volumes gained in the deeper parts, so the ebb-tidal delta as a whole is losing sediment. The erosion of the shallow parts is probably because the shoals are not supplied with sediment by the tide anymore, and waves have started to erode them.

Figure 5 also shows the total cumulative sediment volume relative to 1960 (black circles) of the area inside the polygon shown in Figure 1. Similar to Figure 4, the closure of the Volkerak and the construction of the storm surge barrier mark changes in the trend of the sediment volume. From 1970 onward (closure of the Volkerak channel) the volume grew at a rate of roughly 2 to 3 Mm^3 per year. After the barrier was constructed, the trend changed into an eroding trend with a rate comparable to the rate of growth which existed before 1986. Between 1986 and 2008 the ebb-tidal delta has lost anywhere between 30 and 60 Mm^3 of sediment. This is consistent with the idea of an ebb-tidal delta sediment volume far out of equilibrium with its tidal forcing. A precise value for the loss is difficult to determine due to inaccuracies in the data (Cleveringa, 2008).

However, this strong rate of erosion seems counter-intuitive, as Figure 4 also shows that the morphological activity is much lower, and the basin is not receiving any of this sediment loss. One way to make the observed behaviors of the morphological activity and the sediment volume consistent with each other, is to say that although since 1986 the bed-changes are relatively small, most of them are negative, meaning that erosion is more prevalent than it was before.

It is not exactly clear where the eroded sediment ended up (Cleveringa, 2008). The sedimentation in the channels is too small, and the Eastern Scheldt basin has received virtually no sediment since the barrier has been in place. The dunes adjacent to Eastern Scheldt inlet have not grown significantly since 1986. It is also unlikely that the sediment has been transported seaward, as there is no process present which could plausibly transport these amounts of sediment per year. The most plausible location for the eroded sediment are the abandoned channels of the Grevelingen ebb-tidal delta, which has been filling up with sediment since the closure of Grevelingen inlet. However, the deposition in this area could also come from the eroding shoreface of the Grevelingen ebb-tidal delta, and the entire Grevelingen area show net erosion since 1986.

CONCLUSIONS

From morphological observations of the Eastern Scheldt inlet a view emerges of an ebb-tidal delta which is still far from any kind of equilibrium, and which is steadfastly adapting itself to the new hydraulic forcing regime, even though sediment transport capacities have decreased. The initial response of the ebb-tidal delta is characterized by a reorientation of the channels and a redistribution of sediment from the shallow parts towards deeper areas (Figure 6). The reorientation is most likely related to the changes in cross-shore and alongshore tidal currents. The redistribution is most likely an effect of the waves reworking the shoals coupled to the weakening of the tidal currents and associated sediment supply.

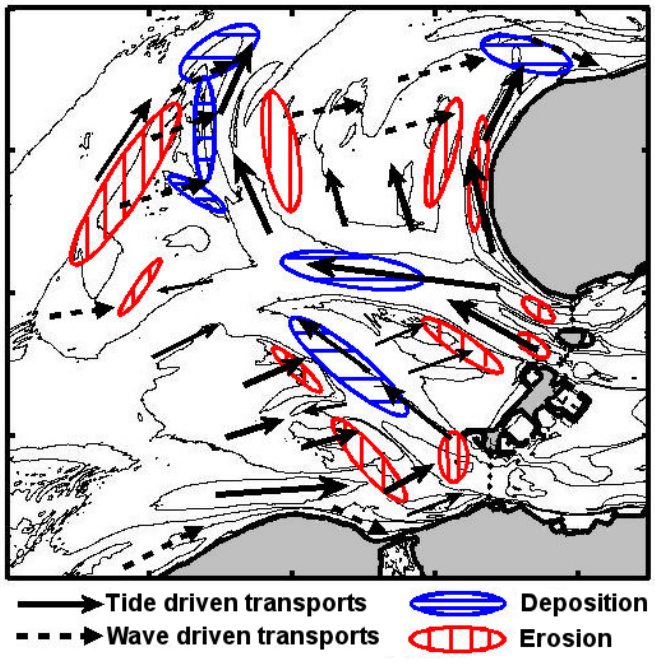

Figure 6. Schematic overview of the main erosion and deposition areas on the ebb-tidal delta.

However, some questions still remain. As mentioned, it is not clear where the eroded sediment ends up. Also, the proposed hypothesis behind the reorientation of the channels related to the alongshore tide remains to be tested. These questions are the subject of ongoing research.

ACKNOWLEDGEMENTS

This study is part of the innovation program Building with Nature. Funding for this particular study was also provided by the Dr. Ir. Cornelis Lely Foundation.

REFERENCES

Aarninkhof, S.G.J., and van Kessel, T., 1999. Data analyse Voordelta: Grootschalige morfologische veranderingen 1960-1996 (Data analysis Outer Delta: Large-scale morphological changes 1960-1996). Delft, the Netherlands: WL|Delft Hydraulics, 33p.

Cleveringa, J., 2008. Morphodynamics of the Delta Coast (south-west Netherlands): Quantitative analysis and phenomenology of the morphological evolution 1964-2004. Alcyon, report number A1881R1r2, 61p.

De Bok, C., 2001. Long-term morphology of the Eastern Scheldt. Rijkswaterstaat, RIKZ, report number RIKZ/2002.108x, 107p.

De Kruif, A.C., 2001. Bodemdieptegegevens van het Nederlandse Kustsysteem (Bed-level data of the Dutch Coastal System). Rijkswaterstaat, RIKZ, report number RIKZ/2001.041, 114p.

Eelkema, M; Wang, Z.B., and Stive, M.J.F., 2012. Impact of back-barrier dams to the development of the ebb-tidal delta of the Eastern Scheldt. *Journal of Coastal Research*, accepted for publication.

Elias, E.P.L., 2006. Morphodynamics of Texel Inlet. IOS Press, Amsterdam, . Ph.D. thesis, 260p.

Mulder, J.P.M., and Louters, T., 1994. Changes in basin geomorphology after implementation of the Oosterschelde estuary project. *Hydrobiologia*, 282/283, 29-39.

Sha, L.P., and Van den Berg, J.H., 1993. Variation in ebb-tidal delta geometry along the coast of the Netherlands and the German Bight. *Journal of Coastal Research*. 9(3), 730-746.

Van den Berg, J.H., 1986. Aspects of sediment- and morphodynamics of subtidal deposits of the Oosterschelde (the Netherlands). Rijkswaterstaat, The Hague, 127p.

Van de Kreeke, J, 2006. An aggregate model for the adaptation of the morphology and sand bypassing after basin reduction of the Frisian Inlet. *Coastal Engineering*, 53, 255-263.

Vroon, J., 1994. Hydrodynamic characteristics of the Oosterschelde in recent decades. *Hydrobiologia,* 282/283, 17-27.

Zimmermann, N., 2009. Stability of morphological cells to dredging-dumping activities. M.Sc.-thesis, Delft University of Technology, The Netherlands.

NCK photo competition

Erik Horstman: Cucumber and anemone in a coastal habitat, Check Jawa, Singapore

DOI: 10.3990/2.185

Vortex tubes in the wave bottom boundary layer

M. Henriquez[1], A.J.H.M. Reniers[2], B.G. Ruessink[3] and M.J.F. Stive[4]

[1]Hydraulic Engineering, Delft University of Technology, P.O. Box 5048, 2600 GA, Delft, The Netherlands, m.henriquez@tudelft.nl

[2]Rosenstiel School of Marine and Atmospheric Science, University of Miami, 4600 Rickenbacker Causeway, Miami, FL 33149, USA

[3]Physical Geography, Utrecht University, Heidelberglaan 2, 3584 CS, Utrecht, The Netherlands

[4]Hydraulic Engineering, Delft University of Technology, P.O. Box 5048, 2600 GA, Delft, The Netherlands

ABSTRACT

The cause of sediment suspension events during flow reversal under waves in the nearshore is not well understood. Vortex tubes and horizontal pressure gradients have been suggested to be the cause of the suspension events. A medium sized wave flume experiment has been conducted to give insight in the hydrodynamics of the wave bottom boundary layer over a fixed single-barred profile. Flow measurements were made with PIV and the swirling strength of the velocity fields were analyzed. Around flow reversal vortex tubes were identified. The vortex tubes had similar size and swirling strength as vortices generated by vortex shedding over a rippled bed. Therefore, vortex tubes under waves in the nearshore could explain the sediment suspension events around flow reversal.

INTRODUCTION

The wave bottom boundary layer exists due to friction between the orbital fluid motion and the bottom. The relatively thin layer plays an important role in the sediment transport by waves in the nearshore. In the layer, sediment is mobilized and transported in various ways, for instance, as sheet flow. There are also observations of sudden suspension events around the reversal of the flow as described in *Madsen* [1974], "just prior to the passage of the crest of a near-breaking wave the bottom seemed to explode". Often pressure gradients are suggested to cause bed failure around flow reversal (see for example *Madsen*, [1974]; *Drake and Calantoni*, [2001]; *Hoefel and Elgar*, [2003]; *Zala Flores and Sleath*, [1998]). Although pressure gradients provide additional forces on sediment particles to aid mobility it does not explain the suspension event (it would rather explain liquefaction of the bed). *Foster et al.* [1994] suggested that the coherent structures, such as vortex tubes [*Carstensen et al.* 2010], are generated in the wave bottom boundary layer under surface waves in the nearshore and could be responsible for sediment suspension events. Vortex tubes are instabilities generated at an inflectional-point of an oscillatory boundary layer. They were observed in the bottom boundary layer of oscillating flow tunnels at flow reversal (see for example *Akhavan et al*. [1991] and *Carstensen et al.* [2010]). *Cartensen et al.* [2010] conducted experiments in an oscillating flow tunnel with a smooth fixed bed and concluded that the impact of the vortex tubes on the bottom shear stress is insignificant. Still, vortex tubes provide a mechanism for the advection of sediment during flow reversal. If, indeed, vortex tubes generate suspension events around flow reversal, the contribution of horizontal pressure gradients to the force balance on sediment particles in the nearshore remains unclear.

Recently, vortex tubes were detected in a wave flume experiment with a fixed bed. The relation between vortex tubes and suspension events is researched by measuring the swirling strength and size of the vortex tubes.

EXPERIMENT

The flume has a length of 40 m, a width of 0.8 m and a water depth of 0.5 m. In the flume a rigid single bar profile was build. The top of the bar is approximately 0.15 m below the mean water level. Granular sediment with a grain size of 0.54 mm was glued to the surface to provide bottom roughness. The hydrodynamic model scale was 1:10 which corresponds to a medium sized wave flume experiment.

The vertical and horizontal flow velocities within the wave bottom boundary layer were measured with Particle Image Velocimetry (PIV) at several locations along the flume [*Henriquez et al*. 2010]. For this study, we limit ourselves to one location just before the bar crest (taken that the wave maker is the origin) and one wave condition. At this location, the water depth was 0.154 m, the root-mean-square wave height was 0.087 m and the wave period of the regular waves was 1.8 s. The wave field consisted of 120 waves. PIV measurements were conducted at a rate of 15 Hz resulting in 27 different phases in one wave cycle.

The laser sheet for PIV was inserted into the water from the water surface using a streamlined window. The camera was placed outside of the flume (flume wall is transparent). The camera had a field of view of approximately 10x10 mm^2. The camera images were processed resulting in a velocity vector for every 0.37x0.37 mm^2. The flow velocity vector is decomposed into a horizontal component u, positive in wave direction, and a vertical component w, positive upwards.

Figure 1 shows the phase-average horizontal velocity $\hat{u}$ at the upper boundary of the velocity vector field which is approximately in the free-stream (outside the wave bottom boundary layer). The shape of the horizontal velocity is skewed and asymmetric indicating that the waves were shoaling.

SWIRLING STRENGTH

Vortices in a shear flow can be identified and quantified with the eigenvalues of the velocity gradient tensor [*Adrian et al.* 2000]. PIV measurements are usually two-dimensional, e.g. in the *xz*-plane, resulting in the velocity gradient tensor:

$$\mathbf{D} = \begin{pmatrix} \frac{\partial u}{\partial x} & \frac{\partial u}{\partial z} \\ \frac{\partial w}{\partial x} & \frac{\partial w}{\partial z} \end{pmatrix}.$$

The characteristic equation of **D** is then

$$\lambda^2 + P\lambda + Q,$$

where P = -tr(**D**) and Q = det(**D**). When written out, P becomes

$$P = -\left(\frac{\partial u}{\partial x} + \frac{\partial w}{\partial z}\right),$$

and Q becomes

$$Q = \frac{\partial u}{\partial x}\frac{\partial w}{\partial z} - \frac{\partial u}{\partial z}\frac{\partial w}{\partial x}.$$

The solutions of the characteristic equation are the eigenvalues of the matrix **D**. Whether the eigenvalues are complex or real can be determined with the discriminant $\Delta = P^2 - 4Q$ and when written out becomes

$$\Delta = \frac{\partial u}{\partial x}^2 + \frac{\partial w}{\partial z}^2 - 2\frac{\partial u}{\partial x}\frac{\partial w}{\partial z} + 4\frac{\partial u}{\partial z}\frac{\partial w}{\partial x}.$$

Now, complex eigenvalues of the velocity gradient tensor indicate the presence of a vortex. Thus, a negative discriminant ($\Delta < 0$) indicates the presence of a vortex. The spiraling motion of a vortex can be quantified by the swirling strength λ_{ci} which is the imaginary part of the complex eigenvalue pair [*Zhou et al.* 1999]. The square of the swirling strength is proportional to the discriminant ($4\lambda_{ci}^2 = -\Delta$). The value of λ_{ci}^{-1} represents the period required to spiral around the origin of the vortex [*Adrian et al.* 2000].

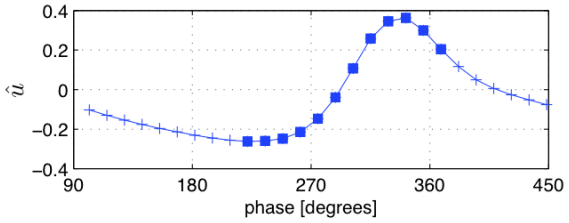

Figure 1. Phase-averaged horizontal velocity at the upper boundary of the velocity vector field. Horizontal axis is phase in degrees and vertical axis is velocity in m/s. The square markers refer to the phases that are shown in Figure 2.

RESULTS

The swirling strength was calculated for all vector fields. Areas with a swirling strength of ≥ 5 s^{-1} were identified as vortices. Statistical properties of vortices such as size, equivalent diameter, average swirling strength and location of centroid were determined for every wave phase.

Generally, the number of vortices decreases exponentially with increasing vortex diameter and, on average, swirling strength of a vortex was between 10 and 20 s^{-1}. Quantities such as average swirling strength, number of vortices and maximum vortex size were larger during positive free-stream velocities than during negative free-stream velocities.

Remarkable was the generation of relatively large vortices with diameters of 3 to 4 mm and an average swirling strength between 15 and 20 s^{-1} at free-stream flow reversal from negative to positive. These vortices were generated close to the bed and originate from one specific location. The consistent temporal and spatial behavior of vortices at one specific location results in the presence of a vortex in the phase-averaged flow field, i.e. it will not be averaged out. Figure 2 shows the appearance of the vortex at phase 275° just prior to flow reversal (which is at phase 288°). After flow reversal, at phase 302°, the swirling strength of the vortex decreases and the shape is less pronounced. At phases 315°, 328° and 342° relatively large patches of high swirling strength are still visible and it is suspected that these originated at locations outside the measuring domain and were transported by the flow.

The fact that the origin coincided with an inflectional-point of a shear layer suggests that these vortices were vortex tubes. Irregularities in the bottom profile of the fixed bed could explain the persistent location of the origin. To put the vortex tube in perspective we use the experimental results of *Nichols and Foster* [2007] who measured the flow field of surface waves above an irregularly rippled movable bed (wavelength ≈0.1 m and height ≈0.01 m and found vortices, generated by vortex shedding, with swirling strengths of ≈10 s^{-1} and diameters of ≈4 mm. It was observed that a sediment plume was entrained into such a vortex. The vortices identified by *Nichols and Foster* [2007] are of similar size and swirling strength as the vortices of this study. This makes it likely that the vortex tubes from the experiment described herein were able to suspend sediment.

CONCLUSIONS

Coherent structures, i.e. vortices, were detected in the wave bottom boundary layer of a medium sized wave flume using swirling strength. The temporal and spatial behavior of some vortices suggested that these were vortex tubes generated by an inflectional-point of a shear layer during flow reversal. Comparison of the vortex tubes with vortices generated by vortex shedding over ripples showed similar swirling strength and size indicating the ability of vortex tubes to cause sediment suspension events around flow reversal. The contribution of horizontal pressure gradients to sediment transport in the nearshore remains unclear.

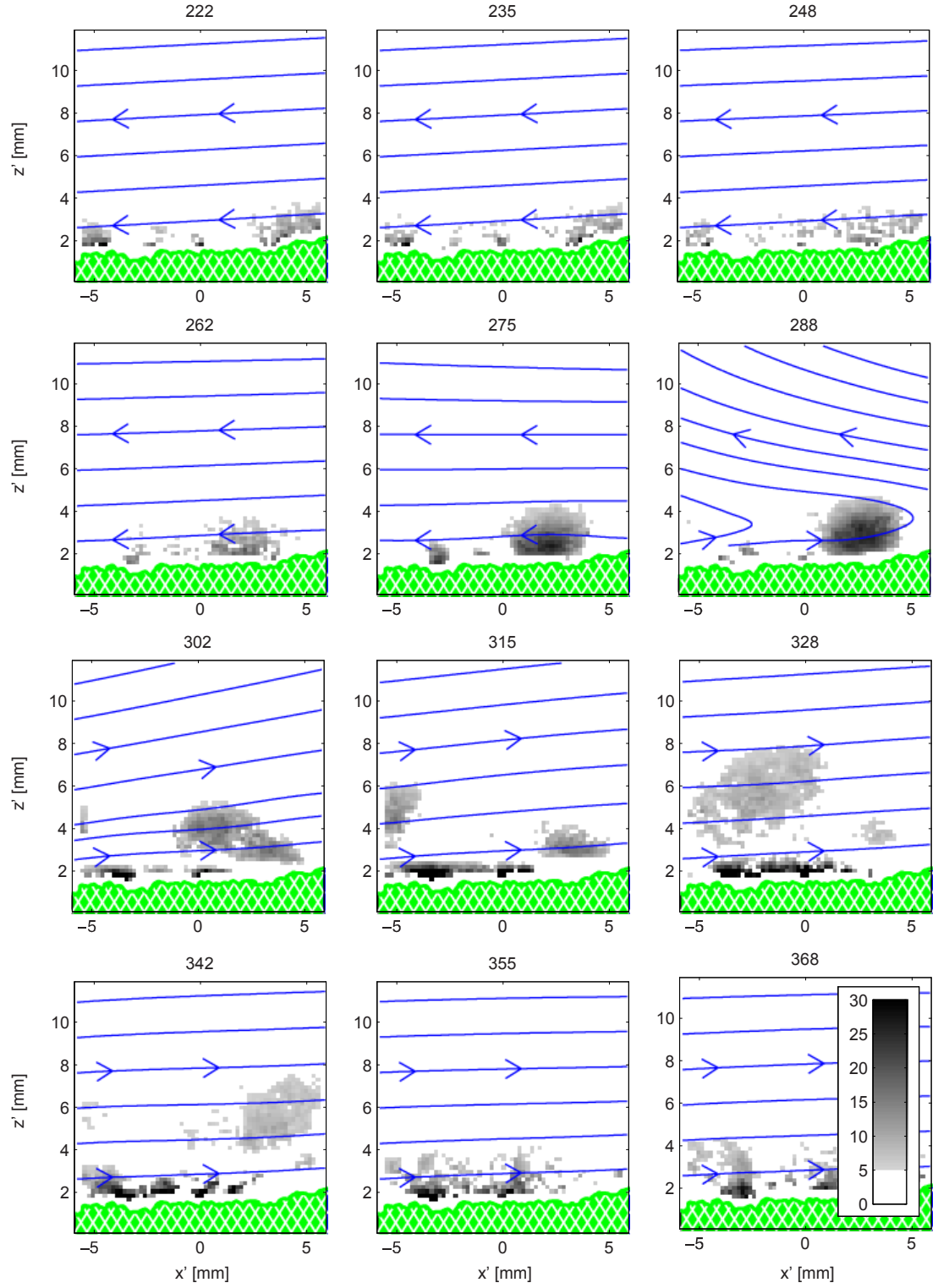

Figure 2. Swirling strength of the phase-average velocity during flow reversal. Color bar indicates swirling strength. Solid blue lines represent streamlines of the flow and green hatched area represents the bottom. The horizontal axis is horizontal distance and the vertical axis is vertical distance with the origin at the center bottom of the PIV vector field. The numbers above subfigures are the wave phases in degrees and correspond with the square markers in Figure 1.

Further research is needed to investigate the existence of vortex tubes at real scales in the nearshore and their role in net sediment transport.

ACKNOWLEDGEMENT

This project is funded by the Technology Foundation STW, applied science division of NWO, in The Netherlands, under project number DCB.07908. The authors are presently supported by the ERC Advanced Grant 291206 – NEMO.

REFERENCES

Adrian, R. J., K. T. Christensen, and Z.-C. Liu. (2000). Analysis and interpretation of instantaneous turbulent velocity fields. Experiments in Fluids 29 (3) (september): 275-290. doi:10.1007/s003489900087.

Akhavan, R., R. D. Kamm, and A. H. Shapiro (2006). An investigation of transition to turbulence in bounded oscillatory Stokes flows Part 1. Experiments. Journal of Fluid Mechanics 225 (-1) (april): 395. doi:10.1017/S0022112091002100.

Carstensen, S., B. M. Sumer, and J. Fredsøe. (2010). Coherent structures in wave boundary layers. Part 1. Oscillatory motion. *Journal of Fluid Mechanics* 646 (March): 169. doi:10.1017/S0022112009992825.

Drake, T. G., and J. Calantoni. (2001). Discrete particle model for sheet flow sediment transport in the nearshore. Journal of Geophysical Research 106 (C9): 868.

Foster, D. L., R. Holman, and R. A. Beach (1994). Sediment suspension events and shear instabilities in the bottom boundary layer. In Proceedings Coastal Dynamics 94, 712-726.

Henriquez, M., A. J. H. M. Reniers, B. G. Ruessink, and M. J. F. Stive (2010). Wave boundary layer hydrodynamics during onshore bar migration. In Proceedings of the 32nd International Conference on Coastal Engineering, Vol. 1, Shanghai, China.

Hoefel, F., and S. Elgar (2003). Wave-Induced Sediment Transport and Sandbar Migration. Science 299 (5614) (maart 21): 1885 -1887. doi:10.1126/science.1081448.

Madsen, O. S. (1974). Stability of a sand bed under breaking waves. In Proceedings of the 14th International Conference on Coastal Engineering, 14:776.

Nichols, C. S., and D. L. Foster (2007). Full-scale observations of wave-induced vortex generation over a rippled bed. Journal of Geophysical Research 112 (oktober 13): 17 PP. doi:200710.1029/2006JC003841.

Zala Flores, N., and J. F. A. Sleath (1998). Mobile layer in oscillatory sheet flow. Journal of Geophysical Research 103: 12783-12793. doi:10.1029/98JC00691.

Zhou, J., R. J. Adrian, S. Balachandar, and T. M. Kendall (1999). Mechanisms for Generating Coherent Packets of Hairpin Vortices in Channel Flow. Journal of Fluid Mechanics 387: 353-396.

DOI: 10.3990/2.186

Flow routing in mangrove forests: field data obtained in Trang, Thailand

E.M. Horstman[1,2], C.M. Dohmen-Janssen[1], T.J. Bouma[2,3,4], S.J.M.H. Hulscher[1]
[1]Water Engineering and Management, University of Twente, P.O. Box 217, 7500 AE Enschede, The Netherlands.
E.M.Horstman@utwente.nl; C.M.Dohmen-Janssen@utwente.nl; S.J.M.H.Hulscher@utwente.nl
[2]Singapore-Delft Water Alliance, National University of Singapore, Engineering Drive 2, 117576 Singapore.
[3]Marine & Coastal Systems, Deltares, P.O. Box 177, 2629 HD Delft, The Netherlands.
[4]Netherlands Institute of Ecology, P.O. Box 140, 4400 AC Yerseke, The Netherlands.
T.Bouma@nioo.knaw.nl

ABSTRACT

Mangroves grow in the intertidal parts of sheltered tropical coastlines, facilitating coastal stabilization and wave attenuation. Mangroves are widely threatened nowadays, although past studies have indicated their contribution to coastal safety. Most of these studies were based on numerical modeling however and a proper database with field observations is lacking yet. This paper presents part of the results of an extensive field campaign in a mangrove area in Trang Province, Thailand. The study area covers the outer border of an estuarine mangrove creek catchment. Data have been collected on elevation, vegetation, water levels, flow directions and flow velocities throughout this study area. Due to the tough conditions in the field, developing a suitable method for data collection and processing has been a major challenge in this study. Analysis of the hydrodynamic data uncovers the change of flow directions and velocities throughout a mangrove creek catchment over one tidal cycle. In the initial stages of flooding and the final stages of ebbing, creeks supply water to the lower elevated parts of the mangroves. In between these stages, the entire forest bordering the estuary is flooded and flow directions are perpendicular to the forest fringe. Flow velocities within the creeks are still substantially higher than those within the forest, as the creeks also supply water to the back mangroves. These insights in flow routing are promising for the future analysis of sediment input and distribution in mangroves.

INTRODUCTION

Mangroves form an indispensable ecosystem in the intertidal area of many tropical and sub-tropical coastlines. Mangrove vegetation consists of salt tolerant trees and shrubs, able to resist the hydrodynamic forces faced in the intertidal parts of sheltered coastlines such as estuaries and lagoons [*Augustinus*, 1995]. Due to their location and persistence, mangroves play an important role in coastal stabilization [*Alongi*, 2008; *Augustinus*, 1995; *Furukawa and Wolanski*, 1996; *Krauss et al.*, 2003; *Van Santen et al.*, 2007] and wave attenuation [*Brinkman*, 2006; *Hong Phuoc and Massel*, 2006; *Mazda et al.*, 2006; *Quartel et al.*, 2007]. Despite this key-function of mangroves in the intertidal area, they are in rapid decline. According to the most recent estimate of global mangrove area there is only 13.8 million ha [*Giri et al.*, 2011] left of the 18.8 million ha of mangrove cover found worldwide in 1980 [*FAO*, 2007]. Hence since 1980 the mangrove area decreased by about 27% and although annual mangrove losses are slowing down, recent annual loss rates are still around 1% [*Bosire et al.*, 2008; *FAO*, 2007]. Therefore there is an urgent need to unravel the contribution of mangroves to long-term coastal safety in order to increase awareness of the need for and hence the success of mangrove preservation.

To date, studies on water flows through mangrove systems are limited. Hydrodynamic studies into flow velocities focus on creek-forest interactions and the consequent tidal asymmetry and self-scouring of tidal mangrove creeks [*Aucan and Ridd*, 2000; *Furukawa et al.*, 1997; *Mazda et al.*, 1995; *Wolanski et al.*, 1980]. This issue gained interest quite a while ago, since flow routing is important for supply of e.g. sediment and nutrients to mangroves [*Wolanski et al.*, 1980]. Most studies investigate mangrove hydrodynamics through numerical models, field data to calibrate and validate these models are sparse. Collection of field data is often limited in time and space; field campaigns usually last for a few days and often only one study site is taken into account [*Aucan and Ridd*, 2000; *Furukawa et al.*, 1997; *Kobashi and Mazda*, 2005]. Comprehensive field studies into hydrodynamics within mangrove forests are really sparse [*Mazda et al.*, 1997], although this information is highly relevant for the distribution of sediments throughout the mangrove area [*Furukawa et al.*, 1997]. Mazda et al. [1997] and Kobashi & Mazda [2005] only made a start by extending knowledge on water flowing through mangrove forests by collecting flow velocity data along transects through mangroves. This procedure is practiced more often for data collection on wave attenuation in mangroves [*Brinkman*, 2006; *Vo-Luong and Massel*, 2008]. Studies linking 2-dimensional flow routing through mangroves to gradients in elevation and vegetation are unprecedented.

A first step forward to increase our understanding of mangrove functioning is to collect an extensive hydrodynamic database in the field. Integrated measurements on elevation, vegetation, water levels, flow velocities and flow directions throughout a mangrove area are required to be able to unravel flow routing through mangroves. This short-paper aims to shed a light on the importance of tidal creeks, which are a common feature in mangroves, for transporting water into mangroves.

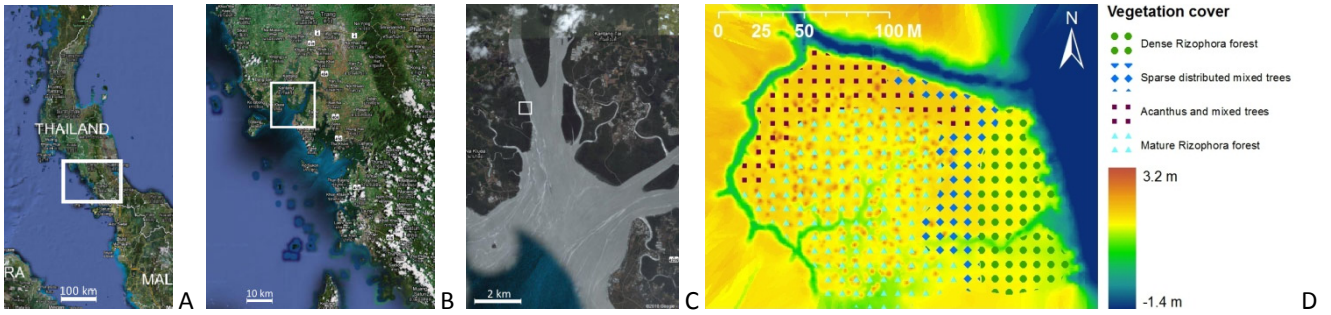

Figure 1. Geography of the study site: (A) Andaman coast of Thailand; (B) Trang province; (C) location of the study site in the Kantang River estuary near Kantang Tai village (opposite the river); (D) elevation and vegetation map of the studied creek catchment.

This paper presents field data obtained during a field campaign in a mangrove catchment in Trang Province, Thailand, from January to May 2011. Section 2 gives an introduction into the geography of this study site. Section 3 presents how hydrodynamic data are obtained within the study area. This section describes procedures for both data collection and data processing. Next, results of the data analysis are presented. These results will be discussed subsequently, leading to some preliminary conclusions following from the analysis of the obtained field data.

STUDY SITE

The study site (7°19'45''N; 99°29'17''E) is located in the Kantang River estuary at the east coast of southern Thailand, in Trang Province (Figure 1A-C). This area is part of the convoluted Thai Andaman coast, consisting of many embayments, islands and islets offering a perfect habitat to mangroves. This paper focusses on data collected in part of a creek catchment directly bordering the Kantang River (Figure 1C). The study area is tide dominated [*Woodroffe*, 1992] being exposed to a mixed semi-diurnal tide with a tidal amplitude of 3.5 m. The study area only covers part of the catchment fed by the main creek bordering the northern edge of the study area (Figure 1D) and forms the fringe of a much more extended mangrove forest extending about 1 km inland.

The geography of the study area has been mapped extensively with Trimble survey equipment (SPS 700-S6 Total Station and R-6 Real Time Kinematic GPS). Obtained elevation data has been interpolated (ordinary kriging with exponential semivariogram model; 0.7 m resolution) and plotted with respect to a datum just in front of the forest fringe (N0 in Figure 3A) in Figure 1D. The study area shows a pronounced 1 m high cliff at the interface with the estuary. Elevation of the forest floor increases while moving further inland, although deep creeks penetrate far into the forest and show incisions bordered by distinct creek banks. The main creek in the north is over 2 m deep. While penetrating deeper into the forest, the creeks tend to get narrower and shallower and they end in a depression in the centre of the study area. The mounds in the sheltered centre and west of the study area are mud mounds built by mud lobsters.

Four distinct vegetation zones are mapped in-situ and are shown in Figure 1D as well. The forest fringe facing the Kantang river is densely covered with *Rizophora* trees. Directly behind this fringe, a less dense forest cover is found consisting of a mix of *Rizophora*, *Avicennia*, *Sonneratia*, *Bruguiera* and *Xylocarpus* trees. Along the main creeks in the study area the same mix of trees is observed with an understory of *Acanthus* shrubs. *Rizophora* trees are dominant in the inner part of the study area.

METHODOLOGY

Data collection

Flow velocities and directions have been monitored throughout the study area with Acoustic Doppler Velocimeters (ADV's, Nortek) with cable probes. ADV's turned out to be very suitable equipment for monitoring hydrodynamics in coastal wetlands [*Horstman et al.*, 2011]. The ADV probes have been mounted downward looking, with one receiver aligned to the north, monitoring flow velocities at just 7 cm above the bed (Figure 2). With this configuration, the probes' sensors were located up to 23 cm above the bed so minimum water depths of 25 cm were required for data collection. End bells of the ADV's battery and memory housing contained pressure sensors and these were mounted to monitor at 7 cm above the substrate as well (Figure 2). Hydrodynamic data have been collected at 16 Hz with a burst length of 4096 samples (i.e. 256 s) and a burst interval of 1500 seconds (25 min). Three ADV's were installed during spring tide (due to the necessity of spring low tide for installation in some locations) and were deployed during an entire spring neap tidal cycle (i.e. 14 days) each time.

Figure 2. Acoustic Doppler Velocimeter during deployment in the field just in front of the mangrove fringe. Downward looking mounting to monitor flow velocities at 7 cm above the bed. Note the black canister in the back, containing the pressure sensor.

Data processing

The output of each ADV deployment contains three velocity components, three correlation values and water pressure. These data have been averaged per burst and low quality data are removed by filtering for correlations lower than 70%. Next, data series collected in four subsequent deployments (due to limited equipment availability) have been combined. ADV's were deployed such that every data series contained one common data collection point. Three data series contained velocities measured in the center of the study area (N3 in Figure 3A). From every data set for this central data collection point, data for one single tidal inundation have been selected showing equal inundation depths and flow velocities. Subsequently, concurrent measurements (internal clocks of the ADV's provided time stamps) have been selected for the surrounding data points from each series (K3 and L3, N0 and N1, N4 and O3 respectively). For the final data series, the reference data point was located in the main creek to the north instead (K3). One tidal peak was selected from these data to resemble inundation depths and velocity components of the representative tidal inundation as it was found before for this location. Then the timestamp of this tidal peak facilitated the selection of concurrent single tide data for the other two data collection points in the minor creeks to the west and south of the catchment (N5 and P1 respectively). By this procedure, three-dimensional flow velocity data have been assembled for nine data points throughout the study area representing equal tidal conditions (tidal stage and amplitude).

RESULTS

Figure 3 presents the resulting temporal sequence of flow velocity patterns throughout the study area (positions are indicated in Figure 3A) for one tidal cycle for which the field data have been merged. High slack tide is around 23:40 h for this instance. Inflow in the main creek to the north of the study area is observed from around 17:30 h onwards, but was not observed at that time yet since the ADV in this creek was located off the thalweg (due to shipping). Data coverage starts at 19 h, when the water depth at K3 exceeds the required minimum depth (i.e. 25 cm). Figure 4 shows the development of the current velocities observed at K3. It shows that on the initial stages of flood (positive current velocities), within creek flow velocities are about 0.1 m/s only. This rapidly changes on initiation of flooding of the mangroves. The lowest areas of the mangrove forest are located at about 1.6 m elevation (w.r.t. N0). When these areas start to inundate, suddenly large volumes of water need to be transported into the mangroves, causing a rapid increase in creek discharge and hence of within creek flow velocities. This situation is shown in figure 3B; water is transported through the creeks into the study area.

At the same instance, however, the mangroves also start to inundate directly from the forest fringe bordering the estuary. Within half an hour after initiation of flow velocity measurements at N3, a change in current directions is observed (see Figure 3C and Figure 4). Once the entire study area is inundated, including the bank separating the forest fringe from the central parts of the catchment, a uniform flow direction perpendicular to the forest fringe is observed. This indicates that water throughout the study area is flowing parallel to the main creek now and that it flows directly from the estuary into the forest. Flow velocities within the creeks stay significantly larger though, since huge quantities of water are required to inundate the extensive mangrove area located to the west of the studied area. Within creek water depths are larger and bottom friction within creeks is negligible compared to shear stresses experienced within the forest vegetation, facilitating the rapid supply of water to the back mangroves through these creeks.

When getting close to high tide, a rapid decrease of flow velocities throughout the study area is observed (Figure 3D) until slack tide. Figure 3E shows that at the turning of the tide, flow velocities throughout the study area have reversed towards the estuary already, while flow velocities observed within the creek are still directed to the west. This is caused by the fact that flow velocities have been monitored at 7 cm above the creek bed. Higher up in the water column at K3 (at levels exceeding the elevation of the forest floor), flow velocities turn concurrently with the flow velocities throughout the studied mangrove forest.

During ebb tide, the inverse sequence of events is observed as during flooding of the forest. Rapidly increasing negative flow velocities are observed on the initiation of ebb tide. Flow velocities throughout the study area are directed perpendicular to the forest fringe again, discharging directly into the estuary (Figure 3F&G). Only in the final stages of ebbing from the forest a change in flow pattern is observed again, with water being discharged via the creeks towards the estuary (Figure 3H).

Although current patterns at ebb and flood show a clear resemblance, current velocities do not. Figure 4 shows that creek flows only show a short-term peak flow velocity (0.3 m/s for this instance) during flood (only one data point, i.e. one burst), while flow velocities at ebb tide maintain a slightly lower maximum speed for a much longer duration (during five bursts). This is caused by a delayed discharge from the forest due to the high vegetation roughness faced by the tidal currents. On incoming tide, the same roughness hampers the inflow of water into the forest causing the delayed velocity peak after flooding of the forest at a water level of 1.6 m. This sequence of flow velocities leads to self-scouring of the creeks, which has been observed in mangrove studies before [*Mazda et al.*, 1995]. In contrary to this asymmetric pattern observed in tidal creek flows, within forest flows do not show such a distinct difference between inflow at flood and outflow at ebb tide (Figure 4).

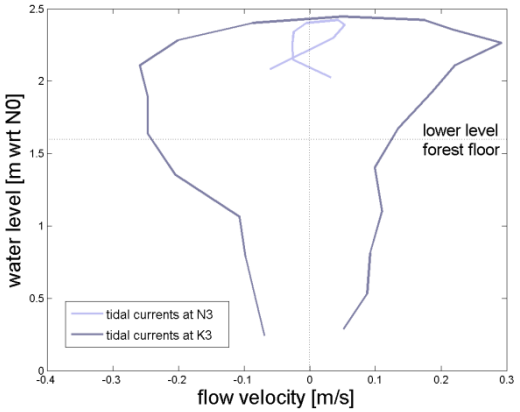

Figure 4. Current velocities observed within the creek (at K3) and in the center of the study area (N3). Velocities plotted are absolute magnitudes of the velocity vectors. Positive values are directed to the west, negative values to the east. The mangroves start to inundate at a water level of 1.6 m.

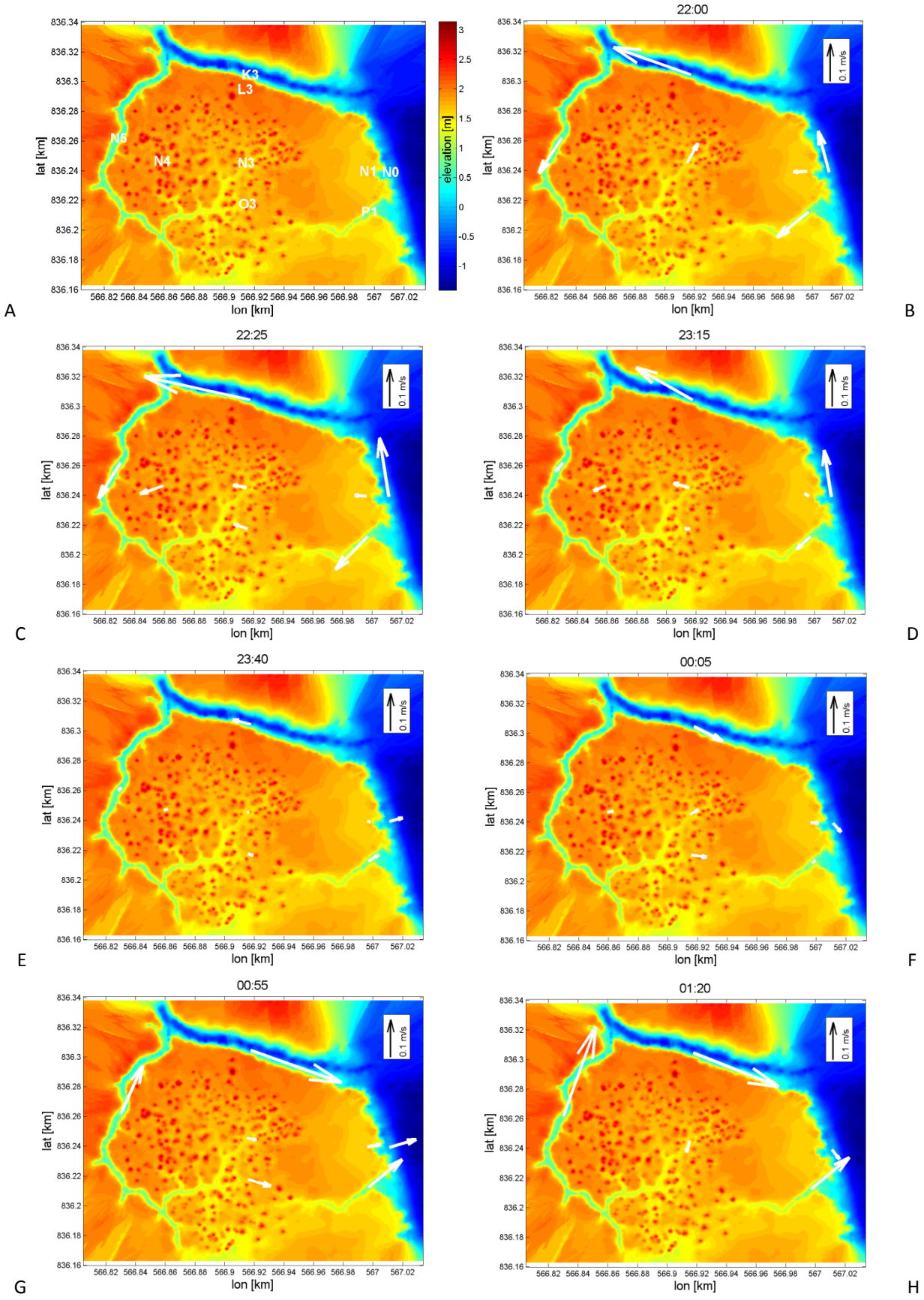

Figure 3. Nine positions for flow velocity measurements are indicated in (A). (B-H) Show the change of flow velocities and directions during an entire tidal cycle (slack high tide at 23:40), from the initial stages of filling of the area to full inundation and subsequent stages of discharge on outgoing tide. L3 does not inundate deeper than about 20 cm and hence flow velocities could not be measured.

DISCUSSION

Although tidal flow patterns through the studied mangrove area are unraveled by showing the flow velocities at different stages of flooding and ebbing, there is no clear-cut conclusion about the importance of tidal creeks in filling and emptying of the mangroves yet. Flow velocities presented in this paper only describe the situation at 7 cm above the bed. This velocity does at first not represent the velocity throughout the entire water column (as near bed flow velocities are significantly lower than those higher up in the water column). Measuring flow velocities at higher levels would have been of little use however as in these cases required water depths for proper ADV functioning would hardly ever occur. Next, it was shown that in the creeks not even the direction of the water current is per se the same throughout the entire water column. So the present analysis does not yet quantify the contribution of creeks to mangrove hydrodynamics.

CONCLUSIONS

The preliminary analysis presented in this paper underlines that creeks are mainly important for the initial stages of tidal filling and final stages of tidal emptying of the mangroves. The near-bed flow velocities presented here are valuable information for the future analysis of sediment transport through mangroves. Concurrently measured suspended sediment concentrations will be related to these flow velocities, so to increase knowledge on sediment routing and deposition in mangroves.

ACKNOWLEDGEMENTS

The authors gratefully acknowledge assistance in planning, facilitating and executing fieldwork by M. Siemerink (University of Twente), N.J.F. van den Berg (University of Twente), D. Galli (National University of Singapore), T. B alke (Deltares/Singapore-Delft Water Alliance), D.A. Friess (National University of Singapore/Singapore-Delft Water Alliance), E.L Webb (National University of Singapore), C. Sudtongkong (Rajamangala University of Technology Srivijaya), Katai, Dumrong and Siron. Fieldwork for this paper has been executed under the NRCT research permit 'Ecology and Hydrodynamics of Mangroves' (Project ID-2565). Also gratefully acknowledged is the support & contributions of the Singapore-Delft Water Alliance (SDWA). The research presented in this work was carried out as part of the SDWA's Mangrove research program (R-264-001-024-414).

REFERENCES

Alongi, D. M. (2008), Mangrove forests: Resilience, protection from tsunamis, and responses to global climate change, Estuar. Coast. Shelf Sci., 76(1), 1-13.

Aucan, J., and P. V. Ridd (2000), Tidal asymmetry in creeks surrounded by saltflats and mangroves with small swamp slopes, Wetlands Ecology and Management, 8(4), 223-232.

Augustinus, P. G. E. F. (1995), Geomorphology and sedimentology of mangroves, in Developments in Sedimentology, edited by G. M. E. Perillo, pp. 333-357, Elsevier.

Bosire, J. O., F. Dahdouh-Guebas, M. Walton, B. I. Crona, R. R. Lewis Iii, C. Field, J. G. Kairo, and N. Koedam (2008), Functionality of restored mangroves: A review, Aquatic Botany, 89(2), 251-259.

Brinkman, R. M. (2006), Wave attenuation in mangrove forests: an investigation through field and theoretical studies, PhD thesis, 146 pp, James Cook University, Townsville.

FAO (2007), The world's mangroves, 1980-2005., 77 pp., Food and Agriculture Organization of the United Nations, Rome.

Furukawa, K., and E. Wolanski (1996), Sedimentation in Mangrove Forests, Mangroves and Salt Marshes, 1(1), 3-10.

Furukawa, K., E. Wolanski, and H. Mueller (1997), Currents and sediment transport in mangrove forests, Estuar. Coast. Shelf Sci., 44(3), 301-310.

Giri, C., E. Ochieng, L. L. Tieszen, Z. Zhu, A. Singh, T. Loveland, J. Masek, and N. Duke (2011), Status and distribution of mangrove forests of the world using earth observation satellite data, Glob. Ecol. Biogeogr., 20(1), 154-159.

Hong Phuoc, V. L., and S. R. Massel (2006), Experiments on wave motion and suspended sediment concentration at Nang Hai, Can Gio mangrove forest, Southern Vietnam, Oceanologia, 48(1), 23-40.

Horstman, E., T. Balke, T. Bouma, M. Dohmen-Janssen, and S. Hulscher (2011), Optimizing methods to measure hydrodynamics in coastal wetlands: evaluating the use and positioning of ADV, ADCP AND HR-ADCP.

Kobashi, D., and Y. Mazda (2005), Tidal Flow in Riverine-Type Mangroves, Wetlands Ecology and Management, 13(6), 615-619.

Krauss, K. W., J. A. Allen, and D. R. Cahoon (2003), Differential rates of vertical accretion and elevation change among aerial root types in Micronesian mangrove forests, Estuar. Coast. Shelf Sci., 56(2), 251-259.

Mazda, Y., N. Kanazawa, and E. Wolanski (1995), Tidal asymmetry in mangrove creeks, Hydrobiologia, 295(1), 51-58.

Mazda, Y., M. Magi, Y. Ikeda, T. Kurokawa, and T. Asano (2006), Wave reduction in a mangrove forest dominated by Sonneratia sp., Wetlands Ecology and Management, 14(4), 365-378.

Mazda, Y., E. Wolanski, B. King, A. Sase, D. Ohtsuka, and M. Magi (1997), Drag force due to vegetation in mangrove swamps, Mangroves and Salt Marshes, 1(3), 193-199.

Quartel, S., A. Kroon, P. G. E. F. Augustinus, P. Van Santen, and N. H. Tri (2007), Wave attenuation in coastal mangroves in the Red River Delta, Vietnam, J. Asian Earth Sci., 29(4), 576-584.

Van Santen, P., P. Augustinus, B. M. Janssen-Stelder, S. Quartel, and N. H. Tri (2007), Sedimentation in an estuarine mangrove system, J. Asian Earth Sci., 29(4), 566-575.

Vo-Luong, P., and S. Massel (2008), Energy dissipation in non-uniform mangrove forests of arbitrary depth, J. Mar. Syst., 74(1-2), 603-622.

Wolanski, E., M. Jones, and J. Bunt (1980), Hydrodynamics of a tidal creek-mangrove swamp system, Mar. Freshw. Res., 31(4), 431-450.

Woodroffe, C. D. (1992), Mangrove sediments and geomorphology, in Tropical mangrove ecosystems, edited by A. I. Robertson and D. M. Alongi, p. 329, American Geophysical Union, Washington DC.

DOI: 10.3990/2.187

Connecting aeolian sediment transport with foredune development

J.G.S. Keijsers[1], A. Poortinga[1], M.J.P.M. Riksen[1] and A.V. de Groot[1]
[1]Land Degradation & Development Group, Wageningen University, P.O. Box 47, 6700AA, Wageningen, The Netherlands
joep.keijsers@wur.nl

ABSTRACT

Foredune volume is an important factor for coastal safety and depends on the balance between erosion through wave attack and sediment input via aeolian transport. Dune erosion can be simulated with good accuracy, but predictions of aeolian sediment transport into the foredunes are still difficult to make. As part of a larger project that aims to model foredune development over decades, the goal of this study is to improve the understanding of the temporal variability in sediment transport at the beach. Measurements of aeolian sediment transport at the beach of barrier island Ameland show that within events, wind velocity and rain are dominant controls. After aggregating wind and precipitation into a single meteorological index, it was found that these controls alone are not sufficient to explain the year-to-year variability in foredune growth rates. In contrast to the volume changes, the variability in the amount of elevation change of the foredune slope can be related to the wind climate and precipitation.

INTRODUCTION

Aeolian sediment transport is an important process in coastal dune development. Together with dune erosion it determines foredune volume, which may form an important factor for coastal safety against flooding. Although dune erosion can be simulated rather well (e.g. Vellinga, 1986; Steetzel, 1993; Van Rijn, 2009), the sediment input to the foredunes is still difficult to predict.

Common equations for aeolian sediment transport as a function of wind speed or friction velocity were established for desert conditions. When these equations are applied in a coastal setting to estimate aeolian sediment fluxes under unsteady and heterogeneous conditions, the results are often dissatisfactory (e.g. Svasek and Terwindt, 1974; Arens, 1996, 1997; Bauer et al., 2009). An important cause for the discrepancy between predicted and measured fluxes is the influence of transport-limiting factors such as, slopes, surface moisture and lag deposits (Sherman and Hotta, 1990; Bauer et al., 2009). Recent approaches to predict sediment input to the foredunes therefore focus on identifying and measuring key variables, and filtering transport events from time series according to these key variables (Delgado-Fernandez, 2011).

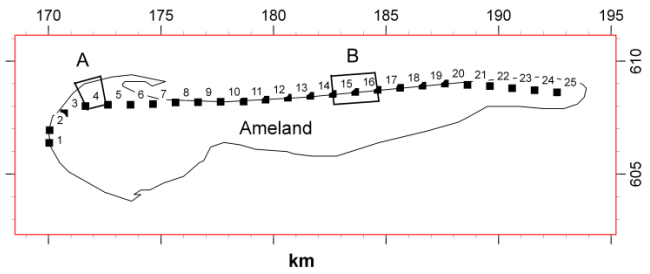

Figure 1. Location of field experiment (A) and the site for profile analysis (B).

The goal of this study is to improve the understanding of the temporal variability in sediment transport at the beach. The hypothesis is that, given a steady beach configuration, temporal variability in sediment input to the foredunes is caused by variability in wind and precipitation. To test this hypothesis, the first part of this study quantifies aeolian sediment fluxes of events and identifies the dominant controls on a time scale of hours. The second part deals with year-to-year sediment input to the foredunes.

METHODS

Study area

This study focuses on the Dutch barrier island Ameland (Figure 1), measuring approximately 25 km in length and oriented west – east. Its northern shore is flanked by a foredune ridge, ranging from 8 to 15 m in height and often backed by a more extensive and vegetated dune field. Storms are frequent in autumn and winter. In case of strong beach erosion during a storm or structural erosion beyond the safety limits, sand nourishments are carried out on the beach and nearshore to maintain or restore the sand volume. The site of the field experiment (A in Figure 1) has a beach width ranging from 150 to 250 m. It is frequently nourished to maintain the 1990 coastline. At the coastal section used for profile analysis, beach width is approximately 100 m.

Short-term aeolian transport

From October to December 2010, a fieldwork experiment was carried out on the beach of western Ameland (A in Figure 1) to measure the magnitude and temporal pattern of aeolian sediment fluxes in relation to meteorological conditions. Sediment transport intensity was measured using two saltiphones, giving the number of grain impacts per time unit. Mass fluxes were measured using Modified Wilson and Cooke catchers. Wind velocity was measured at a height of 2 m above the surface. Wind direction and precipitation were also recorded on site. A digital camera gave

hourly overviews of the general field conditions. Measurements were analyzed per wind event, mostly lasting several hours.

Medium-term dune development

The Jarkus database of annual elevation profiles measured by Rijkswaterstaat was used to calculate annual values of beach width (m), foredune volume above 3 m +NAP (m^3 m^{-1}) and foredune activity index (m). The foredune activity index (cf. Arens, 2004; Levin, 2006) is defined as the sum of absolute vertical elevation changes for all points on the foredune slope, divided by the number of points. Since 1996, the elevation profiles are measured using LiDAR. Therefore only data obtained from 1996 on were used in this analysis. We selected the section between km markers 14 and 16 (containing 11 profiles) as it has a relatively constant beach width throughout the period and shows homogeneous response to storm erosion (B in Figure 1).

Climate-data analysis

Hourly wind and precipitation data for the period 1996 – 2010 were obtained from the Royal Dutch Meteorological Institute. These were measured at the neighboring barrier island Terschelling. To test the validity of these data for Ameland, the data of two other neighboring barrier islands were compared and these showed a high similarity in magnitude and timing of wind and precipitation records. The hourly wind data were aggregated into an annual meteorological index, in this case the onshore component (Davidson-Arnott and Law, 1990):

$$U_{tot} = \sum \cos \alpha_i \cdot (U_i - U_t)^3 \qquad (1)$$

This incorporates the cosine effect of oblique winds (with incident angle α_i) being less effective in transporting sediment across the foredune line than directly onshore winds. Offshore winds were discarded. Only hours having average wind velocity U_i above the threshold velocity U_t and no recorded precipitation were taken into account. The resulting annual values are normalized against the highest occurring annual value.

RESULTS

Field measurements

During the two-month period, 15 aeolian transport events were recorded. A subset of 6 representative events was taken, with fluxes ranging from 3 to 16 kg m^{-1} (Table 1). Within events, the temporal variability was high, with transport intensity picking up as wind speed increases and ceasing when precipitation occurs (Figure 2). At low wind velocities, transport was intermittent and transport was dominated by streamers. At higher wind velocities the saltating particle count was higher and more constant, indicating a continuous and higher transport rate.

Table 1. Recorded data of 6 selected transport events (Poortinga et al., in prep.).

event #	duration (h)	main wind direction	mean and sd wind velocity ($m\ s^{-1}$)	sediment flux ($kg\ m^{-1}\ h^{-1}$)
1	2	E	3.7 ± 0.4	16
2	21	SSW	5.4 ± 1.0	3
3	13	NW	4.6 ± 0.7	3
4	6	W	7.0 ± 1.0	12
5	11	SWW	10.0 ± 1.2	6
6	8	S	5.7 ± 0.7	4

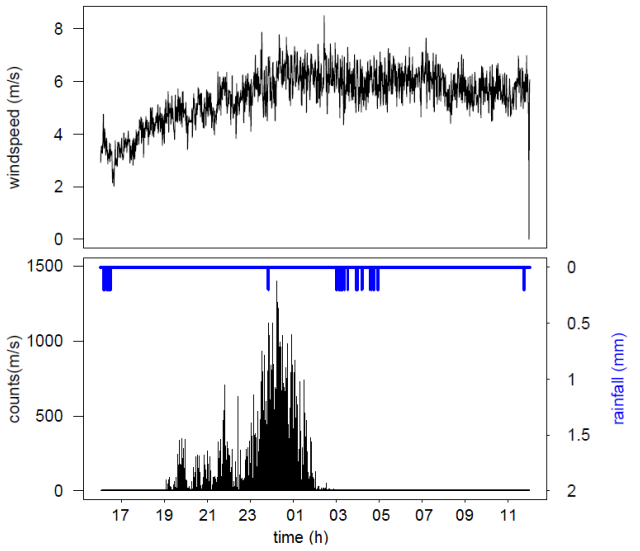

Figure 2. Wind speed (upper panel) and saltating particle count (lower panel) for event 2. Blue bars indicate precipitation (Poortinga et al., in prep.).

Highest fluxes are associated with events with alongshore-directed winds, corresponding with the largest fetch lengths (Table 1). However, these winds are not directed towards the foredune zone, hence not directly contributing to foredune growth. There is no direct correlation between sediment flux and wind speed at this timescale.

Elevation profile analysis

Annual foredune volume changes for the 11 beach-dune profiles are given in Figure 3. Although a homogeneous section of Ameland was selected, the majority of the years contain both volume-gaining and volume-losing profiles. Furthermore, the year-to-year variation in the rates is high. In 1999 and 2008 all profiles have lost considerable volume, which indicates erosion. 1997 and 2009 are all positive. The average rate of foredune growth for this section over the period 1997 – 2010 is 5 m^3 m^{-1} y^{-1}.

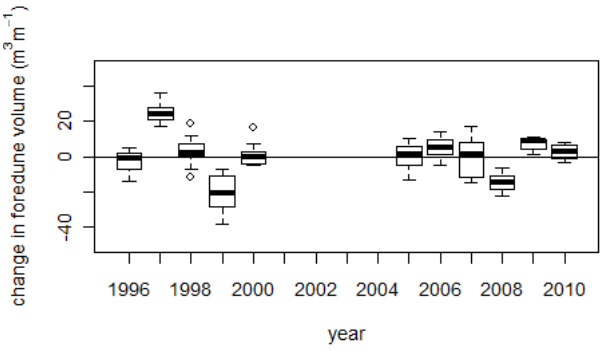

Figure 3. Year-to-year changes in foredune volume for location B.

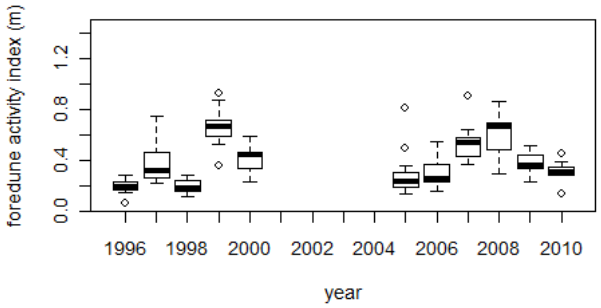

Figure 4. Magnitude and distribution of the foredune activity index at location B.

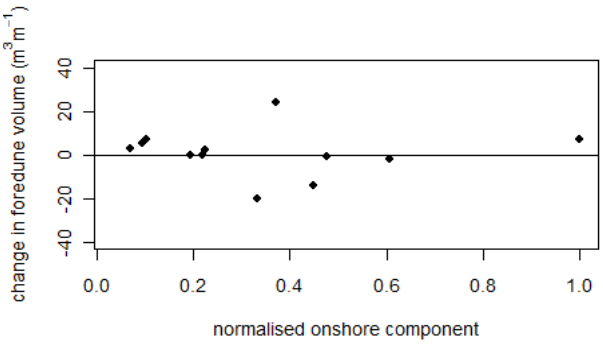

Figure 5. Yearly changes in foredune volume at location B, related to the onshore component of wind velocity.

The annual activity index for the same profiles is given in Figure 4. A completely static foredune slope would have a value of 0. There is considerable difference between the years, with highest values occurring in erosive years (1999 and 2008). In general, the activity index behaves like an absolute of the volume changes. In fact, the correlation between the absolute of the volume changes and the activity index is 0.88 (R^2).

Figure 5 shows the annual foredune volume changes versus the meteorological index. There is no significant relationship between volume changes and the meteorological indices, even when only years with positive or negative volume change are considered.

Correlations improve when activity is considered instead of actual volume changes (R^2=0.52, Figure 6). Activity increases with increasing values of the onshore component, which means that there is more morphological change on the foredune slope for years with stronger onshore winds. For a similar wind index, this was also found for more inland dune profiles by Levin et al. (2006) and a Dutch parabolic dune (Arens, 2004).

The fit improves when hours with recorded rainfall are included in the calculation of the onshore component (R^2=0.66,Figure 6).

DISCUSSION

The year-to-year variability in foredune volume changes is high. By means of Monte Carlo simulation, we estimate the effect of the 0.15 m reported accuracy of the LiDAR technique (De Graaff, 2003; Sallenger, 2003) on the foredune volume calculation at 3 m^3 m^{-1}. This is in the same order of magnitude as the average volume change. The variability per year, illustrated by the width of the boxes in Figure 3, is however much larger, even though an apparently homogeneous stretch of 2 km was selected. This means there are others factors that generate spatial variability, e.g. the average beach height and nearshore morphology. These factors will be analyzed in the future.

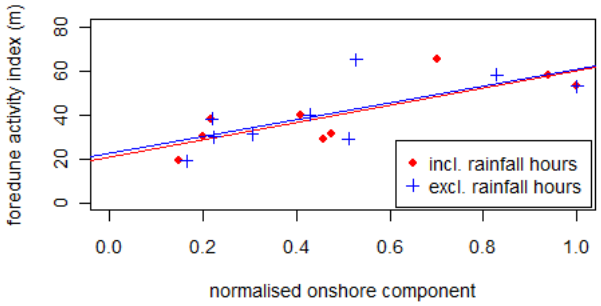

Figure 6. Foredune activity as a function of onshore component. Linear fits for both sets are given.

Disputing the hypothesis, there is no significant correlation between annual foredune volume changes and meteorology in the form of the onshore component of wind. We believe this is mainly caused by foredune erosion. Although in most years the dunes gain volume, this does not mean that no erosion has occurred. In other words, the net foredune volume change is not always equal to the actual aeolian sediment input. To account for this, estimations of annual sediment input into the foredunes may be improved by simulating dune erosion volumes.

Because erosion also induces elevation changes in the foredune, the activity index correlates better to the onshore component of the wind. This means that when the onshore winds are stronger, the expected rate of morphological change or sediment redistribution on the foredune slope is higher. There is however no indication of the direction of the morphological change, i.e. growing or decreasing foredune dimensions.

CONCLUSION

Within aeolian sediment transport events, wind velocity and rainfall are important factors controlling the magnitude of aeolian sediment fluxes. There is however a large variation in transport intensity for events with similar conditions, indicating the presence of complicating factors that were not taken into account in the current measurement campaign.

Based on annual foredune volume changes, the hypothesis that variability in foredune growth rates is primarily caused by variability in wind and precipitation, cannot be confirmed. Although foredune volume gain is caused primarily by aeolian sediment transport into the foredune zone, there is no significant relationship between wind conditions and the volume change on an annual timescale. There is a significant correlation between the onshore component of the wind and the amount of elevation change on the foredune slope, but this does not indicate whether a foredune is growing or eroding.

ACKNOWLEDGMENTS

JK and AdG are funded by Knowledge for Climate. We are grateful to Corjan Nolet and Saskia Visser for their support.

REFERENCES

Arens, S. M. (1996), Rates of aeolian transport on a beach in a temperate humid climate, Geomorphology, 17(1-3 SPEC. ISS.), 3-18.

Arens, S. M. (1997), Transport rates and volume changes in a coastal foredune on a Dutch Wadden island, Journal of Coastal Conservation, 3(1), 49-56.

Bauer, B. O., R. G. D. Davidson-Arnott, P. A. Hesp, S. L. Namikas, J. Ollerhead, and I. J. Walker (2009), Aeolian sediment transport on a beach: Surface moisture, wind fetch, and mean transport, Geomorphology, 105(1-2), 106-116.

De Graaf, H. J. C., S. J. Oude Elberink, A. E. Bollweg, Brügelmann, R., and L. R. A. Richardson (2003), Inwinning droge JARKUS profielen langs Nederlandse kust. Rep. AGI-GAM-2003-40, Rijkswaterstaat.

Delgado-Fernandez, I. (2011), Meso-scale modelling of aeolian sediment input to coastal dunes, Geomorphology, 130(3-4), 230-243.

Levin, N., G. J. Kidron, and E. Ben-Dor (2006), The spatial and temporal variability of sand erosion across a stabilizing coastal dune field, Sedimentology, 53(4), 697-715.

Poortinga, A., J. G. S. Keijsers, S. M. Visser, M. J. P. M. Riksen, and A. C. W. Baas (in prep.), Aeolian sediment transport on the beach of Ameland: measuring aeolian sediment fluxes.

Sallenger, J., A. H., et al. (2003), Evaluation of Airborne Topographic Lidar for Quantifying Beach Changes, Journal of Coastal Research, 19(1), 125-133.

Sherman, D. J., and S. Hotta (1990), Aeolian sediment transport: theory and measurements, in Coastal Dunes: Form and Process, edited by K. F. Nordstrom, Psuty, N.P., Carter, R.W.G., pp. 17-37, John Wiley & Sons, Chichester.

Steetzel, H. (1993), Cross-shore transport during storm surges, University of Technology, Delft.

Svasek, J. N., and J. H. J. Terwindt (1974), Measurements of sand transport by wind on a natural beach, Sedimentology, 21(2), 311-322.

Van Rijn, L. C. (2009), Prediction of dune erosion due to storms, Coastal Engineering, 56(4), 441-457.

Vellinga, P. (1986), Beach and dune erosion during storm surges, University of Technology, Delft.

DOI: 10.3990/2.188

Monitoring silt content in sediments off the Dutch Coast

Ronald L. Koomans[1], Johan de Kok[2], John de Ronde[2], Marcel J.C. Rozemeijer[3, 4], Koos de Vries[1]
[1]Medusa Explorations BV, Verlengde Bremenweg 4, Groningen, the Netherlands, Koomans@medusa-online.com
[2]Deltares, Postbus 177, 2600 MH Delft, The Netherlands
[3]IMARES Wageningen UR, P.O. Box 68, 1970 AB IJmuiden, The Netherlands
[4]Waterdienst, Rijkswaterstaat, Postbus 17, 8200 AA Lelystad

ABSTRACT

Silts, present in sand extraction sites, can potentially mobilize in the water column and result in increased turbidity of the North Sea. The main knowledge gap in assessing this potential risk is the capacity to buffer silts in the sandy sediments. To assess this buffering potential, Rijkswaterstaat and Stichting LaMER started a Monitoring and evaluation program (MEP Sandmining) to monitor, amongst others, the concentration and variation of fines in the sediments off the Dutch Coast.

We monitored the concentration of fines in the sediment along 3 cross-shore tracks, ranging from 0-9 km off the coast, with the Medusa system and by taking sediment samples. The Medusa system results in continuous measurements of the silt content of sediments along a line, the samples have been used for validation purposes.

In the period September 2009 - Oktober 2010, 6 campaigns have been conducted. Measurements show that, although the silt content is very low (<5%), the silt content can vary strongly on small spatial scales. Temporal variations show how the silt content along the profiles change. Comparing silt concentrations to the daily averaged wave height before the measurements, indicates that the silt contents increase with declining wave height.

INTRODUCTION

Silts, present in sand extraction sites, can potentially mobilize in the water column and result in increased turbidity of the North Sea. Computer models predict that this potential effect will not have significant consequences for ecology exploiting current quantities. However, the assumptions of these models have to be verified by a monitoring and evaluation program (MEP Sandmining) (Ellerboek e.a., 2008). The main knowledge gap in assessing this potential risk is the capacity to buffer silts in the sandy sediments. Fine silts present in the water column will settle during calm weather and will be stored in the upper decimeters of the sediment bed. During events, like a storm, these fines will go in suspension. The time scales involved in these processes and the behavior of the fine material in the upper layer of the sediment are part of the MEP of Stichting LaMER and Rijkswaterstaat. Other topics of this MEP relate to the significance of increased suspended silt and decreased amounts of algae on the growth of shellfish like *Ensis directus*. Apart from the sediment-based research presented in this paper, also measurements of concentrations of Suspended Particulate Matter (SPM) in the water column are conducted by taking water samples and by in-situ measuring CTD, suspension concentrations and chlorophyl.

This paper focuses on monitoring changes in the content of fines in the sediments that can (re)suspend into the water column.

MAPPING SEDIMENT COMPOSITION

The Medusa survey system

Traditionally, silt content in the sediment bed is determined by taking sediment samples by (box)coring or taking grab samples. These measurements give accurate information on one spot, but spatial variation in the silt content e.g. due to the presence of small-scale morphological features as ripple structures can result in data that is not representative for large areas. Spatial variation can be mapped by taking large amounts of sediment samples, which is often too expensive.

Different hydrographic methods exist to map the variation in the composition of the sediments on the seafloor. Analysis of the acoustic signals of multi-beam and single-beam echosounders or side-scan sonar, gives high-resolution images of the composition sediments. This information helps to zone the seafloor in a classes with one type of acoustic reflection that can be related to a certain type of sediment. It is though not possible to determine absolute concentrations of silt and sand or absolute values of grain sizes of the sediment bed [du Four et al, 2005]. We propose a method that directly measures some chemical constituents of the seafloor sediments, that can directly be related to sediment composition. This relation is established by a calibration in the laboratory.

This system (named Medusa) is towed over the seafloor behind a vessel. Each second, the system measures concentrations of the natural occurring radionuclides of the seafloor. These radionuclides (^{40}K, ^{232}Th and ^{238}U) are present in rocks and sediments since the origin of the earth and can be measured with a gamma spectrometer. The system measures the background radiation that is emitted by soil and sediments. Various research projects have shown how silt, sand and heavy minerals contain different concentrations and ratios of radionuclides [de Meijer, 1998]. This method is also used to measure median grain size in the field [Nederbracht and Koomans, 2005] and to map the concentration of silts in sediments [Venema and de Meijer, 2001].

The advantage of the proposed system over traditional sediment sampling, is that the detailed maps of sediment composition

determine the spatial variation at a small scale. Moreover, it is a cost effective method for monitoring purposes.

Defining the benchmark

The specific concentrations of radionuclides for each sediment fraction (also called fingerprint) allows the measurements of the radionuclides in the sediment to be translated into maps of sediment composition. To determine fingerprint of the material that will end up in the water column as SPM, we need to 1) define the grain size fraction of the SPM; 2) define the content of SPM in sediments from the site.

Grain size of SPM

SPM has been sampled in the field and was analysed with a Malvern particle sizer [Blok, 2010]. These sediments were not pre-treated to remove organic matter or carbonates. Part of the SPM consists of organic matter. We estimated the carbonate content in the sampled material at maximum 10%, the OM content in the sediment samples is ~1%. It is not clear how much of the OM is involved in the soil-water interaction. The sediment samples located on the position of the PSM samples have been analyzed with the Malvern particle sizer. Because our investigation focuses on the finest fraction of the sediments, the grains >90 µm have been removed. The sediment samples have been pre-treated to remove carbonate and organic matter.

The sieve analyses of these samples from the water column (Figure 1) show that 90% of the SPM is < 35 µm, with a median grain size of 16 µm. The analysis of the sediments show a more bimodal type grain size distribution with a slight increase around 10-20 µm (beware that due to the pre-sieving on 90 µm, a part of the material might be removed. The closer to 90 µm, the more has been removed).

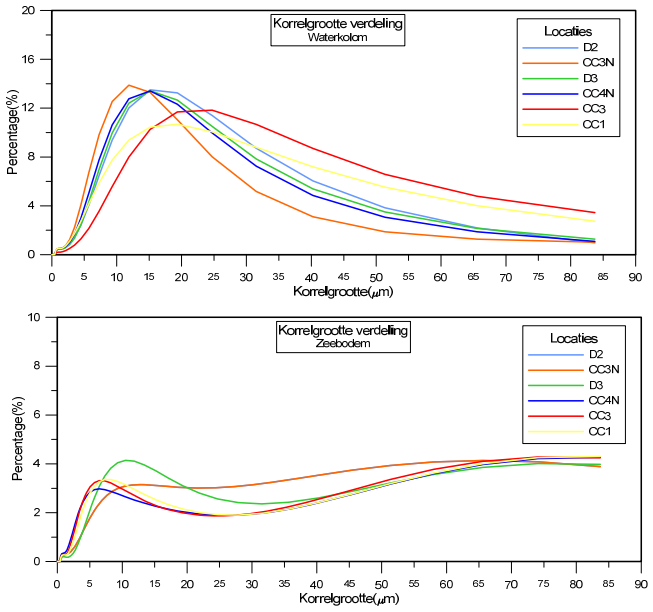

Figure 1: Sieve analysis of sediment in suspension (upper figure) and seafloor sediments. Prior to analysing, the grains >90 µm were removed by sieving

To estimate the mass of fine material that potentially suspends into the water column, we decided to map the content of the fraction <35 µm in the sediment. Therefore, the fraction <35 µm is used as a benchmark for the Medusa measurements.

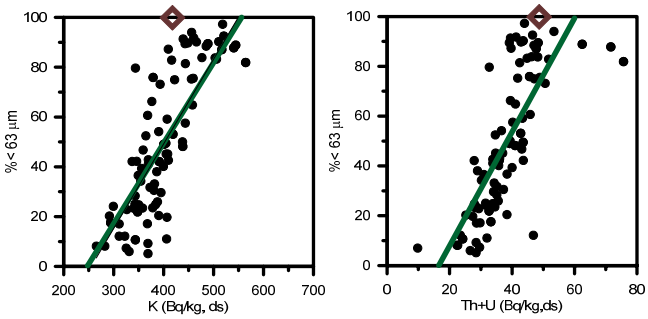

Figure 2: scatterplots of silt content (%<63µm) vs potassium and U+Th for sedimentsamples from various projects around the North Sea..The resulting numbers of clay fraction are derived from different systems (Malvern, sieving).The brown datapoint is based on measurements of SPM. Only datapoints with a silt fraction >3% are plotted.

Measuring SPM in sediment with a content of fines >3%

Previous studies have shown that concentrations of K, U and Th differ between clay and sand (Figure 2). Despite the fact that the samples come from different projects and the samples were analyzed with different sieving methods, a clear correlation exists between silt fraction and radionuclide concentration. The concentration of K in clay is a factor of 2 larger than in sand, the concentration of the sum of U and Th in clay is about a factor 3 larger than in sand. The fingerprint of SPM is determined by taking SPM samples from the water column and by measuring the concentrations of radionuclides of these samples. Also the radionuclide concentration SPM correlates well with the measurements on sediment samples.

Measuring SPM in sediment with a content of fines <3%

The North Sea sediments contain a low content of fines. Malvern analyses of 6 campaigns give an average fraction of 0.9 % (± 1.6) of sediment with a grain size <35µm. Please note that the method of analysis strongly determines the result: all samples have also been analyzed by sieving and sedigraaf. These analyses

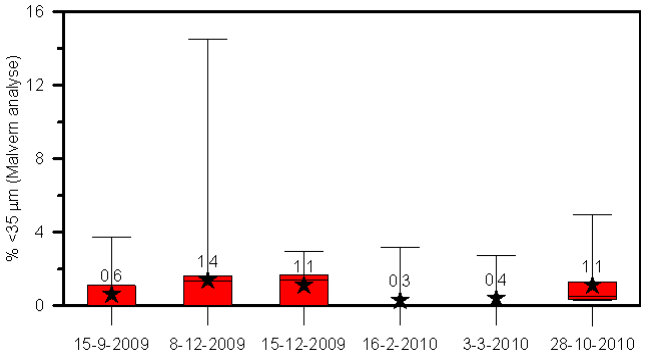

Figure 3: Box-whisker plot of the % <35 µm of sediment samples of different campaigns, measured with the Malvern particle sizer. A star (with number) shows the average.

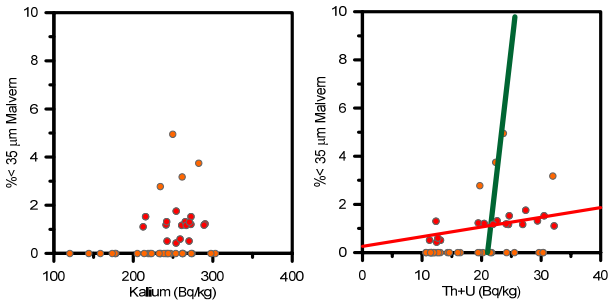

Figure 4: scatterplot of silt content (%<35µm, measured on a Malvern) vs potassium and U+Th for sediment samples taken during the project. The red line present a linear fit of the samples with a silt content >0.3% and <3%. The green line presents the fingerprint of SPM (see Figure 2).

give an average fraction of 1.6 % (± 1.4) of sediment with a grain size <35µm.

The sediment samples have a very low silt content, close to the lower limit of detection of the 'traditional' sample techniques and probably close to the fingerprinting method of the Medusa system. The concentrations of K and the summed concentration of U+Th are compared with Malvern analysis in Figure 4.

A large number of samples have a fraction <35 µm, which is smaller than 0.3%. These samples (orange colored in the graph) are probably below detection limit and are omitted from the analysis. The red line gives a linear fit of the samples with silts measured above detection limit. Figure 4 does not show a correlation between the silt fraction and the concentration K, but does show a correlation between the silt fraction and the concentration of U+Th. However, this correlation deviates strongly from the fingerprint of SPM.

An additional analysis of the chemical composition of these samples shows that heavy minerals are present in the sediments. The concentration of these heavy minerals (with an increased concentration of U+Th) correlate strongly with the silt fraction in the sediments. The correlation between the silt fraction and U+Th is therefore the result of a cross correlation between U+Th, heavy minerals and grain size.

To conclude the fingerprint analyses, we have shown that the concentration of U+Th is enriched in SPM and that the concentration of U+Th is enriched in heavy minerals. For SPM fractions >3%, the enrichment in U+Th due to heavy minerals is negligible and U+Th can be used as a direct proxy for SPM content. For SPM fractions <3%, the determination of absolute concentrations of SPM content is possible with an adapted calibration. Due to their higher density, sediment transport of heavy minerals is smaller than sediment transport rates of quartz and clays. In the region of study, outside the breaker bar system, sorting of heavy minerals is a very slow process [Koomans and de Meijer, 2004] and we can assume that within the time span of our study the content of heavy minerals is constant. With this assumption, changes in the content of U+Th can be attributed to changes in SPM content of the sediments. With this approach, we have a system for quantitatively monitoring the change in the content of fines in the sediment.

MEASUREMENT PROGRAM

The program focused on two line measurements, with a length of 8 km, perpendicular to the coastline (A and C track in Figure 5) and two lines, with a length of 10 km, parallel to the coastline (B and D track in Figure 5). The site was located near Bergen aan Zee. In total 6 campaigns were conducted in the period of September 2009-Oktober 2010.

RESULTS

Figure 6 shows the results of track C. The average silt content is 0.6% with an increased zone of 1.1% around 500 m from the coast. Sample location CC2 is located in this elevated zone.

The change in silt content with respect to the T0 measurement of September 2009 is visible in Figure 6. Almost all measurements show a positive deviation from the September measurements, only the region 2000-3500 m shows lower a lower silt content in T3 and T4 measurements. The total deviation is between -2.5 and 5%.

DISCUSSION

The main goal of the study is to understand the buffering of SPM in the sediment. Since we expect that wave action is an important driving force in the mobilization of the fine material, wave heights of the periods before the measurements have been analyzed. As a first exploration, we compared the average wave height 2 days before the measurement with the averaged silt content in the sediment (Figure 7).

The comparison (Figure 7) shows how in the T1 and T2 measurements, silt content is 4-8% higher than in the T0 measurement. Prior to these campaigns, the wave height is 100-120 cm, which is 80cm lower than the wave height prior to the T0 campaign. This small dataset indicates that after a short period with lower wave height, the silt content in the sediment is higher.

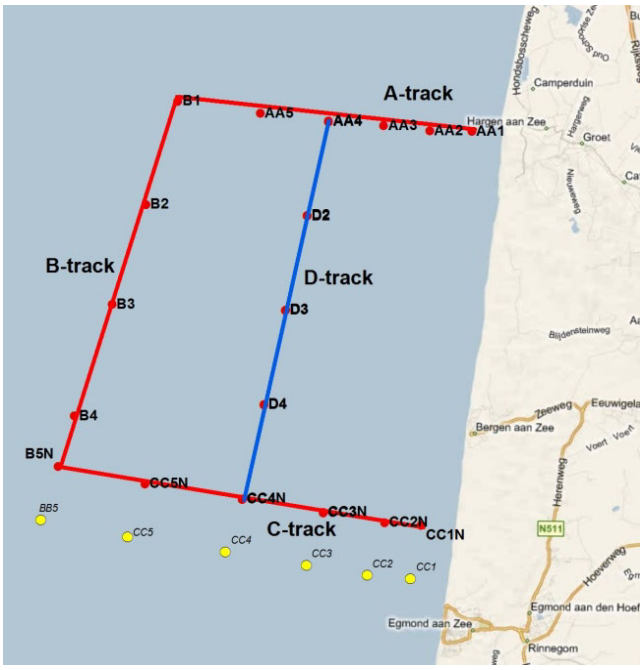

Figure 5: overview of the measured tracks.

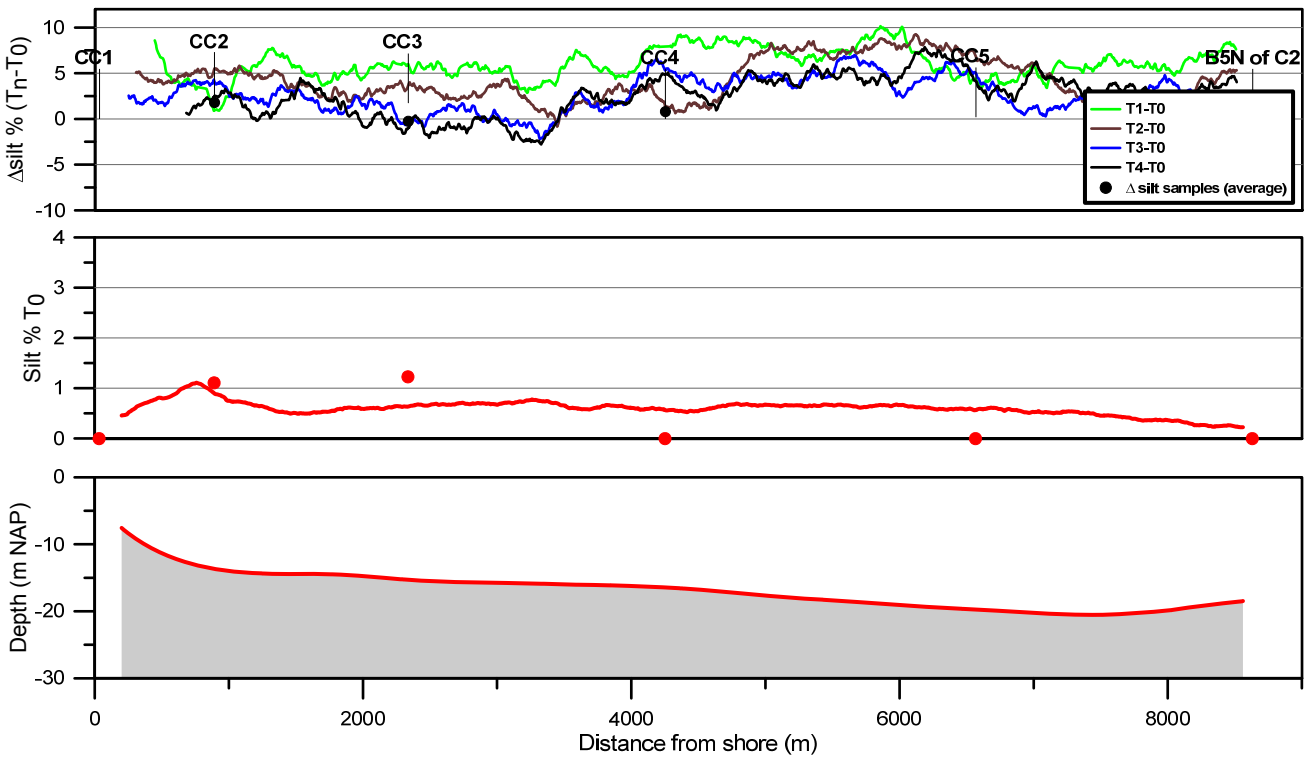

Figure 6: Result of the monitoring of track C, with the change in silt fraction, silt content in the T0 measurement and water depth..

CONCLUSIONS

An intensive study on the grain size distribution and chemical composition of SPM and fine sediments samples from the North Sea, show that the Medusa system is a powerful tool for mapping fine sediments in situ. For silt concentrations >3% a direct relation between the concentration of radionuclides and silt content can be used; for silt concentrations <3% the change in the content of fine silts can be mapped.

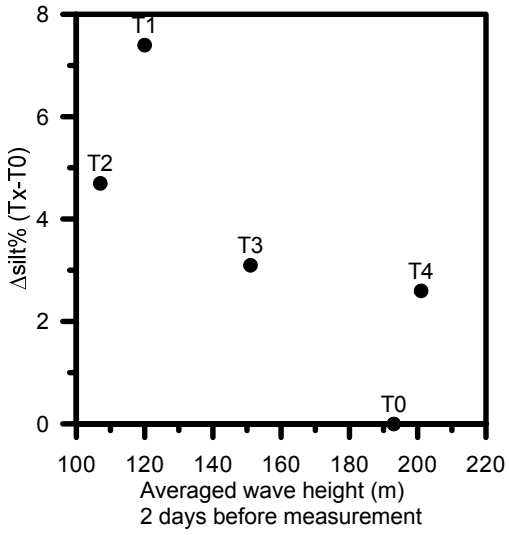

Figure 7: Change in average silt content as function of averaged wave height before the measurement.

A two year monitoring of fine sediments off the coast near Bergen shows that the silt content of sediment changes in space and in time. A first assessment of wave height information and the measured content of fines in the sediment shows how a decrease in wave height, results in a higher silt content in the sediment.

ACKNOWLEDGEMENT

This project was initiated and funded by Stichting LaMER and Rijkswaterstaat.

REFERENCES

Blok, B. 2010. Meetvis, Medusa metingen van september en december 2009. 1201293-000, Deltares, Delft.

Du Four, I., Deleu, S., Darras, I., Roche, M., Koomans, R., & Van Lancker, V. (2005). Comparison between different seabed classification techniques and validation with sediment samples on two shallow-water dumping sites (Belgian continental shelf). Shallow Survey 2005 4th International conference on high resolution surveys in shallow water, Plymouth, Devon, UK.

Koomans, R.L. and de Meijer, R.J. 2004. Density gradation in cross-shore sediment transport. Coastal Engineering, 51: 1105-1115.

de Meijer, R. J. (1998). "Heavy minerals: from 'Edelstein' to Einstein." Journal of Geochemical Exploration 62(1-3): 81-103

Ellerbroek, G., M.J.C. Rozemeijer, J.M. de Kok, J. de Ronde (2008) Evaluatieprogramma MER winning suppletiezand Noordzee 2008-2012. RWS Noord-Holland 16 juli 2008

Nederbracht, G. and R. L. Koomans (2005). Nourishment of the slope of a tidal channel: from experiment to practice. Coastal Dynamics, Barcelona, Spain, ASCE.

Venema, L. B. and R. J. de Meijer (2001). "Natural radionuclides as tracers of the dispersal of dredge spoil dumped at sea." Journal of Environmental Radioactivity 55(3): 221-239.

DOI: 10.3990/2.189

MorphAn: A new software tool to assess sandy coasts

Q.J. Lodder[1] and P.F.C. van Geer[2]
[1]Rijkswaterstaat, waterdienst, P.O.Box 17, 8224 AD, Lelystad, the Netherlands
[2]Deltares, P.O.Box 177, 2600 MH, Delft, the Netherlands, Pieter.vanGeer@deltares.nl

ABSTRACT

We present a new software tool called "MorphAn" that enables easy assessment of sandy coasts. MorphAn provides the possibility to import data of various formats. The software pays special attention to coastal data provided in the so-called Jarkus format. Data can be analyzed with a GIS based map view. Simultaneously an overview of the profile development in time or a more detailed picture of the actual measurements is given. Furthermore, MorphAn includes the possibility to assess coasts for dune safety according the safety assessment rules VTV2006. The software program gives a graphically presentation of the calculation results of dune erosion according to the Duros+ and D++ model as well as calculation results of the normative erosion points. MorphAn also provides the possibility to calculate and visualize the momentary coastline (MKL) and the expected near future coast line position (TKL). The software is freely available and expected to become open source in 2012.

INTRODUCTION

This short paper will introduce you to a new and freely available software tool called "MorphAn". MorphAn enables the user to assess the safety and beach development of sandy coasts.

In 2008 the Dutch Ministry of Infrastructure and the Environment commissioned Deltares to start the build of a new software tool. The aim of this software is to support assessment of dune safety and beach development. Rijkswaterstaat plans to present MorphAn as its official and supported tool for assessment of dune safety in The Netherlands. From the start of the project, one of the main goals has been to release MorphAn as a freely available, preferably open source, software tool. At this moment, the beta version of MorphAn is freely available. Release of the source code is expected at the end of 2012.

Data analysis, Dune safety assessment and coastal development assessment are the three pillars that form the basis of MorphAn. This paper will discuss the figures and tools included in MorphAn to support each of these pillars.

DATA ANALYSES

One of the most important aspects of assessing dune safety or coastal development is analyzing the data that is used to calculate a dune crest retreat point after a storm or momentary coastline. MorphAn offers the ability to import and analyze so-called jarkus measurements (yearly measurements of coastal profiles). A default jarkus dataset that includes most yearly measurements of the Dutch coast between 1965 and 2011 accompanies the software. Next to that, there is also the possibility to import user defined datasets or expand the default dataset with additional measurements.

Once the data is imported, it is possible to specify a list of locations that is used in all operations throughout the program. MorphAn ignores all measurements at locations not in that list.

To accommodate a thorough analysis of the imported data MorphAn provides various types of views that enable the user to analyze the data at different levels of aggregation and along the various dimensions in time and space. This section will introduce you briefly to the types of figures included in MorphAn.

Map overview

The map overview provides a GIS based map that gives a top view of the measurements in space and time. Figure 1 gives an example of the jarkus measurements at Texel for 2011. Blue lines represent the wet parts of the measurements, whereas the sandy colored lines represent dry measurements. Interpolated profile parts can be recognized by the tomato red colored lines. MorphAn also includes a time navigator to control the period that is presented on the map.

Due to its GIS nature it is easy to expand the map by including for example shapefiles as is shown by including the Texel district boundaries and names in Figure 1.

Transect side view

The transect side view (Figure 2) shows a single jarkus measurement in the local coordinate system (RSP). The side view distinguishes wet measurements, dry measurements and the interpolated profile part with the same coloring as the map overview. Furthermore, the side view interrupts the plotted line whenever more than 10 meter separates the measured points. This enables visual assessment of the quality and origin of the jarkus measurements.

Transects comparison view

With the transects comparison view (Figure 3) it is possible to compare jarkus measurements in time for one location or in space for a specific year. This enables the user to look at profile development of a certain feature in time or space. Each measurement is now plotted by a single (unique) color. The tool offers various color scales to customize the image.

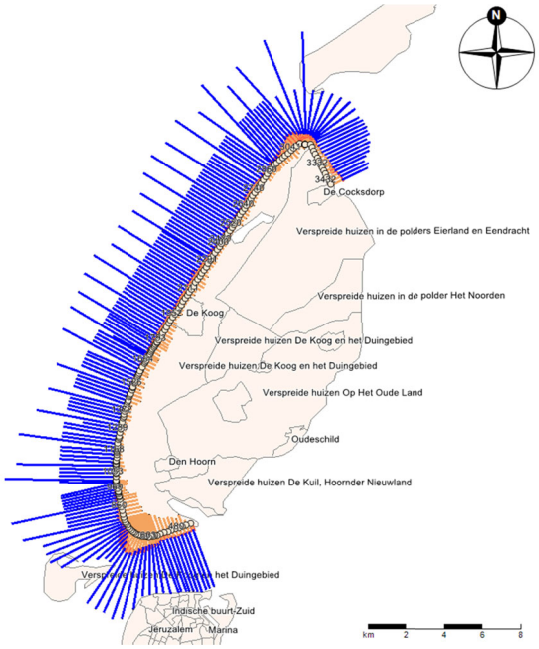

Figure 1. An example of a map in MorphAn showing an overview of the imported jarkus measurements for Texel. The map also contains a layer that shows the districts of Texel according to the Dutch cadastre (http://kadaster.nl/)

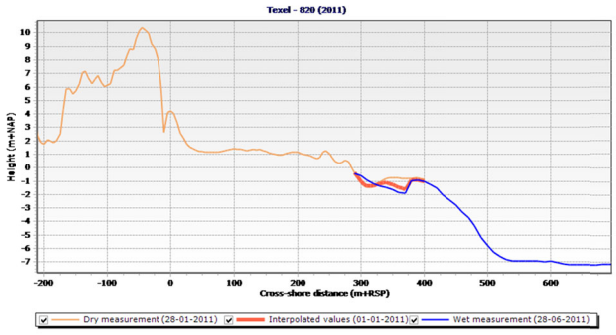

Figure 2. An example of a transect side view in MorphAn. The side view shows differences between measurements taken from land (sandy colored line), measurements taken from a vessel (blue line) and interpolated profile parts that are used to connect the wet and dry measurement when assessing the complete profile (tomato red line)

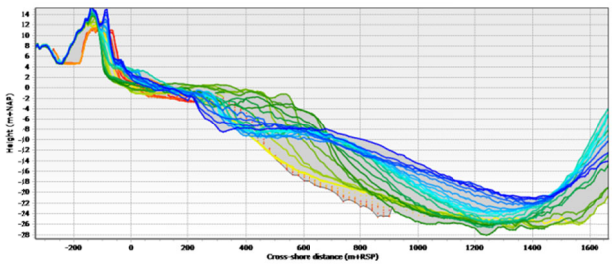

Figure 3. An example of a transect comparison plot in which measurements over a certain period on one location, or measurements for one year over multiple locations can be compared.

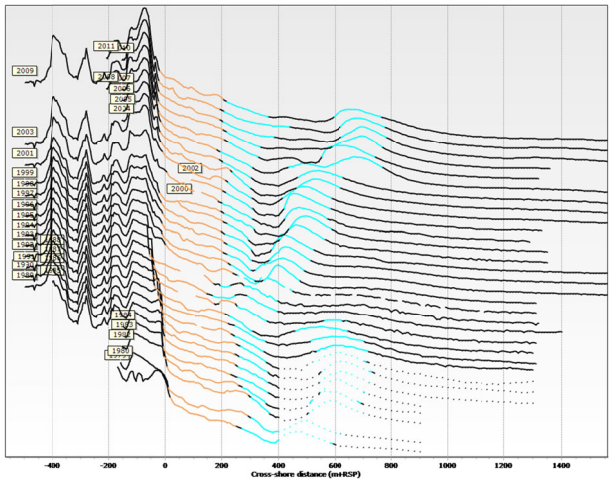

Figure 4. An example of a time stack representation of the beach development at one location. Brown and blue colors accentuate certain height regions of the profile. The blue part clearly shows a bar traveling offshore.

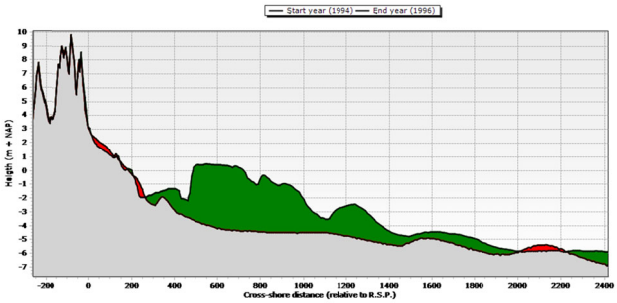

Figure 5. An example of a difference plot between two measurements. Green shows the parts of the profile that have accreted (or have been nourished) since the first measurement. The red parts indicate locations where the profile has eroded relative to the first measurement.

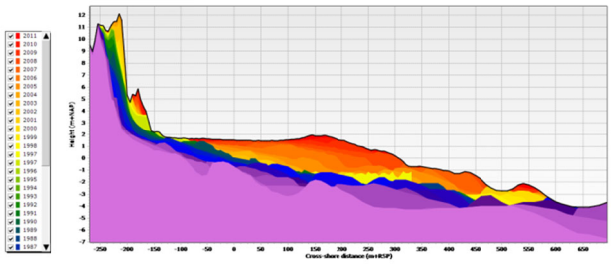

Figure 6. An example of a time history plot. The colored patches indicate the last year in which a change of the bathymetry was measured in that particular part of the profile.

Time stack view

The time stack view is another way of looking at measurements in time at a certain location. In this plot each year is plotted a certain distance higher than the previous year. Due to the highlighting of specific heights in the profile, development of features in the profile becomes more visible. The time stack in Figure 4 for example shows the movement of breaker banks offshore.

Time difference view

Visualization of the morphological change between two years at a certain location can help the user understand the effect of large changes in the bathymetry. The time difference view (Figure 5) shows these differences as green (accretion) or red (erosive) areas. Due to its coupling with a time navigator development of these changes in time is quickly visualized. The example in Figure 6 shows a nourishment just below NAP. By holding the same reference year and changing the year of the compared jarkus measurement the development of the nourishment in time can be analyzed.

Time history view

Time history figures (Figure 6) show the development of the cross-shore profile at one location in time by plotting colored patches. The color represents the last year in which a change occurred in that particular part of the profile. With this tool the user gets an idea of the depth at which the profile actively changes through time.

DUNE SAFETY ASSESSMENT

Dutch dune safety assessment rules (TRDA2006) prescribe the use of Duros+ for calculating dune erosion at the end of an extreme storm event. To assess dune safety, dune erosion due to this extreme event needs to be calculated for profile measurements over a period of fifteen years. To incorporate the yearly variation of the beach profile, the third worst result over these fifteen years is considered the normative erosion point.

MorphAn includes a model to calculate dune erosion with the Duros+ model and visualize the results in order to inspect them (it implements Duros+). Figure 7 shows a representation of such a calculation result for an individual measurement at Ameland. Next to the Duros+ model, MorphAn also implements the D++ model (Deltares, 2010).

To support determination of the normative erosion point, MorphAn also produces Rt-diagrams as described in the assessment rules (Figure 8). An Rt-diagram plots the calculated retreat points (R) in time (t) for a certain location and identifies the third worst point as the normative dune crest retreat point.

One of the added values of MorphAn with respect to existing tools is the ability to interactively display the calculation results on a map as well (Figure 9). This map representation uses the same feature as the previously discussed map overview. Combining the calculation results with other data therefore is relatively easy. Furthermore, selection of one ore more of the results on the map is synchronized with the representations of the calculated erosion and the Rt-diagram. This makes navigating through the results a fun job to do.

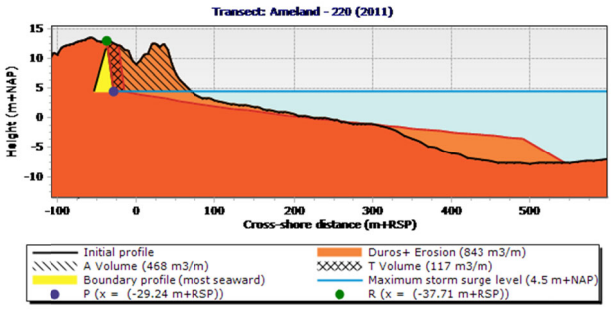

Figure 7. Representation of the result of a dune safety assessment calculation using Duros+ at Ameland as included in MorphAn. The figure also includes the calculated additional erosion and boundary profile.

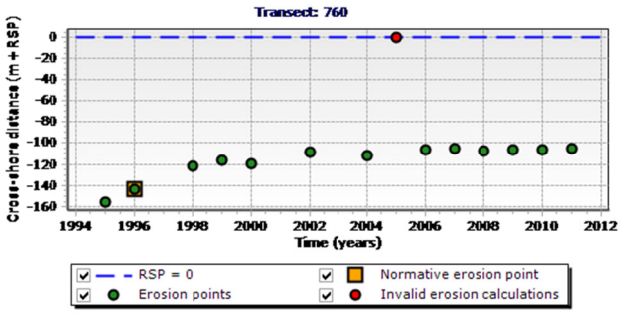

Figure 8. Visualization of the calculated retreat (R) points in time. The normative retreat point is visualized as a squared symbol. MorphAn also distinguishes between questionable (orange), invalid (red) and valid (green) calculation results. This qualification is just a first pointer to the results that need some more examination before trusting the result.

Figure 9. Map overview of the calculated retreat points. The map is coupled to a time navigator, which allows scrolling through time. The MorphAn overview also includes a layer that shows the normative retreat points.

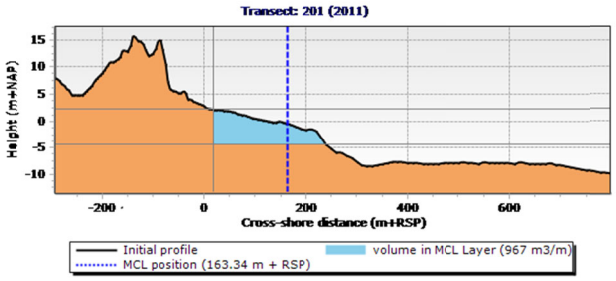

Figure 10. Representation of the calculated momentary coastline position (MKL) as included in MorphAn. The blue area visualizes the volume between the upper and lower boundary for determining the MKL position. The blue dashed line represents the MKL position.

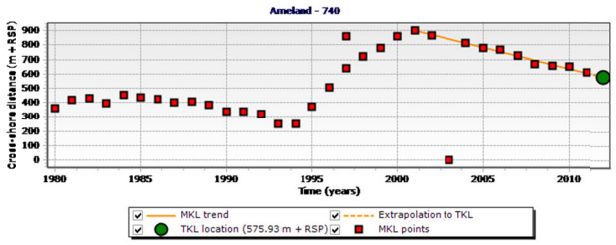

Figure 11. Representation of the MKL point in time for a location at Ameland. MorphAn also includes the calculated trend of the MKL points by plotting an orange line. The green dot represents the predicted coastline TKL.

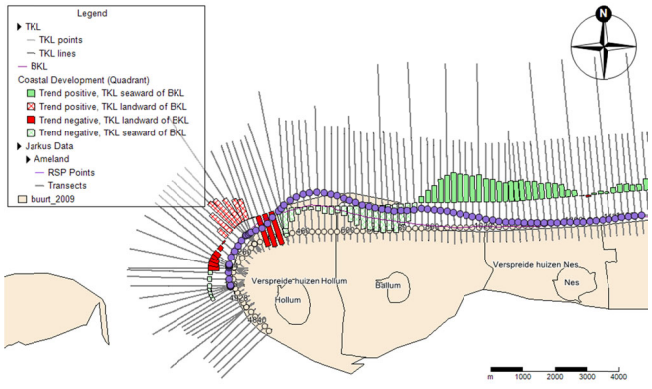

Figure 12. Map overview of the calculated MKL and TKL points. The map also includes a layer that expresses the trend of the MKL relative to the basic coastline (BKL) by means of red and green bars. This layer looks similar to the presentation of MKL trends in the kustlijnkaartenboek published by Rijkswaterstaat at www.kustlijnkaart.nl

COASTAL DEVELOPMENT ASSESSMENT

Next to dune safety assessment, MorphAn offers tools to assess the development of the coastline. A widely used indicator for the beach position is the momentary coastline position (MKL) defined as the volume of sediment between two elevation levels divided by the difference between these two levels. While assessing the development of the coastline these positions in time at a certain location are often used to calculate a trend and determine the expected coastline position (TKL) in a future year. Comparison with a reference coastline (BKL) adds to the decision whether or not there should be nourished at that particular location. Figures 10, 11 and 12 show the way MorphAn represents these calculation results. Figure 12 also contains a representation of the trend of the MKL position and its relation to the TKL similar to kustlijnkaarten produced by the Ministry of Infrastructure and the Environment (www.kustlijnkaart.nl). As the ministry initiated the development of MorphAn, it also plans on assessing the MKL development and determining the TKL with MorphAn in future.

FUTURE DEVELOPMENT

As most users will experience, MorphAn offers a lot of potential for further development of the supported operations. At this moment equipping MorphAn with the necessary tools to assess dune safety according to an expected new version of the assessment rules has a high priority. Next to that, attention is paid to expansion of the functionality to calculate beach development, like including a nourishment database and a module to automatically determine the best period for trend analysis. Although there is no direct coupling between MorphAn and the kustlijnkaarten produced by the ministry, in future calculation results can be written in an output format that can be used for creating these maps.

However, there are also possibilities for adding new features to MorphAn. One can think of including interfaces to other dune erosion models like XBeach (Roelvink et al., 2009) or DurosTA (Steetzel, 1993), but also expanding the capabilities of communication with other programs (export of results to Google Earth for example).

CONCLUSIONS

In this paper, we presented a new software tool, called “MorphAn” to facilitate analysis and assessment of safety and development of sandy coasts. The software is freely available and expected to become open source at the end of 2012. MorphAn supports data analysis in various ways as well as assessment of dune safety according to the Dutch assessment rules denoted in the TRDA2006 and assessment of the development of the momentary coastline. At this moment, MorphAn still offers lots of possibilities for expanding the functionality. We would love to hear all ideas about the possibilities to expand MorphAn in a way we did not think of yet.

REFERENCES

Deltares (2010), Ontwikkeling detailtoest duinen 2011 (D++), tussenrapportage SBW-Duinen. Deltares, 1202124-003).

Dano Roelvink, Ad Reniers, Ap van Dongeren, Jaap van Thiel de Vries, Robert McCall, Jamie Lescinski (2009), Modelling storm impacts on beaches, dunes and barrier islands, Coastal Engineering, 56(11–12),1133-1152, ISSN:0378-3839, 10.1016/j.coastaleng.2009.08.006.

TRDA2006 (2007), Technisch rapport duinafslag, experisenetwerk waterveiligheid.

Henk Steetzel (1993). Cross-shore Transport during Storm Surges.

Short term morphological wave impact on the Zandmotor; A conceptual model

W.Y. Man, S.J.M.H. Hulscher, P.C. Roos, J.P.M. Mulder and A. Luijendijk

Paper confidential

DOI: 10.3990/2.191

Hydrodynamics of the Rhine ROFI near IJmuiden

J.J. Nauw[1] and M. van der Vegt[2]

[1]Royal Netherlands Institute for Sea Research, P.O. Box 59, 1790 AB Den Burg (Texel), the Netherlands, e-mail: Janine.Nauw@nioz.nl

[2]Institute for Marine and Atmospheric Research Utrecht – Physical Geography, Utrecht University, P.O. Box 80.115, 3508 TC Utrecht, The Netherlands

ABSTRACT

The paper will focus on hydrodynamics of the Rhine ROFI in its most northerly extent near IJmuiden. A bottom-mounted ADCP was deployed near IJmuiden and measured for almost 6 months. Observations show that the largest difference in ellipticity between surface and bottom mostly occurred during neap tide, suggesting that the water column was stratified, leading to a cross-shore circulation. However, for 3 out of the 11 neap tides no ellipticity difference was observed and during 1 out of the 10 spring tides a strong ellipticity difference occurred. To understand the causes of these irregularities a model was set up with GOTM. Based on the depth-averaged currents the barotropic pressure gradient is determined. Using a simple advection equation the salinity profile was estimated at the measurement location and used as input for the model. We were able to simulate the overall characteristics of the observed flow patterns. Model results show a strong link between wind stress magnitude and direction and reduced stratification during low energetic neap tides. An increased fresh water discharge was the cause for the strong ellipticity difference during spring tide. The strong effect of wind speed and direction on the onset of stratification of the Rhine ROFI has never been shown before. Furthermore, the results show that during the 150 days of observations the plume always reached IJmuiden.

INTRODUCTION

The focus of this paper is on the effect of the Rhine outflow, tidal conditions and meteorological forcing on the velocity profiles near the port of IJmuiden. A better understanding of the effects of human interventions (for example the construction of Maasvlakte 2) on the transport of freshwater and fines near the Dutch coast is needed and measurements play a crucial role therein. The river Rhine debouches into the North Sea near the port of Rotterdam. It creates a buoyant freshwater plume that drives a coastal current to the north due to the Coriolis force. The resulting cross-shore and alongshore density differences have a clear imprint on the tidal and on the tidally averaged currents. Averaged over tides the freshwater plume drives a mean circulation to the north and a circulation in the cross-shore where currents near the bottom are directed landward and seaward near the surface. This circulation transports suspended matter to the coast and is one of the reasons of the increased mud transport in the nearshore region. The interaction between tides, vertical mixing and stratification may result in periodic stratification. While on the one hand tides cause mixing of the water column, on the other hand the shear in the tidal currents results in transport of fresher water over saline waters, reducing mixing and enhancing stratification. These competing mechanisms can be captured by the Simpson number (horizontal Richardson number) as defined in *Stacey et al.* [2001] based on the earlier work on strain induced periodic stratification (SIPS) of the Rhine ROFI by *Simpson* [1990]:

$$Ri_x = \frac{\beta g S_x H^2}{u_*^2} \qquad (1)$$

where S_x is the horizontal salinity gradient, β=7.7 10^{-4} PSU^{-1} is the influence of salinity on the density, g is gravitational acceleration, H is water depth and u_* is the friction velocity. When the Simpson number is larger than a critical value (typically taken as 0.1) the water column can be stratified near neap tides but well-mixed near spring tides, for smaller than critical values the water column is well-mixed during the entire spring-neap cycle, for much larger than critical values the water column is stratified during the whole spring-neap tidal cycle. When the water column is stratified this strongly impacts on the observed tidal currents. Stratification results in reduced mixing, causing the upper and lower water column to decouple, which results in opposite rotating current vectors in the top and bottom layers [*Souza and Simpson*, 1996]. These counter rotating currents result in periodic up- and downwelling near the coast [*de Boer et al.*, 2009], affecting stratification but also the transport of fines.

The vertical structure of the freshwater plume is also affected by winds. *Munchow and Garvine* [1993] and *Visser* [1994] argue that upwelling winds enhance stratification, while downwelling winds reduce it. *Joordens et al.* [2001] have shown how a period of strong downwelling winds may have limited the freshwater transport and hence intensified density gradients. When the wind relaxed the enhanced density gradients drove a stronger flow, enhancing mean and semi-diurnal stratification. Wind driven currents may also enhance mixing thereby reducing the vertical salinity gradients.

The aim of this paper is to study the effect of tides, winds and waves on the hydrodynamics near IJmuiden. We have a unique half year dataset of observed 1D velocity profiles and for two periods of 26 and 10 days, respectively, also concurrent salinity and temperature observations. Using these data and the model results obtained with the GOTM model we will show the dynamic nature of the plume near IJmuiden and discuss the effects of wind and tides on the onset of stratification and the imprint on the observed velocity profiles.

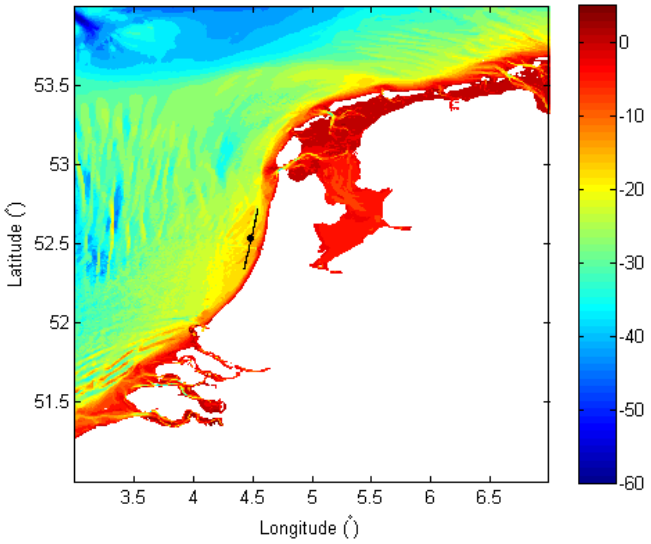

Figure 1. Bathymetry in the Dutch part of the Southern North Sea. The black dot indicates the location of the mooring and the drawn line shows the tidal 'ellipse'.

MEASUREMENTS

A broadband 1200 kHz Acoustic Doppler Current profiler (ADCP) was moored on the bottom at 52° 32'N and 4° 29'E.This is about 7 km offshore from IJmuiden (the Netherlands) and 65 km North East of the Rotterdam harbor. There the bulk of the river Rhine outflow enters the North Sea. The mooring was deployed on August 24, 2007 and recovered on January 22, 2008 leading to a time-series of 150 days. The ADCP has four transducers at an angle of 30°. It uses the Doppler shift to measure the velocity in these four directions. An internal compass is used to transform the velocities into earth coordinates and additionally an estimate of the error is given. The cell size and the blanking distance were 0.5 m. The lowest bin was located at 1.78 m above the bottom. We used 30 pings per ensemble and 25 seconds per ping. The ensembles were stored every 15 minutes.

Within 100 m of the location of the ADCP a lander was placed containing a Sea-Bird SBE37. It recorded every 5 minutes the salinity, temperature and pressure at 1.5 m above the bed from August 23 to September 17, 2007 and from 1 to 10 October, 2007.

Unfortunately, the ADCP was not equipped with a pressure sensor, so the exact depth of the water column was not recorded. For the days the lander and ADCP measured concurrently the water surface was determined by the lander. For the other days the water surface was estimated by determining the cell number at which the backscatter intensity gradient is maximal for each different beam separately. This cell number was corrected for pitch and roll. This leads to four estimates of the cell number in which the surface is located. After despiking the depth estimates with a median filter over a window length of 7 and a detection limit of 1, the average is taken over each of the four beams. However, if the standard deviation between the four estimates is larger than 0.5 the data is discarded. The depth levels and velocities have been corrected for the true speed of sound, which was set at its default value of 1500 m/s. The velocity data was transformed onto sigma coordinates. A total of 25 levels was adopted in the vertical equally distributed over the total

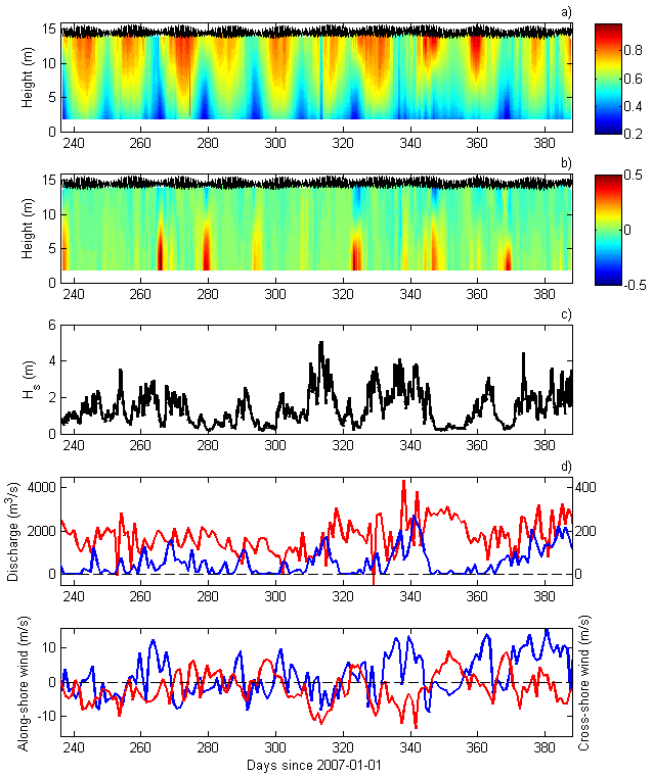

Figure 2. a) Semi-major axis (m/s) and b) ellipticity of the M2 tidal ellipse for each depth cell; c) Significant wave height at IJmuiden; d) fresh water discharge (thin line and left axis: Rhine at Hoek van Holland; thick line and right axis: North Sea Channel at IJmuiden) from www.waterbase.nl e) Wind speed in the alongshore (left, blue) and cross-shore direction (right, red) from www.knmi.nl.

measurement depth, e.g. from the lowest to the highest bin. This leads to an average bin size of about 0.5 m, which is similar to the original bin size.

OBSERVATIONS

First, a least squares harmonic analysis (LSHA) with a window length of 15 days was applied to the depth averaged eastward and northward velocity. For this the T-TIDE package [*Pawlowicz*, 2002] was used. The 35 most important tidal constituents and shallow water constituents were used in the analysis. A total of 84 (94) % of the total variance is explained in the eastward (northward) direction. The residual depth average velocity is only (u_0, v_0) = (0.4, 2.9) cm/s. From the results of the LSHA, the M2 tidal ellipse parameters were determined. The semi-major axis was relatively small: 0.56 m/s. The ellipticity is ε=-6·10^{-3}, indicating that the depth averaged flow was almost rectilinear on the dominant M2 tidal frequency. The inclination was 72.8°, which is comparable to the local orientation of the coast and the bathymetry (Figure 1). The velocities in all sigma layers were rotated over this angle to determine the along- and cross-shore velocity, (u,v).

Next, the depth-varying cross-shore and alongshore currents were analyzed using a running mean LSHA with a window length of 25 hours. Only the M2 tidal constituent was retrieved and

attributed to each sigma level. Also the tidal ellipse parameters were derived. The semi-major axis and the ellipticity for the 150 day time-series are shown in Figure 2a,b. The semi-major axis showed the dominant spring-neap tidal cycle and a decrease in speed over depth. Not all variability of the major axis can be attributed to the spring-neap cycle.

The ellipticity (Figure 2b) showed several events with a large difference between the surface and near bottom value. Such a difference is usually an indication of the presence of stratification [*Souza and Simpson*, 1996]. In these cases the ellipses near the surface (bottom) rotate (counter)clockwise. The largest top-bottom ellipticity differences occurred around days 236, 265, 279, 323, 346 and 369 when the maximum difference in ellipticity between the bottom and the surface exceeded 0.4.

Most events with large ellipticity differences occurred during neap tide, except for the one on day 346 (2007-12-12), which is exactly at maximum spring. The conditions during this event were characterized by weak winds directed offshore and significant wave heights less than 1 m. Moreover, this event was preceded by a peak in fresh water discharged from the North Sea Channel (IJmuiden), likely enhancing the horizontal stratification locally/temporally.

Focusing on the neap tides; only a weak ellipticity difference was found on days 293, 338 and 384 and no significant events occurred on days 249, 307 and 352. The significant wave height and wind speed were small on day 249 and 307, but winds were directed onshore, favoring downwelling and thereby relaxing stratification, if present. Although waves were small and wind direction was offshore on day 352, wind speeds exceeded 10 m/s the day before, which probably induced strong mixing.

MODELING WITH GOTM

In the hydrographic measurements we have observed events of strong ellipticity difference between the surface and the bottom during one spring tide and most but not all neap tides. Although, previous studies suggest this is caused by a stratified water column, we do not have direct measurements to proof this. However, we have observations of the salinity and temperature near the bottom during almost 35 days. Using the available data and a model we try to simulate the hydrodynamics and salinity dynamics in the vertical. For this purpose we used the General Ocean Turbulence Model (GOTM, see *Umlauf and Burchard*, [2005] for a review) to model the hydrodynamic behavior of the currents near IJmuiden under certain conditions. GOTM is a one-dimensional water column model for marine applications. It is coupled to a choice of traditional as well as state-of-the-art parameterizations for vertical turbulent mixing. In the model runs below, we use a standard second order turbulent closure model.

Setup and forcing conditions

The model was set up for a column at the location of the mooring in the North Sea where the total depth was 14.5 m. The column was divided into 35 levels and the time step was set to 100 s. The model was forced with an external pressure gradient which was inferred from the depth averaged velocities measured with the ADCP. A linear equation of state was used:

$$\rho = \rho_0 + \alpha(T - T_0) + \beta(S - S_0) \qquad (2)$$

in which ρ_0=1022 kg/m^3 is a reference density and T_0=17.4 °C and S_0=31.8 are the reference temperature and salinity. These are the averaged values from the measurements of the nearby CTD. The thermal and haline expansion coefficients are α=-0.2316 kgm^{-3}K^{-1} and β=0.7741 kgm^{-3} and were derived by least-squares fitting equation (1) to the data. Note that this definition of β differs from the one used for the horizontal Richardson number in equation (1) in the introduction. Meteorological forcing was obtained from KNMI (Royal Dutch Met Office) and the wind vector was rotated in an alongshore, τ_x, and cross-shore, τ_y, component.

The horizontal temperature and salinity gradients need to be prescribed in GOTM to generate estuarine type velocities. Since we did not have direct measurements of these values we derived them from least squares fitting a simple advection equation to the in-situ measurements of the velocity and (time-derivative) of the salinity or temperature:

$$\frac{\partial \theta}{\partial t} = -u\frac{\partial \theta}{\partial x} - v\frac{\partial \theta}{\partial y} \qquad (3)$$

which was discretized in the following way:

$$\frac{\theta^{n+1} - \theta^n}{\Delta t} = -0.5(u^{n+1} + u^n)\theta_x - 0.5(v^{n+1} + v^n)\theta_y \qquad (4)$$

where θ is T or S and x (y) is in the alongshore (cross-shore) direction and positive to the north northeast (offshore). Assuming that the horizontal gradients are relatively constant near the bottom for a period of two tidal cycles, a running least squares analysis was applied with a window length of 25 hours. The measurements of the CTD were close to the bottom, thus the alongshore and cross-shore velocities in the lowest sigma level were used. To suppress fast variations in the tracers, first a five-point running mean filter is applied to θ, before calculating its time-derivative.

The salinity gradients in the alongshore and cross-shore direction (Figure 3a) show one prominent relatively broad peak around day 279 w

ith a cross-shore gradient of S_y=6·10^{-4} m^{-1}. The R^2 was usually relatively low, except between days 278 and 280, where it was above 0.6. During this period the alongshore gradient, S_x, was negative, suggesting that the downstream salinity was lower. This could be caused by the pulse-like behavior of the river plume [*de*

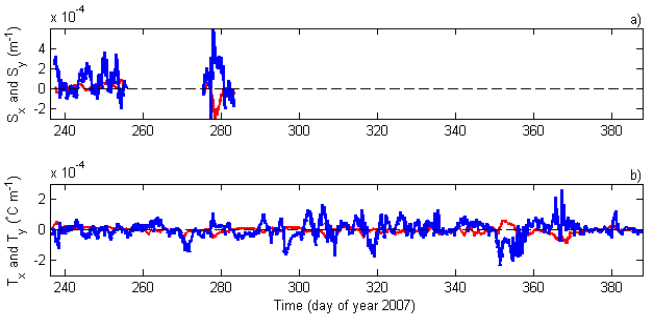

Figure 3. Horizontal gradient in the a) salinity and b) temperature in the alongshore (blue) and cross-shore (red) direction with positive values being to the north northeast in the x-direction and offshore in the y-direction.

Table 1: Experimental setups.

Experiment #	Alongshore salinity gradient, S_x (m^{-1})	Cross-shore salinity gradient, S_y (m^{-1})	Alongshore wind stress, τ_x (Nm^{-2})	Cross-shore wind stress, τ_y (Nm^{-2})
1a	0	$3.75 \cdot 10^{-4}$	0	0
1b	0	$3.75 \cdot 10^{-4}$	Realistic	Realistic
1c	As Fig. 3a	As Fig. 3a	Realistic	Realistic
2a	$-2.0 \cdot 10^{-4}$ to $6.0 \cdot 10^{-4}$	0	0	0
2b	0	$-2.0 \cdot 10^{-4}$ to $6.0 \cdot 10^{-4}$	0	0
3a	0	$3.75 \cdot 10^{-4}$	-0.6 to 0.6	0
3b	0	$3.75 \cdot 10^{-4}$	0	-0.6 to 0.6

Ruijter et al., 1997]. The ellipticity difference at day 237 also seems to be correlated with a peak in the cross-shore salinity gradient, S_y. Note that, of this peak only the second half was captured in the data.

At days 244, 245 and 250 no ellipticity difference was found (Figure 2b), although peaks of similar size were found in the cross-shore salinity gradient, S_y. Especially, the latter is interesting, because it occurred during neap tide. Temperature gradients do not appear to be related to salinity gradients (Figure 3b).

Basic Experiments

We have set up a set of experiments to simulate the hydrodynamics and salinity dynamics as a function of the salinity gradient in the alongshore and cross-shore direction, the local wind stress (Table 1) and the barotropic pressure gradient that drive the tidal flow. In experiment 1a we forced the model with a constant cross-shore salinity gradient of $S_y=3.75 \cdot 10^{-4}$ m^{-1} (other gradients including those for the temperature are set to zero) and an external pressure gradient based on the depth-averaged velocities as in *Burchard* [1999]. A realistic sea level variation based on the measurements was also imposed, but wind and waves were neglected. In experiment 1b, added to this a realistic meteorological forcing was applied, derived from measurements by KNMI in IJmuiden, Wijk aan Zee, Schiphol and de Bilt. In experiment 1c, instead of a constant cross-shore salinity gradient, the horizontal gradients as depicted Figure 3 were imposed (including the temperature gradients). Note that salinity gradients were assumed to be zero in the period for which we do not have measurements, e.g. from day 261 to 274 and from day 284 onwards.

We focus on the model results around day 280. This was a strong event for which we have the meteorological forcing as well as a good estimate of the horizontal temperature and salinity gradients. Figure 4 shows that both a realistic wind stress forcing and a realistic horizontal density gradient are essential to reproduce the phenomenon. If a constant horizontal cross-shore salinity gradient was imposed of $S_y=3.75 \cdot 10^{-4}$ m^{-1} an event with an

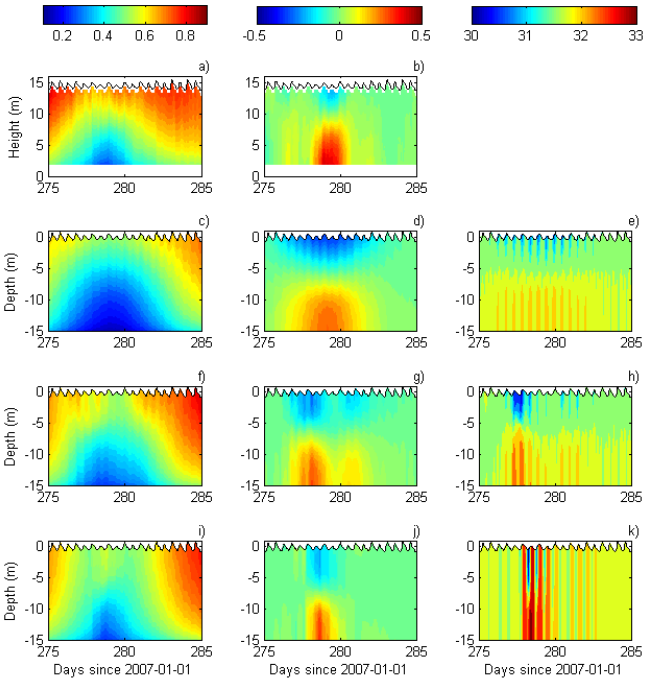

Figure 4. Left: Semi major axis (m/s), middle: ellipticity and right: salinity as a function of depth and time from the measurements (top panel) and the model simulations with constant $S_y=3.75 \cdot 10^{-4}$ m^{-1} (second panel), with realistic wind stress forcing (third panel) and with horizontal gradients from Figure 3 (bottom panel).

ellipticity difference is reproduced, but the negative values of the ellipticity at the surface are too large compared to observations (exp. 1a and Figure 4c,d,e). The period with large ellipticity differences started earlier and continued longer compared with the measurements. Moreover, the semi-major axis showed that the velocities throughout the entire spring-neap tidal cycle and at every sigma level were underestimated by the model. The model output indeed showed a relation between the ellipticity difference

and a periodic (salinity) stratification with a maximum difference of ΔS_{max}=1.6 PSU. Imposing a realistic meteorological forcing (exp. 1b and Figure 4f,g,h), resulted in improved correspondence between modeled and observed semi-major axis. The ellipticity difference became much more comparable to those in the measurements, however the timing of the event was still wrong. In fact, the event seemed to split up into two different events. The periodic stratification became stronger, ΔS_{max}=2.2 PSU, and is still correlated with the ellipticity event(s). When the model was forced by the observed salinity and temperature gradients (exp. 1c and Figure 4i,j,k), the timing and duration of the ellipticity event corresponded much better with the measured ones, although the modeled values of the ellipticity are a little too small, which suggests that the horizontal gradients are slightly different from the ones found in Figure 3. The periodic salinity stratification still only occurs during the ellipticity event and was slightly larger, ΔS_{max}=2.4 PSU. Now also a periodic pattern was observed before and after the event, but with salinity values being constant throughout the entire water column. Overall, the model was quite sensitive to the forcing and best model-data agreement was obtained when the model had the most realistic forcing.

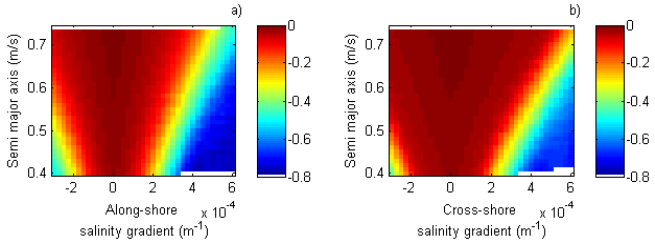

Figure 5. Ellipticity difference between the surface and bottom level for different values of the alongshore and cross-shore salinity gradient, S_x and S_y, as a function of the depth-averaged semi-major axis.

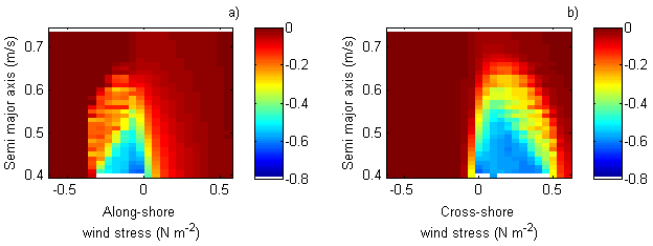

Figure 6. Same as Figure 5 but for the a) alongshore and b) cross-shore wind stress at a constant value of the horizontal salinity gradient $S_y=3.75\cdot10^{-4}$ m^{-1}.

Horizontal salinity gradient

In a second series of experiments the (fixed) alongshore salinity gradient was varied between S_x = -2.0·10^{-4} and 6.0·10^{-4} m^{-1}, while the cross-shore salinity gradient was kept zero (exp. 2a and the other way around in exp. 2b). The M_2 tidal ellipse parameters were calculated for one spring neap tidal cycle. The ellipticity difference between the top and the bottom level was calculated and bin-averaged with respect to the depth-averaged value of the semi-major axis. The results are shown in Figure 5.

The ellipticity difference became increasingly more negative for higher salinity gradients as the ellipticity was negative at the surface and positive near the bottom. The ellipticity difference was close to zero when the salinity gradient was small. For quite a large portion of the phase space, the ellipticity difference was well below -0.1 but became more negative for larger negative values of the gradient. There was a sharp transition from conditions which result in a small difference in ellipticity between surface and bottom and conditions that resulted in large differences. For larger depth-averaged currents this transition occurred for stronger horizontal salinity gradients. The transition from small to large ellipticity differences (stratification) seemed to increase linearly as a function of tidal flow velocity. It occurred for values around $S_{x,y}$=2.0·10^{-4} m^{-1} at neap tide and at S_y=6.0·10^{-4} m^{-1} and S_x=5.0·10^{-4} m^{-1} during spring tide. This figure clearly points out that the existence of an ellipticity difference is not solely connected to the neap tide, but may last throughout an entire spring-neap tidal cycle for horizontal cross-shore salinity gradients above S_y=6.0·10^{-4} m^{-1}. This value corresponds with the maximum observed value during the measurement period (Figure 3a). Obviously, stratification events can be completely absent if the cross-shore salinity gradient remains below S_y=1.0·10^{-4} m^{-1}.

Note that Figure 5a and b are not entirely symmetric around $S_{x,y}$=0 m^{-1}. This is because the system is not entirely symmetric. The barotropic forcing, which is based on the in-situ measurements gives rise to a small positive alongshore current. Besides that, the periodic stratification took place during the flood phase of the tide, if a positive cross-shore salinity gradient was applied and during the ebb phase, if the cross-shore salinity gradient was negative.

Wind stress

The effect of the wind stress on the ellipticity (as a proxy for stratification) was investigated in two series of experiments in which the alongshore (exp. 3a) and cross-shore (exp. 3b) wind stress was varied, respectively. In these experiments the cross-shore horizontal salinity gradient was fixed to S_y = 3.75·10^{-4}, the average value observed during our measurements. The wind-stress was varied from -0.6 to +0.6 Nm^{-2} in both directions separately. The maximum observed wind speed was 16 m/s, which corresponds to a wind stress of about $\tau=\rho_a C_D U^2 \sim 0.5$ Nm^{-2} with the density of air ρ_a=1.3 kgm^{-3} and a drag coefficient C_D=0.0015. Figure 6 shows the ellipticity difference as a function of the alongshore and the cross-shore wind stress at a constant horizontal salinity gradient. The ellipticity difference was small for positive alongshore or downwelling (Figure 6a) and negative cross-shore or onshore winds (Figure 6b). The effect was largest by the cross-shore winds. Onshore winds generated a small net onshore current, which caused saline water to be transported over fresher waters, resulting in enhanced vertical mixing and no stratification.. Negative alongshore winds (northerlies) and offshore winds generated an ellipticity difference. Both were characterized by an estuarine type of circulation around a large part of the neap phase (not shown). This exchange flow was enhanced by advection of fresher water over saline water, increasing stratification. Figures 6a and b are not mirror images, since the effect of a cross-shore current is much more direct than that of an alongshore currents. Thus, by inducing a cross-shore current, wind forcing can either increase or reduce the stratifying effect and thereby control the occurrence of an ellipticity (and stratification) event.

DISCUSSION AND CONCLUSIONS

In an analysis of the ellipse parameters in a unique 150-day long time-series of the horizontal velocity profiles, several events were observed during which a strong ellipticity difference occurred between the bottom and the surface. These events can be related to periodic stratification events, although no direct measurements are available of the stratification. The events seem to occur in regular intervals and to be correlated with the neap phases of the spring-neap tidal cycle. However, during 3 out of 11 neap phases of the tide no ellipticity difference was found, while during 3 others only a small signal could be observed. Moreover, such an ellipticity event was found even during one out of the 10 spring phases of the tide. Hence, the relation between the occurrence of an ellipticity (or stratification) event is more complicated than a simple correlation with the spring-neap tidal cycle.

The gross characteristics of the vertical salinity profile and tidal velocity profile could be simulated using the one-dimensional vertical column General Oceans Turbulence Model (GOTM). The model was forced with observed depth-averaged velocities, horizontal salinity gradients and wind.

A series of experiments showed a quick transition from no ellipticity difference (hence, no stratification) to strong ellipticity

differences (stratified water column) between the surface and bottom. This transition was a function of the horizontal salinity gradient, the magnitude of the depth-averaged currents and wind speed and direction. Stronger tidal currents resulted in less stratification, while increased spatial differences in salinities enhanced stratification. We further showed that wind has a very strong influence on the occurrence of stratification events. Landward directed and downwelling favoring alongshore winds diminished the effect of a significant cross-shore salinity gradient, while seaward directed and upwelling favoring winds enhanced stratification and the presence of ellipticity differences.. The effect of wind will probably even be stronger in 3D models when the presence of a nearby coast poses a boundary for onshore directed currents.

Using the model results, the absence or weakness of events during neap tides could all be explained by unfavorable wind directions or strong wind force. The stratification event that occurred during spring tide was preceded by a discharge event at the sluices of IJmuiden, thereby enhancing horizontal salinity gradients, and occurred during a period with weak offshore directed winds that enhanced the stratification.

Clearly, the existence of these events showed that the stratified region of the Rhine ROFI indeed reaches all the way to IJmuiden. Stratification could lead to an ellipticity event during neap tide, but since the horizontal salinity gradients were relatively small, any counteracting influence, such as the wind force or direction could already suppress such an event.

REFERENCES

de Boer, G. J., Pietrzak, J. D. and Winterwerp, J. C. (2009) SST observations of upwelling induced by tidal straining in the Rhine ROFI. Continental Shelf Research, 29, 263-277.

Burchard, H. (1999) Recalculation of surface slopes as forcing for numerical water column models of tidal flow. Applied Mathematical Modelling, 23, 737-755.

Joordens, J. C. A., Souza, A. J. and Visser, A. (2001) The influence of tidal straining and wind on suspended matter and phytoplankton distribution in the Rhine outflow region Continental Shelf Research, 21, 301 – 325

Münchow, A. and Garvine, R. W. (1993) Buoyancy and wind forcing of a coastal current. Journal of Marine Research, 51, 293-322.

Pawlowicz, R., Beardsley, B. and Lentz, S. (2002) Classical tidal harmonic analysis including error estimates in MATLAB using T_TIDE. Computers and Geosciences, 28, 929-937.

de Ruijter, W.P.M., Visser, A.W. and Bos, W.G. (1997) The Rhine outflow: A prototypical pulsed discharge plume in a high energy shallow sea. Journal of Marine Systems, 12, 263 - 276.

Simpson, J. H., Brown, J., Matthews, J. and Allen, G. (1990) Tidal Straining, Density Currents, and Stirring in the Control of Estuarine Stratification, Estuaries, 13, 125-132.

Souza, A. and Simpson, J. H. (1996) The modification of tidal ellipses by stratification in the Rhine ROFI. Continental Shelf Research, 16, 997-1007.

Stacey, M. T., Burau, J. R. and Monismith, S. G. (2001) Creation of residual flows in a partially stratified estuary. Journal of Geophysical Research, 106, 17013-17037.

Umlauf, L., and Burchard, H. (2005) Second-order turbulence closure models for geophysical boundary layers. A review of recent work, Continental Shelf Research, 25, 795-827.

Visser, A.W., Souza, A. S., Hessner, K. and Simpson J. H. (1994) The effect of stratification on tidal current profiles in a region of freshwater influence. Oceanologica Acta, 17, 369-381.

DOI: 10.3990/2.192

Modeling plan-form deltaic response to changes in fluvial sediment supply

J.H. Nienhuis[1], A.D. Ashton[2], P.C. Roos[1], S.J.M.H. Hulscher[1], L. Giosan[2]

[1] Water Engineering and Management, University of Twente, P.O. Box 17, 7500 AE Enschede. jhnienhuis@gmail.com; P.C.Roos@utwente.nl; S.J.M.H.Hulscher@utwente.nl

[2] Geology and Geophysics Department, Woods Hole Oceanographic Institution, MS #22, 360 Woods Hole Rd., Woods Hole, MA 2543, aashton@whoi.edu

ABSTRACT

This study focuses on the effects of changes in fluvial sediment supply on the plan-form shape of wave-dominated deltas. We apply a one-line numerical shoreline model to calculate shoreline evolution after (I) elimination and (II) time-periodic variation of fluvial input. Model results suggest four characteristic modes of wave-dominated delta development after abandonment. The abandonment mode is determined by the pre-abandonment downdrift shoreline characteristics and wave climate (which are, in turn, determined by previous delta evolution). For asymmetrical deltas experiencing shoreline instability on the downdrift flank, time-periodic variation in fluvial input influences the evolution of downdrift-migrating sandwaves. The frequency and magnitude of the riverine "forcing" can initiate a pattern that migrates away from the river mouth, interacting with the development of shoreline sandwaves. Model results suggest that long-period signals in fluvial delivery can be shredded by autogenic sand waves, whereas shorter-term riverine fluctuations can dominate the signal of the autogenic sandwaves. The insights provided by these exploratory numerical experiments provide a set of hypotheses that can be further tested using natural examples.

INTRODUCTION

River deltas are dynamic and complex depositional landforms, shaped by marine and fluvial processes. This study aims at identifying and characterizing the long-term (centennial to millennial) response of wave-dominated river deltas to temporal changes in fluvial sediment load.

We select two scenarios: (I) fluvial input elimination and (II) periodic fluvial input variation. The first can be the result of delta channel avulsion, which causes sediment to be routed through a new channel [*Roberts*, 1997], or river damming [*Milliman et al.*, 2008], which can effectively reduce sediment delivery. The Ebro Delta, Spain, is an example of a delta that has experienced both avulsions and, recently, the effects of river damming. Periodic fluvial variation can arise from cyclic climate forcing. These scenarios are studied using an 1-line numerical model of Ashton et al. [2006a].

Galloway [1975] recognized that the environmental controls of river discharge, tidal range and wave energy flux have a first-order morphologic control on delta shape. The dominance of one of these factors makes respectively a river-, tide- or wave-dominated delta. Other reported influences are grain size distribution [*Orton and Reading*, 1993], (relative) sea-level rise [*Giosan et al.*, 2006], human engineering [*Syvitski et al.*, 2009], sediment cohesion [*Edmonds and Slingerland*, 2010], and angular distribution of wave energy [*Ashton and Giosan*, 2011]. This last aspect is also the focus of this research.

The selective treatment of one physical process, only wave-sustained littoral transport, makes this research applicable to wave-dominated deltas.

BACKGROUND

Waves primarily control deltaic shape through the alongshore transport of sediment by breaking waves, called the littoral drift [*Komar*, 1973]. Wave height and approach angle affect the amount of transport. Littoral transport in this model is calculated using the CERC formula, relating the direction and height of the breaking waves to the littoral transport [*Ashton and Murray*, 2006a], equation (1).

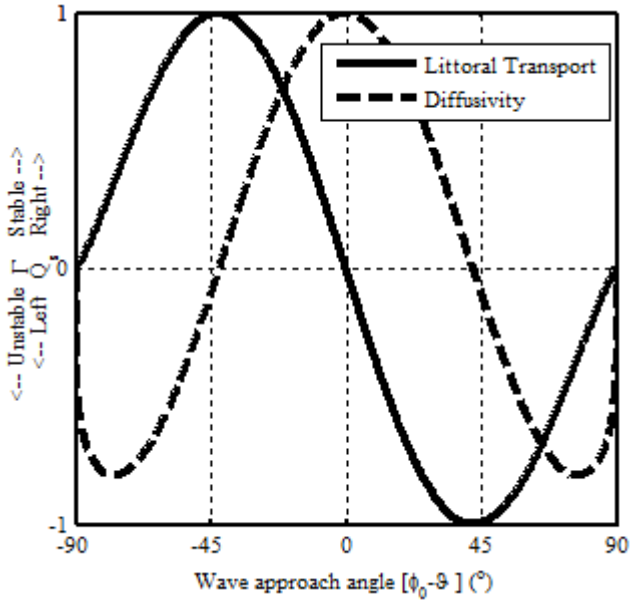

Figure 1: Alongshore sediment transport (Qs) and shoreline diffusivity (I) as a function of wave approach angle (relative between the wave crests and the shoreline).

$$Q_S = K \cdot H_b^{\frac{5}{2}} \cdot \cos(\varphi_b - \vartheta) \cdot \sin(\varphi_b - \vartheta) \qquad (1)$$

K is an empirical constant, which can vary greatly between different sediment types. K is set to 0.34 for all runs. H_b is the breaking wave height. $\varphi_b - \vartheta$ is the difference between the crests of incoming waves (φ_b) and the shoreline orientation (ϑ).

Figure 1 shows the relation between wave approach angle and littoral transport. Transport is zero when waves approach normal to the shore, $\varphi_b - \vartheta$ equals 0°. Maximum transport occurs when deep water waves approach the toe of the shoreface at about 42°.

Appling the Exner equation of sediment continuity along the shoreline gives:

$$D \cdot \frac{\partial \eta}{\partial t} + \frac{\partial Q_S}{\partial x} = f(x,t) \qquad (2)$$

Here, the alongshore derivative in littoral transport $\frac{\partial Q_S}{\partial x}$ (m^2s^{-1}) equals accretion or erosion $\frac{\partial \eta}{\partial t}$ (ms^{-1}) up to the local closure depth D (m), set at 10m. The physical interpretation of this equation, with D constant and one description for the shoreline position η, is that cross-shore dynamics can be superimposed on alongshore behaviour, such that one typical cross-shore profile suffices to describe long-term coastal change. Assuming that sandy, bed-load sediment remains confined close to the shore, erosion or accretion of the shore is proportional to the divergence of this transport [*Ashton and Murray*, 2006a]. The source term $f(x,t)$ (m^2s^{-1}) represents the coarse-grained fluvial sediment kept in the nearshore zone.

The combination of equation (1) and (2) leads to a diffusion equation. The diffusion coefficient, Γ, figure 1, controls the rate that approaching waves can cause plan-view shoreline perturbations to decrease (stable shoreline, $\Gamma>0$) or increase (unstable shoreline, $\Gamma<0$) [*Ashton and Murray*, 2006b].

Previous model results suggest that, as downdrift shorelines experience higher angle waves, they have an increased probability of spit formation and shoreline instability [*Ashton and Giosan*, 2011]. Higher waves increase littoral transport away from the delta, thus decreasing the plan-view cross-shore extent (due to an increased diffusivity) [*Komar*, 1973].

SHORELINE EVOLUTION MODEL

The model uses the "one-contour-line" approach to calculate fluxes of sediment and subsequent shoreline orientation across computational cells. Adding "fluvial" sediment in a cell at a predefined position and time, $f(x,t)$, along the shore simulates the plan-view evolution of a wave-dominated delta [*Ashton and Giosan*, 2011].

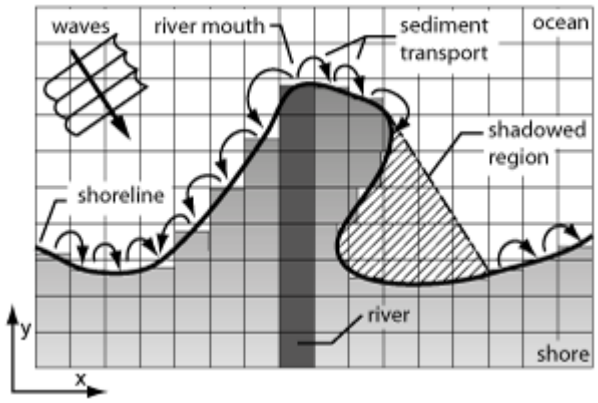

Figure 3: Schematic overview of the model domain. Wave and shoreline orientation determine fluxes between cells, which can be shadowed from other cells. (After Ashton and Murray 2006a)

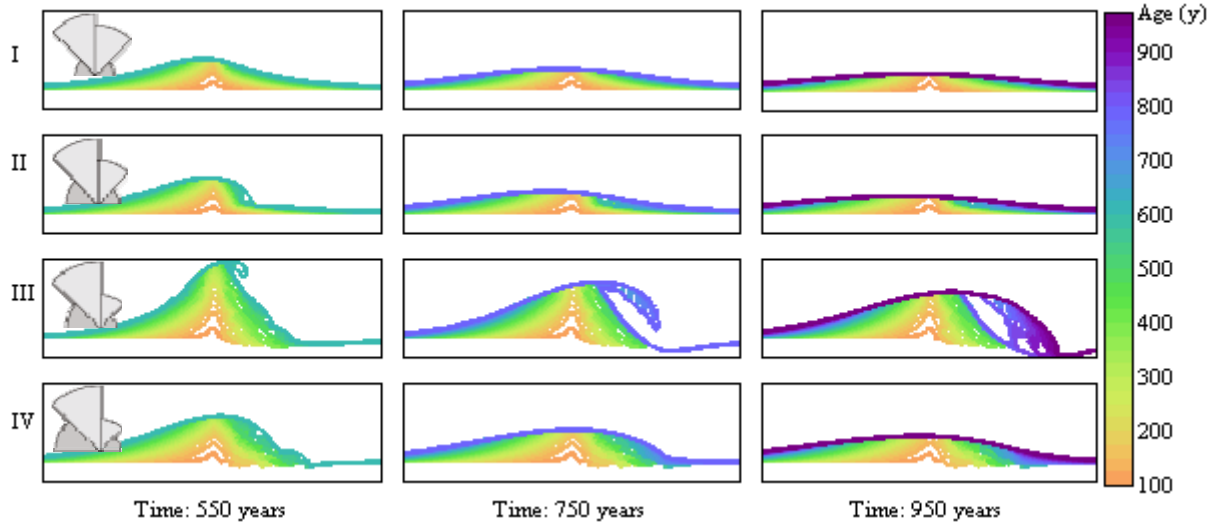

Figure 2: Examples of the four identified modes of lobe abandonment. Lines show the shoreline position, colored according to the time of deposition. Abandonment occurs after 500 years; three snapshots show delta buildup 50, 250 and 450 years after elimination of fluvial sediment supply (at time = 500 years). (I) Diffusive Mode; (II) Discontinuous Mode; (III) Spit Mode; (IV) Sandwave Mode. The wave-rose insets show the angular distribution of wave energy that is used throughout the simulations. NB. All other parameters are left constant between these runs. (fluvial bedload: 100kgs^{-1}; deep water waveheight (1m); wave period (8s))

The plan-view coastal zone is discretized (Figure 3) into 200m square cells. A fractional value F describes the portion of subaerial surface of each cell, being between 0 and 1 if the cell is part of a shoreline. If F equals 1, the cell consists entirely of "land". The algorithm uses F to trace the location and orientation of the shore within a cell. Shore location is a fraction of the cell length perpendicular to the subaerial neighbour. The position of the adjoining shores determines the orientation.

Each time step, set at 1 day, a wave direction is picked from a probability distribution. Wave height is set constant in the simulations. These waves then determine the amount of sediment transport across neighbouring shoreline cells, using equation (1).

RESULTS I: ABANDONMENT BEHAVIOUR

Model runs show four characteristic morphologic scenarios that can develop when deltas are cut off from their sediment supply: (I) diffusive mode, (II) discontinuous mode), (III) spit mode and (IV) a (shoreline) sandwave mode (Figure 2).

The 'diffusive' mode occurs when the initial delta has a classic cuspate shape, and both updrift and downdrift shoreline are stable. The delta shape is flattened by alongshore transport gradients, with erosion around the river mouth, and deposition further away.

The 'discontinuous' mode arises when the downdrift delta shore is near the limit of instability, Γ is close to 0. There is a discontinuity in the shoreline orientation where Γ becomes positive. This discontinuity migrates downdrift, eroding parts of the delta. Infilling of these sections by younger sediments occurs, but flattening of the shoreline happens rapidly, such that it does not result in the formation of a spit.

When a larger downdrift section is unstable (Γ<0), a spit grows that migrates away from the old river mouth. The steeper downdrift shoreline causes spits to shadow and erode deltaic and non-deltaic sediments.

Finally, highly unstable wave climates trigger the formation of shoreline sandwaves (IV) on the downdrift delta even before abandonment. Increased sediment transport away from the river mouth decreases the overall plan-view extent. Abandonment creates a spit that collapses near the river mouth. The influence of the delta geometry before abandonment on the future evolution is demonstrated by plotting two characteristics of the downdrift shoreline, that extends from the river mouth to the delta foot: diffusivity (Γ) and steepness ($\tan^{-1}(\frac{y}{x})$, °) (Figure 4). A steep downdrift shoreline, which is unstable at the current wave conditions, generates a spit.

Along the Mediterranean coast, several deltas show morphologic features that can be placed in this framework. The Ebro delta, Spain, provides a remarkable example of where reworking of lobes has caused the growth of spits [*Canicio and Ibanez*, 1999]. There is also lobe reworking at the Rhone delta, France [*Vella et al.*, 2005], suggesting evidences of a growing discontinuity and a spit. Diffusive reworking seems to take place at the Ombrone River, Italy [*Pranzini*, 2001].

RESULTS II: PERIODIC INPUT VARIATION

Periodic variations in sediment load have several interesting consequences for delta development, particularly when the downdrift coast is experiencing unstable wave conditions. We will discuss the effects on downdrift-extending shoreline sandwaves and general delta stratigraphy.

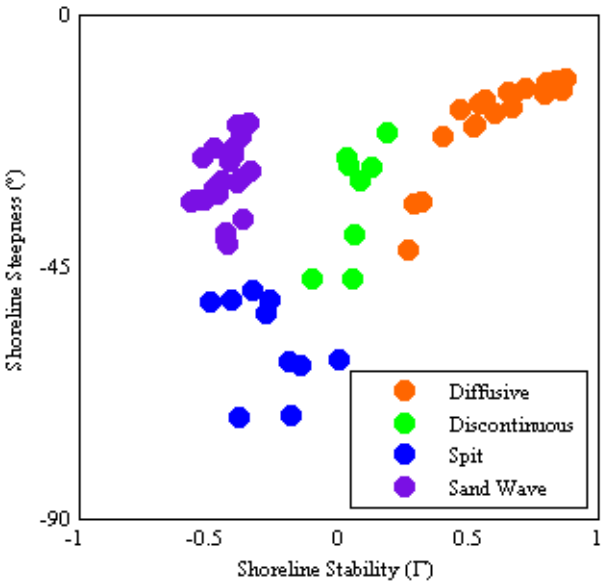

Figure 4: The abandonment framework plots the four visually characterized modes dependent on downdrift shoreline stability (or: net diffusivity) and steepness. Different wave heights (0.8/0.9/1.0m), fluvial input (80,100,120 kgs^{-1}) and wave climates are used to generate these results.

Sandwaves grow when a large portion of the shoreline is unstable (i.e. experiencing predominantly high-angle waves). The frequency and size of these autogenic features depends on wave climate and beach characteristics [*Ashton and Murray*, 2006a]. Sandwaves can also develop allogenically (that is, forced externally), as the river mouth location oscillates between periods of high and low fluvial sediment input.

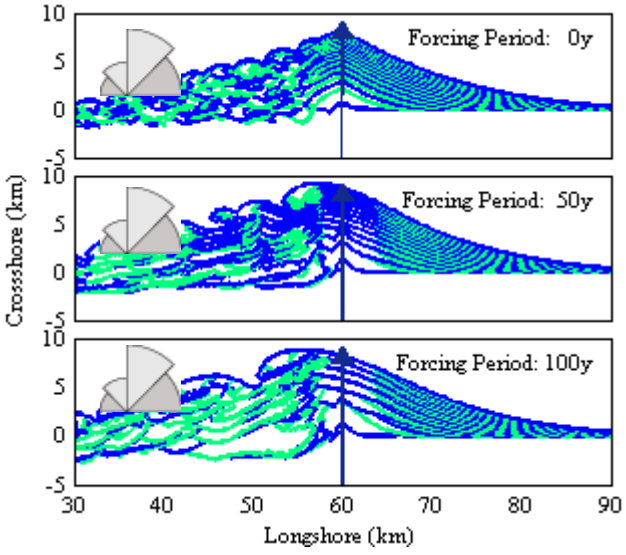

Figure 5: Downdrift (30-60km) and updrift (60-90km) shoreline locations drawn with a 50 year interval for different periods of on-off fluvial variability, 50% in this case (i.e. 150-50-150 kgs^{-1}).The wave-rose insets plot the angular distribution of wave energy.

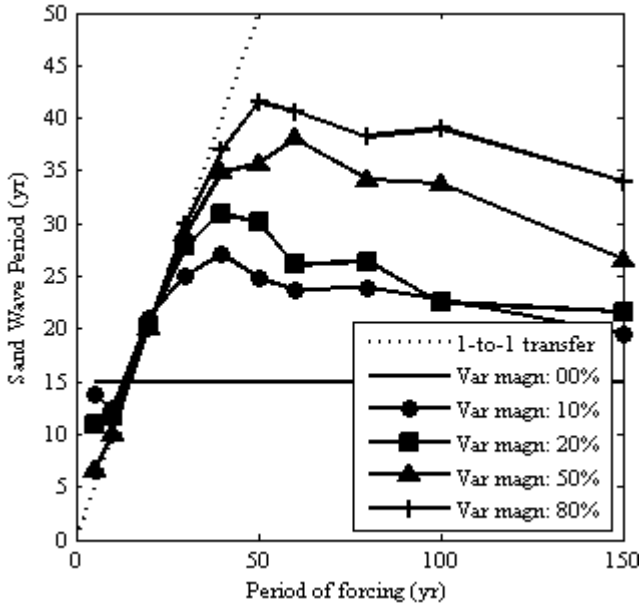

Figure 6: Period of forcing (fluvial sediment load) compared to the measured period of downdrift shoreline sand waves. The percentages indicate the amount of fluctuation (e.g. 50% is: 150-50-150 etc).

Longer forcing periods change the shape of downdrift features, leaving a distinct imprint in the plan-view deltaic stratigraphy, figure 5.

We looked at the generation of these (allogenic) sandwaves in relation with (autogenic) sandwaves that form at the unstable downdrift shoreline (Figure 6). There is a 1-to-1 transfer of frequencies when the forcing period is close to the autogenic period, 15 years in this case. Above and below this period of forcing, different frequency sandwaves interact. The amount of variation and the frequency both determine if a signal can be preserved. These preliminary numerical experiments suggest potential detection limits of climate patterns in marine stratigraphy.

CONCLUSION

Shoreline simulations with different fluvial scenarios provide a series of hypotheses that can be further tested through comparison with natural examples. Features modeled and shown in this paper all arise from one feedback inherent in alongshore littoral transport. Other natural processes can and will change the frameworks and other findings presented here.

We identify four distinct modes in which lobe abandonment can take place. The shoreline shape and wave climate determine how littoral transport reworks the plan-view delta. Going from high to low downdrift instability, abandonment can be characterized by the following modes: diffusive, discontinuity, a spit, or sand waves. These features form primarily during the abandonment phase of the delta.

Time-periodic variations in sediment supply may drastically alter delta development and depositional trends. Signals in sediment input can force their frequency on downdrift autogenic instability. Due to differences in sand wave celerity, self-organization can potentially shred a climate signal. Sediment variability results in concave beach ridges updrift and lagoon formation in downdrift deposits.

Changes in riverine sediment input rework a deltaic shoreline. Several feedbacks between the shoreline and its reworking wave climate create a wide range of potential developments. Understanding these conditions helps determine the style and results of historical, current and future delta evolution. Research is needed to provide further comparison with natural systems.

REFERENCES

Ashton, A. D., and A. B. Murray (2006a), High-angle wave instability and emergent shoreline shapes: Modeling of sand waves, flying spits, and capes, *J. Geophys. Res.*, *111*, F04011.

Ashton, A. D., and A. B. Murray (2006b), High-angle wave instability and emergent shoreline shapes: Wave climate analysis and comparisons to nature, *J. Geophys. Res.*, *111*, F04011.

Ashton, A. D., and L. Giosan (2011), Wave-angle control of delta evolution, *Geophys Res Lett*, *38*, L13405.

Canicio, A., and C. Ibanez (1999), The Holocene Evolution of the Ebro Delta Calalonia, Spain, *Acta Geographica Sinica*, *54*(5), 462-469.

Edmonds, D. A., and R. L. Slingerland (2010), Significant effect of sediment cohesion on delta morphology, *Nature Geoscience*, *3*(2), 105-109.

Galloway, W. D. (1975), Process Framework for describing the morphologic and stratigraphic evolution of deltaic depositional systems, in *Deltas Models for Exploration*, edited, pp. 87-89.

Giosan, L., J. P. Donnelly, S. Constantinescu, F. Filip, I. Ovejanu, A. Vespremeanu-Stroe, E. Vespremeanu, and G. A. T. Duller (2006), Young Danube delta documents stable Black Sea level since the middle Holocene: Morphodynamic, paleogeographic, and archaeological implications, *Geology*, *34*(9), 757-760.

Komar, P. D. (1973), Computer models of delta growth due to sediment input from rivers and longshore transport, *GSA Bulletin*, *84*(7), 2217-2226.

Milliman, J. D., K. L. Farnsworth, P. D. Jones, K. H. Xu, and L. C. Smith (2008), Climatic and anthropogenic factors affecting river discharge to the global ocean, 1951-2000, *Global and Planetary Change*, *62*(3-4), 187-194.

Orton, G. J., and H. G. Reading (1993), Variability of deltaic processes in terms of sediment supply, with particular emphasis on grain size, *Sedimentology*, *40*(3), 475-512.

Pranzini, E. (2001), Updrift river mouth migration on cuspate deltas: two examples from the coast of Tuscany (Italy), *Geomorphology*, *38*(1-2), 125-132.

Roberts, H. H. (1997), Dynamic changes of the Holocene Mississippi River delta plain: The delta cycle, *Journal of Coastal Research*, *13*(3), 605-627.

Syvitski, J. P. M., et al. (2009), Sinking deltas due to human activities, *Nature Geoscience*, *2*(10).

Vella, C., T.-J. Fleury, G. Raccasi, M. Provansal, F. Sabatier, and M. Bourcier (2005), Evolution of the Rhone delta plain in the Holocene, *Marine geology*, *222-223*, 235-265.

Nonlinear response of shoreface-connected sandridges to offshore sand extraction for a realistic inner shelf slope

A. Nnafie, H.E. de Swart, D. Calvete, and R. Garnier

Paper confidential

DOI: 10.3990/2.194

Nearshore evolution at Noordwijk (NL) in response to nourishments, as inferred from Argus video imagery

B.G. Ruessink[1] , R.M. van der Grinten[1], L. Vonhögen-Peeters[2], G. Ramaekers[3] and Q.J. Lodder[3]

[1]Department of Physical Geography, Faculty of Geosciences, Utrecht University, P.O. Box 80.115, 3508 TC Utrecht, The Netherlands, b.g.ruessink@uu.nl, www.coastalresearch.nl/gruessink

[2]Deltares, Subsurface and groundwater systems, Utrecht

[3]Rijkswaterstaat Waterdienst, Lelystad

ABSTRACT

We use an approximately 16-year long data set of daily low-tide video images to examine the effect of three consecutive nourishments on the temporal evolution of the subtidal sandbars and the low-tide water line at Noordwijk, The Netherlands. The data set starts in 1995, with shoreface nourishments implemented in 1998 and in 2006, and a "Zwakke Schakel" beach nourishment in 2007/2008. We find that, consistent with observations elsewhere, the shoreface nourishments halted the interannual, net-seaward migration of the two sandbars. Also, the first nourishment resulted in large-scale sandbar variability known as bar switching. The beach nourishment had no effect on the sandbars, other than an immediate 50-m seaward shift of the low-tide waterline and the inner sandbar. Neither the shoreface nor the beach nourishments were found to result in an increase or decrease in the number and cross-shore extent of rip channels. On the whole, the successive nourishments have reduced the natural dynamics of the Noordwijk coastal system.

INTRODUCTION

Along some 70% of the Dutch coast wind-blown dunes are the last line of natural defense against high waves and water levels during storms. Every six years the safety of these dunes is assessed with an equilibrium-type dune-erosion model, see, for example, Den Heijer et al. (in press). A dune is then considered to be safe when it will not breach during a storm with an occurrence probability of 1 in 10.000 for a given year. Early this century, more than 10 locations along the Dutch coast were considered to be insufficiently safe, especially in view of expected changes in the hydrodynamic boundary conditions induced by climate change. Coastal safety at most of these so-called Zwakke Schakels (Dutch for Weak Links) has been enhanced by large-scale human measures, often including (beach) nourishments.

Noordwijk, located at the central Dutch Holland coast, is an example of a Zwakke Schakel. Here, in winter 2007-2008, the Dijk-in-Duin project was carried out, which involved a massive restructuring of the small and narrow dune field into a wider and higher dune row (see Figure 1). Within the new dune, a 1.1 km long, 9-m high dike was built. Furthermore, the beach was nourished with approximately 3 Mm^3 of sand over a length of 3 km alongshore. This implies a local seaward extension of the beach and the dunes of about 40-50 m.

The nearshore zone of Noordwijk has been monitored with an Argus video-system since 1995. This has resulted in one of the longest (now 16 years), high-resolution (daily) data sets of nearshore evolution with and without human activities. The first 3 years of data contain information on the autonomous nearshore behaviour. In addition to the afore-mentioned Dijk-in-Duin project, shoreface nourishments were implemented in 1998 and 2006. The aim of this paper is to evaluate the effect of the various nourishments, including the Dijk-in-Duin nourishment, on the behaviour of the subtidal sandbars and on the low-tide water line.

Figure 1. A picture of the dunes and beach at Noordwijk (top) before and (bottom) after the Dijk-in-Duin project. Note the striking seaward extension of the dunes and beach.

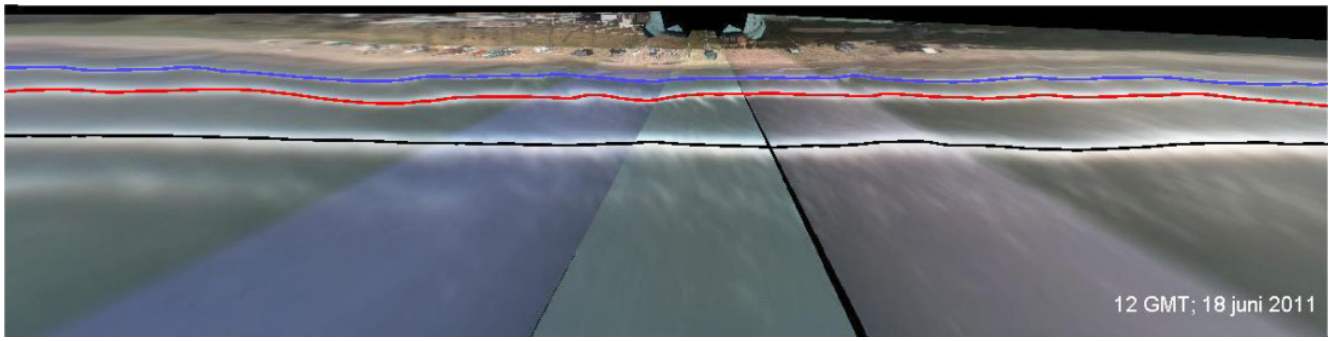

Figure 2. Planview image with an alongshore and cross-shore width of 6 and 1.5 km, respectively. Pixel size is 2.5 x 2.5 m. The black, red and blue lines represent the location of the outer subtidal sandbar, the inner subtial sandbar, and the waterline, respectively. Just seaward of the outer bar, a faint breakerline (not tracked) indicates the position of the 2006 shoreface nourishment.

METHODS AND RESEARCH QUESTIONS

This study was based on the 10-minute time-exposure images collected hourly since 1995, when the Argus system was installed with 5 color cameras. Merging of the images collected during a given hour results in a planview image (Figure 2) that offers an uninterrupted view of the nearshore for some 6 km alongshore and 1.5 km cross-shore. The most striking features in a merged planview image are alongshore continuous, white, high-intensity bands that reflect the wave breaking on subtidal sandbars and nourishments, and on the beach face. These lines are most conspicuous at low tide and we therefore restrict our data set to images collected at low tide.

The alongshore positions of each breakerline were extracted for every available low-tide image in the period March 1995 - August 2011 using the methodology described in Van Enckevort and Ruessink (2001). The colored lines on top of the breakerlines in Figure 2 provide examples of the extracted lines, henceforth called barlines. These lines do not reflect the precise location of the crest of the underlying sandbars. Most importantly, the barlines will shift on/offshore in response to slight day-to-day variations in the low-tide level (Van Enckevort and Ruessink, 2001). These variations were removed following the approach of Pape et al. (2010). Using the obtained data set of barlines, we focused our analyses to answer the following 3 research questions:

1. What is the effect of the nourishments on the alongshore-averaged position of the sandbars and on the low-tide waterline? This implies that we focus on the overall cross-shore (i.e., uniform) sandbar and waterline motion in the entire 6-km width of the study area.
2. What is the effect of the various nourishments on large-scale sandbar and waterline variability within the 6 km study area? Examples of such variability include sandbar switches (e.g., Ojeda et al., 2008) and shoreward propagating accretionary waves (e.g., Wijnberg and Holman, 2007).
3. What is the effect of the nourishments on small-scale sandbar and waterline variability? The focus here is on the number and cross-shore magnitude of rip channels.

RESULTS

Uniform behavior

Figure 3 summarizes our main results for the alongshore-averaged position of the sandbars, the various nourishments and the low-tide water line. Prior to 1998, the two subtidal sandbars migrated offshore. This reflects the autonomous behavior along this stretch of coast (e.g., Wijnberg and Terwindt, 1995). Bathymetric surveys since 1965 demonstrate that the sandbars migrate offshore in a cyclic manner, with bar generation near the shore, net offshore migration and bar decay in roughly 4-5 m water depth. The duration between successive decays is about 4 years. The position reached by the outer bar is just shoreward where it would normally decay (600 - 700 m from the shore).

The 1998 nourishment was implemented as a broad sandbar feature some 300 m seaward of the outer-bar zone. It migrated onshore to reach the location of normal outer-bar decay in about 4 years. From 2004, the nourishment was no longer discernible as a clear breakerline, suggesting that it had flattened out. Bathymetric surveys confirm this (Ojeda et al., 2008). The nourishment stopped the net offshore migration of the inner and outer subtidal sandbars, a sandbar response also seen at other nourished locations (e.g., Van Duin et al., 2004; Grunnet and Ruessink, 2005). The 2006 nourishment was implemented on top of the decaying 1998 nourishment and remained in the same location until the end of the study period. Similarly, the subtidal sandbars did not resume their natural net offshore migration.

The 2008 Dijk-in-Duin nourishment can be seen as a sudden seaward jump of the low-tide waterline and the inner bar. This jump is a direct consequence of the nourishment. The outer subtidal bar and the seaward 2006 nourishment were not affected at all. Since 2008, neither the waterline nor the inner subtidal bar showed much long-term variation and thus did not return to their pre-nourishment position. In more detail, Van der Grinten and Ruessink (2012) observed a northward shift of the northern tip of the beach nourishment by approximately 100 m/year. A similar southward shift of the southern end of the beach nourishment was not observed.

When we consider the time series in Figure 3 in more detail, it is obvious that each series is dominated by slow, multi-year

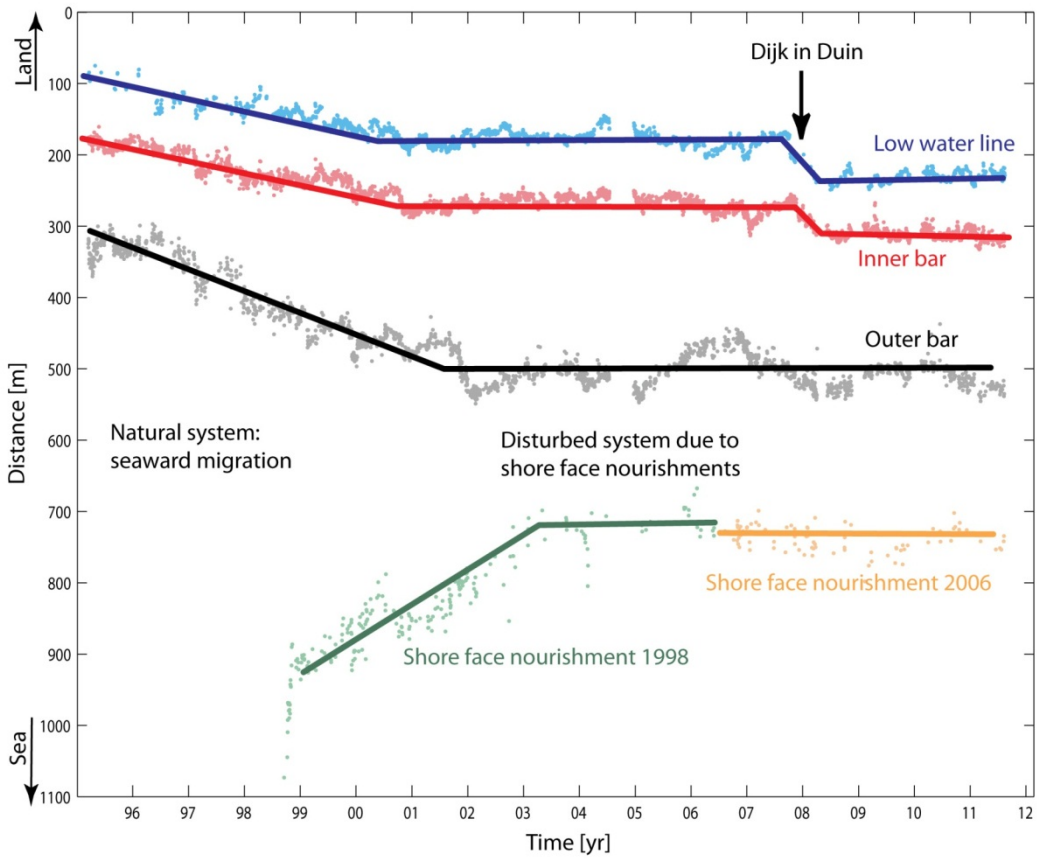

Figure 3. Summary plot of the alongshore-averaged position of the shoreface nourishments, the subtidal sandbars and the low-tide water line versus time. The dots are individual observations, the thick lines are trend lines.

trends. Prior to the first nourishment, this trend was the net-offshore migration, while the first nourishment caused this trend to be replaced by long, irregular oscillations around an otherwise constant position (250 m for the inner bar, and 500 m for the outer bar). Consistent with earlier Noordwijk-based research (e.g., Van Enckevort and Ruessink, 2003), we neither see any marked seasonal variability in sandbar location in response to seasonal variability in the offshore wave conditions, nor a clear response of each bar to storms. The Dijk-in-Duin project has not altered the temporal trends in cross-shore sandbar and waterline behaviour for the time period studied here.

Van der Grinten and Ruessink (2012) further examined the daily migration rate of the two sandbars and the low-tide waterline, where the rate was calculated as the difference in alongshore-averaged position between two consecutive days. The daily migration rates for the outer sandbar were typically largest, while the rates for the low-tide waterline were smallest. Prior to 2007, some 10% of the daily rates for the outer sandbar were 0 m/day, while for the low-tide water line the relative occurrence of 0 m/day was 25%. After 2007, the relative occurrence of 0 m/day was slightly larger for all sandbars and the waterline, for the latter increasing to 35%. Whether this implies that the successive nourishments made the nearshore zone less dynamic, is difficult to say. The increase in 0 m/day occurrences may also correspond to a difference in wave conditions between the two periods.

Large-scale variability

The above-mentioned net-offshore-migration of the subtidal sandbars was not always alongshore uniform prior to the implementation of the 1998 nourishment. This means that at one location the outer bar could be migrating offshore, while at another location it could already be decaying. This alongshore variability in outer sandbar migration sometimes caused an initially alongshore continuous inner bar to break up, with one part realigning with an outer bar and the other part with the beach. This large-scale sandbar variability is known as bar switching and in an Argus image looks like forked breakerlines, or bifurcations. Bar switching is thus due to alongshore variation in outer-bar behavior and is an inherent part of the autonomous sandbar behavior at Noordwijk.

The 1998 nourishment resulted in two nourishment-induced bar switches, one of which is shown in Figure 4. The nourishment did not extend along the entire 6 km of the study area. Shoreward of the nourishment, the sandbars halted their migration, while further to the south and north the net offshore migration continued. At some point, the original inner bar broke at the alongshore location of the head of the nourishment, with the inner bar north and south of the nourishment realigning with the outer bar shoreward of the nourishment. No bar switches were observed following the second shoreface nourishment, probably because it extended along the entire study area and thus did not lead to alongshore variation in

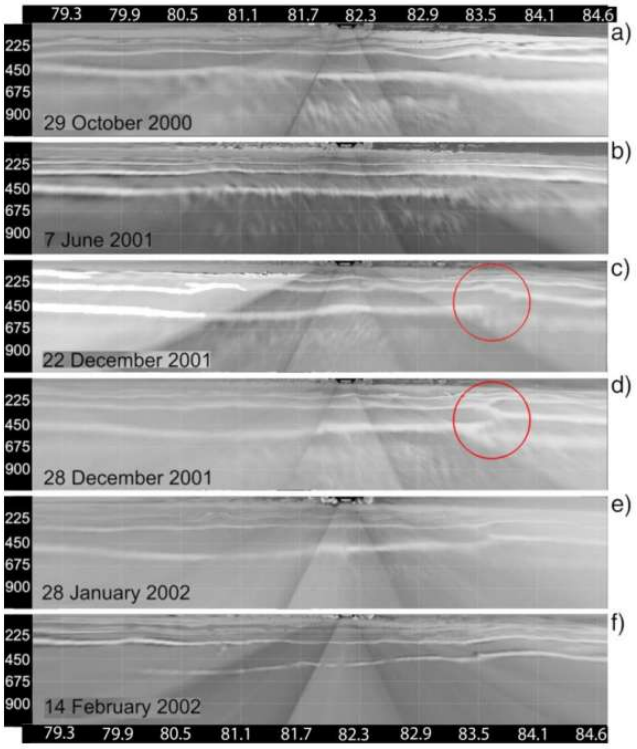

Figure 4. Planview images showing the evolution of a bar switch to the south of the 1998 nourishment. The actual switch is visible as the forked barlines in the red circles. Modified from Ojeda et al. (2008).

outer-bar behaviour. Also, the Dijk-in-Duin nourishment did not result in bar switching, because, as already noted from Figure 3, it did not affect the outer bar.

Another type of large-scale variability is the occasionally loosening of a section of a sandbar (with an alongshore length of several hundreds of meters) and its subsequent onshore migration to merge with a more shoreward sandbar. This loosened part of a sandbar is known as a shoreward propagating accretionary wave (SPAW), and is an inherent part of autonomous sandbar behaviour. We observed one SPAW following the Dijk-in-Duin project, but we believe it to be a natural phenomenon rather than a nourishment-induced feature.

Small-scale variability

The extracted barlines are rarely perfectly straight; instead, they contain all sorts of alongshore variability, ranging from gentle undulations as in Figure 2 to much more pronounced (in the cross-shore) perturbations related to rip channels. Van Enckevort and Ruessink (2003) demonstrated that during the pre-nourishment period rip channels had typical alongshore wavelengths of severalhundreds of meters. Furthermore, the rip features possessed rather long life times, in the order of several months, implying that they did not necessarily disappear during a storm.

Figure 5 shows the standard deviation of the inner-bar lines versus time. The standard deviation is a measure of the magnitude of the alongshore variations in the barline, with larger numbers corresponding to more pronounced variability. The colour coding indicates the number of rips, where a rip was defined as a seaward perturbation with a cross-shore extent of at least 25 m. As can be seen, rather small standard deviations corresponds to a low number of rips. Clearly, the standard deviation and the number of rips vary with time, but there are no breaks in trend in either 2006 (shoreface nourishment) or in 2007/2008 (beach nourishment). From this we can conclude that the nourishments did neither affect the degree of alongshore variation in the inner barline nor the number of rips.

Van der Grinten and Ruessink (2012) additionally observed that, consistent with the observations by Van Enckevort and Ruessink (2003), the rip life times was in the order of months. Furthermore, they observed the rips to migrate both to the north and to the south at rates up to 10 m/day. The migration direction was consistent with the angle of incidence, with waves from the northwest (southwest) causing rip migration to the south (north). This suggests that the alongshore current driven by obliquely incident breaking waves is the main mechanism for alongshore rip migration.

DISCUSSION

When we compare the effect of the various nourishments on sandbar and low-tide waterline evolution, it is obvious that the first shoreface nourishment influenced the coast most. It caused the net offshore sandbar migration to stop and resulted in two bar switches. The second shoreface nourishment, which was more extensive in the alongshore direction, prevented the sandbars from resuming their net offshore trend, but did not result in bar switches. Finally, the beach nourishment affected the inner sandbar and the low-tide waterline only during the actual nourishment implementation. It is possible that the subsequent inert behaviour of the inner bar and low-tide water line is caused by the sand brought into the nearshore system by the shoreface nourishments. Because the sandbars at Noordwijk are, relative to other sites along the Dutch coast, rather small in volume, all this sand has, in a manner of speaking, made the nearshore rather inert, see Ojeda et al. (2008) for further discussion. It is very well possible that beach nourishments unprotected by sandbars and/or shoreface nourishments are much more dynamic.

In Noordwijk, we found that the amount of small-scale alongshore variability (e.g., rips) did not change in response to the various nourishments. This differs from the Terschelling nourishment, which caused a break-up of a shoreward located bar into several sections intersected by deep, obliquely oriented channels (Grunnet and Ruessink, 2005). That nourishment was implemented inside the bar zone, rather than offshore the bar zone as in Noordwijk. It is possible that the location of the nourishment steers the effect on small-scale alongshore variability.

In this work, we have focused primarily on positions, not on volumes. It is possible to use Argus imagery to extract volumes. For example, it is feasible to detect water lines at different stages of the tide to build up a digital elevation model of the intertidal zone (e.g., Aarninkhof et al., 2003). Similarly, breaking patterns can be inverted into depth estimates (e.g., Van Dongeren et al., 2008). Neither of these two techniques are, in their present state, fully automated and are insufficiently validated because of a clear lack of bathymetric monitoring data. Nonetheless, they hold great promise for the future. Ideally, one could combine daily to weekly video-based estimates of bathymetry with a waves-currents-sand transport-coastal evolution model to set up an operational

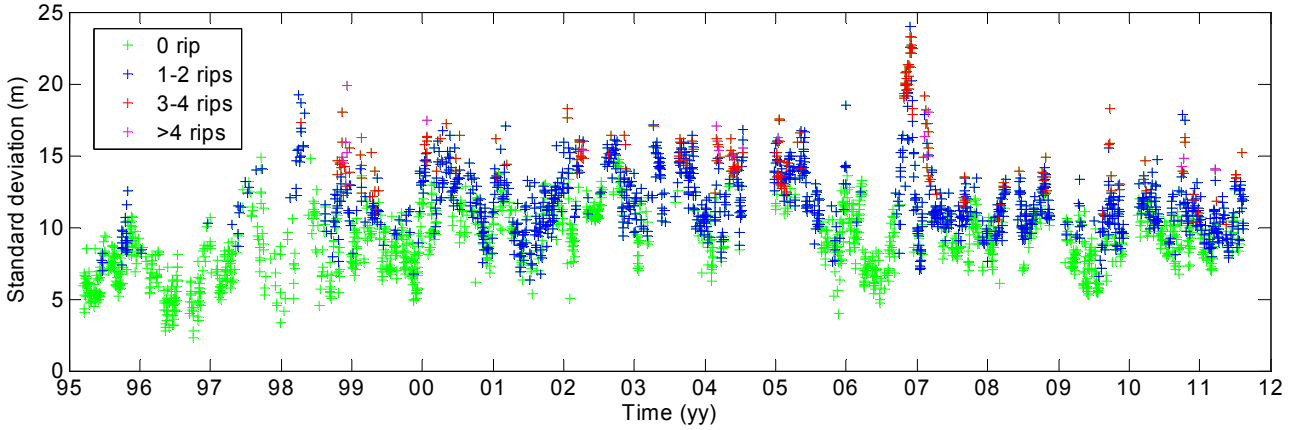

Figure 5. Time series of the standard deviation of inner-bar variability with alongshore wave lengths < 2000 m. The color indicates the number of rips, with a rip being defined as a seaward perturbation of at least 25 m

prediction model for coastal evolution. Such a system might be very useful to predicatively understand large-scale human activities in the coastal zone, such as the Sand Engine.

CONCLUSIONS

Based on the analysis of an approximately 16-year long data set of daily low-tide planview video image, we conclude that the two shoreface nourishments and the Dijk-in-Duin beach nourishment affect the nearshore sandbars and the low-tide water line in the following ways:

1. The first shoreface nourishment, implemented in 1998, stopped the autonomous, net offshore migration of the inner and outer subtidal sandbar. The sandbars did not resume their natural offshore directed trend, probably because of the second (2006) nourishment. The beach nourishment caused an immediate 50-m seaward shift of the low-tide waterline and of the inner bar, but it did not affect the outer bar. By the end of the study period, some 2.5 years after the beach nourishment, neither the low-tide waterline nor the inner bar had returned to their original position. The northern end of the beach nourishment migrated north by approximately 100 m/year. A similar southward shift at the southern end of the nourishment was not observed.
2. The first shoreface nourishment caused alongshore variable cross-shore migration rates of the outer-bar along the coast. In front of the nourishment, the migration rates were near 0, while to the north and south of the nourishment, the net offshore migration continued. After several years, this caused two bar switches. We also observed one shoreward propagating accretionary wave after the beach nourishment, but this feature is likely to be a natural phenomenon rather than nourishment-induced.
3. We did not find any evidence that either the shoreface nourishments or the Dijk-in-Duin beach nourishment affected the small-scale variability in the barlines, for example, in terms of the number of rips.

REFERENCES

Aarninkhof, S.G.J., I.L. Turner, T.D.T. Dronkers, M. Caljouw and L. Nipius, 2003. A video-based technique for mapping intertidal beach bathymetry. *Coastal Engineering*, 49, 275-289.

Den Heijer, C., F. Baart and M. van Koningsveld, in press. Assessment of dune failure along the Dutch coast using a fully probabilistic approach. *Geomorphology*.

Grunnet, N.M. and B.G. Ruessink, 2005. Morphodynamic response of nearshore bars to a shoreface nourishment. Coastal Engineering, *52*, 119-137.

Ojeda, E, B.G. Ruessink and J. Guillen, 2008. Morphodynamic response a two-barred beach to a shoreface nourishment. *Coastal Engineering*, 55, 1185-1196.

Pape, L., N.G. Plant and B.G. Ruessink, 2010. On cross-shore migration and equilibrium states of nearshore sandbars. *Journal of Geophysical Research*, 115, doi:10.1029/2009JF001501.

Van der Grinten, R.M. and B.G. Ruessink, 2012. Evaluatie van de kustversterking bij Noordwijk aan Zee - De invloed van de versterking op de zandbanken. Internal UU Report (In Dutch).

Van Dongeren. A., N. Plant, A. Cohen, D. Roelvink, M.C. Hallar, and P.A. Catalan, 2008. Beach Wizard: nearshore bathymetry estimation through assimilation of model computations and remote observations. *Coastal Engineering*, 55, 1016-1027.

Van Duin, M.J.P., N.R. Wiersma, D.J.R. Walstra, L.C. van Rijn, M.J.F. Stive, 2004. Nourishing the shoreface: observations and hindcasting of the Egmond case, The Netherlands. *Coastal Engineering*, 51, 813-837.

Van Enckevort, I.M.J. and B.G. Ruessink, 2001. Effect of hydrodynamics and bathymetry on video estimates of nearshore sandbar position. *Journal of Geophysical Research*, 106, 16,969-16,980.

Van Enckevort, I.M.J. and B.G. Ruessink, 2003. Video observations of nearshore bar behaviour. Part 2: alongshore non-uniform variability. *Cont. Shelf Research*, 23,513-532.

Wijnberg, K.M. and J.H.J. Terwindt, 1995. Extracting decadal morphological beahaviour from high-resolution, long-term bathymetric surveys along the Holland coast using eigenfucntion analysis. *Marine Geology,* 126, 301-330.

Wijnberg, K.M. and R.A. Holman, 2007. Video-observations of shoreward propagating accretionary waves. *Proceedings of RCEM* 2007, 737-743.

DOI: 10.3990/2.195

Effects of 20 years of nourishments: Quantitative description of the North Holland coast through a coastal indicator approach

G. Santinelli, A. Giardino, A. Bruens

Marine and Coastal Systems, Deltares, P.O. Box 177, 2600 MH Delft, The Netherlands. giorgio.santinelli@deltares.nl; alessio.giardino@deltares.nl; ankie.bruens@deltares.nl

ABSTRACT

The Dutch coast has been eroding over more than a thousand years. Coastal retreat puts coastal functions (e.g. safety against flooding) under pressure. Since 1990, the Dutch policy aims at preventing further retreat of the coastline, but in the meantime taking the valuable dynamical behaviour of the coast into account. Therefore, sand nourishments have been preferred over hard structures to counteract the systematic erosion. In this study, the morphological development of the North-Holland coast since 1965 has been analyzed by looking at a number of indicators. These indicators are 1) representative of the morphological development of the Dutch coast at different temporal and spatial scale and 2) related to policy objectives. The indicators cover the entire coastal profile from dunes to deeper water. The analysis showed how the trends of the different indicators have been affected by the nourishment schemes applied over the last 20 years, by the natural forcings (i.e. yearly storminess), and by the construction of hard structures. From this data-analysis, lessons can be learned regarding future nourishment strategies.

INTRODUCTION

The Netherlands is a low-lying country, where approximately 27 percent of the territory is located below mean sea level and 55 percent is prone to flooding. Protection against flooding is traditionally the primary objective of coastal policy in the Netherlands. However, since 1990 coastal policy has been subject to a number of modifications, and new objectives have been added to cope with the structural erosion problems of the Dutch coast. To fulfill these new objectives, the yearly volume of sand for nourishments was first increased to 6 millions m^3 sand per year in 1990 and then to 12 millions m^3 per year in 2001. Even higher volumes might be necessary in the future to cope with the more severe sea level rise scenarios predicted.

Deltares has been commissioned by Rijkswaterstaat Waterdienst to develop the knowledge needed to carry out an effective nourishment strategy. *Toestand van de Kust* (State of the Coast) is one of the sub-projects of a multi-year program, with the aim of identifying the impact of nourishments for a number of indicators along the Dutch coast. Learned lessons from the past are further used to improve future nourishment strategies. During this first year, the analysis has focused on the North Holland coast. The objective of the present study is twofold. The first objective is to support the Waterdienst in determining where to nourish, by indicating on which spots along the North Holland coast the sediment buffer is limited. This buffer does not only concerns sediment volumes, but also a wider range of coastal indicators. The second objective is to derive the effect of the nourishment strategy in the past to improve the future nourishment schemes.

METHODOLOGY

A number of indicators have been defined that are 1) representative of the morphological development of the Dutch coast at different temporal and spatial scale and 2) related to policy objectives and system function (safety, nature and recreation). An overview of the indicators is given in Table I. The

Table 1: Indicators chosen for describing the morphological development of the coast. Indicators are derived by Rijkswaterstaat (Kustlijnkaartenboeken), Deltares [Giardino et al., 2012], HKV [Van Balen et al., 2011] and Arcadis [Van Santen and Steetzel, 2011].

System function	Policy objective	Indicator
Short term safety	Maintenance of safety	Erosion length Probability of breaching
Medium term safety	Suistainable maintenance of safety	TKL (Toetsen KustLijn) MKL (Momentane KustLijn) BKL (Basis KustLijn) MDL (Momentane DuneLijn)
Long term safety	Suistainable maintenance of safety	Sand volumes at different water depths
Nature and recreation	Suistainable maintenance of dunes	Dune foot position Beach width

Table II: Division of North Holland coast in sub-areas with homogeneous nourishment strategy and autonomous trend.

Area code	Limit sub-region	Length [m]	Nourishment strategy / coastal type	Autonomous trend before 1990	*Wijnberg* [2002] (km from Den Helder)
1	90 – 588	4 980	Mainly beach nourishment	Eroding	~ 3-8 Eroding, profile steepening
2	608 - 1808	12 000	Mainly shoreface nourishment	Eroding	
3	1827 - 2023	1 960	Mainly beach nourishment	Eroding	~ 8-23 Eroding, profile flattening
4	2041 - 2606	5 650	Hondsbossche Zeewering	-	
5	2629 - 3200	5 710	Mainly shoreface nourishment	Eroding	
6	3225 - 3925	7 000	Mainly beach nourishment	Eroding	~ 23-55 Fluctuating
7	3950 - 4975	10 250	Nearly no nourishments	Alternating (erosive-accretive)	
8	5000 - 5500	5 000	Nearly no nourishments – under the effect of IJmuiden jetties	Accretive	

indicators were computed for the entire Dutch coast, for the years between 1965 and 2010. The analysis was subdivided in three periods of time (1965-1990, 1991-2000, 2001-2011), corresponding to radical changes in the nourishment policy. Within these predefined time windows, the study investigated changes in linear trends. The analyses were carried out both, at Jarkus transect level and at larger scale throughout the use of sub-areas, characterized by a homogeneous nourishment policy (e.g. beach nourishments, shoreface nourishments, no nourishment), and a similar autonomous trend erosive or accretive).

STUDY AREA

The North Holland coast is a sandy, microtidal, wave-dominated coast. This stretch of coast has a length of 55 km, and it is bounded in the North by a tidal inlet (the Marsdiep) and in the South by the 2.5 km long jetties of IJmuiden. The plan shape of the coast is slightly concave, with some disturbance near the Petten seawall which protrudes into the sea, giving to the shoreline a local convex curvature.

The alongshore sediment transport along the Holland coast has been derived by several authors using different models, verified by few field measurements [*Kleinhans and Grasmeijer*, 2005].

Studies of *Van Rijn* [1995, 1997] compared these results: despite the wide spreading, the general trend is southward-directed transport between the IJmuiden jetties and approximately km 30, and northward directed transport for the Northern stretch of coast. The magnitude ranges between -200.000 m^3/m/year in the south up to +500.000 m^3/m/ year in the north.

Time variations in sediment volumes at different water depths were computed by several authors [*Van Rijn,* 2010], [*Vermaas* 2010], based on field measurements. A general trend from erosive to accretive can be noticed along the all Holland coast, when comparing periods before and after 1990.

The nourishment policy in the Netherlands has been undergoing several modifications in the last 20 years. Along the North Holland coast, besides the increase in time of total nourishment volumes added, the tendency is towards an increase of shoreface nourishments with respect to beach nourishments. In addition, dune management over the years and man-made constructions (*e.g.* Petten seawall) along the North Holland coast represent the effort made on supporting important coastal functions.

Besides the anthropogenic intervention (nourishments, dune managements, man-made structures), nature plays a main role into the coastline morphological development. Given the complexity of the natural processes in the nearshore area, a unique relation between natural forcing and the different indicators does not exist. Moreover, the interference of the anthropogenic action and especially the huge nourishment volumes deposited on the beach, dune and breaker bars in the last years make even more difficult to distinguish between natural and anthropogenic processes.

The division in sub-areas that is applied in this study is presented in Table II. Sub-areas are characterized by a homogeneous nourishment policy and a similar autonomous trend. The main findings from *Wijnberg* [2002] on morphological trends are included in the last column of the table.

RESULTS

In this paper the results are presented for a number of indicators: the probability of breaching of the first dune row (P), the momentary coastline position (MKL) and the dune foot position (DF). More information concerning the analysis and the results for the complete set of indicators can be found in *Giardino et al.* [2012].

The time variation of the indicators was at first analyzed at Jarkus transect level, in relation with the amount of sand

Table III: Averaged nourishment volumes per sub-area (m^3 per m per year).

Area code	1965-1990	1990-2000	2001-2010
1	0	26	149
2	14	17	88
3	0	47	79
4	0	1	47
5	0	26	81
6	2	80	50
7	0	1	9
8	0	8	0

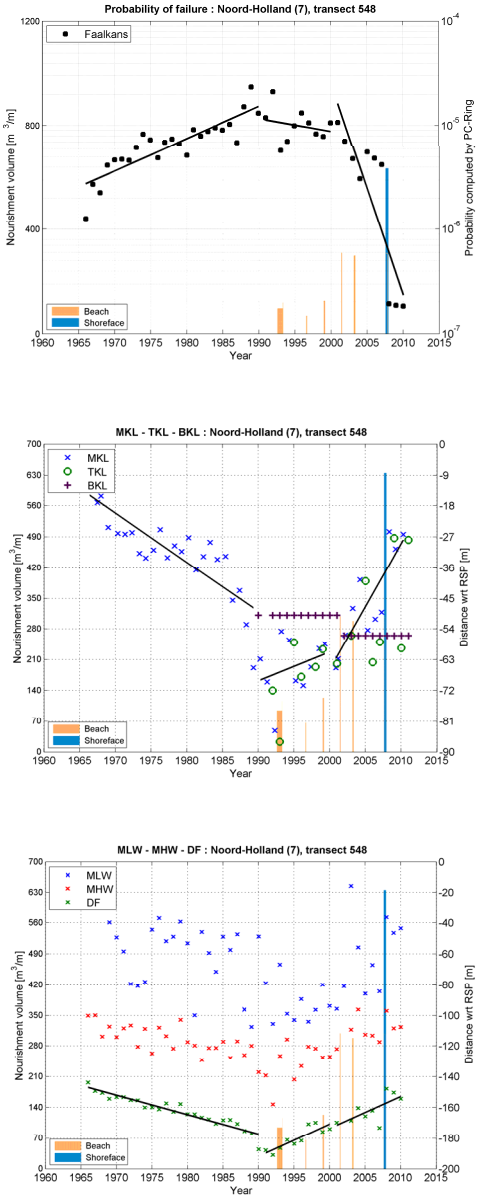

Figure 1. Change in indicators and nourishment volumes (orange and blue bars) in time at Jarkus transect 548. Upper panel: probability of breaching (black dots). Middle panel: Momentary Coastline (MKL, blue crosses), Testing Coastline (TKL, green circles) and Basic Coastline (purple crosses). Lower panel: Dune foot (DF green crosses), mean low water (MLW, blue crosses), mean high water (MHW, red crosses).

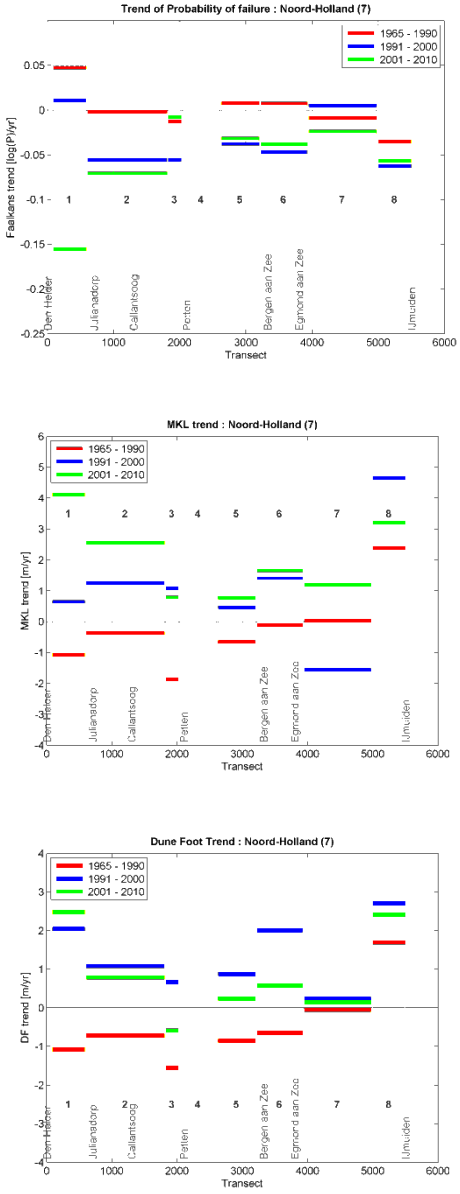

Figure 2. Averaged trend in probability of breaching (upper panel), MKL position (middle panel) and dune foot position (lower panel) within each of the eight areas with homogeneous autonomous trend and nourishment strategy. A relative change in trend of 0.1 year^{-1} on the upper plot, corresponds to a change of one order of magnitude in safety, for a time window of 10 years.

nourished. Figure 1 gives an example, clearly showing that nourishments led to a 'positive' effect in this stretch of coast (decrease in probability of breaching, seaward shift of both MKL and dune foot position). The relation between short term and medium term safety indicators for the all Holland coast, at Jarkus transect level per year, was investigated by *Van Santen* [2011].

The average trends in indicators (a linear trend for the three time windows, averaged over the sub-areas) also show a substantial change towards an average decrease in probability of failure and seaward shift of MKL and dune foot (Figure 2). The change in trend is especially evident for area 1, where mostly beach nourishments were applied. This would suggest that beach nourishments, on this time-scale, have a larger effect than shoreface nourishments. However, shoreface nourishments are built considering a long term prospective (5-10 years), rather then short term effects. On the same line are the modeling results presented in *Giardino* [2010], which showed that a beach or

banquette nourishment of 200 m^3/m would lead to an instant decrease of 35-47 % in dune erosion for a 10 year return period storm, while a 400 m^3/m shoreface nourishment has the potential of reducing it only of 2-5 %. However, the effect of shoreface nourishments may show up later in time. Nourishment volumes for each sub-area and time window are given in Table III.

Also hard structures such as the IJmuiden jetties appear to have an effect on increasing safety levels. Area 7 and 8 are characterized by a decrease in the probability of breaching whereas no nourishment were applied. The trend analysis confirms the previous observation that in general nourishments have led to an improvement of safety (change in trend from positive to negative values) and a seaward shift of MKL and dune foot.

It is important to point out that the probability of breaching only refers to the first dune row, while between transects 2606 and 5200 a multiple dune row system exists. This implies that a decrease in probability of breaching in the more northern transects (*i.e.* between transects 90 and 2041) has a more significant impact on safety against flooding than in the southern transects (*i.e.* between transects 2606 and 5200).

The relations between trends in different indicators and between nourishment volume and indicators have also been derived at the scale of sub-areas (see Figure 3 [*Stronkhorst and Bruens*, 2012]).

CONCLUSIONS

The main objective of the study was to derive the effect of the nourishment strategy in the past. Has the nourishment policy applied since 1990 in The Netherlands led to a 'positive' (seaward) development of the indicators?

The analysis has shown that the nourishment strategy has in general led to positive effects. Short term safety, described by the probability of breaching of the first dune row, has in general increased overall of more than one order of magnitude. The medium term safety has improved, as shown by an average shift of the MKL indicator of 30 m in seaward direction. The dune foot has also been migrating seaward in average of about 18 m since 1990. Moreover, the erosive trends, which were quite common at most locations before 1990, have been replaced starting from 1990 by accretive trends.

Relations between indicators were identified at Jarkus transect level and at the scale of sub-areas. Indicators appeared to be, in general, well correlated. At the scale of sub-areas, relations between nourishment volumes and shift in indicators have been derived as well: nourishments of approximately 1000 m^3 per meter coast per 10 year can result in a seaward shift of MKL of approximately 25 meters per 10 year and a decrease in probability of failure of the first dune row with a factor 10 per 10 year.

A complete database of indicators has been developed, and is now freely available through the Open Earth system. This database can be used as support tool for several projects dealing with coastline morphology in The Netherlands.

The same dataset can now be easily visualized by a number of interfaces which are under development at Deltares (The coastal viewer and Morphan) and be a user friendly support tool for coastal managers.

ACKNOWLEDGEMENT

This study has been carried out in the framework of the KPP-B&O Kust and KPP-Kustbeleid projects, both commissioned by Rijkswaterstaat Waterdienst. In this framework parallel studies have been carried out by HKVlijn in water, ARCADIS and ALTERRA, on the effects of nourishment on short-term safety and they will be presented in one accompanying papers.

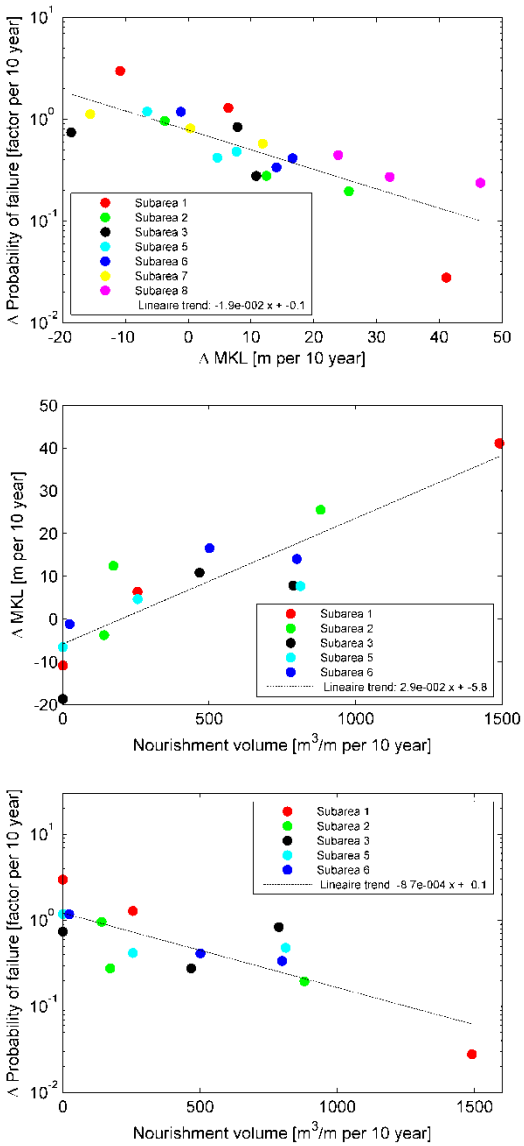

Figure 3. Upper panel: change in probability of failure (factor per 10 year) versus change in MKL position (meter per 10 year). Middle panel: change in MKL position (meter per 10 year) versus nourishment volume (m3 per m per 10 year). Lower panel: change in probability of failure (factor per 10 year) versus nourishment volume (m3 per m per 10 year). Plots for sub-areas in North Holland (see Table II).

Nourishment volumes in sub-area 7 and 8 are negligible and therefore not included in the two lowest panels.

REFERENCES

Bochev-van der Burgh, L.M., Wijnberg, K.M., Hulsher, S.J.M.H., 2011. Decadal-scale morphologic variability of managed coastal dunes. Journal of Coastal Engineering 58 , 927-936 p.

Giardino, A., 2010. The impact of sand nourishmnet design on dune erosion storm conditions BwN HK3.1c. Design aspects pilot Sand Engine Delfland. Deltares memo, reference number 1201770-000-ZKS-0010, Delft, The Netherlands.

Giardino, A., Santinelli, G., Bruens, A., 2012. The state of the coast (Toestand van de Kust). Deltares report, reference number 1206171-003-ZKS-0001, Delft, The Netherlands.

Kleinhans, M.G., and Grasmeijer, B.T., 2005. Alongshore bed load ransport on the shoreface and inner shelf. In L.C. Van Rijn (Editor), EU-Sandpit end-book. Aqua Publications, The Netherlands.

Ruessink, B.G., and Jeuken, C., 2002. Dunefoot dynamics along the Dutch coast. Journal of Earth Surface Processes and Landforms. Vol. 27, Issue 10, 1043 – 1056 p.

Santinelli, G., 2010. Trend analysis of nourishment volumes. Master th. Università degli Studi di Genova – Deltares, 1-70 p.

Stronkhorst, J., and Bruens A., 2012. Kustlijnen voor Dijkringen (concept).

Van Balen, W., Vuik, V., Van Vuren, S., 2011 (draft report). Indicatoren voor kustlijnzorg. Analysie van indicatoren voor veiligheid en recreatie. Project report (PR2063.20), HKV, The Netherlands.

Van Rijn, L.C., 1995. Sand budget and coastline changes of the central coast of Holland between Den Helder and Hoek van Holland period 1964-2040, Delft Hydraulics, Report H2129.

Van Rijn, L.C.,1997. Sediment transport and budget of the central coastal zone of Holland, Coastal Engineering No., 32, 61-90 p.

Van Santen, R.B., Steetzel, H.J., 2011 (draft report). Relatie Kustlijnzorg – Kustveiligheid. Project report, ARCADIS Nederland.

Vermaas, T., 2010. Morphological behaviour of the deeper part of the Holland coast. Master thesis. Deltares, The Netherlands.

Wijnberg, K.M., 2002. Environmental controls on decadal morphologic behaviour of the Holland coast. Marine Geology, 189(3-4): 227-247 p.

NCK photo competition

Luca van Duren: Crater connected to the sea, Faial

DOI: 10.3990/2.196

Simulating the large-scale spatial sand-mud distribution in a schematized process-based tidal inlet system model

F. Scheel[1,2,3], M. van Ledden[1,2], B.C. van Prooijen[1] and M.J.F. Stive[1]

[1] Faculty of Civil Engineering & Geosciences, section Hydraulic Engineering, Delft University of Technology, 2628 CN, Delft, The Netherlands, f.scheel@me.com

[2] Business Line Water, Royal Haskoning, George Hintzenweg 85, 3068 AX, Rotterdam, The Netherlands, m.vanledden@royalhaskoning.com

[3] Sea and Coastal Systems, Unit Morphology and Sedimental Systems, Deltares, 2629 HD, Delft, The Netherlands, info@deltares.nl

ABSTRACT

Tidal basins, as found in the Dutch Wadden Sea, are characterized by strong spatial variations in bathymetry and sediment distribution. In this contribution, the aim is at simulating the spatial sand-mud distribution of a tidal basin. Predicting this spatial distribution is however complicated, due to the non-linear interactions between tides, waves, sediment transport, morphology and biology. To reduce complexity, while increasing physical understanding, an idealized schematization of the Amelander inlet system is considered. Delft3D is applied with a recently developed bed module, containing various sediment layers, combined with formulations for both cohesive and non-cohesive sediment mixtures. Starting with uniform mud content in the spatial domain, the development of the sediment distribution is simulated. Realistic sand-mud patterns are found, with accumulation of mud on the tidal flats. The schematization is further used to determine the sensitivity of the sand-mud patterns to changes in tide, while assessing the influence of tidal dominance on the large-scale sand-mud patterns. The patterns are enhanced/diminished under the influence of higher/lower tides.

INTRODUCTION

Silt and clay particles are present in many tidal basins around the world. Together with sand, these particles often form the total sediment distribution within these systems.

Silt and clay particles (further referred to as mud) respond different to forcing (like waves and currents), compared to sand particles. This results in spatial sand-mud segregation. The differences in settling velocity and critical shear stresses of mud (mixtures), compared to sand, are mainly responsible for this different behavior and response.

The spatial sand-mud segregation patterns are very pronounced in the tidal inlet systems of the Dutch Wadden Sea. When mud particles are available, they tend to settle in less hydrodynamic active areas, like tidal flats. *Van Straaten and Kuenen* [1957] described this behavior in the former Lauwerszee, using Figure 1.

Many morphodynamic researches are aimed at predicting (modelling) the morphological evolution. A 'sand-only' model is often justified here, as sand is by far the main contributor to the morphological evolution in many cases. However, mud particles can have a significant local contribution on morphology, as it gets transported to distinct areas (as supported by Figure 1). Furthermore, the spatial distribution of flora and fauna is highly correlated to the spatial sand-mud distribution, as various species require a certain sand- or mud content to grow/live. Finally, cohesive mud particles tend to attract pollutants. The spatial mud content is therefore an important indicator for the degree of potential pollution.

Assessment of the above mud-related topics, requires prediction (modelling/simulation) of the spatial sand-mud distribution, for instance in a tidal inlet system in the Dutch Wadden Sea. However, this assessment involves non-linear interactions between tides, waves, sediment transport, morphology and biology. This makes it a challenging task.

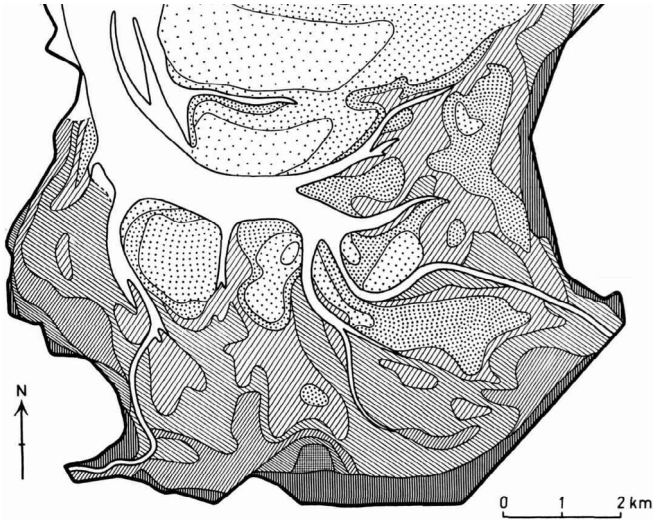

Figure 1. Clay content distribution in the former Lauwerszee, near the current Dutch Wadden Sea, increasing from 0% (white) to >25% (dark grey) clay content [Van Straaten & Kuenen, 1957]

Recent research [*Van Ledden*, 2003] provides us with a tool to model the sand-mud segregation patterns more effectively. While *Van Ledden et al.* [2004] found insightful results in various 1D models, a 3D model of the Friesche Zeegat [*Van Ledden*, 2003] resulted in both similarities and discrepancies compared to reality. But even more important, the physical understanding of the 3D model diminished, mainly due to the complex bathymetry and associated hydrodynamics. *Waeles et al*. [2007] concluded (for a comparable 3D research-model for the Seine River) with the statement that their model is qualitative, rather then quantitative.

From these researches and conclusions, the value to assess the large-scale (general) patterns in the spatial sand-mud distribution, by using a schematized (2DH) tidal inlet system model is given.

Van Ledden [2003] also adopted this advice in his recommendations.

To assess the large-scale sand-mud patterns, some related observations and hypotheses are needed. Mud particles appear to get transported too less hydrodynamic active areas, as found in both observations (Figure 1) and from physical reasoning (e.g. the formulations for (critical) shear stress combined with the decreasing hydrodynamic activity further into a tidal basin).

Furthermore, *Nichols and Boon* [1994] introduced a classification of various systems. Two of these are given in Figure 2. Where Figure 2-A (Mobile Bay) shows a mud basin and a margin that is dominated by sand, indicated by case A. Figure 2-B (Arcachon Bay) features sand-rich channels and intertidal areas with an abundant quantity of mud, indicated with case B. This last behavior can also be found in the former Lauwerszee (Figure 1).

As a hypothesis, which is relating this classification to physics, a (relatively) wave- or tide-dominated system can be proposed for case A and B, respectively. This research is aimed at a tidal basin, and the classification of case B is thus further investigated.

METHODS

A combination of previous studies is used to initiate this research. First, a schematized model of the Amelander inlet system in Delft3D, based on *Dissanayake* [2011], is used for the spatial model domain, as shown in Figure 3. This Amelander inlet system model is combined with a multi-layered sand-mud Delft3D version, which is set-up during the 'Building with Nature' project (BwN-project) by Deltares. This Delft3D version is a combination of the regular Delft3D-FLOW version [*Deltares*, 2011] and formulations by *Van Ledden* [2003], though it also features some (numerical) additions/changes proposed by Deltares.

Schematized Amelander inlet system model

Based on Dissanayake [2011], a schematized Amelander inlet system model is used (Figure 3). The model is forced by the North Sea tide, which is modelled using the M_2, M_4 and M_6 tidal components. At this location, the amplitudes of these tidal components are 0.85, 0.09 and 0.06 meter, respectively.

Using the initial sand-only model and the sand-mud version of Delft3D, a stable bathymetry is generated by simulating a 50-year period of tidally induced forcing (as specified above). This bathymetry (Figure 4-A) is used as the initial bathymetry for all sand-mud simulations, in which mud is supplied by an initial concentration within the water column, initial mud content within the bed and three (continuously supplying) boundary conditions.

Sand-mud version of Delft3D

When comparing to the regular Delf3D version [*Deltares*, 2011], the sand-mud mixture version mainly differs in three parts, being (1) the addition of formulations for sand-mud mixtures with cohesive and non-cohesive regimes, (2) the multi-layered bed (in which biological and physical mixing processes between layers is implemented by using internal diffusion) and (3) the implementation of a fluff layer (a thin layer above the bed, in which most mud settles and can be easily eroded again, before actually consolidating into the (more resistant) bed layers below).

The hydrodynamics (like the shallow water equations) and sediment transport equations within the sand-mud mixture version of Delft3D are identical to the regular Delft3D version.

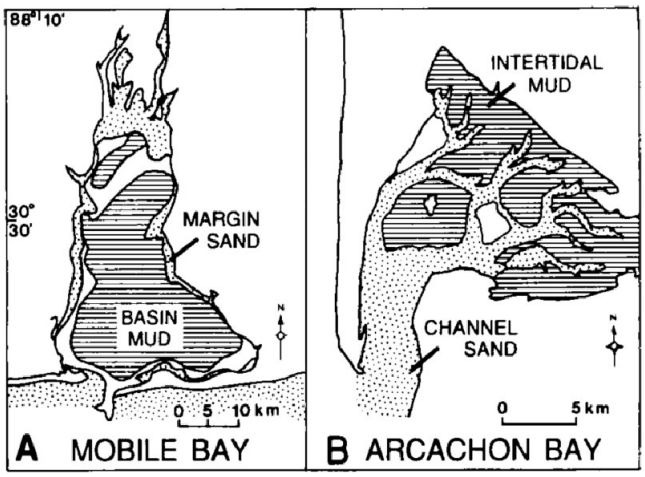

Figure 2. Large-scale sand-mud patterns in basins, with the hypothesis stating that case A is relatively wave- and case B is relatively tidally dominated [after Nichols and Boon, 1994]

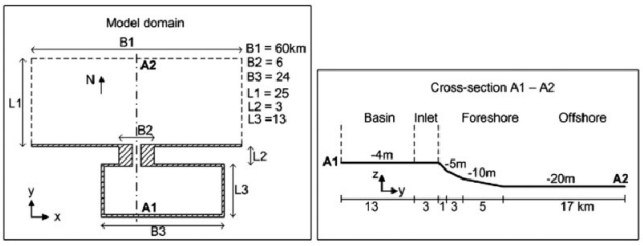

Figure 3. Model domain of schematized Amelander inlet system model, along with cross-section A1-A2 [after Dissanayake, 2011]

Concept of cohesive and non-cohesive sand-mud mixtures

Van Ledden [2003] introduced the concept of formulations for sand-mud mixtures in a cohesive and a non-cohesive regime.

Each mixture features a specific mud content ($0 \leq p_m \leq 1$). By defining a critical mud content ($p_{m,cr}$) a sand-mud mixture is either cohesive ($p_{m,cr} < p_m \leq 1$) or non-cohesive ($0 \leq p_m < p_{m,cr}$). Both regimes feature different formulations, as both regimes show different behavior. The formulations enhance the critical bed shear stress for sand-mud mixtures, depending on the mud content. For the full set of equations, one is referred to *Van Ledden* [2003].

Multi-layered bed and internal diffusion concepts

A multi-layered bed consists of various layers with different sediment mixtures. Each grid-cell in Delft3D features specific layers. The erosion rate in each cell is based on characteristics in the top layer of that cell. Deposition of a mixture, different to the top layer, results in the generation of a new layer. A maximum number of layers is specified and the final underlayer gains content from layers above, if this maximum number is exceeded.

Due to differences between layers (for instance in p_m), mixing could occur due to biological and/or physical processes. This is implemented in the model using internal diffusion between layers.

Fluff layer concept

When mud settles during gentle hydrodynamic conditions, high concentrations of mud appear near the bed, since the mud particles

are not easily consolidated in the bed layers. Because of this behavior, the mud particles near the bed appear like in a hindered settling state, making settling, in the underlying bed layer, a slow process. This high concentrated layer (above the bed) is called the fluff layer. *Van Kessel et al.* [2010] also describes this behavior.

Within the sand-mud version of Delft3D, mud particles first settle to the fluff layer before actually entering the underlying bed layer or re-suspending again into the water column. The critical bed shear stress for erosion is smaller in the fluff layer than in the bed layers. The fluff layer can have significant changes in mud concentration over short timescales (e.g. high concentrations during slack water and low concentrations during ebb- or flood flow), while significant changes for p_m in the bed occur on much larger timescales, which appears to be in line with observations.

Different model scenarios

Initially, the model is simulated with tidal- and wind induced forcing to assess the most realistic scenario, called the reference scenario. Furthermore, scenarios with an increase and decrease in tidal amplitude (and thus tidal prism Ω) are simulated.

Areas within the tidal basin without any morphological influence (Southwest and Southeast areas) were stripped from the spatial domain, to prevent model artifacts to occur (Figure 4-A).

Verification of Delft3D sand-mud version

Before executing the scenarios, verification of the Delft3D sand-mud model is preferred, as changes compared to the original concept by *Van Ledden* [2003] were made.

The model appears to resemble previous models, as indicated by *Scheel* [2012]. The model is therefore considered verified.

RESULTS

Model scenarios were run with a morphological time period of 3 months (also hydrodynamic, as *Morfac* = 1), with mud concentrations at the boundaries running from 10 mg/l (at the North Sea) to 30 mg/l (near the coasts of the Frisian islands). The initial mud content in the bed is 5% and the water column initially features 10 mg/l dissolved mud particles throughout the domain.

Reference scenario

The reference scenario, using realistic tide and average wind conditions, shows realistic results, as observed in the field. With mud abundant on tidal flats and near tidal basin boundaries, while absent in (tidal) channels (see Figure 4-B). Apart from the general sand-mud segregation patterns, the values of mud content and concentrations in the water column, within these patterns, also show realistic values, typical for basins in the Dutch Wadden Sea.

Large tidal range scenario

This large tide scenario is, apart from the tidal amplitudes, which are twice as high, an exact copy of the reference scenario. The behavior, observed by *Nichols and Boon* [1994] in Arcachon Bay (Figure 2-B) and by *Van Straaten and Kuenen* [1957] in the Lauwerszee (Figure 1), is reproduced and, compared to the reference scenario, enhanced (Figure 4-C). This observation supports the hypothesis on tidal dominated basins (as the relative tidal dominance increased compared to the reference scenario).

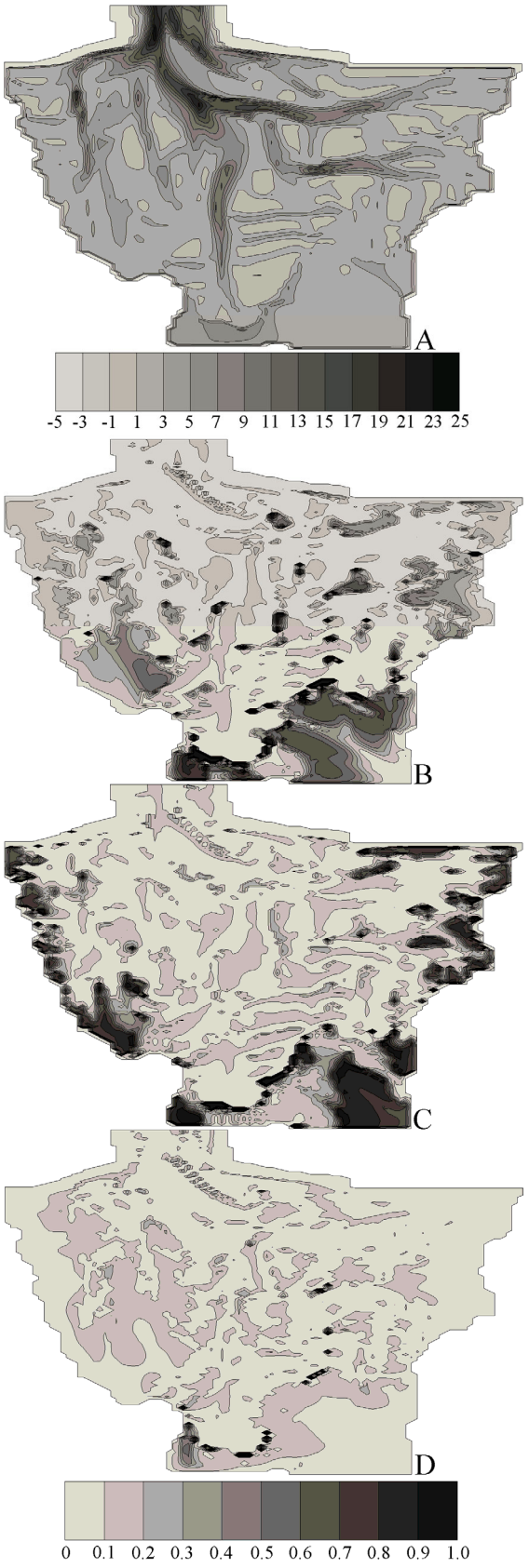

Figure 4. (A) Model bathymetry (depth) and mud content in top layer for scenarios (B) reference, (C) large tide and (D) small tide

Small tidal range scenario

The small tide scenario is an exact copy of the reference scenario, though it features tides with halved tidal amplitudes. As observations no longer show abundance of mud on tidal flats and model boundaries, the expected behavior for a tidal dominated system is no longer met. From the observations, it appears that the tidal dominance is diminishing, also diminishing the associated characteristics. This is again in line with the hypothesis.

ANALYSIS

First, the total mud transport to and through specific sections within the tidal basin is tracked, as mud content observations in the top layer (Figure 4) doesn't provide total transports (content in underlayers is not visible in Figure 4). Different runs are thus compared in a more quantitative manner, rather then qualitative.

Second, the 'hypsolaspy' curve is introduced. This curve relates the mud content to depth (comparable to a hypsometry curve) and therefore indicates the relation between these variables.

Finally, a relation between occurring shear stress and mud content is visualized (using a scatterplot).

Mud transport through the tidal basin

By dividing the tidal basin in equidistant sections from north to south (section A to H), *Scheel* [2012], the mud transport through the tidal basin for the different scenarios is compared.

Looking at Figure 5, the reference scenario shows expected behavior, with mud transported to the southern (boundary) sections (where most tidal flats are found), with mud coming from the North (where mainly channels are found).

The large tide scenario also shows this behavior, though with much larger magnitude. While the low tide scenario supports the previous statements, though it also shows the behavior from the other scenarios on a much smaller scale.

Furthermore, note that the turning point for ex- and import is moving inwards with increasing tidal amplitudes.

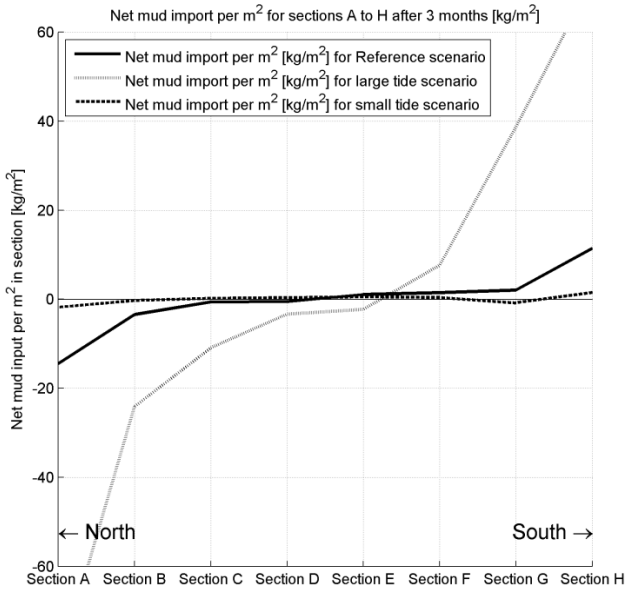

Figure 5. Average mud import [kg/m^2] per (equidistant) section, with sections running from North (section A) to South (section H)

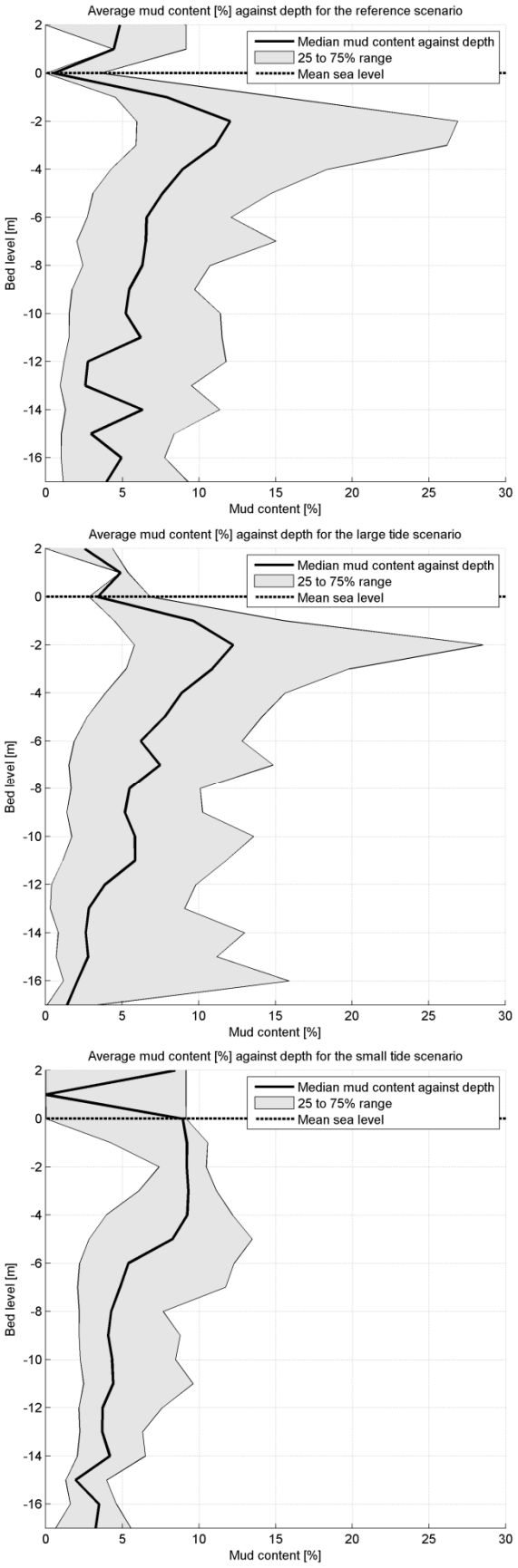

Figure 6. Hypsolaspy curves for all (indicated) scenarios

'Hypsolaspy' curves

Figure 6 introduces hypsolaspy curves for all scenarios. With MSL at 0, the reference situation shows an increase in mud content for shallower areas. This result is as expected, as shallower areas are found further into the tidal basin, these areas are less hydrodynamically active and mud particles are allowed to settle in these regions.

When looking at the large tide scenario, the behavior is comparable to the reference situation, though mud content is smaller in the deeper parts (channels) in the system. While the small tide scenario shows smaller differences, the mud content in shallow areas is still larger compared to the deeper areas.

Occurring shear stress against mud content

By relating the occurring bed shear stress to the mud content for all grid-cells in the tidal basin, a scatterplot (Figure 7) can be constructed. By normalizing the bed shear stress with the critical bed shear stress (for p_m=1, which is the maximal critical shear stress) an interesting distinction can be made. It appears that cohesive mixtures are mainly present when the occurring shear stress is below the critical shear stress. This implies that more mud (cohesive mixtures) is found in shallow areas (e.g. tidal flats), as shear stresses are smaller in these areas *Scheel* [2012]. *Van Ledden* [2003] also observed this behavior.

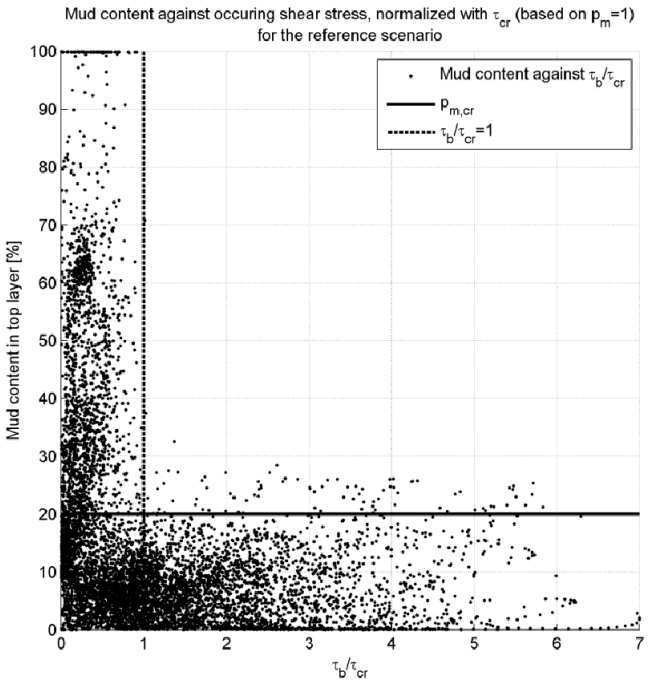

Figure 7. Mud content against occurring bed shear stress (normalized with critical shear stress for p_m=1)

DISCUSSION

In this contribution, research on large-scale sand-mud segregation patterns in a tidal dominated basin is combined with a hypothesis related to tidal- and wave-dominated systems and their relation towards these patterns. While the assessment of the tidally dominated case was considered in this research, the complete assessment of the hypothesis, which requires a wave-dominated system (with wave implementation), is attempted in overlapping research [*Scheel*, 2012].

Large-scale patterns can be assessed much easier with a schematized (2DH) model, just like the approach by *Dissanayake* [2011]. Though, it will not reproduce exact field observations.

CONCLUSIONS

This contribution is one of the first to apply the Delft3D version with sand-mud mixtures, and therefore puts it to the test. It appears a well applicable model, solidly based on work by *Van Ledden* [2003].

A schematized (2DH) model is an advantage for assessing general sand-mud segregation patterns, as observations in the field (e.g. abundant mud in tidal flats and scarce amount of mud in tidal channels) can successfully be reproduced.

Tidally dominated basins (tidal basins) feature mud at intertidal areas (and at tidal basin land-boundaries) and lack mud in tidal channels. These observations are made due to the tidal dominance, as hypothesized. The diminishing tidal (hydrodynamic) influence into the basin is highly responsible for this outcome.

ACKNOWLEDGEMENT

Sincere thanks goes out to Deltares, in particular Thijs van Kessel, for providing a workplace, cluster and the sand-mud version of Delft3D (which is currently under development) free of charge. Furthermore Royal Haskoning and Delft University of Technology are thanked for their workplaces, help and support during the entire (overlapping) M.Sc. research [*Scheel*, 2012].

REFERENCES

Deltares (2011), Delft3D-FLOW, Simulation of multi-dimensional hydrodynamic flows and transport phenomena, including sediments, user manual, version 3.15, 674 p.

Dissanayake, D.M.P.K. (2011), Modelling morphological response of large tidal inlet systems to sea level rise. CRC Press/Balkema, Leiden, 178 p.

Van Ledden, M. (2003), Sand-mud segregation in estuaries and tidal basins, PhD thesis, Repository TU Delft, 221 p.

Van Ledden, M., Z.B. Wang, J.C. Winterwerp, and H. de Vriend (2004), Sand-mud morphodynamics in a short tidal basin, Springer, Ocean Dynamics, Vol. 54, pp. 385-391.

Nichols, M., and J.D. Boon (1994), Sediment transport processes in coastal lagoons, Elsevier Science Publishers, Oceanography Series, Vol. 60, pp. 157-219.

Scheel, F., Simulating the large-scale spatial sand-mud distribution in a schematized process-based tidal inlet system model, M.Sc. thesis, Repository TU Delft, Forthcoming 2012.

Van Straaten, L.M.J.U., and P.H. Kuenen (1957), Accumulation of fine grained sediments in the Dutch Wadden Sea, Lingua Terrae, Geologie en Mijnbouw 19, pp. 329-354.

Waeles, B., P. Le Hir, P. Lesueur, and N. Delsinne (2007), Modelling sand/mud transport and morphodynamics in the Seine River mouth (France): an attempt using a process-based approach, Springer, Hydrobiologia, Vol. 588, no. 1, pp. 69-82.

Van Kessel, T., J.C. Winterwerp, B.C. van Prooijen, M. van Ledden and W. Borst (2010), Modelling the seasonal dynamics of SPM with a simple algorithm for the buffering of fines in a sandy seabed, Continental Shelf Research 31, pp. 124-134.

DOI: 10.3990/2.197

Numerical modeling of physical processes in the North Sea and Wadden Sea with GETM/GOTM

Meinard Tiessen[1,2], Janine Nauw[1], Piet Ruardij[1] and Theo Gerkema[1]
[1] NIOZ Royal Netherlands Institute for Sea Research, PO Box 59, 1790 AB Den Burg (Texel), The Netherlands
[2] Corresponding author: meinard.tiessen@nioz.nl

ABSTRACT

At the Royal Netherlands Institute for Sea Research (NIOZ), several research projects are carried out on the concentration and transport of Suspended Particulate Matter (SPM) in the Southern North Sea and Wadden Sea. So far the focus has been on field data collection and analysis, but in recent years a numerical modeling capacity has been set up, using the GETM/GOTM model. The underlying purpose is twofold. Firstly, a numerical model can provide insight into the hydrodynamics and SPM transport, complementing field observations, helping to interpret and identify the key physical mechanisms. Secondly, it provides a much-needed tool in ecological studies, forming the basic physical core on which the transport of for instance nutrients and larvae depends; thus, these kinds of numerical models provide a valuable bridge in interdisciplinary studies. First steps in the use of the model are reported here, offering a synopsis of its potential.

INTRODUCTION

The historical focus of research carried out at the NIOZ has been towards monitoring physical, biological and geological processes in the North and Wadden Sea. Modeling of physical processes has mainly been used as an additional tool to facilitate the analysis and interpretation of data collected in the field.

Field data are inherently limited in duration and spatial scale. Generally, only specific locations can be studied. Recent developments in remote sensing [as for instance in: *Pietrzak et al., 2011*] and in-situ data collection [as presented in *Nauw et al., 2012*] are greatly expanding the capabilities in data collection. However, the basic limitations still apply to a significant extent. Numerical modeling, on the other hand, can give predictions on wide spatial and temporal scales. However, this type of research can only provide coarse information, lacking the level of detail provided by field data. Moreover, the accuracy of model predictions is greatly dependent on the correctness of the initial model input. By combining field data with numerical modeling, the level of detail obtained by field data could be used to provide more accurate and detailed numerical simulations. The present paper provides an overview of the recent work carried out at the NIOZ in which a numerical modeling techniques are used to study a variety of different physical processes.

The complex circulation pattern in the North Sea mainly arises from the interaction between tides and atmospheric conditions [*Otto et al., 1990*]. The residual current pattern and annual variability in forcing conditions are significant factors determining the sediment transport, distribution of nutrients and pollutants and thus biological development [*Otto et al., 1990; Dyer and Moffat, 1998*]. Furthermore, fresh water inflow from rivers around the North Sea causes stratification and affect the water motion on small and intermediate scale [*De Boer et al., 2006*].

The adjacent Wadden Sea forms a complex estuarine system behind various barrier islands. Several semi-separated tidal basins are drained through tidal channels that are located in between these islands. The dominant tidal behavior is on the semi-diurnal M2 tidal frequency, leading to flooding and drying of large parts of the tidal basins [*Zimmerman, 1976a*]. The tidal currents, along with freshwater inflow from the mainland give rise to complex mixing processes and residual current patterns [*Zimmerman, 1976b*], which have been observed in the field as well as described using computer models over the last decades [*Postma, 1981; Ridderinkhof and Zimmerman, 1992; Stanev et al., 2007; Burchard et al., 2010*].

Suspended Particulate Matter (SPM) is a bulk term encompassing fine-grained substances of organic and inorganic nature, such as silt. It is transported along with the flow while in suspension, but may sink to the bed during calm conditions. High concentrations of SPM can impede sunlight to penetrate the water column, and therefore limit primary production. Moreover, especially in estuarine environments and tidal basins, SPM forms a considerable fraction of the total sediment supply and is therefore of great importance for erosion and accretion of morphological features and their change of form. The transport and concentration of SPM is determined by the prevalent hydrodynamics. Therefore, to understand SPM characteristics, physical aspects such as tides, waves, net currents, and density gradients are of great importance.

Sediment is transported into the North Sea from the English Channel, but also as a result of cliff erosion along the British East coast and river outflow [*Eisma and Kalf, 1987*]. Furthermore, re-suspension of deposited sediments occurs locally as a result of strong currents, due to storm events or during spring tides, for instance at the Flemish Banks [*de Kok, 2004*]. Plumes of sediment can be observed along the coastlines bordering the North Sea captured by estuarine type of circulation due to river outflow, as well as crossing the North Sea [*Pietrzak et al., 2011*].

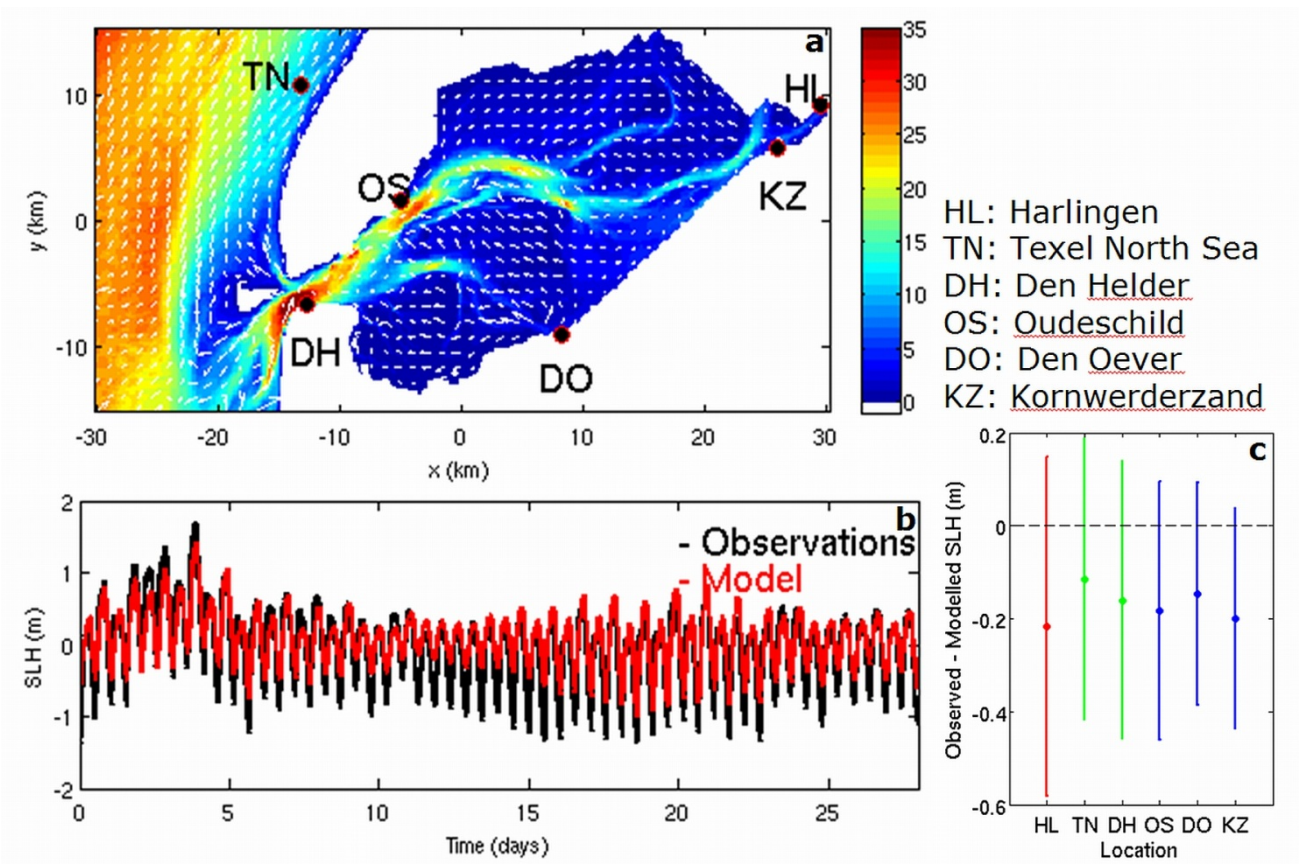

Figure 1. Model set-up for the Marsdiep inlet system: a) Top-view of the bathymetry along with the locations of field-data stations. Sea Level Height (SLH) data from these stations is compared with model predictions (the white arrows indicate the modelled residual current circulation pattern). b) Comparison between predicted (in red) and observed (in black) sea level height over time at Den Helder (DH). c) The mean difference and RMS error between the observed and predicted sea level height for the different stations along the basin-edge.

The transport of nutrients along with favorable water conditions (such as temperature) can give rise to blooms of plankton [*Baars et al., 2002*]. Also, transport of fish-larvae from spawning grounds towards nursery areas is largely driven by flow patterns [*Van der Veer and Witte, 1999*]. Hence, knowledge of the underlying current patterns and their variability is of great importance.

NUMERICAL MODEL

The General Estuarine Transport Model (GETM) is a three-dimensional hydrodynamic model, which is coupled to GOTM (General Ocean Turbulence Model) that includes a variety of vertical turbulence schemes. This public domain model was developed by *Burchard and Bolding [2002]* with an initial focus on estuarine systems, where drying and flooding of parts of the domain are of great importance. However, later also coastal seas (such as the North Sea and the Baltic Sea) were investigated by different research groups using this model. Continually, new modules are being added by the user community. The model can implement the inflow of fresh water and describe the development of stratification in the domain, both as a result of salinity and temperature gradients. The vertical tides and meteo-forcing are prescribed at the open boundaries. Recently, a module for the transport of fine sediments (SPM) has been added to the GETM/GOTM system which is still under development. Initially

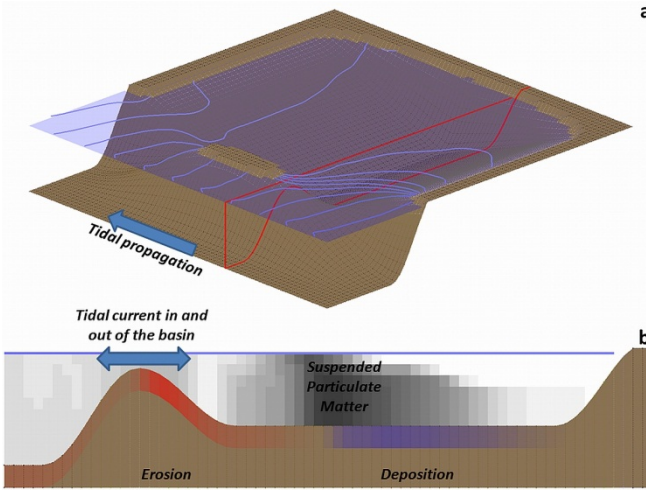

Figure 2. An idealized model set-up of a barrier-island coastline: A tidal wave propagates along the open end of the domain, creating a tidal current in and out of the basin behind the island. b) The strong current results in sediment being eroded from the inlet and transported into the basin, where it deposits.

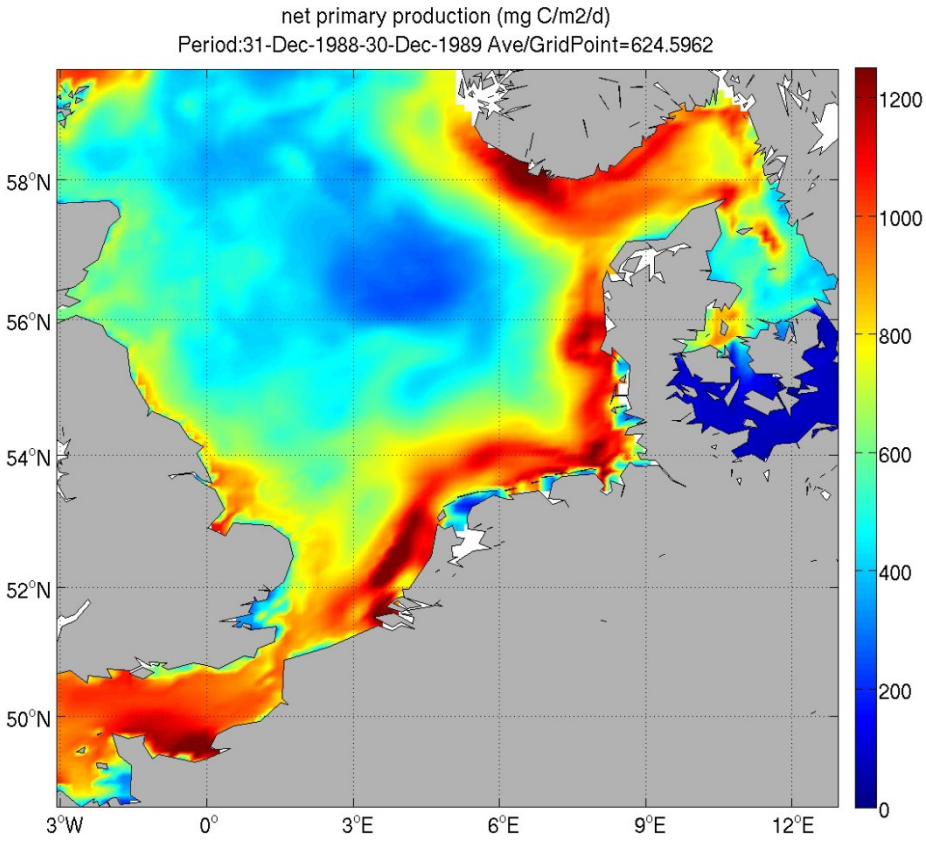

Figure 3. Depicted is the net primary production o of phytoplankton biomass in 1989, calculated with GETM/GOTM and a coupling to ERSEM/BFM, see www.nioz.nl/northsea_model for more results.

the model will be used to describe the hydrodynamics, but subsequently it will be applied to study SPM transport and concentration.

HYDRODYNAMICS

Using long-term ferry based observations, the net SPM transport in the Marsdiep inlet is estimated to be 5 to 10 Mton/year into the Wadden Sea [*Nauw et al., 2012*]. A question that arises from these findings is what happens with this sediment within the Wadden Sea. After all, the Marsdiep inlet forms one of the two main inlets of the Western Wadden Sea, the other one being the Vlie, and so one may expect that part of the imported sediment is partly exported again through the other inlet. As field data is only available from a limited number of stations, numerical modeling results should give a more comprehensive insight into the sediment transport within the Wadden Sea. For the description of SPM characteristics from a numerical model, an accurate description of the hydrodynamics is a prerequisite. An initial set-up can be seen in Fig. 1; here, for simplicity, the Marsdiep basin is taken in isolation, ignoring the neighboring Vlie basin by imposing a 'wall' along the watershed between the basins. Despite these simplifications, a comparison between modeled tidal elevation and data from coastal stations already shows a reasonable correspondence. In the near-future, a similar set-up will be developed for the entire Western Dutch Wadden Sea to investigate the interaction between the Marsdiep and Vlie inlets.

SUSPENDED SEDIMENT TRANSPORT

The transport of fine sediments is important both in relation to biology, and because of bed pattern formation. Currently, a simple experimental version of an SPM-module is available within the model; however this has not yet been applied to actual field-locations. The sensitivities of this sediment module are currently investigated using idealized set-ups; as shown in Fig. 2, where a tidal wave propagating along a coastline passes an idealized estuary. The resulting tidal wave into the estuary causes erosion of the fine sediments at the entrance. This suspended material subsequently deposits further into the estuary. Once a more comprehensive description of the suspended sediment dynamics is developed (involving for instance different sets of grain sizes with their corresponding settling velocities), this module can be applied to a range of different coastal seas and estuaries to investigate the SPM dynamics. Future plans will see the GETM/GOTM model to be applied not only to investigate the SPM transport within the Wadden Sea, but also the dynamics and driving forces behind the East Anglia Plume and plumes along the Dutch coast.

COUPLING TO ECOLOGY

The GETM model is currently already linked to a biological model developed at NIOZ, in collaboration with CEFAS (UK), to study biological processes in the North Sea. The latest version is called BFM, Biogeochemical Flux Model, used to investigate the causes and variability in sub-surface oxygen minima at the Oyster

Grounds, and C and N cycling. An example for the North Sea as a whole is shown in Figure 3: the net primary production (production of new phytoplankton biomass). Fig. 3 shows that the primary production is higher near the coast than in off-shore areas. The high production in the Southern North Sea along the coast is caused by Phaeocystis. These algae can reach very high concentrations through colonies formation which are too large for grazing by mesozooplankton. The relatively high production south of Norway is caused by local conditions in the Skagerrak and the Norwegian Trench and the fact that we dynamically modeled the chlorophyll content, resulting in primary production down to 50 meter. The low production in the Northern off-shore part of the North Sea is caused by relatively low nutrient concentration, a smaller growing season and the stable vertical stratifications.

A second ecological study at NIOZ focuses on the transport of plaice eggs and larvae. Spawning grounds are located in the central (and northern) parts of the North Sea. Residual currents transport the eggs and larvae towards nursery grounds located in the Wadden Sea. Field studies in the Marsdiep inlet have shown strong variability of the plaice concentration over the years. This behavior is partially the result of prevalent forcing conditions, but is also affected by active behavior exhibited by the plaice larvae, such as changing their vertical position in the water column. The transport patterns and inter-annual variability in plaice in the nursery areas forms the basis for this second project. The use of a 3D hydrodynamic model coupled with a particle tracking module (developed at CEFAS [*Van der Molen et al., 2007*]) that can implement active behavior of plaice, can give new insights into the transport routes taken by plaice eggs and larvae. Secondly, the inter-annual variability in forcing conditions will be studied, to identify potential sources of the changes in plaice concentrations in the Marsdiep nursery ground. Additional processes will be studied in a sensitivity analysis, such as water temperature (which might affect plaice development and mortality) and various active behavioral concepts.

CONCLUSIONS

The use of a hydrodynamic model, coupled with various additional components and modules, such as a particle tracking and the SPM module, can give great insights into different processes occurring in the North and Wadden Sea. The large quantity and quality of field-data collected at NIOZ and elsewhere, both of physical processes as well as biological characteristics, can be used to drive model parameters, as well as to judge accuracy of model predictions. Secondly, model predictions can cover large areas and durations that are not covered by the extensive field data-bank. These model data can be used as a basis to study biological, geochemical and ecological processes; the study of SPM in the Wadden Sea, and coupling with primary production being examples of this.

REFERENCES

Baars M, Oosterhuis, S. and Kuipers, B. (2002), Plume & Bloom: water mass patterns and nutrient dynamics in the central part of the Southern Bight. Annual Report 2002, Royal Netherlands Institute for Sea Research, Texel: 11-13

De Boer, G.J., Pietrzak, J.D., Winterwerp, J.C. (2006), On the vertical structure of the Rhine region of freshwater influence. Ocean dynamics 56, 198-216. DOI 10.1007/s10236-005-0042-1

Burchard, H. and Bolding, K. (2002), GETM - a general estuarine transport model. Scientific Documentation, European Commission, rep. EUR 20253 EN, 157 pp.

Burchard, H. and Hetland, R. D. (2010). Quantifying the contributions of tidal straining and gravitational circulation to residual circulation in periodically stratified tidal estuaries. J. phys. oceanogr. 40: 1243-1262, doi:10.1175/2010JPO4270.1

Dyer K. R., Moffat T. J. (1998), Fluxes of Suspended Matter in the East Anglian Plume Southern North Sea. Cont Shelf Res 18:1311–1331

Eisma, D., and Kalf, J. (1987), Dispersal, concentration and deposition of suspended matter in the North Sea, J. Geol. Soc., 144, 161 – 178, doi:10.1144/gsjgs.144.1.0161.

de Kok, J. M. (2004). Slibtransport langs de Nederlandse kust. Bronnen, fluxen en concentraties. RIKZ/OS/2004.148w.

van der Molen, J., Rogers, S. I., Ellis, J. R., Fox, C. J., and McCloghrie, P. (2007), Dispersal patterns of the eggs and larvae of springspawning fish in the Irish Sea, UK. Journal of Sea Research, 58:313– 330.

Nauw, J.J., L.M. Merckelbach, H. Ridderinkhof and H.M. van Aken (2012), Ferry-based observations of the suspended sediment fluxes through the Texel inlet using an acoustic Doppler current profiler, in prep.

Otto, L., Zimmerman, J. T. F., Furnes, G. K., Mork, M., Saetre, R., and Becker, G. (1990), Review of the physical oceanography of the North Sea. Netherlands Journal of Sea Research, 26: 161–238.

Pietrzak, J. D., G. J. de Boer and M. A. Eleveld (2011), Mechanisms controlling the intra-annual mesoscale variability of SST and SPM in the southern North Sea, Continental Shelf Research, 31(6), 594-610

Postma, H. (1981), Exchange of materials between the North Sea and the Wadden Sea. Marine Geology, 40: 199–213.

Ridderinkhof, H. and Zimmerman, J. T. F. (1992), Chaotic stirring in a tidal system. Science. 258,1107-1111

Stanev, E. V., Brink-Spalink, G., and Wolff, J. O., (2007), Sediment dynamics in tidally dominated environments controlled by transport and turbulence: a case study for the east Frisian Wadden Sea. Journal of Geophysical Research—Oceans 112, C04018.

Van der Veer, H. W., and Witte, J. IJ. (1999), Year-class strength of plaice Pleuronectes platessa L. in the Southern Bight of the North Sea: a validation and analysis of the inverse relationship with winter seawater temperature. Marine Ecology Progress Series, 184: 245–257.

Zimmerman, J. T. F. (1976a), Mixing and flushing of tidal embayments in the Western Dutch Wadden Sea, part I: description of salinity distribution and calculation of mixing time scales. Neth J Sea Res 10:149–191

Zimmerman, J. T. F. (1976b), Mixing and flushing of tidal embayments in the Western Dutch Wadden Sea, part II: analysis of mixing processes. Neth J Sea Res 10:397–43

DOI: 10.3990/2.198

Probabilistic assessment of safety against dune retreat along the Northern-Holland coast

W. van Balen[1], V. Vuik[1] and S. van Vuren[1]
[1]HKV Consultants, Botter 11-29, 8232 JN Lelystad, The Netherlands, w.vanbalen@hkv.nl

ABSTRACT

Coastal zone management is a multidisciplinary issue that can be assessed from multiple viewpoints such as safety, recreation, ecology and nature. A possible means for properly maintaining the various functions of the coast is sand nourishments along either the shoreface and/or the beach. To assess the influence of sand nourishments, the time-dependency of appropriate indicators of the various coastal functions can be analyzed.

HKV has conducted a study that focuses on the probability of failure for dune erosion, as an indicator for safety. For this purpose, the yearly JarKus measurements from the online OpenEarth-database are used. HKV has computed the probability of failure for dune erosion for the entire Dutch coast, from 1965 until 2010, using the dune erosion model DUROS+ and the probabilistic method FORM ('First Order Reliability Method'), as implemented in the package PC-Ring. This approach is closely related to the approach of the project Flood Risks in the Netherlands (FLORIS / VNK).

The current paper presents results of these computations, in relation to previous nourishment activities, for the region of Northern-Holland. These gained results can be used to further analyze the effectiveness of nourishments and can hence benefit future nourishment strategies by providing a decision supporting framework.

INTRODUCTION

The major part of the Dutch coast consists of dunes. The sandy dunes form a natural and flexibel sea defense that serves multiple purposes such as safety against flooding of the hinterland, recreation, nature, ecology, drinking water supply, et cetera. However, since the Dutch coast is liable to structural erosion, the multiple functions of the Dutch coast are permanently subject to coastal retreat as a morphologic threat.

In order to properly support the various coastal functions and to counteract the coastal retreat, it has been decided in 1990 to dynamically maintain the shoreline. Therefore, the coastal management strategy has ever since amounted to sand nourishments to achieve the aims following from the coastal functions. Such sand nourishments can either be applied as beach nourishments and as shoreface nourishments. From 2000, the strategy has been focused on maintaining the coastal fundament, based on volumetric arguments.

During the past decades, several studies have been conducted to understand the physical processes underlying dune resilience (cf. *Vellinga* [1986], *Steetzel* [1993]) and several models have been developed to simulate these, such as the 1D dune resilience model DUROS+ and its later adaptations, such as DUROSTA (*Steetzel* [1993]), and the 2D model XBeach (*Roelvink et al.*, [2009]) that simulates dune erosion, overwash and breaching. For each type of model, the availability of measured data of either the bathymetry (as input) and the physical parameters (for calibration and validation) is of key importance.

This paper presents the results of the application of a straightforward 1D dune erosion model, within a probabilistic context, to the dunes along the coast of Northern-Holland (see figure 1). For this, 225 JarKus transects (cf. *Rijkswaterstaat* [2008]) have been subjected to a probabilistic analysis for dune resilience. The main objective of this investigation has been to image the interplay between sand nourishments and dune resilience. For that purpose, the transect data (available in the online database OpenEarth [*Van Koningsveld et al.*, 2010]) with measurements from 1965 until 2010 have been used.

This investigation has been a part of a broader research program in which the entire dune coast of the Netherlands is considered. The final result is failure probabilities for the coast for 1965-2010.

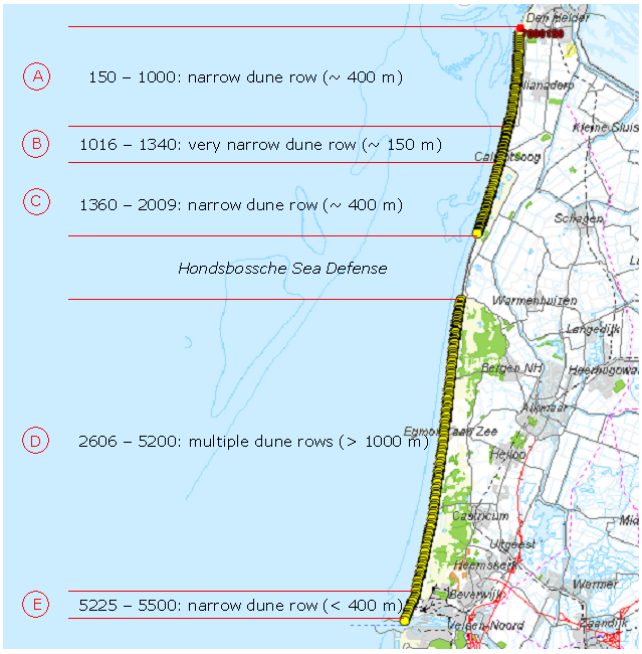

Figure 1. The Northern-Holland coast with distinction between six regions on the basis of dune width and number of dune rows. The yellow dots indicate transects for which a computation has been conducted. The numbers indicate the ID of a transect.

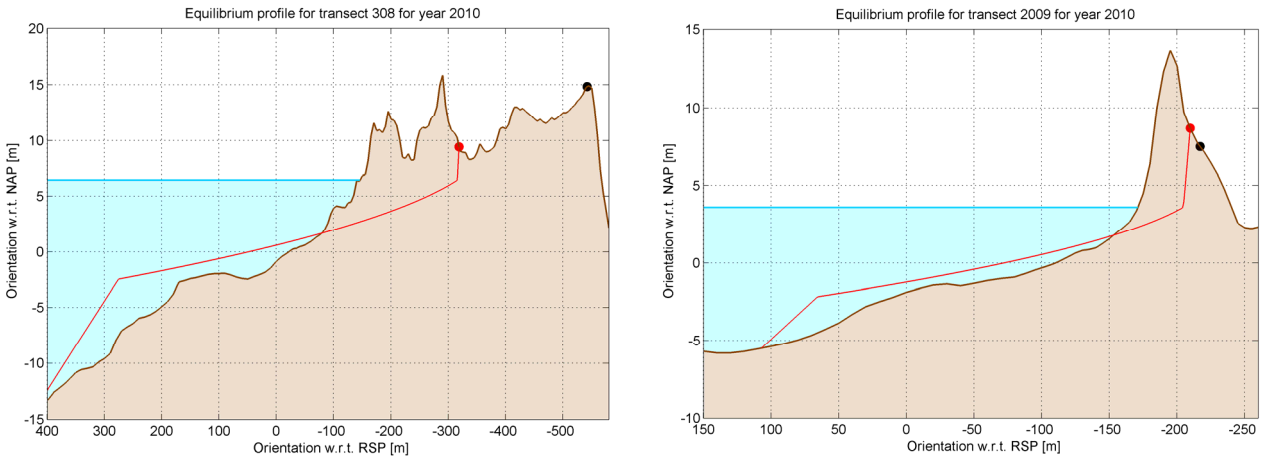

Figure 2. Dune profile and computed equilibrium profile of two JarKus transects in 2010. Left panel: transect 308 in the north of the Northern-Holland coastline; right panel: transect 2009 directly north of the Hondsbossche Sea Defense.

METHODOLOGY

In order to compute failure probabilities, the DUROS+ model for dune erosion is used in combination with the probabilistic level II method FORM ('First Order Reliability Method') as it is implemented in the TNO software package PC-Ring (cf. [*Vrouwenvelder & Steenbergen*, 2003], [*Steenbergen et al.*, 2007]). The DUROS+ model assumes a parabolically shaped equilibrium profile that develops during a storm (cf. [*TAW*, 2007]), thus ignoring time-dependent effects, but assessing a final state in which sand from the dune is deposited seawards.

The probabilistic method FORM is used to take uncertainties regarding the hydraulic loads as well as the strength of the dune into account. Basically, FORM is an optimization method with the constraint of a prevailing limit state function. Uncertainties with respect to dune erosion in this context are considered for key parameters like the wave height, the peak period, the grain size of the sand particles and the geometry.

A serious drawback of the DUROS+ model is the restriction of the dune profile to only a single dune row. In order to fulfill the resulting requirements, only the first dune row of the dune profile is taken into consideration. Figure 1 indicates that this restriction does not have consequences for dunes north of the Hondsbossche Sea Defence, whereas it does have consequences for dunes south of it. The latter category dunes are dunes with a considerable width, generally larger than 1 km, with multiple dune rows.

The software package PC-Ring has been used in a Matlab-batch mode to compute the failure probabilities for each JarKus transect along the entire Dutch coast for the period 1965-2010.

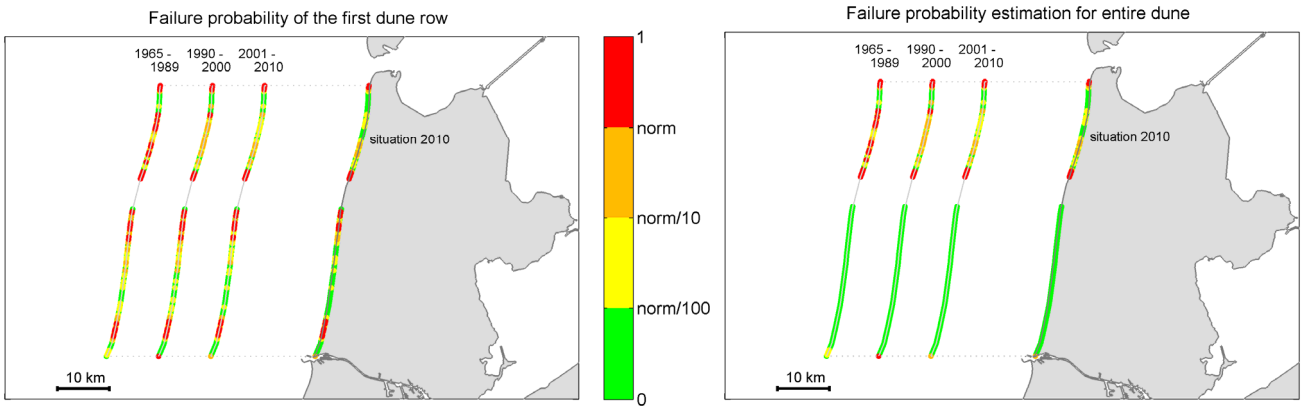

Figure 3. Failure probability of the first dune row (left panel) and estimated failure probability for the entire dune, including multiple dune rows. The failure probability (time-averaged) is normalized by a norm equal to 10^{-4} per year, being the safety standard for the hinterland of dikering 13. Three time windows are chosen: 1965 – 1989 (no nourishments), 1990 – 2000 (nourishment strategy based on maintaining the coast line) and 2001 – 2010 (nourishment strategy based on volumetric arguments).

In total, about 75.000 computations have been carried out (1616 transects for 46 years), based on available profiles from OpenEarth for the entire Dutch coast. From this extensive dataset (actually a useful sequel of the study by *Den Heijer et al.* [2011]), the results for Northern-Holland are highlighted with the particular focus on the development of the failure probability for dune erosion and the role of sand nourishments.

RESULTS

As indicated in figure 1, dunes can consist of multiple dune rows. North of the Hondsbossche Sea Defense, the dunes contain only one row, whereas south of it, the dunes are wide (> 1 km) and high (at some places > 30 m +NAP).

For brevity and conciseness, this paper therefore merely focuses on the northern part, i.e. regions A, B and C in figure 1. Along this region, the dunes are very narrow in the middle part (region B).

An example of a relatively wide dune section is transect 308, whereas an example of a very narrow one is transect 2009 (direct north of the Hondsbossche Sea Defense). The computed equilibrium profiles are shown in figure 2. The calculated failure probabilities are 1.6 10^{-13} for transect 308 and 4.2 10^{-3} for transect 2009, both on a yearly basis. These values can obviously directly be understood from the dune profiles. Also *Den Heijer* [2011] found such a high failure probability for transect 2009.

The results for the entire shoreline are shown in figure 3. In this figure, distinction is made between four sets: the periods from 1965 - 1989 (no nourishments), from 1990 - 2000 (maintaining the shoreline) and from 2001 - 2010 (maintaining the coastal fundament). The situation for 2010 is shown as well.

For the three periods, the probabilities are time-averaged, based on the logarithm of their value. The values are furthermore normalized by the value of 1.0 10^{-4}, being the normative safety standard for the hinterland (dikering 13). This normalization, which is basically arbitrary, is used to distinguish between four levels of safety.

In the left panel of figure 3, the failure probability is shown for the first dune row, whereas in the right panel of figure 3, the estimated failure probability for the entire dune section is shown.

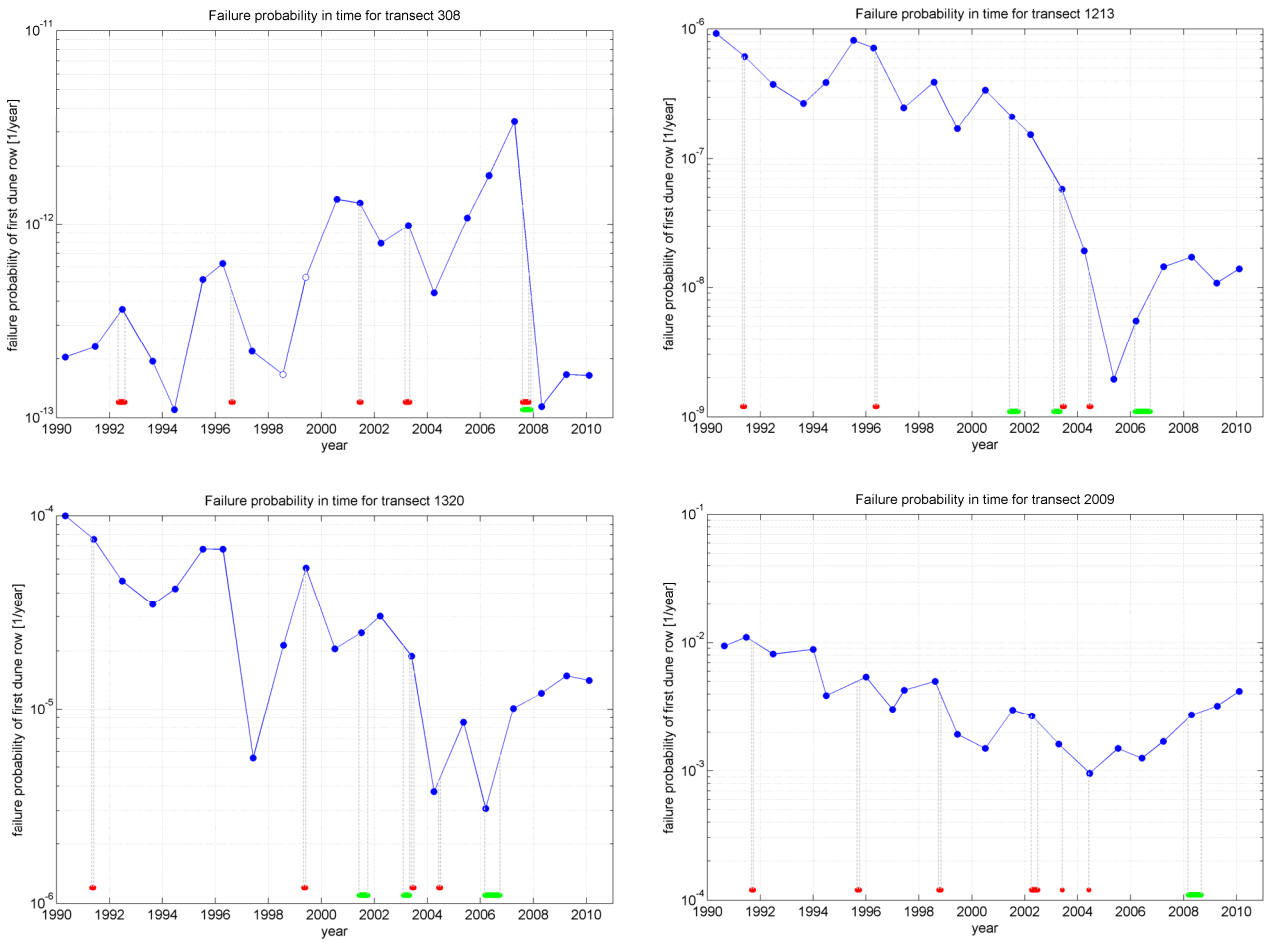

Figure 4. Development of the failure probability of the first dune row in time for four JarKus transects. In lexicographic ordering: transect 308, 1213, 1320 and 2009. The green lines indicate shoreface nourishment periods, the red lines indicate beach nourishment periods. Filled circles refer to correct convergence of the FORM-iteration, open circles refer to bad convergence behavior.

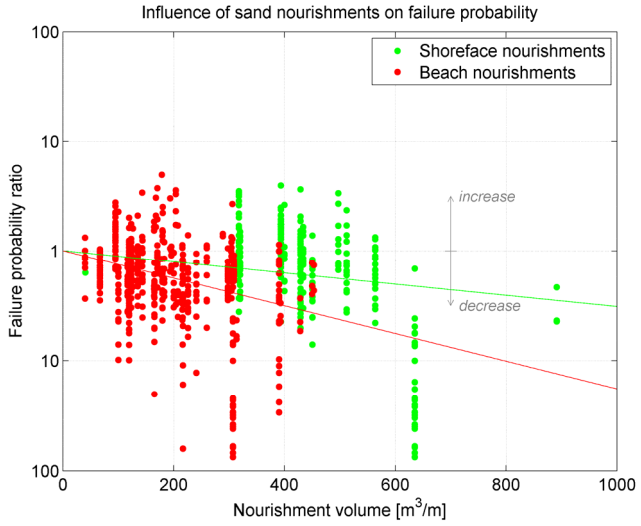

Figure 5. Failure probability ratio, defined as $P_{year\ j}$ / $P_{year\ j-1}$, against the nourishment volume applied, showing the instantaneous effect of sand nourishments, i.e. the effect within one year after application. Green dots refer to shoreface nourishments, red dots refer to beach nourishments. The solid lines present an indication of the orientation of the data.

It is a sure thing that the failure probability of the first dune row is a conservative upper limit for the entire dune section. The basic result is that the part southern of the Hondsbossche Sea Defense can be considered as very safe, considering the huge body of dune mass beyond the first dune row. Generally, the failure probability tends to decrease in due time, which suggests a favorable effect of sand nourishments.

The regions that appear to be the weakest areas are the region in the very north (transects 150, 170 and 190) with failure probabilities of the order of 10^{-4} per year and the region just north of the Hondsbossche Sea Defense (transects 1940 until 2009) with probabilities of the order of 10^{-3} per year. The latter region consists of a relatively narrow dune row with a width sometimes smaller than 100 m.

To gain more insight in the temporal development of the failure probability and, moreover, in the role of sand nourishments, the results for the last 20 years are shown in figure 4. The green bars and red bars indicate periods of shoreface nourishments and beach nourishments, respectively. The points of time correspond with measuring times of the wet bathymetry part of the profile. Information on these times as well as on the nourishment times stem from the OpenEarth database.

From the data only four transects are elected for further analysis, for brevity: transects 308 (in the middle of region A, see figure 1), 1213 (region B), 1320 (region B) and 2009 (most southern point in region C). The equilibrium profiles for transects 308 and 2009 are already shown in figure 2.

From the picture for transect 308 (figure 4), it can be derived that each nourishment has lead to a decrease of the failure probability, directly (instantaneously) in the year after application. Particularly, the nourishment in 2007 appears to be rather effective.

The effectiveness of the sand nourishments is also reflected in the picture for transect 1213. The nourishments between 2000 and 2005 seem to be very effective with a probability decrease of a factor of about 100.

Less effects are seen in the picture for transect 1320. Despite the nourishment between 1998 and 2008, only a decrease by a factor of about 10 is effectuated. The same observation holds for transect 2009, be it even more pronouncedly.

To provide an impression of the *instantaneous* effects of the nourishments, figure 5 is included. This figure displays the failure probability ratio (defined as the probability in year *j* divided by the probability in year *j*-1) against the nourishment volume, for each transect where actually a nourishment has been applied.

For brevity, only the effects *within one year* are shown, which provides a first indication of the effectiveness of the nourishment. Obviously, only a first indication, since this figure discounts long-term, two-dimensional effects. This deficiency is definitely prone to improvement in the near future.

Nonetheless, figure 5 provides an interesting view on the results for the Northern-Holland part of the data. On average, a decrease in failure probability is gained within one year after nourishment, for both the beach nourishments and the shoreface nourishments.

Strict distinction between both types of nourishments can, however, not be made. Within this context, it should be mentioned that in many cases the location of application of a shoreface nourishment is situated outside the domain of the computed equilibrium profile. Moreover, shoreface nourishments are very likely to be important on supra-year timescales, which makes the causes of the effects less easily traceable.

In view of these deficiencies, an image is given of the bottom level difference between 2000 and 2005, on the one hand, and between 2005 and 2009, on the other hand, in figure 6. In these figures, the four selected transects are depicted with a blue marker. These pictures are generated by means of subsequent interpolation and subtraction of 2D bathymetry files.

The strong decrease in failure probability at transect 308 in the year 2007 can directly be understood from the right panel of figure 6: a strong bottom level increase has taken place.

Something similar holds for transects 1213 and 1320, be it less pronouncedly: near the shore the bottom level has increased, whereas further from the shore a decrease and again an increase is seen in seaward direction.

The poor effectiveness of the nourishments near transect 2009 can directly be explained by figure 6 (left panel): in 2005 the bottom level hardly differs from the bottom level in 2000.

CONCLUSIONS AND OUTLOOK

Dune retreat computations have been conducted using the 1D model DUROS+, in combination with the level II probabilistic method FORM. In total, about 75.000 computations have been carried out for the entire Dutch coast, for the last 46 years. In this paper, only some results for the shoreline of Northern-Holland (225 transects considered) are selected and presented.

The obtained results provide an image of the safety of the dune sections along Northern-Holland, by means of a probability of failure of the first dune row. The obtained distribution of the probability is used to identify weak spots.

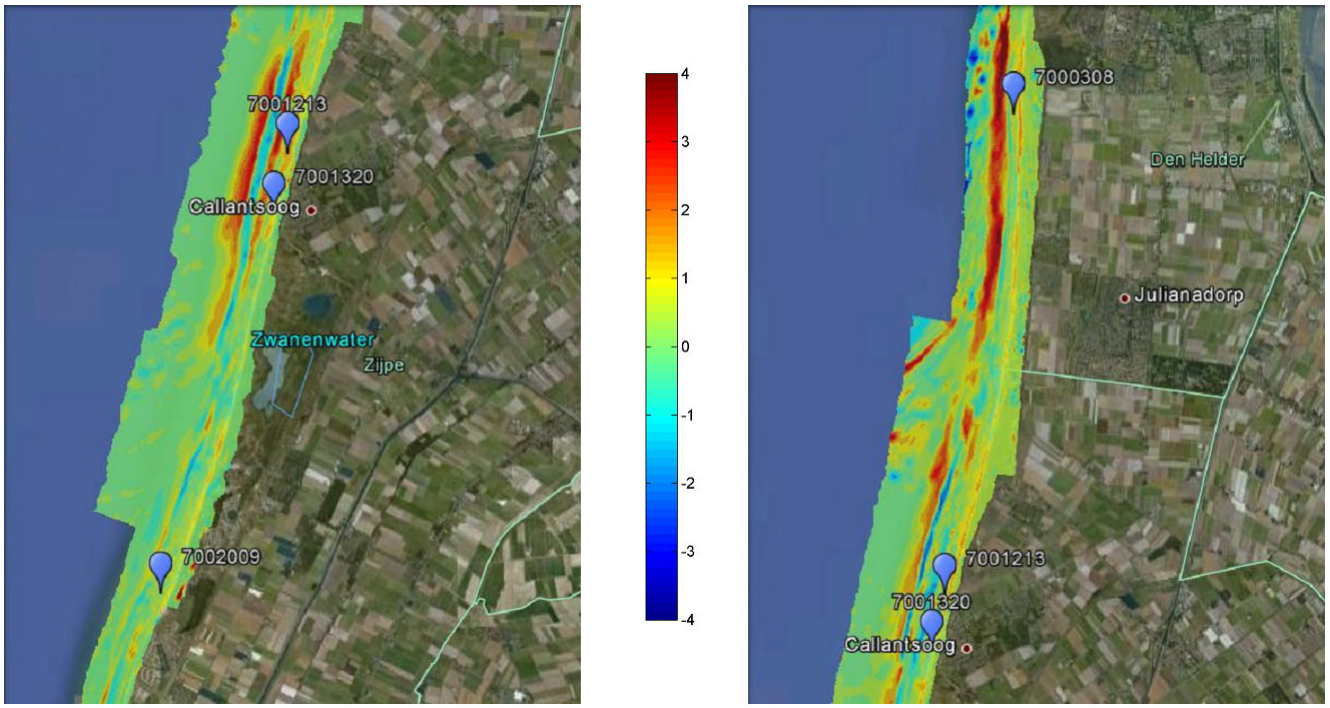

difference between 2005 en 2000

difference between 2009 en 2005

Figure 6. Left panel: bottom level changes in meters between 2005 and 2000 for the regions B and C (cf. figure 1). Right panel: bottom level changes in meters between 2009 and 2005 for the regions A and B (cf. figure 1). The blue markers denote the JarKus transects for which the failure probability development in time is shown in figure 4.

By coupling of the gained results with available information on applied sand nourishments, an image has been sketched of the effectiveness of these nourishments. It turned out that sand nourishments in general, and beach nourishments in particular, on average enhance the safety level of the first dune row.

For the sake of conciseness, the presented results have been restricted to instantaneous effects, i.e. effects gained within one year. Moreover, the two-dimensional aspects have not extensively been addressed. Improvements on both shortcomings should be met in the near future to assess a more general picture of the effectiveness of sand nourishments.

After all, the gained results of about 75.000 computations can largely benefit the insight in the time development of the safety of the coast and its interplay with applied sand nourishments.

ACKNOWLEDGEMENT

This study has been carried out in cooperation with Deltares and Arcadis as a part of the project “KPP-B&O Kust” (Kustlijnzorg), funded by Rijkswaterstaat Waterdienst.

REFERENCES

Heijer, C. den, Baart, F., Koningsveld, M. van, Assessment of dune failure along the Dutch coast using a fully probabilistic approach, Geomorphology (2011), doi:10.1016/j.geomorph. 2011.09.010.

Koningsveld, M. van, Boer, G.J. de, Baart, F., Damsma, T., Heijer, C. den, Geer, P. van, Sonneville, B. de, 2010. OpenEarth — inter-company management of: data, models, tools & knowledge. Proceedings WODCON XIX Conference. Beijing, China.

Rijkswaterstaat, 2008. The yearly coastal measurements (De JAaRlijkse KUStmetingen (JARKUS)). (in Dutch)

Roelvink, D., Reniers, A., van Dongeren, A., van Thiel de Vries, J., McCall, R., Lescinski, J., 2009. Modelling storm impacts on beaches, dunes and barrier islands. Coastal Engineering 56, 1133–1152.

Steenbergen, H.M.G.M., Vrouwenvelder A.C.W.M., and Koster T., Theoriehandleiding PC-Ring Versie 5.0 Deel A: Mechanismenbeschrijvingen. TNO, 2007-D-Rxxxx/A, september 2007. (in Dutch)

Steetzel, H. J., 1993. Cross-shore Transport during Storm Surges. Ph.D. thesis, Delft University of Technology, also published as: Delft Hydraulics communication, no. 476.

TAW. Technische Rapport Duinafslag - Beoordeling van de veiligheid van duinen als waterkering ten behoeve van Voorschrift Toetsen op Veiligheid 2006. WL | Delft Hydraulics, TUDelft en Alkyon, H4357, mei 2007. (in Dutch)

Vellinga, P., 1986. Beach and Dune Erosion during Storm Surges. Ph.D. thesis, Delft University of Technology, also published as: Delft Hydraulics communications, no. 372, 1986.

Vrouwenvelder, A.C.W.M., and Steenbergen, H.M.G.M. Theoriehandleiding PC-Ring Versie 4.0 Deel C: Rekentechnieken. TNO, 2003-CI-R0022, april 2003. (in Dutch)

DOI: 10.3990/2.199

The Lagos coast – Investigation of the long-term morphological impact of the Eko Atlantic City project

K.M. van Bentum[1,2,3], C.W. Hoyng[2], M. Van Ledden[1,2], A.P. Luijendijk[1,3] and M.J.F. Stive[1]

[1]Hydraulic Engineering, Delft University of Technology, Stevinweg 1, 2628 CN , Delft, The Netherlands, kvbentum@gmail.com

[2]Royal Haskoning, George Hintzenweg 85, 3068 AX Rotterdam

[3]Deltares, Rotterdamseweg 185, 2629 HD Delft

ABSTRACT

The Lagos coast has been suffering high rates of erosion since the construction of three harbour moles, i.e. the West Mole, East Mole and the Training Mole, at the tidal inlet connecting the Lagos Lagoon to the South Atlantic Ocean. To provide for a permanent erosion mitigation measure and to create residential and commercial area for circa 400,000 people, the Eko Atlantic City project has been initiated in 2008. In front of the eroded coast, approximately 9 km² of land will be reclaimed and protected by a revetment.

In this study the long-term and large-scale morphological behavior of the Lagos coast is investigated and subsequently the long-term morphological impact of the project is assessed. First, a conceptual model is created, in which the historical development of the coast is discussed. The long-term morphological behavior of the coast downstream of the inlet is determined by two main factors: sediment accumulation at the West Mole and sediment import into the tidal inlet and the lagoon, induced by disturbance of the morphological equilibrium by sea level rise and dredging activities.

Using the numerical simulation model Unibest, the long-term impact of Eko Atlantic City is assessed. It is concluded that the construction of Eko Atlantic City will not change the total erosion volumes downstream of the inlet. However, as the revetment of the project retains the coast, the erosion will be shifted towards downstream. Downdrift of the project, the erosion rates are locally relatively high. The shape of the sea defence has been designed to minimize the local erosion effect. A monitoring and mitigation strategy has been recommended to monitor this effect and instruct coastal protection management actions to be implemented if required.

INTRODUCTION

Lagos is situated at the western part of the Nigerian coast around a tidal inlet which leads to the Lagos Lagoon. In 1908 man started to interfere with the natural coastal system by the construction of three harbour moles at the tidal inlet. These moles are the West Mole, the Training Mole and the East Mole. Nowadays, the tidal inlet is called the Commodore Channel and it constitutes the seaside entrance to the Lagos Harbor, see Figure 1.

As of the completion of the moles, the Lighthouse Beach, situated updrift of the inlet, expanded about 800 meters over circa hundred years due to sediment trapping at the West Mole. Consequently, the Bar Beach, located downdrift of the inlet, suffered enormous rates of erosion. Over roughly hundred years the total retreat of the coast has reached values of more than one kilometer.

To counteract the large loss of beach width due to the erosion, man started to apply nourishments on the Bar Beach around 1960. Enormous volumes of sediment have been supplied to the beach, but it kept on eroding anyhow. An additional problem at Lagos is the growing population, entailing large space demands for residential, commercial and recreational activities.

To cope with this space deficit and the land loss due to the erosion of the Bar Beach, the private project developer South Energyx Nigeria Ltd. (SENL) has initiated the Eko Atlantic City Development Project. This project comprises a land reclamation of 9 km² in front of the Bar Beach, directly east of the East Mole, see Figure 2. The newly reclaimed land is protected against erosion by a revetment, which has a length of roughly 8.4 km. Royal Haskoning provides, among others, the consulting services for the marine works of Eko Atlantic City.

This paper summarizes the results of a study into the long-term morphological impact of Eko Atlantic City on the adjacent coast of Lagos, Nigeria, performed by *van Bentum* [2012]. Three research questions (RQ) have been posed in this project:

RQ1: What are the governing processes and mechanisms determining the long-term and large-scale morphological behavior of the Lagos coast?

RQ2: What was the influence of the construction of the Lagos Harbour Moles and other human interferences on the historical coastline development?

RQ3: How does the construction of Eko Atlantic City change the present morphological processes?

A time span of 10 years after construction of Eko Atlantic City is defined herein as long-term. This work builds upon the analysis from *Royal Haskoning* [2011] in which the initial morphological effects of Eko Atlantic City were assessed.

RESEARCH APPROACH

The study has been divided into two parts. First, the governing processes and mechanisms determining the long-term and large-scale morphological behavior of the Lagos coast have been identified. Information sources have been (scarce) reports, historical maps and nourishment data in the area of interest. Based on these sources, a conceptual model of the historical development

Figure 1: Overview of Lagos [after Google Earth, 2010]

of the Lagos coast has been created. In the conceptual model, the governing sediment fluxes, sources and sinks in the Lagos coastal system are quantified via consideration of the sediment balance at the coast of Lagos. This conceptual model is subsequently used to setup hypotheses regarding the future morphological development of the Lagos coast.

In the second part of the study these hypotheses have been investigated using the numerical simulation model Unibest. The model has been verified against the historical development of the Lagos coast first. Thereafter, the model has been applied to assess the impact of several human interferences such as the construction of Eko Atlantic City. Uncertainties have been dealt with using different scenarios for the magnitude of sea level rise and the sediment sink of the Lagos Lagoon and the Commodore Channel. These simulations provide useful insight into the extent and timescale of erosion along the coast. Recommendations are given on how to mitigate these effects.

HISTORICAL ANALYSIS

The area of interest in this study has been defined by the morphological influence zone of the Lagos Harbor Moles. Using the 'Single line theory' of *Pelnard-Considère* [1956] (see e.g. *Bosboom and Stive* [2010]), the influence of the Lagos Harbor Moles in 2020 (i.e. ten years after construction of Eko Atlantic City) reaches circa 25 km upstream and 25 km downstream.

As the governing processes and mechanisms are not constant over time, the historical development of the Lagos coast has been considered in four periods. The division in time has been made using the historical human interventions at the Lagos coast.

The first significant human intervention at the Lagos coast is the construction of the three harbor moles, between 1908 and 1912. Thereafter, man started to apply nourishments around 1958, which is also the time that man started to dredge the Commodore

Figure 2. Artist's impression of the Eko Atlantic City [made by Royal Haskoning]

Channel, for navigational purposes, and the Lagos Lagoon, to obtain sediment for construction activities. The most recent human act at the Lagos coast is the commencement of the construction of Eko Atlantic City in 2008. Using these data, the historical development is divided in the periods: 'Before 1910', 1910 – 1960, 1960 – 2010 and 'After 2010' [*van Bentum*, 2012].

Governing processes and mechanisms

The wave climate at Lagos consists of persistent, high-energy swell waves, which reach the coast of Lagos with a mean direction of 188°. Hereby, a mean eastward longshore sediment transport of roughly 600,000 m³/year to 700,000 m³/year is induced. It has been assumed that this longshore sediment transport rate was approximately constant over the years.

In general, the whole Lagos coast suffers erosion due to the high rates of relative sea level rise, induced by the Eustatic sea level rise combined with soil subsidence. The rates of subsidence are high, due to natural dewatering and compaction of the soil but also due to human-induced water extraction in het coastal zone.

According to the 'Bruun rule'[*Bruun,* 1962], a cross-shore profile responds in the long-term to an increased mean sea level such that a new equilibrium upper shoreface profile develops relative to the new mean sea level. The coast recedes as result of the (relative) sea level rise, because the sea level rise causes more sediment accommodation space. This induces erosion of the beach, due to the landward shift of the profile. The rate of relative sea level rise is assumed to be constant over time, so this value does not differ between the different periods.

The high rates of erosion downdrift of the inlet, i.e. at the Bar Beach, are not induced by sea level rise alone however. The governing factors inducing the erosion of Bar Beach are the accumulation of sediment by the West Mole and the import of sediment into the Commodore Channel and the Lagos Lagoon. The sediment import into the Commodore Channel and the lagoon occurs due to sea level rise, dredging of the channel and dredging of the lagoon. These processes disturb the morphodynamic equilibrium of the inlet and the lagoon, as they create additional sediment accumulation space by enlarging the depth of the channel respectively the lagoon. This leads to a so-called sediment demand in the lagoon and the tidal inlet.

The result of the sediment trapping at the West Mole and the sediment import into the tidal inlet and the lagoon is that almost no sediment is able to bypass the East Mole. Thereby, a sediment deficit in the longshore current downdrift of the tidal inlet arises. The exact volume of the bypass, however, differs per period. Subsequently, the Bar Beach starts to erode, to provide for a sediment source to the longshore sediment transport. The volume of erosion is thus dependent on the sediment volume able to bypass the East Mole.

Impact human interventions

The impact of the Lagos Harbor Moles on the historical development of the Lagos coast is visible in the differences in beach widths updrift and downdrift of the tidal inlet. The Lighthouse Beach, located updrift of the inlet, expanded about 800 meters over 100 years, due to the sediment accumulation at the West Mole. On the contrary, the Bar Beach, situated downdrift of the inlet, eroded even more than one kilometer since the construction of the moles.

As of 1960, man started to apply mitigation measures at the Bar Beach to counteract the erosion. Because the retreat of the coast had become very severe, mitigation measures were required directly. Although erosion of the Bar Beach was not prevented by the artificial sediment supply with a mean volume of 580,000 m³/year, the nourishments clearly have had an alleviating effect on the erosion. If the nourishments had not been conducted, the erosion of the Bar Beach would have been much worse.

Another human intervention in the Lagos coastal system is the dredging of the Commodore Channel and the dredging of the Lagos Lagoon. The removal of sediment disturbs the morphodynamic equilibrium of the tidal inlet and the lagoon, and additional sediment accumulation space is created. Therefore, the tidal inlet and the lagoon import sediment to restore their dynamic equilibrium. Hereby, the sediment volume bypassing the East Mole is decreased and the Bar Beach suffers even more erosion.

Conceptual sediment balances

Based on the governing processes and mechanisms described above, a sediment balance of the Lagos coast has been set up for each period. In doing this, the sediment fluxes, sources and sinks are expressed as a percentage of the total volume of longshore sediment transport. The assumption underlying the setup of the sediment balances is that far upstream and far downstream of the inlet, beyond the influence of the moles, the volume of longshore sediment transport is hundred per cent, schematised by 'S'. In Figure 3, Figure 4 and Figure 5 the conceptual sediment balances are depicted per period (depicted in [*van Bentum*, 2012]).

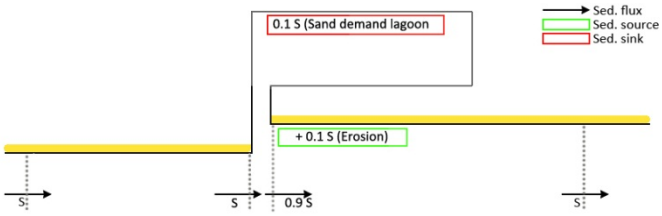

Figure 3. Conceptual sediment balance 'Before 1910'

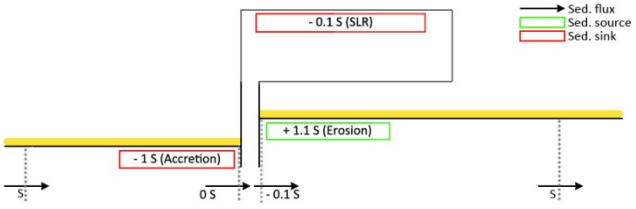

Figure 4. Conceptual sediment balance 1910 – 1960

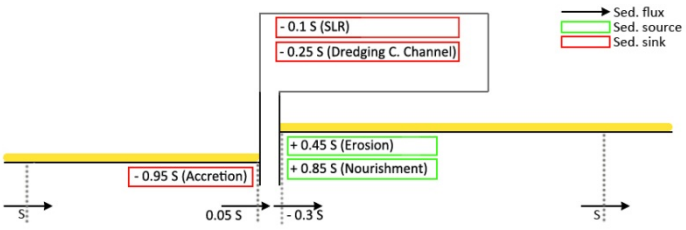

Figure 5. Conceptual sediment balance 1960 – 2010

Using the results of the conceptual model, hypotheses on the long-term morphological development of the Lagos coast with the presence of Eko Atlantic City have been put forward. As discussed earlier, there are two main factors determining the morphological behavior of the Bar Beach: 1) the sediment trapping at the West Mole, and 2) the sediment import into the lagoon and into the Commodore Channel. Due to the sediment sink these processes constitute, the sediment volume bypassing the East Mole is limited.

FUTURE COASTAL DEVELOPMENT

To predict long-term morphological changes, the numerical simulation model Unibest[1] has been applied. In short, the Unibest model can be used to compute longshore and cross-shore processes and the associated morphodynamics of beach profiles and coastline development. The model is especially suited for wave-dominated coasts.

The Unibest model consists of two modules, which run separately from each other: the LT (Longshore Transport) module and the CL (CoastLine) module. First the LT module is run and thereafter the output of the LT module run is used as input in the CL module. The advantage of the use of a 1D model such as the Unibest software is that a large coastal system can be analysed over large time spans. Since data of the Lagos coast is limited, the application of a 1D model is a justified choice in this study.

Using the Unibest model, the hypothetical future scenarios have been simulated. For the area of interest in this study, 11 profiles were defined along the coast, of which four were located in the shadow zone of the East Mole, to take into account the effect of diffraction. Each profile is characterized by a specific initial bathymetry and coastline orientation. In between the defined profiles, the coastal bathymetry has been obtained by linear interpolation between the two profiles. All profiles are defined perpendicular to the coast.

In short, the volumes of longshore sediment transport are computed in the LT module for every cross-section. These volumes provide a certain gradient in the longshore sediment transport between the profiles along the coast. These gradients are used in the CL module to define the accretion or erosion of the coast. Herein it is assumed that the layout of the cross-shore profiles does not change and that behind the (user defined) active depth no sediment transport occurs.

An example of the output of the Unibest model is shown in Figure 6, in which the simulated coastline in 2020 is depicted for both the scenario with the presence of Eko Atlantic City (in red) and without the presence of the project (in yellow). At the location of Eko Atlantic City, a revetment is put at the coastline by which erosion of the coast is prevented.

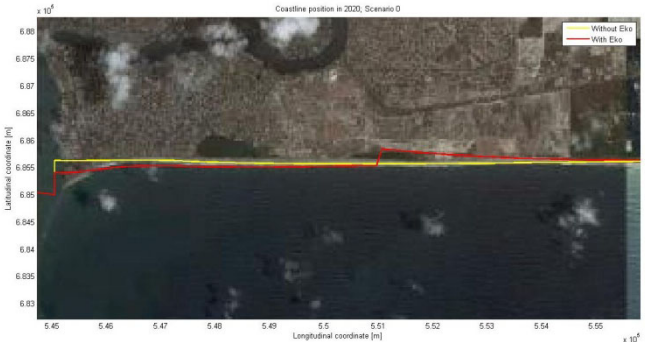

Figure 6. Simulated coastline in 2020. Red is with presence of Eko Atlantic City and yellow without the presence of the project

As stated above, due to the sediment sinks induced by sediment trapping at the West Mole and sediment import into the lagoon and the tidal inlet, the bypass along the East Mole is limited. Therefore, the coast downstream of the tidal inlet, the Bar Beach, erodes. The total volume of erosion occurring downstream of the tidal inlet is not altered by the presence of the Eko Atlantic City project.

The revetment of Eko Atlantic City fixes the coast of the newly reclaimed land, so further erosion of the Bar Beach is prevented. But, the erosion of the Bar Beach is shifted eastward by the construction of the project. As concluded in the conceptual model, the volume of erosion and the corresponding rate of beach retrogression are determined by the volume of sediment bypassing along the East Mole.

The erosion that would occur at the Bar Beach, without the construction of Eko Atlantic City, is spread quite equally over the beach. The erosion that occurs downstream the Eko Atlantic City project, on the contrary, reaches much higher values locally. So, although the total erosion volumes are equal, the erosion rates directly downstream of the project are increased significantly. Because the erosion volume downstream of the project is spread out over a larger distance than the distance over which the erosion is spread out if the project is not constructed, the erosion rates downstream Eko Atlantic City diminish rapidly. Moreover, the transition of the land reclamation towards the original shoreline has been altered into a less abrupt transition to reduce the local higher erosion values.

If the development of the erosion downstream of Eko Atlantic City is considered until 2060, it can be concluded that the erosion rates downstream of the project are highest just after the construction. Over the years, the erosion rates and the erosion

[1] *Unibest is an acronym for UNIform BEach Sediment Transport. The software is developed by Deltares; www.deltaressystems.com. The most recent version is of July 2011.*

volumes decrease somewhat, but the length of the erosion wave increases.

Therefore, keeping the longer-term effects of Eko Atlantic City in mind, and investigating the hinterland of the coast downdrift of Eko Atlantic City, it becomes clear that mitigation measures may be required. It is envisioned that a volume in the order of the longshore sediment transport must be nourished to prevent erosion of the coast downstream of the Eko Atlantic City project.

It is recommended to apply a monitoring campaign at the coast downstream of the Eko Atlantic City project. This is in line with the outcome of the Environmental Impact Assessment study for this project [*Royal Haskoning*, 2011]. Besides the additional advantage of acquiring more data of the Lagos coast, one can also react quickly to undesired scenarios. The analysis of the effects of the construction of Eko Atlantic City reveals the expected shift in erosion by the project, which can be counteracted by nourishments to ensure a stable beach downstream of the Eko Atlantic City project.

CONCLUSIONS

The analysis of the Lagos coast is summarized via answering the research questions.

RQ1: There are five governing processes and mechanisms determining the long-term and large-scale morphological behavior of the Lagos coast:
1) The persistent and high-energy swell waves, inducing a mean eastward longshore sediment transport. 2) The sediment trapping at the West Mole, limiting the sediment bypass along the mole. 3) The high relative sea level rise, creating additional sediment accumulation space. 4) Dredging of the Commodore Channel and the Lagos Lagoon, disturbing the morphodynamic equilibrium and creating extra sediment import. Concluding: the sediment volume bypassing along the East Mole is principally determined by the size of the sink formed by the sediment trapping at the West Mole and the sediment import into the Lagos Lagoon and the Commodore Channel.

RQ2: The influence of the construction of the Lagos Harbour Moles between 1908 and 1912 is visible in: significant accretion of the Lighthouse Beach of more than 800 m, and severe erosion of the Bar Beach of more than one kilometer. Another human interference on the historical coastline development is the performance of nourishments, which had an alleviating effect on the erosion of Bar Beach. On the contrary, the dredging of the Commodore Channel and the Lagos Lagoon has worsened the erosion downstream of the tidal inlet.

RQ3: The construction of Eko Atlantic City does not alter the total volume of erosion occurring downstream of the tidal inlet. However, a shift in the location of erosion is caused by the presence of the revetment of the project. At the location of the project further erosion is prevented but downstream of the project, the erosion will increase locally.

A monitoring and mitigation strategy is recommended to monitor the effects of Eko Atlantic City and instruct coastal erosion protection management actions to be implemented if required.

ACKNOWLEDGEMENT

Royal Haskoning is acknowledged for initiating the study and for providing financial support and all data used in this study. Deltares is also thanked for the financial support and for the support on the Unibest software.

REFERENCES

Bosboom, J. and M.J.F. Stive (2010). Coastal Dynamics I, Delft. VSSD.

Bruun, P. (1962). Sea-Level Rise as a Cause of Shore Erosion. Journal of Waterways and Harbor Division. American Society of Civil Engineers.

Royal Haskoning: Westra, M., O. Scholl, W. de Jong, M. Reneerkens, J. Lansen, M. Lips and C. Hoyng (2011). Eko Atlantic City - Coastal Analysis Report. Nijmegen, Netherlands.

van Bentum, K.M. (2012). The Lagos coast - investigation of the long-term morphological impact of the Eko Atlantic City project. MSc, Delft University of Technology.

DOI: 10.3990/2.200

Observations of suspended matter along the Dutch coast

C.M. van der Hout[1], T. Gerkema[1], J. Nauw[1] and H. Ridderinkhof[1]
[1]Physical Oceanography, Royal Netherlands Institute for Sea Research (NIOZ), P.O. Box 59, 1790 AB, Den Burg (Texel), The Netherlands, carola.van.der.hout@nioz.nl

ABSTRACT

Large amounts of suspended matter are transported through the Dutch coastal zone in the southern North Sea. Current estimates, based on budget studies, are in the order of 15 - 20 Mton per year transported in northward direction, which should take place in a small strip of 5 - 10 km wide. For this study we have performed a series of measurements on total suspended matter in an area in the most northerly extent of the Rhine region of fresh water influence. The measurements focused on observations both in the vertical and in the horizontal on the behavior of suspended matter in the nearshore zone up to 7 km from the shoreline. A peak in bottom concentrations is observed close to the coast along the coastal stretch. This hot spot location is found in the cross-shore direction at about 1.5 km from the coastline at a water depth of 15 m. Here, total suspended matter concentrations near the bottom exceed 200 mg/l. These peak concentrations have not been identified before and add to the suggestion that a large part of the northward suspended matter transport occurs very close to the coast.

INTRODUCTION

The Dutch coastal zone forms a transport path of total suspended matter (TSM) from the Strait of Dover to the Wadden Sea and the Norwegian Trench. On the basis of budget studies, it is estimated that half of the yearly-averaged 30 - 40 Mton from the Strait of Dover is transported along the Belgian and Dutch coast in a small strip of 5 - 10 km wide. No sources and sinks are present along the Belgian and Dutch coast that significantly alter the estimated 15 - 20 Mton/yr [De Kok, 2004; Fettweis et al., 2007]. Main sinks are the Wadden Sea and the Norwegian Trench. Total suspended matter concerns all particles suspended in the water column, being a mixture of silt, clay and organic matter. Inorganic particles are normally smaller than 63 µm, but organic material can grow to sizes > 200 µm. TSM affects primary production by reducing light penetration in the water column, but also by distributing nutrients and organic material. For the Wadden Sea suspended matter is an important contributor for the habitat, e.g. mud content of the shoals, and primary productivity. Nauw and Ridderinkhof [2009] calculated an import of 5 - 10 Mton/yr into the Wadden Sea through the Marsdiep Inlet. This figure is large compared to the current estimate of 15 - 20 Mton/yr along the Dutch coast.

TSM measurements in the Dutch coastal zone are scattered both in time and in space. In the 70's and 80's the focus was on in-situ surface samples of a large area [Visser et al., 1991], in the 90's on the vertical distribution done with in-situ observations with optical instruments and with high time resolution [Joordens et al., 2001; McCandliss et al., 2002], later on extended with acoustic measurements to increase spatial coverage [Merckelbach and Ridderinkhof, 2006], and since the start of the 21st century surface concentrations with high resolution of a large area can be obtained via satellite images [Eleveld et al., 2008] on time and spatial scales similar to current North Sea numerical models. Our project follows the line started in the 90's in order to include information over the full water column. The focus is on the near-shore zone up to 7 km offshore, by doing measurements at vertical cross-sections to the coast, and by examining variations over the tidal cycle as well as at larger time scales, up to seasonal. We present measurements made in 2010 in the northern part of the Dutch coastal zone with R.V. Navicula, as part of the NTW3.1 project in Building with Nature.

MEASUREMENTS

Measurements of total suspended matter (TSM) concentrations, density and current velocities were carried out in spring and autumn 2010 with R.V. Navicula. In this paper we will discuss the results of the cross-sectional measurements done in autumn 2010 on a transect near Egmond aan Zee, 20 km north of the harbor of IJmuiden, and a time-series of part of a tidal cycle done in spring 2010 at an anchor station near the transect at 1.5 km from the coastline (figure 1). The data concerns continuously measured velocities with an acoustic Doppler current profiler (ADCP), complemented with CTD-casts and water samples taken for

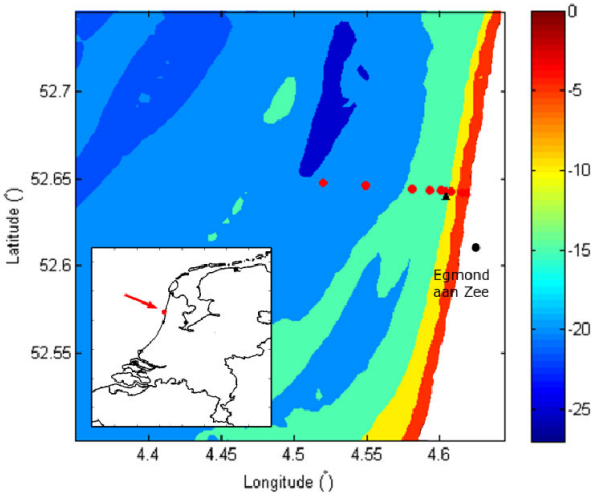

Figure 1. Location of the stations on the transect (red dots) and of the anchor station (black triangle) on the coast of North-Holland. Water depths are in meters below mean sea level.

calibration on stations. At the anchor station the time interval between CTD-casts was 20 minutes. The transect runs from 0.5 km until 7 km from the coastline, with irregularly spaced stations at 0.5, 1, 1.5, 2, 3, 5 and 7 km from the shoreline. The transect was measured on 2010/10/26 during spring tides, average wind force of 5 Bft from the southwest and average wave height of 1.5 m. One week later, on 2010/11/01, the same transect was measured - with an extra station at 1.25 km from the shoreline - during neap tides, under mild meteorological conditions and an average wave height of 0.30 m. Details of the cruise days relevant to this paper are given in Table 1.

The current velocity measurements were done with a vessel-mounted downward looking RDI 1.2 MHz ADCP attached to the side of the ship at a water depth of 1 m. Data was stored with an interval of 2 s with 4 pings per ensemble. The bin height was 0.5 m and blanking distance 0.5 m. At the stations a vertical profile of temperature, salinity, density and optical backscatter was made by lowering a lightweight frame with a Seabird SBE 911plus CTD and a Seapoint OBS from the afterdeck until it would hit the bottom. Only data of the downcast are used for analysis, because of the downward CT-configuration on the frame. The raw data were filtered from peaks, averaged over 25 cm bins and filtered with a running mean over 3 bins.

The optical backscatter sensor (OBS), hereafter called OBS_{frame}, was calibrated with in-situ samples of total suspended matter concentrations. At low scattering values a linear relation can be established between the instruments' voltage and the TSM concentrations [Downing, 2006]. At each station two water samples were taken with a 5 l Niskin bottle; one at about 1 m above the bottom and one at 1 m below the surface. Two subsamples were taken from each sample while stirring thoroughly. The first subsample of a volume between 0.2 and 0.8 l was used to determine the sediment concentration, by 3 bar backpressure filtering over a pre-weighed 0.7 µm glassfiber Whatman filter. The filters were directly rinsed with demi-water to remove the salts and were stored for transport to the lab.

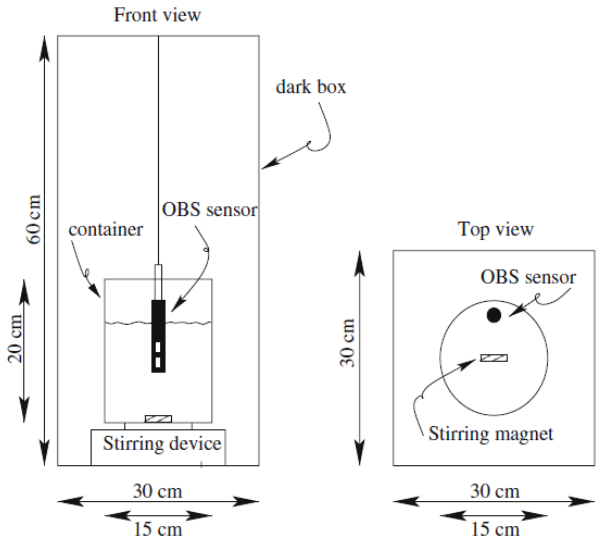

Figure 2. Configuration of voltage measurement of a Seapoint optical backscatter sensor (OBS) in a dark box [Merckelbach and Ridderinkhof, 2006].

Afterwards, the filters were dried at 110° for 2 hours and weighed to determine the concentration of the water sample. The second subsample of 2 l is placed in a dark box, where another OBS, hereafter called OBS_{box}, was placed in the sample (Figure 2). The particulate matter was kept in suspension with a magnetic mixer. When stable, the voltage of the OBS_{box} was notated. The calibration graph of OBS_{box} versus total suspended matter concentration gives a linear relationship shown in figure 3 for the spring measurements and the autumn measurements separately. In spring the range of concentrations observed was between 15 and 210 mg/l, while this was between 3 and 70 mg/l in autumn. The figure shows some scatter as a result of measurement inaccuracies, but with an R^2 of 0.95 a reliable relationship is established for the spring measurements:

$$TSM = 37.11 \cdot OBS_{box} + 3.21 \quad (1)$$

and with an R^2 of 0.94 for the autumn measurements:

$$TSM = 30.24 \cdot OBS_{box} - 3.70 \quad (2)$$

The two lines deviate from each other by an offset of 7 mg/l and an angle. This might be attributed to the difference in TSM composition in spring and autumn. Particles of different material and with a different shape reflect the infrared light of an OBS in a slightly different manner [Downing, 2006]. This implies calibration of the OBS as described above during each cruise.

The OBS_{box} and the OBS_{frame} are also linearly correlated. This relationship is established by performing two CTD-casts in the measurement area on the 26th of October with both instruments attached to the CTD-frame. Data are used from both upcast and downcast, as the signal from an OBS is not influenced by cast direction. The relationship reads:

$$OBS_{box} = 1.21 \cdot OBS_{frame} + 0.02. \quad (3)$$

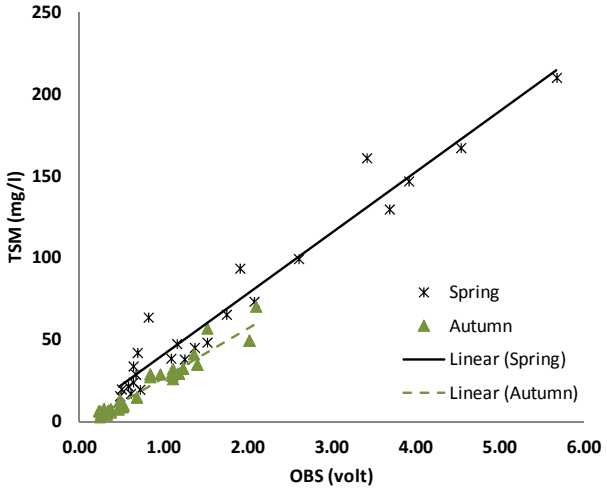

Figure 3. Calibration graph of the optical backscatter sensor (OBS) in the dark box with total suspended matter (TSM) concentration samples for the spring measurements (black line, black crosses) and the autumn measurements (green dashed line, green triangles).

Table 1: Averaged wind, wave and tidal conditions during the measurement periods. Winds are recorded at IJmuiden harbor by the Royal Netherlands Meteorological Institute and waves at IJmuiden munitiestortplaats by the Ministry of Transport, Public Works and Water Management.

Date	Type	Season	Mean wind force (Bft)	Wind direction (^{0})	Wind direction with respect to coastline	Wave height (m)	Spring – Neap
2010/03/29	Anchor station	Spring	3	179	Alongshore from south	1.0	intermediate
2010/10/26	Transect	Autumn	5	216	Alongshore from south	1.5	Spring
2010/11/01	Transect	Autumn	1	66	O fshore	0.3	Neap

The linear relation contains a small offset, probably due to the scatter of the data. The deviation of the angle from 1 has to do with the different age of both sensors. The OBS sensors used are known to age over time. With formulas (1), (2) and (3) the OBS_{frame} data of vertical profiles are converted to TSM concentration.

RESULTS

The cross-sectional views of the concentration distribution of the two transects are shown in Figures 4a and 5a. Both transects were measured during the phase of slack tide after high water. Highest concentrations of 60 mg/l in the first week and 40 mg/l in the second week are found at 1.5 km from the shoreline near the bottom at a water depth of 15 m. These concentrations are not remarkably high as most of the sediments have settled from the water column during the slack phase of the tide. The first transect was measured during a higher turbulent kinetic energy (TKE) period than the second transect. Both tides and waves determine the level of turbulent kinetic energy in this area and thereby the distribution of TSM in the water column [Joordens et al., 2001]. This explains the higher maximum concentration and the overall higher concentrations measured during the first week compared with the second week. In the first week the total volume of suspended matter in the transect was 3 times more than in the second week.

The density distribution in Figure 4b shows well-mixed waters with a horizontal density gradient, with fresher waters close to the shore. The relatively high energy level as a result of waves and spring tides keeps the water column vertically mixed and suppresses a haline cross-shore circulation (Figure 4c). In the second week, under low TKE conditions, the density distribution shows a completely different picture (Figure 5a). Besides a stronger horizontal density difference, the water column is also vertically stratified as much as 0.8 psu at the station furthest offshore. In the cross-shore velocity transect (Figure 5c) a clear upwelling event is seen as a result of both the estuarine circulation as well as the mild offshore directed wind. This upwelling event is

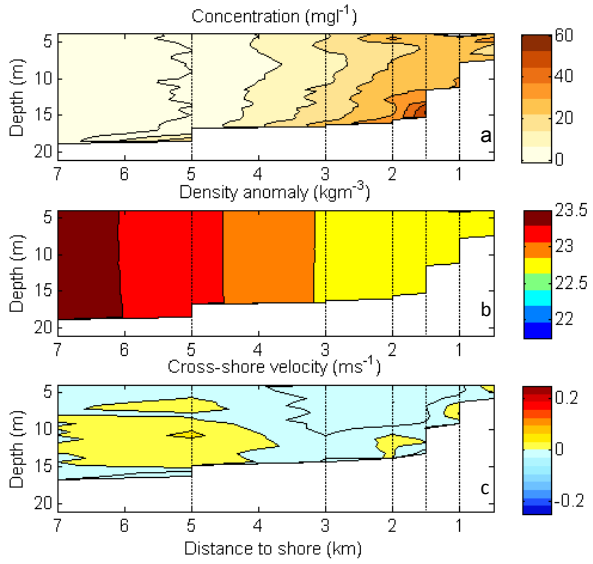

Figure 4. Cross-section perpendicular to the coast of TSM concentration, density-1000 kgm^{-3} and cross-shore velocities (positive in shoreward direction) at CTD casts (vertical dashed lines) on 2010/10/26.Contour lines of concentration are spaced at 7.5 mgl^{-1}, of density anomaly at 0.25 kgm^{-3} and of velocity at 0.025 ms^{-1}.

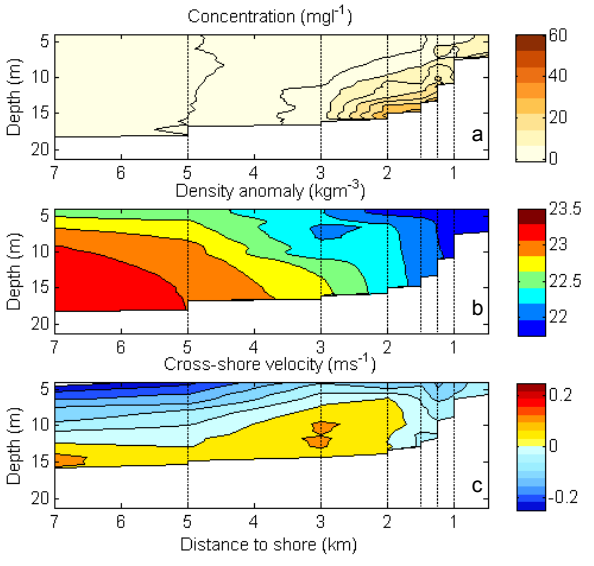

Figure 5. Cross-section perpendicular to the coast of TSM concentration, density-1000 kgm^{-3} and cross-shore velocities (positive in shoreward direction) at CTD casts (vertical dashed lines) on 2010/11/01.Contour lines of concentration are spaced at 7.5 mgl^{-1}, of density anomaly at 0.25 kgm^{-3} and of velocity at 0.050 ms^{-1}.

characteristic for the Rhine region of fresh water influence, though it is less likely to occur further downstream from the Rhine outflow [De Boer et al., 2009].

A time series over part of a tidal cycle is shown in Figure 6. The 4-hour time series was started just before slack after low water, and ends after maximum flood velocity. The water level lags the sea surface height with 45 minutes, indicating the progressive character of the tidal wave in this area. The location of the anchor position is at 1.5 km from the shoreline (Figure 1), which is in the area of highest TSM concentrations, according to Figures 4 and 5. Figure 6 shows the evolution of the TSM concentration as a function of depth and depth-averaged northward velocity. In

general, concentrations increase from the surface to the bottom. Although vertically smoothed, the profiles still show sharp vertical variations and sudden clouds of TSM. Two individual maxima are observed at 11:30 and 13:30. The peak at 11:30 is probably still a remainder of the resuspension by the ebb velocity prior to the start of the measurements. At 13:00 hours UTC, which is one hour after slack tide, concentrations obtain their minimum value due to settling of TSM from the water column. The settling process of suspended matter takes some time leading to a time lag between current velocity and TSM concentration with decreasing currents. The maximum concentration is attained about 45 minutes before the maximum flood velocity in a small layer near the bottom. Resuspension of the recently settled sediments is started. Thereafter, the temporarily settled sediment is resuspended further throughout the water column, decreasing the maximum concentration near the bottom. If only local resuspension and deposition processes would control the volume of total suspended matter in the water column, we would not expect this volume to decrease when flood current velocities maintain strong at 15:00 hours. This indicates that other non-local processes, such as advection in longshore and cross-shore direction are also important in the distribution of TSM in this area.

DISCUSSION AND CONCLUSION

Hot spots of high TSM concentrations are found at 15 m depth at a distance of 1.5 km offshore of Egmond aan Zee. Such hot sport are also found on a similar location in a transect 12 km south and a transect 10 km north of Egmond aan Zee, measured in similar periods. This particular location (1.5 km offshore and 15 m depth) and such high concentrations (> 200 mg/l) have not been identified before along the Dutch coast. Similar research programs focused on an area further offshore, partly because research vessels with a draught of 4-5 m cannot safely operate in this shallow area. R.V. Navicula only has a draught of 1 m and can therefore perform measurements in this area not surveyed before, though safe operation is severely limited by a wave height of 1.5 m.

Turbulence, produced by the tide and meteorological conditions, does not appear to affect the location of the hot spot. This is shown by two transects at the same location measured during different levels of TKE (Figures 4 and 5), though it does increase the total volume in suspension with increasing turbulence as observed in previous studies [Joordens et al., 2001; McCandliss et al., 2002; Fettweis et al., 2006]. Other processes are more likely to maintain the hot spot location whilst diffusion spreads it out in the cross-shore. A possible process concerns the temporary storage on/in the seabed on time scales of the diurnal tidal cycle, the spring-neap tidal cycle and the seasonal cycle. During calm periods - slack tide, neap tide and summer - sediments are accumulated on/in the bed, where bottom processes may rework the material. Preliminary comparison of *Ensis Directus* densities (razor clams) with TSM bottom concentrations show a positive correlation. At the hot spot location, highest densities of *Ensis Directus* in the cross-shore are observed. These bivalves might filter TSM from the water column, rework the sediment or change the cohesive properties of the particles. It is thought that these bivalves have a positive effect on the burial of suspended matter in the bed, though this still has to be verified.

Another process concerns the haline cross-shore circulation measured on the 1st of November 2010 (Figure 5c). Visser et al. [1991] used the estuarine type of circulation in the coastal zone to explain a persistent TSM surface minimum at 25 km from the Dutch coastline as was found in the '70s and' 80s dataset of Rijkswaterstaat. The circulation - due to the horizontal density gradient in the coastal zone (Figures 4b and 5b) - drives surface waters in an offshore direction and bottom waters in an onshore direction perpendicular to the tidal current. This bottom current then transports TSM in the bottom layer in a coastward direction. Why the hot spot location is not closer to the coast could be related to the shallowness of the area shoreward of the hot spot location. There, processes such as wave driven currents start to play a role, bed shear stresses increase and the bed slope gradient increases and with it the gravitational component within the transport equations.

If these hot spots exist at all times - as they appear to do from the results presented in this paper - then they may contribute significantly to the total northward TSM transport. Whether this will change the current estimate of 20 Mton/yr will be subject of further study of observations in this area. However, these measurements do provide more insight in processes transporting large amounts of TSM. This will lead to better assessment of effects of coastal construction works on the natural transport of TSM.

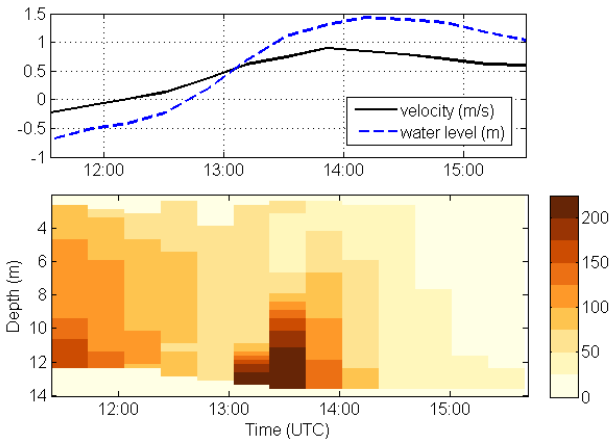

Figure 6. Time-series of depth averaged northward alongshore velocity and water level (top) and concentration over the vertical (bottom). Measured at an anchor station 1.5 km from the shoreline at Egmond aan Zee on the 29th of March 2010 with a 20-minutes interval.

ACKNOWLEDGEMENTS

We gratefully acknowledge the captain and crew of R.V. Navicula as well as the volunteers for their contribution of this research. This research is carried out within the research program Building with Nature, as part of the project NTW3.1.

REFERENCES

Boer, G. J. de, J. D. Pietrzak, and J. C. Winterwerp (2009), SST observations of upwelling induced by tidal straining in the Rhine ROFI, Continental Shelf Research, 29, 263-277, doi:10.1016/j.csr.2007.06.011.

Downing, J. (2006), Twenty-five years with OBS sensors: The good, the bad, and the ugly, Continental Shelf Research, 26(17-18), 2299-2318, doi:10.1016/j.csr.2006.07.018.

Eleveld, M. A., R. Pasterkamp, H. J. van der Woerd, and J. D. Pietrzak (2008), Remotely sensed seasonality in the spatial distribution of sea-surface suspended particulate matter in the southern North Sea, Estuarine, Coastal and Shelf Science, 80(1), 103-113, doi:10.1016/j.ecss.2008.07.015.

Fettweis, M., F. Francken, V. Pison, and D. Van den Eynde (2006), Suspended particulate matter dynamics and aggregate sizes in a high turbidity area, Marine Geology, 235, 63 - 74, doi:10.1016/j.margeo.2006.10.005.

Fettweis, M., B. Nechad, and D. Van den Eynde (2007), An estimate of the suspended particulate matter (SPM) transport in the southern North Sea using SeaWiFS images, in situ measurements and numerical model results, Continental Shelf Research, 27(10-11), 1568-1583, doi:10.1016/j.csr.2007.01.017. [online] Available from:

Joordens, J. C. A., A. J. Souza, and A. Visser (2001), The influence of tidal straining and wind on suspended matter and phytoplankton distribution in the Rhine outflow region, Continental Shelf Research, 21(3), 301-325, doi:10.1016/S0278-4343(00)00095-9.

Kok, J. M. de (2004), Slibtransport langs de Nederlandse kust. Bronnen, fluxen en concentraties. Report RIKZ/OS/2004.148w, Ministry of Transport, Public Works and Water Management (Rijkswaterstaat).

McCandliss, R. R., S. E. Jones, M. Hearn, R. Latter, and C. F. Jago (2002), Dynamics of suspended particles in coastal waters (southern North Sea) during a spring bloom, Journal of Sea Research, 47(3-4), 285-302, doi:10.1016/S1385-1101(02)00123-5.

Merckelbach, L. M., and H. Ridderinkhof (2006), Estimating suspended sediment concentration using backscatterance from an acoustic Doppler profiling current meter at a site with strong tidal currents, Ocean Dynamics, (56), 153-168, doi:10.1007/s10236-005-0036-z.

Nauw, J., and H. Ridderinkhof (2009), Slibtransport door het Marsdiep op basis van veerbootmetingen, NIOZ-Report 2009-7, Royal NIOZ.

Visser, M., W. P. M. de Ruijter, and L. Postma (1991), The distribution of suspended matter in the Dutch coastal zone, Netherlands Journal of Sea Research, 27(2), 127-143.

DOI: 10.3990/2.201

Levee development along tidal channels

M. van der Wegen[1], J. Guo[1], B.E. Jaffe[2], A.J.F. van der Spek[1,3,4] and J.A. Roelvink[1,,3,4]
[1]Water Science and Engineering, UNESCO-IHE, Delft, the Netherlands
[2]USGS Pacific Science Center, Santa Cruz, California, USA.
[3]Delft University of Technology, Delft, the Netherlands.
[4]Deltares, Delft, the Netherlands.

ABSTRACT

Levees are small elevation ridges found on the edge between channels and shoals. They are known to develop along river channels during floods and along channels in alluvial deep water fans. Levees in tidal environments such as the Waddenzee are less pronounced (with a typical height in the order of 10 cm) and may be recognized by the fact that they become dry earlier than the surrounding mudflats, due to their higher elevation and coarser material. Levees form an essential link in the morphological interaction between tidal channels and shoals, although their development is yet poorly understood and requires further research.

We explore levee development by a process-based approach (Delft3D) both under highly schematized conditions and a realistic case study. The schematized approach concerns morphological development of a 2km long 100 m wide tidal channel with surrounding tidal flats. The levees develop during flood and further analysis shows the sensitivity to model parameters such as the diffusion coefficient, shoal width, grain size, and initial channel depth. The realistic case study concerns a tidal channel in a sub-embayment of San Francisco Estuary. 150 Years of bathymetric observations are coupled to a process-based morphodynamic modeling exercise explaining the levee development. Model results of the schematized setup and teh San Pablo Bay case have in common that major accreation of the levees and the channel slopes occurs during flooding conditions.

INTRODUCTION

Levees are small elevation, coarse material ridges found on the edge between channels and shoals. They are known to develop along river channels during floods [*Adams et al*., 2004, *Rowland et al.,* 2009, *Brierley et al,* 1997], along channels in alluvial deep water fans during high turbidity flow events [*Normark et al*.,2002, *Fildani et al.,* 2006, *Straub and Mohrig,* 2008], and along creek systems in salt marshes and mudflats during regular tidal forcing [*Perillo and Iribarne,* 2003, *Temmerman et al.,* 2005, *Wells et al.,* 1990].

Levees in tidal environments such as the Waddenzee are less pronounced (with a typical height in the order of 10 cm) and may be recognized by the fact that they become dry earlier than the surrounding mudflats, due to their higher elevation and coarser material. In a muddier environment *Jaffe et al.* [2007] report continuous measured narrowing of the tidal channel in San Pablo Bay over 150 years which may be interpreted as an expansion of the intertidal mudflats. Accretion takes place at the steep slope between channel and shoal, rather than at the edge of the shoal itself. It is not clear whether or not levee development and slope accretion are governed by similar processes and to what extent the sediment characteristics play a role in these types of channel shoal interaction.

AIM AND METHODOLOGY

Levee development forms an essential part in the morphodynamic interaction between channels and shoals although the governing processes are yet poorly understood and require further research. The aim of the current work is to investigate channel shoal interactions in more detail. Use is made of a process-based numerical model (Delft3D).

Delft 3D solves the Reynolds averaged Navier Stokes equations, including the k-ε turbulence closure model, and applies a horizontal curvilinear grid with sigma layers for vertical grid resolution. It allows for salt-fresh water density variations, separate formulae for mud transport and sand transport, and variations in bed composition and specification (for example, bed layers with different percentages of mud and sand and spatial variation of critical shear stress). The impact of wind and waves can be added, so that, for example, the effects of wind set up and increased shear stress due to waves are taken into account. The applied wave model is SWAN of which a detailed description and its application in Delft 3D can be found respectively at the SWAN homepage (http://vlm089.citg.tudelft.nl/swan/index.htm), Booij et al. (1999) and Lesser et al. (2004). For every hydrodynamic time step (1 minute in this case) the flow module calculates water levels and velocities from the shallow water equations. Based on these hydrodynamic conditions and the wind field, the wave module calculates a wave field every hour and adds wave induced shear stresses to the shear stresses calculated from the flow module. The wave field is considered to be constant during one hour. Sediment transport is calculated from the resulting flow field and the bed is updated based on the divergence of the sediment transport field [Roelvink, 2006].

Our first step is to investigate channel shoal interaction under (very) schematized circumstances, i.e. by means of a 2 km long channel forced by tidal flow and additional sensitivity analysis on input parameters and processes. We will subsequently relate the outcome of the schematized model to a case study, i.e. San Pablo Bay, California, USA [Van der Wegen et al, 2010, 2011].

MODEL SETUP

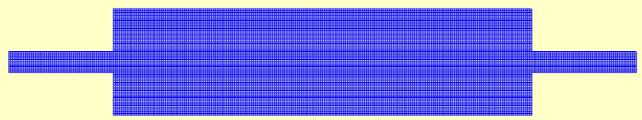

Figure 1. Model grid for schematized conditions

Schematised model

Figure 1 shows the grid applied for the schematized model. The grid cell size is 10m in transverse direction and 5m in longitudinal direction. The channel has a width of the boundary limits. In the wider middle part of the model domain the channel is flanked by shoals. We suppose that the tide propagates from left to right. The boundary conditions on the west side and the eastside are described by a tidally varying water level with an amplitude of 1.75m and a period of 12 hours with a small water level phase difference between the boundaries to drive the tidal current defined by

$$\Delta\varphi = \frac{360^0}{T\sqrt{gh}}L \qquad (1)$$

in which T (s) is the tidal period, g (m/s^2) is the gravitational acceleration, L is the length of the model grid (m), h is the initial water depth in the channel (m). The standard settings apply Van Rijn transport formulations with constant D50.

San Pablo Bay model

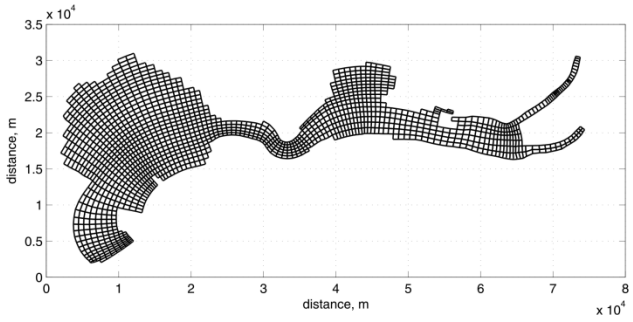

Figure 2. Numerical grid of model covering San Pablo Bay and Suisun Bay. The upper branch at the landward side represents the Sacramento River and the lower branch the San Joaquin River.

Figure 2 shows the model domain applied in the San Pablo Bay case study. A curvilinear grid is applied on the domain and the condition for a stable and accurate computation (Courant number < 10) is met with a grid cell size of approximately 100 by 150 m and a time step of 2 minutes. Density currents and wave effects are included as well as 15 sigma layers describing the vertical grid distribution. The initial bathymetry is a measured (see Figure 3) and bed composition was derived as described by Van der Wegen et al. [2010].

The river discharge regime is modeled by a high river discharge 'wet' season and a low river discharge 'dry' season. This high level of schematization reduced river inflow to three practical 'tuning' parameters (i.e. duration of high discharge compared to low discharge and the magnitudes of the high and low river discharges). The landward river boundary conditions a derived from a larger 3D hydrodynamic model (Delft3D) covering a model domain ranging from the Delta to 20 km offshore including all sub-embayments of San Francisco Estuary [Van der Wegen et al. 2011]. In accordance with general observations salt concentration is set constant at zero at the landward boundary and at 31 psu at the seaward boundary. Prevailing wind conditions are schematized by a diurnal sinusoidal signal varying from 0 at midnight to 7 m/s at noon uniformly distributed over the domain. Every hour the SWAN model uses wind and hydrodynamic data from the flow calculation to generate a wave field and returns resulting adapted hydrodynamic parameters to the flow module. We apply 3 sand fractions modeled by Van Rijn transport formulation and five mud fractions modeled by the Krone-Patheniades formulation. Van der Wegen et al. [2011] provide further detail on the applied model formulations and schematizations.

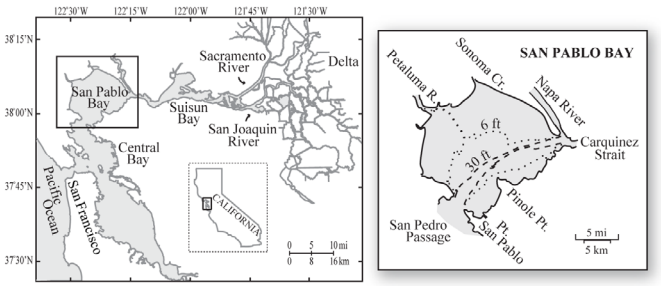

Figure 3. Location of San Pablo Bay in California

MODEL RESULTS

Schematised model

Figures 4 and 5 present model results after 100 days of morphodynamic development. Clearly one can observe the levee development occuring at the shoals. The channel become more shallow and the levee develop up to more than 0.5 m in height. There is a significant variation along the channel, because the western levees have developed first. Small channels have evolved at ebb. The channels are located irregular intervals to drain the shoals at ebb, but aslo enhance flooding efficiency. Sensitivity analysis has been carried out on D50, sediment transport fomulation, the bed slope factor, shoal dimensions (height, width and slope), height of mean water level and tidal amplitude, multiple sediment fractions including mud, application of wind and waves as well as channel curvature.

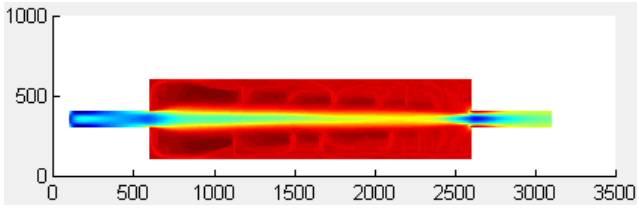

Figure 4. Model results: Bed level after 1000 days of morphodynamic development (blue refers to 8 m below mean water and dark red refers to1.5 m above mean water).

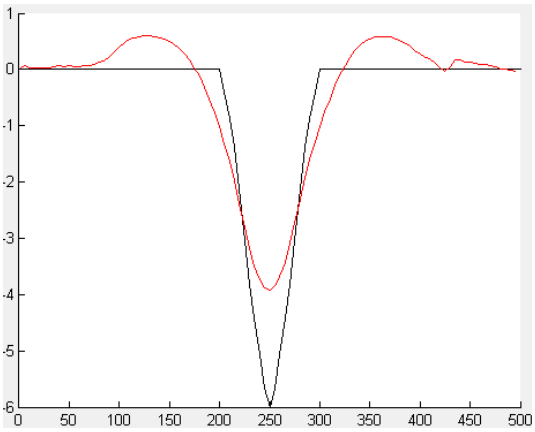

Figure 5. Model results: Mid domain bed level after 1000 days of morphodynamic development (black refers initial channel profile and red refers to profile after 1000 days).

San Pablo Bay model

Figure 6 shows the measured and modeled morphodynamimc developments of the San Pablo Bay model over two different 30 year periods. One may clearly observe the resemblence between modeled and measured erosion and sedimentation patterns. Also, the development of the channel banks is pronounced and well reproduced by the model. This gives confidence to further analyse the underlying conditions and processes that govern channel slope and levee development by means of the (detailed) data generated by the model.

DISCUSSION AND CONCLUSION

Closer analysis of the model results shows that levee development in the schematized model and slope accretion in the San Pablo Bay model both occur mainly during flooding of the shoal area. The explanation is twofold. Rising water levels flood the shoals and transverse flow velocities (perpendicular to the channel) reduce considerably while entering the shoals so that sediment settles. Secondly, sediment concentrations increase because sediment transported in the large channel water column now enters a smaller water depth. The higher sediment concentration enhances settling of sediment as well. Especially the San Pablo Bay case includes more complexity since water flows are not nicely alligned with the channel direction and much more processes are included such as wind waves and multiple sediment fractions. Accretion and erosion occur both during different phases of the tidal cycle. However, main accreation of the slopes occurs during flooding conditions. The process-baed modeling approach allows for a proper sensitivity analysis that enables to distinguish governing processes from secondary processes. For example, for the San Pablo Bay case study wind wave resuspension on the mudflats is necessary to let the westerly channel slopes accrete, whereas slope accretion on the easterly shoals is governed by dpoeistion during high river flow conditions.

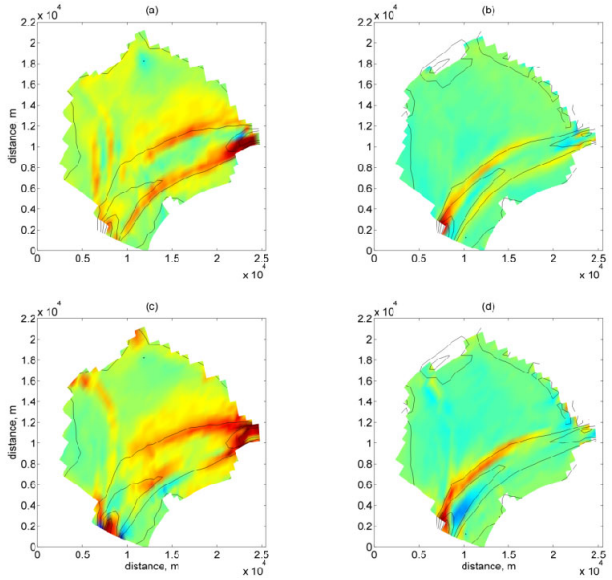

Figure 6. Erosion and sedimentation patterns (red is 5m deposition and blue is 5 m erosion) measured (a,b) and modeled (c,d) for 1856-1887 depositional period (a,c) and 1951-1983 erosional period (b,d) (Figure is partly from Van der Wegen [2011]).

ACKNOWLEDGEMENT

The research is part of the US Geological Survey CASCaDE climate change project (CASCaDE contribution *). The authors acknowledge the US Geological Survey Priority Ecosystem Studies, CALFED and Deltares for making this research financially possible.

REFERENCES

Adams, PN, RL Slingerland & ND Smith, 2004. Variations in natural levee morphology in anastomosed channel flood palin complexes. Geomorphology, 61: 127-142.

Booij, N., R.C. Ris and L.H. Holthuijsen, (1999), A third-generation wave model for coastal regions, Part I, Model description and validation, *J.Geoph.Research*, 104, C4, 7649-7666)

Lesser, G.R., Roelvink, J.A. Van Kester, J.A.T.M., Stelling, G.S., (2004), Development and validation of a three-dimensional morphological model. Coastal Engineering 51, 883-915.

Brierley, GJ, RJ Ferguson & KJ Woolfe, 1997. What is a fluvial levee? Sedimentary geology, 114: 1-9.

Fildani, A., Normark, W.R., Kostic S. and Parker, G. (2006), Channel formation by flow stripping: large-scale scour features along the Monterey East Channel and their relation to sediment waves, Sedimentology, 53, pp 1265–1287 doi: 10.1111/j.1365-3091.2006.00812.x.

Jaffe, B. E., R. E. Smith, and A. C. Foxgrover (2007), Anthropogenic influence on sedimentation and intertidal mudflat change in San Pablo Bay, California: 1856–1983, Estuarine Coastal Shelf Sci., 73, 175–187, doi:10.1016/j.ecss.2007.02.017.

Normark, W.R., Piper, D.J.W., Posamentier, H., Pirmez, C., Migeon, S. (2002), Variability in form and growth of sediment waves on turbidite channel levees, Marine Geology 192, 23-58.

Perillo, GME & OO Iribarne, 2003. Processes of tidal channel development in salt and freshwater marshes. Earth Surface Processes and Landforms, 28: 1473-1482.

Straub, K. M., and D. Mohrig (2008), Quantifying the morphology and growth of levees in aggrading submarine channels, J. Geophys. Res., 113, F03012, doi:10.1029/2007JF000896

Roelvink, J. A. (2006), Coastal morphodynamic evolution techniques, J. Coastal Eng., 53, 177–187.

Rowland, JC, WE Dietrich, G Day& G Parker, 2009. Formation and maintenance of single-thread tie channels entering floodplain lakes: Observations from three diverse river systems. J. Geophysical Research, 114, F02013. (doi:10.1029/2008JF001073)

Temmerman, S.; Bouma, T.J.; Govers, G.; Wang, Z.B.; de Vries, M.B.; Herman, P.M.J. (2005). Impact of vegetation on flow routing and sedimentation patterns: Three dimensional modeling for a tidal marsh *J. Geophys. Res. 110*: F04019. dx.doi.org/10.1029/2005JF000301

Van der Wegen, M., Jaffe, B. E., and Roelvink, J. A., 2011. Process-based, morphodynamic hindcast of decadal deposition patterns in San Pablo Bay, California, 1856–1887, J. Geophys. Res., 116, F02008, doi:10.1029/2009JF001614.

Van der Wegen, M., A. Dastgheib, B.E. Jaffe, J.A. Roelvink, (2010), Bed composition generation for morphodynamic modeling: case study of San Pablo Bay in California, U.S.A.,Ocean Dynamics DOI: 10.1007/s10236-010-0314-2

Wells, JT, CE Adams, YA Park & EW Frankenberg, 1990. Morphology, sedimentology and tidal channel processes on a high-tide-range mudflat, west coast of South Korea. Marine geology, 95: 111-130.

DOI: 10.3990/2.202

Quantified and applied sea-bed dynamics of the Netherlands Continental Shelf and the Wadden Sea

Thaiënne A.G.P. van Dijk[1a,2], M.H.P. Kleuskens[3], L.L. Dorst[4], C. van der Tak[5], P.J. Doornenbal[1a], A.J.F. van der Spek[1a,6], R.M. Hoogendoorn[1a], D. Rodriguez Aguilera[1b], P.J. Menninga[7] and R.P. Noorlandt[1a,8]

[1a]Applied Geology and Geophysics, Deltares, P.O. Box 85467, 3508 AL, Utrecht, The Netherlands, thaienne.vandijk@deltares.nl
[1b]Soil and Groundwater Quality, Deltares, P.O. Box 85467, 3508 AL, Utrecht, The Netherlands
[2]Water Engineering and Management, University of Twente, P.O. Box 217, 7500 AE, Enschede, The Netherlands
[3]Alten PTS, 5651 CD Eindhoven, The Netherlands
[4]Hydrographic Service, Royal Netherlands Navy, P.O. Box 90701, 2509 LS, The Hague, The Netherlands
[5]MARIN, P.O. Box 28, 6700 AA Wageningen, The Netherlands
[6]Netherlands Centre for Coastal Research (NCK), Delft University of Technology, Faculty of Civil Engineering and Geosciences, P.O. Box 5048, 2600 GA, Delft, The Netherlands
[7]Institute for Marine and Atmospheric research Utrecht (IMAU), Utrecht University, P.O. Box 80.005, 3508 TA, Utrecht, The Netherlands
[8]Department of Geotechnology, Delft University of Technology, P.O. Box 5048, 2600 GA, Delft, The Netherlands

ABSTRACT

Sedimentary coasts and shallow-sea beds may be dynamic. The large-scaled spatial variation in these dynamics and the smaller-scaled behaviour of individual marine bedforms are largely unknown. Sea-bed dynamics are relevant for the safety of shipping, and therefore for monitoring strategies, and for offshore engineering projects and archaeological investigations. To date, sea-bed dynamic studies in the North Sea that are based on high-resolution echo soundings are mostly local. Recently, sufficient time series of modern, digital echo sounder surveys have become available to allow for a Netherlands Continental Shelf-wide quantification of vertical dynamic trends as well as for the detailed analysis of the morphodynamics of marine bedforms. Results show that *(i)* tidal channels, estuaries and longshore bars are particularly dynamic, *(ii)* the shelf offshore is less dynamic in general, and *(iii)* the most dynamic zones offshore are the zones where marine bedforms occur. The occurrence of superimposed sand banks, long bed waves, sand waves and megaripples is limited to the sandy shelf and sand wave migration rates vary spatially between 0 to 20 m/year. This spatial knowledge of morphodynamics is used in combination with environmental conditions and sea traffic to validate and to optimise re-survey policies.

INTRODUCTION

Sandy continental shelves and sedimentary coasts may be dynamic. Most sandy sea beds of shallow seas are characterized by marine bedforms of different spatial scales, such as sand banks, long bed waves, sand waves and megaripples. Each of these bedforms has its own dynamic time scale. These dynamics are relevant for navigation safety, especially in seas with critical depths for shipping, such as the southern North Sea. In order to keep nautical maps up-to-date, dynamic sea beds need to be re-surveyed in an appropriate frequency. Guidelines for horizontal and vertical accuracy of the data are provided by the International Hydrographic Organization [*IHO*, 2008], but no guidelines for the validation and optimization of re-survey policies exist. Other applications are offshore engineering projects, such as wind farms, and archaeological investigations.

Previous empirical studies of seabed morphodynamics focused on the analysis of marine bedforms of small sites with specific local conditions [e.g. *Duffy and Hughes-Clarke*, 2005; *Knaapen*, 2005; *Van Dijk and Kleinhans*, 2005; *Winter and Ernstsen*, 2007; *Buijsman and Ridderinkhof*, 2008; *Van Dijk et al.*, 2008; *Dorst et al.*, 2009; *Dorst et al.*, 2011]. Although recently performed for the German coastal zone [*Winter*, 2011], a large-scaled study of the morphodynamics of the Netherlands Continental Shelf (NCS) does not exist. Such a study provides an overview of the spatial variation in seabed dynamics that increases our insight and understanding of the processes of bed evolution.

Only recently, the coverage of multiple datasets (time series) of digital bathymetric data, which are required for the study of sea-bed morphodynamics, has become sufficient for the NCS to perform this study. In addition, the horizontal precision of these modern data is adequate for the detailed and quantitative analyses of bed changes and bedform mobility.

The aim of this paper is to present the vertical sea-bed dynamics of the Netherlands Continental Shelf and the Wadden Sea, based on a quantitative analysis on a 25 x 25 m resolution. Detailed analyses of selected locations serve to describe the local morphology and dynamics of individual bedforms.

DATA AND METHODS

Bathymetric data

All data that are contained in the digital Bathymetric Archive System (BAS) of the Hydrographic Service of the Royal

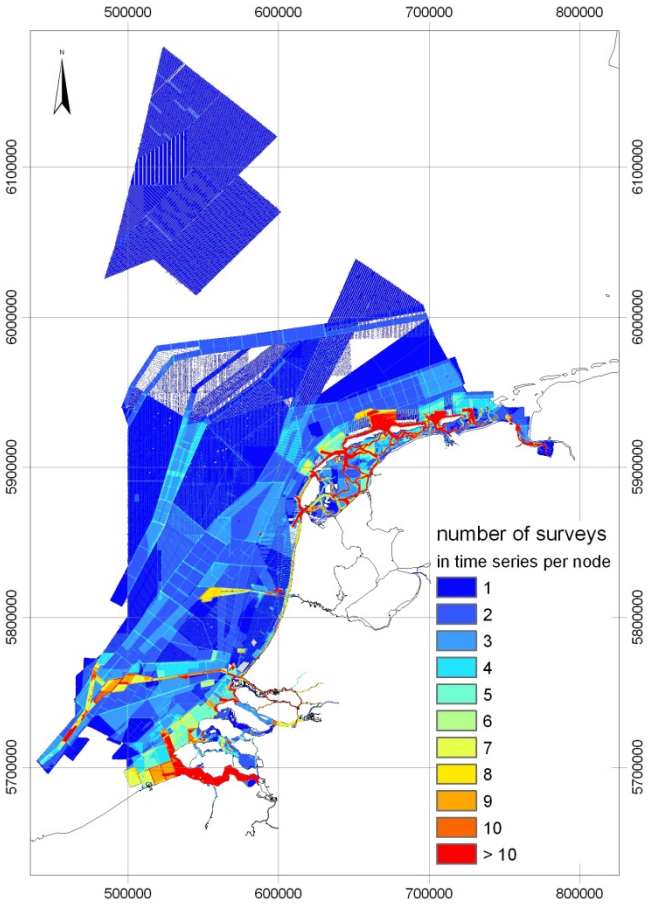

Figure 1. Number of digital datasets included in a time series per grid node (UTM31 WGS84 co-ordinates). In most areas where only one dataset was available, fair sheets were digitized to create a time series of 2 datasets.

Netherlands Navy below the 10 m isobath [*Righolt et al.*, 2010] were used in this study. This database includes data acquired by Rijkswaterstaat for the shallower coastal zone. Digital data in BAS comprise both single-beam echo soundings (SBES) and multi-beam echo soundings (MBES), that were collected according to the Order 1 standards for hydrographic surveys of the International Hydrographic Organization [*IHO*, 2008].

The overlap of surveys creates time series of various spatial extents and different periods. Most time series comprise two or three datasets; at few locations on the NCS, time series of more than 5 datasets exist (Figure 1). In locations where time series did not exist, historical echo soundings were digitized from plotted or hand-written fair sheets in order to create a bathymetric time series. The data density and precision (horizontal positioning and echo sounding beams) differ per method and in time. The digital datasets used in this study were acquired between the late 1980s and June 2010. The fair sheets date from before that. Data density used in this study is at most 1 observation per 3 x 5 m.

Digital Elevation Models (DEMs) were created from these bathymetric data by interpolating to a 25 x 25 m grid, using the Inverse Distance Weighting algorithm with a search radius of 100 m. This 25 m resolution was chosen to still represent sand waves (hundreds of meters in length) well and to minimize the introduction of interpolation artefacts of single beam echo soundings in track lines. Megaripples cannot be characterized at this resolution, but are often not captured by single beam data in the first place.

Vertical nodal dynamic analysis

Because we deal with numerous overlaps of various extents, different numbers of surveys and different periods, it is insufficient to use average values of bed elevation change in meters. For the quantitative analysis of vertical dynamic trends (m/yr) for each grid node, we developed a fully automated linear regression of all bed elevations in the stacked time series per node (Figure 2). Based on visual inspection of the nodal bed elevations in time, linear regression is justified within in the periods that are covered by the time series. We used an averaged date of collection per survey, because the periods of acquisition are relatively short and never were a problem for the precision of the calculations. Because the correction for tides and ship movements provided differences between surveys that are larger than the (natural) vertical dynamics, we corrected for this discrepancy by subtracting the averaged vertical dynamics for each specific stacked combination of surveys from the vertical dynamics at each node (Figure 3).

Geometry and mobility of individual bedforms

For the detailed morphological and dynamic analyses of individual sand waves and long bed waves, the bathymetric signal is separated into bedform types of different spatial scales by truncating a Fourier approximation at certain frequencies [for details, see *Van Dijk et al.*, 2008]. This way, the more dynamic

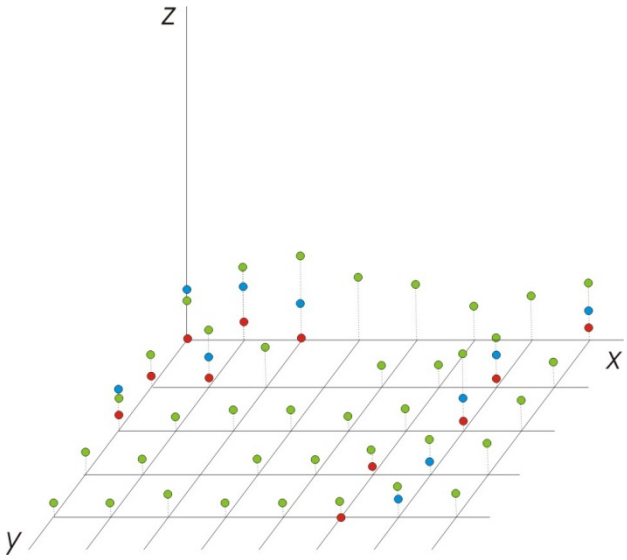

Figure 2. Illustration of different bathymetric datasets in a time series, displaying two sets of single-bean echo soundings (red and blue) distributed in track lines that do not exactly overlap and one set of multibeam echo soundings (green). The stacked time series for node (0,0) comprises three data points (red, green, blue).

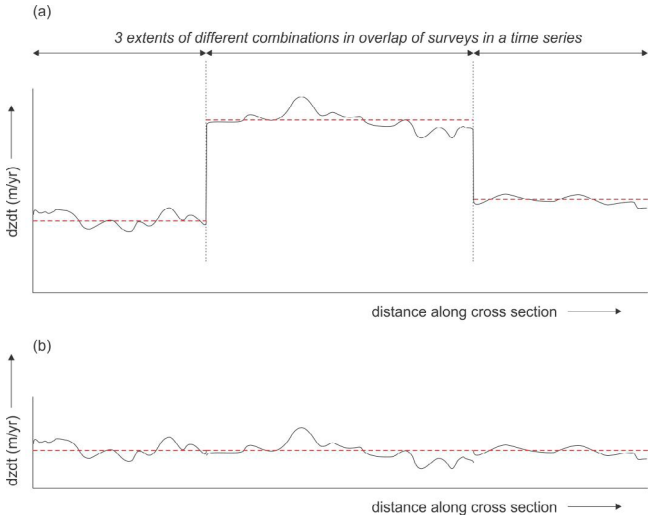

Figure 3. Applied correction in calculating the vertical nodal dynamics of the NCS. (a) The calculated dynamics (black solid line) are corrected by subtracting the average dynamics for each combination of survey overlap (red dashed lines) (b) Resulting morphodynamics in which the patchwork is removed and the natural seabed dynamics are revealed.

megaripples (contained in multibeam data), which may obscure the sand wave or long bed wave dynamics, are removed. From the smoothed bedform signal, locations of crest, trough and inflection points are then determined in a semi-automated way, from which the geometry and dynamics of individual bedforms is calculated.

RESULTS

Vertical dynamics trends

The quantified vertical nodal dynamic trends for the Netherlands Continental Shelf (Figure 4) provide an overview of regions of contrasting dynamics on the NCS. In this map, vertical dynamic trends are simplified into classes of absolute values in order to amplify the dynamic contrasts. Thus, this map does not display the full range of dynamic trends, which apart from extremes may range between few decimeters per year degradation or aggradation.

In general, the coastal zone is more dynamic than the continental shelf. Three zones of contrasting (natural) dynamics may be distinguished. First, the highly dynamic coastal zone includes estuaries, tidal inlets with ebb-tidal deltas, tidal channels in the Wadden sea and near-shore Zeeland, and breaker bars. Dynamic trends in these environments typically range between absolute values of 0.1 and 0.35 m/yr with extremes up to 1.5 m/yr.

Second, areas of moderate dynamics occur offshore on mostly sandy parts of the NCS, where rhythmic bedforms are present. Here, values typically range between -0.1 to 0.1 m/yr with extremes of an absolute 0.3 m/yr in the sand wave fields. The appearance of bedform patterns in the vertical dynamics map indicates that the measure of vertical dynamics is controlled by the migration and/or growth of individual bedforms. Clear fields of relatively high dynamics are the sand wave field west of Texel, a long bed wave field north of Texel and Vlieland, and the entire sand wave field in the Southern Bight including tidal ridges and long bed waves. The tidal ridges 75 km offshore Texel, where sand waves seem to be absent, also display large vertical dynamics, although these results may in part be due to the low-resolution data of digitized fair sheets.

Third, offshore areas of very low sea-bed dynamics (around 0 m/yr; light blue) occur mostly in parts of the NCS where rhythmic bedforms are absent. Although the dynamics map is scarcely filled in these zones, the largest areas of low dynamics occur in the deeper parts of the NCS, farther offshore. The low-dynamic area north of de Wadden islands is unexpectedly stable in the sense that the shore-face connected ridges that occur here could have been susceptible to migration or growth/decay. In addition, areas of low seabed dynamics appear in a zone between the sand wave field west of Texel and the offshore sand banks, and in small patches along the coast offshore Den Haag, offshore Voorne and the Vlakte van de Raan (ebb-tidal delta of the Western Scheldt).

Other small parts of high vertical dynamics in Figure 4 are anthropogenic areas, such as sand extraction sites, and due to artefacts caused by the data in the time series. The latter are most prominent in the shipping lane in the centre of the map (Deep Water Route East) and in the zones of low dynamics north of the Wadden islands. The effect of data precision is also recognized in the contrasts of dynamics for the separate survey overlaps.

Bedform size and mobility

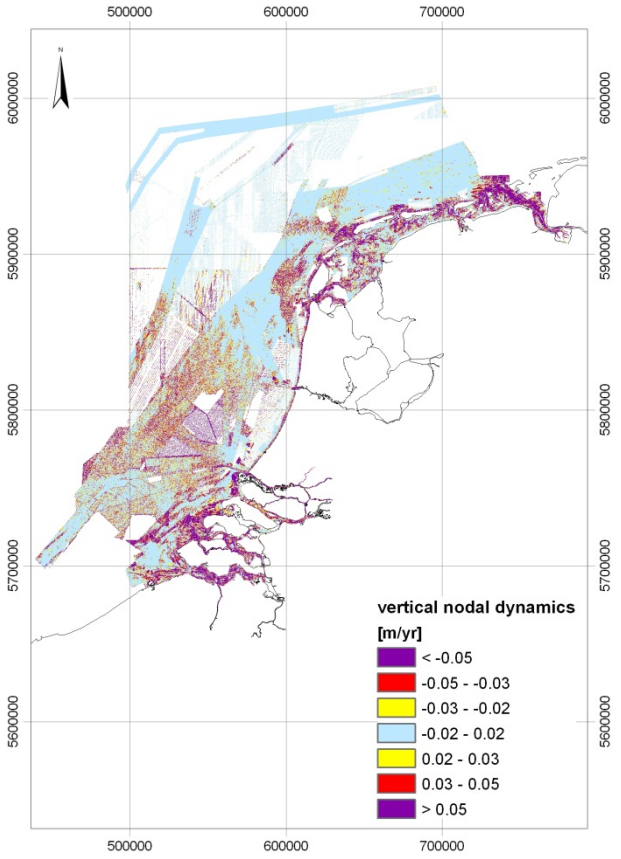

Figure 4. Vertical nodal dynamic trends of the Netherlands Continental Shelf (absolute values) show that the coastal zone is significantly more dynamic than the shelf, and that bed form fields offshore are the most dynamic zones on the shelf. Choice of classes is to amplify the morphodynamic contrasts; values range between -0.35 and 0.35 m/yr.

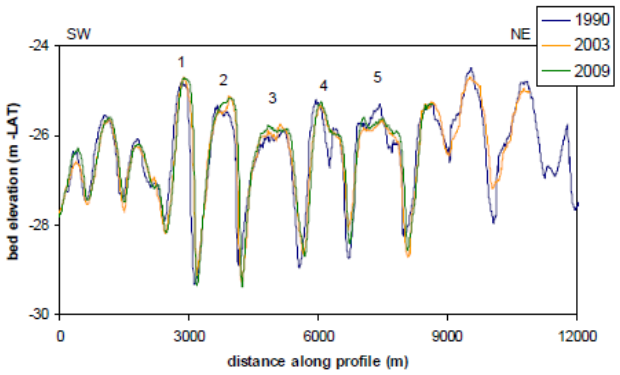

Figure 5. Profiles (SE to NW) of long bed waves north of Texel and Vlieland from the 1990, 2003 and 2009 datasets.

Detailed analyses of individual bedforms provide more information on the geometry, mobility and morphodynamics of bedforms. Three areas that are characterized by three different types of bedforms are here described.

Firstly, the sand wave field west of Texel comprises sand waves with an average wavelength of 345 m and an average wave height of 1.4 m. With an average sand wave migration rate of 16 to 19 m/yr to the northeast, this area is exceptionally dynamic compared to other sand wave fields on the NCS, where migration rates are mostly less than 5 m/yr [*Van Dijk et al.*, 2008; *Dorst et al.*, 2011; *Van Dijk et al.*, 2011].

Secondly, five long bed waves in the dynamic field north of Texel and Vlieland were analyzed. Long bed waves were first identified by *Knaapen et al.* [2001], but migration rates were never reported. The long bed waves north of Texel have an average wavelength of 1125 m and an average wave height of 3.4 m. Net migration rates, based on 3 surveys between 1990 and 2009 (Figure 5), range from 10.5 to 18.4 m/yr, with an average of 12.4 m/yr to the northeast.

Thirdly, the shoreface-connected ridges north of Wadden islands were analyzed based on profiles of two datasets only (Figure 6). The average wavelength of the ridges is 4614 m and the average height is 4.3 m. Present-day knowledge on migration rates and vertical morphodynamics of shoreface-connected ridges on the NCS is limited. Changes in dimensions are negligible and the average migration rate is 1.0 m/yr to the southwest.

DISCUSSION

A large-scaled study of vertical bed level changes of a wide coastal zone of the German Continental Shelf was recently performed by *Winter* [2011]. His calculations are based on a large number of annual datasets near the coast (up to 30 for two estuaries) and a small number of datasets (less than 5) farther offshore. Although his results are presented as bed elevation range (difference between the maximum and minimum bed levels) per node (in meters) and are thus not directly comparable to our dynamic trends (in m/yr), the overall pattern of dynamics is in good agreement with our findings of the NCS. *Winter* also describes highly dynamic estuaries and tidal inlets between the Wadden islands and areas of low dynamics offshore, which connects very well to the vertical dynamics map of the Dutch Wadden presented in this paper.

A regional bed dynamics study for the Wadden Sea, using a time series from 1926 to 2006, was carried out by *Vonhögen et al.* [2010]. They expressed dynamics in terms of the net deposition (cm), thus the difference between the latest and the lowest bed levels in the time series. Although these values are also not directly comparable to our dynamic trends in m/yr, the pattern of highly-dynamic tidal channels corresponds well and therewith corroborates our findings.

For the shoreface-connected ridges, in comparison, shoreface-connected ridges at the north coast of Spiekeroog, one of the German Wadden islands, also migrate landwards, but are much more dynamic [*Antia*, 1996]. The maximum migration rate of 100-200 m/yr is a factor 100 – 200 higher than the migration we find, and 4 to 40 times higher than rates reported from ridges in North-America, which range from nearly stable to 6 m/yr [*Antia,* 1996, and references therein]. Although the environment of the

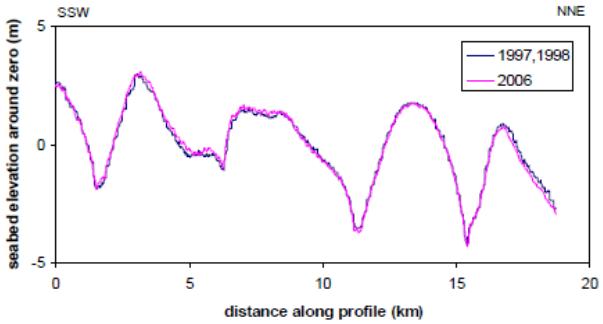

Figure 6. Profiles (SSW to NNE) of the shoreface-connected ridges north of the Wadden islands indicate that these bedforms have neither grown nor migrated in almost a decade.

banks at Spiekeroog seems similar to the shoreface-connected ridges at Ameland and Schiermonnikoog, the former banks are shorter and lower.

As the controlling parameters of the spatial variation in sea-bed dynamics, we hypothesise that:

- grain size affects the presence of sand waves and also may be a proxy for spatial variation in bedform migration rates, since an overlay of median grain sizes and bed morphology & dynamics correspond very well;
- current velocity seems the dominant factor for dimensions of sand waves [for wave length, see also *Van Santen et al.*, 2011] and sediment transport potential seems related to the migration rate of sand waves and long bed waves, when we compare modeled sediment transport rates of the North Sea [*Van der Molen and De Swart*, 2001] and an overview study of *Bearman* [1999] to our sand wave migration rates.

The vertical dynamic trends are sensitive to data quality issues, such as data density and precision. Low-resolution data, especially the older datasets, may underestimate the bedform heights and also affect the location of crests and troughs. In general, a lower data resolution of one dataset results in a higher vertical dynamics when comparing to another dataset.

APPLICATIONS

Without knowledge of the sea-bed dynamics, re-survey policies of continental shelves and rivers cannot be validated. The above analysis was used to validate and to optimize the survey-policy of the Netherlands Hydrographic Office. Hereto, we combined the morphodynamics and the predicted grounding dangers for shipping, based on shipping intensity, predicted water depth and the probability of unknown objects at the bed. An ongoing study on the river- and sea-bed dynamics for Rijkswaterstaat includes the investigation of cause and effects, including the interaction between dredging activities and sand waves.

Other applications are advice on sea-bed stability for regional planning and offshore engineering projects, such as the allocation, construction and maintenance of offshore wind farms. Bedform mobility may affect the depth of wind piles into the sea bed by maximally the bedform height, which may be up to several meters.

Finally, knowledge on the morphodynamics of tidal channels and sand banks is crucial in refining the 3D geological model of the subsurface, the evolution of the marine palaeolandscape and the prediction of archaeological remnants, such as shipwrecks and subrecent archaeology (e.g. WOII-remnants). Sea-bed dynamics also play a role in the burial and exposure of shipwrecks, so establishing the affected depths and time-scales of these dynamics provide information on the preservation potential of these archaeological items.

CONCLUSIONS

Vertical nodal dynamic trends of the Netherlands Continental Shelf typically vary between -0.35 and 0.35 m/yr. The coastal zone is significantly more dynamic than the offshore zone. Especially estuaries, tidal inlets, tidal channels and breaker bars are dynamic (abs. values of 0.1 – 0.35 m/yr, with extremes up to 1.5 m/yr). Offshore the most dynamic parts are the fields of mobile marine bedforms, such as sand waves and long bed waves, where vertical bed levels are caused by bedform migration and/or growth (levels between -0.1 and 0.1 m/s with extremes up to an abs. 0.35 m/yr). Deeper parts and north of the Wadden islands, vertical dynamics are very low (~0 m/yr).

Vertical trends in sea-bed dynamics are crucial in the re-survey policies of hydrographic surveyors. By combining the (predicted) sea-bed dynamics with predicted grounding dangers for sea traffic, monitoring policies can be optimized so that measuring efforts are low while safety is still the highest. To offshore engineers, managers and marine archaeologists, morphodynamics support the decision-making on regional planning, marine protected areas and archaeological values and the potential risks to offshore structures and maintenance.

ACKNOWLEDGEMENT

All data were provided by the Hydrographic Office, Royal Netherlands Navy, and Rijkswaterstaat, Ministry of Infra Structure and the Environment. Most of this work was carried out within a research project financed by the Ministry of Defense. Within this project, the Maritime Research Institute of the Netherlands (MARIN) quantified the grounding dangers for shipping.

REFERENCES

Antia, E.E. (1996), Rates and patterns of migration of shoreface-connected ridges along the sourthern North Sea coast, Journal of Coastal Research, 12, 38-46.

Bearman, G. (Ed.) (1999), Waves, tides and shallow-water processes, second ed., 227 pp., Butterworth-Heinemann, Oxford.

Buijsman, M.C. and Ridderinkhof, H. (2008), Long-term evolution of sand waves in the Marsdiep inlet, II: relation to hydrodynamics, Continental Shelf Research, 28, 1202-1215.

Dorst, L.L., Roos, P.C. and Hulscher, S.J.M.H. (2011), Spatial differences in sand wave dynamics between the Amsterdam and the Rotterdam region in the Southern North Sea, Continental Shelf Research, 31, 1096-1105.

Dorst, L.L., Roos, P.C., Hulscher, S.J.M.H. and Lindenbergh, R.C. (2009), The estimation of sea floor dynamics from bathymetric surveys of a sand wave area, Journal of Applied Geodesy, 3, 97-120.

Duffy, G.P. and Hughes-Clarke, J.E. (2005), Application of spatial cross correlation to detection of migration of submarine sand dunes, Journal of Geophysical Research, 110.

IHO (2008), IHO Standards for Hydrographic Surveys, edited, International Hydrographic Bureau, Monaco.

Knaapen, M.A.F. (2005), Sandwave migration predictor based on shape information Journal of Geophysical Research, 110, 9.

Knaapen, M.A.F., Hulscher, S.J.M.H., de Vriend, H.J. and Stolk, A. (2001), A new type of sea bed waves, Geophysical Research Letters, 28, 1323-1326.

Righolt, R.H., Schaap, J., Dorst, L.L. and Vos, E.M. (2010), Needle in a haystack, in Management of massive point cloud data: wet and dry, edited by P.J.M. Van Oosterom, M.G. Vosselman, T.A.G.P. Van Dijk and M. Uitentuis, p. 104, Nederlandse Commissie voor Geodesie, Delft.

Van der Molen, J. and De Swart, H.E. (2001), Holocene wave conditions and wave-induced sand transport in the southern North Sea, Continental Shelf Research, 21, 1723-1749.

Van Dijk, T.A.G.P. and Kleinhans, M.G. (2005), Processes controlling the dynamics of compound sand waves in the North Sea, Netherlands, Journal of Geophysical Research, 110.

Van Dijk, T.A.G.P., Lindenbergh, R.C. and Egberts, P.J.P. (2008), Separating bathymetric data representing multi-scale rhythmic bedforms: a geostatistical and spectral method compared, Journal of Geophysical Research, 113.

Van Dijk, T.A.G.P., Van der Tak, C., De Boer, W.P., Kleuskens, M.H.P., Doornenbal, P.J., Noorlandt, R.P. and Marges, V.C. (2011), The scientific validation of the hydrographic survey policy of the Netherlands Hydrographic Office, Royal Netherlands Navy, 165 pp, Deltares.

Van Santen, R.B., De Swart, H.E. and Van Dijk, T.A.G.P. (2011), Sensitivity of tidal sand wavelength to environmental parameters: A combined data analysis and modelling approach, Continental Shelf Research, 31, 966-978.

Vonhögen, L.M., Van Heteren, S., Marges, V.C., Wiersma, A.P. and De Kleine, M.P.E. (2010), Comparison between the internal dynamics of the Dutch Wadden Sea and the volumes involved by subsidence areas, paper presented at NCK days 2010, West-Kapelle, Netherlands.

Winter, C. (2011), Macro scale morphodynamics of the German North Sea coast, Journal of Coastal Research, SI 64, 706 - 710.

Winter, C. and Ernstsen, V.B. (2007), Spectral analysis of compound dunes, paper presented at 5th IAHR Symposium on River, Coastal and Estuarine Morphodynamics (RCEM 2007), Taylor & Francis, University of Twente, Enschede, The Netherlands

DOI: 10.3990/2.203

Assessing dune erosion: 1D or 2DH? The Noorderstrand case study

P.F.C. van Geer[1] and M. Boers[1]
[1]Deltares, P.O.Box 177, 2600 MH, Delft, the Netherlands, Pieter.vanGeer@deltares.nl

ABSTRACT

The Dutch safety assessment rules primarily focus on the cross-shore processes related to dune erosion during an extreme storm. A case study of the Noorderstrand (Schouwen) reminds us of the importance of taking into account effects of these alongshore processes. Both a study of the available (GIS) data and an extensive study with the numerical model XBeach show various processes that influence the amount of dune erosion during an extreme storm. Long-term processes that lead to migration of sand waves on the beach as well as the edge of the nearby channel building out seaward are present in both the measurement data and the model simulations. The resulting variation in the beach geometry causes a strong redistribution of sediment in alongshore direction during an extreme storm, leading to a sediment balance difference up to 100 m^3/m measured along a cross-shore transect. Redistribution of the sediment alongshore proves not only to be dependent on the beach geometry, but also on the wind direction during the storm.

INTRODUCTION

Each primary sea defense in The Netherlands needs to be assessed for safety on a regular basis. Currently, the assessment rules for dune erosion prescribe a 1D model Duros+ to calculate dune erosion, despite the fact that it is outside the range of validity for some locations. Recently, during the second assessment round, a dune section at the Noorderstrand did not pass the assessment. During the search for a solution to this safety problem, also 2D simulations were performed to assess dune erosion in this area. These simulations reminded us once again of the importance of taking into account alongshore processes when looking at dune erosion. This paper describes and discusses several findings obtained from these simulations.

The Noorderstrand lies right South of the Brouwensdam (Figure 1). Before this dam was built, a relatively deep channel positioned itself close to the shoreline. After closing off the Grevelingen, this channel remained near the coastline and started filling up. The channel is still present, but the rate sediment is deposited in the former tidal channel is rapidly decreasing nowadays. Furthermore, there is only one dune row. At one particular location, the dune is relatively narrow, causing the dune section not to reach the required level of safety.

APPROACH

To investigate dune erosion as a 2D process we used an XBeach model [Roelvink et al. 2009] that we setup for the area of the Noorderstrand. XBeach is a two-dimensional, numerical, wave group resolving, morphological model that supports slumping of dune faces. It can therefore calculate hydrodynamics and dune erosion for an area like the Noorderstrand. Since we do not have data that quantifies the impact of a storm in that area, it is hard to calibrate the model quantitatively. There are, however, many measurements of the bathymetry of that area, which allows us to qualitatively verify the model by matching observed long-term developments with processes that occur during a simulated storm. This paper shows that several of the physical processes that occur during an XBeach simulation support the long-term development we retrieved from the measurement data. Having confidence in the model outcome in a qualitative sense, we can now look at the qualitative effect of assessing dune erosion as a 2D process instead of a 1D process only.

Figure 1: Overview of the location and orientation of the Noorderstrand area.

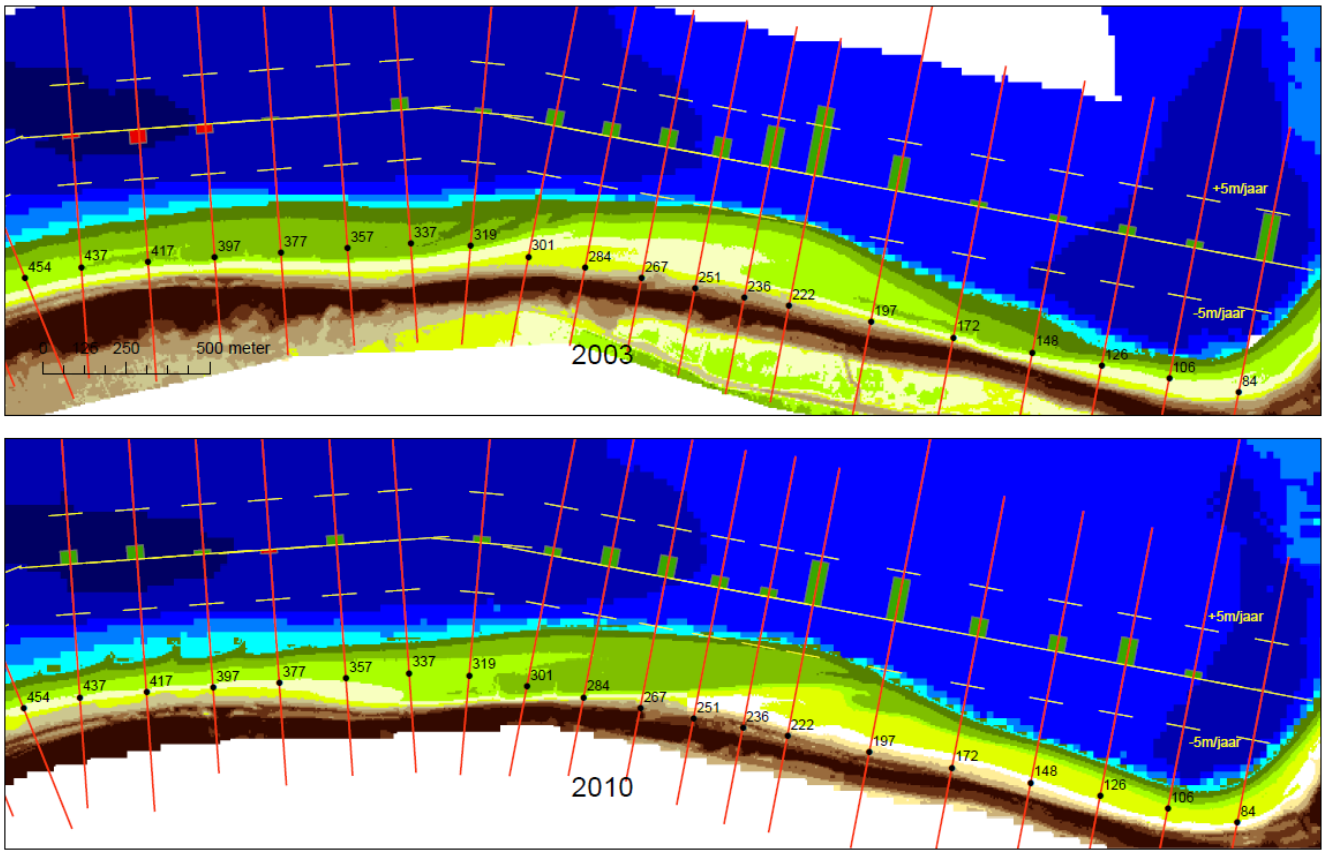

Figure 2: Development of the beach and channel near the Noorderstrand. The light green areas show a sand wave moving eastward and a new one entering at the western side of the area. The green bars denote the seaward movement rate of the edge of the channel.

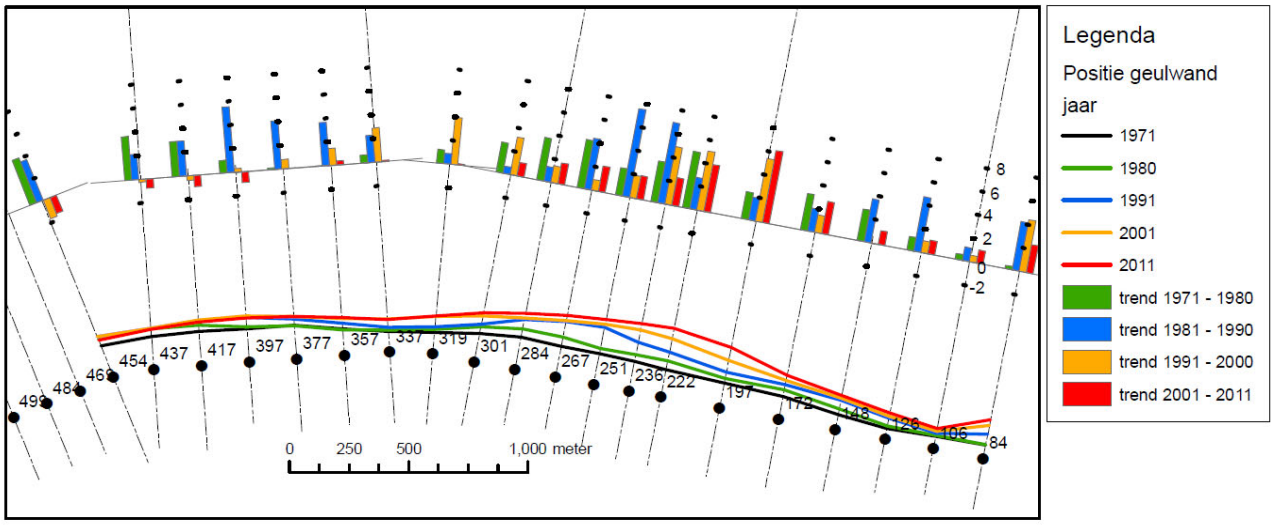

Figure 3: Development of the edge of the channel in time. The lines show the averaged position of the slice between -3m + NAP and -5m + NAP for a specific year. The bars denote the movement of that line at a particular location (in m/year).

MORPHOLOGICAL DEVELOPMENT NOORDERSTRAND

Measurements of the bathymetry near the Noorderstand have been carried out on a yearly basis. From these measurements, several trends can be identified. From the moment of finishing the Brouwersdam, the channel, for example, started filling up. This process slowed down in the past 10 years. Two trends draw our attention with respect to verifying XBeach calculation.

First, there appears to be a so-called sand wave on the upper (dry) part of the beach. Between 3 m + NAP and 1.5 m + NAP sand waves travel from West to East. Figure 2 shows the measured bathymetry of 2003 in comparison with the bathymetry of 2010. The dry part of the beach (yellow and light green colors) shows a bulk of sand moving from transect 251 eastward to 222 / 197. A new wave is starting to develop near transect 357. The magnitude of the bulks of sand traveling along the coast increased after the nourishments of 1994 and 1995 and slightly decreased again due to another nourishment in 2000.

The second trend is related to the movement of the edge of the channel near the Noorderstrand. Figure 3 shows the averaged position of the channel in time. This line tends to gradually build out seaward (and to the east) between transect 267 and 197.

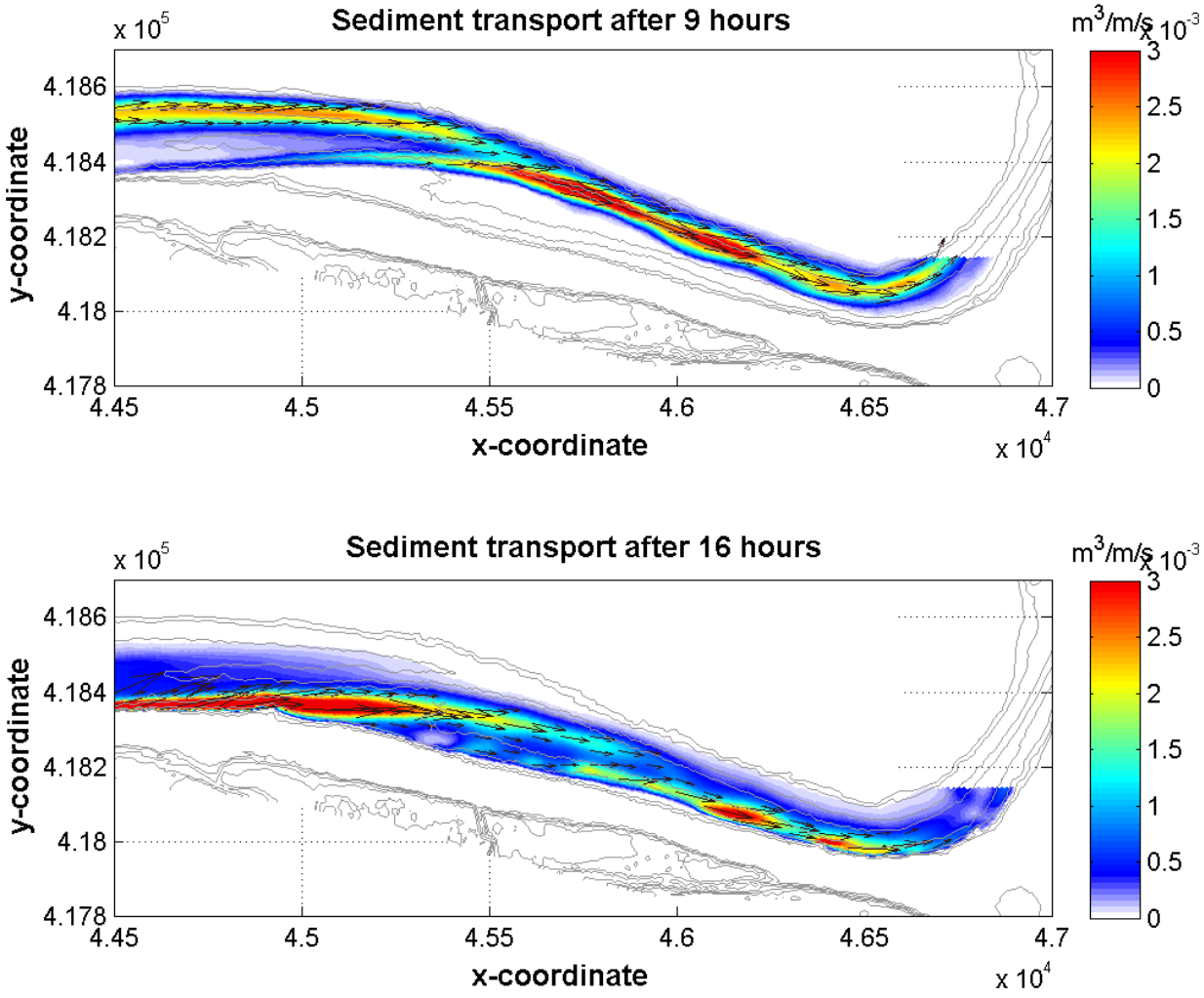

Figure 4: Sediment transport direction and magnitude near the Noorderstrand at two stages during a once in 10 years storm as calculated by XBeach.

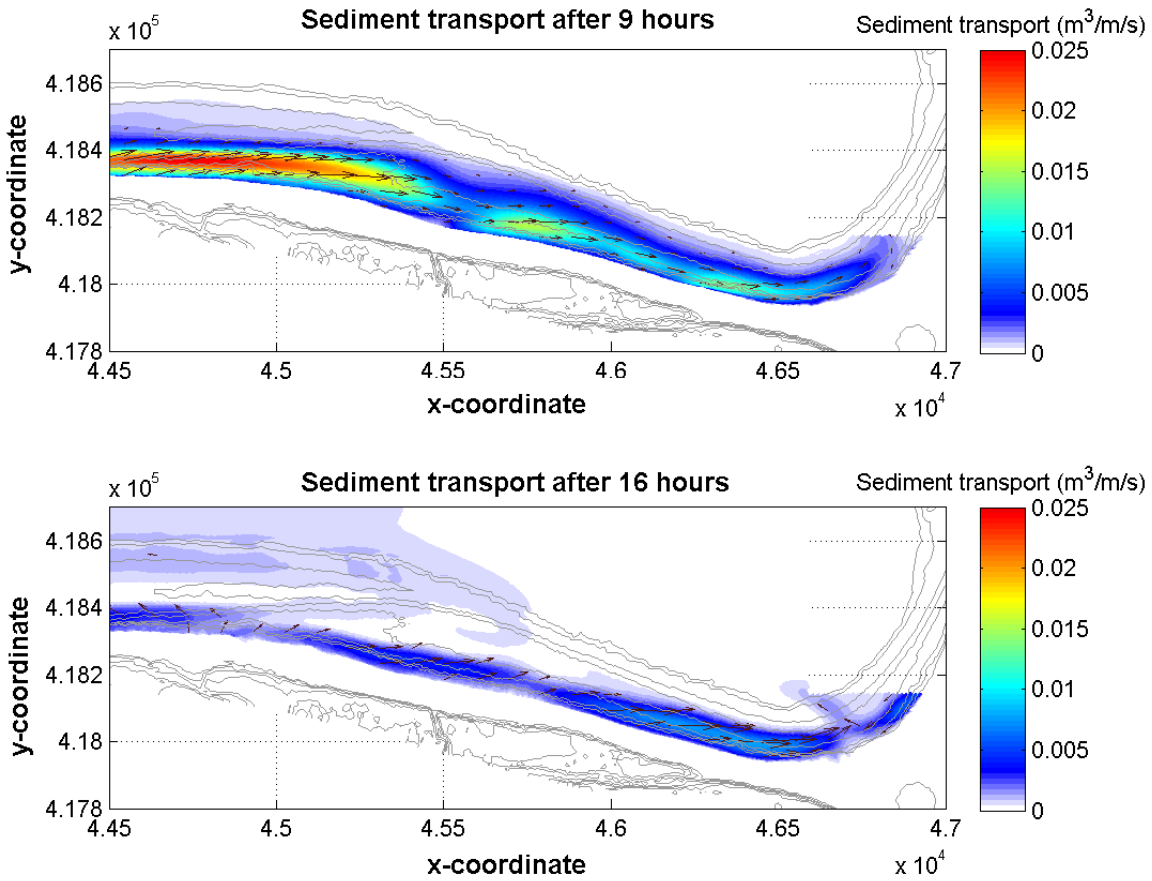

Figure 5: Sediment transport direction and magnitude near the Noorderstrand during a storm from north west and a northern storm.

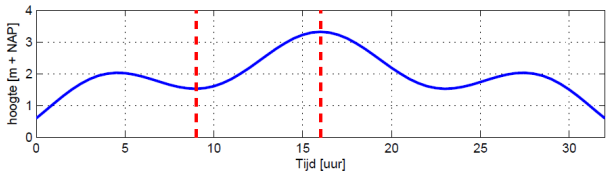

Figure 6: Applied storm surge for a once in 10 years storm.

VERIFICATION OF XBEACH

On the XBeach model, we imposed a storm surge and wave boundary conditions that varied in time. Figure 6 visualizes the used storm surge, which corresponds with a storm with a probability of occurrence of once in 10 years. We used a similar surge to simulate an extreme storm that matches the conditions that we use to assess the safety of the dunes at the Noorderstrand.

The lack of measurement data before and after storm events makes it impossible to calibrate any dune erosion model for the Noorderstrand area. While analyzing the results of the uncalibrated model, we did however identify processes in our simulations that support the observed long-term development of the bathymetry.

Figure 4 shows calculated sediment transport patterns after 9 and 16 hours of storm (also indicated by red dashed lines in Figure 6). After 9 hours of storm (when the water levels are still relatively low) sediment transport mainly occurs right at the edge of the channel, causing sediment to drop over the edge into the channel. Mostly between transect 236 and 197. This process supports a seaward displacement of the edge of the channel.

The calculating sediment transport at the peak of the storm (after 16 hours) mainly occurs higher on the beach and initiates movement of the sediment from East to West. Also this process supports the measured long-term bathymetrical changes.

MORPHODYNAMICS DURING AN EXTREME STORM

When assessing dune erosion with a 1D model, sediment that erodes from the dune face is assumed to settle on the beach further offshore, without interacting with neighboring transects. This assumption does not necessarily have to be valid for any location.

In case of the Noorderstrand, oblique wind and waves force an alongshore current that varies in direction and magnitude as shown in Figure 4. This causes sediment transport not just in cross-shore direction, but also along the coastline. Gradients in

this longshore sediment transport cause not all cross-shore transects to have a balance between the amount of eroded sediment and the amount of accreted sediment. Eroded sediment in the western part of the area travels eastwards and contributes to the accretion in another transect.

Alongshore redistribution of sediment

Figure 7 shows the difference between accretion and erosion along transects from west to east in the study area, interpolated from the model bathymetry at the end of the simulation with a northwestern wind. The figure shows that the difference between the amount of eroded sediment and the amount of accreted sediment in the calculation can reach 100 m^3/m. At some locations, this doubles the amount of eroded sediment above storm surge level.

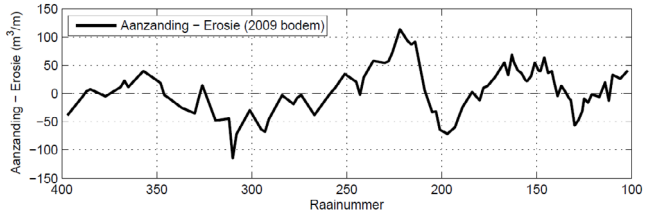

Figure 7: Accretion – erosion along the coastline of the Noorderstrand as calculated by XBeach with an extreme storm from NW.

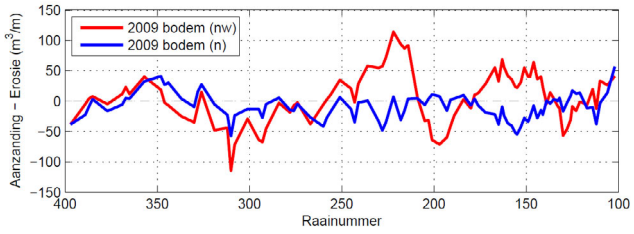

Figure 8: Accretion – Erosion along the coastline as calculated by XBeach. The red line shows the sediment balance after calculation with a northwestern storm. The blue line shows the sediment balance along the coastline after calculating a northern storm.

Sensitivity of disturbed sediment balance

The redistribution of sediment along the coast appears to be driven by the alongshore current gradients that exist during a northwestern storm. Calculations with varying wind direction, but similar characterization of the surge level in time, revealed that the redistribution of sediment in alongshore direction changes dramatically with changing wind direction. Figure 5 compares sediment transport during a northwestern storm with sediment transport calculated for a northern storm. Due to the change if the angle of incident of the waves, the northern storm primarily causes sediment to travel cross-shore (as assumed in a 1D model), whereas the northeastern storm mainly induced sediment transport in the alongshore direction. This change of the sediment transport processes and corresponding gradients also have an effect on the redistribution of sediment in the alongshore direction. Figure 8 (red line) shows the same redistribution during a northwestern storm as displayed in Figure 7. The blue line shows that redistribution of sediment during the northern storm reached just around 40 m^3/m.

DISCUSSION

The case study of the Noorderstrand shows that 2D processes can have a significant influence on the calculated amount of dune erosion. Especially while assessing dune safety at locations with a complex foreshore, such as the Noorderstrand, one should be cautious with applying a 1D model only. Redistribution of sediment in the alongshore direction can have an important effect on the height of the beach in neighboring transects and therefore also the amount of eroded sediment.

The Dutch assessment rules for dune safety [TRDA2006, 2007] prescribe the assessment of dune erosion during an extreme storm with the help of the 1D Duros+ model. Although the assessment rules do indicate that the remaining (boundary) profile after a storm should be continuous along the coastline to prevent flooding, alongshore processes are not taken into account while assessing the amount of erosion during an extreme storm event. The rules do not encourage assessors to judge the importance of alongshore processes. The Noorderstrand case study showed a contribution of redistribution of sediment can influence the amount of eroded sediment significantly and should be something to look after when assessing dune safety in areas with a complex foreshore.

Due to the absence of a proper calibration of the model, results presented in this study can only be interpreted qualitatively. Any definite conclusions regarding the safety of the Noorderstrand area would be one step ahead of reality.

ACKNOWLEDGEMENT

Waterschap Scheldestromen is kindly acknowledged for commissioning Deltares to carry out this study. Next to that we would like to thank dhr. ir. Hans van de Sande (Waterschap Scheldestromen) for his valuable input, that helped us reaching the results presented in this paper.

REFERENCES

Dano Roelvink, Ad Reniers, Ap van Dongeren, Jaap van Thiel de Vries, Robert McCall, Jamie Lescinski (2009), Modelling storm impacts on beaches, dunes and barrier islands, Coastal Engineering, 56(11–12),1133-1152, ISSN:0378-3839, 10.1016/j.coastaleng.2009.08.006.

TRDA2006 (2007), Technisch rapport duinafslag, experisenetwerk waterveiligheid

DOI: 10.3990/2.204

Highlights of Dutch and US coastal graduation projects in the Mississippi Delta after Hurricane Katrina

M. van Ledden[1,3], M. Kluyver[2], A.J. Lansen[1] and R. Kluskens[1]
[1]Royal Haskoning, George Hintzenweg 85, Rotterdam, The Netherlands, m.vanledden@royalhaskoning.com
[2]Moffatt & Nichol, 301 Main Street, Suite 800, Baton Rouge, LA 70825, USA
[3]Delft University of Technology, Stevinweg 1, Delft, The Netherlands

ABSTRACT

This paper presents the highlights of coastal graduation projects conducted in New Orleans after Hurricane Katrina from students of universities in The Netherlands (Delft, Twente, Groningen, Amsterdam, Wageningen) and Louisiana (LSU, UNO). The intent is to show good examples of how knowledge and modeling tools in the field of coastal engineering, typical to the Netherlands, is applied in an international context. Three illustrative examples are summarized. The first example is the development of an innovative forecasting tool for predicting storm surge in the Louisiana coastal zone. This tool has successfully been applied during training exercises and real-life applications in New Orleans. Second, an in-depth study has been carried out to increase the understanding of the effectiveness of diversions to restore wetlands. Practical recommendations were provided for the choice of location and size of diversions in the Lower Mississippi. A third example is the long-term morphological modeling of the Wax Lake Delta. Various characteristics of this delta development were reproduced by the model, but also limitations of the predictive performance of the model were detected. This paper will close with an outlook on further collaboration between Louisiana and The Netherlands.

INTRODUCTION

In 2005 Hurricane Katrina showed the Gulf Coast's extreme vulnerability to coastal flooding. After the first landfall in Florida, Hurricane Katrina intensified to a Category 5 hurricane in the Gulf of Mexico. The second landfall took place near Buras in Louisiana. It generated storm surge levels at the coast with a maximum water level of 9m+MSL near Biloxi (Mississippi). Over 50 breaches in the levee system around New Orleans resulted in major flooding of the city. With a total property damage estimated at $81 billion (2005), it was the costliest natural disaster in US history, and 1836 people lost their lives in this tragedy.

The coastal flooding during Katrina has initiated various federal and state programs to reduce flood risk in this area. The US Army Corps of Engineers has been responsible for executing a program to improve the levee system around New Orleans to the 100-yr design standard. This 6-year program was focusing on flood risk reduction in the short term and has resulted in a $15 billion investment program in levees, pump stations and storm surge barriers to provide the necessary level of protection.

The Louisiana Coastal Protection and Restoration Project (LACPR) from the US Army Corps of Engineers and Louisiana's Comprehensive Master Plan for a Sustainable Coast from the State of Louisiana have been focusing on the long-term flood risk reduction. A range of measures were evaluated for different levels of protection. These measures included structural measures such as the further raising of levees and barriers but also a range of non-structural measures such as wetland restoration, evacuation and changing building codes to further reduce flood risk. Both projects have resulted in various flood risk reduction strategies for coastal Louisiana.

According to the authors, these programs have provided a unique opportunity for students to experience how people in this delta gain their livelihoods from the resources of the coast and how they are dependent on manmade flood protection infrastructure and the natural coastal habitat that protect their homes and business from storm flooding. About 20 graduation projects have been initiated with Dutch and US students on various coastal engineering topics in and around New Orleans and in the Mississippi River Delta. These students originated from various universities in The Netherlands (Delft, Twente, Groningen, Amsterdam, Wageningen) and Louisiana (UNO, LSU).

This paper shows highlights of coastal graduation projects in Louisiana. Three illustrative examples are summarized from the coastal graduation projects on how knowledge and modeling tools in the field of coastal engineering, typical to the Netherlands, are applied in an international context. These examples are focusing on two central coastal challenges in Louisiana: hurricane storm surge and wetland restoration. This paper will close with a discussion of coastal research topics for further collaboration between Louisiana and The Netherlands.

HURRICANE SURGE FORECASTING

As a coastal city, New Orleans is threatened by tropical storms or hurricanes every year. Both intense hurricane force winds and associated high water levels (storm surges) threaten this city. After Hurricane Katrina flooded the majority of the city in 2005, there has been a keen interest to obtain better insight into the storm surges produced by tropical systems. In order to adequately protect and prepare the city of New Orleans, forecasted surge levels for an approaching storm could provide a crucial piece of information. Forecasted surge levels are necessary to make decisions about safety measures, distribution of information to the public, evacuation of residents and emergency sandbag placement.

To predict these surge levels, the U.S. Army Corps of Engineers

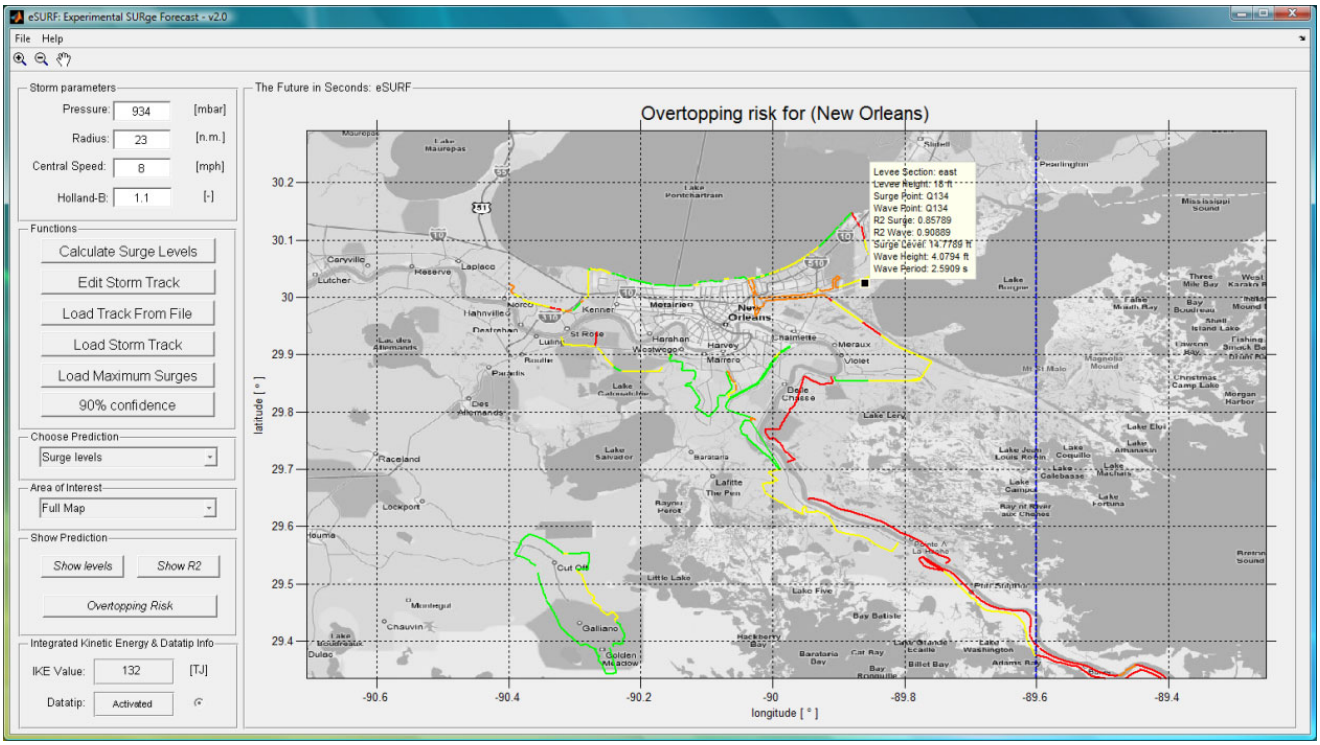

Figure 1. Overtopping risk for the New Orleans Hurricane Risk Reduction System

(USACE) utilizes the ADCIRC model (see e.g. Westerink et al. 2008), a numerical model that calculates free surface elevation due to tides, winds, river discharges, precipitation and more. The ADCIRC model captures the physical processes during a storm event to a high level of detail.

The ADCIRC model is physically very detailed, and almost all relevant aspects regarding hurricanes and storm surge are used to create a forecast. This however comes at a certain cost. The high level of detail requires a computer to do a significant amount of calculations. Depending on the complexity of the storm and used (super)computer resources, it could take ADCIRC more than 6 hours to finalize a single model run. Due to the changeable nature of these complicated weather systems, a hurricane may already have completely changed in size or its course within the time frame to complete a model run.

The goal of the eSURF project was to make a fast forecasting model that can predict surge levels caused by hurricanes. eSURF stands for Experimental Surge Forecast. Van den Berg (2008), Lin (2009) and Smits (2009) worked on the project and through various stages of iteration developed the program in the attempt to reduce the dependency on elaborate, time consuming model calculations in the critical hours before a Hurricane makes landfall. Their contributions during their graduation projects resulted in the eSURF program that can now make a surge level prediction in seconds, without significant reductions in accuracy. The program uses an innovative algorithm to come up with a fast and relative accurate prediction of surge levels. The model is a prediction model that uses multiple linear regression on a dataset of model results. At the base are the ADCIRC results from 152 synthetic storms for the Louisiana coast, 2566 surge level prediction points, the parameters of the forecasted hurricane and the eSURF algorithm. In addition, eSURF can also predict wave heights and wave periods and provide a risk classification based upon the forecasted hydraulic parameters in combination with known levee heights for the Greater New Orleans Metropolitan area (Figure 1).

The user-friendly interface created by the students, at last, makes the program accessible to anyone with basic coastal engineering skills and a desktop computer. The eSURF project provided an opportunity for students to perform an in-depth study of the physical processes of hurricanes and storm surge and its relevancy to society. The contribution of the students to the project has been greatly appreciated. The USACE can use this tool in conjunction with other sources of information available prior to a storm making landfall. The multitude of sources available helps to establish a better informed and more reliable risk assessment. Future development of eSURF includes the expansion of the programs use to all neighboring states situated on the Gulf of Mexico.

WETLAND RESTORATION

The wetlands of Louisiana are a unique habitat with high ecological, recreational and economical value. The marshes and swamps of South-Eastern Louisiana are, however, deteriorating at an alarming rate. In the past, the Mississippi River was able to carry sediment to the marshes every flood season, but now the river is isolated from its floodplains because of human interventions. Over the years, a levee system has been built, alongside the downstream portion of the Mississippi River to prevent flooding of the adjacent land. The river mouth is confined to a number of canalized channels protruding into the Gulf of Mexico, and sediment is therefore immediately delivered to the

edge of the continental shelf, isolated from the current bird foot shaped sub-delta and the up and down-drift coasts of the deltaic plain. The sediment deposits off the continental shelf and is no longer replenished into the marshes. Furthermore, increased rates of subsidence in the region have been correlated to withdrawal of hydrocarbons and groundwater in the delta plain. The relative sea-level rise in this region is at a rate of 10 mm per year. The result is a staggering loss of marshland over the past century.

The impact of the marshland degradation on the attractiveness and sustainability of the Louisiana coastal plain is significant. It is predicted that hurricane surge elevations at the toe of the Greater New Orleans levee system will increase substantially if the process of wetland degradation continues at the current rate. Therefore, a long term investment to protect the great city of New Orleans is to start revitalizing the marsh area of Southern Louisiana. Allowing river water rich with sediments to enter the marshes through diversions is considered to be a promising option which could slow down or even reverse this trend. Both the work from Hillen et al. (2007) in this section and Hanegan (2011) in the next section focus on this option.

Hillen et al. (2007) studied the feasibility and effects of marsh restoration by a diversion in the Mississippi River near Port Sulphur (see Figure 2 for locations), diverting water into the adjacent Barataria Bay and Breton Sound. The main research objective was to determine the land building potential of a diversion in the Mississippi River near Port Sulphur and if accreted land will contribute to surge reduction and a safer New Orleans in the long term. The subject has been studied with a qualitative physical model and detailed numerical simulations with a quantitative 3D numerical model.

A literature survey showed that there still is a knowledge gap on the subject of engineering large scale effective sediment diversion. Some of the diversions built in the past along the Mississippi River work well, while others do not function as originally planned. The reasons of malfunctioning and the complex physical processes are not well understood. Another knowledge gap is the complex interaction between marshes and storm surge propagation and the effect of marshes on the storm surge reduction. A historical rule-of-thumb exists from USACE (1963) for surge level reduction over marshes (ca. 1 m per 14.5 km) but various researchers utilizing detailed numerical computations show that the effect of marshes for extreme events is limited (see e.g. Resio and Westerink, 2008).

First-order calculations for the Port Sulpher project area show that a significant amount of water needs to be diverted from the Mississippi River to introduce sufficient sediment into the system for substantial marsh restoration. It was estimated that a yearly average discharge through the diversion of approximately 50.000 m^3/s is needed. This is about one third of the total yearly average Mississippi River discharge. Although these effects have not been quantified in detail, it is safe to state that such a large change in the hydrodynamics would have an effect on the salinity intrusion and morphodynamics of the Mississippi River.

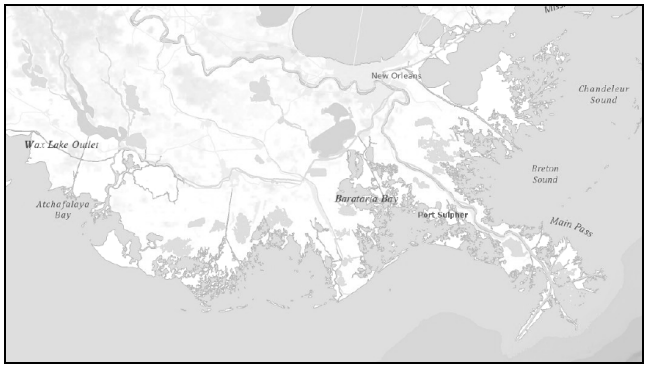

Figure 2. South Eastern Louisiana with the Mississippi Delta and the Atchafalaya Basin and Delta (including the Wax Lake Outlet) in the West

To gain insight in the influence zone and possible effects of a diversion, a physical model at the Louisiana State University (LSU) was utilized. This physical model represents the lower part of the Mississippi River Delta (The Birdfoot Delta). Model runs simulated changes over a 30 year time frame for three different diversions. The students were able to study the influence zone of a diversion and the sediment movement through the river. The model indicated that the location and orientation of a diversion in the river are important factors that need to be taken into consideration when designing a diversion. The data obtained from the physical model was used as input for more detailed calculations with a numerical model.

For quantitative modeling on storm surge reduction, the numerical modeling suite Delft3D was used. Several model runs with different schematizations of the project area were completed. Boundary conditions were based on the storm conditions of hurricane Katrina to provide a first insight and to study possible effects on a case by case basis. The modeled storm surge levels for the base conditions are higher than the actual measured storm surges. However, this model does approximate the results of the actual storm surge and can, therefore, be used to determine relative effects of storm surge reduction of the marsh area created by a diversion near Port Sulphur.

Different scenarios which represent various marsh types are modeled: the existing situation, a situation with an area of solid marshes, a marsh area with 35% open water, a marsh area with canals, a gently sloped marsh area and a shallow water area. The increased roughness and vegetation parameters are applied in a special vegetation (marsh) module of the model. The model results show that marshes do have a positive effect on storm surge reduction. The influence area of the marshes on storm surge is limited to the Mississippi Birdfoot, and there is no storm surge reduction in Lake Borgne or Lake Pontchartrain. The model shows that the storm surge reduction is identical for solid marshes and for marshes with canals or marsh areas with 35% open water. For Hurricane Katrina type conditions, 30km of marshland will reduce the storm surge elevation by about 0.5m to 1m.

Hillen et al. (2007) showed that creating a large-scale sediment diversion to increase the long-term safety of New Orleans and its surrounding areas is a promising possibility but also identified its challenges. Substantial amounts of sediment rich water need to be diverted from the main channel to slow down or reverse marsh degradation. This will in turn affect the river bed morphology and

could have an impact on the shipping function of the main channel. It is recommended to study this effect in more detail.

If enough sediment is diverted from the Mississippi River, land building and marsh restoration will occur which in turn can reduce storm surge levels. The storm surge reduction is primarily of local nature and depends largely on the characteristics of the storm, such as path and storm intensity. For this case study, marshes that will be created by the diversion near Port Sulphur will locally reduce the storm surge and therefore increase the safety of the residents of Plaquemines Parish. These marshes do not directly lead to a reduction in the storm surge levels near New Orleans. If no interventions occur in coastal Louisiana, the marsh deterioration will continue at the current alarming rate and because this deterioration is at such a high rate and in such a large area, it will severely reduce the storm surge reduction capacity of the Mississippi deltaic plain in the long term. A large-scale diversion is a good option as a sustainable part of a long-term master plan for the future of New Orleans and its surroundings.

WAX LAKE DELTA MORPHOLOGY

Hanegan (2011) also focused on the option of constructing diversions to restore marshlands. His focus was the delta formation over long-term timescales taking place after the construction of a river diversion. The most beneficial impact of an outlet to the marsh area depends on the formation of a new delta at the seaward side of the outlet by deposition of diverted sediment. In his thesis work "Modeling the Evolution of the Wax Lake Delta in Atchafalaya Bay, Louisiana", the results of process-based, hydrodynamic and morphologic modeling using Delft3D are presented, focusing on the Wax Lake Delta in Atchafalaya Bay. The model was developed to simulate a five year period of delta development from the beginning of 1998 to the end of 2002. The purpose of this modeling study was to further validate the ability of process-based modeling tools to successfully simulate typical delta-building processes and the resulting morphologic and stratigraphic characteristics of such a delta. With the ability to reliably predict the resulting deltaic deposition, the investments in the outlets for restoration of the Louisiana marshlands can be optimized.

The model applied in this study was generally successful in simulating the growth typical of river dominant systems (Figure 3). The Wax Lake Delta is clearly river-dominant according to traditional classification schemes; however, the deposition of fine sediments is influenced by basin processes that resuspend and export significant quantities from the Atchafalaya Bay. The processes contributing to the coarse sediment depositional features that dominate the Wax Lake Delta are qualitatively simulated under purely riverine forcings, but the fine sediment dynamics cannot be accurately simulated in the present, process-limited model. Recommendations for improving morphological simulation include model redevelopment with an alternative, total load transport formulation and the inclusion of limited marine forcings that inhibit fine-sediment deposition.

The accurate simulation of the actual development of a real delta requires a corresponding accurate representation of dominant processes, model domain bathymetry and sediment composition, and the calibration of hydrodynamics and sediment transport. Though the hydrodynamic calibration process was fairly straightforward, the subsequent need to alter calibrated sediment transport parameters for more accurate long-term simulation highlights the difficulty of transport calibration based on a single, discrete measured event. In this case, the possible storage of fine sediment in the prototype upstream channel during low flows, hysteresis in transport and discharge peaks at the upstream boundary, and the limited model representation of marine processes create significant complications for calibration.

The results of this study indicate that successful simulation of delta development along the typically low-energy Louisiana coast requires inclusion of marine processes beyond those included in this assumed river-dominant simulation. The inclusion of two sediment fractions, necessary to assess the validity of depositional body stratigraphy, likely results in a less accurate morphologic simulation than if only the coarse sediment fraction was included because of the neglected processes and their effect on fine sediment deposition. Though it was thought that the use of process-based, depth-averaged morphological modeling in Delft3D would offer an ideal method for assessing the expected land-building arising from large-scale sediment diversions in the transgressive Mississippi Delta, the necessary inclusion of multiple marine processes for accurate delta development simulation, especially the difficult to implement wind forcings from periodic cold front passages, makes the use of this modeling technique somewhat inefficient. At the moment, more simplified models that assume delta radial symmetry are more suited for the evaluation of expected diversion land-building for preliminary studies where multiple location alternatives are still in consideration. Detailed process-based modeling, such as that presented in this study, is more suited for much higher level evaluations in the diversion design process that justify the increased effort to adequately represent all processes involved. For situations in which the exact stratigraphy of depositional bodies is of no interest, simulation of the development of the mostly sand-dominant delta features in the Southeast Louisiana Coast may be more efficiently achieved with a single fraction sediment schematization.

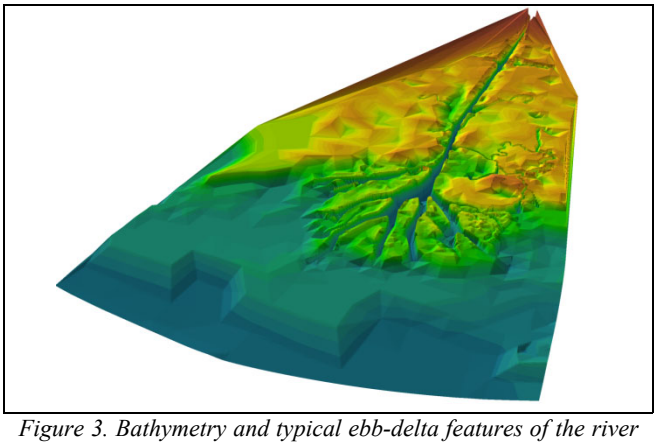

Figure 3. Bathymetry and typical ebb-delta features of the river dominant Wax Lake Delta

OUTLOOK

In the aftermath of Hurricane Katrina, New Orleans and the Mississippi River Delta Region has invested more money than any time in history of the State of Louisiana in rebuilding levees and wetlands. This investment has nourished world class science, research and engineering expertise in which the Dutch Coastal Engineering community and its students have taken part. This paper has shown three examples of graduation projects after Katrina by Dutch and US students. The projects have been welcomed with high interest by local stakeholders because of the high quality and innovative ideas.

Now is the time to use this momentum to continue the exchange of students and build upon academic and scientific relationships. Especially in light of the just published Louisiana's Master Plan for a sustainable Coast (State of Louisiana, 2012), this is a solid foundation on which the State plans to continue building Louisiana's Coastal Program. Within the plan, structural and non-structural projects and programs are proposed, many of which have been conceptually studied by the Dutch students with a few selected for more in depth study (e.g. river diversions).

As Louisiana moves forward with the implementation of the Master Plan and associated in-depth research of feasibility of the proposed projects within the plan, the exchange of Dutch and US students should be continued in our view. Potential topics for further collaboration are:

- System interaction between river and marshes. Long-term strategies for the coast of Louisiana include marsh restoration and its interaction with the Mississippi River and its tributaries. Balancing the needs for redistribution of fresh water and sediments through diversions should be weighed against other important (economical) functions of the Mississippi River. Dutch expertise in River Management and supporting modeling tools can support weighing of various interests and alternatives.
- Long-term morphology of the Louisiana Coast. The morphology of the coastline is governed by various marine and alluvial processes which are complex in nature. The impact of human interventions of any sort need to be studied for optimization of any coastal strategy. The Dutch knowledge and experience in both short-term and long-term coastal modeling can play a key role in evaluating and optimizing these interventions.
- Hurricane surge prediction. Emergency Management will be a major subject in the overall flood protection strategy of the Southern Louisiana coastal region, in which accurate prediction will highly impact the effectiveness of any emergency measure. The Dutch knowledge in modeling of storm surges and the experience in operational flood forecasting can be shared with the Louisiana coastal community to improve emergency management

Climate change and the challenges it poses to society are making newspaper headlines in not only The Netherlands and Louisiana, but in many coastal communities. With increasing globalization of research and consultancy services students should be part of the international dialogue in an early stage to familiarize and offer them a global perspective on the international coastal engineering community.

ACKNOWLEDGEMENT

The editors thank the students for their enormous enthusiasm and motivation shown during their projects. It has been rewarding to work with high-talented and very motivated students during their projects in New Orleans. The students hosted in New Orleans projects were (in alphabetical order): Marcel van de Berg, Anja Bos, Tjeerd Driessen, Kevin Hanegan, Sanne van de Heuvel, Marten Hillen, Freek Kranen, Jos Kuilboer, ChuHui Lin, Alissa Miller, Pieter Nordbeck, Tom Smits, Roald Treffers, Mats Vosse and Marcel van der Waart. The US Army Corps of Engineers in New Orleans is highly acknowledged for hosting the Dutch students. The discussions at the New Orleans District have been very fruitful and enriched the projects to a large extent. The financial and logistical support from Royal Haskoning is highly appreciated.

REFERENCES

Hanegan, K., Modeling the evolution of the Wax Lake Delta in Atchafalaya Bay, Louisiana, Erasmus Mundus Msc Programme, Coastal and Marine Engineering and Management (CoMeM), 2011.

Hillen, M., Kuilboer, J., Nordbeck, P., Treffers, R. The effects of a diversion in the Mississippi River near Port Sulphur on the long-term safety of New Orleans, Delft University of Technology, 2007.

Lin, C. The future in seconds: eSURF, University of Twente, 2009.

Resio, D.T., and J.J. Westerink, "Modeling the physics of storm surges", Physics Today, September 2008, pp. 33-38.

Smits, T., Internship Report - Internship at Royal Haskoning in New Orleans, Delft University of Technology, 2009.

State of Louisiana, Louisiana's Master Plan for a sustainable Coast (draft), http://www.coastalmasterplan.louisiana.gov/2012-master-plan/draft-2012-master-plan/, 2012.

US Army Corps of Engineers, US Army Engineer District, New Orleans, Interim Survey Report, Morgan City, Louisiana and Vicinity, serial no. 63, US Army Engineer District, New Orleans, LA (November 1963).

Van Den Berg, M. A predictive model for hurricane surge levels in New Orleans, University of Twente, 2008.

Westerink, J. J., J. C. Feyen, J. H. Atkinson, H. J. Roberts, E. J. Kubatko, R. A. Luettich, C. Dawson, M. D. Powell, J. P. Dunion, and H. Pourtuheri (2008), A basin- to channel-scale unstructured grid hurricane storm surge model applied to southern Louisiana, Mon. Weather Rev., 136, 833–864, doi:10.1175/2007MWR1946.1.

DOI: 10.3990/2.205

Tidal divides

J. Vroom[1] and Z.B. Wang[1,2]
[1]Deltares, P.O. Box 177, 2600 MH, Delft, The Netherlands, Julia.Vroom@deltares.nl
[2]Delft University of Technology, Faculty of Civil Engineering and Geosciences

ABSTRACT

The Wadden Sea consists of a series of tidal basins which are connected to the North Sea by tidal inlets. Each lagoon has as boundaries the mainland coast, the barrier islands on both side of the tidal inlet, and the tidal divides behind the two barrier islands. Behind each Wadden Island there is a tidal divide separating two adjacent tidal basins. The locations of the tidal divides in the Wadden Sea are not fixed. Especially after a human interference, a tidal divide can move and thereby influences the distribution of area between the basins, which is important for the morphological development of the basins. Two types of tidal divides can actually be identified behind each island: the hydraulic tidal divide and the morphological tidal divide. These do not necessarily have the same position, and their location is an indicator for the equilibrium of the adjacent basins. This paper describes theoretical analyses meant for improve the insights into the location of the tidal divides and their movements, as are observed in the Dutch part of the Wadden Sea in the last 80 years.

INTRODUCTION

In a series of tidal basins, like the Wadden Sea, a tidal watershed or tidal divide forms the separation between two adjacent tidal basins. Tidal divides are characterized by lower flow velocities and an elevated bed level. They are important for the morphological development of the basins, because by moving they change the surface area of the adjacent basins. In this paper we study the movement of the tidal divides in the Dutch Wadden Sea in the last 80 years by analyzing flow velocities from DELFT3D-model results and bathymetries collected by Rijkswaterstaat. A simplified case is used to study the factors influencing the position of the tidal divide. First, we will give a clear description of a tidal divide, which will be used throughout this paper.

METHODS

Movement of tidal divides

First, clear definitions of the tidal divides are needed for determining positions of the tidal divides in different years. We make a distinction between hydraulic and morphological tidal divides. A hydraulic tidal divide is the separation between the basins in terms of drainage. It can be defined as the line where the standard deviation of the flow velocity is minimal. In reality, we do not see such a line, but a transitional area with lower flow velocities consisting of interconnected tidal flats. However, a line is desired to be able to use the hydraulic tidal divide as a basin boundary for example in computations. The morphological tidal divide is an elevated spine-like structure in bed, see Figure 1 (inset). The centre-line of the spine-shape is the line representation of the morphological tidal divide; this is not necessarily the highest point in the bed, as can been seen from the morphological tidal divide behind Ameland.

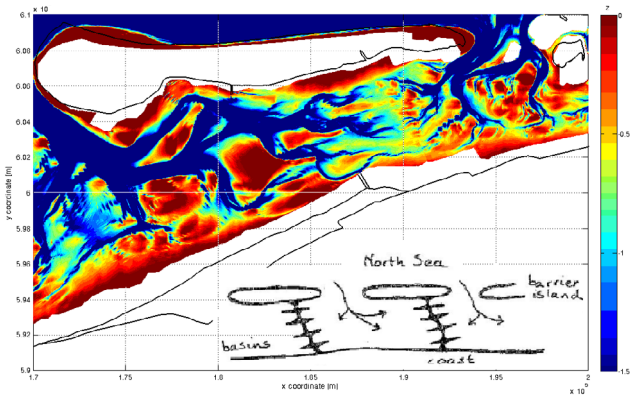

Figure 1. The spine-shaped morphological tidal divide behind Ameland

Simplified case

In order to obtain more understanding about the behaviour of the hydraulic tidal divide we analyse a simple case: The region between two adjacent tidal inlets, i.e. the area behind a barrier island, is considered as a prismatic channel. The problem is then simplified to the tidal propagation through a channel with constant water depth. We consider the propagation of a single tidal component. At one side of the channel the water level is then described by a cosine function and at the other side of the channel the amplitude as well as the phase may be different.

We now ask our self the question will there be a hydraulic tidal divide, i.e. a place in the channel where the amplitude of the flow velocity is minimal? Which factors determine whether or not a

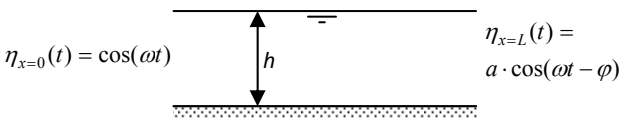

Figure 2. Sketch of the simplified case

hydraulic tidal divide is present? What is the position of the hydraulic tidal divide? Which factors determine the position of the hydraulic tidal divide?

First we try to answer the questions using an analytical approach. To do this we solve the linear equation for tidal propagation with linearized bottom friction (*Wang et al.*, 2011, *Vroom*, 2011):

$$\frac{\partial^2 \eta}{\partial t^2} - c^2 \frac{\partial^2 \eta}{\partial x^2} + \kappa \frac{\partial \eta}{\partial t} = 0$$

Herein

η	Water level [m]
t	Time [s]
c	Propagation velocity of tidal wave [m/s]
x	Coordinate along the channel (island) [m]
κ	Linearized friction factor [s^{-1}]

The solution of this equation satisfying the boundary conditions as shown in Figure 1 is:

$$\tilde{\eta}(x) = \frac{\sinh[p(L-x)]}{\sinh(pL)} + \frac{\sinh(px)}{\sinh(pL)} a \cdot e^{-i\varphi}$$

With:

$\tilde{a} = a \cdot e^{-i\varphi}$, the complex amplitude at the channel end x=L.

$p = \mu + ik = ik_0\sqrt{1 - i\sigma}$

$$\sigma = \frac{\kappa}{\omega}$$

Herein

L	Length of channel / island [m]
a	Amplitude ratio between the two ends of the channel [-]
φ	Phase lag between the two ends of the channel
ω	Frequency of the tidal wave [rad/s]
μ	Damping factor [-]
k	Wave number [-] (= 2π/λ)
k_0	Frictionless wave number [-] (=ω/c)

The solution for the flow velocity is:

$$u(x,t) = \frac{i\omega}{ph}\left(\frac{\cosh[p(L-x)]}{\sinh(pL)} - \frac{\cosh(px)}{\sinh(pL)} a \cdot e^{-i\varphi}\right) \cdot e^{i\omega t}$$

$$\tilde{u}(x) = \frac{i\omega}{ph}\left(\frac{\cosh[p(L-x)]}{\sinh(pL)} - \frac{\cosh(px)}{\sinh(pL)} a \cdot e^{-i\varphi}\right)$$

The further elaboration of this equation algebraically is done by neglecting the bottom friction (σ=0). The amplitude of the flow velocity is then

$$\hat{u}(x) = \frac{\omega}{k_0 h}\sqrt{\left(\frac{\cos[k_0(L-x)] - a\cos(k_0 x)\cos\varphi}{\sin(k_0 L)}\right)^2 + \left(\frac{a\cos(k_0 x)\sin\varphi}{\sin(k_0 L)}\right)^2}$$

Solving the equation that the derivative of the amplitude of the flow velocity is zero yields:

$$\tan(2k_0 x) = \frac{\sin(2k_0 L) - 2a\cos\varphi\sin(k_0 L)}{\cos(2k_0 L) - 2a\cos\varphi\cos(k_0 L) + a^2}$$

This is the equation determining the location of the hydraulic tidal divide for the frictionless case.

RESULTS

Movement of tidal divides

The positions of the hydraulic and morphological tidal divides in the Dutch Wadden Sea are determined for different years according to the definitions described in the previous section.

Regarding the hydraulic tidal divide, the largest changes are observed near the Afsluitdijk. The simulation for 1926, including the Afsluitdijk, shows that the hydraulic tidal divide has not moved yet. The standard deviation of the flow velocity is lowest at this position, but also very low at the later position of the hydraulic tidal divide. Probably, this used to be a local hydraulic tidal divide, splitting the drainage area of two branches of the Vlie

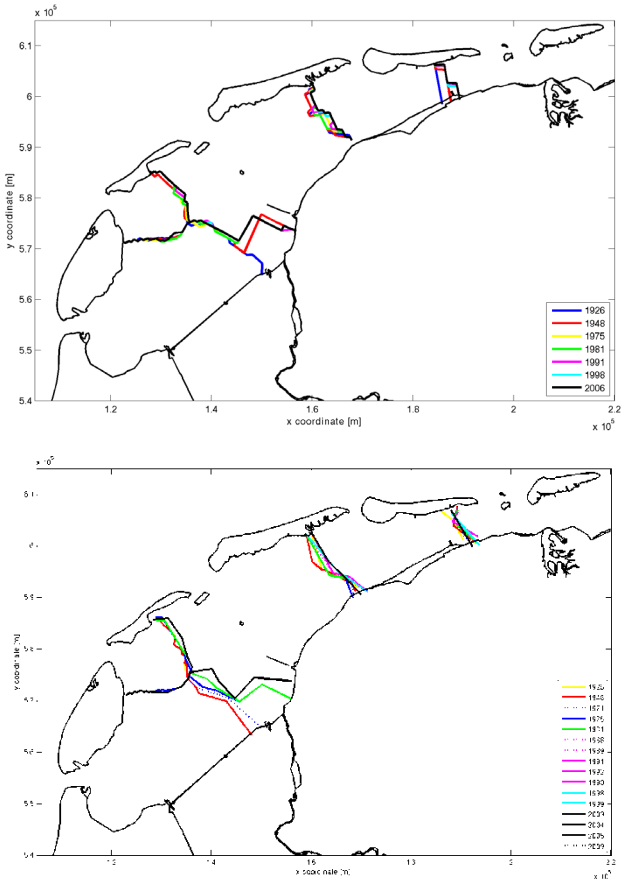

Figure 3 (top): Hydraulic tidal divides in the Dutch Wadden Sea, note that the 1926 simulation also includes the Afsluitdijk and therefore resembles the 1932 situation (post closure).

Figure 4 (bottom): Morphological tidal divides in the Dutch Wadden Sea

basin. The Eierlandse Gat basin has slightly increased in size, due to an eastward expansion of the hydraulic tidal divide between Eierlandse Gat and Vlie. Although the Eierlandse Gat basin is relatively close to the Afsluitdijk, the movement of the tidal divides bordering the basin is very small. The tidal divide behind Terschelling shows a shift in eastward direction.

Looking at the lines representing the morphological tidal divides in Figure 4, we can see that the morphological tidal divide between Marsdiep and Vlie adjusts much slower than the hydraulic tidal divide. It is remarkable that for the situation just after closure, the hydraulic and morphological tidal divide have more or less the same position. Apparently, the elevated bed level of the morphological tidal divide hinders the movement of the hydraulic tidal divide first. Due to higher flow velocities at the morphological tidal divide, the topographic high erodes and the hydraulic tidal divide can move. When the morphological tidal divide has moved close to the position of the hydraulic tidal divide, the bed level can get higher again. For the other tidal divides we study in this paper, we see a smaller movement of the tidal divides. Because the movement is more gradual, the morphological tidal divide can keep pace with the hydraulic tidal divide more easily.

Simplified case

For the simplified case we can make a distinction between a frictionless derivation and a derivation including linearized friction.

Frictionless case

Figure 5 shows the position of the hydraulic tidal divide in the rectangular channel in case without friction.

The following observations are made from the analytical solution:

If the tidal amplitudes at the two ends are the same, a tidal divide exists and is located in the middle for the case that there is no phase difference between the two ends. This is the trivial case that the tides at the two ends are exactly the same.

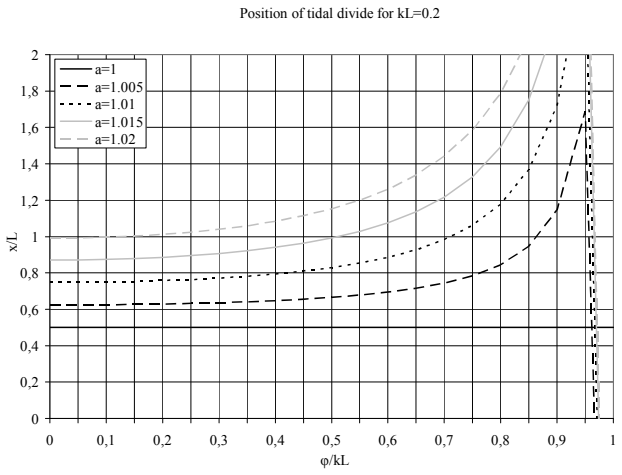

Figure 5: Position of the tidal divide versus the relative phase difference (kL=0.2) for increasing wave amplitude a (lighter gray lines). Note that a tidal divide is only present if x/L is in the realistic domain between 0 and 1.

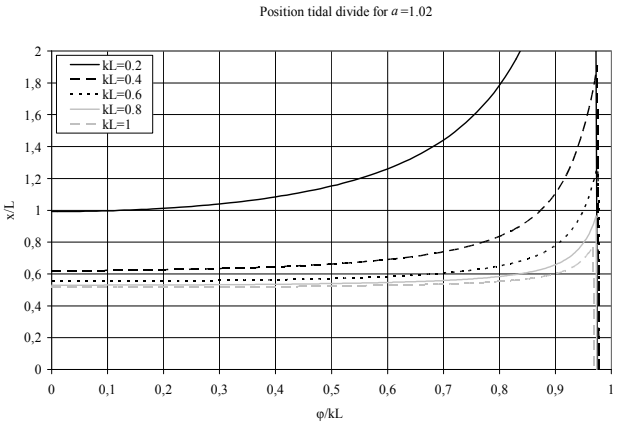

Figure 6. Position of the tidal divide versus the relative phase difference for increasing relative channel length (kL) (lighter gray lines).

It is remarkable that the phase difference has no influence on the position of the tidal divide in case the incoming waves have equal amplitudes. But the phase difference does have an influence on the absolute value of the minimum of the flow velocity amplitude in this case. The phase difference has to be smaller than *kL*, if it is equal to *kL* a purely propagating wave will be present.

Even more remarkable is the influence of the amplitude difference between the two ends. The tidal divide is closer to the side with larger tidal amplitude than the side with smaller amplitude. According to the linear solution the amplitude ratio has even more influence on the existence and the position of tidal divides than the relative phase difference. This means that it is not the propagation of the tidal wave but the spatial variation of the tidal range that has the most influence on the location of the tidal divide behind a barrier island.

There is not always a tidal divide. If the tidal amplitudes at the two ends are not equal there is a limit to the phase difference between the two ends for the existence of a tidal divide. When the relative phase difference between the two ends becomes larger than the limit, no tidal divide can be found (no solution for x in the realistic domain 0<x<L). The limit for the phase difference becomes smaller if the amplitude increases in the direction of tidal propagation. Interpreted for the Wadden Sea case this means that a tidal divide only can exists if the propagation of the tidal wave on the sea side of a barrier island is much faster than the propagation in the basin behind the island. In other words, the tidal divide can only exist if the Wadden Sea is relatively shallow.

The phase difference limit for the existence of the tidal divide becomes larger if the island is longer and/or the basin behind the island is shallower. It seems thus that the barrier islands should have lengths above a certain limit depending on the characteristics of the tide and the tidal propagation at the North Sea side.

Case with linearized friction

In Figure 7 the contribution of the bottom friction term on the importance of the phase difference and the amplitude ratio is clearly visible. If the bottom friction is small, the amplitude ratio is dominant over the phase difference. With larger friction the phase difference is the governing mechanism for determining the

position of the hydraulic tidal divide. In Figure 8 we see that with the inclusion of the bottom friction, the phase difference does have an influence on the position of the tidal divide, even if the incoming waves have equal amplitudes. For larger relative channel lengths, the limits for the phase difference and amplitude ratio are less strict.

DISCUSSION

The determination of the position of the line representing the hydraulic and morphological tidal divide will always be somewhat arbitrary, which means the exact position of the line will differ from person to person. This is influencing the surface areas of the basins and can be important for the determination of the equilibrium state of the basins. The movement of the tidal divides however, can also be observed from the bathymetric data itself and the observations made in this paper are not strongly dependent on this line representation.

CONCLUSIONS

The movement of the tidal divides in the Dutch Wadden Sea show an interrelated behavior of the hydraulic and morphological tidal divide. After large changes in the basins, the morphological tidal divide might be high enough to hinder the movement of the hydraulic tidal divide. After erosion of the topographic high, the hydraulic tidal divide can move more freely, afterwards the morphological tidal divide will follow.

In order to obtain more insights into the locations of the tidal divides a theoretical analysis has been carried out for a simplified case. The tidal propagation behind an island is schematised into a simple channel flow with two open boundaries representing the two inlets where the tidal variation of water level is represented by a single tidal component with different amplitudes and phases at the two boundaries. The hydraulic tidal divide is defined at the location where the amplitude of the flow velocity is minimal. The analytical solution of the linear tidal propagation equation shows that a tidal divide does not always exist. It can only exist when the island is relatively long and / or the back barrier basin is relatively shallow. The analytical solution shows further surprisingly that the difference in tidal amplitude between the two ends of the channel (island) has more influence on the location of the tidal divide than the phase difference in case of small bottom friction. When the tidal amplitudes at the two ends are the same and bottom friction is neglected, the tidal divide is always in the middle, independent of the phase difference. When friction is included, the phase difference becomes more important. It is further surprising that the tidal divide moves to the end with larger tidal amplitude when the amplitudes at the two ends are not equal. The limit for the phase difference between the two ends for existence of tidal divide becomes smaller if the amplitude increases in the direction of tidal propagation. If the difference between the amplitudes at the two ends is too large and / or the phase difference between the two ends is too large no tidal divide exists because the amplitude of the flow velocity will be monotonously changing along the channel.

Our final conclusion is that the variation of the tidal amplitude as well as the direction of the tidal wave propagation on the sea side of the islands have influence on the location of the hydraulic tidal divides in the Wadden Sea, but which parameter is more dominant is depending on the water depth - wave height ratio.

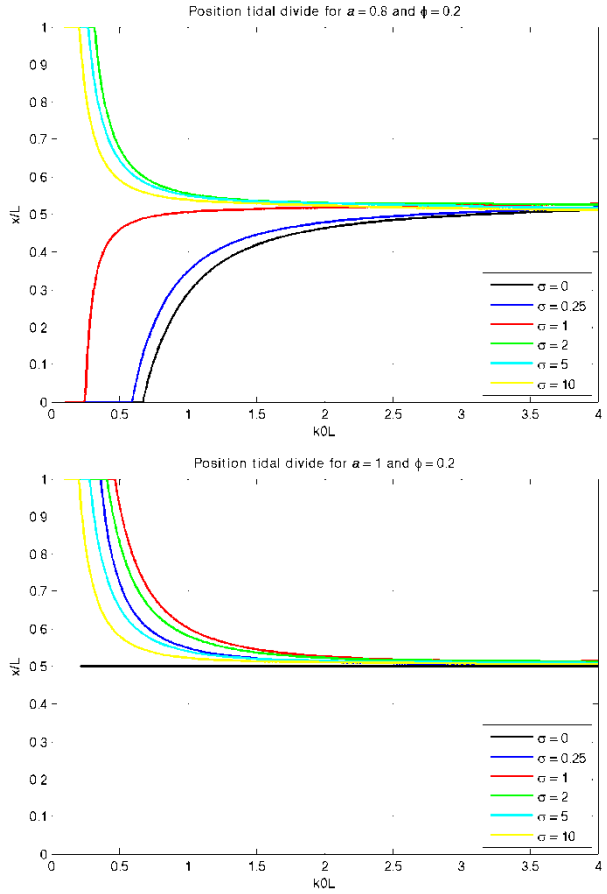

Figure 7 (top): Position of the tidal divide versus the relative channel length for an amplitude ratio of 0.8 and phase difference of 0.2 for different values of the bottom friction factor σ

Figure 8 (bottom): Position of the tidal divide versus the relative channel length for equal amplitudes and a phase difference of 0.2 for different values of the bottom friction factor σ

ACKNOWLEDGEMENTS

This study has been executed as part of a Master Thesis at TU Delft. The supervisors, prof.dr.ir. M.J.F. Stive, dr.ir. R.J. Labeur, dr.ir. B.C. van Prooijen and ir. M.P.H. Janssen, are acknowledged for their discussions and valuable input.

REFERENCES

Ippen, A.T., and Harleman, D.R.F. (1966), Tidal Dynamics in Estuaries, Part I: Estuaries of rectangular section and Part II: Real estuaries, Chapter 10 of 'Estuary and Coastline Hydrodynamics', Mc-GrawHill, New York

Wang, Z.B., Vroom, J., Van Prooijen, B.C., Labeur, R.J., Stive, M.J.F. and Jansen, M.H.P. (2011), Development of tidal watersheds in the Wadden Sea, Conference Proceedings of River, Coastal and Estuarine Morphodynamics: RCEM 2011.

Vroom, J.(2011), Tidal divides, A study on a simplified case and the Dutch Wadden Sea, Master Thesis TU Delft

DOI: 10.3990/2.206

Rip Current Observations at Egmond aan Zee

G. Winter[1,2*], A.R. van Dongeren[2], M.A. de Schipper[1] and J.S.M. van Thiel de Vries[1,2]
[1]Faculty of Civil Engineering and Geosciences, Delft University of Technology, Delft, The Netherlands
[2]Deltares, Marine and Coastal Systems, P.O. Box 177, 2600 MH Delft, The Netherlands
*corresponding author: Gundula.Winter@deltares.nl

ABSTRACT

Rip currents are narrow, seaward directed flows in the surf zone that can pose a serious threat to swimmers. This issue has received attention particularly on swell dominated coasts (such as the US, Australia, France and UK) where numerous field experiments have been undertaken. However, the threat of rip currents is less recognised on wind-sea dominated coasts such as the North Sea, even though a consistent number of swimmers drift offshore (in rip currents) and require rescue by surf lifeguards each year (for example at Egmond aan Zee, The Netherlands). In August 2011, a five day field experiment SEAREX (Swimmer Safety at Egmond – A Rip current Experiment) was conducted. Lagrangian velocity measurements were taken with drifter instruments and human drifters that were tracked via GPS. Three flow patterns were observed in the experiment: (1) a locally governed circulation cell, (2) a pattern in which the drifter initially floats offshore and then is advected by a strong tidal alongshore-directed current and (3) a meandering longshore current between the shoreline and the bar. A variety of rip current velocities were measured with the strongest being approximately 0.6 m/s. The field data was hindcasted with the numerical model XBeach. Based on this model the sensitivity of rip currents towards wave height, water level and rip channel depth was investigated. Both field and model data show that offshore velocities in a rip increase with increasing wave height and decreasing water level, but that the rip channel depth imposes an upper limit on the rip current velocity.

INTRODUCTION

Rip currents are narrow, offshore directed flows that are generated by wave interaction or structural interaction mechanisms [*Dalrymple*, 1978]. The latter group consists of rip currents induced by the bottom topography, coastal boundaries (such as breakwaters and groins) as well as barred coastlines and are referred to bathymetrically controlled rip currents. This type of rip currents are found to be stronger than their non-morphologically controlled counterparts, the so-called transient rip currents [*Dalrymple et al.*, 2011]. This paper will focus on barred coastlines and the rip currents induced in this context.

The location of rip currents on a barred coast line is tied to a rip channel that interrupts the sand bar (Figure 1). Waves break over the bar, and exert a force on the water column through radiation stress gradients [*Longuet-Higgins and Stewart*, 1964]. This force causes a relatively high water level set-up in the trough between the beach and the bar. However, in the channel the waves break later (due to the deeper water) and induce less set up. The alongshore water level gradient initiates a longshore flow parallel to the beach that is referred to as feeder current. The feeder currents converge onshore of the rip channel into an offshore flow, the so-called rip neck. Outside the surf zone the rip current diffuses in the rip head. Together with the onshore mass transport over the sand bar the rip current forms a closed circulation cell.

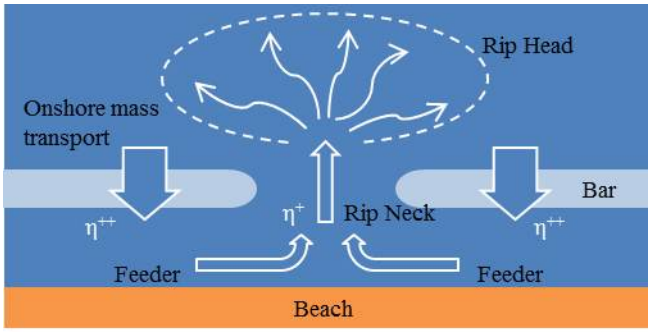

Figure 1. Rip current circulation cell. η++ indicates a relatively large water level set-up and η+ a relatively small set-up.

A number of field experiments have been undertaken to measure rip currents in the field with fixed instruments [*Aagaard et al.*, 1997; *Brander*, 1999; *Callaghan et al.*, 2004; *Dette et al.*, 1995; *MacMahan et al.*, 2005]. Current meters deployed in cross shore and/or longshore transects provide Eulerian flow measurements and give insight in the temporal variations of rip currents. However, the installation of these instruments in the surf zone is problematic and this experimental set-up provides limited spatial information about flow patterns of rip currents.

In more recent field studies GPS tracked drifters have been used to obtain a more comprehensive image of the flow patterns in a rip current and to overcome the limitations associated with fixed instrument transects [*Austin et al.*, 2010; *Johnson and Pattiaratchi*, 2004; *MacMahan et al.*, 2010]. People were also utilised as human drifters and were tracked either with two theodolites from the beach [*Brander and Short*, 2000] or with GPS trackers mounted to the people's heads [*MacMahan et al.*, 2010].

The results of GPS drifter tracking have shown that floating objects are mainly retained in the surf zone [*Reniers et al.*, 2009]. Observed flow patterns include eddies and meandering long shore currents [*MacMahan et al.*, 2010] and only infrequently is drifting material ejected offshore or washed on the beach.

This paper describes rip current characteristics on the Dutch coast and the results of the field experiment at Egmond aan Zee. The objectives of this research were to describe the rip current

flow patterns and to investigate the correlation of typical rip current velocities with hydrodynamic forcing.

A five day field experiment was conducted and the collected data was used to identify the governing parameters of rip current speed and to validate a hindcast model. The identified parameters were then subjected to a sensitivity analysis in the validated model.

This study contributes to the ultimate goal to predict rip currents based on forecasted hydrodynamic parameters given that an accurate bathymetry is available.

FIELD METHODS

In August 2011 (yeardays 234 – 238), a five day field experiment SEAREX (Swimmer safety in Egmond aan Zee – A Rip current Experiment) was conducted. The beach at the site is fronted by three bars of which the first and second are interrupted by several rip channels. Measurements were performed in two distinct rip channels in the second bar (Figure 2).

Lagrangian velocities in the surf zone were measured with drifter instruments that were similar to the design by *Schmidt et al.* [2003] (Figure 3). The drifters were tracked by GPS dataloggers and post-processed with data from a static base station to sub-meter accuracy following *MacMahan et al.* [2009]. In addition to the drifter instruments, human drifters were equipped with the same GPS units.

To distinguish regions of different flow intensities, the drifters were deployed in matrices consisting of two drifter rows either in alongshore or cross-shore direction. The drifters were deployed in cross-shore arrays when the updrift feeder was dominating.

A high resolution bathymetry survey was conducted using jetski and wheel-barrel mounted RTK-GPS instruments. Offshore wave data was recorded by an existing directional wave rider buoy at

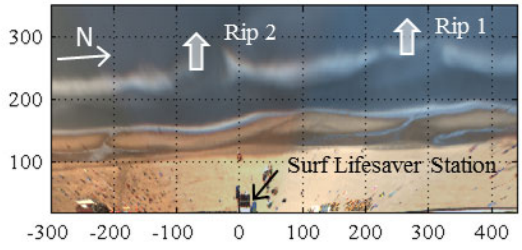

Figure 2. Argus plan view of the field site (derived from camera images taken from the lighthouse). The northern (Rip 1) and southern (Rip 2) rip channel are indicated.

Figure 3. Drifter instruments used during SEAREX.

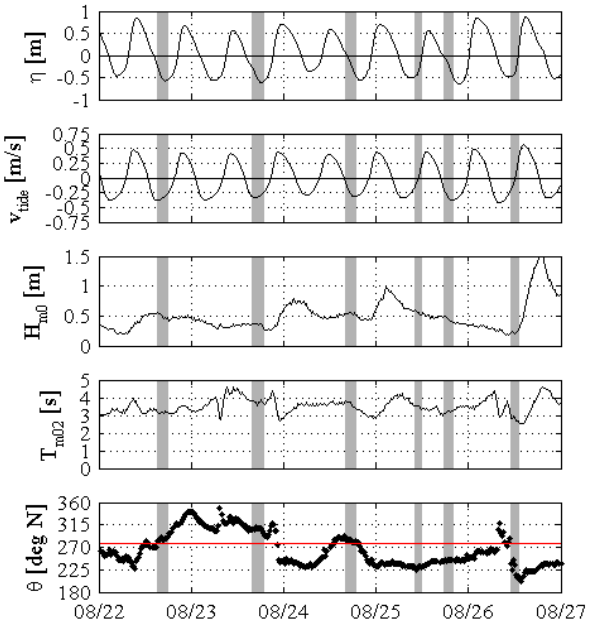

Figure 4. Hydrodynamic conditions during the field experiment from top to bottom: Water level (η) [m], tidal current (v_{tide}) [m/s], wave height (H_{m0}) [m], wave period (T_{m02}) [s] and wave angle (θ) [°N]. The red line in the bottom panel indicates the shore normal. The grey bars mark drifter experiments (with four to five deployments each).

Petten (maintained by Rijkswaterstaat) located 21 km North and 8.3 km offshore of the field site. Due to the relative uniformity of the coastal profile, wave data from this location is assumed representative for the offshore conditions at Egmond.

FIELD RESULTS

Hydrodynamic Conditions

The wave conditions were moderate throughout the experiment with the offshore wave height H_{m0} ranging from 0.35 to 0.7 m and the wave period T_{m02} ranging from 2.4 to 3.8 s. The field campaign coincided with neap tide with the smallest astronomical tidal range of 1.15 m on August 24. During the deployments the water level was around or below NAP +0 m. An overview of the tidal and wave conditions is provided in Figure 4.

Rip Current Velocities

An extensive dataset of rip current measurements in a Lagrangian framework was collected. In total, 28 drifter deployments were performed and 21 of these observations were classified as rip events. A rip event is defined as a flow pattern in which the drifters floated through the rip channel offshore.

The maximum drifter velocity of 0.60 m/s was measured on August 26 when also the highest offshore wave heights were recorded. The wave height H_{m0} was as large as 0.7 m and the offshore wave period T_{m02} was 3.6 s.

The offshore extent of the measured rip currents was in the order of 100 m offshore of the bar crest and stretched as far as 150 m. Large offshore extents were associated with strong offshore flows in which the drifters exited the surf zone. When the

drifters were retained in the surf zone the offshore extent was only 30 to 60 m offshore of the bar crest.

Observed Flow Pattern

In the experiment three flow patterns were observed: (1) a locally governed circulation cell (2) a pattern in which the drifter initially floats offshore and is then advected by the tidal longshore current and (3) a meandering longshore current. Pattern (1) and (2) describe rip events.

(1) The local circulation cell was always confined to the surf zone and was centred over the end of the downdrift bar (Figure 5). Only one circulation cell was observed downdrift of the channel while at no time during the experiment was a counter rotating eddy updrift of the rip channel observed.

(2) The drifters floated through the channel, exited the surf zone and were advected by a tidal longshore current offshore (Figure 6). The observed flow direction offshore of the bar was consistent with the tidal flow during those deployments. In case of weak tidal currents the drift direction was governed by the angle of wave incidence and/or the prevailing wind direction.

Flow pattern 2 was observed with rather high flow velocities in the rip channel (on average $u_{drifter}$ = 0.31 m/s compared to $u_{drifter}$ =

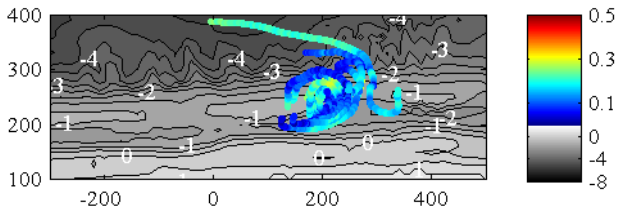

Figure 6. Local circulation cell measured during one deployment on August 22: The velocities are indicated by the colours and the bathymetry is plotted underneath in grey.

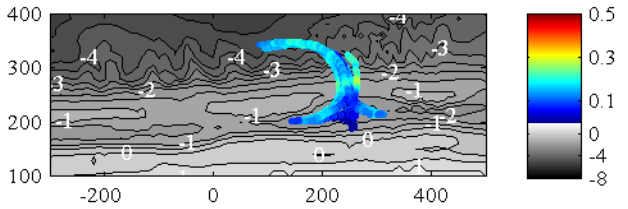

Figure 7. Offshore directed drifter paths during one deployment on August 23: The velocities are indicated by the colours and the bathymetry is plotted underneath in grey.

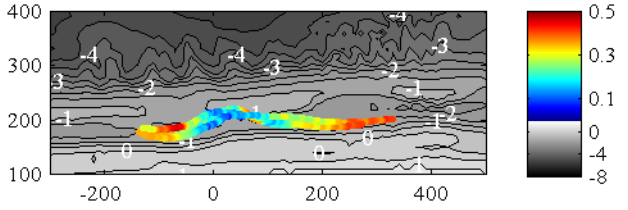

Figure 8. Meandering longshore current during one deployment on August 25: The velocities are indicated by the colours and the bathymetry is plotted underneath in grey.

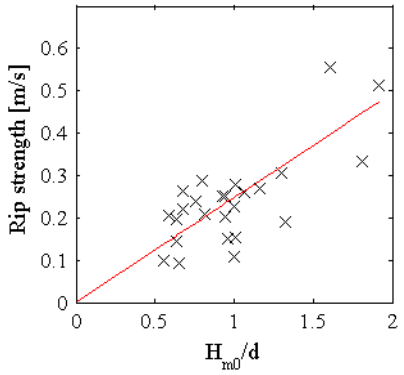

Figure 5. Rip strength versus H_{m0}/d. The solid red line represents the linear regression line.

0.18 m/s observed with flow pattern 1) and suggests that stronger currents possess enough inertia to enable the current (and the drifter) to exit the surf zone.

(3) The meandering longshore current is separated from (2) in the way that drifter paths are confined to the zone between the breaker bar and the beach (Figure 7).

This pattern was observed with water levels around or above NAP +0 m. The measurements were conducted in the presence of a northward directed tidal current. Both wind and waves came from southern directions and were likely to enhance the northward drifter movement.

FIELD DATA ANALYSIS

Correlation of rip currents with hydrodynamic forcing

Rip current flow is conditional upon wave dissipation. An indicator for the intensity of wave breaking is the ratio of the offshore wave height H_{m0} over the water depth on the bar d. The rip currents were evaluated in terms of the rip strength which represents the offshore velocity in a rip current. The rip strength is calculated by taking the maximum offshore velocities of each drifter that floated offshore in the rip channel and then averaging those values over one deployment.

A linear least squares regression was fit to the data with H_{m0}/d as independent variable and the rip strength as response variable (Figure 8). The R^2 value of the regression model is 0.68 and the p-value is 0.0048 and thus, a statistically significant correlation between the rip strength and wave height over water depth ratio is existent.

Correlation with Argus video images

The size of the data set does not allow drawing definite conclusions from a statistical analysis. In particular, it cannot be decided whether the high velocities measured on August 26 are outliers or indicate a trend (here they were not treated as outliers).

Therefore, a series of video images (Argus) that reveal areas of wave dissipation was used to examine the relation between H_{m0}/d and the rip strength. Figure 9 shows three images recorded on August 25 with low water level (large H_{m0}/d), intermediate water level and high water level (small H_{m0}/d).

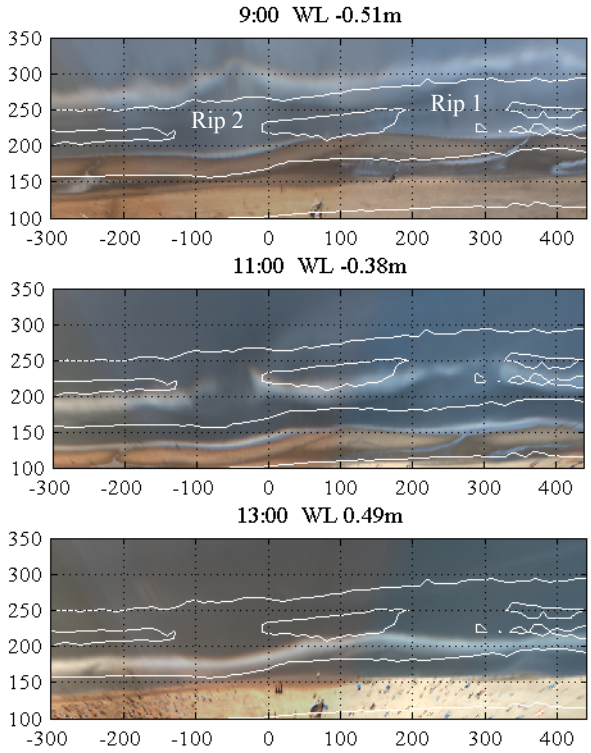

Figure 9. Series of Argus images on August 25. The water level increases from top to bottom and therewith the wave breaking shifts from offshore of the first surf zone bar to the swash bar. Wave breaking takes place slightly offshore of the white band that indicates the bores of the broken waves.

The statistical analysis indicated that the rip strength decreased with decreasing H_{m0} /*d*. The video images show that with higher water levels, the waves propagate over the surf zone bar and are not dissipated until they reach the swash bar (bottom panel). This interrupts the driving mechanism for rip currents on the first surf zone bar and explains the low rip activity with low values of H_{m0} /*d*. Similar observations were made in previous field studies where weak or no rip currents were measured at high tide [*Aagaard et al.*, 1997; *Austin et al.*, 2010; *Brander*, 1999].

However, the linear relation suggested in the statistical analysis may not hold for very low water levels (large H_{m0} /*d*) when the waves are also dissipated in the channel (top panel). As a consequence the longshore variation in wave dissipation and water level set up (which drive the rip current circulation) are weakened (Rip 2) or completely absent (Rip 1). An offshore current in Rip 2 is evident from the protuberance in the wave dissipation band. The opposing current causes the waves to refract towards the current and causes a non-uniform wave dissipation band.

The influence of the wave dissipation was further investigated in a sensitivity analysis using a numerical model (see below).

NUMERICAL MODEL

Hindcast

A hindcast model of the rip current system was built using XBeach [see *Roelvink et al.*, 2009 for a model description] in stationary mode (no wave group forcing). The drifter option was used to validate the model against flow patterns and rip current velocities observed in the field. From four out of five days one representative deployment was chosen to replicate in the hindcast model.

The hindcast model reproduced the field observations with respect to the rip strength well (Table 1). The large offshore velocities measured on August 25 are attributed to a cross-offshore wind that was not implemented in the model.

Likewise, the drifter trajectories were replicated well. Figure 10 shows the modelled drifter paths of a deployment on August 22 and August 23. The circulation and advection of the drifters to the South is reproduced well (compare with Figure 5 and Figure 6).

However, all hindcast models had in common that the offshore extent of the rip current was underestimated. This is attributed to the distinct vertical flow structure offshore of the rip channel with large offshore directed velocities near the surface and weak or slight onshore directed velocities near the bed [*Haas and Svendsen*, 2002]. This particular flow structure is not accounted for in a 2DH model and therefore, the offshore velocities in the upper water layer were underestimated. As a consequence, the drifters that floated in the upper water layer were advected less far offshore in the model than they were observed in the field.

Table 1. Rip strength calculated from the measured and modelled drifter data.

Deployment Day	Measured [m/s]	Model [m/s]
August 22	0.29	0.25
August 23	0.24	0.20
August 24	0.21	0.26
August 25	0.55	0.36

Sensitivity Analysis

The validated model was used to investigate the relation between H_{m0} /*d* and the rip strength in more detail. Several combinations of wave height, rip channel depth (with respect to the bar crest) and water level were tested (Figure 11). The model results also show an increase in rip strength with increasing H_{m0} /*d*. But the maximum possible rip strength is limited by the rip channel depth because it determines when wave breaking commences in the channel. It is thus not the wave dissipation on the bar, but the dissipation gradient from the bar to the channel that governs the strength of a rip current.

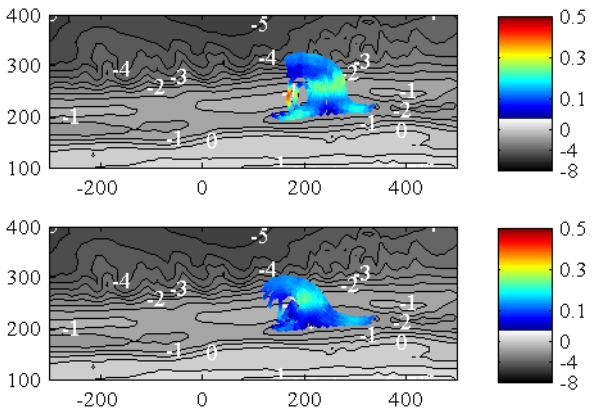

Figure 10. Modelled drifter paths of a deployment on August 22 (top) and August 23 (bottom).

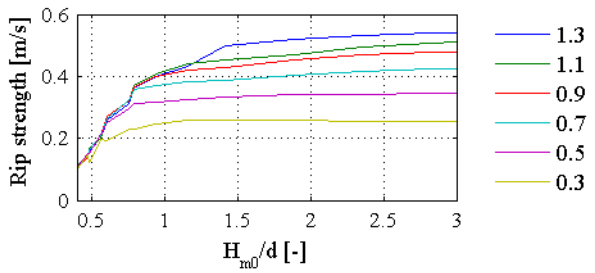

Figure 11. Rip strength vs. H_{m0}/d for various rip channel depths ranging from 0.3 m to 1.3 m.

CONCLUSIONS

A field experiment demonstrated the existence of rip currents at the wind-sea dominated coast of Egmond aan Zee with water levels below NAP +0 m. With water levels around or above NAP +0 m meandering longshore currents prevailed. Under moderate wave conditions (H_{m0} = 0.35 to 0.7 m) these rip currents reached a considerable strength of up to 0.6 m/s.

A statistically significant correlation between the measured rip current strength and the ratio of offshore wave height over water depth on the bar was identified. Video images indicate that this relation is not linear but stagnates for large values of H_{m0}/d when wave breaking commences in the rip channel.

A hindcast of the measurements was performed in the numerical model XBeach. The model showed good agreement with the field data in terms of the rip strength. The flow patterns were also replicated fairly well though the offshore extent of the rip current was consistently underestimated.

In the validated model the sensitivity of the rip strength to wave height, water level and channel depth was analysed and confirmed the conclusions drawn from the field data that rip strength increases with increasing H_{m0}/d until wave breaking commences in the rip channel which retards the rip current flow.

ACKNOWLEDGEMENT

We thank the many volunteers who assisted in collecting the field data: Andrew Pomeroy, Antoon Hendriks, Arnold van Rooijen, Brice Blossier, Claire Bouchigny, Cilia Swinkels, Dano Roelvink, Dirk Knipping, Erwin Bergsma, Giorgio Santinelli, Greta van Velzen, Hesseltje Roelvink, Ivan Garcia, Jamie Lescinski, Jeroen Stark, Lisa de Graaf, Leo Sembiring, Maarten van Ormondt, Roland Vlijm, Timon Pekkeriet and in particular Willem Verbeek whose experience with rip currents at Egmond aan Zee was valued highly.

We appreciate the help and equipment provided by Shore Monitoring and the bathymetry survey that was conducted by them. On site Shore Monitoring was represented by Roeland de Zeeuw and Sierd de Vries.

Rijkswaterstaat is gratefully acknowledged for the use of the wave buoy data taken at Petten that was provided to us by Andre Jansen.

The research was funded by Flood Control 2015 (Realtime Safety on Sedimentary Coasts program) and Building with Nature (Swimmer Safety project), Deltares Strategic Funding in the framework of the System Tools for Prevention and Preparation program (project 1202362).

M.A. de Schipper was funded by Building with Nature under project code NTW 3.2.

REFERENCES

Aagaard, T., B. Greenwood, and J. Nielsen (1997), Mean currents and sediment transport in a rip channel, Marine Geology, 140(1-2), 25-45.

Austin, M., T. M. Scott, J. W. Brown, J. A. Brown, J. H. MacMahan, G. Masselink, and P. Russell (2010), Temporal observations of rip current circulation on a macro-tidal beach, Continental Shelf Research, 30(1149-1165).

Brander, R. W. (1999), Field observations on the morphodynamic evolution of a low-energy rip current system, Marine Geology, 157(3-4), 199-217.

Brander, R. W., and A. D. Short (2000), Morphodynamics of a large-scale rip current system at Muriwai Beach, New Zealand, Marine Geology, 165(Compendex), 27-39.

Callaghan, D. P., T. E. Baldock, and P. Nielsen (2004), Pulsing and Circulation in Rip Current System, in International Conference Coastal Engineering, edited by J. M. Smith, pp. 1493-1505, American Society of Civil Engineers, Lisbon.

Dalrymple, R. A. (1978), Rip currents and their causes, in International Conference on Coastal Engineering, edited, pp. 1414-1427, American Society of Civil Engineers, Hamburg.

Dalrymple, R. A., J. H. MacMahan, A. J. H. M. Reniers, and V. Nelko (2011), Rip Currents, Annual Review of Fluid Mechanics, 43(1), 551-581.

Dette, H. H., K. Peters, and F. Spignat (1995), About rip currents at a meso-tidal coast, in Coastal Dynamics '95, edited, pp. 477-488, American Society of Civil Engineers, Gdansk, Poland.

Haas, K. A., and I. A. Svendsen (2002), Laboratory measurements of the vertical structure of rip currents, J. Geophys. Res., 107(C5), 3047.

Johnson, D., and C. Pattiaratchi (2004), Transient rip currents and nearshore circulation on a swell-dominated beach, J. Geophys. Res., 109(C2), C02026.

Longuet-Higgins, M. S., and R. W. Stewart (1964), Radiation stresses in water waves; a physical discussion, with applications, Deep Sea Research and Oceanographic Abstracts, 11(4), 529-562.

MacMahan, J. H., J. Brown, and E. Thornton (2009), Low-Cost Handheld Global Positioning System for Measuring Surf-Zone Currents, Journal of Coastal Research, 744-754.

MacMahan, J. H., E. B. Thornton, T. P. Stanton, and A. J. H. M. Reniers (2005), RIPEX: Observations of a rip current system, Marine Geology, 218(Compendex), 113-134.

MacMahan, J. H., et al. (2010), Mean Lagrangian flow behavior on an open coast rip-channeled beach: A new perspective, Marine Geology, 268(1-4), 1-15.

Reniers, A. J. H. M., J. H. MacMahan, E. B. Thornton, T. P. Stanton, M. Henriquez, J. W. Brown, J. A. Brown, and E. Gallagher (2009), Surf zone surface retention on a rip-channeled beach, J. Geophys. Res., 114(C10), C10010.

Roelvink, D., A. Reniers, A. van Dongeren, J. van Thiel de Vries, R. McCall, and J. Lescinski (2009), Modelling storm impacts on beaches, dunes and barrier islands, Coastal Engineering, 56(11-12), 1133-1152.

Schmidt, W. E., B. T. Woodward, K. S. Millikan, R. T. Guza, B. Raubenheimer, and S. Elgar (2003), A GPS-tracked surf zone drifter, Journal of Atmospheric and Oceanic Technology, 20(Compendex), 1069-1075.

NCK photo competition

Thorsten Balke: Oostkapelle, Zeeland

Acknowledgements

As local organizing committee we thankfully acknowledge the contribution of a number of people to these Jubilee Conference Proceedings. First of all, we would like to thank all keynote speakers for accepting the invitation and for putting so much effort in preparing their keynote papers. We thank Job Dronkers and Ad van der Spek for their special contributions to these proceedings. Thanks also to all other authors for submitting so many interesting short papers.

The short papers have been assessed by a team of reviewers. We are happy the reviewers could find time to do this in a rather short time span. Thanks for your contribution. The beautiful pictures included in these proceedings were submitted for the special NCK jubilee photo competition. Thanks to all photographers for their participation and to Martin Baptist, Theo Gerkema and Ad van der Spek for realizing this initiative and for being the jury.

Finally, the organization of these NCK-days would not have been possible without support from both NCK and our Water Engineering & Management colleagues. Thanks to the NCK-organization in person of Ad van der Spek, Claire van Oeveren and Jolien Mans. From our WEM-colleagues we especially acknowledge Brigitte Leurink and Anke Wigger for keeping us on track and arranging so many things we did not think of.

Photo index

Author index